

DEEP *Chandra* MONITORING OBSERVATIONS OF NGC 4278: CATALOG OF SOURCE PROPERTIES

N. J. BRASSINGTON, G. FABBIANO, D.-W. KIM, A. ZEAS
Harvard-Smithsonian Center for Astrophysics, 60 Garden Street, Cambridge, MA 02138

S. ZEPF, A. KUNDU
Department of Physics and Astronomy, Michigan State University, East Lansing, MI 48824-2320

L. ANGELINI
Laboratory for X-Ray Astrophysics, NASA Goddard Space Flight Center, Greenbelt, MD 20771

R. L. DAVIES
Sub-Department of Astrophysics, University of Oxford, Oxford OX1 3RH, UK

J. GALLAGHER
Department of Astronomy, University of Wisconsin, Madison, WI 53706-1582

V. KALOGERA, T. FRAGOS
Department of Physics and Astronomy, Northwestern University, Evanston, IL 60208

A. R. KING
Theoretical Astrophysics Group, University of Leicester, Leicester LE1 7RH, UK

S. PELLEGRINI
Dipartimento di Astronomia, Università di Bologna, Via Ranzani 1, 40127 Bologna, Italy

G. TRINCHIERI
INAF-Osservatorio Astronomico di Brera, Via Brera 28, 20121 Milan, Italy
Draft version October 24, 2018

ABSTRACT

We present the properties of the discrete X-ray sources detected in our monitoring program of the globular cluster (GC) rich elliptical galaxy, NGC 4278, observed with *Chandra* ACIS-S in six separate pointings, resulting in a co-added exposure of 458-ks. From this deep observation, 236 sources have been detected within the region overlapped by all observations, 180 of which lie within the D_{25} ellipse of the galaxy. These 236 sources range in L_X from 3.5×10^{36} erg s^{-1} (with 3σ upper limit $\leq 1 \times 10^{37}$ erg s^{-1}) to $\sim 2 \times 10^{40}$ erg s^{-1} , including the central nuclear source which has been classified as a LINER. From optical data, 39 X-ray sources have been determined to be coincident with a globular cluster, these sources tend to have high X-ray luminosity, with ten of these sources exhibiting $L_X > 1 \times 10^{38}$ erg s^{-1} . From X-ray source photometry, it has been determined that the majority of the 236 point sources that have well constrained colors, have values that are consistent with typical LMXB spectra, with 29 of these sources expected to be background objects from the $\log N - \log S$ relation. There are 103 sources in this population that exhibit long-term variability, indicating that they are accreting compact objects. 3 of these sources have been identified as transient candidates, with a further 3 possible transients. Spectral variations have also been identified in the majority of the source population, where a diverse range of variability has been identified, indicating that there are many different source classes located within this galaxy.

Subject headings: galaxies: individual (NGC 4278) — X-rays: galaxies — X-ray: binaries

1. INTRODUCTION

NGC 4278 is the second of two nearby, isolated, normal elliptical galaxies for which we were awarded deep monitoring observations with *Chandra* ACIS-S (Weisskopf *et al.* 2000). The purpose of these observations was to study the low-mass

X-ray binary (LMXB) population down to limiting luminosities of a few (0.3–8.0 keV) 10^{36} erg s^{-1} , well in the range of those LMXBs in the Galaxy and M31. LMXBs are the only direct fossil evidence of the formation and evolution of binary stars in the old stellar populations of early-type galaxies. First discovered in the Milky Way (see Giacconi 1974), these binaries are composed of a compact accretor, neutron star or black

hole, and a late-type stellar donor. The origin and evolution of Galactic LMXBs has been the subject of much discussion, centered on two main evolution paths (see Grindlay 1984; review by Verbunt & Van den Heuvel 1995): the evolution of primordial binary systems in the stellar field, or formation and evolution in Globular Cluster.

With the advent of *Chandra*, many LMXB populations have been discovered in early-type galaxies (see review Fabbiano 2006), and the same evolutionary themes (field or GC formation and evolution) have again surfaced, supported and stimulated by a considerably larger and growing body of data. With our unique observations of NGC 3379 (Brassington *et al.* 2008) and NGC 4278 (this paper), we can now take a fresh look at these issues. Moreover, our observations have a time sampling that permits variability studies and the identification of X-ray transients. Such data will extend the limited sample of existing multi-epoch observations (albeit with higher limiting luminosities; e.g. Irwin 2006; Sivakoff *et al.* 2008), where a variety of different variability behaviours of LMXBs have already been observed. Both multi-epoch observations and low luminosity thresholds are important aspects of the observational characteristics of Galactic LMXBs and are needed for constraining the evolution of these populations (e.g., Piro & Bildsten 2002, Bildsten & Deloye 2004).

The first galaxy that was observed in this program was NGC 3379, in the nearby poor group Leo ($D=10.6$ Mpc; Tonry *et al.* 2001). This system was chosen for this study because it is a relatively isolated unperturbed ‘typical’ elliptical galaxy, with an old stellar population (age of 9.3 Gyr, Terlevich & Forbes 2002) and a poor globular cluster system ($S_{GC} = 1.3 \pm 0.7$, Harris 1991; where $S_{GC} = \text{No.GC} \times 10^{(0.4(M_v+15))}$). From the 324-ks *Chandra* observation, reported in detail in Brassington *et al.* (2008), 132 X-ray point sources were detected, 98 of which were found to lie within the D_{25} ellipse of the galaxy. Through *HST* observations of the galaxy the globular cluster system was identified in the central region and ten GC-LMXBs detected. These GC-LMXB associations were found to have high luminosities, with three sources exhibiting $L_X \geq 1 \times 10^{38} \text{ erg s}^{-1}$. Also from studying this population it was determined that 48% of the detected LMXBs were found to show some type of long-term variability, with 5 of these sources being classified as transients and a further 3 of these as possible transients.

The characteristics of NGC 4278 are similar to those of NGC 3379 in all but the GC population, where NGC 4278 has a rich globular cluster system ($S_{GC} = 6.1 \pm 1.5$, Harris 1991), making it an ideal galaxy to explore the evolution of LMXB from primordial field binaries in a rich environment. Like NGC 3379, NGC 4278 is a nearby ($D=16.1$ Mpc; Tonry *et al.* 2001) relatively isolated, unperturbed ‘typical’ elliptical galaxy with an old stellar population (age of 10.7 Gyr, Terlevich & Forbes 2002).

Observationally, NGC 4278 is an ideal target for LMXB population studies, because of its proximity, resulting in a resolution of ~ 36 pc with *Chandra*, and its lack of a prominent hot gaseous halo. These characteristics optimize the detection of fainter LMXBs, and minimize source confusion; because of its angular diameter ($D_{25} = 4.0$ arcmin, RC3), NGC 4278 is entirely contained in the ACIS-S3 CCD chip, and is not affected by the degradation of the *Chandra* PSF at large radii.

Here we publish the catalog of LMXBs with their properties resulting from the entire observational campaign of NGC 4278 (five observations between March 2006 and February

2007, for a total of ~ 430 ks), which has been recently completed, and includes the first 37 ks observation taken in 2005, from the *Chandra* archive. In addition to this catalog paper, further highlights from the X-ray binary population of NGC 4278 will be presented in forthcoming papers. In the first (Kim *et al.* 2009, in prep) we compare the X-ray luminosity function of GC and field LMXBs detected in both NGC 4278 and NGC 3379. This will be followed by a paper presenting the properties of the transient population of both galaxies (Brassington *et al.* 2009, in prep). Further papers will be presented on: the properties of the nuclear source and the diffuse emission of NGC 4278, as well as the nonuniform distribution of the LMXBs within the galaxy and the intensity and spectral variability of the luminous X-ray binary population.

This paper is organized as follows: §2. details the observational program and describes the data analysis methods and results, including pipeline processing of the data, source detection, astrometry and matching of sources from the different observations, X-ray photometry and overall population results, variability analysis and optical counterpart matching (GC and background objects); §3. is the source catalog, including the results from the individual observations and the co-added data; §4 presents the discussion of the properties of the sources catalog; §5 summarizes the conclusions of this work.

2. OBSERVATIONS AND DATA ANALYSIS

The six separate *Chandra* observations of NGC 4278 have been carried out over a two year baseline, with the first of these, a 37 ks pointing, being performed in February 2005. This observation has been followed by five deeper pointings, all carried out between March 2006 and February 2007, resulting in a total exposure time of 471-ks.

The initial data processing to correct for the motion of the spacecraft and apply instrument calibration was carried out with the Standard Data Processing (SDP) at the *Chandra* X-ray Center (CXC). The data products were then analysed using the CXC CIAO software suite (v3.4)¹ and HEASOFT (v5.3.1). The data were reprocessed, screened for bad pixels, and time filtered to remove periods of high background. Following the methods of Kim *et al.* (2004a), time filtering was done by making a background light curve and then excluding those time intervals beyond a 3σ fluctuation above the mean background count rate, where the mean rate was determined iteratively after excluding the high background intervals. This resulted in a total corrected exposure time of 458-ks, the log of these exposures is presented in Table 1.

From the six individual data sets, a combined observation was produced, using the script *merge_all*², where the reprocessed level 2 event files from each observation were reprojected to a given RA and Dec, and then combined, and a combined exposure map was also created. Each of the individual observations used in the *merge_all* script were first corrected for relative astrometry before being reprocessed and reprojected. These corrections were done by using the CIAO tool *reproject_aspect*³ to update the aspect solution files by comparing the source list from an individual observation to the source list from a single reference observation (in this case the longest cleaned exposure obs-7078). These corrected aspect solution files were then used in all subsequent analysis.

¹ <http://asc.harvard.edu/ciao>

² http://asc.harvard.edu/ciao/ahelp/merge_all.html

³ http://asc.harvard.edu/ciao/threads/reproject_aspect/

From the co-added dataset of these six observations, a 0.3–8.0 keV (from here on referred to as ‘full band’) *Chandra* image was created and adaptively smoothed using the CIAO task *csmooth*. This uses a smoothing kernel to preserve an approximately constant signal to noise ratio across the image, which was constrained to be between 2.4σ and 4σ . In Figure 1, both the optical image, with the full band X-ray contours overlaid (top), and the ‘true color’ image of the galaxy system (bottom) are shown. The ‘true color’ image was created by combining three separate smoothed, and exposure corrected, images in three energy bands; 0.3–0.9 keV, 0.9–2.5 keV and 2.5–8.0 keV, using the same smoothing scale for each image. These energy bands correspond to red, green and blue respectively.

2.1. Source Detection and Count Extraction Regions

Discrete X-ray sources were searched for over each observation (the six single observations and the co-added observation) using the CIAO tool *wavdetect*, where the full band, with a significance threshold parameter of 1×10^{-6} , corresponding to roughly one spurious source over one CCD, was searched over. This CIAO tool searches for localized enhancements of the X-ray emission, and does not set any a priori thresholds on the S/N of each source (in contrast to sliding cell algorithms: Freeman *et al.* 2002). In Kim *et al.* (2004a) simulations were carried out to investigate the number of false detections compared to the expected ~ 1 false source per image provided by the threshold significance of 1×10^{-6} . These simulations and results are detailed in §4 of the paper, where they find that the performance of *wavdetect* is as expected, resulting in ~ 1 spurious source per image. These simulations cover the values of background (~ 0.28 counts/pixel) of our co-added observation. Further to this, these simulations were compared to *Chandra* observations with relatively long exposures (~ 100 ks), where 0.3 spurious sources per exposure were detected, fully consistent with the simulation results. A similar approach was also used by Kenter *et al.* (2005).

Following the results of these simulations it is clear that, when setting a detection threshold of 1×10^{-6} in *wavdetect*, only one of the formally identified sources is expected to be a false detection per image and so this prescription has been followed here. We reiterate that using this method does not set any a priori thresholds on the S/N of each source, it is therefore possible to include sources that have a high detection significance but at the same time a low flux significance, or S/N, therefore resulting in sources with poorly constrained flux.

When running *wavdetect* a range of 1, 2, 4, 8, 16 and 32 pixel wavelet scales were selected (where pixel width is $0.49''$), with all other parameters set at the default values. Exposure maps were created for the S3 chip from each observation, at 1.5 keV. The *wavdetect* tool was used in preference to other source detection software, as this detection package can be used within the low counts regime, as it does not require a minimum number of background counts per pixel for the accurate computation of source detection thresholds. Further to this, *wavdetect* also performs better in confused regions, which is the case in the nuclear region of elliptical galaxies (Freeman *et al.* 2002).

Once the X-ray sources had been detected, and their position had been determined by *wavdetect*, counts were extracted from a circular region, centered on the *wavdetect* position, with background counts determined locally, in an annulus surrounding the source, following the prescription of Kim *et al.*

(2004a). The extraction radius for each source was chosen to be the 95% encircled energy radius at 1.5 keV (which varies as a function of the off-axis angle⁴), with a minimum of $3''$ near the aim point. Similarly, background counts for each source were estimated from a concentric annulus, with inner and outer radii of two and five times the source radius respectively.

When nearby sources were found within the background region, they were excluded before measuring the background counts. Net count rates were then calculated with the effective exposure (including vignetting) for both the source and background regions. Errors on counts were derived following Gehrels (1986). For cases where sources have fewer than 4 counts, the Gehrels approximation begins to differ to Poissonian errors. However, these error values are still accurate to 1%, and, if anything, provide a more conservative estimate as Gehrels approximation does not account for the smaller error value at the lower limit. When the source extraction regions of nearby regions were found to overlap, to avoid an overestimate of their source count rates, counts were calculated from a pie-sector, excluding the nearby source region, and then rescaled, based on the area ratio of the chosen pie to the full circular region. Once the correction factor was determined, it was applied to correct the counts in all energy bands. For a small number of sources that overlapped with nearby sources in a more complex way (e.g. overlapped with more than 2 sources), instead of correcting the aperture photometry, the source cell determined by *wavdetect* was used to extract the source counts in each energy band.

From these source counts, fluxes and luminosities were calculated in the 0.3–8.0 keV band, with an energy conversion factor (ECF) corresponding to an assumed power law spectral shape, with $\Gamma = 1.7$ and Galactic N_{H}^5 (see Figure 11 for a justification of this assumption). The ECF was calculated with the *arf* (auxiliary response file) and the *rmf* (redistribution matrix file) generated for each source in each observation. For each source, the spatial and temporal quantum efficiency variations⁶ were accounted for by calculating the ECF in each observation and then taking an exposure-weighted mean ECF. The ECF over the 0.3–8.0 keV band varied by only $\sim 2\%$ between all six of the observations taken between 2005 and 2007⁷. This procedure was applied to each single observation and to the total co-added exposure.

In the instances where *wavdetect* did not formally identify a source in a single observation, source counts have been extracted from a circle with a 95% encircled energy radius, centered on the position from the co-added observation (or in cases where the source was not formally detected in the co-added observation, the source position from the single observation was used). The definition of background regions and the treatment of overlapping sources are outlined above. From these extracted source counts, a Bayesian approach, developed by Park *et al.* (2006), has been used to provide 68% source intensity upper confidence bounds on the full band counts. These values have then been used to calculate upper limits on the flux and luminosity of these sources.

2.2. Source Correlation

⁴ see <http://cxc.harvard.edu/cal/Hrma/psf/index.html>

⁵ $N_{\text{H}} = 1.76 \times 10^{20} \text{ cm}^{-2}$ (from COLDEN: <http://cxc.harvard.edu/toolkit/colden.jsp>).

⁶ See http://cxc.harvard.edu/cal/Acis/Cal_prods/qeDeg/ for the low energy QE degradation.

⁷ <http://asc.harvard.edu/ciao/why/acisqedeg.html>

From the co-added observation only, 271 sources were detected by *wavdetect*. From this list, sources external to the overlapping area covered by the S3 chip in all six individual observations were excluded, reducing this total number to 220 point sources. Using this source list from the co-added observation, sources detected in the individual observations were matched with this list, where source correlations were searched for up to a separation of $2''$. In the cases where multiple matches were detected for a source, the closer correlation was selected. From these matches, a histogram of source separations, shown in the left panel of Figure 2, was produced. In this figure it is clear that the peak separation between sources lies $\sim 0.15''$, with the number of correlated sources dropping at $\sim 1.0''$, and this is therefore the value we set for maximum separation when cross-correlating sources.

Once a cut of $1.0''$ had been applied to the cross-matched source list, the remaining unmatched sources, detected in the separate pointings only, were investigated individually, resulting in further potential matches being established. These potential matches correspond to sources with fewer counts, and hence a greater positional uncertainty, leading to larger values of separation. These potential source correlations were then further investigated by calculating the ratio of the source separation and the combined position uncertainty. Where the position uncertainty at the 95% confidence level has been defined by Kim *et al.* (2007a), as:

$$\log PU = \begin{cases} 0.1145 \times OAA - 0.4958 \times \log C + 0.1932, & 0.0000 < \log C \leq 2.1393, \\ 0.0968 \times OAA - 0.2064 \times \log C - 0.4260, & 2.1393 < \log C \leq 3.3000 \end{cases} \quad (1)$$

where the position uncertainty, PU , is in arcseconds, and the off axis angle, OAA , is in arcminutes. Source counts, C , are as extracted by *wavdetect*. Using this ratio of source separation and position uncertainty allows low L_X source correlations to be identified. Often these sources, particularly at greater off axis angles, cannot be matched by source separation cuts alone, due to the increasing PSF spread out and asymmetry at larger OAA ⁸. Therefore, by using this source separation - PU ratio, the greater position uncertainties in these weak sources can be accounted for, resulting in smaller ratios, and thereby identifying correlations that would otherwise be missed with source separation cuts alone.

In the right panel of Figure 2, a histogram of the ratio of separation and the combined position uncertainty is shown, where sources with a ratio of greater than 1 were investigated individually. In all but one instance it was found that these higher ratio sources lie in the central region of the galaxy, where both source confusion is likely and diffuse gas may be present. This emission results in higher background fluctuations, which can lead to the PU of these sources to be underestimated, therefore resulting in a falsely high ratio value. The source that was detected outside the central region is too faint (*net counts* $< \sim 100$ counts) to allow its radial profiles to be compared with a corresponding model PSF profile, generated for the source position using the CIAO tool *mkpsf*, and has been flagged as a possible double source.

After confirming that these additional sources with separation $\geq 1''$, were correlated with sources detected in the co-added observation, the remaining list of sources detected in individual observation was reduced to sixteen. All of these

sixteen sources were determined to be well separated from the sources detected in the co-added observation, and were therefore included in the final list of detected sources, increasing the total number to 236. These 236 sources are presented in Figure 3, where the unsmoothed full band image from the co-added dataset, with regions overlaid in white, is shown.

2.3. Hardness Ratios and X-ray colors

Within NGC 4278, the range of net counts for the point-like sources in the co-added observation is $\sim 7-48772$ (with signal-to-noise ratio (S/N) values ranging from 1.1 to 218.8), corresponding to 0.3–8.0 keV luminosities of 3.5×10^{36} erg s^{-1} (3σ upper limit $\leq 1 \times 10^{37}$ erg s^{-1}) – 2×10^{40} erg s^{-1} , when using the energy conversion factor described in §2.1. Most of these sources are too faint for detailed spectral analysis, therefore their hardness ratio and X-ray colors were calculated in order to characterize their spectral properties. The X-ray hardness ratio is defined as $HR = (Hc - Sc) / (Hc + Sc)$, where Sc and Hc are the net counts in the 0.5–2.0 keV and 2.0–8.0 keV band respectively. Following the prescription of Kim *et al.* (2004b), the X-ray colors are defined as $C21 = \log(S_1/S_2)$ and $C32 = \log(S_2/H)$, where S_1 , S_2 and H are the net counts respectively in the energy bands of 0.3–0.9 keV, 0.9–2.5 keV and 2.5–8.0 keV (energy bands and definitions are summarized in Table 2). These counts were corrected for the spatial and temporal QE variation, referring them all to the aim point of the first, recent observing epoch (Feb. 2006, Table 1), and for the effect of the Galactic absorption, using $N_H = 1.76 \times 10^{20} \text{cm}^{-2}$ (from COLDEN: <http://cxc.harvard.edu/toolkit/colden.jsp>).

By definition, as the X-ray spectra become harder, the HR increases and the X-ray colors decrease. For faint sources with a small number of counts, the formal calculation of the HR and colors often results in unreliable errors, because of negative net counts in one band and an asymmetric Poisson distribution. Therefore a Bayesian approach has been applied to derive the uncertainties associated with the HR and colors. This model was developed by Park *et al.* (2006) and calculates values using a method based on the Bayesian estimation of the ‘real’ source intensity, which takes into account the Poisson nature of the probability distribution of the source and background counts, as well as the effective area at the position of the source (van Dyk *et al.* 2001), resulting in HR and color values that are more accurate than the classical method, especially in the small-number-of-counts regime (less than 10 counts), where the Poisson distributions become distinctly asymmetric.

2.4. Source Variability

Due to the monitoring approach that has been used when observing NGC 4278, both long-term and short-term variations have been able to be searched for in the galaxy’s LMXB population. Long-term variability was defined by the chi-squared test, where a straight line model was fitted to the luminosities derived for each individual observation, with errors based on the Gehrels approximation (Gehrels 1986). For the cases where sources only had upper limit values of L_X , the associated error was defined to be the standard deviation of the upper limit from the mode value attained from the Bayesian estimates method, resulting in a conservatively large error, due to the nature of the Poissonian statistics. From these best fit models, sources were determined to be variable if $\chi^2_\nu > 1.2$, and those with fits with $\chi^2_\nu < 1.2$ were defined as non-variable

⁸ See §5 in Kim *et al.* (2004a) for a full discussion

sources. For sources that were only detected in the co-added observation, long-term variability was not searched for. This long-term behaviour will be further investigated in a forthcoming paper, where full Poissonian error treatment will be applied to sources with very low observed counts.

In addition to the chi-squared test variability criterion, transient candidates (TC), sources that either appear or disappear, or are only detected for a limited amount of ‘contiguous’ time during the observations, were searched for. Typically, sources are defined to be TCs if the ratio between the ‘on-state’, the peak L_X luminosity, and the ‘off-state’, the lower L_X luminosity or non-detection upper limit, is greater than a certain value (usually between 5–10; e.g. Williams *et al.* 2008). However, such a criterion can overestimate the number of transient candidates, when the ‘on-state’ X-ray luminosity is poorly constrained. To address this, the Bayesian model developed by Park *et al.* (2006) was used to derive the uncertainties associated with the ratio between ‘on-state’ and ‘off-state’. In this model, source and background counts from both the peak L_X luminosity and the non-detection observations were used to estimate the ratio, where the differences in both the exposure and ECF values were also accounted for. From this Bayesian approach a value of peak L_X /non-detection upper limit was calculated, along with a lower bound value of this ratio. This lower bound value was then used to determine the transient nature of the source, where a ratio of greater than 10 indicated a TC and sources with a ratio between 5 and 10 were labeled as possible transient candidates (PTC). This transient behavior was only searched for in sources that were only detected for a limited amount of ‘contiguous’ time during the observations and were determined to be variable using the chi-squared test.

Further to these four long-term variability classifications, the variation of the source luminosity between each observation was also investigated, by comparing the significance (in σ) of the change in luminosity between exposures, where the significance has been estimated by:

$$\text{signif} = \frac{|L_{X1} - L_{X2}|}{\sqrt{(\sigma_1^2 + \sigma_2^2)}}, \quad (2)$$

where σ_n is the error value of the luminosity from that individual observation, based on the Gehrels approximation, or, where upper limits have been used, the standard deviation of the estimated luminosity.

Short-term variations in each source were investigated when *net counts* > 20 in a single observation. In these instances, the variability was identified by using the Kolmogorov-Smirnov test (K-S test), where sources with variability values >90% confidence were labeled as possible variable sources and sources with values >99% confidence were defined as variable sources. This short-term variability was also quantified by using the Bayesian blocks method (BB) (Scargle 1998; Scargle *et al.* 2009, in prep). This method searches for abrupt changes in the source intensity during an observation, and therefore is very efficient for detecting bursts or state changes. Because it is based on the Poisson likelihood it can be used on the unbinned lightcurves of sources with very few counts. The implementation of the method used in this analysis is the same as in the ChaMP pipeline (see §3.3.2 in Kim *et al.* 2004a). This assumes a prior of $\gamma = 4.0$ which *roughly* translates to a significance level of $\sim 99\%$ for each detected block (however see Scargle *et al.*

(2009, in prep)⁹, for a caveat on this interpretation of the value of the prior).

2.5. Radial Profile

From the complete source list from the co-added observation a radial distribution of LMXBs has been created, using annuli centered on the nucleus of the galaxy (source 117). This profile has been compared to a multi-Gaussian expansion model of the I-band optical data (Cappellari *et al.* 2006), which is assumed to follow the stellar mass of the galaxy (Gilfanov 2004). This X-ray source density profile is presented in Figure 4, where the optical profile has been normalized to the X-ray data by way of a χ^2 fit. The central 1'' profile of the galaxy has not been plotted due to the excess of optical light, arising from the LINER that lies at the center of NGC 4278. Also indicated in this figure is the D_{25} ellipse and the number of background sources, which has been estimated from the hard-band *ChaMP*+*CDF* $\log N - \log S$ relation (Kim *et al.* 2007b), where ~ 29 sources are expected to be objects not associated with NGC 4278. From this figure it can be seen that the X-ray profile follows the optical surface density profile at larger radii, with the flattening in the central region ($r \leq 15''$) a consequence of source confusion. This indicates that the number and spatial distribution of LMXBs follows that of their parent population, the old stellar population.

2.6. Optical Counterparts

The globular cluster system of NGC 4278, observed with WFPC2, on-board *HST*, is reported in Kundu & Whitmore (2001), where images in both the *V* and *I* bands have been analyzed. In addition to this GC system identified in the *HST* data, background objects have also been classified (Kundu, A. 2007, private communication). These have been identified as objects that were well resolved in the *HST* images and were clearly more extended than any known globular cluster. Further to this, these background objects often had other features, such as visible disks, indicative of a galaxy rather than a globular cluster.

Right ascension and declination corrections have been applied to the astrometry of the *HST* data, relative to the co-added *Chandra* observation. This was done by comparing the positions of all GC-LMXB correlations with separations $\leq 1''$ and with net counts ≥ 50 , resulting in 37 matches. From these matches relative offsets of $\Delta RA = 0.48''$ and $\Delta Dec = 0.22''$ were identified and removed from the *HST* data.

After correcting the astrometry of these optical data, correlations up to an offset of 3'' with the X-ray sources, were searched for. When multiple matches were found, the closer matching object was selected. In the left panel of Figure 5, a histogram of these matches is shown, where it can be seen that the number of source correlations decreases at $\sim 1''$ before increasing at greater separations. Because of this clear distinction, the source radius was set to 1'' and sources between 1'' and 3'' were defined as ‘excluded matches’. This cut off radius value was then tested by comparing these correlations with the ratio of the separation divided by the combined position uncertainty from the co-added X-ray point sources (the definition of this is given in equation 1) and the uncertainty in the astrometry in the optical data, which has been conservatively set at 0.2''.

These ratios are shown in the right panel in Figure 5, where a histogram of all optical-X-ray correlations is presented, with

⁹ see also <http://space.mit.edu/CXC/analysis/SITAR/functions.html>

a shaded histogram of the background correlations only, overlaid. From this figure, it is shown that the majority of the confirmed GC correlated sources have a separation-position uncertainty ratio of less than 1.4. All of the sources with a ratio of greater than 1.4 were visually inspected and only two sources are found to have small separations $<0.5''$. The remaining sources all have separations $>0.6''$ and have been identified as excluded matches. From this further analysis the separation value cut off was redefined to be $0.6''$. This results in 45 X-ray-optical correlations, 6 of which have been classified as background objects, which is consistent with the number of sources that are expected to be background objects from the $\log N - \log S$ relation (5). This leaves 39 GC-X-ray source that are classified as correlations. The optical properties of these GC-LMXB sources, and the ‘excluded matches’ are shown in Tables 11 and 12 respectively (Full descriptions of these tables are given in §3).

In order to estimate the chance coincidence probability of the sources within the *HST* FOV, the same method as in Zezas *et al.* (2002) was followed, where the positions of the globular clusters were randomized by adding a random shift between $0.6''$ and $30''$, and for each new fake dataset the cross-correlation was performed using the same search radius as for the observed list of globular clusters. The limits of the shifts were chosen so that the new positions did not fall within the search radius and that they follow the general spatial distribution of the globular clusters. 500 such simulations were performed, resulting in 2.05 ± 1.43 associations expected by chance. If the cross-correlation radius is increased to $1''$, the chance associations rises to 4.96 ± 2.10 . Increasing this radius to $3''$ results in 35.85 ± 6.00 associations expected by chance, which is slightly higher than the 31 ‘excluded matches’ that have been found within this radius.

In Figure 6 the confirmed GC and X-ray sources, as well associated correlations, are indicated. In the top image circular regions indicating the X-ray sources with no GC counterpart are overlaid on a full band X-ray image, where the confirmed GCs are indicated by white ‘X’ marks. Also in this image the D_{25} ellipse and *HST* field of view are also shown. In the bottom image a full band X-ray image covering the *HST* FOV is presented, where the correlated X-ray sources are indicated by box regions and the white ‘X’ marks indicate the confirmed GCs. In both images X-ray luminosities are indicated by color, where sources with $L_X \geq 1 \times 10^{38} \text{ erg s}^{-1}$ are shown in yellow, sources with $1 \times 10^{38} \geq L_X \geq 1 \times 10^{37} \text{ erg s}^{-1}$ are shown in red and sources with $L_X \leq 1 \times 10^{37} \text{ erg s}^{-1}$ are indicated in cyan.

3. SOURCE CATALOG AND VARIABILITY ATLAS

Table 3 presents the properties of the master list of the 236 X-ray sources detected within NGC 4278, from the co-added observation of 458-ks. This table has been divided into two sections, where the first part presents all sources with $S/N > 3$ in at least one observation, and the second part lists all sources with $S/N < 3$. In this table column (1) gives the source number used through out this series of papers, column (2) gives the IAU name (following the convention “CXOU Jhhmmss.s+/-ddmmss”), columns (3) and (4) give the R.A. and Dec. of the source aperture, columns (5) and (6) give the radius and the position uncertainty (PU) of the source (both in arcseconds), column (7) gives the S/N , column (8) gives the log value of the co-added luminosity in the 0.3–8.0 keV energy band (for sources with $S/N < 3$, 3σ upper limit values are also presented in brackets). For sources detected in a single

observation only, 1σ upper limit from the co-added observation are shown, with 3σ upper limit values from the detected observation presented in brackets. Column (9) provides information about the long-term variability of the source, indicating if the source is non-variable (N), variable (V), a transient candidate (TC) or a possible transient (PTC). In all other cases the source was only detected in the combined observation, providing insufficient information to investigate long-term variability. In columns (10) and (11) the short-term variability of the source is indicated from both Bayesian block analysis (BB) and the Kolmogorov-Smirnov test (K-S), where ‘V’ indicates that the source is variable in at least one observation and ‘N’ indicates that it has been found to be non-variable in all six observations. In the K-S column, sources have also been labeled as possible variable sources (P) (see §2.4 for further information). In all other cases there were insufficient counts to investigate the short-term variability. In column (12) the optical associations with the X-ray source are indicated, where ‘GC’ indicates that the associated optical sources has been confirmed as a globular cluster, and ‘BG’ indicates that the sources has been classified as a background object. ‘corr’ denotes matches that have been defined as correlations, and ‘exmt’ denotes the ‘excluded matches’, between $0.8''$ and $3''$ in separation. Sources with a ‘none’ label were inside the field of view of the *HST* observation, but have no optical counterpart. All other sources were external to the *HST* FOV. Column (13) gives the distance from the galactic center (in arcseconds), where values in bold type face indicate sources that lie within the D_{25} ellipse. Column (14) provides source flag information, indicating sources that have been detected in a single observation only (X), overlapping sources (O1 for single overlaps and O2 for more complicated cases) and possible double sources (double?).

In this table, the 236 sources presented are the complete list detected by *wavdetect*, for which we estimate that ~ 1 source is a spurious detection (see §2.1). Since this catalog of X-ray sources is intended to be as complete a study as possible, all detected sources are included in the complete list, although for sources with $S/N < 3$ source parameters such as flux, hardness ratio and color values are not as well constrained as sources with higher flux significance. We have therefore separated the table into two sections, where the first part presents sources with $S/N > 3$ in at least one observation and well constrained properties, and the second part lists the sources with low S/N values.

Table 4 presents the detailed source parameters from the co-added observation; column (1) gives the source number, columns (2)–(8) give the net counts, in each of the 7 energy bands (see Table 2 for definitions of these bands), column (9) indicates the hardness ratio, columns (10) and (11) show the color-color values and column (12) gives the log value of the luminosity in the 0.3–8.0 keV energy band. Where sources were not detected in the co-added observation, upper limits for net broad band counts and L_X are given.

Tables 5–10 present the source parameters, measured for each observation, where columns (1)–(11) provide the same information presented in Table 4, but further provided in this table is source variability information, where columns (12)–(14) present results of Bayesian block analysis (BB), the Kolmogorov-Smirnov test (K-S) and the significance of the change in L_X between the previous observation and the current observation respectively. Column (15) indicates the log value of the luminosity in the 0.3–8.0 keV energy band.

Table 11 presents the optical properties of the counterparts

found from the optical data of NGC 4278, where 39 GCs and 6 background objects have been found to be coincident with X-ray sources. Table 12 summarizes the results for the ‘excluded matches’ sources. In both tables column (1) gives the X-ray source number, column (2) the V band magnitude, column (3) the I band magnitude, column (4) $V-I$ colors, column (5) the separation between the X-ray source and the GC and column (6) the ratio between separation and the combined position error. The horizontal line in both tables separates the confirmed GCs (top section of table) from the background objects (bottom section of table).

Figure 7 presents the intensity and spectral variability of each of the 236 X-ray sources, over all six pointings, where the temporal properties of each point source are shown in four separate panels. In the top panel the long-term light curve of each source is presented, with errorbars indicating the 1σ uncertainty in the intensity of the source, with upper limit values provided for sources that were not detected in a single observation. The second panel shows the hardness ratio variation of each source, and panels three and four, show the temporal properties of C21 and C32 respectively. In all four panels, the co-added values are also indicated, by a horizontal dashed green line. In instances where the source was not detected in the co-added observation, a blue line indicates the upper limit of the source luminosity.

Figure 8 presents the L_X -HR plots for sources with measured hardness ratios in at least two observations. Each point shows the X-ray luminosity and hardness ratio value of a source during each pointing, as well as the values derived from the co-added observation. Each point is labeled and color coded, where magenta, green, blue, red, cyan and dark green indicate observations 1–6 respectively, and black represents the co-added observation value. Similarly, Figure 9 presents the color-color values for sources with measured color-color values in at least two observations, where again individual observations are labeled and color coded (following the same color scheme as in Figure 8), with the co-added observation indicated in black.

4. DISCUSSION

4.1. X-ray Source Population

In the previous sections the data analysis methods, used to determine the properties of the X-ray binary population of NGC 4278, have been presented. From the six individual *Chandra* pointings, taken between February 2005 and February 2007, a co-added observation, totaling an exposure time of 458-ks, has been produced. From this deep observation of the galaxy, 236 X-ray point sources have been detected in the region overlapped by all of the individual pointings, with 180 of these sources residing within the D_{25} ellipse of the system. These 236 sources are presented in Figure 3 where a raw, full band image from the co-added observation, with the overlap region and D_{25} ellipse overlaid, is presented in the main image, with source regions also indicated. The two following images present the central region of the galaxy, where the dense population of sources can be more clearly seen. Of these 236 sources, based on the hard-band *ChAMP*+*CDF* $\log N - \log S$ relation (Kim *et al.* 2007b), ~ 29 sources detected in the co-added observation are expected to be objects not associated with NGC 4278. Within the D_{25} ellipse of the galaxy it is expected that ~ 12 of these sources are background objects. In Figure 4 the number of expected background objects is indicated in the X-ray source number density profile of the

galaxy and appears consistent with the flattening of the profile at larger radii.

The total number of LMXBs residing in NGC 4278 is much greater than that of NGC 3379 (notwithstanding the 90% completeness limit of $L_X \sim 5 \times 10^{36}$ erg s $^{-1}$ compared to $L_X \sim 1 \times 10^{37}$ erg s $^{-1}$ in NGC 4278), where only 98 sources were detected within the D_{25} ellipse of the galaxy, compared to 180 in the D_{25} ellipse of NGC 4278. This increase in the total LMXB population in NGC 4278 follows the known correlation of increasing X-ray luminosity arising from LMXBs (normalized by L_B) with increasing globular cluster specific frequency (S_{GC}) (e.g Kim *et al.* 2006, Irwin 2005). Such a relationship confirms the importance of LMXB formation in GCs, and through the deep observations that have presented here and in Brassington *et al.* (2008) this correlation will be further investigated in a forthcoming paper, where the hypothesis that all LMXBs were formed in GCs will be tested.

The X-ray luminosity of the sources detected within NGC 4278 ranges from 3.5×10^{36} erg s $^{-1}$ (with 3σ upper limit $\leq 1 \times 10^{37}$ erg s $^{-1}$) up to $\sim 2 \times 10^{40}$ erg s $^{-1}$, where the brightest source, 117, lies at the nucleus of the galaxy and has been classed as a LINER with $H\alpha$ emission (Ho *et al.* 1997). The full X-ray data analysis of this source from these six observations will be reported in a forthcoming paper. Apart from this central source, no LMXBs exceeding 1×10^{39} erg s $^{-1}$ have been detected in this galaxy, unlike NGC 3379, where a ULX source with a co-added X-ray luminosity of $\sim 2 \times 10^{39}$ erg s $^{-1}$ was discovered. This lack of ULXs in NGC 4278 is unsurprising as it is rare to find such a high luminosity object (external to the nuclear region) in E and S0 galaxies (Irwin, Bregman & Athey 2004).

The L_X distribution of all of the detected X-ray sources within NGC 4278 is shown in Figure 10, where the GC associations are also indicated. In this figure the main histogram presents the calculated L_X values from all sources (with 1σ upper limits from the co-added observation provided for sources only detected in a single observation), except for the central bright source 117. The bottom left histogram presents these same sources, but for those with $S/N < 3$, 3σ upper limits are shown, these upper limit values are then presented separately in the bottom right histogram. From the main figure it can be seen that the majority of sources detected from this observation lie in the luminosity range of 1×10^{37} erg s $^{-1}$ – 6×10^{37} erg s $^{-1}$, with a mode luminosity of $\sim 1.5 \times 10^{37}$ erg s $^{-1}$ and with source incompleteness beginning to affect the source distribution $L_X \leq 1 \times 10^{37}$ erg s $^{-1}$. From the histogram including 3σ upper limit values, this mode value remains the same, as does source incompleteness.

In the forthcoming paper Kim *et al.* (2009, in prep), the X-ray luminosity function (XLF) of NGC 4278 will be investigated, and a correction to allow for source incompleteness will be applied. Some preliminary results, investigating the XLF of NGC 4278, alongside NGC 3379, have been reported in Kim *et al.* (2006), where sources, down to a 90% completeness limit of $L_X \sim 3 \times 10^{37}$ erg s $^{-1}$, from the first two observations, have been detected. From the even greater sensitivity afforded to us by combining the six separate pointings, we can investigate the XLF close to the X-ray luminosity range of normal Galactic LMXBs. Previously, this has only been possible for the nearby radio galaxy Centaurus A (NGC 5128), where the XLF has been measured down to $\sim 2 \times 10^{36}$ erg s $^{-1}$ (Kraft *et al.* 2001; Voss & Gilfanov 2006). With our greater

sensitivity we can compare our results to these studies, allowing us to investigate the shape of the low luminosity LMXB XLF, although it should be noted that both NGC 3379 and NGC 4278 are much more ‘normal’ galaxy than Centaurus A.

In addition to the X-ray point sources that have been presented in this catalog, the optical sources within NGC 4278 have also been identified. These were detected in a WFPC2 *HST* observation, where 266 confirmed globular clusters have been identified. From these 266 sources, 39 GC-LMXB, with separations $< 0.6''$, have been detected. From Figure 10 it can be seen that these 39 GC-LMXB sources appear to predominantly lie at the high X-ray luminosity end of this distribution. The luminosity function of these GC-LMXB sources from both galaxies and its implications for the understanding of LMXB evolution will also be presented in Kim *et al.* (2009, in prep), where the X-ray luminosity functions of both GC and field LMXBs will be compared.

4.2. X-ray Colors

In Figure 11 the LMXB population color-color diagram, based on the photometry of the co-added observation, is presented. In the top panel color-color values are plotted, with the sources divided into luminosity bins, with symbols of each bin indicated by the labeling in the panel. In the bottom panel, the errorbars for each of these points are plotted. Also in this figure source variability is indicated, where variable sources are plotted in blue, non-variable sources are shown in green and sources with undetermined variability are indicated in cyan. Additionally, in both of the panels a grid has been overlaid to indicate the predicted locations of the sources at redshift $z=0$ for different spectra, described by a power law with various photon indices ($0 \leq \Gamma_{ph} \leq 4$, from top to bottom.) and absorption column densities ($10^{20} \leq N_H \leq 10^{22} \text{ cm}^{-2}$, from right to left). In Figure 12 the L_X -HR, L_X -C21 and L_X -C32 population plots are presented, where variability is again indicated by color, with variable sources shown in blue, non-variable sources are plotted in green and sources with undetermined variability are shown in cyan.

From the color-color diagram, presented in Figure 11, it can be seen that most of the well defined colors lie within the area of a typical LMXB spectrum of $\Gamma = 1.5 - 2.0$, with no intrinsic absorption (e.g. Irwin, Athey & Bregman 2003; Fabbiano 2006). However, there also appears to be a population of sources that have much harder spectra, again with either no intrinsic absorption, or sources with a possible soft excess, albeit with colors that are not as well defined. The L_X -HR distribution of this subpopulation was explored to identify sources with higher hardness ratios than one would expect from LMXBs but it was found that the sources that were identified in the color-color diagram did not exhibit harder HR values (see the top panel of Figure 12). Because of this, while it is possible that these sources could be absorbed background AGN, the poorly constrained colors of this subpopulation alone do not provide adequate information to confirm this interpretation. The overall color-color and L_X -HR distributions of the LMXB population within NGC 4278 is very similar to that of NGC 3379, where again, most of the sources with well constrained colors were determined to lie within the area of a typical LMXB spectrum. Also in NGC 3379, like NGC 4278, a subpopulation of sources with harder spectra with either no intrinsic absorption, or a soft excess, was identified. However, unlike the subpopulation of NGC 4278, these sources were determined to show not only color-color values

indicating their harder spectra, but also exhibited higher HR values and for this reason were flagged as possible absorbed background AGN.

4.3. Source Variability

A characteristic of compact accretion sources such as LMXBs is variability, and, as a result of the monitoring nature of the observing campaign, we have been able to search for this variability, in both the long-term regime, and also over short-term baselines, where changes over hours and days have been identified. One of the specific aims of our monitoring campaign has been to identify transient candidate sources as it has been suggested that field LMXBs are expected to be transients (Piro & Bildsten 2002; King 2002) and low luminosity ultracompact binaries in GCs are also expected to be transient in nature (Bildsten & Deloye 2004). In the forthcoming paper Brassington *et al.* (2009, in prep) we investigate the subpopulation of transient candidates that has been discovered in both NGC 4278 and NGC 3379.

Our data represent the most complete variability study for an extragalactic LMXB population (see Fabbiano 2006; Xu *et al.* 2005), investigating both long and short term behaviour. In the case of the long-term variability, sources have been separated into four different classifications; non-variable and variable sources, and also transient candidates (TC) or possible transients candidates (PTC). These two latter definitions have been applied to sources that either appear or disappear, or are only detected for a limited amount of ‘contiguous’ time during the observations, with a lower bound ratio of greater than 10 between the ‘on-state’ and the ‘off-state’, for TCs, or a lower bound ratio between 5 and 10 for the PTCs (see §2.4 for a full discussion of this definition).

The 13 sources that were investigated for transient behavior are presented in Table 13, where both the ratio and lower bound ratio, calculated from Bayesian modeling, are presented, along with each source’s variability classification. From this table it can be seen that many of these sources appear to be PTCs and TCs from their ratio alone, but when allowing for the uncertainties from their source and background counts, they can only be classified as variable sources. Including the uncertainties when determining TCs is particularly important when dealing with sources with low S/N values, as is the case for a number of sources in this catalog.

Out of the 236 sources, 97, 41% of the sources within NGC 4278, have been defined as variable sources. A further 3 sources are TCs, and 3 are PTCs, with 97 sources found to be non-varying in intensity over the six observations. The remaining 36 sources have insufficient data to investigate their long-term variability. These levels of long-term variability observed in NGC 4278 are very similar to those of NGC 3379, where 42% of the sources were determined to be variable, with a further 5 sources identified as TCs and 3 as PTCs. This similar number of TCs/PTCs in both galaxies is maybe somewhat surprising, given the larger number of LMXBs detected within NGC 4278. However, from theory it has been suggested that transient sources will predominantly be field LMXBs (Piro & Bildsten 2002) and in fact, in NGC 4278 five of the six TC/PTC sources have been determined to be field sources and in NGC 3379 three of the four TC/PTCs that we have optical coverage for are also field sources (the remaining 4 TC/PTCs are external to the *HST* FOV). Both NGC 3379 and NGC 4278 were selected for this study as they have very similar L_B values ($1.35 \times 10^{10} L_\odot$, $1.63 \times 10^{10} L_\odot$), and by comparing the number of field TCs/PTCs in each galaxy to their

field population we find similar values of 11% and 9% respectively, compared to 8% and 3% when including the whole X-ray source population within the D_{25} ellipse. These values are consistent with the suggestion that transient sources will be predominantly found in the field, and this result will be further explored in the forthcoming paper Brassington *et al.* (2009, in prep).

The long and short-term variability of the X-ray sources with NGC 4278, are summarized in Table 14, where these two variability parameters have been cross-correlated, to indicate the number of sources exhibiting both long and short-term variations, although, the majority of these sources do not have sufficient counts in each observation to determine their short-term variability. The numbers within this table indicate the number of sources from the whole observation and the numbers in brackets represent the sources within the D_{25} ellipse. From this table it can be seen that, for the sources with a defined short-term variability measure, both long-term variable and non-variable sources have a variety of short-term behavior. For the transient candidates no observations had sufficient counts with which to investigate their short-term variability. Also, as an additional point, all of the TCs, and PTCs found within NGC 4278 reside well within the D_{25} ellipse of the galaxy, indicating that they are likely LMXBs associated with NGC 4278.

In addition to the L_X variability, spectral variations have also been investigated. These are presented in Figures 8 and 9, where L_X -HR and color-color plots for each source are shown. From these figures it is clear that the majority of sources within NGC 4278 exhibit some sort of variability, with a variety of different spectral variations shown within this population. This spectral variability is similar to behaviour discussed in McClintock & Remillard (2006), with a significant number of sources emitting softer spectra as L_X increases (e.g sources 76 and 147). It has been suggested that this increasing softness represents a thermal state, where the flux is dominated by the heat radiation from the inner accretion disk. Conversely, sources exhibiting spectral hardening with increasing L_X are also present within the galaxy (e.g sources 14 and 119). This harder state has been explained as a steep power law state, where a highly energized corona is present (e.g. Feng & Kaaret 2006). In addition to these spectral behaviors, sources that show little to no spectral variation with increasing luminosity (e.g. sources 40 and 169), and sources that show no discernible pattern at all (e.g. sources 118 and 158) have also been detected. A more detailed discussion of the spectral variability of all of these X-ray sources presented in this catalog will be the subject of a forthcoming paper.

5. CONCLUSIONS

We have presented a source catalog and variability atlas resulting from our monitoring deep observations of the nearby elliptical NGC 4278 with *Chandra* ACIS-S. Our results can be summarized as follows:

- 236 X-ray point sources have been detected within NGC 4278, ranging in luminosity from 3.5×10^{36} erg s⁻¹ (with 3σ upper limit $\leq 1 \times 10^{37}$

erg s⁻¹) to $\sim 2 \times 10^{40}$ erg s⁻¹, with 180 of these sources residing within the D_{25} ellipse of the galaxy.

- The nuclear source in this galaxy has been classified as a LINER with H α emission (Ho *et al.* 1997) and has a luminosity of $\sim 2 \times 10^{40}$ erg s⁻¹ from the co-added observation.
- 39 globular clusters have been identified to be coincident with X-ray sources, all of which lie within the D_{25} ellipse of the galaxy. These GC-LMXB associations tend to have high X-ray luminosities, with ten of these sources exhibiting $L_X > 1 \times 10^{38}$ erg s⁻¹.
- From source photometry, it has been determined that the majority of source with well constrained colors have values that are consistent with a typical LMXB spectrum of $\Gamma = 1.5 - 2.0$, with no intrinsic absorption.
- 103 sources, 44% of the X-ray source population, have been found to exhibit some type of long-term variability, which clearly identifies them as accreting compact objects. 3 of these variable sources have been identified as transient candidates, with a further 3 identified as possible transients.
- Spectral variability analysis has revealed that the sources within NGC 4278 exhibit a range of variability patterns, where both high/soft–low/hard and low/soft–high/hard spectral transitions have been observed, as well as sources that vary in luminosity, but exhibit no spectral variation, indicating that there are many different source classes within this galaxy.

Following this catalog paper we will be presenting highlights from the X-ray binary population of this galaxy in forthcoming papers. The first will compare the X-ray luminosity function of GC and field LMXBs detected in both NGC 4278 and NGC 3379 (Kim *et al.* 2009, in prep). This will be followed by a paper presenting the properties of the transient population of both galaxies (Brassington *et al.* 2009, in prep). In addition to these we will also present papers on: the properties of the nuclear source and the diffuse emission of NGC 4278, as well as the nonuniform distribution of the sources within the galaxy and the intensity and spectral variability of the luminous X-ray binary population.

We thank the CXC DS and SDS teams for their efforts in reducing the data and developing the software used for the reduction (SDP) and analysis (CIAO). We would also like to thank the referee, Jimmy Irwin, for his helpful comments which have improved this paper. This work was supported by *Chandra* G0 grant G06-7079A (PI:Fabbiano) and subcontract G06-7079B (PI:Kalogera). We acknowledge partial support from NASA contract NAS8-39073(CXC). A. Zezas acknowledges support from NASA LTSA grant NAG5-13056. S. Pellegrini acknowledges partial financial support from the Italian Space Agency ASI (Agenzia Spaziale Italiana) through grant ASI-INAF I/023/05/0.

REFERENCES

Bildsten, L. & Deloye, C. J. 2004, ApJ, 607, L119
 Brassington, N., J., *et al.* 2008, ApJS, 179, 142
 Cappellari, M., *et al.* 2006, MNRAS, 366, 1126
 Fabbiano, G. 2006, ARAA, 44, 323

Feng, H. & Kaaret, P. 2006 ApJL, 650, L75
 Freeman, P. E., Kashyap, V., Rosner, R. & Lamb D. Q., 2002, ApJS, 138, 185
 Gehrels, N. 1986, ApJ, 303, 336

- Giacconi, R. 1974, in *X-ray Astronomy*, eds. R. Giacconi & H. Gursky, p.155, Dordrecht: Reidel
- Gilfanov, M. 2004, *MNRAS*, 349, 146
- Grindlay, J. E. 1984, *Adv. Space Res.*, 3, 19
- Harris, W. E. 1991, *ARAA*, 29, 543
- Ho, L. C., Filippenko, A. V., Sargent, W. L. W. & Peng, C. Y. 1997, *ApJS*, 112, 391
- Irwin, J. A., Athey, A. E. & Bregman, J. N. 2003, *ApJ*, 587, 356
- Irwin, J. A., Bregman, J. N. & Athey, A. E. 2004, *ApJ*, 601, L143
- Irwin, J. 2005, *ApJ*, 631, 511
- Irwin, J. 2006, *MNRAS*, 371, 1903
- Kenter, A., *et al.* 2005, *ApJS*, 161, 9
- Kim, D.-W., Cameron, R. A., Drake, J. J., *et al.* 2004a, *ApJS*, 150, 19
- Kim, D.-W., Wilkes, B., Green, P., *et al.* 2004b, *ApJ*, 600, 59
- Kim, D.-W., *et al.* 2006, *ApJ*, 652, 1090
- Kim, M., *et al.* 2007a, *ApJS*, 169, 401
- Kim, M., *et al.* 2007b, *ApJ*, 659, 29
- King, A. R. 2002, *MNRAS*, 335, L13
- Kraft, R. P., *et al.* 2001, *ApJ*, 560, 675
- Kundu, A., Whitmore, B. C. 2001, *ApJ*, 121, 2950
- McClintock, J. E., & Remillard, R. A. 2006, in *Compact Stellar X-Ray Sources*, ed. W. H. G. Lewin & M. van der Klis (Cambridge: Cambridge Univ. Press), in press
- Park, T., Kashyap, V., Siemiginowska, A., van Dyk, D., Zezas, A., Heinke, C., Wargelin, B. 2006, *ApJ*, 652, 610
- Piro, A. L. & Bildsten, L. 2002, *ApJ*, 571, L103
- Scargle, J.D. 1998, *ApJ*, 504, 405
- Sivakoff, G. R., Jordán, A., Juett, A. M., Sarazin, C. L., & Irwin, J. A., 2008, astro-ph/0806.0627
- Terlevich, A. I. & Forbes, D. A. 2002, *MNRAS*, 330, 547
- Tonry J., *et al.* 2001, *ApJ*, 546, 681
- van Dyk, D., *et al.* 2001, *ApJ*, 548, 224
- Verbunt, F. & van den Heuvel, E. P. J. 1995, in *X-ray Binaries*, eds. Lewin, W. H. G., van Paradijs, J., van den Heuvel, E. P. J., Cambridge, UK: CUP, p.457
- Voss, R. & Gilfanov, M. 2006, *A&A*, 447, 71
- Weisskopf, M. C., Tananbaum, H. D., Van Speybroeck, L. P. & O'Dell, S. L. 2000, *Proc. SPIE*, 4012, 2
- Williams, B. F., *et al.* 2008, *ApJ*, 680, 1120
- Xu, Y., Xu, H., Zhang, Z., Kundu, A., Wang, Y. & Wu, X.-P., 2005, 631, 809
- Zezas, A., Fabbiano, G., Rots, A. H., Murray, S. S. 2002, *ApJ*, 577, 710

TABLE 1
OBSERVATION LOG

Obs. Num.	OBSID	Date	Exposure (sec)	Cleaned Exposure (sec)
1	4741	2005-02-03	37462.0	37264.5
2	7077	2006-03-16	110303.8	107736.7
3	7078	2006-07-25	51433.2	48076.2
4	7079	2006-10-24	105071.7	102504.6
5	7081	2007-02-20	110724.0	107564.5
6	7080	2007-04-20	55824.8	54837.5
Total	-	-	470819.5	457984.0

NOTE. — The pointing OBSID 7181 was taken before OBSID 7080, so to maintain the time sequence of the exposures these observation numbers have been labeled as above in this paper.

TABLE 2
DEFINITION OF ENERGY BANDS AND X-RAY COLORS

Band	Definition
Broad (B)	0.3–8 keV
Soft (S)	0.3–2.5 keV
Hard (H)	2.5–8 keV
Soft 1 (S_1)	0.3–0.9 keV
Soft 2 (S_2)	0.9–2.5 keV
Conventional Broad (Bc)	0.5–8 keV
Conventional Soft (Sc)	0.5–2 keV
Conventional Hard (Hc)	2–8 keV
Hardness Ratio HR	$(Hc-Sc)/(Hc+Sc)$
X-ray Color C21	$-\log(S_2) + \log(S_1) = \log(S_1/S_2)$
X-ray Color C32	$-\log(H) + \log(S_2) = \log(S_2/H)$

TABLE 3
MASTER SOURCE LIST

Masterid	CXOU Name	RA (J2000)	Dec (J2000)	Radius ('')	PU ('')	S/N	Log L_x (0.3–8.0 keV) (erg s^{-1})	Variability			Opt Corr (12)	DG ('')	Flag (14)
								LT (9)	BB (10)	K-S (11)			
(1)	(2)	(3)	(4)	(5)	(6)	(7)	(8)	(9)	(10)	(11)	(12)	(13)	(14)
1	J122023.6+291614	12:20:23.640	+29:16:13.92	4.13	0.39	9.2	37.8	V	-	-	-	223.1	-
2	J122023.0+291453	12:20:23.021	+29:14:52.76	4.57	0.34	15.8	38.2	V	-	P	-	242.6	O1
4	J122022.6+291458	12:20:22.570	+29:14:58.08	4.36	0.36	12.6	38.1	V	-	P	-	234.8	O1
5	J122022.6+291536	12:20:22.558	+29:15:35.89	4.09	0.27	24.9	38.5	V	N	V	-	219.1	-
8	J122019.4+291448	12:20:19.435	+29:14:47.98	3.87	0.45	8.8	37.8	N	-	-	-	205.7	-
9	J122019.3+291412	12:20:19.262	+29:14:12.11	4.17	0.87	4.0	37.3	V	-	-	-	227.3	-
11	J122018.0+291655	12:20:17.988	+29:16:54.97	3.00	0.45	6.1	37.5	N	-	-	-	146.1	-
13	J122017.8+291422	12:20:17.753	+29:14:22.22	3.84	0.24	31.6	38.7	V	N	N	-	206.2	-
14	J122017.3+291450	12:20:17.263	+29:14:49.82	3.50	0.29	14.0	38.0	N	V	N	-	182.4	-
15	J122017.2+291612	12:20:17.208	+29:16:12.43	3.00	0.41	6.8	37.5	N	-	-	-	141.2	-
16	J122017.1+291705	12:20:17.110	+29:17:05.00	3.00	0.67	3.4	37.1	V	-	-	-	135.3	-
17	J122016.7+291410	12:20:16.673	+29:14:10.15	3.81	0.34	10.2	37.8	V	-	P	-	205.9	-
19	J122015.8+291758	12:20:15.823	+29:17:58.43	3.00	0.45	5.4	37.4	V	-	-	-	135.8	-
21	J122015.5+291553	12:20:15.521	+29:15:52.59	3.00	0.57	3.7	37.2	N	-	-	-	127.8	-
23	J122014.7+291901	12:20:14.695	+29:19:01.26	3.00	0.51	4.6	37.3	V	-	-	-	166.2	-
24	J122014.5+291854	12:20:14.503	+29:18:54.26	3.00	0.71	4.0	37.2	N	-	-	-	159.2	-
26	J122013.7+291611	12:20:13.661	+29:16:10.64	3.00	0.36	6.8	37.5	V	-	-	-	98.0	-
27	J122013.5+291653	12:20:13.469	+29:16:53.27	3.00	0.61	4.6	37.0	V	-	-	-	87.0	O1
28	J122013.4+291656	12:20:13.433	+29:16:56.03	3.00	0.66	4.5	37.1	-	-	-	-	86.6	O1
29	J122013.3+291848	12:20:13.286	+29:18:47.62	3.00	0.32	8.3	37.7	N	-	P	-	144.2	-
30	J122013.1+291910	12:20:13.066	+29:19:10.28	3.00	0.64	3.3	37.1	V	-	-	-	161.7	-
31	J122012.7+291622	12:20:12.730	+29:16:21.94	3.00	0.18	19.7	38.3	N	V	N	-	82.5	-
32	J122012.5+291742	12:20:12.480	+29:17:42.08	3.00	0.51	2.2	36.9	V	-	-	-	90.1	-
35	J122012.4+291906	12:20:12.384	+29:19:06.18	3.00	0.25	11.0	37.9	N	-	-	-	153.7	-
36	J122011.9+291651	12:20:11.930	+29:16:50.76	3.00	0.44	3.5	37.1	V	-	-	-	66.8	-
38	J122011.7+291622	12:20:11.712	+29:16:22.02	3.00	0.36	6.7	37.4	N	-	-	-	70.1	O2
39	J122011.5+291624	12:20:11.458	+29:16:23.51	3.00	0.24	10.4	37.8	V	-	P	-	66.5	O2
40	J122011.3+291625	12:20:11.316	+29:16:24.53	3.00	0.25	9.9	37.7	V	-	P	-	64.4	O2
41	J122010.9+291628	12:20:10.879	+29:16:28.02	3.00	0.15	24.1	38.5	N	N	N	-	57.8	-
42	J122010.8+291911	12:20:10.814	+29:19:10.75	3.00	0.19	19.1	38.3	N	-	P	-	149.4	-
43	J122010.8+291546	12:20:10.807	+29:15:46.49	3.00	0.23	9.8	37.8	V	-	-	-	82.8	-
44	J122010.4+291421	12:20:10.438	+29:14:21.18	3.00	0.68	3.4	37.1	-	-	-	-	156.9	-
45	J122010.2+291758	12:20:10.236	+29:17:58.47	3.00	0.42	3.8	37.2	N	-	-	none	81.1	-
46	J122010.1+291625	12:20:10.118	+29:16:25.47	3.00	0.40	3.9	37.2	N	-	-	-	50.0	-
48	J122010.1+291703	12:20:10.056	+29:17:02.88	3.00	0.31	5.7	37.5	V	-	-	-	44.0	O1
50	J122010.0+291532	12:20:09.953	+29:15:32.24	3.00	0.22	10.3	37.8	N	-	-	-	88.6	-
51	J122009.9+291741	12:20:09.936	+29:17:40.65	3.00	0.34	5.3	37.4	V	-	-	GCcorr	64.4	-
53	J122009.8+291658	12:20:09.797	+29:16:58.48	3.00	0.29	7.1	37.5	N	-	P	-	39.7	O2
54	J122009.8+291649	12:20:09.778	+29:16:48.81	3.00	0.33	5.5	37.4	N	-	-	-	38.7	-
55	J122009.5+291738	12:20:09.511	+29:17:38.41	3.00	0.41	3.3	37.1	N	-	-	none	59.2	-
56	J122009.4+291634	12:20:09.415	+29:16:34.47	3.00	0.25	7.2	37.6	V	-	-	-	37.6	-
57	J122009.4+291614	12:20:09.413	+29:16:14.25	3.00	0.34	5.0	37.4	N	-	-	-	49.8	-
60	J122009.2+291509	12:20:09.221	+29:15:08.64	3.00	0.47	4.9	37.3	N	-	-	-	106.8	-
62	J122009.2+291643	12:20:09.185	+29:16:43.07	3.00	0.50	3.7	37.0	-	-	-	-	31.8	O2
63	J122009.1+291758	12:20:09.142	+29:17:58.02	3.00	0.19	9.9	37.8	N	-	P	GCcorr	73.8	-
64	J122009.0+291725	12:20:09.012	+29:17:24.59	3.00	0.45	4.1	37.1	-	-	-	none	44.3	O2
65	J122008.9+291702	12:20:08.940	+29:17:01.94	3.00	0.23	8.7	37.6	N	-	-	-	29.9	O2
66	J122008.9+291660	12:20:08.914	+29:16:59.67	3.00	0.18	11.1	37.8	V	N	P	-	28.8	O2
67	J122008.9+291840	12:20:08.856	+29:18:39.70	3.00	0.21	9.8	37.8	N	-	-	-	112.1	-
68	J122008.9+291729	12:20:08.851	+29:17:28.99	3.00	0.17	10.9	38.0	N	N	N	GCcorr	46.5	O1
69	J122008.8+291855	12:20:08.770	+29:18:55.14	3.00	0.32	6.8	37.5	N	-	-	-	126.9	-
70	J122008.8+291645	12:20:08.760	+29:16:44.62	3.00	0.39	3.1	37.2	V	-	-	-	26.1	O1
71	J122008.7+291453	12:20:08.702	+29:14:52.99	3.00	0.30	8.5	37.7	N	-	P	-	120.3	-
72	J122008.7+291432	12:20:08.690	+29:14:32.50	3.00	0.24	13.8	38.0	N	-	-	-	140.4	-

TABLE 3 — *Continued*

Masterid	CXOU Name	RA	Dec	Radius	PU	S/N	Log $L_X(0.3-8.0 \text{ keV})$	Variability			Opt Corr	DG	Flag
		(J2000)	(J2000)	($''$)	($''$)	($''$)	(erg s^{-1})	LT	BB	K-S	($''$)		
(1)	(2)	(3)	(4)	(5)	(6)	(7)	(8)	(9)	(10)	(11)	(12)	(13)	(14)
73	J122008.7+291619	12:20:08.678	+29:16:18.65	3.00	0.20	8.9	37.8	V	-	-	-	40.3	O1
74	J122008.7+291613	12:20:08.662	+29:16:13.20	3.00	0.29	7.4	37.5	V	-	-	-	44.6	O2
75	J122008.6+291820	12:20:08.623	+29:18:20.11	3.00	0.55	3.0	37.1	V	-	-	GCexmt	92.4	-
76	J122008.4+291717	12:20:08.390	+29:17:16.83	3.00	0.16	11.2	38.0	V	-	-	GCcorr	33.2	O1
78	J122008.4+291754	12:20:08.354	+29:17:54.05	3.00	0.17	13.7	38.0	N	V	N	BGexmt	66.4	-
79	J122008.3+291719	12:20:08.338	+29:17:18.82	3.00	-	-	37.3	V	-	-	none	34.3	X
80	J122008.2+291628	12:20:08.167	+29:16:27.72	3.00	0.34	5.8	37.4	N	-	-	-	29.0	O2
81	J122008.2+291660	12:20:08.153	+29:16:59.89	3.00	0.27	6.5	37.5	N	-	-	GCcorr	19.6	O2
82	J122008.1+291633	12:20:08.141	+29:16:32.55	3.00	0.48	3.7	37.0	N	-	-	BGexmt	25.1	O2
83	J122008.1+291717	12:20:08.138	+29:17:17.08	3.00	0.16	10.5	38.0	TC	-	-	GCcorr	31.4	O1
84	J122008.1+291644	12:20:08.076	+29:16:43.73	3.00	0.18	11.5	37.9	V	-	-	GCcorr	17.8	O2
85	J122008.0+291642	12:20:08.050	+29:16:41.97	3.00	0.18	10.9	37.8	N	-	P	GCcorr	18.3	O2
86	J122008.0+291654	12:20:08.045	+29:16:54.44	3.00	0.30	5.7	37.4	V	-	-	none	16.4	O2
87	J122008.0+291758	12:20:08.028	+29:17:58.47	3.00	0.30	7.1	37.4	N	-	-	none	69.5	O1
88	J122008.0+291652	12:20:07.994	+29:16:52.20	3.00	0.26	6.6	37.5	N	-	-	GCexmt	15.4	O2
91	J122007.9+291657	12:20:07.930	+29:16:57.20	3.00	0.22	7.5	37.6	PTC	-	-	none	15.8	O2
92	J122007.9+291632	12:20:07.913	+29:16:31.92	3.00	0.49	3.7	37.0	V	-	-	-	23.6	O2
94	J122007.8+291758	12:20:07.848	+29:17:58.03	3.00	0.38	7.2	37.2	V	-	-	none	68.6	O1
96	J122007.8+291720	12:20:07.752	+29:17:20.47	3.00	0.12	27.5	38.6	N	N	P	GCcorr	32.1	-
97	J122007.7+291503	12:20:07.745	+29:15:03.38	3.00	0.43	4.5	37.3	V	-	-	-	108.1	-
98	J122007.7+291644	12:20:07.706	+29:16:44.10	3.00	0.15	15.4	38.1	V	-	P	GCcorr	13.3	O2
99	J122007.7+291654	12:20:07.661	+29:16:53.60	3.00	0.15	12.7	38.0	V	N	N	GCexmt	11.3	O2
100	J122007.5+291634	12:20:07.534	+29:16:33.81	3.00	0.23	7.3	37.7	V	-	-	BGexmt	19.3	O1
101	J122007.5+291654	12:20:07.457	+29:16:53.89	3.00	0.16	9.9	37.9	V	-	-	none	8.8	O2
103	J122007.4+291609	12:20:07.368	+29:16:08.79	3.00	0.18	11.0	37.9	V	-	P	-	42.6	-
104	J122007.3+291656	12:20:07.298	+29:16:56.15	3.00	0.17	8.7	37.8	N	-	-	GCexmt	8.2	O2
106	J122007.2+291652	12:20:07.174	+29:16:52.04	3.00	0.16	8.0	37.8	-	-	-	GCexmt	4.8	O2
107	J122007.2+291410	12:20:07.166	+29:14:10.02	3.00	0.60	4.7	37.3	N	-	-	-	160.8	-
108	J122007.2+291739	12:20:07.164	+29:17:38.74	3.00	0.19	9.4	37.8	V	-	-	GCcorr	48.2	-
109	J122007.1+291639	12:20:07.145	+29:16:39.14	3.00	0.29	4.5	37.5	V	-	-	none	12.4	O1
110	J122007.1+291709	12:20:07.123	+29:17:09.32	3.00	0.22	5.2	37.5	V	-	-	none	19.0	O1
111	J122007.0+291629	12:20:07.042	+29:16:29.13	3.00	0.25	6.3	37.5	V	-	-	-	21.8	-
114	J122006.9+291660	12:20:06.914	+29:16:59.52	3.00	0.16	11.3	37.9	N	-	-	none	8.8	O2
116	J122006.9+291701	12:20:06.900	+29:17:01.22	3.00	0.20	6.6	37.6	-	-	-	none	10.5	O2
117	J122006.8+291651	12:20:06.823	+29:16:50.78	3.00	0.05	218.8	40.3	V	V	V	BGcorr	0.0	O2 NUCLEUS
118	J122006.8+291637	12:20:06.816	+29:16:36.66	3.00	0.14	17.2	38.2	N	N	N	GCcorr	14.1	O2
119	J122006.8+291656	12:20:06.804	+29:16:55.94	3.00	0.10	30.7	38.7	V	N	N	GCexmt	5.2	O2
120	J122006.8+291646	12:20:06.787	+29:16:45.67	3.00	0.12	18.5	38.4	N	N	N	GCexmt	5.1	O2
121	J122006.8+291857	12:20:06.782	+29:18:56.60	3.00	0.33	4.6	37.4	V	-	-	-	125.8	O1
123	J122006.7+291646	12:20:06.691	+29:16:45.92	3.00	-	-	38.0	V	-	-	none	5.2	X
124	J122006.6+291641	12:20:06.629	+29:16:41.22	3.00	0.16	9.6	37.8	N	-	-	GCexmt	9.9	O2
125	J122006.6+291714	12:20:06.607	+29:17:14.21	3.00	0.21	7.1	37.6	N	-	-	GCexmt	23.6	O1
126	J122006.6+291629	12:20:06.552	+29:16:29.32	3.00	0.32	5.0	37.5	N	-	-	-	21.7	O1
127	J122006.5+291706	12:20:06.538	+29:17:05.98	3.00	0.24	6.6	37.5	N	-	-	GCexmt	15.7	O2
128	J122006.5+291645	12:20:06.514	+29:16:44.84	3.00	0.17	7.6	37.7	-	-	-	BGcorr	7.2	O2
129	J122006.5+291659	12:20:06.504	+29:16:58.65	3.00	0.19	8.3	37.7	V	-	-	BGcorr	8.9	O2
130	J122006.4+291624	12:20:06.439	+29:16:23.58	3.00	0.33	5.4	37.4	V	-	-	-	27.7	-
131	J122006.4+291709	12:20:06.434	+29:17:08.64	3.00	0.38	4.0	37.1	V	-	-	none	18.6	O2
132	J122006.4+291649	12:20:06.398	+29:16:48.61	3.00	0.14	11.3	38.0	V	V	V	BGexmt	6.0	O2
133	J122006.4+291843	12:20:06.372	+29:18:43.14	3.00	0.17	15.9	38.1	N	N	N	-	112.5	-
134	J122006.3+291710	12:20:06.324	+29:17:09.91	3.00	0.26	6.6	37.4	V	-	-	GCcorr	20.2	O2
135	J122006.3+291644	12:20:06.324	+29:16:43.66	3.00	0.19	8.3	37.7	-	-	-	GCexmt	9.7	O2
137	J122006.3+291656	12:20:06.283	+29:16:56.06	3.00	0.21	8.1	37.6	V	-	-	GCexmt	8.8	O2
138	J122006.2+291651	12:20:06.245	+29:16:51.30	3.00	0.21	6.3	37.5	-	-	-	none	7.6	O2
139	J122006.2+291658	12:20:06.218	+29:16:57.53	3.00	0.16	10.9	37.8	TC	-	-	GCexmt	10.4	O2

TABLE 3 — *Continued*

Masterid	CXOU Name	RA	Dec	Radius	PU	S/N	Log $L_X(0.3\text{--}8.0\text{ keV})$	Variability			Opt Corr	DG	Flag
		(J2000)	(J2000)	($''$)	($''$)	($''$)		($''$)	(7)	LT			
(1)	(2)	(3)	(4)	(5)	(6)	(7)	(8)	(9)	(10)	(11)	(12)	(13)	(14)
140	J122006.2+291631	12:20:06.218	+29:16:31.45	3.00	0.15	15.6	38.1	V	V	-	-	20.9	O2
141	J122006.2+291608	12:20:06.206	+29:16:08.48	3.00	0.24	6.7	37.6	V	-	P	-	43.1	O1
142	J122006.1+291414	12:20:06.149	+29:14:14.32	3.00	0.59	4.8	37.3	N	-	-	-	156.7	-
143	J122006.1+291813	12:20:06.098	+29:18:13.47	3.00	0.22	7.9	37.6	V	-	P	none	83.2	-
144	J122006.1+291601	12:20:06.082	+29:16:00.64	3.00	0.34	3.6	37.2	N	-	-	-	51.1	O1
145	J122006.1+291637	12:20:06.060	+29:16:36.54	3.00	0.33	3.7	37.4	-	-	-	BGexmt	17.4	O1
146	J122006.0+291648	12:20:06.031	+29:16:48.39	3.00	0.11	31.3	38.7	V	N	V	none	10.6	O2
147	J122006.0+291651	12:20:05.998	+29:16:50.53	3.00	0.13	17.2	38.2	V	-	V	BGcorr	10.8	O2
148	J122005.9+291709	12:20:05.945	+29:17:08.92	3.00	0.14	15.7	38.1	N	N	P	GCcorr	21.5	O2
149	J122005.9+291652	12:20:05.921	+29:16:51.81	3.00	-	-	37.7	V	-	-	GCexmt	11.8	X
150	J122005.9+291605	12:20:05.914	+29:16:05.39	3.00	0.42	4.4	37.1	-	-	-	-	46.9	O2
152	J122005.7+291710	12:20:05.729	+29:17:09.97	3.00	0.39	4.1	37.1	V	-	-	GCexmt	24.0	O2
153	J122005.7+291659	12:20:05.717	+29:16:59.06	3.00	0.40	3.1	37.2	V	-	-	GCcorr	16.7	double?
154	J122005.7+291650	12:20:05.698	+29:16:49.97	3.00	0.14	13.6	38.0	N	-	P	GCcorr	14.7	O2
155	J122005.7+291555	12:20:05.681	+29:15:55.36	3.00	0.20	9.7	37.8	N	-	-	-	57.4	-
156	J122005.7+291716	12:20:05.669	+29:17:15.89	3.00	0.26	3.9	37.4	PTC	-	-	none	29.3	O1
157	J122005.5+291706	12:20:05.508	+29:17:05.58	3.00	0.14	13.3	38.1	V	-	P	GCexmt	22.7	O1
158	J122005.5+291641	12:20:05.486	+29:16:40.77	3.00	0.11	26.3	38.7	V	N	P	GCexmt	20.2	O1
159	J122005.4+291717	12:20:05.388	+29:17:17.01	3.00	0.35	4.4	37.2	PTC	-	-	none	32.3	O2
160	J122005.3+291610	12:20:05.335	+29:16:10.33	3.00	0.23	7.8	37.6	V	-	-	none	44.9	-
162	J122005.2+291653	12:20:05.234	+29:16:52.74	3.00	0.21	7.7	37.6	V	-	-	GCcorr	20.9	-
163	J122005.2+291640	12:20:05.230	+29:16:39.93	3.00	0.12	17.8	38.4	V	N	P	GCcorr	23.5	O1
164	J122005.2+291539	12:20:05.218	+29:15:38.84	3.00	0.34	4.7	37.3	N	-	-	-	74.9	-
165	J122005.1+291715	12:20:05.083	+29:17:15.30	3.00	0.25	6.5	37.4	N	-	-	GCcorr	33.5	O2
166	J122005.0+291704	12:20:05.021	+29:17:03.89	3.00	0.22	7.6	37.6	N	-	P	GCexmt	27.0	-
167	J122004.9+291602	12:20:04.855	+29:16:01.67	3.00	0.38	4.9	37.2	N	-	-	GCcorr	55.4	O2
168	J122004.9+291714	12:20:04.853	+29:17:14.43	3.00	0.30	5.0	37.3	N	-	-	GCexmt	35.0	O2
169	J122004.8+291737	12:20:04.798	+29:17:37.33	3.00	0.16	9.7	37.8	V	-	V	none	53.6	-
170	J122004.8+291728	12:20:04.793	+29:17:28.46	3.00	0.18	8.3	37.7	N	-	P	GCexmt	46.1	-
171	J122004.8+291744	12:20:04.769	+29:17:43.57	3.00	0.24	5.7	37.4	N	-	-	GCexmt	59.2	-
172	J122004.7+291607	12:20:04.699	+29:16:07.33	3.00	0.46	3.3	37.2	N	-	-	GCcorr	51.6	O1
179	J122004.5+291612	12:20:04.531	+29:16:12.18	3.00	0.21	9.2	37.7	V	-	-	GCcorr	48.9	O2
181	J122004.5+291602	12:20:04.469	+29:16:01.79	3.00	0.28	5.1	37.4	N	-	-	none	57.9	O1
182	J122004.5+291648	12:20:04.457	+29:16:48.22	3.00	0.27	6.1	37.4	V	-	-	none	31.1	O2
183	J122004.3+291421	12:20:04.337	+29:14:21.38	3.00	0.41	5.9	37.5	N	-	-	-	152.9	-
184	J122004.3+291736	12:20:04.330	+29:17:36.01	3.00	0.10	31.8	38.7	V	N	N	GCexmt	55.8	-
185	J122004.2+291651	12:20:04.229	+29:16:51.49	3.00	0.12	18.5	38.4	V	N	N	GCcorr	33.9	O1
186	J122004.1+291624	12:20:04.142	+29:16:23.61	3.00	0.28	4.4	37.3	V	-	-	none	44.4	-
187	J122004.1+291615	12:20:04.102	+29:16:15.24	3.00	0.17	9.7	37.8	V	-	-	GCcorr	50.3	-
189	J122003.8+291638	12:20:03.830	+29:16:37.96	3.00	0.17	8.7	37.8	V	-	P	BGcorr	41.2	O1
190	J122003.8+291610	12:20:03.773	+29:16:09.71	3.00	0.19	9.7	37.8	N	-	-	GCcorr	57.3	-
191	J122003.7+291630	12:20:03.727	+29:16:29.85	3.00	0.19	7.9	37.6	N	-	-	GCcorr	45.6	-
192	J122003.7+291720	12:20:03.710	+29:17:19.72	3.00	0.32	3.4	37.1	V	-	-	none	50.0	-
193	J122003.5+291618	12:20:03.545	+29:16:17.61	3.00	0.37	3.0	37.1	N	-	-	GCcorr	54.2	-
194	J122003.4+291640	12:20:03.434	+29:16:39.50	3.00	0.12	21.1	38.4	V	N	V	GCcorr	45.7	O1
195	J122003.3+291743	12:20:03.278	+29:17:42.94	3.00	0.16	8.7	37.7	N	-	-	none	69.8	-
196	J122003.2+291405	12:20:03.202	+29:14:05.22	3.00	0.92	4.4	37.3	-	-	-	-	172.2	-
197	J122003.2+291632	12:20:03.170	+29:16:31.98	3.00	0.27	5.4	37.4	V	-	P	BGexmt	51.3	-
199	J122002.5+291625	12:20:02.486	+29:16:24.73	3.00	0.34	3.6	37.2	V	-	-	GCcorr	62.4	-
201	J122002.1+291550	12:20:02.098	+29:15:50.08	3.00	0.36	4.3	37.3	V	-	-	-	86.6	-
202	J122002.0+291730	12:20:01.999	+29:17:29.79	3.00	0.17	7.5	37.6	N	-	-	GCcorr	74.2	-
203	J122001.9+291758	12:20:01.850	+29:17:58.29	3.00	0.23	6.4	37.5	N	-	-	GCcorr	93.8	-
204	J122001.6+291626	12:20:01.582	+29:16:26.16	3.00	0.14	16.6	38.2	TC	-	-	none	72.9	-
205	J122001.4+291704	12:20:01.428	+29:17:04.43	3.00	0.19	6.6	37.5	N	-	-	none	71.9	-
206	J122001.3+291656	12:20:01.344	+29:16:55.94	3.00	0.33	3.4	37.1	N	-	-	none	71.9	-

TABLE 3 — *Continued*

Masterid (1)	CXOU Name (2)	RA	Dec	Radius	PU	S/N	Log $L_X(0.3-8.0 \text{ keV})$ (8)	Variability			Opt Corr (12)	DG ($''$) (13)	Flag (14)
		(J2000) (3)	(J2000) (4)	($''$) (5)	($''$) (6)	(7)		LT (9)	BB (10)	K-S (11)			
208	J122001.1+291724	12:20:01.085	+29:17:23.50	3.00	0.26	4.5	37.3	N	-	-	GCcorr	81.9	-
209	J122000.9+291515	12:20:00.931	+29:15:15.11	3.00	0.20	12.1	37.9	N	-	P	-	122.9	-
210	J122000.7+291748	12:20:00.746	+29:17:48.14	3.00	0.27	5.7	37.3	N	-	-	none	98.0	O2
211	J122000.7+291529	12:20:00.746	+29:15:29.05	3.00	0.34	5.4	37.4	V	-	-	-	114.0	-
213	J122000.6+291808	12:20:00.598	+29:18:08.47	3.00	0.21	6.9	37.6	V	-	-	BGcorr	112.6	O1
214	J122000.4+291746	12:20:00.398	+29:17:46.12	3.00	0.45	3.1	36.9	-	-	-	GCcorr	100.6	O2
216	J122000.3+291705	12:20:00.314	+29:17:05.06	3.00	0.17	7.9	37.6	N	-	-	GCcorr	86.3	-
217	J122000.3+291812	12:20:00.274	+29:18:12.25	3.00	0.29	4.4	37.3	V	-	-	GCcorr	118.2	O1
219	J121959.7+291612	12:19:59.678	+29:16:12.45	3.00	0.37	3.2	37.1	N	-	-	-	101.0	-
220	J121959.7+291426	12:19:59.666	+29:14:25.63	3.00	0.22	16.8	38.2	V	-	P	-	172.7	-
223	J121958.6+291544	12:19:58.565	+29:15:43.66	3.00	0.28	6.9	37.5	V	-	-	-	127.2	-
225	J121958.5+291608	12:19:58.490	+29:16:08.16	3.00	0.17	11.7	37.9	N	-	P	-	117.0	-
226	J121958.2+291836	12:19:58.174	+29:18:36.41	3.00	0.33	4.9	37.3	V	-	-	-	154.8	-
227	J121958.1+291712	12:19:58.099	+29:17:11.81	3.00	0.14	15.5	38.1	V	V	V	-	116.1	O1
228	J121957.7+291715	12:19:57.708	+29:17:14.56	3.00	0.13	19.9	38.3	V	-	-	-	121.6	O1
229	J121957.6+291725	12:19:57.634	+29:17:24.93	3.00	0.17	10.6	37.8	N	-	-	-	125.0	-
230	J121957.1+291620	12:19:57.108	+29:16:19.64	3.00	0.23	8.2	37.7	V	-	-	-	130.9	-
231	J121956.9+291639	12:19:56.858	+29:16:38.77	3.00	0.21	9.0	37.7	V	-	-	-	130.9	-
232	J121956.7+291631	12:19:56.690	+29:16:31.35	3.00	0.37	3.2	37.2	V	-	-	-	134.0	O1
233	J121956.4+291637	12:19:56.419	+29:16:37.02	3.00	0.30	4.7	37.4	N	-	-	-	136.8	O1
234	J121956.4+291633	12:19:56.405	+29:16:33.40	3.00	0.36	5.2	37.3	N	-	-	-	137.4	O2
236	J121955.0+291654	12:19:55.042	+29:16:53.58	3.00	0.73	3.2	37.1	-	-	-	-	154.2	-
Master Source List for sources with S/N<3													
3	J122022.6+291551	12:20:22.589	+29:15:51.22	4.02	1.03	0.7	36.5 (≤ 37.1)	-	-	-	-	214.7	O1
6	J122022.2+291554	12:20:22.236	+29:15:54.36	3.94	1.06	1.5	36.9 (≤ 37.2)	-	-	-	-	209.4	O1
7	J122020.9+291647	12:20:20.904	+29:16:46.88	3.49	-	-	36.7 (≤ 37.9)	N	-	-	-	184.3	X
10	J122018.1+291555	12:20:18.077	+29:15:55.01	3.15	1.00	1.0	36.5 (≤ 37.0)	-	-	-	-	157.4	-
12	J122017.8+291440	12:20:17.762	+29:14:39.96	3.67	-	-	36.3 (≤ 36.9)	N	-	-	-	193.9	X
18	J122016.1+291718	12:20:16.121	+29:17:18.40	3.00	-	-	36.5 (≤ 37.0)	N	-	-	-	124.7	X
20	J122015.5+291519	12:20:15.538	+29:15:19.16	3.00	0.73	2.6	37.0 (≤ 37.3)	-	-	-	-	146.3	-
22	J122014.7+291741	12:20:14.702	+29:17:41.07	3.00	0.67	2.7	37.0 (≤ 37.3)	N	-	-	-	114.7	-
25	J122014.5+291751	12:20:14.462	+29:17:50.62	3.00	0.68	2.5	37.0 (≤ 37.3)	-	-	-	-	116.5	-
33	J122012.4+291707	12:20:12.439	+29:17:07.43	3.00	0.65	1.7	36.8 (≤ 37.1)	-	-	-	-	75.4	-
34	J122012.4+291438	12:20:12.410	+29:14:37.93	3.00	1.07	2.2	36.8 (≤ 37.1)	N	-	-	-	151.6	O2
37	J122011.8+291515	12:20:11.767	+29:15:14.71	3.00	0.63	2.7	37.0 (≤ 37.3)	V	-	-	-	115.8	-
47	J122010.1+291646	12:20:10.068	+29:16:46.19	3.00	-	-	37.0 (≤ 37.2)	N	-	-	-	42.7	X
49	J122010.0+291427	12:20:09.998	+29:14:27.46	3.00	1.00	2.5	37.0 (≤ 37.2)	-	-	-	-	149.2	-
52	J122009.8+291655	12:20:09.811	+29:16:54.99	3.00	0.49	1.5	36.9 (≤ 37.2)	-	-	-	none	39.3	O1
58	J122009.4+291723	12:20:09.401	+29:17:23.41	3.00	0.49	1.8	36.9 (≤ 37.2)	N	-	-	none	46.9	O1
59	J122009.4+291645	12:20:09.401	+29:16:45.06	3.00	0.41	2.7	37.2 (≤ 37.4)	V	-	-	-	34.2	O1
61	J122009.2+291707	12:20:09.214	+29:17:06.62	3.00	-	-	36.9 (≤ 37.2)	N	-	-	none	35.1	X
77	J122008.4+291614	12:20:08.378	+29:16:13.85	3.00	0.56	1.4	36.8 (≤ 37.2)	-	-	-	-	42.2	O1
89	J122008.0+291603	12:20:07.994	+29:16:03.25	3.00	-	-	36.4 (≤ 36.9)	N	-	-	-	49.9	X
90	J122007.9+291546	12:20:07.939	+29:15:45.69	3.00	0.46	2.6	37.0 (≤ 37.3)	-	-	-	-	66.7	-
93	J122007.9+291727	12:20:07.862	+29:17:27.48	3.00	0.61	2.7	37.0 (≤ 37.3)	-	-	-	GCexmt	39.1	-
95	J122007.8+291537	12:20:07.800	+29:15:37.33	3.00	0.64	1.5	36.7 (≤ 37.1)	-	-	-	-	74.5	-
102	J122007.4+291708	12:20:07.442	+29:17:07.63	3.00	0.36	2.0	37.0 (≤ 37.4)	-	-	-	none	18.7	O1
105	J122007.2+291648	12:20:07.250	+29:16:47.90	3.00	-	-	37.6 (≤ 37.7)	V	-	P	GCexmt	6.3	X
112	J122007.0+291852	12:20:06.986	+29:18:52.41	3.00	0.61	1.0	36.5 (≤ 37.0)	N	-	-	-	121.7	O1
113	J122006.9+291726	12:20:06.941	+29:17:25.59	3.00	0.45	1.5	36.8 (≤ 37.1)	V	-	-	GCexmt	34.8	-
115	J122006.9+291622	12:20:06.902	+29:16:22.23	3.00	0.35	3.0	37.1 (≤ 37.4)	N	-	-	-	28.6	-
122	J122006.8+291809	12:20:06.763	+29:18:08.55	3.00	0.42	2.5	37.0 (≤ 37.2)	N	-	-	none	77.8	-
136	J122006.3+291715	12:20:06.283	+29:17:15.03	3.00	-	-	37.1 (≤ 37.3)	N	-	-	GCexmt	25.3	X

TABLE 3 — *Continued*

Masterid	CXOU Name	RA	Dec	Radius	PU	S/N	Log $L_X(0.3-8.0 \text{ keV})$	Variability			Opt Corr	DG	Flag
		(J2000)	(J2000)	($''$)	($''$)	($''$)	(erg s^{-1})	LT	BB	K-S	(12)	($''$)	(14)
(1)	(2)	(3)	(4)	(5)	(6)	(7)	(8)	(9)	(10)	(11)	(12)	(13)	(14)
151	J122005.9+291822	12:20:05.899	+29:18:21.52	3.00	0.39	2.6	37.0 (≤ 37.3)	N	-	-	GCexmt	91.5	-
161	J122005.3+291602	12:20:05.256	+29:16:01.68	3.00	0.44	2.3	37.0 (≤ 37.3)	-	-	-	GCcorr	53.2	O1
173	J122004.6+291634	12:20:04.618	+29:16:34.48	3.00	-	-	36.8 (≤ 37.0)	V	-	-	GCcorr	33.1	X
174	J122004.6+291615	12:20:04.594	+29:16:15.37	3.00	0.32	2.6	37.1 (≤ 37.4)	N	-	-	GCcorr	45.9	O1
175	J122004.6+291714	12:20:04.562	+29:17:14.47	3.00	0.27	2.8	37.2 (≤ 37.4)	V	-	-	none	37.9	O1
176	J122004.6+291820	12:20:04.555	+29:18:20.19	3.00	0.44	2.0	36.8 (≤ 37.2)	N	-	-	GCexmt	94.2	-
177	J122004.5+291625	12:20:04.538	+29:16:24.95	3.00	-	-	37.0 (≤ 37.2)	N	-	-	GCexmt	39.5	X
178	J122004.5+291637	12:20:04.534	+29:16:36.89	3.00	0.44	2.9	37.1 (≤ 37.4)	V	-	-	none	33.0	-
180	J122004.5+291644	12:20:04.522	+29:16:44.12	3.00	0.41	2.6	37.1 (≤ 37.4)	-	-	-	GCexmt	30.8	O1
188	J122004.1+291744	12:20:04.075	+29:17:43.57	3.00	0.44	1.6	36.7 (≤ 37.1)	-	-	-	none	63.9	-
198	J122003.0+291815	12:20:02.978	+29:18:14.96	3.00	0.50	1.9	36.8 (≤ 37.1)	-	-	-	GCexmt	98.1	-
200	J122002.2+291526	12:20:02.222	+29:15:26.02	3.00	0.58	1.9	36.8 (≤ 37.2)	-	-	-	-	103.9	-
207	J122001.3+291609	12:20:01.325	+29:16:09.05	3.00	0.44	1.6	36.7 (≤ 37.1)	-	-	-	none	83.2	-
212	J122000.7+291753	12:20:00.660	+29:17:53.04	3.00	0.40	2.3	37.0 (≤ 37.3)	-	-	-	none	101.9	O1
215	J122000.3+291722	12:20:00.348	+29:17:21.98	3.00	0.33	2.9	37.0 (≤ 37.3)	-	-	-	GCcorr	90.3	-
218	J122000.1+291750	12:20:00.120	+29:17:49.81	3.00	0.40	2.4	37.0 (≤ 37.3)	-	-	-	BGexmt	105.7	O1
221	J121959.3+291847	12:19:59.282	+29:18:47.34	-	-	-	36.6 (≤ 37.0)	N	-	-	-	152.7	X
222	J121959.2+291901	12:19:59.213	+29:19:01.05	-	-	-	36.5 (≤ 37.0)	N	-	-	-	164.0	X
224	J121958.5+291642	12:19:58.517	+29:16:42.09	-	-	-	37.1 (≤ 37.3)	V	-	-	-	109.0	X
235	J121956.4+291804	12:19:56.393	+29:18:03.67	3.00	0.70	1.1	36.5 (≤ 37.0)	N	-	-	-	154.7	-

NOTE. — Table has been divided into two parts. The first part lists all sources with $S/N > 3$, in at least one observation. The second section lists the remaining sources, that have $S/N < 3$ in all observations. Col. (1): source number, col. (2): IAU name (following the convention “CXOU Jhhmmss.s+/-ddmmss”), cols. (3) and (4): right ascension and declination, col. (5): source extraction radius in arcseconds, col. (6): position uncertainty (from section 2.2, equation 1), col. (7): signal-to-noise ratio, col. (8): $\log L_X$ (0.3–8.0 keV) assuming $D=16.1$ Mpc (for the sources with $S/N < 3$, 3σ upper limits are also quoted in brackets). For sources only detected in a single observation, 1σ upper limits from the co-added observation are quoted (with 3σ upper limits from the detected observation presented in brackets), col. (9): long-term source variability - (N) indicates non-variable sources, (V) indicates variable sources, (TC) transient candidates, (PTC) possible transients, cols. (10) and (11): short-term variability, where (BB) indicates Bayesian block analysis and (K-S) indicates the Kolmogorov-Smirnov test, in both columns symbols indicate - (N) non-variable in all observations, (V) variable in at least one observation, (P) possible variability in at least one observation, col. (12): optical associations - ‘GC’ indicates that the optical source is a confirmed globular cluster, ‘BG’ indicates that optical source is a background objects. ‘corr’ denotes matches that have been defined as correlations, and ‘exmt’ denotes matches between $0.8''$ and $3''$ in separation, ‘none’ indicates sources inside the field of view of the *HST* observation, but have no optical counterpart. All other sources are external to the *HST* FOV. Col. (13): distance from the galactic center (in arcseconds), where values in bold type face indicate sources that lie within the D_{25} ellipse. Col. (14): flag information - (X) sources detected in a single observation only, O1 and O2 overlapping sources (single and complicated cases respectively) and (double?) possible double sources.

TABLE 4 — *Continued*

MID	B-band	S1-band	S2-band	Net Counts S-band	H-band	Sc-band	Hc-band	HR	C21	C32	Log L_X (0.3–8.0 keV)
(1)	(2)	(3)	(4)	(5)	(6)	(7)	(8)	(9)	(10)	(11)	(12)
236	28.9±9.0	-0.7±4.0	18.8±6.3	18.1±7.0	10.9±6.3	16.6±6.4	14.1±6.7	-0.15 ^{+0.29} _{-0.26}	-1.02 ^{+0.62} _{-0.76}	0.25 ^{+0.31} _{-0.26}	37.1

NOTE. — Col. (1): Master ID, cols. (2)–(8): net counts, in each of the 7 energy bands (see Table 2 for definitions of these bands), col. (9): hardness ratio, cols. (10) and (11) color values, col. (12): log L_X (0.3–8.0 keV). Upper limit L_X values are at the 68% confidence level.

TABLE 5
SOURCE COUNTS, HARDNESS RATIOS, COLOR-COLOR VALUES AND VARIABILITY:
OBSERVATION 1

Masterid	B-band	S1-band	S2-band	Net Counts			H-band	Sc-band	Hc-band	HR	C21	C32	Variability			Log L_X
(1)	(2)	(3)	(4)	S-band	(6)	(7)	(8)	(9)	(10)	(11)	BB	k-S	signif.	(15)		
1	9.8±4.7	-1.0±1.9	1.1±2.7	0.1±2.7	9.7±4.4	0.0±2.3	10.5±4.6	0.94 ^{+0.06} _{-0.08}	-0.38 ^{+0.91} _{-1.15}	-0.72 ^{+0.43} _{-0.67}	-	-	-	37.7		
2	11.3±5.0	3.0±3.2	5.1±3.6	8.0±4.3	3.3±3.4	7.9±4.1	3.0±3.4	-0.58 ^{+0.24} _{-0.28}	-0.08 ^{+0.35} _{-0.43}	0.19 ^{+0.45} _{-0.38}	-	-	-	37.8		
3	<3.9	-	-	-	-	-	-	-	-	-	-	-	-	<37.3		
4	15.5±5.5	6.2±3.8	9.1±4.3	15.3±5.2	0.3±2.7	12.9±4.8	2.1±3.2	-0.81 ^{+0.11} _{-0.19}	-0.05 ^{+0.24} _{-0.24}	0.84 ^{+0.84} _{-0.46}	-	-	-	37.9		
5	64.3±9.3	19.8±5.7	35.3±7.1	55.1±8.6	9.1±4.4	49.9±8.2	13.0±5.0	-0.63 ^{+0.09} _{-0.10}	-0.10 ^{+0.08} _{-0.16}	0.59 ^{+0.18} _{-0.17}	N	N	-	38.6		
6	<2.0	-	-	-	-	-	-	-	-	-	-	-	-	<37.0		
7	<0.6	-	-	-	-	-	-	-	-	-	-	-	-	<36.5		
8	12.6±5.0	2.2±2.9	6.3±3.8	8.6±4.3	4.0±3.4	5.3±3.6	6.8±4.0	0.06 ^{+0.30} _{-0.30}	-0.29 ^{+0.34} _{-0.46}	0.19 ^{+0.32} _{-0.30}	-	-	-	37.8		
9	<1.5	-	-	-	-	-	-	-	-	-	-	-	-	<36.9		
10	<1.3	-	-	-	-	-	-	-	-	-	-	-	-	<36.8		
11	<11.4	-	-	-	-	-	-	-	-	-	-	-	-	<37.8		
12	<3.2	-	-	-	-	-	-	-	-	-	-	-	-	<37.2		
13	50.2±8.3	14.1±5.0	26.3±6.3	40.4±7.5	9.8±4.4	33.0±6.9	14.7±5.1	-0.43 ^{+0.12} _{-0.14}	-0.19 ^{+0.15} _{-0.14}	0.43 ^{+0.16} _{-0.16}	N	N	-	38.4		
14	22.3±6.1	4.3±3.4	14.6±5.0	18.8±5.6	3.5±3.4	14.4±5.0	7.4±4.1	-0.37 ^{+0.20} _{-0.21}	-0.43 ^{+0.24} _{-0.27}	0.56 ^{+0.38} _{-0.27}	N	N	-	38.1		
15	12.7±5.0	2.1±2.9	6.4±3.8	8.5±4.3	4.2±3.4	7.1±4.0	6.1±3.8	-0.14 ^{+0.27} _{-0.30}	-0.32 ^{+0.37} _{-0.48}	0.19 ^{+0.32} _{-0.27}	-	-	-	37.8		
16	<2.1	-	-	-	-	-	-	-	-	-	-	-	-	>37.1		
17	<8.4	-	-	-	-	-	-	-	-	-	-	-	-	>37.7		
18	<1.1	-	-	-	-	-	-	-	-	-	-	-	-	>36.8		
19	<1.0	-	-	-	-	-	-	-	-	-	-	-	-	>36.7		
20	<1.1	-	-	-	-	-	-	-	-	-	-	-	-	>36.8		
21	3.7±3.6	0.5±2.3	2.1±2.9	2.5±3.2	1.1±2.7	3.2±3.2	0.8±2.7	-0.67 ^{+0.25} _{-0.33}	-0.31 ^{+0.69} _{-0.91}	0.19 ^{+0.80} _{-0.67}	-	-	-	37.3		
22	<1.6	-	-	-	-	-	-	-	-	-	-	-	-	>36.9		
23	6.6±4.1	3.4±3.2	4.1±3.4	7.5±4.1	-0.9±1.9	6.1±3.8	-0.2±2.3	-0.93 ^{+0.11} _{-0.07}	0.00 ^{+0.38} _{-0.35}	0.99 ^{+1.00} _{-0.61}	-	-	-	37.5		
24	<10.7	-	-	-	-	-	-	-	-	-	-	-	-	>37.7		
25	<4.7	-	-	-	-	-	-	-	-	-	-	-	-	>37.4		
26	<9.4	-	-	-	-	-	-	-	-	-	-	-	-	>37.7		
27	<0.5	-	-	-	-	-	-	-	-	-	-	-	-	>36.4		
28	<1.1	-	-	-	-	-	-	-	-	-	-	-	-	>36.7		
29	11.9±4.9	3.5±3.2	7.5±4.0	11.0±4.6	0.9±2.7	9.3±4.3	1.8±2.9	-0.76 ^{+0.14} _{-0.24}	-0.21 ^{+0.26} _{-0.33}	0.69 ^{+0.76} _{-0.38}	-	-	-	37.8		
30	<1.4	-	-	-	-	-	-	-	-	-	-	-	-	<37.1		
31	40.6±7.6	9.3±4.3	19.0±5.6	28.3±6.5	12.2±4.7	23.9±6.1	16.0±5.2	-0.25 ^{+0.13} _{-0.17}	-0.21 ^{+0.16} _{-0.19}	0.21 ^{+0.17} _{-0.15}	N	N	-	38.3		
32	<0.5	-	-	-	-	-	-	-	-	-	-	-	-	>36.4		
33	<0.9	-	-	-	-	-	-	-	-	-	-	-	-	>36.7		
34	<0.7	-	-	-	-	-	-	-	-	-	-	-	-	>36.6		
35	13.1±5.0	3.6±3.2	9.6±4.3	13.1±4.8	-0.1±2.3	13.7±4.8	-0.3±2.3	-0.98 ^{+0.05} _{-0.02}	-0.32 ^{+0.27} _{-0.30}	1.07 ^{+0.84} _{-0.54}	-	-	-	37.9		
36	<2.3	-	-	-	-	-	-	-	-	-	-	-	-	>37.1		
37	<0.5	-	-	-	-	-	-	-	-	-	-	-	-	>36.5		
38	<7.5	-	-	-	-	-	-	-	-	-	-	-	-	>37.6		
39	11.8±3.5	1.4±2.7	6.4±3.8	7.7±4.1	4.2±3.4	7.2±4.0	4.2±3.4	-0.33 ^{+0.28} _{-0.31}	-0.46 ^{+0.41} _{-0.59}	0.19 ^{+0.29} _{-0.30}	-	-	-	37.8		
40	7.7±2.4	0.7±2.3	4.4±3.4	5.1±3.6	2.5±2.9	5.3±3.6	3.4±3.2	-0.29 ^{+0.31} _{-0.36}	-0.53 ^{+0.53} _{-0.69}	0.24 ^{+0.40} _{-0.37}	-	-	-	37.6		
41	56.7±8.7	10.6±4.4	30.9±6.7	41.5±7.6	15.2±5.1	35.7±7.1	20.1±5.7	-0.34 ^{+0.11} _{-0.13}	-0.38 ^{+0.15} _{-0.16}	0.32 ^{+0.17} _{-0.11}	N	N	-	38.5		
42	16.7±5.3	3.8±3.2	8.6±4.1	12.4±4.7	4.3±3.4	11.7±4.6	5.1±3.6	-0.44 ^{+0.22} _{-0.24}	-0.27 ^{+0.27} _{-0.27}	0.29 ^{+0.30} _{-0.24}	-	-	-	38.2		
43	16.0±5.3	6.5±3.8	8.6±4.1	15.1±5.1	0.9±2.7	12.4±4.7	0.8±2.7	-0.92 ^{+0.08} _{-0.08}	-0.03 ^{+0.22} _{-0.24}	0.75 ^{+0.75} _{-0.43}	-	-	-	37.9		
44	<9.7	-	-	-	-	-	-	-	-	-	-	-	-	>37.7		
45	<4.7	-	-	-	-	-	-	-	-	-	-	-	-	>37.4		
46	<4.8	-	-	-	-	-	-	-	-	-	-	-	-	>37.4		
47	<0.9	-	-	-	-	-	-	-	-	-	-	-	-	>36.7		
48	<10.0	-	-	-	-	-	-	-	-	-	-	-	-	>37.7		
49	<1.4	-	-	-	-	-	-	-	-	-	-	-	-	>36.9		
50	14.3±5.2	4.1±3.4	8.3±4.1	12.5±4.8	1.8±2.9	9.0±4.3	3.7±3.4	-0.49 ^{+0.26} _{-0.29}	-0.21 ^{+0.26} _{-0.30}	0.56 ^{+0.57} _{-0.37}	-	-	-	37.9		

TABLE 5 — *Continued*

Masterid	B-band	S1-band	S2-band	Net Counts	H-band	Sc-band	Hc-band	HR	C21	C32	BB	Variability	Log L_X
(1)	(2)	(3)	(4)	S-band (5)	(6)	(7)	(8)	(9)	(10)	(11)	(12)	k-S signif. (14)	(0.3–8.0 keV) (15)
51	<1.3	-	-	-	-	-	-	-	-	-	-	-	<36.8
52	<4.9	-	-	-	-	-	-	-	-	-	-	-	<37.4
53	<6.0	-	-	-	-	-	-	-	-	-	-	-	<37.5
54	<4.2	-	-	-	-	-	-	-	-	-	-	-	<37.3
55	<4.0	-	-	-	-	-	-	-	-	-	-	-	<37.3
56	<8.0	-	-	-	-	-	-	-	-	-	-	-	<37.6
57	<2.7	-	-	-	-	-	-	-	-	-	-	-	<37.2
58	<3.1	-	-	-	-	-	-	-	-	-	-	-	<37.2
59	<0.7	-	-	-	-	-	-	-	-	-	-	-	<36.6
60	<2.0	-	-	-	-	-	-	-	-	-	-	-	<37.0
61	<6.9	-	-	-	-	-	-	-	-	-	-	-	<37.6
62	<0.5	-	-	-	-	-	-	-	-	-	-	-	<36.4
63	8.9±4.6	2.2±2.9	4.1±3.4	6.2±4.0	2.7±3.2	5.9±3.8	3.4±3.4	-0.36 ^{+0.34} _{-0.36}	-0.13 ^{+0.42} _{-0.51}	0.16 ^{+0.51} _{-0.43}	-	-	37.7
64	<2.3	-	-	-	-	-	-	-	-	-	-	-	<37.1
65	<10.5	-	-	-	-	-	-	-	-	-	-	-	<37.7
66	23.1±6.3	9.0±4.3	11.4±4.7	20.4±5.9	2.6±3.2	15.7±5.3	5.5±3.8	-0.53 ^{+0.18} _{-0.21}	-0.03 ^{+0.22} _{-0.18}	0.59 ^{+0.46} _{-0.32}	N	N	38.1
67	11.8±4.9	3.4±3.2	5.5±3.6	8.8±4.3	3.0±3.2	5.3±3.6	4.8±3.6	-0.11 ^{+0.33} _{-0.35}	-0.11 ^{+0.30} _{-0.35}	0.24 ^{+0.40} _{-0.35}	-	-	37.8
68	21.0±6.0	3.9±3.4	8.2±4.1	12.1±4.8	9.0±4.3	11.7±4.7	9.8±4.4	-0.15 ^{+0.21} _{-0.23}	-0.21 ^{+0.29} _{-0.33}	0.00 ^{+0.21} _{-0.21}	N	N	38.0
69	8.0±4.3	1.4±2.7	4.7±3.4	6.1±3.8	1.9±2.9	6.3±3.8	1.9±2.9	-0.64 ^{+0.17} _{-0.24}	-0.35 ^{+0.43} _{-0.59}	0.35 ^{+0.56} _{-0.43}	-	-	37.6
70	4.6±4.2	0.2±2.7	3.6±3.4	3.8±3.8	0.8±2.7	4.3±3.8	0.7±2.7	-0.73 ^{+0.23} _{-0.27}	-0.38 ^{+0.53} _{-1.00}	0.46 ^{+0.76} _{-0.61}	-	-	37.4
71	9.7±4.6	0.3±2.3	4.7±3.4	5.0±3.6	4.7±3.6	4.5±3.4	4.6±3.6	-0.06 ^{+0.37} _{-0.36}	-0.61 ^{+0.53} _{-0.84}	0.03 ^{+0.29} _{-0.32}	-	-	37.7
72	18.3±5.7	7.3±4.0	7.4±4.0	14.7±5.1	3.6±3.4	12.1±4.7	4.5±3.6	-0.51 ^{+0.22} _{-0.24}	0.08 ^{+0.21} _{-0.24}	0.29 ^{+0.38} _{-0.29}	-	-	38.0
73	8.2±5.0	2.1±2.9	3.7±3.4	5.8±4.0	1.8±2.9	1.2±2.9	3.6±3.4	0.48 ^{+0.52} _{-0.29}	-0.11 ^{+0.46} _{-0.56}	0.27 ^{+0.64} _{-0.51}	-	-	37.6
74	13.6±5.6	2.3±2.9	7.0±4.0	9.3±4.4	4.1±3.4	8.8±4.3	3.8±3.4	-0.46 ^{+0.26} _{-0.29}	-0.35 ^{+0.35} _{-0.43}	0.24 ^{+0.30} _{-0.29}	-	-	37.8
75	<2.8	-	-	-	-	-	-	-	-	-	-	-	<37.2
76	19.3±5.9	4.8±3.6	5.6±3.8	10.4±4.7	8.9±4.3	8.9±4.4	9.6±4.4	-0.02 ^{+0.24} _{-0.26}	0.03 ^{+0.29} _{-0.32}	-0.16 ^{+0.24} _{-0.27}	-	-	38.0
77	<0.7	-	-	-	-	-	-	-	-	-	-	-	<36.6
78	21.8±6.1	5.1±3.6	9.9±4.4	15.0±5.2	6.7±4.0	14.6±5.1	6.5±4.0	-0.44 ^{+0.20} _{-0.22}	-0.19 ^{+0.24} _{-0.27}	0.19 ^{+0.24} _{-0.22}	N	N	38.1
79	<1.1	-	-	-	-	-	-	-	-	-	-	-	<36.7
80	<6.0	-	-	-	-	-	-	-	-	-	-	-	<37.5
81	<7.0	-	-	-	-	-	-	-	-	-	-	-	<37.6
82	<1.1	-	-	-	-	-	-	-	-	-	-	-	<36.8
83	<1.9	-	-	-	-	-	-	-	-	-	-	-	<37.0
84	36.6±8.8	5.4±4.3	24.0±6.1	29.3±7.0	7.5±4.2	24.0±6.4	13.5±5.0	-0.33 ^{+0.16} _{-0.17}	-0.51 ^{+0.24} _{-0.40}	0.51 ^{+0.21} _{-0.19}	N	N	38.3
85	<19.2	-	-	-	-	-	-	-	-	-	-	-	<38.0
86	<2.1	-	-	-	-	-	-	-	-	-	-	-	<37.1
87	<8.7	-	-	-	-	-	-	-	-	-	-	-	<37.7
88	<5.7	-	-	-	-	-	-	-	-	-	-	-	<37.5
89	<0.9	-	-	-	-	-	-	-	-	-	-	-	<36.7
90	<9.1	-	-	-	-	-	-	-	-	-	-	-	<37.7
91	<1.1	-	-	-	-	-	-	-	-	-	-	-	<36.8
92	<0.5	-	-	-	-	-	-	-	-	-	-	-	<36.4
93	<2.1	-	-	-	-	-	-	-	-	-	-	-	<37.0
94	<6.3	-	-	-	-	-	-	-	-	-	-	-	<37.5
95	<0.9	-	-	-	-	-	-	-	-	-	-	-	<36.7
96	70.0±9.7	14.8±5.1	39.9±7.5	54.7±8.6	15.3±5.2	47.0±8.1	19.3±5.7	-0.47 ^{+0.10} _{-0.12}	-0.30 ^{+0.09} _{-0.18}	0.44 ^{+0.14} _{-0.14}	N	N	38.6
97	<8.6	-	-	-	-	-	-	-	-	-	-	-	<37.7
98	22.6±7.9	2.5±4.0	17.0±5.5	19.5±6.3	3.6±3.6	15.3±5.7	6.6±4.2	-0.46 ^{+0.22} _{-0.24}	-0.59 ^{+0.38} _{-0.67}	0.64 ^{+0.43} _{-0.32}	-	-	38.1
99	37.2±8.4	9.3±5.1	20.9±6.1	30.2±7.5	7.0±4.3	24.8±6.8	10.6±4.9	-0.46 ^{+0.17} _{-0.18}	-0.31 ^{+0.26} _{-0.22}	0.48 ^{+0.24} _{-0.24}	N	N	38.3
100	<3.1	-	-	-	-	-	-	-	-	-	-	-	<37.2
101	<27.6	-	-	-	-	-	-	-	-	-	-	-	<38.2
102	<1.2	-	-	-	-	-	-	-	-	-	-	-	<36.8

TABLE 5 — *Continued*

Masterid	B-band	S1-band	S2-band	Net Counts		H-band	Sc-band	Hc-band	HR	C21	C32	Variability			Log L_x	
(1)	(2)	(3)	(4)	S-band	(5)	(6)	(7)	(8)	(9)	(10)	(11)	BB	k-S	signif.	(14)	(15)
103	17.6±5.7	7.2±4.0	5.9±3.8	13.1±5.0	4.4±3.6	10.5±4.6	5.3±3.8	-0.39 ^{+0.24} _{-0.27}	0.16 ^{+0.24} _{-0.27}	0.13 ^{+0.35} _{-0.29}	-	-	-	-	38.0	
104	≤14.3	-	-	-	-	-	-	-	-	-	-	-	-	-	-	≤37.9
105	≤27.9	-	-	-	-	-	-	-	-	-	-	-	-	-	-	≤38.2
106	≤18.0	-	-	-	-	-	-	-	-	-	-	-	-	-	-	≤38.0
107	8.1±4.3	3.6±3.2	0.5±2.3	4.1±3.4	4.1±3.4	4.3±3.4	4.0±3.4	-0.12 ^{+0.38} _{-0.38}	0.61 ^{+0.77} _{-0.53}	-0.53 ^{+0.53} _{-0.85}	-	-	-	-	37.6	
108	9.1±4.6	3.2±3.2	3.4±3.2	6.6±4.0	2.5±3.2	7.0±4.0	2.3±3.2	-0.62 ^{+0.17} _{-0.27}	0.05 ^{+0.38} _{-0.40}	0.13 ^{+0.54} _{-0.45}	-	-	-	-	37.7	
109	≤2.8	-	-	-	-	-	-	-	-	-	-	-	-	-	-	≤37.2
110	≤1.9	-	-	-	-	-	-	-	-	-	-	-	-	-	-	≤37.0
111	13.1±5.3	5.7±3.8	4.7±3.6	10.4±4.7	2.7±3.2	6.9±4.1	2.5±3.2	-0.57 ^{+0.21} _{-0.33}	0.16 ^{+0.32} _{-0.32}	0.21 ^{+0.51} _{-0.40}	-	-	-	-	37.8	
112	≤2.1	-	-	-	-	-	-	-	-	-	-	-	-	-	-	≤37.0
113	≤1.1	-	-	-	-	-	-	-	-	-	-	-	-	-	-	≤36.8
114	≤15.4	-	-	-	-	-	-	-	-	-	-	-	-	-	-	≤37.9
115	7.8±4.6	3.0±3.2	3.5±3.4	6.4±4.1	1.4±2.9	7.1±4.1	1.1±2.9	-0.81 ^{+0.17} _{-0.19}	0.03 ^{+0.48} _{-0.49}	0.29 ^{+0.78} _{-0.58}	-	-	-	-	37.6	
116	≤4.4	-	-	-	-	-	-	-	-	-	-	-	-	-	-	≤37.4
117	6979.8±84.8	2002.4±45.9	3571.8±60.9	5574.1±75.9	1405.7±38.6	4668.9±69.5	1899.4±44.7	-0.47 ^{+0.01} _{-0.01}	-0.18 ^{+0.02} _{-0.01}	0.44 ^{+0.01} _{-0.02}	N	N	-	-	40.6	
118	34.2±7.9	7.8±4.8	21.2±6.0	29.0±7.2	5.3±3.8	24.1±6.6	8.0±4.3	-0.55 ^{+0.15} _{-0.10}	-0.32 ^{+0.21} _{-0.39}	0.59 ^{+0.30} _{-0.71}	N	N	-	-	38.2	
119	103.9±14.9	14.8±7.0	58.3±9.7	73.0±11.6	31.2±7.3	56.6±10.5	45.3±8.4	-0.17 ^{+0.10} _{-0.13}	-0.54 ^{+0.25} _{-0.19}	0.28 ^{+0.12} _{-0.09}	N	N	-	-	38.7	
120	50.8±12.9	17.1±7.7	24.7±8.0	41.8±10.7	8.4±5.1	39.0±10.1	10.2±5.6	-0.65 ^{+0.15} _{-0.18}	-0.03 ^{+0.17} _{-0.32}	0.49 ^{+0.29} _{-0.27}	N	N	-	-	38.4	
121	≤0.8	-	-	-	-	-	-	-	-	-	-	-	-	-	-	≤36.6
122	≤1.1	-	-	-	-	-	-	-	-	-	-	-	-	-	-	≤36.7
123	≤26.8	-	-	-	-	-	-	-	-	-	-	-	-	-	-	≤38.1
124	≤20.2	-	-	-	-	-	-	-	-	-	-	-	-	-	-	≤38.0
125	10.1±4.7	2.3±2.9	6.3±3.8	8.6±4.3	1.5±2.9	7.9±4.1	2.4±3.2	-0.64 ^{+0.16} _{-0.26}	-0.29 ^{+0.37} _{-0.43}	0.51 ^{+0.67} _{-0.43}	-	-	-	-	37.7	
126	≤2.3	-	-	-	-	-	-	-	-	-	-	-	-	-	-	≤37.1
127	≤3.6	-	-	-	-	-	-	-	-	-	-	-	-	-	-	≤37.3
128	≤19.8	-	-	-	-	-	-	-	-	-	-	-	-	-	-	≤38.0
129	≤3.1	-	-	-	-	-	-	-	-	-	-	-	-	-	-	≤37.2
130	≤2.3	-	-	-	-	-	-	-	-	-	-	-	-	-	-	≤37.1
131	≤1.8	-	-	-	-	-	-	-	-	-	-	-	-	-	-	≤37.0
132	≤27.0	-	-	-	-	-	-	-	-	-	-	-	-	-	-	≤38.1
133	27.5±6.6	3.2±3.2	17.4±5.3	20.6±5.8	6.9±4.0	18.1±5.4	9.8±4.4	-0.35 ^{+0.17} _{-0.19}	-0.59 ^{+0.24} _{-0.35}	0.40 ^{+0.22} _{-0.19}	N	N	-	-	38.2	
134	≤1.6	-	-	-	-	-	-	-	-	-	-	-	-	-	-	≤36.9
135	≤10.6	-	-	-	-	-	-	-	-	-	-	-	-	-	-	≤37.7
136	≤1.2	-	-	-	-	-	-	-	-	-	-	-	-	-	-	≤36.8
137	8.3±6.6	1.4±3.9	7.3±5.1	8.8±5.9	-0.5±3.3	5.6±5.5	1.2±3.7	-0.60 ^{+0.27} _{-0.40}	-0.38 ^{+0.61} _{-0.84}	0.69 ^{+0.99} _{-0.61}	-	-	-	-	37.6	
138	≤5.6	-	-	-	-	-	-	-	-	-	-	-	-	-	-	≤37.5
139	≤0.8	-	-	-	-	-	-	-	-	-	-	-	-	-	-	≤36.6
140	46.7±8.2	11.3±4.7	25.6±6.3	36.9±7.4	9.8±4.4	31.6±6.9	13.7±5.0	-0.45 ^{+0.13} _{-0.14}	-0.27 ^{+0.16} _{-0.16}	0.43 ^{+0.16} _{-0.16}	N	N	-	-	38.4	
141	≤2.8	-	-	-	-	-	-	-	-	-	-	-	-	-	-	≤37.2
142	≤3.9	-	-	-	-	-	-	-	-	-	-	-	-	-	-	≤37.3
143	6.6±4.1	0.5±2.3	3.4±3.2	3.8±3.4	2.7±3.2	1.2±2.7	5.6±3.8	0.67 ^{+0.33} _{-0.21}	-0.46 ^{+0.54} _{-0.84}	0.11 ^{+0.48} _{-0.46}	-	-	-	-	37.5	
144	≤4.1	-	-	-	-	-	-	-	-	-	-	-	-	-	-	≤37.3
145	≤8.7	-	-	-	-	-	-	-	-	-	-	-	-	-	-	≤37.7
146	113.3±14.6	23.1±6.6	63.4±9.5	86.5±11.1	26.8±6.6	75.9±10.5	34.5±7.3	-0.43 ^{+0.08} _{-0.09}	-0.36 ^{+0.12} _{-0.12}	0.41 ^{+0.11} _{-0.10}	N	N	-	-	38.8	
147	≤27.4	-	-	-	-	-	-	-	-	-	-	-	-	-	-	≤38.2
148	23.2±6.4	6.5±4.0	14.1±5.1	20.6±6.0	2.6±3.2	19.3±5.8	4.3±3.6	-0.69 ^{+0.16} _{-0.18}	-0.24 ^{+0.21} _{-0.24}	0.67 ^{+0.46} _{-0.32}	N	P	-	-	38.1	
149	≤1.0	-	-	-	-	-	-	-	-	-	-	-	-	-	-	≤36.8
150	≤7.5	-	-	-	-	-	-	-	-	-	-	-	-	-	-	≤37.6
151	≤2.1	-	-	-	-	-	-	-	-	-	-	-	-	-	-	≤37.0
152	≤1.2	-	-	-	-	-	-	-	-	-	-	-	-	-	-	≤36.8
153	13.3±5.6	1.3±3.3	9.3±4.5	10.6±5.0	2.8±3.2	9.5±4.8	3.3±3.5	-0.58 ^{+0.22} _{-0.29}	-0.53 ^{+0.38} _{-0.77}	0.48 ^{+0.46} _{-0.35}	-	-	-	-	37.9	
154	17.9±7.4	1.4±3.5	8.6±4.6	10.1±5.3	7.6±4.2	8.1±4.9	10.6±4.6	0.11 ^{+0.28} _{-0.33}	-0.46 ^{+0.46} _{-0.76}	0.08 ^{+0.24} _{-0.27}	-	-	-	-	38.0	

TABLE 5 — *Continued*

Masterid	B-band	S1-band	S2-band	Net Counts	H-band	Sc-band	Hc-band	HR	C21	C32	BB	Variability	Log L_x	
(1)	(2)	(3)	(4)	S-band (5)	(6)	(7)	(8)	(9)	(10)	(11)	(12)	k-S (13)	signif. (14)	(0.3–8.0 keV) (15)
155	17.4±5.7	5.1±3.6	9.7±4.4	14.8±5.2	2.6±3.2	13.3±5.0	3.4±3.4	-0.66 ^{+0.18} _{-0.22}	-0.19 ^{+0.24} _{-0.27}	0.54 ^{+0.45} _{-0.35}	-	-	-	38.0
156	≤1.7	-	-	-	-	-	-	-	-	-	-	-	-	≤36.9
157	19.2±6.0	6.4±4.0	8.2±4.3	14.6±5.3	4.6±3.6	11.2±4.8	7.4±4.1	-0.27 ^{+0.24} _{-0.24}	-0.03 ^{+0.27} _{-0.24}	0.27 ^{+0.29} _{-0.30}	-	-	-	38.1
158	108.9±15.1	20.3±5.8	60.5±8.9	80.7±10.2	28.4±6.5	71.3±9.6	36.3±7.2	-0.38 ^{+0.08} _{-0.10}	-0.39 ^{+0.11} _{-0.12}	0.35 ^{+0.11} _{-0.09}	N	N	-	38.7
159	≤1.0	-	-	-	-	-	-	-	-	-	-	-	-	≤36.7
160	≤7.8	-	-	-	-	-	-	-	-	-	-	-	-	≤37.6
161	≤3.4	-	-	-	-	-	-	-	-	-	-	-	-	≤37.2
162	≤9.4	-	-	-	-	-	-	-	-	-	-	-	-	≤37.7
163	67.3±12.4	15.0±5.2	38.3±7.4	53.3±8.6	14.4±5.1	48.9±8.3	15.3±5.2	-0.57 ^{+0.10} _{-0.11}	-0.30 ^{+0.12} _{-0.16}	0.45 ^{+0.13} _{-0.15}	N	P	-	38.5
164	10.0±4.7	3.3±3.2	5.2±3.6	8.5±4.3	1.5±2.9	6.9±4.0	2.4±3.2	-0.59 ^{+0.20} _{-0.31}	-0.11 ^{+0.35} _{-0.35}	0.43 ^{+0.67} _{-0.46}	-	-	-	37.7
165	7.5±4.5	3.3±3.2	5.6±3.8	8.8±4.4	-1.4±1.9	7.5±4.1	0.3±2.7	-0.90 ^{+0.12} _{-0.10}	-0.13 ^{+0.34} _{-0.38}	1.07 ^{+1.07} _{-0.54}	-	-	-	37.6
166	≤11.0	-	-	-	-	-	-	-	-	-	-	-	-	≤37.8
167	≤7.3	-	-	-	-	-	-	-	-	-	-	-	-	≤37.6
168	≤5.0	-	-	-	-	-	-	-	-	-	-	-	-	≤37.4
169	19.4±5.8	6.1±3.8	12.3±4.7	18.4±5.6	1.0±2.7	14.8±5.1	2.8±3.2	-0.74 ^{+0.15} _{-0.19}	-0.21 ^{+0.21} _{-0.25}	0.89 ^{+0.72} _{-0.41}	-	-	-	38.0
170	15.5±5.3	5.2±3.6	9.1±4.3	14.3±5.1	1.2±2.7	13.1±4.8	1.8±2.9	-0.84 ^{+0.10} _{-0.16}	-0.13 ^{+0.24} _{-0.27}	0.75 ^{+0.64} _{-0.43}	-	-	-	37.9
171	≤6.6	-	-	-	-	-	-	-	-	-	-	-	-	≤37.5
172	≤2.5	-	-	-	-	-	-	-	-	-	-	-	-	≤37.1
173	≤1.2	-	-	-	-	-	-	-	-	-	-	-	-	≤36.8
174	≤1.1	-	-	-	-	-	-	-	-	-	-	-	-	≤36.7
175	≤1.2	-	-	-	-	-	-	-	-	-	-	-	-	≤36.8
176	≤1.7	-	-	-	-	-	-	-	-	-	-	-	-	≤37.0
177	≤3.5	-	-	-	-	-	-	-	-	-	-	-	-	≤37.3
178	≤0.5	-	-	-	-	-	-	-	-	-	-	-	-	≤36.4
179	16.3±5.7	5.1±3.6	7.5±4.1	12.6±5.0	3.7±3.6	11.1±4.7	5.6±4.0	-0.41 ^{+0.25} _{-0.27}	-0.08 ^{+0.27} _{-0.30}	0.29 ^{+0.41} _{-0.34}	-	-	-	37.9
180	≤3.1	-	-	-	-	-	-	-	-	-	-	-	-	≤37.2
181	7.5±4.5	0.8±2.7	4.9±3.6	5.7±4.0	1.8±2.9	4.4±3.6	3.7±3.4	-0.17 ^{+0.40} _{-0.43}	-0.46 ^{+0.54} _{-0.76}	0.38 ^{+0.59} _{-0.46}	-	-	-	37.6
182	≤12.1	-	-	-	-	-	-	-	-	-	-	-	-	≤37.8
183	10.0±4.6	2.5±2.9	7.5±4.0	10.0±4.4	0.0±2.3	7.4±4.0	0.8±2.7	-0.86 ^{+0.14} _{-0.14}	-0.35 ^{+0.32} _{-0.37}	0.92 ^{+0.91} _{-0.46}	-	-	-	37.7
184	98.2±11.1	20.1±5.7	53.1±8.4	73.1±9.7	25.1±6.2	65.6±9.2	29.8±6.6	-0.43 ^{+0.08} _{-0.10}	-0.31 ^{+0.08} _{-0.15}	0.35 ^{+0.12} _{-0.09}	N	N	-	38.7
185	48.9±8.3	9.4±4.4	27.7±6.5	37.1±7.4	11.9±4.7	29.6±6.7	16.8±5.3	-0.33 ^{+0.12} _{-0.16}	-0.38 ^{+0.17} _{-0.18}	0.39 ^{+0.15} _{-0.16}	N	N	-	38.4
186	10.9±5.0	2.7±3.2	5.0±3.6	7.6±4.3	3.3±3.4	7.3±4.1	4.1±3.6	-0.36 ^{+0.32} _{-0.34}	-0.13 ^{+0.40} _{-0.49}	0.19 ^{+0.43} _{-0.40}	-	-	-	37.7
187	2.9±3.8	-0.3±2.3	1.7±2.9	1.4±3.2	1.6±2.9	2.1±3.2	1.4±2.9	-0.25 ^{+0.34} _{-0.75}	-0.31 ^{+0.84} _{-1.07}	0.05 ^{+0.81} _{-0.80}	-	-	-	37.2
188	≤1.0	-	-	-	-	-	-	-	-	-	-	-	-	≤36.7
189	12.8±5.5	6.7±4.0	2.3±3.2	9.0±4.6	3.1±3.2	5.6±4.0	5.9±3.8	-0.01 ^{+0.32} _{-0.37}	0.46 ^{+0.53} _{-0.41}	-0.05 ^{+0.51} _{-0.62}	-	-	-	37.8
190	11.8±5.0	1.7±2.9	7.0±4.0	8.7±4.4	3.0±3.2	9.3±4.4	2.9±3.2	-0.60 ^{+0.22} _{-0.27}	-0.40 ^{+0.40} _{-0.62}	0.35 ^{+0.40} _{-0.32}	-	-	-	37.8
191	12.3±5.1	1.6±2.9	7.8±4.1	9.3±4.6	2.9±3.2	8.8±4.4	3.8±3.4	-0.47 ^{+0.26} _{-0.29}	-0.48 ^{+0.43} _{-0.65}	0.40 ^{+0.40} _{-0.32}	-	-	-	37.8
192	≤7.7	-	-	-	-	-	-	-	-	-	-	-	-	≤37.6
193	≤4.2	-	-	-	-	-	-	-	-	-	-	-	-	≤37.3
194	66.6±10.0	12.0±4.7	41.7±7.6	53.7±8.5	12.0±4.7	42.2±7.7	18.8±5.6	-0.44 ^{+0.10} _{-0.12}	-0.46 ^{+0.15} _{-0.14}	0.56 ^{+0.15} _{-0.14}	N	P	-	38.5
195	≤9.2	-	-	-	-	-	-	-	-	-	-	-	-	≤37.7
196	≤9.7	-	-	-	-	-	-	-	-	-	-	-	-	≤37.7
197	≤9.8	-	-	-	-	-	-	-	-	-	-	-	-	≤37.7
198	≤2.5	-	-	-	-	-	-	-	-	-	-	-	-	≤37.1
199	≤2.0	-	-	-	-	-	-	-	-	-	-	-	-	≤37.0
200	≤1.1	-	-	-	-	-	-	-	-	-	-	-	-	≤36.8
201	≤4.7	-	-	-	-	-	-	-	-	-	-	-	-	≤37.4
202	4.4±3.8	-0.7±1.9	4.3±3.4	3.7±3.4	0.7±2.7	2.2±2.9	2.5±3.2	-0.01 ^{+0.54} _{-0.52}	-0.92 ^{+0.61} _{-0.99}	0.53 ^{+0.77} _{-0.53}	-	-	-	37.4
203	5.6±4.0	2.4±2.9	1.4±2.7	3.8±3.4	1.8±2.9	4.2±3.4	1.7±2.9	-0.56 ^{+0.23} _{-0.44}	0.24 ^{+0.67} _{-0.59}	-0.05 ^{+0.72} _{-0.75}	-	-	-	37.5
204	339.4±19.5	100.4±11.1	194.2±15.0	294.5±18.2	44.8±7.8	252.0±16.9	68.7±9.4	-0.61 ^{+0.04} _{-0.01}	-0.19 ^{+0.03} _{-0.07}	0.68 ^{+0.06} _{-0.08}	N	N	-	39.2
205	9.2±4.6	2.4±2.9	6.1±3.8	8.5±4.3	0.7±2.7	5.0±3.6	2.6±3.2	-0.44 ^{+0.31} _{-0.38}	-0.27 ^{+0.35} _{-0.43}	0.69 ^{+0.76} _{-0.46}	-	-	-	37.7

TABLE 5 — *Continued*

Masterid	B-band	S1-band	S2-band	Net Counts		H-band	Sc-band	Hc-band	HR	C21	C32	Variability			Log L_X	
(1)	(2)	(3)	(4)	S-band	(5)	(6)	(7)	(8)	(9)	(10)	(11)	BB	k-S	signif.	(14)	(15)
206	<3.1	-	-	-	-	-	-	-	-	-	-	-	-	-	-	<37.2
207	<3.3	-	-	-	-	-	-	-	-	-	-	-	-	-	-	<37.2
208	<3.5	-	-	-	-	-	-	-	-	-	-	-	-	-	-	<37.3
209	14.7±5.2	0.5±2.3	10.3±4.4	10.8±4.6	3.8±3.4	11.1±4.6	3.8±3.4	-0.55 ^{+0.22} _{-0.25}	-0.84 ^{+0.38} _{-0.84}	0.40 ^{+0.32} _{-0.27}	-	-	-	-	37.9	
210	<6.4	-	-	-	-	-	-	-	-	-	-	-	-	-	-	<37.5
211	<8.5	-	-	-	-	-	-	-	-	-	-	-	-	-	-	<37.6
212	<2.0	-	-	-	-	-	-	-	-	-	-	-	-	-	-	<37.0
213	<7.6	-	-	-	-	-	-	-	-	-	-	-	-	-	-	<37.6
214	<1.3	-	-	-	-	-	-	-	-	-	-	-	-	-	-	<36.8
215	<1.1	-	-	-	-	-	-	-	-	-	-	-	-	-	-	<36.8
216	8.8±4.4	1.3±2.7	7.2±4.0	8.5±4.3	0.2±2.3	8.1±4.1	1.1±2.7	-0.84 ^{+0.13} _{-0.16}	-0.54 ^{+0.43} _{-0.61}	0.92 ^{+0.76} _{-0.54}	-	-	-	-	37.7	
217	<2.3	-	-	-	-	-	-	-	-	-	-	-	-	-	-	<37.1
218	<3.3	-	-	-	-	-	-	-	-	-	-	-	-	-	-	<37.2
219	<1.6	-	-	-	-	-	-	-	-	-	-	-	-	-	-	<36.9
220	18.9±5.8	2.0±2.9	14.2±5.0	16.3±5.3	2.6±3.2	13.8±5.0	5.4±3.8	-0.50 ^{+0.21} _{-0.22}	-0.67 ^{+0.35} _{-0.48}	0.67 ^{+0.46} _{-0.32}	-	-	-	-	38.0	
221	<1.7	-	-	-	-	-	-	-	-	-	-	-	-	-	-	<37.0
222	<2.4	-	-	-	-	-	-	-	-	-	-	-	-	-	-	<37.7
223	1.2±3.0	1.4±2.7	-0.7±1.9	0.7±2.7	0.5±2.3	1.2±2.7	0.4±2.3	-0.42 ^{+0.28} _{-0.58}	0.61 ^{+1.15} _{-0.76}	-0.31 ^{+1.00} _{-1.14}	-	-	-	-	36.8	
224	<10.8	-	-	-	-	-	-	-	-	-	-	-	-	-	-	<37.8
225	15.8±5.3	5.5±3.6	7.4±4.0	12.9±4.8	2.9±3.2	12.3±4.7	3.7±3.4	-0.60 ^{+0.20} _{-0.24}	-0.03 ^{+0.24} _{-0.26}	0.38 ^{+0.40} _{-0.33}	-	-	-	-	37.9	
226	<1.9	-	-	-	-	-	-	-	-	-	-	-	-	-	-	<37.0
227	34.1±7.4	5.4±3.6	18.3±5.4	23.7±6.1	10.1±4.4	21.0±5.8	13.1±4.8	-0.30 ^{+0.16} _{-0.17}	-0.43 ^{+0.22} _{-0.21}	0.28 ^{+0.18} _{-0.17}	N	N	-	-	38.3	
228	13.5±5.3	1.5±2.7	6.2±3.8	7.7±4.1	4.7±3.6	8.1±4.1	5.5±3.8	-0.27 ^{+0.27} _{-0.27}	-0.43 ^{+0.40} _{-0.54}	0.13 ^{+0.33} _{-0.26}	-	-	-	-	37.8	
229	12.7±5.0	0.4±2.3	8.3±4.1	8.7±4.3	4.0±3.4	9.2±4.3	3.8±3.4	-0.50 ^{+0.25} _{-0.27}	-0.76 ^{+0.38} _{-0.84}	0.32 ^{+0.32} _{-0.27}	-	-	-	-	37.8	
230	<9.8	-	-	-	-	-	-	-	-	-	-	-	-	-	-	<37.7
231	11.5±4.9	3.1±3.2	7.3±4.0	10.5±4.6	1.0±2.7	9.1±4.3	1.8±2.9	-0.77 ^{+0.13} _{-0.23}	-0.24 ^{+0.32} _{-0.35}	0.67 ^{+0.72} _{-0.43}	-	-	-	-	37.8	
232	<2.7	-	-	-	-	-	-	-	-	-	-	-	-	-	-	<37.2
233	<7.3	-	-	-	-	-	-	-	-	-	-	-	-	-	-	<37.6
234	<1.8	-	-	-	-	-	-	-	-	-	-	-	-	-	-	<37.0
235	<5.1	-	-	-	-	-	-	-	-	-	-	-	-	-	-	<37.4
236	<1.1	-	-	-	-	-	-	-	-	-	-	-	-	-	-	<36.8

NOTE. — Col. (1): Master ID, cols. (2)–(8): net counts, in each of the 7 energy bands (see Table 2 for definitions of these bands), col. (9): hardness ratio, cols. (10) and (11) color values, errors are given as 1σ , cols. (12) and (13): short-term variability, where (BB) indicate Bayesian block analysis and (K-S) indicates the Kolmogorov-Smirnov test, in both columns symbols indicate - (N) non-variable in all observations, (V) variable in at least one observation, (P) possible variability in at least one observation, col. (14): the significance of the change in L_X between the previous observation and the current observation respectively (equation 2), col. (15): $\log L_X$ (0.3–8.0 keV). Upper limit values of net B and L_X are at the 68% confidence level.

TABLE 6
SOURCE COUNTS, HARDNESS RATIOS, COLOR-COLOR VALUES AND VARIABILITY:
OBSERVATION 2

Masterid (1)	B-band (2)	S1-band (3)	S2-band (4)	Net Counts			Hc-band (8)	HR (9)	C21 (10)	C32 (11)	Variability			Log L_X (0.3–8.0 keV) (15)	
				S-band (5)	H-band (6)	Sc-band (7)					BB (12)	k-S (13)	signif. (14)		
1	30.6±7.9	1.3±3.4	9.1±4.6	10.4±5.2	20.2±6.5	9.0±4.6	21.2±6.6	0.35 ^{+0.21} _{-0.20}	-0.48 ^{+0.42} _{-0.83}	-0.30 ^{+0.19} _{-0.22}	N	N	0.2	37.8	
2	64.6±10.8	4.3±4.0	45.5±8.1	49.8±8.6	14.9±6.0	42.9±7.9	18.0±6.4	-0.47 ^{+0.15} _{-0.12}	-0.88 ^{+0.28} _{-0.37}	0.49 ^{+0.19} _{-0.14}	N	P	1.7	38.1	
3	<6.6	-	-	-	-	-	-	-	-	-	-	-	-	0.0	<37.1
4	71.0±11.2	23.3±6.2	35.4±7.3	58.7±9.1	12.1±5.7	52.3±8.5	14.2±6.0	-0.62 ^{+0.13} _{-0.11}	-0.06 ^{+0.09} _{-0.15}	0.43 ^{+0.25} _{-0.13}	N	P	1.3	38.1	
5	170.3±14.7	48.7±8.3	93.7±10.9	142.3±13.2	28.0±7.1	120.1±12.2	41.2±8.1	-0.54 ^{+0.07} _{-0.06}	-0.17 ^{+0.06} _{-0.10}	0.55 ^{+0.10} _{-0.11}	N	N	0.4	38.5	
6	<1.8	-	-	-	-	-	-	-	-	-	-	-	-	0.0	<36.5
7	<4.4	-	-	-	-	-	-	-	-	-	-	-	-	0.0	<36.9
8	32.2±7.7	11.0±4.7	23.0±6.2	34.0±7.3	-1.8±3.4	28.9±6.7	0.4±4.0	-0.97 ^{+0.06} _{-0.03}	-0.22 ^{+0.16} _{-0.18}	1.30 ^{+0.92} _{-0.46}	N	N	0.2	37.8	
9	<8.6	-	-	-	-	-	-	-	-	-	-	-	-	0.0	<37.2
10	<2.2	-	-	-	-	-	-	-	-	-	-	-	-	0.0	<36.6
11	11.2±5.5	2.1±3.2	5.2±3.8	7.3±4.4	3.8±4.0	3.6±3.6	7.5±4.6	0.34 ^{+0.39} _{-0.37}	-0.21 ^{+0.45} _{-0.62}	0.11 ^{+0.53} _{-0.40}	-	-	1.1	37.3	
12	4.2±3.6	-0.3±1.9	1.5±2.7	1.2±2.7	3.0±3.2	1.5±2.7	2.8±3.2	0.24 ^{+0.57} _{-0.37}	-0.53 ^{+0.76} _{-1.07}	-0.19 ^{+0.51} _{-0.61}	-	-	0.4	36.9	
13	385.3±21.0	99.0±11.1	225.8±16.2	324.8±19.2	60.5±9.2	273.8±17.7	88.5±10.8	-0.56 ^{+0.04} _{-0.04}	-0.25 ^{+0.03} _{-0.07}	0.59 ^{+0.07} _{-0.06}	N	N	7.6	38.9	
14	69.7±10.0	17.3±5.4	31.3±6.9	48.6±8.3	21.1±6.3	44.5±7.9	24.0±6.6	-0.36 ^{+0.12} _{-0.12}	-0.16 ^{+0.13} _{-0.14}	0.18 ^{+0.15} _{-0.12}	N	N	0.3	38.1	
15	25.0±6.8	3.6±3.4	14.7±5.2	18.3±5.8	6.7±4.4	16.7±5.4	9.0±4.8	-0.37 ^{+0.22} _{-0.22}	-0.48 ^{+0.27} _{-0.35}	0.35 ^{+0.27} _{-0.24}	N	N	0.7	37.7	
16	<6.6	-	-	-	-	-	-	-	-	-	-	-	-	0.0	<37.1
17	47.5±8.8	9.4±4.6	32.5±7.1	41.9±8.0	5.6±4.4	36.1±7.4	9.5±5.1	-0.64 ^{+0.15} _{-0.13}	-0.43 ^{+0.16} _{-0.19}	0.72 ^{+0.35} _{-0.24}	N	N	2.6	38.0	
18	1.8±4.2	1.0±2.9	-0.7±2.3	0.3±3.2	1.5±3.4	0.7±2.9	1.2±3.4	0.10 ^{+0.90} _{-0.05}	0.46 ^{+1.07} _{-0.99}	-0.46 ^{+0.99} _{-1.07}	-	-	0.3	36.5	
19	12.3±5.5	4.0±3.6	8.2±4.3	12.3±5.1	0.0±2.9	11.1±4.7	0.6±3.2	-0.91 ^{+0.11} _{-0.09}	-0.19 ^{+0.30} _{-0.37}	0.76 ^{+0.92} _{-0.45}	-	-	2.0	37.4	
20	<12.1	-	-	-	-	-	-	-	-	-	-	-	-	1.6	<37.4
21	<14.1	-	-	-	-	-	-	-	-	-	-	-	-	0.1	<37.4
22	<11.2	-	-	-	-	-	-	-	-	-	-	-	-	1.2	<37.4
23	15.8±6.0	5.7±4.0	12.4±4.8	18.1±5.8	-2.3±2.7	15.9±5.3	-0.7±3.2	-0.97 ^{+0.07} _{-0.03}	-0.21 ^{+0.24} _{-0.27}	1.22 ^{+0.92} _{-0.53}	-	-	0.2	37.5	
24	<12.4	-	-	-	-	-	-	-	-	-	-	-	-	1.4	<37.4
25	<2.4	-	-	-	-	-	-	-	-	-	-	-	-	1.3	<36.7
26	14.3±5.8	0.2±2.7	10.9±4.7	11.1±5.0	3.2±3.8	8.8±4.4	5.6±4.3	-0.33 ^{+0.34} _{-0.31}	-0.84 ^{+0.46} _{-0.84}	0.46 ^{+0.53} _{-0.35}	-	-	0.3	37.4	
27	<8.1	-	-	-	-	-	-	-	-	-	-	-	-	1.7	<37.2
28	<5.6	-	-	-	-	-	-	-	-	-	-	-	-	0.8	<37.1
29	23.6±6.8	1.0±2.9	8.4±4.3	9.4±4.7	14.2±5.4	8.1±4.3	16.9±5.8	0.29 ^{+0.23} _{-0.21}	-0.53 ^{+0.38} _{-0.85}	-0.19 ^{+0.22} _{-0.21}	N	N	0.7	37.6	
30	<2.7	-	-	-	-	-	-	-	-	-	-	-	-	0.0	<36.7
31	93.8±11.1	20.4±5.8	53.1±8.5	73.6±9.8	20.2±5.9	62.1±9.0	31.7±7.0	-0.38 ^{+0.09} _{-0.10}	-0.30 ^{+0.10} _{-0.13}	0.45 ^{+0.13} _{-0.11}	N	N	0.1	38.3	
32	23.9±6.8	24.6±6.3	-2.1±1.9	22.5±6.3	1.4±3.4	7.8±4.4	1.1±3.4	-0.82 ^{+0.18} _{-0.18}	1.76 ^{+0.91} _{-0.54}	-0.61 ^{+0.99} _{-1.15}	N	N	3.5	37.6	
33	<2.2	-	-	-	-	-	-	-	-	-	-	-	-	0.0	<36.6
34	<2.6	-	-	-	-	-	-	-	-	-	-	-	-	0.0	<36.7
35	28.3±7.2	4.1±3.8	19.9±5.8	24.0±6.5	4.3±4.0	21.2±6.0	6.7±4.4	-0.59 ^{+0.19} _{-0.19}	-0.54 ^{+0.27} _{-0.37}	0.62 ^{+0.40} _{-0.27}	N	N	0.9	37.7	
36	<10.5	-	-	-	-	-	-	-	-	-	-	-	-	0.8	<37.3
37	8.8±5.0	1.5±2.9	8.5±4.3	10.1±4.7	-1.3±2.7	7.9±4.3	-0.6±2.9	-0.93 ^{+0.11} _{-0.07}	-0.51 ^{+0.40} _{-0.64}	0.99 ^{+0.92} _{-0.53}	-	-	1.7	37.2	
38	20.9±7.7	5.9±4.0	13.2±5.0	19.2±5.9	1.2±3.2	9.6±4.6	6.7±4.3	-0.25 ^{+0.29} _{-0.27}	-0.24 ^{+0.21} _{-0.37}	0.80 ^{+0.78} _{-0.40}	N	N	0.7	37.6	
39	24.3±6.2	8.5±4.1	11.5±4.6	20.0±5.7	4.3±3.4	16.3±5.2	7.2±4.0	-0.43 ^{+0.17} _{-0.20}	-0.05 ^{+0.18} _{-0.19}	0.40 ^{+0.30} _{-0.21}	N	N	0.8	37.6	
40	28.7±4.7	6.1±4.0	16.4±5.3	22.5±6.2	5.9±4.0	17.5±5.6	9.7±4.6	-0.34 ^{+0.18} _{-0.20}	-0.32 ^{+0.21} _{-0.24}	0.43 ^{+0.27} _{-0.25}	N	N	0.8	37.7	
41	154.7±13.8	23.1±6.2	96.0±10.9	119.1±12.2	35.6±7.3	95.4±11.0	52.4±8.5	-0.35 ^{+0.07} _{-0.08}	-0.56 ^{+0.14} _{-0.07}	0.46 ^{+0.08} _{-0.09}	N	N	0.2	38.4	
42	92.7±11.1	22.0±6.0	48.8±8.2	70.7±9.7	22.0±6.2	58.2±8.9	30.4±7.0	-0.37 ^{+0.09} _{-0.11}	-0.23 ^{+0.10} _{-0.13}	0.36 ^{+0.13} _{-0.11}	N	N	0.0	38.2	
43	42.1±8.2	9.7±4.6	19.0±5.8	28.7±6.9	13.4±5.2	25.1±6.5	14.7±5.4	-0.32 ^{+0.18} _{-0.15}	-0.18 ^{+0.17} _{-0.22}	0.15 ^{+0.19} _{-0.15}	N	N	0.2	37.9	
44	<11.8	-	-	-	-	-	-	-	-	-	-	-	-	0.9	<37.4
45	9.0±5.3	0.5±2.9	4.1±3.6	4.6±4.1	4.4±4.0	1.3±3.2	7.0±4.4	0.71 ^{+0.29} _{-0.23}	-0.38 ^{+0.61} _{-0.84}	0.00 ^{+0.48} _{-0.46}	-	-	0.2	37.2	
46	<14.5	-	-	-	-	-	-	-	-	-	-	-	-	0.2	<37.4
47	17.4±7.3	9.7±4.7	7.5±4.3	17.2±5.9	0.3±3.2	15.7±5.6	1.0±3.4	-0.92 ^{+0.09} _{-0.08}	0.19 ^{+0.27} _{-0.24}	0.69 ^{+0.91} _{-0.54}	-	-	2.2	37.5	
48	9.4±5.8	4.1±3.8	5.8±4.0	9.8±5.0	-0.3±3.2	9.6±4.7	-1.0±3.2	-0.94 ^{+0.10} _{-0.06}	-0.05 ^{+0.40} _{-0.43}	0.61 ^{+0.54} _{-0.53}	-	-	0.8	37.2	

TABLE 6 — Continued

Masterid	B-band	S1-band	S2-band	Net Counts	H-band	Sc-band	Hc-band	HR	C21	C32	BB	Variability	Log L_X	
(1)	(2)	(3)	(4)	S-band (5)	(6)	(7)	(8)	(9)	(10)	(11)	(12)	k-S signif. (14)	(0.3–8.0 keV) (15)	
49	<1.5	-	-	-	-	-	-	-	-	-	-	-	0.0	≤36.5
50	34.0±7.6	7.2±4.1	22.6±6.1	29.8±6.9	4.2±4.0	28.1±6.6	5.6±4.3	-0.73 ^{+0.15} _{-0.15}	-0.40 ^{+0.19} _{-0.22}	0.70 ^{+0.37} _{-0.30}	N	N	0.4	37.8
51	27.5±7.7	4.3±3.8	19.9±5.8	24.2±6.5	3.4±3.8	19.8±5.9	5.9±4.3	-0.62 ^{+0.20} _{-0.19}	-0.54 ^{+0.27} _{-0.35}	0.70 ^{+0.51} _{-0.30}	N	N	3.2	37.7
52	≤7.3	-	-	-	-	-	-	-	-	-	-	-	0.6	≤37.1
53	15.3±6.6	0.7±3.2	8.5±4.4	9.3±5.0	5.5±4.3	4.0±4.0	8.8±4.8	0.38 ^{+0.35} _{-0.38}	-0.53 ^{+0.38} _{-0.92}	0.19 ^{+0.37} _{-0.30}	-	-	0.5	37.4
54	17.6±7.4	2.6±3.6	12.2±5.0	14.8±5.7	1.6±3.6	14.6±5.4	4.0±4.1	-0.68 ^{+0.17} _{-0.22}	-0.48 ^{+0.37} _{-0.57}	0.67 ^{+0.75} _{-0.40}	-	-	1.3	37.5
55	11.2±6.1	2.4±3.4	4.7±3.8	7.1±4.6	4.3±4.0	5.9±4.1	3.7±4.0	-0.36 ^{+0.37} _{-0.39}	-0.13 ^{+0.51} _{-0.65}	0.05 ^{+0.49} _{-0.45}	-	-	0.9	37.3
56	20.7±6.9	5.7±4.3	13.4±5.2	19.1±6.3	1.6±3.6	13.8±5.6	5.1±4.3	-0.56 ^{+0.25} _{-0.26}	-0.24 ^{+0.27} _{-0.35}	0.72 ^{+0.76} _{-0.40}	N	N	0.6	37.6
57	14.5±6.0	0.1±2.9	7.2±4.3	7.3±4.7	7.2±4.4	2.6±3.8	10.8±5.0	0.66 ^{+0.34} _{-0.19}	-0.61 ^{+0.46} _{-0.92}	0.03 ^{+0.29} _{-0.30}	-	-	1.5	37.4
58	2.9±4.6	-0.3±2.9	4.5±3.8	4.2±4.3	-1.4±2.7	4.0±4.0	-1.9±2.7	-0.87 ^{+0.19} _{-0.13}	-0.46 ^{+0.54} _{-0.99}	0.76 ^{+1.00} _{-0.61}	-	-	0.3	36.7
59	<1.5	-	-	-	-	-	-	-	-	-	-	-	0.0	≤36.4
60	8.1±5.1	5.2±3.8	1.1±2.9	6.3±4.3	1.8±3.6	4.5±3.8	1.3±3.6	-0.61 ^{+0.27} _{-0.39}	0.54 ^{+0.77} _{-0.51}	-0.13 ^{+0.91} _{-0.94}	-	-	1.0	37.2
61	9.9±6.1	5.0±4.0	7.9±4.4	12.9±5.4	-3.4±2.3	11.3±5.1	-2.9±2.7	-0.98 ^{+0.05} _{-0.02}	-0.11 ^{+0.32} _{-0.35}	1.15 ^{+0.99} _{-0.54}	-	-	0.1	37.3
62	≤3.7	-	-	-	-	-	-	-	-	-	-	-	0.0	≤36.8
63	37.8±7.9	9.4±4.6	13.8±5.1	23.2±6.4	14.6±5.3	23.7±6.3	15.1±5.4	-0.28 ^{+0.17} _{-0.16}	-0.07 ^{+0.20} _{-0.22}	-0.05 ^{+0.23} _{-0.12}	N	N	0.8	37.8
64	≤12.3	-	-	-	-	-	-	-	-	-	-	-	1.1	≤37.3
65	31.8±7.1	12.6±4.8	13.9±5.0	26.4±6.5	5.4±3.8	22.1±6.0	7.1±4.1	-0.56 ^{+0.15} _{-0.18}	0.04 ^{+0.17} _{-0.17}	0.40 ^{+0.27} _{-0.21}	N	N	0.8	37.8
66	33.6±7.1	6.8±4.0	21.1±5.8	27.9±6.5	5.7±3.8	27.5±6.5	5.5±3.8	-0.70 ^{+0.11} _{-0.15}	-0.38 ^{+0.19} _{-0.21}	0.56 ^{+0.24} _{-0.18}	N	N	1.8	37.8
67	31.5±7.4	-1.5±2.3	19.9±5.8	18.4±5.9	13.1±5.2	15.4±5.3	17.7±5.8	0.01 ^{+0.17} _{-0.21}	-1.48 ^{+0.67} _{-0.81}	0.21 ^{+0.16} _{-0.18}	N	N	0.2	37.8
68	52.1±9.0	15.7±5.4	26.5±6.5	42.2±8.0	10.0±4.8	29.9±6.9	16.5±5.7	-0.35 ^{+0.21} _{-0.15}	-0.11 ^{+0.13} _{-0.17}	0.44 ^{+0.18} _{-0.19}	N	N	0.4	38.0
69	28.3±7.1	3.7±3.6	20.2±5.8	24.0±6.4	4.3±4.0	18.4±5.7	8.1±4.6	-0.46 ^{+0.20} _{-0.20}	-0.59 ^{+0.30} _{-0.38}	0.64 ^{+0.38} _{-0.29}	N	N	0.4	37.7
70	9.4±6.0	-0.5±3.2	8.8±4.7	8.2±5.2	1.2±3.6	4.4±4.4	4.2±4.3	-0.10 ^{+0.44} _{-0.54}	-0.69 ^{+0.46} _{-0.99}	0.59 ^{+0.83} _{-0.46}	-	-	0.3	37.2
71	25.1±6.8	7.3±4.1	14.0±5.1	21.3±6.1	3.7±4.0	15.7±5.3	5.1±4.3	-0.61 ^{+0.23} _{-0.22}	-0.19 ^{+0.22} _{-0.21}	0.54 ^{+0.48} _{-0.33}	N	P	0.2	37.7
72	50.4±8.6	11.4±4.7	35.0±7.1	46.4±8.1	4.0±3.8	39.4±7.5	9.7±4.7	-0.65 ^{+0.11} _{-0.13}	-0.38 ^{+0.15} _{-0.16}	0.91 ^{+0.40} _{-0.27}	N	N	0.1	38.0
73	39.1±9.0	9.4±4.7	23.9±6.3	33.3±7.4	5.8±4.3	27.9±6.8	8.2±4.7	-0.60 ^{+0.16} _{-0.17}	-0.29 ^{+0.16} _{-0.22}	0.59 ^{+0.32} _{-0.27}	N	N	0.9	37.8
74	8.5±6.0	4.3±3.8	3.3±3.6	7.6±4.7	1.0±3.4	4.1±4.0	1.4±3.6	-0.53 ^{+0.29} _{-0.47}	0.16 ^{+0.56} _{-0.51}	0.27 ^{+0.94} _{-0.67}	-	-	1.8	37.2
75	17.6±6.2	3.9±3.6	9.6±4.6	13.4±5.3	4.2±4.0	6.9±4.3	7.0±4.4	-0.07 ^{+0.35} _{-0.35}	-0.27 ^{+0.32} _{-0.37}	0.35 ^{+0.40} _{-0.35}	-	-	1.7	37.5
76	85.6±10.9	24.8±6.5	46.9±8.1	71.6±9.9	14.0±5.3	62.5±9.3	19.6±6.0	-0.57 ^{+0.35} _{-0.10}	-0.24 ^{+0.17} _{-0.06}	0.56 ^{+0.35} _{-0.16}	N	N	1.5	38.2
77	≤2.4	-	-	-	-	-	-	-	-	-	-	-	0.0	≤36.6
78	55.9±9.1	10.4±4.7	29.2±6.7	39.6±7.8	16.3±5.6	34.1±7.1	20.2±6.1	-0.32 ^{+0.13} _{-0.14}	-0.34 ^{+0.16} _{-0.19}	0.27 ^{+0.15} _{-0.14}	N	N	0.3	38.0
79	≤16.5	-	-	-	-	-	-	-	-	-	-	-	2.4	≤37.5
80	18.1±7.5	2.3±3.8	14.4±5.3	16.7±6.1	0.7±3.4	15.6±5.8	2.2±3.8	-0.85 ^{+0.12} _{-0.15}	-0.56 ^{+0.37} _{-0.67}	0.86 ^{+0.83} _{-0.43}	-	-	0.7	37.5
81	20.8±7.2	4.8±4.5	3.0±4.0	7.8±5.5	13.0±5.1	8.2±5.3	13.4±5.2	0.22 ^{+0.28} _{-0.37}	0.30 ^{+0.72} _{-0.72}	-0.51 ^{+0.41} _{-0.59}	-	-	0.8	37.6
82	2.9±6.1	3.8±4.1	3.0±3.8	6.8±5.1	-4.1±2.3	4.9±4.6	-3.8±2.7	-0.91 ^{+0.15} _{-0.09}	0.16 ^{+0.73} _{-0.70}	0.76 ^{+1.07} _{-0.84}	-	-	0.4	36.7
83	≤1.5	-	-	-	-	-	-	-	-	-	-	-	0.0	≤36.4
84	52.2±8.5	7.5±4.1	29.1±6.5	36.5±7.3	15.6±5.2	33.2±7.0	18.4±5.6	-0.35 ^{+0.14} _{-0.12}	-0.49 ^{+0.19} _{-0.20}	0.28 ^{+0.17} _{-0.11}	N	N	2.0	38.0
85	36.4±7.4	7.7±4.1	23.9±6.1	31.6±6.9	4.8±3.6	29.1±6.6	5.6±3.8	-0.71 ^{+0.11} _{-0.14}	-0.38 ^{+0.17} _{-0.21}	0.70 ^{+0.24} _{-0.24}	N	N	0.3	37.8
86	≤15.6	-	-	-	-	-	-	-	-	-	-	-	1.4	≤37.4
87	18.3±4.3	0.9±2.9	11.1±4.7	12.0±5.1	6.8±4.3	9.8±4.6	8.2±4.6	-0.16 ^{+0.27} _{-0.28}	-0.69 ^{+0.38} _{-0.84}	0.21 ^{+0.27} _{-0.24}	N	N	0.2	37.5
88	31.4±9.8	2.9±4.7	20.7±6.2	23.5±7.3	8.2±4.8	20.0±6.9	10.9±5.2	-0.36 ^{+0.20} _{-0.24}	-0.59 ^{+0.38} _{-0.70}	0.40 ^{+0.27} _{-0.21}	-	-	1.8	37.8
89	≤0.8	-	-	-	-	-	-	-	-	-	-	-	0.0	≤36.2
90	≤9.9	-	-	-	-	-	-	-	-	-	-	-	1.1	≤37.3
91	≤2.7	-	-	-	-	-	-	-	-	-	-	-	0.0	≤36.7
92	≤1.1	-	-	-	-	-	-	-	-	-	-	-	0.0	≤36.3
93	≤11.7	-	-	-	-	-	-	-	-	-	-	-	0.9	≤37.3
94	16.1±3.8	0.1±2.7	9.4±4.4	9.6±4.7	6.1±4.1	9.0±4.4	7.6±4.4	-0.16 ^{+0.28} _{-0.29}	-0.76 ^{+0.45} _{-0.84}	0.21 ^{+0.27} _{-0.26}	N	N	0.6	37.5
95	≤2.4	-	-	-	-	-	-	-	-	-	-	-	0.0	≤36.6
96	223.3±16.4	49.1±8.3	126.6±12.4	175.8±14.6	47.5±8.3	143.6±13.2	72.1±9.8	-0.39 ^{+0.06} _{-0.07}	-0.31 ^{+0.06} _{-0.09}	0.45 ^{+0.08} _{-0.08}	N	N	0.7	38.6
97	7.6±5.1	2.2±3.2	2.7±3.4	4.9±4.1	2.7±3.8	3.3±3.6	4.1±4.1	0.02 ^{+0.34} _{-0.49}	0.03 ^{+0.67} _{-0.70}	0.00 ^{+0.98} _{-0.70}	-	-	0.7	37.1

TABLE 6 — *Continued*

Masterid	B-band	S1-band	S2-band	Net Counts		H-band	Sc-band	Hc-band	HR	C21	C32	BB	Variability	Log L_X	
(1)	(2)	(3)	(4)	S-band	(5)	(6)	(7)	(8)	(9)	(10)	(11)	(12)	k-S	signif.	(15)
98	72.7±10.1	6.6±4.3	45.2±8.0	51.8±8.7	20.9±5.9	40.7±7.9	30.5±6.8	-0.21 ^{+0.11} _{-0.13}	-0.73 ^{+0.21} _{-0.37}	0.38 ^{+0.11} _{-0.17}	N	N	0.3	38.1	
99	44.1±8.6	6.5±4.6	25.7±6.6	32.2±7.6	11.8±4.8	30.8±7.3	11.6±4.9	-0.50 ^{+0.13} _{-0.16}	-0.48 ^{+0.24} _{-0.32}	0.36 ^{+0.17} _{-0.16}	N	N	2.6	37.9	
100	27.9±7.8	8.6±4.8	14.6±5.5	23.3±6.8	4.6±4.2	17.3±6.1	8.9±4.9	-0.40 ^{+0.24} _{-0.24}	-0.13 ^{+0.24} _{-0.30}	0.46 ^{+0.45} _{-0.30}	N	N	2.4	37.7	
101	31.1±7.5	4.5±4.1	21.3±6.1	25.7±6.9	5.4±3.8	18.8±6.2	8.1±4.3	-0.45 ^{+0.17} _{-0.21}	-0.54 ^{+0.30} _{-0.40}	0.59 ^{+0.27} _{-0.21}	N	N	2.0	37.7	
102	≤13.3	-	-	-	-	-	-	-	-	-	-	-	-	1.4	≤37.4
103	33.0±7.7	7.3±4.3	20.9±6.0	28.3±6.9	4.7±4.1	26.0±6.5	4.1±4.1	-0.80 ^{+0.09} _{-0.14}	-0.35 ^{+0.19} _{-0.24}	0.62 ^{+0.40} _{-0.27}	N	N	1.0	37.8	
104	22.2±6.6	9.2±4.7	8.2±4.4	17.4±6.0	4.7±3.6	15.3±5.7	5.6±3.8	-0.52 ^{+0.19} _{-0.22}	0.13 ^{+0.25} _{-0.26}	0.24 ^{+0.32} _{-0.27}	N	N	0.6	37.6	
105	39.3±13.3	26.5±8.8	6.8±8.4	33.3±11.7	6.0±5.4	30.4±11.0	6.2±5.9	-0.74 ^{+0.12} _{-0.26}	0.47 ^{+0.72} _{-0.32}	0.15 ^{+0.68} _{-0.86}	N	P	1.1	37.8	
106	≤46.3	-	-	-	-	-	-	-	-	-	-	-	-	0.3	≤37.9
107	≤12.9	-	-	-	-	-	-	-	-	-	-	-	-	1.1	≤37.4
108	22.0±6.8	2.3±3.4	15.7±5.3	18.0±5.9	4.1±4.1	17.0±5.6	5.4±4.4	-0.61 ^{+0.22} _{-0.22}	-0.62 ^{+0.35} _{-0.61}	0.54 ^{+0.48} _{-0.30}	N	N	0.3	37.6	
109	30.1±8.9	12.0±5.4	10.3±5.1	22.3±6.9	7.6±4.9	17.2±6.1	9.5±5.3	-0.37 ^{+0.28} _{-0.23}	0.14 ^{+0.26} _{-0.25}	0.13 ^{+0.35} _{-0.29}	-	-	2.5	37.7	
110	20.4±7.6	4.2±4.5	14.0±5.6	18.2±6.7	2.2±3.9	14.9±6.1	4.7±4.3	-0.63 ^{+0.20} _{-0.25}	-0.35 ^{+0.35} _{-0.56}	0.67 ^{+0.70} _{-0.40}	-	-	2.2	37.6	
111	11.0±6.3	2.8±4.0	10.3±5.0	13.0±5.9	-2.0±3.0	11.8±5.6	-1.5±3.2	-0.96 ^{+0.08} _{-0.04}	-0.38 ^{+0.41} _{-0.64}	1.07 ^{+0.92} _{-0.54}	-	-	1.6	37.3	
112	≤3.5	-	-	-	-	-	-	-	-	-	-	-	-	0.0	≤36.8
113	≤1.7	-	-	-	-	-	-	-	-	-	-	-	-	0.0	≤36.5
114	57.8±13.4	19.2±7.0	29.6±8.1	48.8±10.3	9.5±5.1	43.3±9.8	9.4±5.2	-0.69 ^{+0.15} _{-0.13}	-0.11 ^{+0.17} _{-0.19}	0.50 ^{+0.25} _{-0.21}	N	N	1.3	38.0	
115	≤5.1	-	-	-	-	-	-	-	-	-	-	-	-	1.6	≤37.0
116	≤28.3	-	-	-	-	-	-	-	-	-	-	-	-	1.4	≤37.7
117	8782.9±95.2	3338.2±59.1	4502.8±68.4	7841.1±89.9	941.9±31.9	6832.4±84.0	1361.1±38.1	-0.70 ^{+0.00} _{-0.01}	-0.05 ^{+0.01} _{-0.01}	0.71 ^{+0.01} _{-0.02}	N	Y	42.9	40.2	
118	101.1±11.7	20.2±6.1	55.1±8.7	75.3±10.2	25.7±6.4	63.0±9.4	31.2±6.9	-0.39 ^{+0.09} _{-0.10}	-0.34 ^{+0.12} _{-0.13}	0.33 ^{+0.06} _{-0.06}	N	N	0.1	38.3	
119	330.3±20.9	53.4±9.9	168.9±15.1	222.3±17.6	108.0±11.7	196.2±16.6	125.9±12.6	-0.28 ^{+0.05} _{-0.06}	-0.43 ^{+0.10} _{-0.07}	0.22 ^{+0.06} _{-0.05}	N	N	0.4	38.8	
120	107.7±14.5	28.1±8.4	54.7±10.3	82.8±12.8	24.9±6.8	70.5±12.1	32.5±7.6	-0.43 ^{+0.10} _{-0.11}	-0.20 ^{+0.13} _{-0.17}	0.35 ^{+0.15} _{-0.11}	N	N	0.9	38.3	
121	≤5.3	-	-	-	-	-	-	-	-	-	-	-	-	0.0	≤37.0
122	≤10.8	-	-	-	-	-	-	-	-	-	-	-	-	1.2	≤37.3
123	≤253.6	-	-	-	-	-	-	-	-	-	-	-	-	6.8	≤38.7
124	39.7±8.6	13.7±5.7	23.5±6.6	37.2±8.2	2.6±3.4	31.7±7.7	6.2±4.1	-0.72 ^{+0.12} _{-0.14}	-0.18 ^{+0.22} _{-0.15}	0.89 ^{+0.54} _{-0.35}	N	N	0.1	37.9	
125	16.2±7.5	2.4±3.6	10.0±4.8	12.4±5.6	3.6±4.0	11.4±5.2	5.3±4.3	-0.47 ^{+0.30} _{-0.29}	-0.40 ^{+0.40} _{-0.65}	0.40 ^{+0.31} _{-0.37}	-	-	0.8	37.5	
126	≤16.1	-	-	-	-	-	-	-	-	-	-	-	-	1.4	≤37.5
127	24.6±8.1	7.8±4.9	12.9±5.8	20.7±7.1	3.9±4.2	19.9±6.8	3.8±4.4	-0.78 ^{+0.12} _{-0.22}	-0.11 ^{+0.30} _{-0.35}	0.46 ^{+0.56} _{-0.38}	-	-	1.8	37.6	
128	≤33.0	-	-	-	-	-	-	-	-	-	-	-	-	1.0	≤37.8
129	≤16.7	-	-	-	-	-	-	-	-	-	-	-	-	1.0	≤37.5
130	≤19.4	-	-	-	-	-	-	-	-	-	-	-	-	1.6	≤37.5
131	≤10.5	-	-	-	-	-	-	-	-	-	-	-	-	1.1	≤37.3
132	51.1±10.8	23.7±7.4	14.5±6.8	38.2±9.6	12.9±5.2	32.7±9.1	16.3±5.7	-0.39 ^{+0.13} _{-0.19}	0.24 ^{+0.30} _{-0.18}	0.06 ^{+0.29} _{-0.23}	N	N	0.4	38.0	
133	75.5±10.2	14.7±5.2	39.1±7.5	53.8±8.7	21.7±6.2	49.3±8.3	26.2±6.6	-0.37 ^{+0.10} _{-0.12}	-0.31 ^{+0.12} _{-0.16}	0.27 ^{+0.14} _{-0.11}	N	N	0.0	38.2	
134	≤15.8	-	-	-	-	-	-	-	-	-	-	-	-	1.8	≤37.5
135	≤27.1	-	-	-	-	-	-	-	-	-	-	-	-	0.2	≤37.7
136	9.7±6.6	0.9±3.2	9.7±4.7	10.6±5.2	-0.4±3.2	9.5±4.8	0.2±3.4	-0.89 ^{+0.13} _{-0.11}	-0.61 ^{+0.46} _{-0.77}	0.84 ^{+0.92} _{-0.46}	-	-	1.3	37.2	
137	25.5±9.5	12.0±6.2	11.7±6.6	23.7±8.6	1.8±3.9	25.6±8.4	2.1±4.3	-0.91 ^{+0.09} _{-0.09}	0.09 ^{+0.40} _{-0.37}	0.70 ^{+0.77} _{-0.61}	-	-	0.0	37.7	
138	≤34.2	-	-	-	-	-	-	-	-	-	-	-	-	1.9	≤37.8
139	≤13.4	-	-	-	-	-	-	-	-	-	-	-	-	1.9	≤37.4
140	80.6±10.8	25.6±6.6	43.3±8.0	69.0±9.9	11.6±5.1	54.6±8.9	19.7±6.1	-0.52 ^{+0.11} _{-0.10}	-0.11 ^{+0.09} _{-0.14}	0.58 ^{+0.19} _{-0.15}	N	N	2.1	38.2	
141	13.8±6.0	4.5±4.0	6.1±4.1	10.7±5.2	3.2±3.8	10.2±5.0	4.6±4.1	-0.49 ^{+0.29} _{-0.31}	-0.03 ^{+0.38} _{-0.43}	0.27 ^{+0.56} _{-0.46}	-	-	1.4	37.4	
142	14.6±5.8	3.4±3.4	4.9±3.8	8.3±4.6	6.3±4.3	8.6±4.4	5.8±4.3	-0.31 ^{+0.33} _{-0.31}	-0.03 ^{+0.41} _{-0.45}	-0.05 ^{+0.34} _{-0.38}	-	-	1.2	37.4	
143	28.4±7.1	-0.7±2.3	10.1±4.6	9.5±4.7	18.9±5.9	8.5±4.4	20.7±6.1	0.37 ^{+0.21} _{-0.19}	-0.90 ^{+0.46} _{-1.00}	-0.23 ^{+0.17} _{-0.19}	N	P	0.8	37.7	
144	5.9±5.0	5.6±4.0	2.2±3.4	7.8±4.7	-1.9±2.7	6.2±4.3	-0.4±3.2	-0.87 ^{+0.18} _{-0.13}	0.40 ^{+0.65} _{-0.48}	0.53 ^{+1.07} _{-0.84}	-	-	0.5	37.0	
145	≤23.9	-	-	-	-	-	-	-	-	-	-	-	-	0.1	≤37.6
146	165.6±14.5	40.6±7.9	93.4±11.0	134.0±13.1	31.6±6.9	118.5±12.4	44.3±7.9	-0.51 ^{+0.07} _{-0.07}	-0.27 ^{+0.08} _{-0.09}	0.50 ^{+0.10} _{-0.08}	N	N	3.6	38.5	
147	84.9±10.6	26.4±6.5	45.4±8.0	71.9±9.8	13.0±4.8	66.3±9.5	16.9±5.3	-0.63 ^{+0.07} _{-0.10}	-0.13 ^{+0.10} _{-0.12}	0.57 ^{+0.13} _{-0.15}	N	N	0.6	38.2	

TABLE 6 — *Continued*

Masterid	B-band	S1-band	S2-band	Net Counts	H-band	Sc-band	Hc-band	HR	C21	C32	BB	Variability	Log L_X			
(1)	(2)	(3)	(4)	S-band (5)	(6)	(7)	(8)	(9)	(10)	(11)	(12)	k-S signif. (14)	(0.3–8.0 keV) (15)			
148	62.3±9.7	15.9±5.5	30.3±6.9	46.2±8.3	16.2±5.6	38.7±7.7	21.5±6.2	-0.35 ^{+0.12} _{-0.14}	-0.17 ^{+0.13} _{-0.17}	0.32 ^{+0.12} _{-0.11}	N	N	0.2	38.0		
149	44.9±8.2	21.4±6.0	19.6±5.8	41.0±7.8	3.9±3.4	37.4±7.5	5.8±3.8	-0.76 ^{+0.09} _{-0.11}	0.11 ^{+0.18} _{-0.11}	0.63 ^{+0.35} _{-0.21}	N	N	5.1	37.9		
150	≤8.5	-	-	-	-	-	-	-	-	-	-	-	-	1.1	≤37.2	
151	4.2±4.6	-0.2±2.7	5.9±4.0	5.8±4.3	-1.6±2.7	6.4±4.1	-1.0±2.9	-0.91 ^{+0.13} _{-0.09}	-0.61 ^{+0.53} _{-0.92}	0.84 ^{+0.99} _{-0.53}	-	-	-	0.6	36.9	
152	≤3.5	-	-	-	-	-	-	-	-	-	-	-	-	-	0.5	≤36.8
153	≤22.5	-	-	-	-	-	-	-	-	-	-	-	-	-	1.3	≤37.6
154	67.1±9.5	15.1±5.2	31.8±6.9	46.9±8.2	20.2±5.7	41.6±7.8	22.1±5.9	-0.37 ^{+0.11} _{-0.13}	-0.22 ^{+0.14} _{-0.15}	0.22 ^{+0.14} _{-0.11}	N	N	0.5	38.1		
155	41.3±8.2	15.2±5.3	18.9±5.8	34.0±7.4	7.3±4.4	32.6±7.1	7.8±4.6	-0.66 ^{+0.13} _{-0.15}	-0.02 ^{+0.19} _{-0.13}	0.44 ^{+0.23} _{-0.25}	N	N	0.5	37.9		
156	50.5±9.0	11.6±5.0	34.1±7.2	45.7±8.3	4.8±4.1	36.9±7.6	11.3±5.1	-0.58 ^{+0.12} _{-0.14}	-0.37 ^{+0.16} _{-0.17}	0.80 ^{+0.41} _{-0.24}	N	N	5.0	38.0		
157	68.2±10.1	16.1±5.6	37.0±7.5	53.1±8.9	15.1±5.5	46.9±8.4	18.5±5.9	-0.49 ^{+0.11} _{-0.12}	-0.25 ^{+0.11} _{-0.18}	0.42 ^{+0.14} _{-0.16}	N	N	0.2	38.1		
158	235.4±21.2	41.2±7.8	159.7±13.9	200.9±15.6	35.0±7.3	175.2±14.6	54.1±8.7	-0.58 ^{+0.06} _{-0.05}	-0.50 ^{+0.07} _{-0.08}	0.69 ^{+0.09} _{-0.08}	N	P	1.6	38.6		
159	≤1.6	-	-	-	-	-	-	-	-	-	-	-	-	0.0	≤36.5	
160	13.4±6.1	3.6±3.8	6.9±4.4	10.6±5.3	2.9±3.8	6.9±4.7	4.4±4.1	-0.33 ^{+0.37} _{-0.43}	-0.16 ^{+0.43} _{-0.51}	0.32 ^{+0.62} _{-0.45}	-	-	-	0.0	37.4	
161	≤6.6	-	-	-	-	-	-	-	-	-	-	-	-	-	0.0	≤37.1
162	≤7.4	-	-	-	-	-	-	-	-	-	-	-	-	-	1.4	≤37.1
163	134.7±16.7	21.3±6.2	77.5±10.1	98.8±11.4	36.1±7.4	82.0±10.5	47.3±8.3	-0.33 ^{+0.07} _{-0.10}	-0.47 ^{+0.12} _{-0.11}	0.36 ^{+0.10} _{-0.08}	N	N	1.5	38.4		
164	11.3±5.5	3.2±3.4	5.5±4.0	8.7±4.7	2.6±3.6	9.0±4.6	2.0±3.6	-0.75 ^{+0.10} _{-0.25}	-0.11 ^{+0.40} _{-0.48}	0.27 ^{+0.64} _{-0.46}	-	-	-	1.2	37.3	
165	17.2±6.3	9.7±4.7	6.1±4.1	15.8±5.8	1.4±3.4	14.4±5.4	0.8±3.4	-0.92 ^{+0.10} _{-0.08}	0.27 ^{+0.29} _{-0.27}	0.46 ^{+0.80} _{-0.49}	-	-	-	0.2	37.5	
166	32.8±7.8	9.4±4.7	12.5±5.1	21.8±6.5	11.0±5.0	18.5±6.0	11.4±5.1	-0.30 ^{+0.19} _{-0.21}	0.01 ^{+0.19} _{-0.27}	0.06 ^{+0.24} _{-0.19}	N	N	0.7	37.8		
167	≤12.6	-	-	-	-	-	-	-	-	-	-	-	-	0.5	≤37.4	
168	≤5.7	-	-	-	-	-	-	-	-	-	-	-	-	0.7	≤37.0	
169	21.9±6.7	7.6±4.3	10.3±4.7	17.9±5.9	3.9±4.0	18.5±5.8	3.3±4.0	-0.80 ^{+0.11} _{-0.09}	-0.05 ^{+0.24} _{-0.24}	0.38 ^{+0.48} _{-0.33}	N	N	1.8	37.6		
170	23.1±6.8	6.4±4.1	11.4±4.8	17.8±5.9	5.3±4.1	17.3±5.7	4.8±4.1	-0.65 ^{+0.20} _{-0.21}	-0.13 ^{+0.24} _{-0.27}	0.32 ^{+0.32} _{-0.27}	N	N	1.2	37.6		
171	10.0±5.4	3.0±3.4	6.4±4.1	9.4±4.8	0.6±3.2	9.0±4.6	1.0±3.4	-0.85 ^{+0.15} _{-0.15}	-0.19 ^{+0.40} _{-0.51}	0.61 ^{+0.84} _{-0.53}	-	-	-	0.0	37.3	
172	≤5.8	-	-	-	-	-	-	-	-	-	-	-	-	-	0.0	≤37.0
173	≤4.5	-	-	-	-	-	-	-	-	-	-	-	-	-	0.5	≤36.9
174	14.7±7.6	4.2±3.8	9.5±4.7	13.7±5.6	0.5±3.2	11.2±5.1	1.9±3.6	-0.82 ^{+0.15} _{-0.18}	-0.24 ^{+0.35} _{-0.38}	0.76 ^{+0.84} _{-0.45}	-	-	-	1.8	37.4	
175	7.5±5.3	2.8±3.6	7.2±4.3	9.9±5.1	-2.5±2.3	9.9±4.8	-2.2±2.7	-0.97 ^{+0.06} _{-0.03}	-0.24 ^{+0.40} _{-0.59}	1.07 ^{+0.99} _{-0.54}	-	-	-	1.2	37.1	
176	5.0±4.8	-0.9±2.3	2.7±3.4	1.9±3.6	3.1±3.8	0.0±2.9	5.8±4.3	0.79 ^{+0.21} _{-0.25}	-0.53 ^{+0.76} _{-1.07}	-0.03 ^{+0.70} _{-0.67}	-	-	-	0.7	37.0	
177	5.3±3.8	2.5±2.9	1.4±2.7	4.0±3.4	1.4±2.7	3.2±3.2	1.3±2.7	-0.54 ^{+0.13} _{-0.46}	0.27 ^{+0.62} _{-0.54}	0.05 ^{+0.73} _{-0.72}	-	-	-	0.5	37.0	
178	≤2.1	-	-	-	-	-	-	-	-	-	-	-	-	-	0.0	≤36.6
179	21.8±8.4	5.7±4.1	10.6±4.8	16.3±5.9	5.8±4.1	14.7±5.6	5.2±4.1	-0.56 ^{+0.23} _{-0.24}	-0.16 ^{+0.27} _{-0.32}	0.27 ^{+0.32} _{-0.27}	N	N	1.4	37.6		
180	≤4.7	-	-	-	-	-	-	-	-	-	-	-	-	-	0.0	≤36.9
181	10.2±5.6	0.0±2.9	7.6±4.4	7.6±4.8	2.5±3.6	8.2±4.7	2.2±3.6	-0.70 ^{+0.19} _{-0.30}	-0.61 ^{+0.46} _{-0.92}	0.40 ^{+0.65} _{-0.43}	-	-	-	0.8	37.3	
182	16.6±7.6	1.3±3.4	12.0±5.1	13.3±5.7	3.4±3.8	11.2±5.2	4.8±4.1	-0.50 ^{+0.28} _{-0.30}	-0.61 ^{+0.38} _{-0.77}	0.51 ^{+0.51} _{-0.35}	-	-	-	0.9	37.5	
183	≤10.8	-	-	-	-	-	-	-	-	-	-	-	-	-	1.6	≤37.3
184	229.4±16.5	50.3±8.3	123.7±12.3	174.0±14.4	55.5±8.7	143.8±13.2	77.9±10.1	-0.36 ^{+0.07} _{-0.06}	-0.29 ^{+0.06} _{-0.09}	0.38 ^{+0.07} _{-0.07}	N	N	0.9	38.7		
185	152.0±16.1	29.8±6.8	90.4±10.7	120.2±12.3	31.6±7.0	107.0±11.6	46.9±8.2	-0.45 ^{+0.07} _{-0.07}	-0.39 ^{+0.10} _{-0.09}	0.49 ^{+0.09} _{-0.09}	N	N	0.4	38.5		
186	8.3±5.8	-0.1±2.7	7.1±4.3	7.0±4.6	1.1±3.4	9.2±4.7	0.7±3.4	-0.87 ^{+0.13} _{-0.13}	-0.69 ^{+0.54} _{-0.91}	0.54 ^{+0.83} _{-0.46}	-	-	-	1.5	37.2	
187	26.1±6.9	3.6±3.6	17.0±5.4	20.5±6.1	5.6±4.1	16.7±5.6	9.3±4.7	-0.36 ^{+0.21} _{-0.21}	-0.54 ^{+0.33} _{-0.40}	0.48 ^{+0.30} _{-0.24}	N	N	1.4	37.7		
188	≤6.7	-	-	-	-	-	-	-	-	-	-	-	-	-	0.0	≤37.1
189	32.2±8.2	8.8±4.6	18.3±5.7	27.1±6.8	5.6±4.1	24.7±6.5	5.2±4.1	-0.72 ^{+0.16} _{-0.16}	-0.21 ^{+0.18} _{-0.22}	0.51 ^{+0.29} _{-0.24}	N	N	0.2	37.8		
190	35.8±7.7	6.2±4.0	26.7±6.5	32.9±7.1	3.0±3.8	30.9±6.9	4.6±4.1	-0.81 ^{+0.11} _{-0.13}	-0.51 ^{+0.19} _{-0.24}	0.86 ^{+0.56} _{-0.32}	N	N	0.1	37.8		
191	21.6±6.6	6.4±4.1	10.4±4.7	16.8±5.8	4.8±4.0	13.0±5.2	6.5±4.3	-0.41 ^{+0.13} _{-0.26}	-0.11 ^{+0.24} _{-0.27}	0.32 ^{+0.38} _{-0.29}	N	N	0.7	37.6		
192	≤1.4	-	-	-	-	-	-	-	-	-	-	-	-	-	1.5	≤36.4
193	8.1±5.2	2.5±3.4	0.8±2.9	3.2±4.0	4.8±4.0	2.3±3.6	4.6±4.0	0.33 ^{+0.39} _{-0.28}	0.31 ^{+0.91} _{-0.77}	-0.46 ^{+0.61} _{-0.84}	-	-	-	0.7	37.2	
194	119.6±13.3	35.8±7.2	66.6±9.4	102.4±11.4	17.5±5.7	90.6±10.7	24.0±6.4	-0.63 ^{+0.07} _{-0.07}	-0.15 ^{+0.07} _{-0.12}	0.59 ^{+0.15} _{-0.10}	N	P	2.1	38.3		
195	28.9±7.2	6.0±4.0	12.9±5.0	18.9±5.9	10.0±4.8	15.4±5.3	12.6±5.2	-0.17 ^{+0.19} _{-0.22}	-0.21 ^{+0.21} _{-0.27}	0.13 ^{+0.23} _{-0.20}	N	N	1.0	37.7		
196	≤11.4	-	-	-	-	-	-	-	-	-	-	-	-	-	0.9	≤37.3

TABLE 6 — *Continued*

Masterid	B-band	S1-band	S2-band	Net Counts		H-band	Sc-band	Hc-band	HR	C21	C32	Variability			Log L_X
(1)	(2)	(3)	(4)	S-band	(5)	(6)	(7)	(8)	(9)	(10)	(11)	BB	k-S	signif.	(15)
197	13.2±5.7	1.9±3.2	9.5±4.6	11.4±5.1	1.8±3.4	6.6±4.3	6.3±4.3	-0.10 ^{+0.36} _{-0.37}	-0.48 ^{+0.40} _{-0.62}	0.59 ^{+0.70} _{-0.43}	-	-	0.3	37.4	
198	≤5.9	-	-	-	-	-	-	-	-	-	-	-	-	0.0	≤37.0
199	9.6±5.3	-0.2±2.7	8.0±4.3	7.9±4.6	1.7±3.4	7.9±4.4	2.4±3.6	-0.67 ^{+0.19} _{-0.33}	-0.76 ^{+0.45} _{-0.92}	0.54 ^{+0.72} _{-0.43}	-	-	1.3	37.3	
200	≤6.2	-	-	-	-	-	-	-	-	-	-	-	-	0.0	≤37.1
201	18.0±6.2	2.7±3.4	6.0±4.0	8.7±4.7	9.3±4.7	6.2±4.1	10.7±5.0	0.21 ^{+0.30} _{-0.30}	-0.19 ^{+0.40} _{-0.59}	-0.13 ^{+0.26} _{-0.30}	-	-	1.3	37.5	
202	27.1±6.9	4.0±3.4	18.0±5.6	22.0±6.1	5.0±4.1	17.9±5.6	7.5±4.6	-0.48 ^{+0.21} _{-0.21}	-0.54 ^{+0.37} _{-0.26}	0.54 ^{+0.35} _{-0.27}	N	N	1.1	37.7	
203	14.2±5.9	6.2±4.0	9.2±4.4	15.5±5.4	-1.2±3.2	14.6±5.2	-0.6±3.4	-0.96 ^{+0.08} _{-0.04}	-0.08 ^{+0.24} _{-0.27}	0.92 ^{+0.91} _{-0.54}	-	-	0.1	37.4	
204	≤1.7	-	-	-	-	-	-	-	-	-	-	-	-	17.4	≤36.5
205	12.8±5.7	1.2±2.9	8.9±4.4	10.1±4.8	2.7±3.8	10.4±4.7	3.1±4.0	-0.68 ^{+0.16} _{-0.14}	-0.61 ^{+0.46} _{-0.69}	0.43 ^{+0.64} _{-0.38}	-	-	1.0	37.4	
206	≤4.6	-	-	-	-	-	-	-	-	-	-	-	-	0.0	≤36.9
207	≤4.2	-	-	-	-	-	-	-	-	-	-	-	-	0.0	≤36.9
208	9.8±5.4	-0.5±2.3	9.6±4.6	9.0±4.7	0.8±3.4	10.1±4.7	0.2±3.4	-0.90 ^{+0.12} _{-0.10}	-0.90 ^{+0.53} _{-0.92}	0.70 ^{+0.83} _{-0.46}	-	-	0.9	37.2	
209	39.8±8.0	1.9±3.2	20.9±5.9	22.9±6.3	17.0±5.7	19.3±5.8	20.6±6.1	-0.04 ^{+0.16} _{-0.18}	-0.86 ^{+0.44} _{-0.53}	0.09 ^{+0.19} _{-0.11}	N	N	0.0	37.9	
210	11.6±5.5	1.5±2.9	8.0±4.3	9.5±4.7	2.1±3.6	8.6±4.4	2.7±3.8	-0.66 ^{+0.18} _{-0.24}	-0.48 ^{+0.33} _{-0.65}	0.46 ^{+0.67} _{-0.43}	-	-	0.0	37.3	
211	15.4±5.9	-1.8±1.9	10.8±4.7	9.0±4.7	6.4±4.3	8.9±4.6	7.0±4.4	-0.21 ^{+0.30} _{-0.31}	-1.30 ^{+0.61} _{-0.92}	0.24 ^{+0.30} _{-0.24}	-	-	0.0	37.4	
212	≤2.9	-	-	-	-	-	-	-	-	-	-	-	-	0.0	≤36.7
213	25.2±7.5	7.4±4.1	8.1±4.3	15.5±5.4	9.4±4.8	15.9±5.3	9.8±5.0	-0.31 ^{+0.22} _{-0.21}	0.05 ^{+0.24} _{-0.24}	-0.03 ^{+0.24} _{-0.24}	N	N	1.0	37.7	
214	≤11.6	-	-	-	-	-	-	-	-	-	-	-	-	1.6	≤37.3
215	≤11.5	-	-	-	-	-	-	-	-	-	-	-	-	1.4	≤37.3
216	25.3±6.8	2.6±3.2	15.3±5.2	18.0±5.7	7.3±4.4	16.7±5.4	8.1±4.6	-0.42 ^{+0.20} _{-0.22}	-0.59 ^{+0.30} _{-0.49}	0.32 ^{+0.27} _{-0.21}	N	N	0.0	37.7	
217	14.7±6.4	3.1±3.4	11.8±4.8	14.8±5.4	0.9±3.4	13.3±5.1	2.1±3.8	-0.83 ^{+0.14} _{-0.17}	-0.43 ^{+0.39} _{-0.46}	0.75 ^{+0.81} _{-0.43}	-	-	1.6	37.4	
218	≤4.8	-	-	-	-	-	-	-	-	-	-	-	-	0.0	≤36.9
219	6.8±4.9	-0.6±2.3	4.9±3.8	4.2±4.0	2.6±3.6	4.2±3.8	3.2±3.8	-0.26 ^{+0.37} _{-0.48}	-0.69 ^{+0.54} _{-0.99}	0.24 ^{+0.65} _{-0.48}	-	-	1.0	37.1	
220	102.5±11.5	31.7±6.8	52.0±8.4	83.6±10.4	18.9±5.8	72.6±9.7	25.4±6.5	-0.55 ^{+0.08} _{-0.09}	-0.10 ^{+0.11} _{-0.09}	0.48 ^{+0.13} _{-0.12}	N	N	2.8	38.3	
221	≤4.1	-	-	-	-	-	-	-	-	-	-	-	-	0.0	≤36.9
222	≤1.3	-	-	-	-	-	-	-	-	-	-	-	-	0.0	≤36.4
223	14.1±5.8	0.1±2.7	5.7±4.0	5.9±4.3	8.2±4.6	7.7±4.3	7.3±4.6	-0.12 ^{+0.34} _{-0.31}	-0.61 ^{+0.53} _{-0.92}	-0.11 ^{+0.30} _{-0.29}	-	-	1.0	37.4	
224	6.6±4.9	2.8±3.2	3.1±3.4	5.9±4.1	0.7±3.4	5.0±3.8	0.2±3.4	-0.78 ^{+0.22} _{-0.22}	0.03 ^{+0.56} _{-0.54}	0.27 ^{+0.94} _{-0.65}	-	-	1.7	37.1	
225	43.5±8.3	13.9±5.1	14.5±5.2	28.5±6.8	15.0±5.4	24.8±6.4	16.6±5.7	-0.26 ^{+0.15} _{-0.17}	0.12 ^{+0.14} _{-0.21}	0.00 ^{+0.20} _{-0.15}	N	N	0.1	37.9	
226	11.4±5.4	3.3±3.4	5.4±3.8	8.7±4.6	2.7±3.6	9.1±4.4	2.3±3.6	-0.73 ^{+0.17} _{-0.27}	-0.11 ^{+0.40} _{-0.43}	0.24 ^{+0.62} _{-0.43}	-	-	1.5	37.3	
227	97.4±11.7	13.4±5.0	49.5±8.3	62.9±9.2	33.6±7.1	54.8±8.7	42.0±7.8	-0.20 ^{+0.11} _{-0.10}	-0.46 ^{+0.12} _{-0.16}	0.20 ^{+0.11} _{-0.09}	N	Y	0.1	38.2	
228	43.3±8.6	7.9±4.3	25.3±6.4	33.3±7.2	10.7±4.8	31.4±7.0	12.2±5.1	-0.50 ^{+0.13} _{-0.17}	-0.40 ^{+0.19} _{-0.19}	0.39 ^{+0.19} _{-0.17}	N	N	0.2	37.9	
229	32.4±7.4	10.2±4.6	11.8±4.8	22.0±6.2	10.4±4.8	21.8±6.1	11.0±5.0	-0.39 ^{+0.17} _{-0.19}	0.03 ^{+0.18} _{-0.22}	0.08 ^{+0.21} _{-0.21}	N	N	0.3	37.8	
230	40.7±8.0	4.4±3.6	27.7±6.5	32.1±7.1	8.6±4.6	27.2±6.5	13.1±5.2	-0.41 ^{+0.16} _{-0.14}	-0.67 ^{+0.24} _{-0.37}	0.51 ^{+0.21} _{-0.16}	N	N	1.7	37.9	
231	30.8±7.9	6.5±4.0	18.1±5.6	24.6±6.4	5.8±4.1	20.8±5.9	7.2±4.4	-0.55 ^{+0.14} _{-0.19}	-0.35 ^{+0.22} _{-0.21}	0.48 ^{+0.30} _{-0.24}	N	N	0.3	37.7	
232	≤5.7	-	-	-	-	-	-	-	-	-	-	-	-	0.0	≤37.0
233	13.8±6.1	2.4±3.2	11.4±4.7	13.8±5.2	1.1±3.2	13.9±5.1	0.7±3.2	-0.93 ^{+0.10} _{-0.07}	-0.51 ^{+0.38} _{-0.48}	0.75 ^{+0.78} _{-0.43}	-	-	0.1	37.4	
234	≤12.9	-	-	-	-	-	-	-	-	-	-	-	-	1.5	≤37.4
235	6.6±4.8	2.2±3.2	3.3±3.4	5.5±4.1	1.0±3.2	2.4±3.4	1.7±3.4	-0.24 ^{+0.25} _{-0.76}	-0.05 ^{+0.56} _{-0.67}	0.29 ^{+0.89} _{-0.61}	-	-	0.2	37.1	
236	≤4.6	-	-	-	-	-	-	-	-	-	-	-	-	0.0	≤36.9

NOTE. — Col. (1): Master ID, cols. (2)–(8): net counts, in each of the 7 energy bands (see Table 2 for definitions of these bands), col. (9): hardness ratio, cols. (10) and (11) color values, errors are given as 1σ , cols. (12) and (13): short-term variability, where (BB) indicate Bayesian block analysis and (K-S) indicates the Kolmogorov-Smirnov test, in both columns symbols indicate - (N) non-variable in all observations, (V) variable in at least one observation, (P) possible variability in at least one observation, col. (14): the significance of the change in L_X between the previous observation and the current observation respectively (equation 2), col. (15): $\log L_X$ (0.3–8.0 keV). Upper limit values of net B and L_X are at the 68% confidence level.

TABLE 7
SOURCE COUNTS, HARDNESS RATIOS, COLOR-COLOR VALUES AND VARIABILITY:
OBSERVATION 3

Masterid (1)	B-band (2)	S1-band (3)	S2-band (4)	Net Counts			HR (9)	C21 (10)	C32 (11)	Variability			Log L_X (0.3–8.0 keV) (15)	
				S-band (5)	H-band (6)	Sc-band (7)				Hc-band (8)	BB (12)	k-S (13)		signif. (14)
1	22.5±6.2	0.1±2.3	11.1±4.6	11.2±4.7	11.3±4.7	8.3±4.1	14.8±5.2	0.14 ^{+0.22} _{-0.22}	-0.84 ^{+0.46} _{-0.92}	0.06 ^{+0.18} _{-0.19}	N	N	1.4	38.0
2	37.1±7.5	3.3±3.2	20.1±5.7	23.4±6.1	13.7±5.1	19.9±5.7	16.4±5.4	-0.24 ^{+0.16} _{-0.17}	-0.55 ^{+0.29} _{-0.29}	0.21 ^{+0.20} _{-0.12}	N	N	1.4	38.3
3	<1.4	-	-	-	-	-	-	-	-	-	-	-	0.0	<36.8
4	36.6±7.5	10.5±4.4	21.9±5.9	32.4±6.9	4.2±3.8	32.1±6.8	3.7±3.8	-0.87 ^{+0.07} _{-0.09}	-0.11 ^{+0.15} _{-0.17}	0.72 ^{+0.35} _{-0.26}	N	N	1.0	38.2
5	64.5±9.3	17.5±5.3	34.9±7.1	52.4±8.4	12.1±4.8	47.9±8.1	12.7±5.0	-0.66 ^{+0.09} _{-0.10}	-0.09 ^{+0.13} _{-0.13}	0.51 ^{+0.16} _{-0.15}	N	N	0.6	38.5
6	<2.1	-	-	-	-	-	-	-	-	-	-	-	0.0	<37.0
7	<1.3	-	-	-	-	-	-	-	-	-	-	-	0.0	<36.8
8	12.4±5.0	5.5±3.6	4.3±3.4	9.8±4.4	2.6±3.2	8.0±4.1	3.5±3.4	-0.49 ^{+0.27} _{-0.30}	0.21 ^{+0.33} _{-0.26}	0.21 ^{+0.49} _{-0.42}	-	-	0.2	37.7
9	<5.7	-	-	-	-	-	-	-	-	-	-	-	0.0	<37.4
10	<0.6	-	-	-	-	-	-	-	-	-	-	-	0.0	<36.4
11	9.1±4.6	-0.7±1.9	6.4±3.8	5.8±3.8	3.3±3.4	4.2±3.4	5.2±3.8	0.02 ^{+0.38} _{-0.37}	-1.07 ^{+0.61} _{-0.92}	0.27 ^{+0.43} _{-0.32}	-	-	0.8	37.6
12	<2.6	-	-	-	-	-	-	-	-	-	-	-	0.6	<37.0
13	151.0±13.4	43.0±7.7	74.5±9.7	117.5±11.9	33.4±7.0	104.0±11.3	43.2±7.8	-0.48 ^{+0.06} _{-0.08}	-0.11 ^{+0.07} _{-0.10}	0.37 ^{+0.11} _{-0.08}	N	N	1.1	38.8
14	28.1±6.6	10.3±4.4	12.1±4.7	22.4±6.0	5.7±3.8	17.9±5.4	8.6±4.3	-0.42 ^{+0.16} _{-0.19}	0.03 ^{+0.19} _{-0.19}	0.35 ^{+0.24} _{-0.24}	N	N	0.3	38.1
15	<10.1	-	-	-	-	-	-	-	-	-	-	-	0.8	<37.7
16	<7.2	-	-	-	-	-	-	-	-	-	-	-	1.0	<37.5
17	15.2±5.5	2.7±3.2	10.1±4.4	12.9±5.0	2.3±3.2	13.3±5.0	2.1±3.2	-0.82 ^{+0.12} _{-0.18}	-0.40 ^{+0.32} _{-0.43}	0.56 ^{+0.54} _{-0.35}	-	-	0.9	37.8
18	<0.9	-	-	-	-	-	-	-	-	-	-	-	0.4	<36.6
19	8.8±4.6	0.2±2.3	6.3±3.8	6.6±4.0	2.2±3.2	6.2±3.8	1.9±3.2	-0.66 ^{+0.19} _{-0.34}	-0.69 ^{+0.46} _{-0.91}	0.40 ^{+0.57} _{-0.40}	-	-	0.6	37.6
20	<7.3	-	-	-	-	-	-	-	-	-	-	-	0.2	<37.5
21	<1.9	-	-	-	-	-	-	-	-	-	-	-	1.5	<36.9
22	<2.3	-	-	-	-	-	-	-	-	-	-	-	1.1	<37.0
23	<9.3	-	-	-	-	-	-	-	-	-	-	-	0.3	<37.6
24	<9.2	-	-	-	-	-	-	-	-	-	-	-	0.5	<37.6
25	<2.9	-	-	-	-	-	-	-	-	-	-	-	0.0	<37.1
26	<0.8	-	-	-	-	-	-	-	-	-	-	-	2.3	<36.6
27	<2.0	-	-	-	-	-	-	-	-	-	-	-	1.1	<36.9
28	<7.4	-	-	-	-	-	-	-	-	-	-	-	1.0	<37.5
29	<14.7	-	-	-	-	-	-	-	-	-	-	-	0.1	<37.8
30	<4.0	-	-	-	-	-	-	-	-	-	-	-	0.0	<37.2
31	41.6±7.8	11.4±4.6	24.1±6.1	35.5±7.1	6.1±4.0	32.1±6.8	7.9±4.3	-0.65 ^{+0.12} _{-0.13}	-0.23 ^{+0.15} _{-0.16}	0.59 ^{+0.24} _{-0.19}	N	N	0.9	38.2
32	<2.6	-	-	-	-	-	-	-	-	-	-	-	2.7	<37.0
33	<4.5	-	-	-	-	-	-	-	-	-	-	-	0.0	<37.3
34	<1.1	-	-	-	-	-	-	-	-	-	-	-	0.0	<36.7
35	14.9±5.5	4.9±3.6	7.8±4.1	12.7±5.0	2.2±3.2	11.6±4.7	1.7±3.2	-0.83 ^{+0.12} _{-0.17}	-0.11 ^{+0.30} _{-0.29}	0.48 ^{+0.54} _{-0.40}	-	-	0.4	37.8
36	<8.3	-	-	-	-	-	-	-	-	-	-	-	0.5	<37.5
37	<7.9	-	-	-	-	-	-	-	-	-	-	-	0.1	<37.5
38	5.4±5.2	0.3±2.3	-0.2±2.3	0.1±2.7	4.8±3.8	-0.4±2.3	5.6±4.0	0.89 ^{+0.11} _{-0.15}	0.15 ^{+1.07} _{-1.07}	-0.69 ^{+0.54} _{-0.99}	-	-	0.6	37.3
39	18.2±5.4	5.8±3.6	8.8±4.1	14.6±5.0	3.6±3.2	11.7±4.6	6.6±3.8	-0.34 ^{+0.20} _{-0.22}	-0.08 ^{+0.21} _{-0.24}	0.38 ^{+0.29} _{-0.25}	N	N	1.2	37.9
40	21.8±4.3	4.2±3.4	13.1±4.8	17.3±5.4	4.5±3.6	14.7±5.1	6.3±4.0	-0.46 ^{+0.19} _{-0.22}	-0.38 ^{+0.25} _{-0.26}	0.46 ^{+0.32} _{-0.25}	N	N	1.9	37.9
41	66.7±9.5	14.8±5.1	30.8±6.7	45.7±8.0	21.0±5.9	39.1±7.5	26.9±6.5	-0.25 ^{+0.10} _{-0.14}	-0.21 ^{+0.15} _{-0.16}	0.20 ^{+0.13} _{-0.12}	N	N	0.2	38.4
42	44.0±8.0	9.8±4.4	28.0±6.5	37.8±7.4	6.2±4.0	33.7±7.0	9.9±4.6	-0.59 ^{+0.12} _{-0.13}	-0.35 ^{+0.14} _{-0.19}	0.64 ^{+0.25} _{-0.18}	N	N	0.3	38.3
43	17.7±5.7	6.1±3.8	8.0±4.1	14.2±5.1	3.6±3.4	14.0±5.0	4.3±3.6	-0.60 ^{+0.20} _{-0.22}	-0.03 ^{+0.24} _{-0.24}	0.35 ^{+0.35} _{-0.32}	-	-	0.2	37.9
44	<4.0	-	-	-	-	-	-	-	-	-	-	-	0.8	<37.2
45	<1.6	-	-	-	-	-	-	-	-	-	-	-	1.4	<36.8
46	<2.3	-	-	-	-	-	-	-	-	-	-	-	1.4	<37.0
47	<1.2	-	-	-	-	-	-	-	-	-	-	-	2.2	<36.7
48	<2.3	-	-	-	-	-	-	-	-	-	-	-	1.2	<37.0
49	<5.5	-	-	-	-	-	-	-	-	-	-	-	1.3	<37.4
50	13.2±5.1	5.2±3.6	4.4±3.4	9.6±4.4	3.6±3.4	7.0±4.0	6.5±4.0	-0.12 ^{+0.29} _{-0.30}	0.16 ^{+0.30} _{-0.32}	0.11 ^{+0.37} _{-0.38}	-	-	0.3	37.7

TABLE 7 — *Continued*

Masterid	B-band	S1-band	S2-band	Net Counts		Sc-band	Hc-band	HR	C21	C32	Variability			Log L_X
(1)	(2)	(3)	(4)	S-band	H-band	(7)	(8)	(9)	(10)	(11)	BB	k-S	signif.	(0.3–8.0 keV)
				(5)	(6)						(12)	(13)	(14)	(15)
51	<5.6	-	-	-	-	-	-	-	-	-	-	-	2.2	<37.4
52	<0.5	-	-	-	-	-	-	-	-	-	-	-	1.3	<36.3
53	<10.0	-	-	-	-	-	-	-	-	-	-	-	0.1	<37.6
54	10.2±5.1	4.1±3.6	4.5±3.6	8.6±4.6	1.6±3.2	6.8±4.1	2.3±3.4	-0.62 ^{+0.19} _{-0.19}	0.05 ^{+0.38} _{-0.43}	0.35 ^{+0.72} _{-0.51}	-	-	0.4	37.6
55	<1.1	-	-	-	-	-	-	-	-	-	-	-	1.7	<36.7
56	14.4±5.7	0.0±2.7	9.0±4.4	9.0±4.7	5.4±4.0	5.1±4.0	9.3±4.6	0.25 ^{+0.32} _{-0.34}	-0.76 ^{+0.45} _{-0.92}	0.24 ^{+0.30} _{-0.29}	-	-	0.8	37.8
57	<10.5	-	-	-	-	-	-	-	-	-	-	-	0.1	<37.6
58	<7.5	-	-	-	-	-	-	-	-	-	-	-	0.7	<37.5
59	<3.7	-	-	-	-	-	-	-	-	-	-	-	0.0	<37.2
60	<10.8	-	-	-	-	-	-	-	-	-	-	-	0.8	<37.6
61	<0.6	-	-	-	-	-	-	-	-	-	-	-	1.6	<36.4
62	<2.8	-	-	-	-	-	-	-	-	-	-	-	0.0	<37.1
63	9.0±4.7	2.6±3.2	4.7±3.6	7.3±4.3	1.6±2.9	6.0±4.0	1.5±2.9	-0.70 ^{+0.20} _{-0.30}	-0.13 ^{+0.42} _{-0.51}	0.38 ^{+0.64} _{-0.49}	-	-	1.3	37.6
64	<6.0	-	-	-	-	-	-	-	-	-	-	-	0.1	<37.4
65	<15.8	-	-	-	-	-	-	-	-	-	-	-	0.4	<37.8
66	27.0±6.8	3.7±3.6	14.4±5.1	18.1±5.8	8.9±4.4	12.4±5.0	14.8±5.2	0.02 ^{+0.21} _{-0.21}	-0.46 ^{+0.30} _{-0.40}	0.24 ^{+0.19} _{-0.21}	N	P	1.6	38.0
67	13.5±5.4	-0.1±2.3	14.6±5.1	14.5±5.2	-1.0±2.3	14.3±5.1	-0.3±2.7	-0.97 ^{+0.05} _{-0.03}	-1.07 ^{+0.46} _{-0.92}	1.30 ^{+0.92} _{-0.54}	-	-	0.0	37.7
68	20.8±6.2	2.7±3.2	9.7±4.4	12.4±5.0	8.4±4.4	10.2±4.6	9.0±4.6	-0.14 ^{+0.26} _{-0.25}	-0.40 ^{+0.33} _{-0.43}	0.08 ^{+0.24} _{-0.21}	N	N	0.3	37.9
69	<9.3	-	-	-	-	-	-	-	-	-	-	-	1.4	<37.6
70	<3.9	-	-	-	-	-	-	-	-	-	-	-	0.9	<37.2
71	<10.1	-	-	-	-	-	-	-	-	-	-	-	1.0	<37.6
72	24.4±6.4	8.1±4.1	8.6±4.3	16.8±5.4	7.6±4.1	13.4±5.0	8.3±4.3	-0.30 ^{+0.21} _{-0.22}	0.05 ^{+0.22} _{-0.21}	0.08 ^{+0.24} _{-0.24}	N	N	0.2	38.0
73	16.5±6.3	5.3±3.8	7.2±4.1	12.4±5.1	4.2±3.6	11.3±4.8	4.2±3.6	-0.53 ^{+0.24} _{-0.26}	-0.03 ^{+0.27} _{-0.29}	0.24 ^{+0.35} _{-0.32}	-	-	0.0	37.8
74	12.9±5.7	4.6±3.6	7.0±4.0	11.5±4.8	1.1±2.9	7.3±4.1	3.1±3.4	-0.51 ^{+0.28} _{-0.32}	-0.08 ^{+0.23} _{-0.32}	0.59 ^{+0.75} _{-0.46}	-	-	1.5	37.7
75	<0.8	-	-	-	-	-	-	-	-	-	-	-	2.7	<36.6
76	24.3±6.6	6.7±4.1	15.4±5.2	22.1±6.2	2.2±3.2	18.1±5.7	5.0±3.8	-0.63 ^{+0.17} _{-0.19}	-0.27 ^{+0.22} _{-0.24}	0.75 ^{+0.56} _{-0.35}	N	N	1.7	38.0
77	<2.0	-	-	-	-	-	-	-	-	-	-	-	0.0	<36.9
78	26.7±6.7	6.2±3.8	13.8±5.0	19.9±5.8	6.8±4.1	17.6±5.4	8.5±4.4	-0.41 ^{+0.19} _{-0.20}	-0.24 ^{+0.21} _{-0.22}	0.32 ^{+0.24} _{-0.21}	N	N	0.3	38.0
79	<0.9	-	-	-	-	-	-	-	-	-	-	-	2.7	<36.5
80	<7.9	-	-	-	-	-	-	-	-	-	-	-	0.7	<37.5
81	7.6±5.0	4.3±3.8	2.9±3.4	7.2±4.6	0.5±2.7	4.0±4.0	1.5±3.0	-0.51 ^{+0.27} _{-0.49}	0.21 ^{+0.62} _{-0.53}	0.38 ^{+1.00} _{-0.69}	-	-	0.3	37.5
82	<4.6	-	-	-	-	-	-	-	-	-	-	-	0.4	<37.3
83	<2.3	-	-	-	-	-	-	-	-	-	-	-	0.0	<37.0
84	27.3±6.5	5.4±3.6	12.2±4.7	17.6±5.4	9.7±4.3	12.8±4.8	13.7±4.8	-0.03 ^{+0.19} _{-0.20}	-0.24 ^{+0.21} _{-0.24}	0.13 ^{+0.19} _{-0.18}	N	N	0.5	38.0
85	15.6±5.2	4.4±3.4	9.4±4.3	13.9±5.0	1.8±2.7	10.1±4.4	2.7±2.9	-0.62 ^{+0.18} _{-0.24}	-0.21 ^{+0.24} _{-0.27}	0.67 ^{+0.43} _{-0.32}	N	N	0.1	37.8
86	<5.7	-	-	-	-	-	-	-	-	-	-	-	0.5	<37.4
87	<8.4	-	-	-	-	-	-	-	-	-	-	-	0.7	<37.5
88	<8.1	-	-	-	-	-	-	-	-	-	-	-	1.7	<37.5
89	<1.1	-	-	-	-	-	-	-	-	-	-	-	0.0	<36.7
90	<7.1	-	-	-	-	-	-	-	-	-	-	-	0.5	<37.5
91	<0.9	-	-	-	-	-	-	-	-	-	-	-	0.0	<36.6
92	<1.0	-	-	-	-	-	-	-	-	-	-	-	0.0	<36.6
93	<5.2	-	-	-	-	-	-	-	-	-	-	-	0.5	<37.3
94	<2.9	-	-	-	-	-	-	-	-	-	-	-	2.2	<37.1
95	<3.8	-	-	-	-	-	-	-	-	-	-	-	0.0	<37.2
96	79.2±10.3	10.9±4.7	56.2±8.7	67.1±9.5	12.1±4.8	60.2±9.0	16.7±5.4	-0.61 ^{+0.09} _{-0.10}	-0.61 ^{+0.14} _{-0.17}	0.68 ^{+0.15} _{-0.14}	N	N	1.6	38.5
97	<3.2	-	-	-	-	-	-	-	-	-	-	-	0.9	<37.1
98	37.8±7.5	9.5±4.4	20.6±5.8	30.1±6.8	7.7±4.0	29.1±6.6	9.5±4.3	-0.55 ^{+0.12} _{-0.14}	-0.24 ^{+0.16} _{-0.19}	0.46 ^{+0.16} _{-0.19}	N	N	0.6	38.2
99	33.5±8.7	7.6±5.4	18.6±6.1	26.1±7.7	7.4±4.5	17.7±6.7	10.4±5.0	-0.32 ^{+0.22} _{-0.26}	-0.32 ^{+0.36} _{-0.32}	0.37 ^{+0.30} _{-0.20}	N	N	1.5	38.1
100	5.5±5.1	-0.5±2.7	3.5±3.8	3.0±4.2	2.5±3.4	2.2±3.8	2.7±3.6	0.03 ^{+0.34} _{-0.52}	-0.46 ^{+0.69} _{-1.07}	0.13 ^{+0.76} _{-0.67}	-	-	1.1	37.3
101	<23.8	-	-	-	-	-	-	-	-	-	-	-	0.6	<38.0
102	<13.5	-	-	-	-	-	-	-	-	-	-	-	1.3	<37.7

TABLE 7 — *Continued*

Masterid	B-band	S1-band	S2-band	Net Counts		H-band	Sc-band	Hc-band	HR	C21	C32	BB	Variability	Log L_x	
(1)	(2)	(3)	(4)	S-band	(5)	(6)	(7)	(8)	(9)	(10)	(11)	(12)	k-S	signif.	(15)
													(13)	(14)	
103	24.5±6.4	1.0±2.7	15.0±5.1	15.9±5.3	8.6±4.3	14.4±5.1	9.5±4.4	-0.27 ^{+0.19} _{-0.21}	-0.84 ^{+0.38} _{-0.69}	0.27 ^{+0.19} _{-0.19}	N	N	1.5	38.0	
104	≤24.3	-	-	-	-	-	-	-	-	-	-	-	-	1.4	≤38.0
105	≤7.5	-	-	-	-	-	-	-	-	-	-	-	-	1.8	≤37.5
106	≤15.8	-	-	-	-	-	-	-	-	-	-	-	-	0.9	≤37.8
107	≤4.3	-	-	-	-	-	-	-	-	-	-	-	-	0.1	≤37.5
108	26.9±6.7	4.8±3.6	16.2±5.2	21.0±5.9	5.9±4.0	18.6±5.6	6.6±4.1	-0.53 ^{+0.18} _{-0.20}	-0.40 ^{+0.21} _{-0.27}	0.43 ^{+0.27} _{-0.22}	N	N	2.3	38.0	
109	≤5.7	-	-	-	-	-	-	-	-	-	-	-	-	1.9	≤37.4
110	≤2.6	-	-	-	-	-	-	-	-	-	-	-	-	2.1	≤37.0
111	≤1.5	-	-	-	-	-	-	-	-	-	-	-	-	1.5	≤36.8
112	≤2.7	-	-	-	-	-	-	-	-	-	-	-	-	0.0	≤37.0
113	≤2.1	-	-	-	-	-	-	-	-	-	-	-	-	0.0	≤36.9
114	≤21.1	-	-	-	-	-	-	-	-	-	-	-	-	1.2	≤37.9
115	≤6.5	-	-	-	-	-	-	-	-	-	-	-	-	1.2	≤37.4
116	≤13.1	-	-	-	-	-	-	-	-	-	-	-	-	0.0	≤37.7
117	7623.0±88.7	2499.0±51.3	4013.0±64.6	6512.0±82.1	1111.0±34.5	5499.4±75.5	1643.6±41.7	-0.59 ^{+0.01} _{-0.00}	-0.12 ^{+0.01} _{-0.01}	0.59 ^{+0.01} _{-0.02}	N	N	37.7	40.5	
118	44.7±9.5	7.2±4.6	23.5±6.3	30.7±7.4	13.3±5.0	26.0±6.9	16.0±5.4	-0.30 ^{+0.15} _{-0.17}	-0.41 ^{+0.23} _{-0.30}	0.29 ^{+0.15} _{-0.18}	N	N	0.0	38.3	
119	143.4±16.5	27.3±8.0	78.8±11.2	106.1±13.3	37.2±7.6	86.2±12.3	56.8±9.1	-0.27 ^{+0.08} _{-0.10}	-0.40 ^{+0.15} _{-0.10}	0.35 ^{+0.10} _{-0.09}	N	N	0.2	38.8	
120	42.1±9.8	3.0±5.1	33.8±8.1	36.9±9.1	5.2±4.1	21.7±7.9	14.3±5.5	-0.26 ^{+0.20} _{-0.22}	-0.92 ^{+0.48} _{-0.63}	0.79 ^{+0.33} _{-0.27}	N	N	0.5	38.2	
121	≤2.5	-	-	-	-	-	-	-	-	-	-	-	-	0.0	≤37.0
122	≤1.8	-	-	-	-	-	-	-	-	-	-	-	-	1.0	≤36.9
123	≤18.7	-	-	-	-	-	-	-	-	-	-	-	-	9.3	≤37.9
124	18.6±6.4	5.4±4.1	13.5±5.3	18.9±6.3	-0.3±2.3	17.9±6.1	-0.7±2.3	-0.99 ^{+0.03} _{-0.01}	-0.27 ^{+0.27} _{-0.35}	1.22 ^{+0.92} _{-0.46}	-	-	0.1	37.9	
125	4.8±4.3	-1.2±2.3	2.1±3.2	0.9±3.4	3.9±3.4	-0.2±2.9	4.8±3.6	0.79 ^{+0.21} _{-0.23}	-0.46 ^{+0.84} _{-1.07}	-0.16 ^{+0.48} _{-0.64}	-	-	0.4	37.3	
126	≤8.2	-	-	-	-	-	-	-	-	-	-	-	-	0.2	≤37.5
127	≤11.4	-	-	-	-	-	-	-	-	-	-	-	-	0.6	≤37.7
128	≤21.8	-	-	-	-	-	-	-	-	-	-	-	-	0.8	≤37.9
129	≤5.2	-	-	-	-	-	-	-	-	-	-	-	-	0.9	≤37.3
130	13.8±5.6	4.5±3.8	4.1±3.6	8.5±4.7	5.3±3.8	6.7±4.3	4.8±3.8	-0.24 ^{+0.35} _{-0.38}	0.13 ^{+0.43} _{-0.45}	-0.05 ^{+0.34} _{-0.43}	-	-	1.4	37.8	
131	≤9.8	-	-	-	-	-	-	-	-	-	-	-	-	1.3	≤37.6
132	≤9.0	-	-	-	-	-	-	-	-	-	-	-	-	2.2	≤37.6
133	37.0±7.5	3.8±3.4	24.9±6.2	28.7±6.6	8.3±4.3	24.5±6.2	11.9±4.8	-0.40 ^{+0.15} _{-0.16}	-0.67 ^{+0.24} _{-0.32}	0.48 ^{+0.19} _{-0.19}	N	N	0.3	38.2	
134	≤12.6	-	-	-	-	-	-	-	-	-	-	-	-	0.9	≤37.7
135	≤22.4	-	-	-	-	-	-	-	-	-	-	-	-	1.5	≤38.0
136	≤2.9	-	-	-	-	-	-	-	-	-	-	-	-	1.0	≤37.1
137	≤8.0	-	-	-	-	-	-	-	-	-	-	-	-	1.2	≤37.5
138	≤10.0	-	-	-	-	-	-	-	-	-	-	-	-	1.4	≤37.6
139	≤4.3	-	-	-	-	-	-	-	-	-	-	-	-	0.9	≤37.2
140	18.1±6.1	1.5±3.2	13.5±5.1	15.1±5.6	3.1±3.4	13.1±5.2	3.5±3.6	-0.67 ^{+0.19} _{-0.23}	-0.67 ^{+0.40} _{-0.70}	0.59 ^{+0.46} _{-0.30}	-	-	2.3	37.9	
141	9.0±4.9	2.2±3.2	7.6±4.1	9.9±4.7	-0.9±2.3	9.8±4.6	-0.3±2.7	-0.95 ^{+0.08} _{-0.05}	-0.35 ^{+0.38} _{-0.56}	1.07 ^{+0.92} _{-0.54}	-	-	0.6	37.6	
142	≤3.7	-	-	-	-	-	-	-	-	-	-	-	-	1.0	≤37.4
143	8.3±4.4	0.3±2.3	4.1±3.4	4.4±3.6	3.9±3.4	1.9±2.9	5.8±3.8	0.53 ^{+0.33} _{-0.21}	-0.53 ^{+0.53} _{-0.85}	0.05 ^{+0.38} _{-0.37}	-	-	0.6	37.6	
144	≤8.1	-	-	-	-	-	-	-	-	-	-	-	-	0.6	≤37.5
145	≤5.2	-	-	-	-	-	-	-	-	-	-	-	-	1.2	≤37.3
146	126.6±15.5	20.1±6.8	83.6±10.8	103.7±12.3	23.2±6.4	90.7±11.5	37.3±7.7	-0.47 ^{+0.09} _{-0.08}	-0.55 ^{+0.15} _{-0.12}	0.57 ^{+0.13} _{-0.10}	N	P	3.1	38.7	
147	≤53.5	-	-	-	-	-	-	-	-	-	-	-	-	0.9	≤38.3
148	39.4±8.0	6.3±4.1	21.3±6.0	27.6±6.8	11.9±4.8	25.1±6.5	14.3±5.2	-0.34 ^{+0.16} _{-0.16}	-0.40 ^{+0.21} _{-0.27}	0.28 ^{+0.16} _{-0.17}	N	N	1.3	38.2	
149	≤15.6	-	-	-	-	-	-	-	-	-	-	-	-	1.5	≤37.8
150	≤6.0	-	-	-	-	-	-	-	-	-	-	-	-	0.7	≤37.4
151	≤2.8	-	-	-	-	-	-	-	-	-	-	-	-	0.5	≤37.1
152	≤1.8	-	-	-	-	-	-	-	-	-	-	-	-	0.4	≤36.9
153	≤1.9	-	-	-	-	-	-	-	-	-	-	-	-	2.1	≤36.9
154	24.4±8.4	1.7±3.7	14.2±5.4	15.9±6.0	8.7±4.8	12.5±5.4	13.7±5.5	-0.02 ^{+0.25} _{-0.23}	-0.61 ^{+0.38} _{-0.77}	0.21 ^{+0.27} _{-0.21}	N	N	0.6	38.0	

TABLE 7 — *Continued*

Masterid	B-band	S1-band	S2-band	Net Counts	H-band	Sc-band	Hc-band	HR	C21	C32	BB	Variability	Log L_x		
(1)	(2)	(3)	(4)	S-band (5)	(6)	(7)	(8)	(9)	(10)	(11)	(12)	k-S (13)	signif. (14)	(0.3–8.0 keV) (15)	
155	11.6±5.1	2.8±3.2	5.4±3.8	8.2±4.4	3.4±3.4	4.0±3.6	5.0±3.8	0.07 ^{+0.41} _{-0.45}	-0.16 ^{+0.40} _{-0.43}	0.21 ^{+0.43} _{-0.40}	-	-	1.1	37.7	
156	≤4.4	-	-	-	-	-	-	-	-	-	-	-	-	3.8	≤37.3
157	15.7±6.3	1.2±3.2	9.7±4.7	10.9±5.2	4.5±3.8	11.3±5.1	3.8±3.8	-0.60 ^{+0.22} _{-0.27}	-0.53 ^{+0.38} _{-0.85}	0.32 ^{+0.38} _{-0.29}	-	-	1.9	37.8	
158	104.6±14.5	25.0±6.3	48.2±8.2	73.2±9.9	31.6±6.9	63.2±9.2	35.9±7.3	-0.34 ^{+0.10} _{-0.09}	-0.17 ^{+0.09} _{-0.13}	0.21 ^{+0.11} _{-0.10}	N	N	0.0	38.6	
159	≤3.7	-	-	-	-	-	-	-	-	-	-	-	-	1.0	≤37.2
160	≤8.4	-	-	-	-	-	-	-	-	-	-	-	-	0.2	≤37.6
161	≤3.1	-	-	-	-	-	-	-	-	-	-	-	-	0.0	≤37.1
162	14.8±5.9	9.7±4.6	5.0±3.8	14.7±5.5	0.1±3.0	10.3±4.9	1.0±3.2	-0.87 ^{+0.13} _{-0.13}	0.35 ^{+0.32} _{-0.27}	0.61 ^{+0.92} _{-0.53}	-	-	2.2	37.8	
163	75.2±12.6	14.1±5.1	46.2±8.1	60.3±9.1	13.9±5.1	56.3±8.8	18.4±5.7	-0.56 ^{+0.10} _{-0.10}	-0.42 ^{+0.15} _{-0.13}	0.54 ^{+0.15} _{-0.13}	N	N	1.0	38.5	
164	≤10.7	-	-	-	-	-	-	-	-	-	-	-	-	0.4	≤37.6
165	≤7.9	-	-	-	-	-	-	-	-	-	-	-	-	0.7	≤37.5
166	8.8±5.3	1.1±2.9	8.4±4.4	9.5±4.8	-0.5±2.7	9.6±4.7	-1.3±2.7	-0.96 ^{+0.07} _{-0.04}	-0.53 ^{+0.45} _{-0.77}	0.92 ^{+0.91} _{-0.54}	-	-	0.9	37.6	
167	1.1±3.8	1.0±2.7	-0.1±2.7	0.9±3.2	0.2±2.9	1.7±3.2	-0.2±2.9	-0.49 ^{+0.27} _{-0.51}	0.23 ^{+1.07} _{-0.92}	-0.08 ^{+1.07} _{-1.07}	-	-	0.7	36.7	
168	≤9.1	-	-	-	-	-	-	-	-	-	-	-	-	1.4	≤37.6
169	≤12.9	-	-	-	-	-	-	-	-	-	-	-	-	0.2	≤37.7
170	7.2±4.7	-0.5±2.3	4.6±3.8	4.2±4.0	3.0±3.4	5.3±4.0	2.6±3.4	-0.45 ^{+0.23} _{-0.40}	-0.69 ^{+0.61} _{-0.99}	0.19 ^{+0.51} _{-0.48}	-	-	0.6	37.5	
171	7.2±4.6	0.8±2.7	7.4±4.1	8.2±4.4	-1.0±2.3	7.2±4.1	-0.2±2.7	-0.92 ^{+0.11} _{-0.08}	-0.61 ^{+0.46} _{-0.77}	0.99 ^{+1.00} _{-0.46}	-	-	0.5	37.5	
172	≤8.7	-	-	-	-	-	-	-	-	-	-	-	-	1.2	≤37.5
173	≤0.5	-	-	-	-	-	-	-	-	-	-	-	-	0.9	≤36.3
174	≤3.3	-	-	-	-	-	-	-	-	-	-	-	-	1.4	≤37.1
175	≤4.1	-	-	-	-	-	-	-	-	-	-	-	-	0.7	≤37.2
176	≤2.3	-	-	-	-	-	-	-	-	-	-	-	-	0.7	≤37.0
177	≤11.9	-	-	-	-	-	-	-	-	-	-	-	-	1.5	≤37.7
178	≤3.0	-	-	-	-	-	-	-	-	-	-	-	-	0.0	≤37.1
179	≤5.7	-	-	-	-	-	-	-	-	-	-	-	-	1.4	≤37.4
180	≤1.6	-	-	-	-	-	-	-	-	-	-	-	-	0.0	≤36.8
181	≤3.1	-	-	-	-	-	-	-	-	-	-	-	-	1.1	≤37.1
182	≤8.0	-	-	-	-	-	-	-	-	-	-	-	-	0.5	≤37.5
183	6.2±4.3	0.8±2.7	0.0±2.3	0.8±2.9	5.4±3.8	0.4±2.7	5.2±3.8	0.78 ^{+0.22} _{-0.21}	0.31 ^{+1.07} _{-1.00}	-0.76 ^{+0.53} _{-0.92}	-	-	0.7	37.4	
184	108.4±11.7	24.0±6.1	52.2±8.4	76.2±9.9	32.2±6.9	67.0±9.4	39.0±7.5	-0.32 ^{+0.08} _{-0.10}	-0.21 ^{+0.07} _{-0.15}	0.23 ^{+0.11} _{-0.09}	N	N	0.2	38.6	
185	37.2±7.6	1.8±2.9	29.6±6.6	31.3±6.9	5.8±4.0	26.8±6.5	9.5±4.6	-0.53 ^{+0.14} _{-0.16}	-0.99 ^{+0.35} _{-0.57}	0.70 ^{+0.24} _{-0.22}	N	N	3.2	38.2	
186	4.9±4.3	0.9±2.7	1.8±3.2	2.7±3.6	2.2±3.2	3.6±3.6	1.7±3.2	-0.45 ^{+0.27} _{-0.55}	-0.08 ^{+0.84} _{-0.91}	-0.03 ^{+0.75} _{-0.80}	-	-	0.3	37.3	
187	16.2±5.8	4.5±3.6	8.8±4.4	13.3±5.2	2.9±3.4	13.3±5.1	2.5±3.4	-0.78 ^{+0.12} _{-0.11}	-0.16 ^{+0.27} _{-0.32}	0.43 ^{+0.51} _{-0.35}	-	-	0.8	37.8	
188	≤1.4	-	-	-	-	-	-	-	-	-	-	-	-	0.0	≤36.8
189	21.4±6.7	3.7±3.4	11.6±4.7	15.4±5.3	6.8±4.1	9.2±4.4	11.4±4.8	0.04 ^{+0.24} _{-0.24}	-0.38 ^{+0.30} _{-0.32}	0.24 ^{+0.27} _{-0.21}	-	-	0.8	37.9	
190	17.0±5.8	3.1±3.2	9.0±4.4	12.1±5.0	4.9±3.8	10.7±4.7	5.5±4.0	-0.40 ^{+0.26} _{-0.27}	-0.32 ^{+0.29} _{-0.38}	0.27 ^{+0.32} _{-0.37}	-	-	0.2	37.8	
191	16.2±5.7	5.0±3.6	6.3±4.0	11.3±4.8	4.9±3.8	10.0±4.6	4.5±3.8	-0.46 ^{+0.27} _{-0.29}	0.00 ^{+0.38} _{-0.29}	0.13 ^{+0.37} _{-0.32}	-	-	0.9	37.8	
192	≤0.8	-	-	-	-	-	-	-	-	-	-	-	-	0.0	≤36.5
193	≤9.3	-	-	-	-	-	-	-	-	-	-	-	-	0.5	≤37.6
194	78.8±10.9	9.6±4.4	44.9±7.8	54.5±8.6	24.0±6.2	54.4±8.5	24.6±6.3	-0.44 ^{+0.10} _{-0.10}	-0.58 ^{+0.17} _{-0.16}	0.30 ^{+0.13} _{-0.10}	N	N	1.8	38.5	
195	7.7±4.6	2.0±2.9	5.6±3.8	7.6±4.3	0.0±2.7	7.1±4.1	1.0±2.9	-0.83 ^{+0.16} _{-0.17}	-0.29 ^{+0.42} _{-0.51}	0.69 ^{+0.91} _{-0.46}	-	-	0.9	37.5	
196	≤0.5	-	-	-	-	-	-	-	-	-	-	-	-	1.8	≤-inf
197	≤1.7	-	-	-	-	-	-	-	-	-	-	-	-	1.9	≤36.8
198	≤2.7	-	-	-	-	-	-	-	-	-	-	-	-	0.0	≤37.1
199	≤2.0	-	-	-	-	-	-	-	-	-	-	-	-	1.4	≤36.9
200	≤7.2	-	-	-	-	-	-	-	-	-	-	-	-	1.0	≤37.5
201	≤1.3	-	-	-	-	-	-	-	-	-	-	-	-	2.7	≤36.7
202	4.9±4.2	1.5±2.9	0.8±2.7	2.3±3.4	2.5±3.2	3.0±3.4	2.4±3.2	-0.19 ^{+0.39} _{-0.57}	0.23 ^{+0.92} _{-0.84}	-0.23 ^{+0.69} _{-0.92}	-	-	1.4	37.3	
203	≤4.0	-	-	-	-	-	-	-	-	-	-	-	-	1.3	≤37.2
204	≤1.6	-	-	-	-	-	-	-	-	-	-	-	-	0.0	≤36.8
205	3.8±4.0	-0.4±2.3	3.8±3.4	3.5±3.6	0.4±2.7	4.6±3.6	0.1±2.7	-0.85 ^{+0.18} _{-0.15}	-0.61 ^{+0.61} _{-0.92}	0.53 ^{+0.92} _{-0.53}	-	-	0.4	37.2	

TABLE 7 — *Continued*

Masterid	B-band	S1-band	S2-band	Net Counts			Hc-band	HR	C21	C32	Variability			Log L_X
(1)	(2)	(3)	(4)	S-band	H-band	Sc-band	(8)	(9)	(10)	(11)	BB	k-S	signif.	(0.3–8.0 keV)
				(5)	(6)	(7)					(12)	(13)	(14)	(15)
206	<3.7	-	-	-	-	-	-	-	-	-	-	-	0.0	<37.2
207	<2.9	-	-	-	-	-	-	-	-	-	-	-	0.0	<37.1
208	<7.8	-	-	-	-	-	-	-	-	-	-	-	0.1	<37.5
209	15.5±5.5	0.9±2.7	7.0±4.0	7.9±4.3	7.6±4.1	8.6±4.3	7.2±4.1	-0.16 ^{+0.26} _{-0.27}	-0.53 ^{+0.38} _{-0.77}	0.00 ^{+0.24} _{-0.24}	-	-	0.5	37.8
210	<4.6	-	-	-	-	-	-	-	-	-	-	-	0.8	<37.3
211	9.0±4.7	3.1±3.2	6.7±4.0	9.8±4.6	-0.8±2.3	7.3±4.1	0.0±2.7	-0.92 ^{+0.12} _{-0.08}	-0.21 ^{+0.34} _{-0.38}	0.99 ^{+0.92} _{-0.53}	-	-	0.4	37.6
212	<1.0	-	-	-	-	-	-	-	-	-	-	-	0.0	<36.6
213	<5.1	-	-	-	-	-	-	-	-	-	-	-	2.1	<37.3
214	<1.1	-	-	-	-	-	-	-	-	-	-	-	2.0	<36.6
215	<2.3	-	-	-	-	-	-	-	-	-	-	-	1.1	<37.0
216	4.6±4.2	-0.4±2.3	2.6±3.2	2.2±3.4	2.3±3.2	3.4±3.4	1.9±3.2	-0.39 ^{+0.28} _{-0.36}	-0.46 ^{+0.69} _{-1.07}	0.05 ^{+0.67} _{-0.59}	-	-	1.3	37.3
217	5.8±4.1	1.4±2.7	2.9±3.2	4.2±3.6	1.5±2.9	3.9±3.4	1.1±2.9	-0.64 ^{+0.25} _{-0.36}	-0.16 ^{+0.39} _{-0.67}	0.19 ^{+0.75} _{-0.59}	-	-	0.0	37.4
218	<1.3	-	-	-	-	-	-	-	-	-	-	-	0.0	<36.7
219	<9.5	-	-	-	-	-	-	-	-	-	-	-	0.6	<37.6
220	34.0±7.2	12.8±4.8	16.4±5.2	29.3±6.6	4.8±3.6	26.9±6.4	5.5±3.8	-0.70 ^{+0.13} _{-0.14}	-0.02 ^{+0.15} _{-0.17}	0.51 ^{+0.29} _{-0.22}	N	N	1.8	38.1
221	<1.1	-	-	-	-	-	-	-	-	-	-	-	0.0	<36.7
222	<3.9	-	-	-	-	-	-	-	-	-	-	-	0.0	<37.2
223	<8.3	-	-	-	-	-	-	-	-	-	-	-	0.3	<37.5
224	<1.5	-	-	-	-	-	-	-	-	-	-	-	1.1	<36.8
225	15.0±5.5	3.0±3.2	7.2±4.0	10.2±4.6	4.8±3.8	8.8±4.3	4.7±3.8	-0.39 ^{+0.29} _{-0.29}	-0.24 ^{+0.32} _{-0.38}	0.19 ^{+0.32} _{-0.30}	-	-	0.7	37.8
226	<3.4	-	-	-	-	-	-	-	-	-	-	-	1.2	<37.2
227	25.6±6.8	7.7±4.1	12.1±4.7	19.8±5.8	6.9±4.1	17.0±5.3	8.5±4.4	-0.40 ^{+0.19} _{-0.20}	-0.11 ^{+0.22} _{-0.21}	0.27 ^{+0.24} _{-0.24}	N	N	2.1	38.0
228	12.9±5.5	3.7±3.4	8.2±4.1	11.9±4.8	0.8±2.9	11.9±4.7	1.7±3.2	-0.84 ^{+0.12} _{-0.16}	-0.21 ^{+0.29} _{-0.35}	0.70 ^{+0.78} _{-0.46}	-	-	1.0	37.7
229	10.5±5.0	2.6±3.2	8.1±4.1	10.7±4.7	-0.2±2.7	10.6±4.6	-0.3±2.7	-0.96 ^{+0.08} _{-0.04}	-0.35 ^{+0.35} _{-0.45}	0.92 ^{+0.84} _{-0.54}	-	-	0.7	37.6
230	<5.5	-	-	-	-	-	-	-	-	-	-	-	3.4	<37.4
231	12.4±5.2	0.4±2.7	10.1±4.4	10.4±4.7	1.9±3.2	9.9±4.4	2.6±3.4	-0.69 ^{+0.14} _{-0.21}	-0.76 ^{+0.45} _{-0.84}	0.62 ^{+0.61} _{-0.38}	-	-	0.2	37.7
232	<1.3	-	-	-	-	-	-	-	-	-	-	-	0.0	<36.7
233	<12.4	-	-	-	-	-	-	-	-	-	-	-	0.6	<37.7
234	<6.8	-	-	-	-	-	-	-	-	-	-	-	0.0	<37.5
235	<0.8	-	-	-	-	-	-	-	-	-	-	-	1.3	<36.5
236	<5.7	-	-	-	-	-	-	-	-	-	-	-	1.0	<37.4

NOTE. — Col. (1): Master ID, cols. (2)–(8): net counts, in each of the 7 energy bands (see Table 2 for definitions of these bands), col. (9): hardness ratio, cols. (10) and (11) color values, errors are given as 1σ , cols. (12) and (13): short-term variability, where (BB) indicate Bayesian block analysis and (K-S) indicates the Kolmogorov-Smirnov test, in both columns symbols indicate - (N) non-variable in all observations, (V) variable in at least one observation, (P) possible variability in at least one observation, col. (14): the significance of the change in L_X between the previous observation and the current observation respectively (equation 2), col. (15): $\log L_X$ (0.3–8.0 keV). Upper limit values of net B and L_X are at the 68% confidence level.

TABLE 8
SOURCE COUNTS, HARDNESS RATIOS, COLOR-COLOR VALUES AND VARIABILITY:
OBSERVATION 4

Masterid (1)	B-band (2)	S1-band (3)	S2-band (4)	Net Counts			Hc-band (8)	HR (9)	C21 (10)	C32 (11)	Variability			Log L_X (0.3–8.0 keV) (15)	
				S-band (5)	H-band (6)	Sc-band (7)					BB (12)	k-S (13)	signif. (14)		
1	22.1±6.1	-0.8±1.9	8.4±4.1	7.6±4.1	14.5±5.1	5.2±3.6	17.4±5.4	0.50 ^{+0.21} _{-0.18}	-1.15 ^{+0.54} _{-0.99}	-0.21 ^{+0.18} _{-0.19}	N	N	0.0	38.0	
2	97.9±11.3	11.4±4.7	68.0±9.4	79.4±10.2	18.4±5.8	69.9±9.5	27.8±6.7	-0.50 ^{+0.08} _{-0.09}	-0.62 ^{+0.13} _{-0.16}	0.61 ^{+0.11} _{-0.13}	N	N	0.5	38.3	
3	<0.9	-	-	-	-	-	-	-	-	-	-	-	-	0.0	≤36.3
4	45.5±8.4	11.4±4.7	24.8±6.3	36.1±7.4	9.4±4.7	29.8±6.7	13.8±5.3	-0.44 ^{+0.13} _{-0.16}	-0.20 ^{+0.16} _{-0.17}	0.43 ^{+0.21} _{-0.16}	N	N	2.0	38.0	
5	131.6±12.8	42.5±7.7	63.8±9.2	106.3±11.5	25.4±6.5	88.4±10.6	31.0±7.0	-0.53 ^{+0.07} _{-0.08}	-0.06 ^{+0.08} _{-0.10}	0.42 ^{+0.11} _{-0.10}	N	Y	0.5	38.4	
6	≤10.4	-	-	-	-	-	-	-	-	-	-	-	-	0.8	≤37.3
7	≤2.6	-	-	-	-	-	-	-	-	-	-	-	-	0.0	≤36.7
8	23.8±6.7	3.4±3.4	17.3±5.4	20.7±6.0	3.1±3.8	17.1±5.4	5.7±4.3	-0.59 ^{+0.21} _{-0.22}	-0.54 ^{+0.30} _{-0.37}	0.67 ^{+0.56} _{-0.32}	N	N	0.3	37.7	
9	≤5.5	-	-	-	-	-	-	-	-	-	-	-	-	0.0	≤37.1
10	≤2.3	-	-	-	-	-	-	-	-	-	-	-	-	0.0	≤36.7
11	16.4±6.0	2.4±3.2	9.0±4.4	11.4±5.0	5.0±4.1	11.6±4.8	5.5±4.3	-0.46 ^{+0.29} _{-0.28}	-0.40 ^{+0.37} _{-0.51}	0.24 ^{+0.38} _{-0.29}	-	-	0.3	37.5	
12	≤1.8	-	-	-	-	-	-	-	-	-	-	-	-	0.0	≤36.6
13	222.7±16.2	49.7±8.3	117.7±12.0	167.4±14.1	55.4±8.7	154.0±13.6	66.0±9.4	-0.47 ^{+0.06} _{-0.06}	-0.24 ^{+0.07} _{-0.08}	0.36 ^{+0.08} _{-0.07}	N	N	2.6	38.7	
14	50.8±8.7	10.1±4.6	34.1±7.1	44.1±8.0	6.6±4.3	39.8±7.5	9.3±4.7	-0.67 ^{+0.11} _{-0.12}	-0.40 ^{+0.16} _{-0.16}	0.70 ^{+0.27} _{-0.19}	N	N	0.6	38.0	
15	16.1±6.1	2.6±3.2	6.5±4.1	9.1±4.7	7.0±4.6	6.2±4.1	7.5±4.7	0.01 ^{+0.38} _{-0.35}	-0.24 ^{+0.40} _{-0.48}	0.00 ^{+0.32} _{-0.32}	-	-	0.1	37.5	
16	≤2.9	-	-	-	-	-	-	-	-	-	-	-	-	1.3	≤36.7
17	33.4±7.6	8.4±4.4	14.6±5.2	23.0±6.4	10.4±4.8	19.3±5.8	14.9±5.4	-0.21 ^{+0.17} _{-0.19}	-0.11 ^{+0.22} _{-0.21}	0.18 ^{+0.20} _{-0.20}	N	N	0.1	37.8	
18	≤3.1	-	-	-	-	-	-	-	-	-	-	-	-	0.0	≤36.8
19	18.6±6.1	3.9±3.4	16.4±5.3	20.3±5.9	-1.6±2.7	19.3±5.7	-1.1±2.9	-0.98 ^{+0.04} _{-0.02}	-0.48 ^{+0.24} _{-0.32}	1.30 ^{+0.92} _{-0.54}	-	-	0.0	37.6	
20	≤6.4	-	-	-	-	-	-	-	-	-	-	-	-	1.0	≤37.1
21	≤10.5	-	-	-	-	-	-	-	-	-	-	-	-	0.9	≤37.3
22	6.6±5.0	2.2±3.2	5.6±4.0	7.8±4.6	-1.2±2.9	7.3±4.3	0.2±3.4	-0.86 ^{+0.16} _{-0.14}	-0.24 ^{+0.45} _{-0.59}	0.76 ^{+1.00} _{-0.61}	-	-	0.9	37.1	
23	9.5±5.0	2.9±3.2	5.4±3.8	8.3±4.4	1.2±3.2	9.2±4.4	0.9±3.2	-0.87 ^{+0.14} _{-0.13}	-0.16 ^{+0.40} _{-0.43}	0.46 ^{+0.76} _{-0.46}	-	-	0.1	37.4	
24	≤11.3	-	-	-	-	-	-	-	-	-	-	-	-	0.6	≤37.3
25	≤18.3	-	-	-	-	-	-	-	-	-	-	-	-	1.7	≤37.5
26	19.1±6.3	2.4±3.2	9.5±4.6	11.9±5.1	7.2±4.4	8.6±4.4	8.4±4.7	-0.09 ^{+0.30} _{-0.29}	-0.43 ^{+0.38} _{-0.48}	0.13 ^{+0.30} _{-0.24}	-	-	2.9	37.6	
27	≤6.6	-	-	-	-	-	-	-	-	-	-	-	-	0.7	≤37.1
28	≤6.4	-	-	-	-	-	-	-	-	-	-	-	-	0.9	≤37.1
29	23.7±6.7	2.4±3.2	16.0±5.3	18.4±5.8	5.3±4.1	17.7±5.6	6.8±4.4	-0.52 ^{+0.21} _{-0.21}	-0.64 ^{+0.35} _{-0.46}	0.46 ^{+0.34} _{-0.25}	N	N	0.0	37.7	
30	≤5.0	-	-	-	-	-	-	-	-	-	-	-	-	0.0	≤37.0
31	91.4±11.0	13.8±5.0	55.3±8.7	69.1±9.6	22.3±6.2	58.3±8.9	32.8±7.1	-0.34 ^{+0.10} _{-0.10}	-0.47 ^{+0.09} _{-0.18}	0.42 ^{+0.12} _{-0.11}	Y	N	0.1	38.2	
32	≤3.7	-	-	-	-	-	-	-	-	-	-	-	-	0.0	≤36.9
33	≤10.9	-	-	-	-	-	-	-	-	-	-	-	-	0.6	≤37.3
34	≤1.0	-	-	-	-	-	-	-	-	-	-	-	-	0.0	≤36.3
35	51.5±8.7	6.5±4.0	27.4±6.5	33.9±7.1	17.6±5.7	28.7±6.6	22.2±6.2	-0.20 ^{+0.14} _{-0.14}	-0.53 ^{+0.23} _{-0.19}	0.22 ^{+0.14} _{-0.14}	N	N	1.3	38.0	
36	8.9±5.3	3.7±3.4	2.6±3.4	6.3±4.3	2.6±3.8	4.3±3.8	4.0±4.1	-0.17 ^{+0.47} _{-0.46}	0.19 ^{+0.61} _{-0.48}	0.00 ^{+0.80} _{-0.70}	-	-	0.2	37.2	
37	≤3.2	-	-	-	-	-	-	-	-	-	-	-	-	1.3	≤36.8
38	9.5±6.6	6.5±4.0	3.3±3.6	9.8±4.8	-0.3±3.2	10.3±4.7	-1.2±3.2	-0.95 ^{+0.09} _{-0.05}	0.32 ^{+0.48} _{-0.37}	0.46 ^{+0.99} _{-0.69}	-	-	0.1	37.3	
39	66.7±11.7	16.2±5.3	36.6±7.3	52.8±8.6	13.8±5.3	43.4±7.8	20.2±6.1	-0.42 ^{+0.10} _{-0.13}	-0.26 ^{+0.14} _{-0.13}	0.43 ^{+0.17} _{-0.13}	N	P	1.8	38.1	
40	≤35.4	-	-	-	-	-	-	-	-	-	-	-	-	1.4	≤37.8
41	133.7±13.0	27.9±6.5	78.3±10.0	106.3±11.6	27.5±6.7	91.9±10.8	34.8±7.4	-0.50 ^{+0.07} _{-0.08}	-0.33 ^{+0.08} _{-0.12}	0.48 ^{+0.11} _{-0.09}	N	N	0.1	38.4	
42	112.5±12.0	27.2±6.5	70.2±9.5	97.4±11.1	15.1±5.3	85.4±10.4	22.7±6.2	-0.63 ^{+0.08} _{-0.07}	-0.30 ^{+0.08} _{-0.12}	0.70 ^{+0.12} _{-0.14}	N	N	0.9	38.3	
43	15.3±6.1	1.0±3.2	10.2±4.7	11.2±5.2	4.1±4.0	12.6±5.1	3.2±4.0	-0.74 ^{+0.15} _{-0.11}	-0.61 ^{+0.38} _{-0.84}	0.38 ^{+0.45} _{-0.33}	-	-	1.7	37.5	
44	≤11.0	-	-	-	-	-	-	-	-	-	-	-	-	0.8	≤37.3
45	10.9±5.4	-1.0±2.3	7.8±4.3	6.8±4.4	4.0±3.8	3.9±3.8	7.7±4.4	0.33 ^{+0.36} _{-0.39}	-0.92 ^{+0.54} _{-0.91}	0.27 ^{+0.43} _{-0.32}	-	-	1.7	37.3	
46	≤5.4	-	-	-	-	-	-	-	-	-	-	-	-	0.0	≤37.0
47	≤2.3	-	-	-	-	-	-	-	-	-	-	-	-	0.0	≤36.7
48	16.1±6.7	4.4±3.8	10.0±4.6	14.3±5.4	2.5±3.8	11.7±5.0	3.0±4.0	-0.72 ^{+0.15} _{-0.28}	-0.24 ^{+0.29} _{-0.38}	0.51 ^{+0.62} _{-0.40}	-	-	2.0	37.5	
49	≤6.6	-	-	-	-	-	-	-	-	-	-	-	-	0.8	≤37.1

TABLE 8 — *Continued*

Masterid	B-band	S1-band	S2-band	Net Counts			HR	C21	C32	Variability			Log L_x		
(1)	(2)	(3)	(4)	S-band	H-band	Sc-band	Hc-band	(9)	(10)	(11)	BB	k-S	signif.	(0.3–8.0 keV)	
				(5)	(6)	(7)	(8)	(9)	(10)	(11)	(12)	(13)	(14)	(15)	
50	34.8±7.7	11.2±4.8	18.9±5.7	30.1±7.0	4.8±4.1	31.2±6.9	4.3±4.1	-0.82 ^{+0.09} _{-0.13}	-0.13 ^{+0.17} _{-0.18}	0.56 ^{+0.38} _{-0.27}	N	N	0.5	37.8	
51	15.2±6.0	5.9±4.0	7.4±4.3	13.3±5.3	1.9±3.6	14.1±5.2	0.9±3.6	-0.91 ^{+0.11} _{-0.09}	0.00 ^{+0.29} _{-0.29}	0.46 ^{+0.75} _{-0.46}	-	-	1.0	37.5	
52	≤12.3	-	-	-	-	-	-	-	-	-	-	-	-	2.0	≤37.4
53	12.2±6.3	4.4±3.8	7.9±4.3	12.3±5.2	0.1±3.4	11.8±5.0	-0.4±3.4	-0.94 ^{+0.10} _{-0.06}	-0.13 ^{+0.32} _{-0.38}	0.69 ^{+0.91} _{-0.46}	-	-	0.3	37.4	
54	16.0±6.3	6.8±4.3	7.7±4.4	14.5±5.7	1.5±3.6	12.2±5.2	2.9±4.0	-0.74 ^{+0.15} _{-0.26}	0.03 ^{+0.29} _{-0.30}	0.51 ^{+0.78} _{-0.46}	-	-	0.4	37.5	
55	≤11.5	-	-	-	-	-	-	-	-	-	-	-	-	1.5	≤37.3
56	≤8.1	-	-	-	-	-	-	-	-	-	-	-	-	2.0	≤37.2
57	9.9±5.8	-0.7±2.9	7.7±4.4	7.0±4.8	2.9±4.0	5.4±4.3	5.3±4.4	-0.11 ^{+0.47} _{-0.47}	-0.76 ^{+0.53} _{-0.92}	0.35 ^{+0.64} _{-0.40}	-	-	0.5	37.3	
58	≤1.6	-	-	-	-	-	-	-	-	-	-	-	-	1.1	≤36.5
59	≤1.1	-	-	-	-	-	-	-	-	-	-	-	-	0.0	≤36.3
60	≤10.7	-	-	-	-	-	-	-	-	-	-	-	-	1.1	≤37.3
61	≤2.5	-	-	-	-	-	-	-	-	-	-	-	-	0.0	≤36.7
62	≤16.5	-	-	-	-	-	-	-	-	-	-	-	-	1.7	≤37.5
63	23.4±6.8	1.9±3.2	15.3±5.3	17.3±5.8	6.1±4.3	16.5±5.6	6.7±4.4	-0.51 ^{+0.22} _{-0.22}	-0.67 ^{+0.38} _{-0.62}	0.40 ^{+0.30} _{-0.24}	N	P	0.3	37.6	
64	≤11.3	-	-	-	-	-	-	-	-	-	-	-	-	0.2	≤37.4
65	23.0±6.2	6.0±3.8	14.1±5.0	20.2±5.8	2.8±3.2	19.6±5.7	3.7±3.4	-0.73 ^{+0.14} _{-0.17}	-0.27 ^{+0.22} _{-0.21}	0.67 ^{+0.38} _{-0.32}	N	N	0.0	37.7	
66	35.4±7.2	6.2±3.8	22.3±5.9	28.5±6.5	6.9±4.0	24.8±6.2	10.8±4.6	-0.45 ^{+0.16} _{-0.16}	-0.43 ^{+0.19} _{-0.21}	0.51 ^{+0.21} _{-0.17}	N	N	1.3	37.8	
67	40.3±7.9	1.0±2.9	18.4±5.6	19.4±5.9	20.9±6.0	17.5±5.6	23.4±6.3	0.07 ^{+0.16} _{-0.18}	-1.03 ^{+0.52} _{-0.67}	0.01 ^{+0.12} _{-0.18}	N	N	0.8	37.9	
68	43.7±8.4	12.2±5.0	25.5±6.4	37.8±7.6	5.9±4.3	32.4±7.1	10.4±5.0	-0.57 ^{+0.14} _{-0.15}	-0.22 ^{+0.15} _{-0.17}	0.62 ^{+0.32} _{-0.22}	N	N	0.2	38.0	
69	10.4±5.2	5.5±3.8	4.7±3.8	10.2±4.8	0.2±2.9	7.5±4.3	1.6±3.4	-0.76 ^{+0.15} _{-0.24}	0.13 ^{+0.38} _{-0.32}	0.53 ^{+0.92} _{-0.53}	-	-	0.2	37.3	
70	≤19.2	-	-	-	-	-	-	-	-	-	-	-	-	1.5	≤37.6
71	25.0±6.8	6.0±4.0	7.3±4.3	13.3±5.3	11.6±5.0	13.2±5.1	11.7±5.1	-0.13 ^{+0.23} _{-0.22}	0.00 ^{+0.31} _{-0.29}	-0.13 ^{+0.22} _{-0.27}	N	N	1.1	37.7	
72	56.4±9.1	14.3±5.1	31.6±6.9	45.9±8.1	10.5±4.8	41.7±7.7	11.7±5.1	-0.61 ^{+0.11} _{-0.12}	-0.24 ^{+0.14} _{-0.15}	0.51 ^{+0.17} _{-0.19}	N	N	0.3	38.0	
73	34.6±8.6	7.3±4.4	18.0±5.7	25.3±6.7	9.7±4.8	22.5±6.3	11.0±5.1	-0.41 ^{+0.18} _{-0.18}	-0.27 ^{+0.19} _{-0.19}	0.28 ^{+0.22} _{-0.19}	N	N	0.1	37.8	
74	14.4±6.7	0.9±3.2	10.5±4.7	11.4±5.2	3.4±4.0	10.6±4.8	5.9±4.4	-0.40 ^{+0.18} _{-0.29}	-0.61 ^{+0.38} _{-0.84}	0.43 ^{+0.34} _{-0.35}	-	-	1.0	37.4	
75	≤13.6	-	-	-	-	-	-	-	-	-	-	-	-	1.9	≤37.4
76	54.9±12.2	6.9±4.3	36.8±7.5	43.7±8.2	11.2±5.0	37.5±7.6	16.5±5.7	-0.45 ^{+0.13} _{-0.13}	-0.61 ^{+0.20} _{-0.25}	0.54 ^{+0.17} _{-0.17}	N	N	0.3	38.0	
77	≤5.2	-	-	-	-	-	-	-	-	-	-	-	-	0.0	≤37.0
78	53.0±8.9	12.0±4.8	29.9±6.7	41.9±7.8	11.1±5.0	40.2±7.6	11.6±5.1	-0.61 ^{+0.12} _{-0.12}	-0.27 ^{+0.13} _{-0.19}	0.44 ^{+0.19} _{-0.16}	N	N	0.3	38.0	
79	≤62.0	-	-	-	-	-	-	-	-	-	-	-	-	6.8	≤38.1
80	≤13.2	-	-	-	-	-	-	-	-	-	-	-	-	0.1	≤37.4
81	≤14.0	-	-	-	-	-	-	-	-	-	-	-	-	0.6	≤37.4
82	≤6.1	-	-	-	-	-	-	-	-	-	-	-	-	0.3	≤37.1
83	249.7±22.5	64.8±9.3	144.9±13.2	209.7±15.8	41.3±7.8	179.7±14.6	64.4±9.4	-0.52 ^{+0.05} _{-0.06}	-0.29 ^{+0.10} _{-0.03}	0.58 ^{+0.07} _{-0.09}	N	N	10.9	38.7	
84	58.5±11.2	13.4±5.6	26.1±6.8	39.5±8.3	19.4±6.0	36.4±8.0	20.9±6.2	-0.33 ^{+0.12} _{-0.15}	-0.22 ^{+0.19} _{-0.17}	0.14 ^{+0.18} _{-0.12}	N	N	0.0	38.0	
85	≤34.5	-	-	-	-	-	-	-	-	-	-	-	-	0.4	≤37.8
86	20.5±6.0	4.9±3.6	14.6±5.1	19.5±5.8	1.1±2.7	14.8±5.2	6.0±3.8	-0.48 ^{+0.19} _{-0.21}	-0.35 ^{+0.22} _{-0.27}	0.97 ^{+0.67} _{-0.43}	N	N	1.7	37.6	
87	≤16.6	-	-	-	-	-	-	-	-	-	-	-	-	0.0	≤37.5
88	≤28.2	-	-	-	-	-	-	-	-	-	-	-	-	1.2	≤37.7
89	≤2.3	-	-	-	-	-	-	-	-	-	-	-	-	0.0	≤36.6
90	≤3.6	-	-	-	-	-	-	-	-	-	-	-	-	1.3	≤36.8
91	93.5±11.2	42.3±7.8	48.0±8.2	90.3±10.9	3.2±3.4	77.3±10.2	8.2±4.3	-0.83 ^{+0.05} _{-0.07}	0.04 ^{+0.08} _{-0.11}	1.08 ^{+0.43} _{-0.25}	N	N	8.2	38.2	
92	≤3.0	-	-	-	-	-	-	-	-	-	-	-	-	0.0	≤36.7
93	≤2.2	-	-	-	-	-	-	-	-	-	-	-	-	0.0	≤36.6
94	≤8.3	-	-	-	-	-	-	-	-	-	-	-	-	0.8	≤37.2
95	≤1.1	-	-	-	-	-	-	-	-	-	-	-	-	0.0	≤36.3
96	176.6±14.8	34.9±7.2	100.3±11.2	135.2±12.9	41.4±7.8	113.1±11.9	55.7±8.9	-0.40 ^{+0.07} _{-0.08}	-0.36 ^{+0.08} _{-0.09}	0.42 ^{+0.08} _{-0.09}	N	N	0.3	38.5	
97	≤6.7	-	-	-	-	-	-	-	-	-	-	-	-	0.0	≤37.1
98	67.6±12.0	16.5±6.1	38.8±7.9	55.3±9.5	12.3±5.3	47.1±8.9	16.6±5.8	-0.53 ^{+0.12} _{-0.13}	-0.31 ^{+0.19} _{-0.14}	0.53 ^{+0.17} _{-0.17}	N	N	0.6	38.1	
99	53.1±9.6	21.1±6.5	24.0±6.6	45.2±8.8	7.9±4.4	39.2±8.3	8.4±4.6	-0.69 ^{+0.11} _{-0.16}	0.03 ^{+0.15} _{-0.20}	0.48 ^{+0.24} _{-0.20}	N	N	0.9	38.0	
100	23.2±7.3	7.2±4.5	10.8±5.0	18.0±6.2	5.2±4.3	15.1±5.7	6.1±4.6	-0.53 ^{+0.27} _{-0.25}	-0.08 ^{+0.27} _{-0.30}	0.29 ^{+0.43} _{-0.32}	-	-	0.9	37.6	

TABLE 8 — *Continued*

Masterid	B-band	S1-band	S2-band	Net Counts		H-band	Sc-band	Hc-band	HR	C21	C32	Variability			Log L_x	
(1)	(2)	(3)	(4)	S-band	(5)	(6)	(7)	(8)	(9)	(10)	(11)	BB	k-S	signif.	(14)	(15)
151	<10.2	-	-	-	-	-	-	-	-	-	-	-	-	-	0.8	<37.3
152	<3.2	-	-	-	-	-	-	-	-	-	-	-	-	-	0.0	<36.8
153	10.2±7.0	2.5±4.3	3.6±4.6	6.0±5.7	4.2±4.2	7.2±5.5	3.7±4.4	-0.41 ^{+0.25} _{-0.37}	0.00 ^{+0.80} _{-0.91}	0.00 ^{+0.70} _{-0.78}	-	-	-	-	1.3	37.3
154	60.1±9.3	14.5±5.3	33.9±7.1	48.4±8.4	11.7±4.7	39.2±7.7	18.3±5.6	-0.42 ^{+0.11} _{-0.13}	-0.24 ^{+0.12} _{-0.18}	0.49 ^{+0.15} _{-0.16}	N	P		0.4	38.1	
155	28.1±7.3	6.4±4.1	13.7±5.2	20.1±6.2	8.1±4.6	19.8±6.0	8.4±4.7	-0.47 ^{+0.19} _{-0.21}	-0.21 ^{+0.24} _{-0.27}	0.24 ^{+0.24} _{-0.21}	N	N		0.3	37.7	
156	<2.0	-	-	-	-	-	-	-	-	-	-	-	-	-	0.0	<36.6
157	67.5±10.0	10.9±4.8	41.2±7.8	52.1±8.7	15.4±5.6	45.2±8.2	19.0±6.0	-0.47 ^{+0.12} _{-0.05}	-0.45 ^{+0.13} _{-0.08}	0.44 ^{+0.17} _{-0.12}	N	P		2.0	38.1	
158	269.8±22.2	39.2±7.8	172.6±14.3	211.8±15.9	58.4±9.0	177.9±14.7	85.7±10.6	-0.41 ^{+0.05} _{-0.06}	-0.55 ^{+0.08} _{-0.08}	0.49 ^{+0.08} _{-0.06}	N	N		1.3	38.7	
159	<3.3	-	-	-	-	-	-	-	-	-	-	-	-	-	0.8	<36.8
160	20.0±6.8	4.7±4.0	9.6±4.8	14.3±5.8	5.7±4.3	11.1±5.2	6.9±4.6	-0.32 ^{+0.30} _{-0.30}	-0.19 ^{+0.32} _{-0.37}	0.24 ^{+0.35} _{-0.32}	N	N		0.9	37.6	
161	<2.2	-	-	-	-	-	-	-	-	-	-	-	-	-	0.0	<36.6
162	24.3±7.3	7.7±4.6	10.2±5.1	17.9±6.4	6.4±4.3	18.8±6.3	5.5±4.3	-0.63 ^{+0.21} _{-0.21}	-0.03 ^{+0.27} _{-0.29}	0.21 ^{+0.33} _{-0.29}	-	-	-	0.5	37.7	
163	134.0±16.5	31.4±7.1	65.6±9.4	97.0±11.4	37.0±7.5	80.9±10.5	48.5±8.4	-0.31 ^{+0.08} _{-0.09}	-0.23 ^{+0.11} _{-0.09}	0.27 ^{+0.10} _{-0.09}	N	N		0.8	38.4	
164	<6.1	-	-	-	-	-	-	-	-	-	-	-	-	-	1.5	<37.1
165	17.1±6.4	9.3±4.6	6.5±4.3	15.9±5.8	1.2±3.6	10.1±5.0	3.8±4.1	-0.60 ^{+0.20} _{-0.27}	0.21 ^{+0.30} _{-0.26}	0.46 ^{+0.85} _{-0.49}	-	-	-	0.7	37.5	
166	15.3±6.4	5.6±4.0	3.4±4.0	8.9±5.1	6.4±4.4	8.5±4.8	5.6±4.4	-0.31 ^{+0.37} _{-0.37}	0.24 ^{+0.39} _{-0.45}	-0.19 ^{+0.48} _{-0.61}	-	-	-	0.3	37.5	
167	<10.5	-	-	-	-	-	-	-	-	-	-	-	-	-	0.6	<37.3
168	<10.5	-	-	-	-	-	-	-	-	-	-	-	-	-	0.8	<37.3
169	34.2±7.7	13.4±5.0	20.4±5.9	33.8±7.2	0.4±3.4	31.2±6.9	2.8±4.0	-0.90 ^{+0.07} _{-0.10}	-0.09 ^{+0.16} _{-0.17}	1.07 ^{+0.76} _{-0.46}	N	Y		1.3	37.8	
170	32.2±7.4	3.1±3.4	13.1±5.1	16.1±5.7	16.1±5.4	14.3±5.3	16.6±5.6	0.01 ^{+0.19} _{-0.21}	-0.61 ^{+0.46} _{-0.37}	-0.14 ^{+0.27} _{-0.09}	N	N		1.3	37.8	
171	16.8±6.1	7.2±4.1	6.3±4.1	13.5±5.3	3.3±3.8	12.9±5.1	3.5±4.0	-0.70 ^{+0.15} _{-0.20}	0.13 ^{+0.35} _{-0.26}	0.24 ^{+0.36} _{-0.43}	-	-	-	0.1	37.5	
172	<6.2	-	-	-	-	-	-	-	-	-	-	-	-	-	1.2	<37.1
173	<65.2	-	-	-	-	-	-	-	-	-	-	-	-	-	6.9	<38.1
174	<6.7	-	-	-	-	-	-	-	-	-	-	-	-	-	0.5	<37.1
175	13.6±5.9	5.4±4.0	5.8±4.1	11.1±5.2	2.5±3.6	6.3±4.4	4.0±4.0	-0.34 ^{+0.37} _{-0.43}	0.05 ^{+0.38} _{-0.34}	0.29 ^{+0.68} _{-0.48}	-	-	-	1.3	37.4	
176	<9.7	-	-	-	-	-	-	-	-	-	-	-	-	-	0.8	<37.3
177	<7.4	-	-	-	-	-	-	-	-	-	-	-	-	-	1.7	<37.1
178	16.7±6.6	7.9±4.6	6.5±4.4	14.4±5.9	2.3±3.8	10.8±5.3	3.5±4.1	-0.64 ^{+0.17} _{-0.21}	0.16 ^{+0.35} _{-0.32}	0.35 ^{+0.75} _{-0.48}	-	-	-	1.8	37.5	
179	24.8±7.2	6.8±4.3	13.9±5.4	20.7±6.5	4.1±4.0	14.9±5.7	7.1±4.6	-0.44 ^{+0.25} _{-0.24}	-0.21 ^{+0.24} _{-0.27}	0.51 ^{+0.46} _{-0.32}	N	N		1.9	37.7	
180	<13.5	-	-	-	-	-	-	-	-	-	-	-	-	-	1.5	<37.4
181	<17.5	-	-	-	-	-	-	-	-	-	-	-	-	-	1.6	<37.5
182	<13.7	-	-	-	-	-	-	-	-	-	-	-	-	-	0.2	<37.4
183	11.8±5.7	3.4±3.6	7.7±4.3	11.2±5.1	0.6±3.4	10.1±4.7	1.2±3.6	-0.85 ^{+0.15} _{-0.15}	-0.21 ^{+0.34} _{-0.46}	0.61 ^{+0.84} _{-0.46}	-	-	-	0.1	37.4	
184	230.0±16.5	40.9±7.6	128.5±12.5	169.4±14.2	60.6±9.0	138.7±12.9	82.1±10.3	-0.32 ^{+0.06} _{-0.07}	-0.39 ^{+0.07} _{-0.09}	0.35 ^{+0.07} _{-0.06}	N	N		0.0	38.6	
185	96.9±11.5	17.9±5.8	56.8±8.8	74.7±10.1	22.2±6.3	64.4±9.4	29.6±7.0	-0.43 ^{+0.10} _{-0.09}	-0.39 ^{+0.12} _{-0.14}	0.43 ^{+0.12} _{-0.11}	N	N		0.9	38.3	
186	14.3±6.1	6.8±4.3	8.6±4.6	15.4±5.8	-1.1±2.9	7.0±4.6	1.3±3.6	-0.74 ^{+0.21} _{-0.26}	0.00 ^{+0.27} _{-0.29}	0.92 ^{+0.91} _{-0.54}	-	-	-	0.3	37.4	
187	36.8±8.1	9.6±4.7	19.8±6.0	29.5±7.1	7.3±4.6	28.3±6.9	8.7±4.8	-0.59 ^{+0.16} _{-0.17}	-0.21 ^{+0.18} _{-0.19}	0.43 ^{+0.27} _{-0.22}	N	N		0.1	37.8	
188	<2.6	-	-	-	-	-	-	-	-	-	-	-	-	-	0.0	<36.7
189	23.4±7.6	8.7±4.7	14.0±5.2	22.7±6.5	0.9±3.4	20.6±6.2	2.4±3.8	-0.88 ^{+0.10} _{-0.12}	-0.11 ^{+0.22} _{-0.24}	0.83 ^{+0.81} _{-0.43}	N	N		1.4	37.6	
190	20.1±6.7	4.2±3.8	8.2±4.6	12.5±5.4	7.6±4.6	6.4±4.4	12.8±5.3	0.30 ^{+0.29} _{-0.30}	-0.16 ^{+0.35} _{-0.40}	0.05 ^{+0.30} _{-0.29}	N	N		1.2	37.6	
191	16.4±6.3	3.8±3.8	10.1±4.7	13.8±5.6	2.6±3.8	15.8±5.6	2.0±3.8	-0.86 ^{+0.12} _{-0.14}	-0.29 ^{+0.34} _{-0.43}	0.48 ^{+0.65} _{-0.54}	-	-	-	1.3	37.5	
192	11.7±5.6	3.8±3.6	6.6±4.1	10.4±5.0	1.3±3.4	8.7±4.6	1.9±3.6	-0.76 ^{+0.14} _{-0.24}	-0.13 ^{+0.37} _{-0.41}	0.48 ^{+0.81} _{-0.45}	-	-	-	2.0	37.3	
193	<6.9	-	-	-	-	-	-	-	-	-	-	-	-	-	1.2	<37.1
194	89.6±11.9	23.9±6.3	50.9±8.3	74.8±10.0	15.2±5.4	61.4±9.1	23.8±6.4	-0.49 ^{+0.09} _{-0.10}	-0.24 ^{+0.13} _{-0.10}	0.56 ^{+0.12} _{-0.16}	N	N		3.0	38.2	
195	25.8±6.9	7.4±4.1	13.7±5.1	21.1±6.1	4.7±4.1	15.5±5.3	7.9±4.7	-0.41 ^{+0.23} _{-0.23}	-0.16 ^{+0.21} _{-0.22}	0.46 ^{+0.46} _{-0.30}	N	N		0.8	37.7	
196	<19.5	-	-	-	-	-	-	-	-	-	-	-	-	-	2.8	<37.6
197	<10.2	-	-	-	-	-	-	-	-	-	-	-	-	-	1.2	<37.3
198	<6.3	-	-	-	-	-	-	-	-	-	-	-	-	-	0.0	<37.1
199	<4.3	-	-	-	-	-	-	-	-	-	-	-	-	-	0.0	<36.9
200	<13.1	-	-	-	-	-	-	-	-	-	-	-	-	-	0.1	<37.5

TABLE 8 — *Continued*

Masterid	B-band	S1-band	S2-band	Net Counts			HR	C21	C32	Variability			Log L_X	
(1)	(2)	(3)	(4)	S-band (5)	H-band (6)	Sc-band (7)	Hc-band (8)	(9)	(10)	(11)	BB (12)	k-S (13)	signif. (14)	(0.3–8.0 keV) (15)
201	<2.2	-	-	-	-	-	-	-	-	-	-	-	0.0	<36.7
202	15.9±6.0	2.3±3.2	11.8±4.8	14.2±5.3	1.7±3.6	14.5±5.2	2.1±3.8	-0.84 ^{+0.12} _{-0.16}	-0.51 ^{+0.35} _{-0.51}	0.67 ^{+0.72} _{-0.40}	-	-	0.5	37.5
203	14.5±5.7	3.6±3.4	7.1±4.1	10.7±4.8	3.8±3.8	9.0±4.4	5.4±4.1	-0.36 ^{+0.32} _{-0.30}	-0.19 ^{+0.35} _{-0.35}	0.27 ^{+0.45} _{-0.38}	-	-	1.4	37.4
204	<1.2	-	-	-	-	-	-	-	-	-	-	-	0.0	<36.3
205	22.8±6.7	5.2±3.8	15.3±5.3	20.5±6.1	2.3±3.6	20.1±5.9	1.6±3.6	-0.92 ^{+0.09} _{-0.22}	-0.35 ^{+0.24} _{-0.59}	0.70 ^{+0.64} _{-0.82}	N	N	1.4	37.6
206	9.3±5.3	2.2±3.2	3.5±3.6	5.7±4.3	3.6±3.8	6.4±4.1	2.8±3.8	-0.55 ^{+0.22} _{-0.23}	-0.05 ^{+0.59} _{-0.70}	0.00 ^{+0.82} _{-0.56}	-	-	1.0	37.2
207	<2.2	-	-	-	-	-	-	-	-	-	-	-	0.0	<36.7
208	11.8±5.6	1.4±2.9	7.6±4.3	9.0±4.7	2.8±3.8	5.1±4.0	5.2±4.3	-0.09 ^{+0.45} _{-0.44}	-0.48 ^{+0.45} _{-0.67}	0.38 ^{+0.59} _{-0.43}	-	-	0.3	37.4
209	44.5±8.4	0.1±2.7	25.8±6.5	25.9±6.6	18.6±5.9	16.4±5.6	27.8±6.8	0.20 ^{+0.17} _{-0.16}	-1.30 ^{+0.55} _{-0.77}	0.16 ^{+0.15} _{-0.14}	N	P	0.8	37.9
210	<10.8	-	-	-	-	-	-	-	-	-	-	-	0.5	<37.3
211	<20.9	-	-	-	-	-	-	-	-	-	-	-	0.3	<37.6
212	<8.5	-	-	-	-	-	-	-	-	-	-	-	1.5	<37.2
213	23.2±6.7	9.1±4.4	5.9±4.0	14.9±5.4	8.2±4.6	11.2±4.8	8.7±4.7	-0.21 ^{+0.26} _{-0.26}	0.27 ^{+0.27} _{-0.27}	-0.11 ^{+0.30} _{-0.29}	N	N	2.1	37.7
214	<7.0	-	-	-	-	-	-	-	-	-	-	-	1.0	<37.1
215	<17.0	-	-	-	-	-	-	-	-	-	-	-	1.8	<37.5
216	31.9±7.4	8.0±4.3	20.8±5.9	28.8±6.8	3.1±3.8	25.8±6.5	5.7±4.3	-0.70 ^{+0.16} _{-0.17}	-0.32 ^{+0.19} _{-0.22}	0.75 ^{+0.54} _{-0.32}	N	N	1.9	37.8
217	<2.2	-	-	-	-	-	-	-	-	-	-	-	1.4	<36.6
218	<8.0	-	-	-	-	-	-	-	-	-	-	-	0.9	<37.2
219	9.8±5.5	2.5±3.4	4.7±3.8	7.2±4.6	2.6±3.8	5.8±4.1	3.9±4.1	-0.34 ^{+0.39} _{-0.39}	-0.11 ^{+0.49} _{-0.64}	0.19 ^{+0.70} _{-0.51}	-	-	0.2	37.3
220	46.9±8.6	7.3±4.3	25.9±6.4	33.2±7.2	13.8±5.4	30.1±6.8	15.1±5.7	-0.39 ^{+0.15} _{-0.15}	-0.47 ^{+0.23} _{-0.20}	0.30 ^{+0.17} _{-0.16}	N	P	1.4	38.0
221	<1.8	-	-	-	-	-	-	-	-	-	-	-	0.0	<36.6
222	<1.3	-	-	-	-	-	-	-	-	-	-	-	0.0	<36.4
223	<16.1	-	-	-	-	-	-	-	-	-	-	-	0.2	<37.5
224	<2.7	-	-	-	-	-	-	-	-	-	-	-	0.0	<36.8
225	53.2±8.9	13.9±5.1	30.6±6.7	44.4±8.0	8.8±4.7	41.4±7.7	10.6±5.0	-0.64 ^{+0.11} _{-0.13}	-0.22 ^{+0.14} _{-0.16}	0.56 ^{+0.19} _{-0.21}	N	N	1.5	38.0
226	20.7±6.3	2.6±3.2	12.1±4.8	14.7±5.3	6.0±4.1	10.0±4.6	10.4±4.8	-0.07 ^{+0.25} _{-0.25}	-0.48 ^{+0.32} _{-0.46}	0.32 ^{+0.30} _{-0.24}	N	N	2.1	37.6
227	53.1±9.1	17.4±5.4	23.1±6.1	40.4±7.7	12.3±5.1	35.7±7.2	17.8±5.8	-0.40 ^{+0.13} _{-0.13}	-0.03 ^{+0.15} _{-0.15}	0.32 ^{+0.15} _{-0.19}	N	N	0.2	38.0
228	23.8±7.0	4.1±3.6	13.7±5.1	17.8±5.8	6.2±4.3	15.5±5.3	8.7±4.7	-0.36 ^{+0.22} _{-0.13}	-0.38 ^{+0.27} _{-0.14}	0.35 ^{+0.29} _{-0.24}	N	N	0.1	37.7
229	38.7±7.8	11.5±4.7	20.4±5.8	31.9±7.0	6.8±4.3	26.9±6.5	9.4±4.7	-0.54 ^{+0.15} _{-0.16}	-0.16 ^{+0.17} _{-0.16}	0.48 ^{+0.24} _{-0.21}	N	N	1.5	37.9
230	19.7±6.4	5.1±3.8	9.9±4.6	15.0±5.4	4.8±4.1	13.2±5.1	5.4±4.3	-0.51 ^{+0.26} _{-0.26}	-0.19 ^{+0.27} _{-0.29}	0.29 ^{+0.41} _{-0.29}	-	-	1.5	37.6
231	27.6±7.0	6.9±4.1	13.9±5.1	20.8±6.1	6.8±4.3	17.4±5.6	9.2±4.7	-0.38 ^{+0.20} _{-0.20}	-0.19 ^{+0.22} _{-0.24}	0.32 ^{+0.27} _{-0.21}	N	N	0.1	37.7
232	<16.0	-	-	-	-	-	-	-	-	-	-	-	2.1	<37.5
233	<18.6	-	-	-	-	-	-	-	-	-	-	-	0.5	<37.6
234	18.4±6.2	0.4±2.7	8.7±4.4	9.1±4.7	9.3±4.7	9.3±4.6	9.7±4.8	-0.06 ^{+0.28} _{-0.27}	-0.69 ^{+0.46} _{-0.84}	0.00 ^{+0.24} _{-0.24}	-	-	1.0	37.6
235	<0.7	-	-	-	-	-	-	-	-	-	-	-	0.0	<36.1
236	<16.2	-	-	-	-	-	-	-	-	-	-	-	0.7	<37.5

NOTE. — Col. (1): Master ID, cols. (2)–(8): net counts, in each of the 7 energy bands (see Table 2 for definitions of these bands), col. (9): hardness ratio, cols. (10) and (11) color values, errors are given as 1σ , cols. (12) and (13): short-term variability, where (BB) indicate Bayesian block analysis and (K-S) indicates the Kolmogorov-Smirnov test, in both columns symbols indicate - (N) non-variable in all observations, (V) variable in at least one observation, (P) possible variability in at least one observation, col. (14): the significance of the change in L_X between the previous observation and the current observation respectively (equation 2), col. (15): $\log L_X$ (0.3–8.0 keV). Upper limit values of net B and L_X are at the 68% confidence level.

TABLE 9
SOURCE COUNTS, HARDNESS RATIOS, COLOR-COLOR VALUES AND VARIABILITY:
OBSERVATION 5

Masterid	B-band	S1-band	S2-band	Net Counts		H-band	Sc-band	Hc-band	HR	C21	C32	Variability			Log L_X
(1)	(2)	(3)	(4)	S-band	(5)	(6)	(7)	(8)	(9)	(10)	(11)	BB	k-S	signif.	(15)
												(12)	(13)	(14)	
1	49.4±9.0	0.4±3.2	13.1±5.1	13.6±5.6	35.8±7.5	10.6±4.8	37.1±7.7	0.51 ^{+0.15} _{-0.14}	-0.76 ^{+0.47} _{-0.85}	-0.38 ^{+0.14} _{-0.17}	N	N	0.4	38.0	
2	129.3±13.2	22.1±6.3	79.4±10.2	101.5±11.5	27.8±7.1	83.1±10.4	44.1±8.4	-0.36 ^{+0.08} _{-0.09}	-0.45 ^{+0.11} _{-0.12}	0.48 ^{+0.11} _{-0.11}	N	N	1.3	38.4	
3	<2.3	-	-	-	-	-	-	-	-	-	-	-	-	0.0	<36.6
4	76.2±10.6	22.0±6.2	41.7±7.8	63.7±9.5	12.6±5.6	53.7±8.7	18.9±6.3	-0.53 ^{+0.11} _{-0.12}	-0.19 ^{+0.14} _{-0.10}	0.53 ^{+0.19} _{-0.16}	N	N	1.9	38.2	
5	204.7±15.8	49.8±8.4	118.2±12.0	168.0±14.3	36.7±7.6	140.7±13.1	54.1±8.9	-0.49 ^{+0.06} _{-0.07}	-0.28 ^{+0.08} _{-0.07}	0.53 ^{+0.09} _{-0.09}	N	N	2.7	38.6	
6	<1.8	-	-	-	-	-	-	-	-	-	-	-	-	1.2	<36.5
7	<2.1	-	-	-	-	-	-	-	-	-	-	-	-	0.0	<36.6
8	26.4±7.4	6.0±4.1	16.9±5.6	22.9±6.5	3.5±4.4	23.5±6.3	2.8±4.4	-0.88 ^{+0.11} _{-0.12}	-0.32 ^{+0.21} _{-0.30}	0.59 ^{+0.59} _{-0.35}	N	N	0.1	37.7	
9	21.2±7.1	6.3±4.3	12.5±5.1	18.8±6.2	2.4±4.3	19.3±5.9	2.5±4.4	-0.87 ^{+0.12} _{-0.13}	-0.19 ^{+0.24} _{-0.29}	0.56 ^{+0.70} _{-0.40}	N	N	2.3	37.6	
10	<7.3	-	-	-	-	-	-	-	-	-	-	-	-	0.0	<37.1
11	<19.8	-	-	-	-	-	-	-	-	-	-	-	-	0.3	<37.6
12	<4.1	-	-	-	-	-	-	-	-	-	-	-	-	0.0	<36.9
13	207.0±15.9	56.3±8.8	107.0±11.6	163.3±14.1	43.7±8.1	141.7±13.1	57.8±9.1	-0.47 ^{+0.06} _{-0.07}	-0.17 ^{+0.05} _{-0.09}	0.40 ^{+0.10} _{-0.07}	N	N	1.8	38.6	
14	62.5±9.7	19.4±5.8	27.5±6.6	46.9±8.3	15.7±5.7	43.4±7.9	16.7±5.9	-0.50 ^{+0.12} _{-0.12}	-0.06 ^{+0.14} _{-0.13}	0.26 ^{+0.15} _{-0.16}	Y	N	0.7	38.1	
15	10.9±5.4	1.4±2.9	7.2±4.1	8.6±4.6	2.3±3.6	8.0±4.3	2.9±3.8	-0.61 ^{+0.21} _{-0.21}	-0.46 ^{+0.46} _{-0.43}	0.40 ^{+0.65} _{-0.43}	-	-	0.2	37.4	
16	18.4±6.3	2.7±3.4	5.0±3.8	7.8±4.6	10.6±5.0	4.8±3.8	11.9±5.2	0.39 ^{+0.30} _{-0.28}	-0.13 ^{+0.45} _{-0.57}	-0.27 ^{+0.27} _{-0.32}	-	-	2.6	37.5	
17	35.1±8.2	3.6±3.8	17.1±5.7	20.7±6.4	14.4±5.8	21.2±6.1	15.1±6.0	-0.24 ^{+0.17} _{-0.21}	-0.52 ^{+0.32} _{-0.47}	0.08 ^{+0.20} _{-0.17}	N	P	0.1	37.8	
18	<2.7	-	-	-	-	-	-	-	-	-	-	-	-	0.0	<36.7
19	9.0±5.4	-0.6±2.7	6.0±4.0	5.4±4.3	3.6±4.0	6.3±4.1	4.2±4.1	-0.34 ^{+0.40} _{-0.37}	-0.69 ^{+0.54} _{-0.91}	0.21 ^{+0.54} _{-0.42}	-	-	1.3	37.2	
20	<3.9	-	-	-	-	-	-	-	-	-	-	-	-	0.0	<36.9
21	<11.4	-	-	-	-	-	-	-	-	-	-	-	-	0.4	<37.4
22	9.5±5.4	5.3±4.0	4.0±3.6	9.3±4.8	0.2±3.2	7.0±4.3	0.0±3.2	-0.88 ^{+0.16} _{-0.12}	0.19 ^{+0.43} _{-0.40}	0.46 ^{+0.92} _{-0.61}	-	-	0.3	37.2	
23	<2.9	-	-	-	-	-	-	-	-	-	-	-	-	1.8	<36.7
24	5.2±4.9	4.4±3.6	1.0±3.2	5.3±4.3	-0.1±3.2	4.8±4.0	-0.7±3.2	-0.83 ^{+0.21} _{-0.17}	0.46 ^{+0.85} _{-0.54}	0.15 ^{+1.07} _{-0.99}	-	-	0.4	37.0	
25	<1.6	-	-	-	-	-	-	-	-	-	-	-	-	2.7	<36.5
26	24.3±6.7	0.6±2.7	13.1±5.0	13.6±5.2	10.7±4.8	11.9±4.8	11.3±5.0	-0.09 ^{+0.23} _{-0.23}	-0.84 ^{+0.38} _{-0.84}	0.10 ^{+0.21} _{-0.19}	N	N	0.5	37.6	
27	22.9±6.7	2.8±3.4	12.7±5.0	15.5±5.6	7.4±4.4	13.3±5.1	8.7±4.7	-0.28 ^{+0.24} _{-0.24}	-0.48 ^{+0.35} _{-0.49}	0.24 ^{+0.27} _{-0.21}	N	N	2.6	37.6	
28	<10.0	-	-	-	-	-	-	-	-	-	-	-	-	0.7	<37.3
29	23.2±6.7	3.5±3.4	13.5±5.1	17.0±5.7	6.2±4.3	15.4±5.3	6.7±4.4	-0.48 ^{+0.23} _{-0.23}	-0.43 ^{+0.27} _{-0.37}	0.32 ^{+0.30} _{-0.24}	N	P	0.2	37.6	
30	17.4±6.0	5.5±3.8	7.0±4.1	12.6±5.1	4.8±4.0	6.8±4.1	8.4±4.6	0.04 ^{+0.30} _{-0.31}	0.00 ^{+0.27} _{-0.29}	0.16 ^{+0.38} _{-0.32}	-	-	2.2	37.5	
31	121.3±12.4	30.2±6.7	66.0±9.3	96.2±11.0	25.1±6.5	78.6±10.0	36.6±7.5	-0.42 ^{+0.09} _{-0.08}	-0.23 ^{+0.09} _{-0.11}	0.43 ^{+0.12} _{-0.09}	N	N	1.6	38.3	
32	<0.9	-	-	-	-	-	-	-	-	-	-	-	-	0.0	<36.2
33	<3.0	-	-	-	-	-	-	-	-	-	-	-	-	1.3	<36.7
34	3.2±4.6	2.6±3.4	0.8±2.9	3.5±4.0	-0.3±3.2	0.5±2.9	0.1±3.4	-0.06 ^{+0.31} _{-0.34}	0.31 ^{+0.99} _{-0.69}	0.08 ^{+1.07} _{-0.00}	-	-	0.7	36.8	
35	41.0±8.1	8.0±4.3	19.8±5.8	27.7±6.7	13.3±5.2	26.4±6.5	15.7±5.6	-0.32 ^{+0.15} _{-0.17}	-0.30 ^{+0.21} _{-0.20}	0.17 ^{+0.19} _{-0.14}	N	N	1.1	37.9	
36	13.9±5.9	3.4±3.6	11.8±4.8	15.2±5.6	-1.4±2.9	15.2±5.3	-2.0±2.9	-0.98 ^{+0.04} _{-0.02}	-0.38 ^{+0.30} _{-0.45}	1.07 ^{+0.92} _{-0.54}	-	-	0.6	37.4	
37	<2.0	-	-	-	-	-	-	-	-	-	-	-	-	0.0	<36.6
38	<9.1	-	-	-	-	-	-	-	-	-	-	-	-	0.6	<37.2
39	26.3±4.4	5.0±3.6	14.8±5.1	19.8±5.8	7.0±4.1	16.6±5.3	9.7±4.6	-0.32 ^{+0.18} _{-0.20}	-0.35 ^{+0.22} _{-0.27}	0.32 ^{+0.24} _{-0.19}	N	P	3.4	37.7	
40	26.4±4.4	4.9±3.6	14.9±5.1	19.8±5.8	7.1±4.1	16.6±5.3	8.8±4.4	-0.37 ^{+0.19} _{-0.20}	-0.35 ^{+0.22} _{-0.27}	0.32 ^{+0.24} _{-0.19}	N	N	0.7	37.7	
41	157.7±14.0	31.2±6.9	89.7±10.6	120.9±12.3	36.8±7.5	102.0±11.3	51.1±8.5	-0.39 ^{+0.07} _{-0.08}	-0.37 ^{+0.10} _{-0.09}	0.41 ^{+0.10} _{-0.08}	N	N	0.6	38.5	
42	101.6±11.5	17.3±5.4	52.9±8.5	70.2±9.6	31.4±7.0	65.5±9.3	33.0±7.1	-0.39 ^{+0.09} _{-0.09}	-0.39 ^{+0.14} _{-0.11}	0.26 ^{+0.10} _{-0.10}	N	P	1.0	38.3	
43	39.0±7.9	8.3±4.3	21.3±5.9	29.6±6.8	9.4±4.7	28.0±6.5	10.8±5.0	-0.50 ^{+0.15} _{-0.16}	-0.29 ^{+0.16} _{-0.22}	0.38 ^{+0.18} _{-0.19}	N	N	2.7	37.9	
44	<2.3	-	-	-	-	-	-	-	-	-	-	-	-	1.6	<36.6
45	9.8±5.4	1.1±2.9	4.6±3.8	5.7±4.3	4.1±4.0	3.3±3.6	6.5±4.4	0.32 ^{+0.42} _{-0.39}	-0.31 ^{+0.54} _{-0.84}	0.05 ^{+0.51} _{-0.45}	-	-	0.2	37.2	
46	14.0±5.9	1.0±3.2	9.9±4.6	10.9±5.1	3.1±3.8	8.6±4.6	5.7±4.3	-0.30 ^{+0.34} _{-0.33}	-0.61 ^{+0.46} _{-0.77}	0.46 ^{+0.53} _{-0.38}	-	-	1.7	37.4	
47	<2.3	-	-	-	-	-	-	-	-	-	-	-	-	0.0	<36.6
48	10.4±3.5	2.3±3.2	5.2±3.8	7.5±4.4	2.5±3.4	7.7±4.3	3.1±3.6	-0.55 ^{+0.24} _{-0.31}	-0.19 ^{+0.43} _{-0.59}	0.27 ^{+0.59} _{-0.43}	N	N	0.9	37.3	

TABLE 9 — *Continued*

Masterid	B-band	S1-band	S2-band	Net Counts	H-band	Sc-band	Hc-band	HR	C21	C32	BB	Variability	Log L_X	
(1)	(2)	(3)	(4)	S-band (5)	(6)	(7)	(8)	(9)	(10)	(11)	(12)	k-S signif. (14)	(15)	
49	<14.1	-	-	-	-	-	-	-	-	-	-	-	1.3	≤37.4
50	41.8±8.1	8.4±4.3	24.9±6.3	33.2±7.1	8.5±4.6	26.9±6.5	12.7±5.2	-0.42 ^{+0.15} _{-0.16}	-0.38 ^{+0.19} _{-0.18}	0.46 ^{+0.24} _{-0.17}	N	N	1.1	38.0
51	<14.4	-	-	-	-	-	-	-	-	-	-	-	0.7	≤37.4
52	<15.0	-	-	-	-	-	-	-	-	-	-	-	0.2	≤37.4
53	11.6±3.9	3.5±3.6	3.9±3.6	7.3±4.6	5.1±4.0	3.8±3.8	6.7±4.3	0.27 ^{+0.39} _{-0.42}	0.05 ^{+0.49} _{-0.53}	-0.08 ^{+0.43} _{-0.43}	N	P	0.2	37.3
54	<13.4	-	-	-	-	-	-	-	-	-	-	-	1.1	≤37.4
55	<10.2	-	-	-	-	-	-	-	-	-	-	-	0.2	≤37.3
56	29.8±7.5	6.3±4.3	17.0±5.6	23.3±6.5	6.5±4.4	19.6±6.0	9.7±5.0	-0.41 ^{+0.20} _{-0.20}	-0.32 ^{+0.24} _{-0.27}	0.40 ^{+0.30} _{-0.24}	N	N	3.0	37.7
57	16.9±6.2	2.4±3.4	7.7±4.3	10.2±5.0	6.8±4.4	10.5±4.8	6.4±4.4	-0.34 ^{+0.31} _{-0.29}	-0.32 ^{+0.40} _{-0.59}	0.08 ^{+0.29} _{-0.29}	-	-	0.8	37.5
58	4.1±4.9	2.5±3.4	0.8±3.2	3.3±4.1	0.8±3.4	2.3±3.6	1.1±3.6	-0.29 ^{+0.23} _{-0.71}	0.31 ^{+0.99} _{-0.77}	0.00 ^{+0.99} _{-0.99}	-	-	0.8	36.9
59	19.8±6.8	2.3±3.6	16.4±5.6	18.7±6.2	1.1±3.6	15.7±5.7	4.5±4.3	-0.66 ^{+0.19} _{-0.22}	-0.62 ^{+0.35} _{-0.67}	0.86 ^{+0.78} _{-0.43}	-	-	2.9	37.6
60	16.5±5.9	5.6±3.8	7.2±4.1	12.8±5.1	3.7±3.8	8.8±4.4	5.4±4.1	-0.34 ^{+0.33} _{-0.31}	-0.03 ^{+0.30} _{-0.26}	0.27 ^{+0.43} _{-0.38}	-	-	1.4	37.5
61	<3.8	-	-	-	-	-	-	-	-	-	-	-	0.0	≤36.8
62	≤8.3	-	-	-	-	-	-	-	-	-	-	-	1.5	≤37.2
63	43.2±8.3	8.0±4.3	27.7±6.5	35.7±7.4	7.5±4.6	32.7±7.1	9.1±4.8	-0.62 ^{+0.14} _{-0.15}	-0.43 ^{+0.16} _{-0.21}	0.56 ^{+0.27} _{-0.18}	N	N	1.7	37.9
64	≤5.8	-	-	-	-	-	-	-	-	-	-	-	1.3	≤37.0
65	22.9±6.2	6.0±3.8	14.1±5.0	20.1±5.8	2.8±3.2	15.6±5.2	4.7±3.6	-0.59 ^{+0.17} _{-0.20}	-0.27 ^{+0.22} _{-0.19}	0.67 ^{+0.38} _{-0.19}	N	N	0.4	37.6
66	34.1±7.1	6.0±3.8	21.2±5.8	27.2±6.5	6.9±4.0	24.8±6.2	7.8±4.1	-0.57 ^{+0.13} _{-0.15}	-0.43 ^{+0.19} _{-0.21}	0.51 ^{+0.22} _{-0.22}	N	N	0.4	37.8
67	28.5±7.1	3.4±3.4	15.6±5.3	19.0±5.9	9.6±4.7	14.3±5.2	11.7±5.1	-0.17 ^{+0.20} _{-0.23}	-0.51 ^{+0.27} _{-0.40}	0.24 ^{+0.19} _{-0.21}	N	N	1.3	37.7
68	40.8±8.3	13.1±5.1	21.4±6.1	34.5±7.5	6.3±4.4	28.7±6.8	8.6±4.8	-0.60 ^{+0.16} _{-0.16}	-0.11 ^{+0.17} _{-0.17}	0.53 ^{+0.31} _{-0.25}	N	N	0.6	37.9
69	15.4±5.9	1.7±3.2	9.9±4.6	11.6±5.1	3.8±3.8	10.5±4.7	6.2±4.3	-0.35 ^{+0.29} _{-0.28}	-0.51 ^{+0.40} _{-0.67}	0.38 ^{+0.45} _{-0.33}	-	-	0.5	37.4
70	≤1.5	-	-	-	-	-	-	-	-	-	-	-	3.0	≤36.4
71	30.0±7.2	6.5±4.0	14.0±5.1	20.6±6.0	9.4±4.7	15.8±5.3	12.7±5.2	-0.18 ^{+0.21} _{-0.20}	-0.21 ^{+0.21} _{-0.25}	0.19 ^{+0.21} _{-0.19}	N	N	0.4	37.7
72	65.3±9.6	19.1±5.7	26.0±6.4	45.2±8.1	20.1±6.0	40.7±7.6	23.5±6.4	-0.33 ^{+0.12} _{-0.12}	-0.05 ^{+0.14} _{-0.13}	0.14 ^{+0.13} _{-0.14}	N	N	0.5	38.1
73	15.8±3.8	3.1±3.4	10.3±4.6	13.5±5.2	3.8±3.6	11.4±4.8	4.5±3.8	-0.52 ^{+0.25} _{-0.26}	-0.38 ^{+0.33} _{-0.42}	0.40 ^{+0.40} _{-0.29}	N	N	2.1	37.5
74	8.5±3.2	1.4±2.9	4.8±3.6	6.2±4.1	2.8±3.4	5.2±3.8	3.5±3.6	-0.32 ^{+0.39} _{-0.40}	-0.29 ^{+0.48} _{-0.70}	0.21 ^{+0.51} _{-0.42}	-	-	0.8	37.2
75	≤1.2	-	-	-	-	-	-	-	-	-	-	-	2.0	≤36.3
76	57.0±9.5	14.7±5.4	33.2±7.1	48.0±8.5	9.1±4.8	44.2±8.1	11.4±5.2	-0.64 ^{+0.12} _{-0.12}	-0.26 ^{+0.15} _{-0.16}	0.60 ^{+0.19} _{-0.22}	N	N	0.2	38.0
77	≤1.6	-	-	-	-	-	-	-	-	-	-	-	0.0	≤36.5
78	62.4±9.5	19.2±5.7	32.1±6.9	51.3±8.5	11.1±5.1	43.2±7.8	16.9±5.8	-0.49 ^{+0.11} _{-0.13}	-0.11 ^{+0.12} _{-0.14}	0.50 ^{+0.16} _{-0.20}	N	N	0.5	38.1
79	≤9.2	-	-	-	-	-	-	-	-	-	-	-	5.9	≤37.2
80	≤10.7	-	-	-	-	-	-	-	-	-	-	-	0.6	≤37.3
81	≤21.1	-	-	-	-	-	-	-	-	-	-	-	0.8	≤37.6
82	≤11.9	-	-	-	-	-	-	-	-	-	-	-	0.9	≤37.3
83	≤10.0	-	-	-	-	-	-	-	-	-	-	-	10.8	≤37.3
84	≤35.9	-	-	-	-	-	-	-	-	-	-	-	2.4	≤37.8
85	33.6±5.0	9.5±4.6	19.8±5.8	29.4±6.9	3.3±3.4	28.0±6.6	4.8±3.8	-0.75 ^{+0.12} _{-0.14}	-0.21 ^{+0.18} _{-0.19}	0.75 ^{+0.40} _{-0.29}	N	P	0.5	37.8
86	≤11.8	-	-	-	-	-	-	-	-	-	-	-	1.8	≤37.3
87	≤15.0	-	-	-	-	-	-	-	-	-	-	-	0.4	≤37.4
88	≤24.5	-	-	-	-	-	-	-	-	-	-	-	0.5	≤37.6
89	6.8±5.0	0.9±2.9	5.6±4.0	6.5±4.4	0.3±3.2	3.9±3.8	0.7±3.4	-0.63 ^{+0.29} _{-0.37}	-0.38 ^{+0.46} _{-0.84}	0.53 ^{+1.00} _{-0.53}	-	-	1.2	37.1
90	≤1.5	-	-	-	-	-	-	-	-	-	-	-	0.0	≤36.4
91	≤6.0	-	-	-	-	-	-	-	-	-	-	-	7.4	≤37.0
92	8.8±3.3	1.0±2.9	4.9±3.8	5.9±4.3	3.5±3.6	6.0±4.1	3.1±3.6	-0.45 ^{+0.28} _{-0.38}	-0.38 ^{+0.53} _{-0.77}	0.16 ^{+0.48} _{-0.43}	-	-	1.9	37.2
93	≤6.6	-	-	-	-	-	-	-	-	-	-	-	0.0	≤37.1
94	≤3.3	-	-	-	-	-	-	-	-	-	-	-	1.2	≤36.8
95	≤11.0	-	-	-	-	-	-	-	-	-	-	-	1.6	≤37.3
96	212.0±16.0	39.5±7.6	121.2±12.2	160.7±14.0	51.3±8.5	142.1±13.2	63.4±9.4	-0.44 ^{+0.06} _{-0.07}	-0.37 ^{+0.06} _{-0.10}	0.41 ^{+0.07} _{-0.08}	N	N	1.1	38.6
97	17.6±6.0	4.6±3.6	9.2±4.4	13.8±5.2	3.7±3.8	9.8±4.6	6.2±4.3	-0.31 ^{+0.29} _{-0.29}	-0.19 ^{+0.27} _{-0.30}	0.35 ^{+0.45} _{-0.30}	-	-	2.1	37.6
98	29.8±5.1	4.7±4.1	14.8±5.3	19.5±6.3	9.9±4.6	18.6±6.0	11.5±4.9	-0.30 ^{+0.30} _{-0.20}	-0.35 ^{+0.40} _{-0.40}	0.20 ^{+0.20} _{-0.20}	N	P	3.0	37.7
99	52.4±9.2	16.9±5.8	27.5±6.7	44.4±8.4	8.0±4.4	37.2±7.8	13.3±5.2	-0.52 ^{+0.12} _{-0.14}	-0.12 ^{+0.15} _{-0.15}	0.54 ^{+0.22} _{-0.19}	N	N	0.2	38.0

TABLE 9 — *Continued*

Masterid	B-band	S1-band	S2-band	Net Counts	H-band	Sc-band	Hc-band	HR	C21	C32	BB	Variability	k-S	signif.	Log L_x
(1)	(2)	(3)	(4)	S-band (5)	(6)	(7)	(8)	(9)	(10)	(11)	(12)	(13)	(14)	(15)	(15)
100	14.3±4.0	0.8±3.2	9.9±4.6	10.8±5.1	4.1±3.6	7.3±4.6	6.9±4.1	-0.07 ^{+0.32} _{-0.37}	-0.61 ^{+0.46} _{-0.77}	0.38 ^{+0.37} _{-0.30}	N	N	1.2	37.4	
101	34.2±7.9	10.9±5.1	14.1±5.4	25.0±7.0	9.2±4.4	19.5±6.4	10.7±4.7	-0.35 ^{+0.18} _{-0.20}	-0.04 ^{+0.25} _{-0.18}	0.21 ^{+0.21} _{-0.22}	N	N	1.9	37.8	
102	≤2.6	-	-	-	-	-	-	-	-	-	-	-	-	0.0	≤36.7
103	27.8±7.3	6.4±4.1	12.9±5.1	19.3±6.1	8.5±4.7	17.2±5.7	9.5±5.0	-0.36 ^{+0.22} _{-0.21}	-0.19 ^{+0.24} _{-0.27}	0.19 ^{+0.24} _{-0.22}	N	N	2.1	37.7	
104	34.2±7.7	11.2±5.1	17.9±5.7	29.1±7.2	5.1±3.8	25.1±6.7	7.0±4.1	-0.61 ^{+0.19} _{-0.16}	-0.12 ^{+0.19} _{-0.19}	0.58 ^{+0.24} _{-0.29}	N	N	0.6	37.8	
105	≤15.1	-	-	-	-	-	-	-	-	-	-	-	-	0.8	≤37.4
106	≤39.1	-	-	-	-	-	-	-	-	-	-	-	-	0.5	≤37.8
107	11.1±5.8	4.6±3.8	7.7±4.4	12.3±5.3	-1.2±3.2	11.3±5.0	0.1±3.6	-0.92 ^{+0.12} _{-0.08}	-0.11 ^{+0.32} _{-0.37}	0.84 ^{+0.92} _{-0.53}	-	-	0.0	37.3	
108	17.4±6.2	5.5±4.0	9.6±4.6	15.1±5.6	2.2±3.6	13.7±5.2	2.7±3.8	-0.79 ^{+0.13} _{-0.21}	-0.13 ^{+0.26} _{-0.30}	0.54 ^{+0.64} _{-0.41}	-	-	3.0	37.5	
109	10.9±4.0	4.8±4.0	5.8±4.2	10.7±5.3	0.7±3.0	9.1±4.9	1.2±3.2	-0.83 ^{+0.15} _{-0.17}	0.03 ^{+0.40} _{-0.46}	0.53 ^{+0.92} _{-0.45}	-	-	0.4	37.3	
110	30.5±8.1	4.6±4.3	17.4±5.9	22.0±6.9	8.5±4.8	20.1±6.4	11.2±5.3	-0.36 ^{+0.20} _{-0.22}	-0.43 ^{+0.32} _{-0.46}	0.32 ^{+0.27} _{-0.21}	N	N	0.9	37.7	
111	23.7±7.3	7.0±4.4	16.0±5.6	23.0±6.6	0.8±3.6	22.6±6.5	0.8±3.8	-0.95 ^{+0.07} _{-0.05}	-0.24 ^{+0.24} _{-0.30}	0.86 ^{+0.86} _{-0.40}	N	N	1.0	37.6	
112	3.4±5.1	-1.6±1.9	-0.8±2.3	-2.5±2.3	5.8±4.3	-2.3±1.9	6.5±4.4	0.96 ^{+0.04} _{-0.09}	-0.08 ^{+0.61} _{-1.14}	-0.84 ^{+0.51} _{-0.99}	-	-	0.7	36.8	
113	≤1.7	-	-	-	-	-	-	-	-	-	-	-	-	2.4	≤36.5
114	41.5±6.1	8.9±5.4	23.8±6.7	32.7±8.1	9.4±4.6	28.4±7.6	12.0±5.0	-0.46 ^{+0.15} _{-0.17}	-0.28 ^{+0.22} _{-0.31}	0.43 ^{+0.19} _{-0.21}	N	N	0.9	37.9	
115	6.7±5.5	0.7±3.4	5.6±4.1	6.4±4.8	0.3±3.4	6.3±4.6	-0.6±3.4	-0.85 ^{+0.19} _{-0.15}	-0.38 ^{+0.33} _{-0.84}	0.53 ^{+0.92} _{-0.53}	-	-	0.6	37.1	
116	≤7.2	-	-	-	-	-	-	-	-	-	-	-	-	3.0	≤37.1
117	7200.9±86.4	2734.7±53.7	3689.3±62.0	6424.1±81.6	776.8±29.1	5592.5±76.2	1134.2±34.9	-0.70 ^{+0.01} _{-0.01}	-0.04 ^{+0.01} _{-0.01}	0.71 ^{+0.01} _{-0.02}	N	P	53.1	40.1	
118	77.0±10.3	19.1±5.8	46.9±8.1	66.0±9.5	11.0±4.7	57.1±8.9	16.8±5.5	-0.59 ^{+0.09} _{-0.10}	-0.27 ^{+0.10} _{-0.15}	0.67 ^{+0.14} _{-0.07}	N	N	0.0	38.1	
119	252.1±18.3	41.3±8.8	153.8±14.2	195.1±16.3	57.1±8.9	175.3±15.5	71.1±9.8	-0.48 ^{+0.10} _{-0.06}	-0.47 ^{+0.08} _{-0.10}	0.45 ^{+0.08} _{-0.06}	N	N	1.5	38.7	
120	95.7±13.4	24.3±8.0	51.1±9.6	75.4±12.0	20.3±6.2	72.9±11.6	21.3±6.5	-0.60 ^{+0.09} _{-0.11}	-0.22 ^{+0.15} _{-0.15}	0.42 ^{+0.15} _{-0.12}	N	N	1.4	38.2	
121	6.3±2.9	2.1±2.9	4.0±3.4	6.0±4.0	0.7±2.9	5.6±3.8	1.6±3.2	-0.69 ^{+0.21} _{-0.31}	-0.13 ^{+0.45} _{-0.54}	0.46 ^{+0.84} _{-0.54}	-	-	2.3	37.1	
122	≤2.0	-	-	-	-	-	-	-	-	-	-	-	-	1.2	≤36.6
123	70.6±10.7	23.1±6.8	31.8±7.5	54.9±9.7	15.7±5.3	43.5±8.8	23.0±6.2	-0.37 ^{+0.12} _{-0.13}	-0.07 ^{+0.15} _{-0.13}	0.33 ^{+0.15} _{-0.19}	N	N	6.6	38.1	
124	41.5±8.8	18.0±6.2	20.4±6.2	38.5±8.3	3.0±3.6	36.1±7.9	5.4±4.1	-0.79 ^{+0.11} _{-0.13}	0.02 ^{+0.19} _{-0.15}	0.76 ^{+0.32} _{-0.35}	N	N	1.4	37.9	
125	14.4±3.6	2.4±3.2	9.5±4.4	11.9±5.0	2.0±3.2	8.8±4.4	4.7±3.8	-0.39 ^{+0.29} _{-0.31}	-0.43 ^{+0.38} _{-0.51}	0.59 ^{+0.59} _{-0.40}	N	N	0.9	37.4	
126	5.4±3.0	0.7±2.9	2.2±3.2	2.9±3.8	2.5±3.4	3.1±3.6	3.1±3.6	-0.07 ^{+0.31} _{-0.56}	-0.15 ^{+0.76} _{-0.92}	-0.03 ^{+0.73} _{-0.72}	-	-	0.4	37.0	
127	9.8±4.2	4.1±4.2	4.5±4.2	8.6±5.4	1.2±3.0	9.8±5.3	1.3±3.2	-0.83 ^{+0.15} _{-0.17}	0.05 ^{+0.62} _{-0.61}	0.43 ^{+0.86} _{-0.67}	-	-	0.2	37.2	
128	≤29.2	-	-	-	-	-	-	-	-	-	-	-	-	1.7	≤37.7
129	≤25.7	-	-	-	-	-	-	-	-	-	-	-	-	0.8	≤37.7
130	10.7±6.0	0.9±3.4	10.3±4.8	11.2±5.5	-0.6±3.2	11.2±5.2	-0.4±3.4	-0.93 ^{+0.10} _{-0.07}	-0.61 ^{+0.46} _{-0.77}	0.92 ^{+0.84} _{-0.54}	-	-	0.3	37.3	
131	≤1.4	-	-	-	-	-	-	-	-	-	-	-	-	2.6	≤36.4
132	65.5±11.1	24.8±7.3	31.7±7.8	56.5±10.2	9.0±4.7	50.4±9.7	11.0±5.1	-0.69 ^{+0.10} _{-0.11}	-0.05 ^{+0.18} _{-0.21}	0.55 ^{+0.23} _{-0.19}	N	N	0.5	38.1	
133	82.1±10.5	19.4±5.7	36.5±7.3	55.8±8.8	26.3±6.5	50.8±8.4	29.9±6.9	-0.32 ^{+0.10} _{-0.11}	-0.16 ^{+0.11} _{-0.15}	0.16 ^{+0.14} _{-0.10}	N	N	1.6	38.2	
134	13.3±5.0	4.5±3.4	6.5±3.8	10.9±4.6	2.4±2.9	11.3±4.6	2.2±2.9	-0.73 ^{+0.14} _{-0.22}	-0.05 ^{+0.26} _{-0.27}	0.40 ^{+0.43} _{-0.32}	-	-	0.8	37.4	
135	≤31.6	-	-	-	-	-	-	-	-	-	-	-	-	0.7	≤37.8
136	≤3.4	-	-	-	-	-	-	-	-	-	-	-	-	0.0	≤36.8
137	≤19.0	-	-	-	-	-	-	-	-	-	-	-	-	1.9	≤37.5
138	≤15.8	-	-	-	-	-	-	-	-	-	-	-	-	1.2	≤37.5
139	≤4.5	-	-	-	-	-	-	-	-	-	-	-	-	10.4	≤36.9
140	29.1±4.8	9.5±4.6	14.1±5.1	23.7±6.4	5.9±4.0	22.9±6.2	6.6±4.1	-0.61 ^{+0.16} _{-0.17}	-0.08 ^{+0.19} _{-0.21}	0.38 ^{+0.26} _{-0.22}	N	N	2.9	37.7	
141	19.0±6.7	3.8±3.8	15.1±5.4	18.9±6.2	0.0±3.4	20.8±6.2	-0.8±3.4	-0.98 ^{+0.06} _{-0.02}	-0.46 ^{+0.33} _{-0.43}	0.92 ^{+0.91} _{-0.39}	-	-	1.0	37.5	
142	≤13.9	-	-	-	-	-	-	-	-	-	-	-	-	0.6	≤37.4
143	19.0±6.3	-0.5±2.3	8.4±4.4	7.9±4.6	11.1±5.0	5.2±4.0	13.4±5.3	0.41 ^{+0.27} _{-0.28}	-0.92 ^{+0.54} _{-0.91}	-0.08 ^{+0.21} _{-0.24}	-	-	1.4	37.5	
144	≤11.5	-	-	-	-	-	-	-	-	-	-	-	-	0.0	≤37.3
145	≤5.3	-	-	-	-	-	-	-	-	-	-	-	-	1.5	≤37.0
146	308.3±19.2	59.1±9.2	183.0±14.9	242.0±17.1	66.3±9.4	214.9±16.1	88.7±10.7	-0.47 ^{+0.05} _{-0.05}	-0.40 ^{+0.07} _{-0.07}	0.47 ^{+0.07} _{-0.06}	N	Y	0.2	38.7	
147	52.7±9.0	13.8±5.3	33.0±7.1	46.8±8.5	5.9±4.0	39.1±7.8	11.5±4.8	-0.59 ^{+0.11} _{-0.13}	-0.30 ^{+0.18} _{-0.14}	0.75 ^{+0.25} _{-0.22}	N	Y	0.7	38.0	
148	72.3±9.8	17.9±5.4	34.8±7.1	52.6±8.5	19.6±5.7	41.4±7.6	26.3±6.4	-0.29 ^{+0.10} _{-0.13}	-0.20 ^{+0.13} _{-0.13}	0.27 ^{+0.14} _{-0.11}	N	N	0.1	38.1	
149	≤5.1	-	-	-	-	-	-	-	-	-	-	-	-	4.7	≤37.0

TABLE 9 — Continued

Masterid	B-band	S1-band	S2-band	Net Counts		H-band	Sc-band	Hc-band	HR	C21	C32	BB	Variability	Log L_x	
(1)	(2)	(3)	(4)	S-band	(5)	(6)	(7)	(8)	(9)	(10)	(11)	(12)	k-S	signif.	(15)
150	<9.4	-	-	-	-	-	-	-	-	-	-	-	-	0.3	≤37.2
151	≤10.5	-	-	-	-	-	-	-	-	-	-	-	-	0.2	≤37.3
152	22.5±6.1	15.2±5.1	5.3±3.6	20.5±5.8	2.0±2.9	16.9±5.3	1.9±2.9	-0.86 ^{+0.08} _{-0.14}	0.51 ^{+0.24} _{-0.22}	0.38 ^{+0.53} _{-0.41}	N	N	3.3	37.6	
153	≤5.3	-	-	-	-	-	-	-	-	-	-	-	-	1.2	≤37.0
154	45.0±8.5	12.5±5.1	19.1±5.8	31.6±7.2	13.3±5.1	28.5±6.9	16.3±5.4	-0.33 ^{+0.13} _{-0.17}	-0.09 ^{+0.18} _{-0.18}	0.18 ^{+0.17} _{-0.16}	N	N	1.4	37.9	
155	20.4±6.6	7.5±4.3	9.8±4.7	17.2±5.9	3.1±3.8	10.4±5.0	5.7±4.3	-0.39 ^{+0.31} _{-0.31}	-0.03 ^{+0.27} _{-0.24}	0.43 ^{+0.56} _{-0.35}	N	N	0.9	37.6	
156	≤1.5	-	-	-	-	-	-	-	-	-	-	-	-	0.0	≤36.4
157	36.3±5.2	7.2±4.1	21.2±5.9	28.4±6.7	7.6±4.3	25.1±6.4	10.4±4.7	-0.47 ^{+0.15} _{-0.17}	-0.35 ^{+0.19} _{-0.21}	0.46 ^{+0.21} _{-0.19}	N	N	2.9	37.8	
158	161.8±9.7	31.5±6.9	98.2±11.0	129.7±12.6	31.4±6.9	109.6±11.7	46.1±8.1	-0.46 ^{+0.06} _{-0.08}	-0.38 ^{+0.08} _{-0.11}	0.53 ^{+0.09} _{-0.09}	N	N	4.8	38.5	
159	≤4.8	-	-	-	-	-	-	-	-	-	-	-	-	0.7	≤37.0
160	33.1±7.8	7.0±4.3	21.8±6.2	28.8±7.1	4.3±4.1	24.0±6.5	7.1±4.7	-0.62 ^{+0.19} _{-0.18}	-0.38 ^{+0.22} _{-0.24}	0.67 ^{+0.46} _{-0.29}	N	N	1.2	37.8	
161	≤5.0	-	-	-	-	-	-	-	-	-	-	-	-	0.0	≤37.0
162	35.3±8.0	13.7±5.2	19.9±5.9	33.6±7.4	1.8±3.8	26.1±6.6	4.4±4.3	-0.80 ^{+0.10} _{-0.14}	-0.08 ^{+0.18} _{-0.13}	0.92 ^{+0.68} _{-0.46}	N	N	0.9	37.8	
163	97.5±7.7	12.4±5.0	62.1±9.0	74.5±9.9	23.0±6.2	61.4±9.1	34.7±7.2	-0.34 ^{+0.08} _{-0.11}	-0.60 ^{+0.14} _{-0.16}	0.45 ^{+0.46} _{-0.10}	N	N	2.3	38.2	
164	≤10.6	-	-	-	-	-	-	-	-	-	-	-	-	0.7	≤37.3
165	11.2±3.6	3.6±3.4	8.3±4.3	11.9±5.0	-0.3±2.7	11.5±4.8	-0.5±2.7	-0.96 ^{+0.06} _{-0.04}	-0.24 ^{+0.32} _{-0.35}	0.92 ^{+0.84} _{-0.54}	N	N	0.8	37.3	
166	21.6±6.9	10.9±4.8	5.3±4.1	16.2±5.9	5.4±4.3	10.6±5.1	7.9±4.7	-0.23 ^{+0.30} _{-0.31}	0.38 ^{+0.34} _{-0.30}	0.03 ^{+0.45} _{-0.43}	N	P	0.6	37.6	
167	≤10.1	-	-	-	-	-	-	-	-	-	-	-	-	0.3	≤37.3
168	15.5±5.3	2.4±2.9	10.1±4.4	12.5±4.8	3.0±3.2	11.8±4.7	3.8±3.4	-0.57 ^{+0.20} _{-0.24}	-0.46 ^{+0.30} _{-0.40}	0.51 ^{+0.38} _{-0.30}	-	-	1.3	37.5	
169	49.3±8.7	20.2±5.8	27.3±6.5	47.5±8.3	1.8±3.6	41.8±7.8	5.3±4.3	-0.83 ^{+0.11} _{-0.10}	-0.04 ^{+0.14} _{-0.12}	0.98 ^{+0.75} _{-0.35}	N	N	1.1	37.9	
170	25.4±6.9	8.0±4.3	14.3±5.2	22.3±6.3	3.1±3.8	20.6±6.0	3.6±4.0	-0.80 ^{+0.10} _{-0.12}	-0.16 ^{+0.21} _{-0.22}	0.59 ^{+0.34} _{-0.35}	N	P	0.8	37.7	
171	16.3±6.0	5.2±3.8	10.0±4.6	15.3±5.4	1.0±3.4	12.4±5.0	1.7±3.6	-0.85 ^{+0.13} _{-0.15}	-0.16 ^{+0.24} _{-0.30}	0.70 ^{+0.78} _{-0.46}	-	-	0.2	37.5	
172	10.7±6.3	5.6±4.0	3.6±3.8	9.2±5.0	1.3±3.6	8.6±4.7	0.5±3.6	-0.86 ^{+0.16} _{-0.14}	0.24 ^{+0.31} _{-0.43}	0.24 ^{+0.91} _{-0.67}	-	-	1.2	37.3	
173	≤1.5	-	-	-	-	-	-	-	-	-	-	-	-	6.8	≤36.4
174	≤1.6	-	-	-	-	-	-	-	-	-	-	-	-	1.2	≤36.5
175	8.0±3.2	1.7±2.9	3.1±3.4	4.7±4.0	2.7±3.4	4.6±3.8	3.4±3.6	-0.25 ^{+0.41} _{-0.47}	-0.11 ^{+0.62} _{-0.72}	0.05 ^{+0.65} _{-0.59}	-	-	0.8	37.2	
176	≤1.4	-	-	-	-	-	-	-	-	-	-	-	-	1.3	≤36.4
177	≤2.6	-	-	-	-	-	-	-	-	-	-	-	-	0.0	≤36.7
178	≤3.9	-	-	-	-	-	-	-	-	-	-	-	-	2.2	≤36.8
179	9.4±3.3	-0.5±2.3	7.2±4.1	6.7±4.3	1.6±3.2	3.6±3.6	5.3±4.0	0.16 ^{+0.44} _{-0.45}	-0.84 ^{+0.53} _{-0.92}	0.54 ^{+0.69} _{-0.46}	-	-	2.0	37.2	
180	≤10.2	-	-	-	-	-	-	-	-	-	-	-	-	0.5	≤37.3
181	19.6±6.4	4.5±3.8	9.5±4.6	14.0±5.4	5.6±4.1	10.5±4.8	6.0±4.3	-0.36 ^{+0.29} _{-0.30}	-0.21 ^{+0.29} _{-0.35}	0.24 ^{+0.32} _{-0.29}	-	-	0.8	37.6	
182	4.4±2.8	2.5±3.2	2.8±3.2	5.3±4.0	-0.3±2.7	3.1±3.4	1.6±3.2	-0.42 ^{+0.30} _{-0.58}	0.05 ^{+0.37} _{-0.59}	0.46 ^{+1.07} _{-0.61}	-	-	1.3	36.9	
183	16.1±6.0	2.0±3.2	6.1±4.0	8.0±4.6	8.0±4.6	7.4±4.3	8.5±4.7	-0.01 ^{+0.32} _{-0.31}	-0.29 ^{+0.45} _{-0.62}	-0.08 ^{+0.29} _{-0.30}	-	-	0.4	37.5	
184	295.1±18.5	37.0±7.3	188.2±14.8	225.3±16.2	69.8±9.6	197.7±15.2	94.2±11.0	-0.42 ^{+0.05} _{-0.05}	-0.60 ^{+0.06} _{-0.10}	0.46 ^{+0.07} _{-0.06}	N	N	2.1	38.7	
185	65.3±6.5	11.6±4.7	39.7±7.5	51.3±8.4	14.5±5.2	45.9±8.0	18.3±5.7	-0.49 ^{+0.10} _{-0.12}	-0.44 ^{+0.15} _{-0.15}	0.46 ^{+0.14} _{-0.14}	N	N	2.7	38.1	
186	≤4.5	-	-	-	-	-	-	-	-	-	-	-	-	1.9	≤36.9
187	39.1±8.2	9.4±4.6	21.6±6.1	31.1±7.1	8.1±4.7	27.8±6.7	11.3±5.2	-0.49 ^{+0.17} _{-0.16}	-0.27 ^{+0.19} _{-0.19}	0.43 ^{+0.24} _{-0.22}	N	N	0.0	37.9	
188	≤7.2	-	-	-	-	-	-	-	-	-	-	-	-	1.2	≤37.1
189	14.0±3.7	1.4±2.9	10.6±4.6	12.1±5.0	2.7±3.4	10.9±4.7	3.4±3.6	-0.63 ^{+0.21} _{-0.25}	-0.62 ^{+0.41} _{-0.67}	0.54 ^{+0.51} _{-0.35}	N	P	1.2	37.4	
190	32.3±7.5	10.3±4.6	18.6±5.7	28.8±6.8	3.5±4.0	22.3±6.1	6.8±4.6	-0.61 ^{+0.19} _{-0.19}	-0.16 ^{+0.16} _{-0.19}	0.67 ^{+0.51} _{-0.32}	N	N	1.1	37.8	
191	20.9±6.7	7.0±4.3	9.2±4.6	16.2±5.8	4.7±4.1	11.5±5.1	6.3±4.4	-0.38 ^{+0.29} _{-0.30}	-0.03 ^{+0.27} _{-0.27}	0.29 ^{+0.41} _{-0.32}	N	N	0.4	37.6	
192	17.9±6.2	0.1±2.7	9.1±4.6	9.2±4.8	8.7±4.6	8.5±4.6	10.2±4.8	0.02 ^{+0.28} _{-0.28}	-0.76 ^{+0.45} _{-0.92}	0.05 ^{+0.24} _{-0.24}	-	-	0.7	37.5	
193	5.5±5.0	1.7±3.2	2.5±3.4	4.1±4.1	1.4±3.6	2.4±3.6	3.0±4.0	0.02 ^{+0.47} _{-0.45}	-0.03 ^{+0.78} _{-0.83}	0.11 ^{+0.94} _{-0.75}	-	-	0.6	37.0	
194	70.5±6.7	14.4±5.1	37.8±7.3	52.2±8.5	17.6±5.6	44.1±7.8	23.3±6.2	-0.37 ^{+0.11} _{-0.12}	-0.30 ^{+0.13} _{-0.15}	0.36 ^{+0.13} _{-0.13}	N	Y	1.7	38.1	
195	27.5±7.0	6.7±4.0	19.9±5.8	26.6±6.5	0.8±3.4	23.7±6.2	2.4±3.8	-0.89 ^{+0.08} _{-0.11}	-0.38 ^{+0.22} _{-0.18}	0.99 ^{+0.83} _{-0.40}	N	N	0.0	37.7	
196	≤4.9	-	-	-	-	-	-	-	-	-	-	-	-	2.0	≤37.0
197	21.2±6.6	4.4±3.8	12.3±5.0	16.7±5.8	4.5±4.0	12.1±5.1	7.7±4.6	-0.30 ^{+0.26} _{-0.27}	-0.32 ^{+0.29} _{-0.35}	0.43 ^{+0.37} _{-0.32}	N	P	1.9	37.6	
198	≤3.1	-	-	-	-	-	-	-	-	-	-	-	-	0.0	≤36.8
199	16.2±6.1	6.7±4.1	6.5±4.1	13.2±5.3	3.0±3.8	10.5±4.8	5.6±4.3	-0.41 ^{+0.31} _{-0.29}	0.11 ^{+0.29} _{-0.30}	0.29 ^{+0.60} _{-0.42}	-	-	2.1	37.5	

TABLE 9 — *Continued*

Masterid	B-band	S1-band	S2-band	Net Counts			HR	C21	C32	Variability			Log L_X	
(1)	(2)	(3)	(4)	S-band	H-band	Sc-band	Hc-band	(9)	(10)	(11)	BB	k-S	signif.	(0.3–8.0 keV)
				(5)	(6)	(7)	(8)				(12)	(13)	(14)	(15)
200	<1.4	-	-	-	-	-	-	-	-	-	-	-	1.8	≤36.4
201	15.4±6.0	1.7±3.2	3.8±3.6	5.5±4.3	10.0±4.8	1.7±3.4	11.5±5.1	0.78 ^{+0.22} _{-0.17}	-0.16 ^{+0.59} _{-0.78}	-0.35 ^{+0.35} _{-0.40}	-	-	2.4	37.5
202	29.1±7.1	5.3±3.8	17.8±5.4	23.1±6.2	6.0±4.3	21.3±5.9	6.7±4.4	-0.59 ^{+0.18} _{-0.19}	-0.40 ^{+0.21} _{-0.37}	0.46 ^{+0.32} _{-0.22}	N	N	1.3	37.7
203	22.6±6.6	5.3±3.8	11.8±4.8	17.1±5.7	5.5±4.1	14.6±5.2	5.8±4.3	-0.52 ^{+0.24} _{-0.24}	-0.24 ^{+0.34} _{-0.27}	0.32 ^{+0.32} _{-0.27}	N	N	0.8	37.6
204	≤2.4	-	-	-	-	-	-	-	-	-	-	-	0.0	≤36.6
205	14.3±5.9	2.2±3.2	10.4±4.7	12.5±5.2	1.8±3.6	10.9±4.8	3.2±4.0	-0.68 ^{+0.16} _{-0.18}	-0.48 ^{+0.37} _{-0.57}	0.59 ^{+0.72} _{-0.40}	-	-	1.1	37.4
206	≤11.9	-	-	-	-	-	-	-	-	-	-	-	0.2	≤37.4
207	≤3.9	-	-	-	-	-	-	-	-	-	-	-	0.0	≤36.8
208	11.2±5.5	-0.6±2.3	10.2±4.6	9.7±4.7	1.5±3.6	8.6±4.4	3.1±4.0	-0.63 ^{+0.19} _{-0.19}	-0.99 ^{+0.46} _{-1.00}	0.62 ^{+0.77} _{-0.43}	-	-	0.2	37.3
209	60.7±9.3	3.1±3.4	32.3±6.9	35.3±7.3	25.4±6.5	27.9±6.5	33.0±7.1	0.01 ^{+0.13} _{-0.13}	-0.81 ^{+0.56} _{-0.48}	0.13 ^{+0.12} _{-0.12}	N	N	1.1	38.1
210	13.2±5.7	5.7±3.8	6.6±4.1	12.3±5.1	0.8±3.4	10.6±4.7	3.2±4.0	-0.67 ^{+0.16} _{-0.19}	0.03 ^{+0.29} _{-0.30}	0.54 ^{+0.85} _{-0.49}	-	-	0.7	37.4
211	≤5.6	-	-	-	-	-	-	-	-	-	-	-	2.0	≤37.0
212	≤3.2	-	-	-	-	-	-	-	-	-	-	-	1.3	≤36.8
213	12.0±3.4	2.3±2.9	2.8±3.2	5.1±3.8	7.0±4.1	5.8±3.8	6.6±4.1	-0.02 ^{+0.32} _{-0.33}	0.03 ^{+0.51} _{-0.54}	-0.32 ^{+0.37} _{-0.43}	N	N	1.6	37.3
214	≤5.6	-	-	-	-	-	-	-	-	-	-	-	0.3	≤37.0
215	≤1.6	-	-	-	-	-	-	-	-	-	-	-	2.4	≤36.5
216	24.1±6.9	9.1±4.4	9.5±4.6	18.5±5.9	5.6±4.4	14.7±5.3	6.2±4.6	-0.52 ^{+0.26} _{-0.24}	0.08 ^{+0.21} _{-0.24}	0.24 ^{+0.38} _{-0.32}	N	N	0.9	37.6
217	7.3±3.0	1.1±2.7	4.9±3.6	6.0±4.0	1.8±3.2	5.8±3.8	2.5±3.4	-0.55 ^{+0.21} _{-0.29}	-0.38 ^{+0.36} _{-0.69}	0.35 ^{+0.67} _{-0.46}	-	-	2.0	37.1
218	≤10.9	-	-	-	-	-	-	-	-	-	-	-	0.4	≤37.3
219	≤3.4	-	-	-	-	-	-	-	-	-	-	-	1.5	≤36.8
220	91.7±11.0	31.1±6.8	48.4±8.1	79.5±10.2	12.2±5.1	73.4±9.8	12.9±5.2	-0.74 ^{+0.07} _{-0.08}	-0.12 ^{+0.14} _{-0.06}	0.61 ^{+0.16} _{-0.15}	N	N	3.3	38.3
221	5.8±3.8	-0.2±1.9	2.7±2.9	2.5±2.9	3.4±3.2	0.6±2.3	5.3±3.6	0.79 ^{+0.13} _{-0.18}	-0.69 ^{+0.51} _{-0.99}	-0.05 ^{+0.37} _{-0.41}	-	-	1.4	37.0
222	≤1.0	-	-	-	-	-	-	-	-	-	-	-	0.0	≤36.7
223	31.9±7.3	3.7±3.4	20.7±5.9	24.3±6.4	7.6±4.4	20.5±5.9	10.1±4.8	-0.41 ^{+0.17} _{-0.19}	-0.59 ^{+0.24} _{-0.35}	0.46 ^{+0.21} _{-0.22}	N	N	2.3	37.8
224	≤2.8	-	-	-	-	-	-	-	-	-	-	-	0.0	≤36.8
225	45.8±8.4	9.6±4.6	28.6±6.6	38.2±7.6	7.6±4.4	30.7±6.9	13.2±5.2	-0.46 ^{+0.14} _{-0.14}	-0.35 ^{+0.16} _{-0.19}	0.59 ^{+0.24} _{-0.19}	N	P	0.8	37.9
226	≤2.9	-	-	-	-	-	-	-	-	-	-	-	3.0	≤36.7
227	74.4±10.2	15.4±5.2	47.1±8.1	62.5±9.2	11.9±5.2	54.4±8.6	18.7±6.0	-0.54 ^{+0.09} _{-0.12}	-0.36 ^{+0.12} _{-0.15}	0.62 ^{+0.16} _{-0.17}	N	N	1.0	38.1
228	276.2±17.9	36.8±7.2	162.1±13.8	198.9±15.2	77.2±10.1	166.8±14.0	105.8±11.6	-0.29 ^{+0.05} _{-0.07}	-0.53 ^{+0.06} _{-0.10}	0.35 ^{+0.07} _{-0.05}	N	N	12.8	38.7
229	37.5±7.8	6.9±4.0	22.8±6.1	29.7±6.8	7.8±4.6	26.5±6.5	10.4±5.0	-0.50 ^{+0.16} _{-0.16}	-0.40 ^{+0.19} _{-0.22}	0.48 ^{+0.22} _{-0.21}	N	N	0.6	37.8
230	22.5±6.5	5.9±4.0	12.6±4.8	18.6±5.8	3.9±3.8	14.1±5.1	6.6±4.3	-0.45 ^{+0.23} _{-0.23}	-0.21 ^{+0.24} _{-0.25}	0.48 ^{+0.43} _{-0.29}	N	N	0.3	37.6
231	10.3±3.1	1.4±2.7	7.1±4.0	8.5±4.3	2.1±3.2	8.1±4.1	2.6±3.4	-0.64 ^{+0.16} _{-0.25}	-0.48 ^{+0.40} _{-0.57}	0.46 ^{+0.59} _{-0.41}	N	N	2.3	37.3
232	9.7±5.1	8.4±4.3	2.1±3.2	10.5±4.8	-0.8±2.7	4.7±3.8	-0.3±2.9	-0.84 ^{+0.19} _{-0.16}	0.59 ^{+0.59} _{-0.40}	0.46 ^{+1.07} _{-0.84}	-	-	0.2	37.3
233	5.9±2.6	2.3±2.9	4.2±3.4	6.5±4.0	0.0±2.7	6.1±3.8	-0.4±2.7	-0.92 ^{+0.15} _{-0.08}	-0.11 ^{+0.40} _{-0.45}	0.61 ^{+0.92} _{-0.53}	-	-	1.6	37.0
234	≤14.0	-	-	-	-	-	-	-	-	-	-	-	1.2	≤37.4
235	≤1.6	-	-	-	-	-	-	-	-	-	-	-	0.0	≤36.5
236	≤2.9	-	-	-	-	-	-	-	-	-	-	-	2.3	≤36.7

NOTE. — Col. (1): Master ID, cols. (2)–(8): net counts, in each of the 7 energy bands (see Table 2 for definitions of these bands), col. (9): hardness ratio, cols. (10) and (11) color values, errors are given as 1σ , cols. (12) and (13): short-term variability, where (BB) indicate Bayesian block analysis and (K-S) indicates the Kolmogorov-Smirnov test, in both columns symbols indicate - (N) non-variable in all observations, (V) variable in at least one observation, (P) possible variability in at least one observation, col. (14): the significance of the change in L_X between the previous observation and the current observation respectively (equation 2), col. (15): $\log L_X$ (0.3–8.0 keV). Upper limit values of net B and L_X are at the 68% confidence level.

TABLE 10
SOURCE COUNTS, HARDNESS RATIOS, COLOR-COLOR VALUES AND VARIABILITY:
OBSERVATION 6

Masterid (1)	B-band (2)	S1-band (3)	S2-band (4)	Net Counts			Hc-band (8)	HR (9)	C21 (10)	C32 (11)	Variability			Log L_X (0.3–8.0 keV) (15)	
				S-band (5)	H-band (6)	Sc-band (7)					BB (12)	k-S (13)	signif. (14)		
1	10.1±5.4	-1.0±2.3	7.3±4.1	6.4±4.3	3.7±4.0	5.9±4.0	4.2±4.1	-0.33 ^{+0.41} _{-0.37}	-0.92 ^{+0.54} _{-0.91}	0.27 ^{+0.51} _{-0.38}	-	-	2.1	37.6	
2	47.4±8.4	9.8±4.4	24.2±6.2	34.0±7.1	13.3±5.2	31.0±6.8	14.9±5.4	-0.46 ^{+0.13} _{-0.14}	-0.16 ^{+0.15} _{-0.20}	0.31 ^{+0.16} _{-0.16}	N	N	1.1	38.3	
3	<3.0	-	-	-	-	-	-	-	-	-	-	-	-	0.0	<37.1
4	20.7±6.3	3.8±3.4	13.5±5.0	17.3±5.6	3.4±3.8	13.2±5.0	4.9±4.1	-0.60 ^{+0.23} _{-0.23}	-0.32 ^{+0.27} _{-0.32}	0.56 ^{+0.49} _{-0.32}	N	N	1.8	37.9	
5	85.8±10.7	22.6±6.0	51.1±8.3	73.7±9.8	12.1±5.1	58.5±8.9	20.9±6.1	-0.54 ^{+0.09} _{-0.10}	-0.20 ^{+0.10} _{-0.12}	0.66 ^{+0.14} _{-0.17}	N	N	1.1	38.5	
6	<4.7	-	-	-	-	-	-	-	-	-	-	-	-	0.0	<37.3
7	6.8±4.6	2.1±2.9	2.6±3.2	4.7±3.8	2.1±3.4	1.6±2.9	3.7±3.8	0.34 ^{+0.39} _{-0.28}	0.03 ^{+0.59} _{-0.67}	0.08 ^{+0.75} _{-0.67}	-	-	1.4	37.4	
8	21.7±6.2	7.4±4.0	8.9±4.3	16.3±5.3	5.5±4.0	11.8±4.7	9.2±4.6	-0.23 ^{+0.22} _{-0.24}	0.08 ^{+0.21} _{-0.21}	0.24 ^{+0.30} _{-0.27}	N	N	1.3	37.9	
9	<7.8	-	-	-	-	-	-	-	-	-	-	-	-	1.1	<37.5
10	<4.2	-	-	-	-	-	-	-	-	-	-	-	-	0.0	<37.2
11	<11.0	-	-	-	-	-	-	-	-	-	-	-	-	0.0	<37.6
12	<1.3	-	-	-	-	-	-	-	-	-	-	-	-	0.0	<36.7
13	88.8±10.7	17.0±5.3	48.5±8.1	65.4±9.3	23.3±6.2	55.2±8.6	31.1±6.9	-0.39 ^{+0.09} _{-0.10}	-0.26 ^{+0.11} _{-0.14}	0.35 ^{+0.13} _{-0.09}	N	N	0.5	38.6	
14	26.4±6.6	6.9±4.0	15.3±5.1	22.2±6.0	4.2±3.6	18.9±5.6	6.0±4.0	-0.59 ^{+0.16} _{-0.18}	-0.19 ^{+0.19} _{-0.21}	0.56 ^{+0.33} _{-0.27}	N	N	0.5	38.0	
15	12.1±5.1	2.3±2.9	5.3±3.6	7.6±4.1	4.6±3.8	6.1±3.8	5.4±4.0	-0.16 ^{+0.35} _{-0.33}	-0.21 ^{+0.37} _{-0.46}	0.08 ^{+0.38} _{-0.32}	-	-	0.8	37.7	
16	<10.6	-	-	-	-	-	-	-	-	-	-	-	-	0.5	<37.6
17	24.6±6.4	-0.1±2.3	16.4±5.2	16.3±5.3	8.3±4.3	12.8±4.8	12.2±4.8	-0.15 ^{+0.20} _{-0.21}	-1.07 ^{+0.46} _{-0.92}	0.35 ^{+0.19} _{-0.19}	N	N	1.1	38.0	
18	<4.0	-	-	-	-	-	-	-	-	-	-	-	-	0.0	<37.2
19	<13.3	-	-	-	-	-	-	-	-	-	-	-	-	1.0	<37.7
20	<2.1	-	-	-	-	-	-	-	-	-	-	-	-	0.0	<36.9
21	<4.9	-	-	-	-	-	-	-	-	-	-	-	-	0.8	<37.3
22	<1.2	-	-	-	-	-	-	-	-	-	-	-	-	1.6	<36.6
23	<5.8	-	-	-	-	-	-	-	-	-	-	-	-	1.1	<37.3
24	<2.6	-	-	-	-	-	-	-	-	-	-	-	-	0.7	<37.0
25	<3.1	-	-	-	-	-	-	-	-	-	-	-	-	0.0	<37.1
26	15.7±5.6	0.1±2.3	13.0±4.8	13.1±5.0	2.6±3.4	11.8±4.7	3.3±3.6	-0.67 ^{+0.17} _{-0.23}	-0.99 ^{+0.46} _{-0.84}	0.62 ^{+0.53} _{-0.33}	-	-	0.5	37.8	
27	<0.9	-	-	-	-	-	-	-	-	-	-	-	-	3.3	<36.5
28	<0.9	-	-	-	-	-	-	-	-	-	-	-	-	1.8	<36.5
29	12.1±5.1	4.0±3.4	8.1±4.1	12.0±4.8	0.0±2.7	7.8±4.1	1.9±3.2	-0.72 ^{+0.16} _{-0.28}	-0.19 ^{+0.27} _{-0.32}	0.84 ^{+0.92} _{-0.46}	-	-	0.1	37.6	
30	<3.3	-	-	-	-	-	-	-	-	-	-	-	-	2.0	<37.1
31	64.8±9.4	11.9±4.7	36.7±7.2	48.6±8.2	16.2±5.3	37.3±7.3	25.9±6.4	-0.25 ^{+0.12} _{-0.13}	-0.36 ^{+0.11} _{-0.19}	0.41 ^{+0.12} _{-0.15}	N	N	0.3	38.4	
32	<2.0	-	-	-	-	-	-	-	-	-	-	-	-	0.0	<36.9
33	<2.4	-	-	-	-	-	-	-	-	-	-	-	-	0.0	<36.9
34	<2.6	-	-	-	-	-	-	-	-	-	-	-	-	0.5	<37.0
35	17.9±5.8	0.9±2.7	13.3±4.8	14.2±5.1	3.8±3.6	12.7±4.8	5.7±4.0	-0.45 ^{+0.23} _{-0.24}	-0.84 ^{+0.46} _{-0.69}	0.51 ^{+0.38} _{-0.30}	-	-	0.4	37.8	
36	<0.7	-	-	-	-	-	-	-	-	-	-	-	-	2.3	<36.4
37	<12.0	-	-	-	-	-	-	-	-	-	-	-	-	2.1	<37.6
38	<11.9	-	-	-	-	-	-	-	-	-	-	-	-	1.5	<37.6
39	16.4±3.5	4.4±3.4	6.3±3.8	10.6±4.6	4.8±3.6	11.0±4.6	4.7±3.6	-0.46 ^{+0.22} _{-0.26}	-0.05 ^{+0.26} _{-0.30}	0.13 ^{+0.30} _{-0.26}	N	P	0.7	37.8	
40	16.1±3.5	4.5±3.4	6.4±3.8	10.9±4.6	5.2±3.6	11.2±4.6	5.1±3.6	-0.44 ^{+0.22} _{-0.24}	-0.05 ^{+0.26} _{-0.27}	0.11 ^{+0.29} _{-0.24}	N	P	0.6	37.8	
41	88.9±10.7	18.9±5.6	50.5±8.3	69.4±9.5	19.6±5.8	61.2±9.0	25.1±6.4	-0.47 ^{+0.08} _{-0.11}	-0.32 ^{+0.11} _{-0.13}	0.46 ^{+0.11} _{-0.13}	N	N	0.7	38.5	
42	61.6±9.2	15.8±5.2	35.0±7.1	50.8±8.3	10.8±4.7	41.5±7.6	15.6±5.3	-0.50 ^{+0.09} _{-0.13}	-0.21 ^{+0.09} _{-0.18}	0.52 ^{+0.16} _{-0.16}	N	P	1.0	38.4	
43	12.7±5.1	5.1±3.6	7.0±4.0	12.1±4.8	0.5±2.7	10.8±4.6	0.4±2.7	-0.94 ^{+0.09} _{-0.06}	-0.03 ^{+0.24} _{-0.29}	0.76 ^{+0.84} _{-0.45}	-	-	1.6	37.7	
44	<3.4	-	-	-	-	-	-	-	-	-	-	-	-	0.0	<37.1
45	<3.5	-	-	-	-	-	-	-	-	-	-	-	-	1.1	<37.1
46	<5.5	-	-	-	-	-	-	-	-	-	-	-	-	1.1	<37.3
47	<1.6	-	-	-	-	-	-	-	-	-	-	-	-	0.0	<36.7
48	<4.7	-	-	-	-	-	-	-	-	-	-	-	-	1.0	<37.2
49	<2.6	-	-	-	-	-	-	-	-	-	-	-	-	1.5	<37.0
50	14.1±5.4	4.0±3.4	6.9±4.0	10.9±4.7	3.3±3.4	5.6±3.8	5.8±4.0	-0.06 ^{+0.35} _{-0.35}	-0.13 ^{+0.29} _{-0.33}	0.32 ^{+0.43} _{-0.35}	-	-	1.5	37.7	

TABLE 10 — *Continued*

Masterid	B-band	S1-band	S2-band	Net Counts S-band	H-band	Sc-band	Hc-band	HR	C21	C32	BB	Variability k-S	signif.	Log L_x (0.3–8.0 keV)	
(1)	(2)	(3)	(4)	(5)	(6)	(7)	(8)	(9)	(10)	(11)	(12)	(13)	(14)	(15)	
51	≤ 5.2	-	-	-	-	-	-	-	-	-	-	-	-	0.9	≤ 37.3
52	≤ 3.2	-	-	-	-	-	-	-	-	-	-	-	-	1.3	≤ 37.1
53	≤ 6.1	-	-	-	-	-	-	-	-	-	-	-	-	0.7	≤ 37.3
54	≤ 5.6	-	-	-	-	-	-	-	-	-	-	-	-	0.7	≤ 37.3
55	≤ 3.7	-	-	-	-	-	-	-	-	-	-	-	-	0.8	≤ 37.1
56	11.8 ± 5.4	0.0 ± 2.7	11.4 ± 4.7	11.4 ± 5.0	0.4 ± 2.9	11.8 ± 4.8	1.0 ± 3.2	$-0.89^{+0.11}_{-0.11}$	$-0.92^{+0.54}_{-0.84}$	$0.92^{+0.84}_{-0.46}$	-	-	-	0.5	37.6
57	≤ 8.0	-	-	-	-	-	-	-	-	-	-	-	-	0.9	≤ 37.5
58	≤ 3.3	-	-	-	-	-	-	-	-	-	-	-	-	0.5	≤ 37.1
59	10.0 ± 5.3	1.4 ± 3.2	8.4 ± 4.4	9.8 ± 5.0	0.2 ± 2.7	7.1 ± 4.4	1.6 ± 3.2	$-0.73^{+0.19}_{-0.27}$	$-0.46^{+0.38}_{-0.76}$	$0.84^{+0.92}_{-0.46}$	-	-	-	0.0	37.6
60	6.5 ± 4.3	2.3 ± 2.9	4.8 ± 3.6	7.1 ± 4.1	-0.6 ± 2.3	5.9 ± 3.8	0.0 ± 2.7	$-0.90^{+0.14}_{-0.10}$	$-0.19^{+0.40}_{-0.45}$	$0.84^{+0.92}_{-0.61}$	-	-	-	0.3	37.4
61	≤ 2.5	-	-	-	-	-	-	-	-	-	-	-	-	0.0	≤ 36.9
62	≤ 3.7	-	-	-	-	-	-	-	-	-	-	-	-	0.3	≤ 37.1
63	18.7 ± 5.9	1.6 ± 2.9	8.8 ± 4.3	10.4 ± 4.7	8.3 ± 4.3	7.4 ± 4.1	11.0 ± 4.7	$0.14^{+0.26}_{-0.26}$	$-0.51^{+0.40}_{-0.62}$	$0.05^{+0.22}_{-0.24}$	-	-	-	0.4	37.8
64	≤ 2.9	-	-	-	-	-	-	-	-	-	-	-	-	0.5	≤ 37.0
65	≤ 14.4	-	-	-	-	-	-	-	-	-	-	-	-	0.1	≤ 37.7
66	30.1 ± 7.2	7.6 ± 4.3	16.5 ± 5.4	24.1 ± 6.5	6.0 ± 4.0	20.2 ± 6.0	8.6 ± 4.4	$-0.46^{+0.17}_{-0.19}$	$-0.24^{+0.21}_{-0.22}$	$0.46^{+0.24}_{-0.25}$	N	N	-	1.6	38.0
67	13.3 ± 5.2	-0.9 ± 1.9	8.9 ± 4.3	8.0 ± 4.3	5.3 ± 3.8	5.8 ± 3.8	8.1 ± 4.3	$0.11^{+0.30}_{-0.30}$	$-1.22^{+0.61}_{-0.92}$	$0.24^{+0.27}_{-0.27}$	-	-	-	0.4	37.8
68	21.5 ± 6.3	4.5 ± 3.6	9.1 ± 4.4	13.6 ± 5.2	7.8 ± 4.3	10.7 ± 4.7	10.5 ± 4.7	$-0.08^{+0.24}_{-0.24}$	$-0.19^{+0.32}_{-0.27}$	$0.08^{+0.27}_{-0.21}$	N	N	-	0.1	37.9
69	10.3 ± 4.9	1.1 ± 2.7	5.0 ± 3.6	6.1 ± 4.0	4.2 ± 3.6	5.9 ± 3.8	4.8 ± 3.8	$-0.19^{+0.36}_{-0.35}$	$-0.38^{+0.46}_{-0.69}$	$0.08^{+0.38}_{-0.35}$	-	-	-	0.7	37.7
70	≤ 2.4	-	-	-	-	-	-	-	-	-	-	-	-	0.0	≤ 36.9
71	13.7 ± 5.2	0.3 ± 2.3	7.9 ± 4.1	8.2 ± 4.3	5.5 ± 3.8	7.0 ± 4.0	7.1 ± 4.1	$-0.08^{+0.29}_{-0.29}$	$-0.76^{+0.45}_{-0.84}$	$0.19^{+0.27}_{-0.27}$	-	-	-	0.3	37.7
72	31.5 ± 7.0	7.1 ± 4.0	9.8 ± 4.4	16.9 ± 5.4	14.5 ± 5.1	13.6 ± 5.0	16.2 ± 5.3	$0.01^{+0.18}_{-0.20}$	$-0.03^{+0.21}_{-0.25}$	$-0.14^{+0.19}_{-0.19}$	N	N	-	0.2	38.1
73	9.4 ± 3.3	-0.1 ± 2.3	6.7 ± 4.0	6.6 ± 4.1	2.6 ± 3.2	5.5 ± 3.8	4.3 ± 3.6	$-0.20^{+0.36}_{-0.38}$	$-0.76^{+0.53}_{-0.92}$	$0.38^{+0.48}_{-0.38}$	-	-	-	0.3	37.5
74	4.8 ± 2.5	1.3 ± 2.7	2.1 ± 2.9	3.4 ± 3.4	2.0 ± 2.9	3.9 ± 3.4	1.8 ± 2.9	$-0.50^{+0.23}_{-0.33}$	$-0.05^{+0.64}_{-0.75}$	$0.05^{+0.65}_{-0.64}$	-	-	-	0.2	37.2
75	≤ 2.4	-	-	-	-	-	-	-	-	-	-	-	-	0.0	≤ 36.9
76	13.9 ± 5.0	0.6 ± 2.3	3.7 ± 3.2	4.3 ± 3.4	9.6 ± 4.3	3.5 ± 3.2	10.5 ± 4.4	$0.44^{+0.28}_{-0.23}$	$-0.46^{+0.54}_{-0.69}$	$-0.35^{+0.24}_{-0.29}$	N	N	-	2.2	37.7
77	≤ 7.6	-	-	-	-	-	-	-	-	-	-	-	-	1.1	≤ 37.4
78	23.4 ± 6.5	6.7 ± 4.0	14.3 ± 5.1	21.0 ± 6.0	2.4 ± 3.4	17.9 ± 5.6	4.0 ± 3.8	$-0.71^{+0.16}_{-0.19}$	$-0.21^{+0.18}_{-0.25}$	$0.67^{+0.56}_{-0.35}$	Y	N	-	1.0	37.9
79	16.6 ± 5.3	7.6 ± 4.0	8.6 ± 4.1	16.2 ± 5.2	0.5 ± 2.3	14.4 ± 5.0	1.5 ± 2.7	$-0.87^{+0.08}_{-0.13}$	$0.03^{+0.21}_{-0.22}$	$0.92^{+0.76}_{-0.46}$	N	N	-	2.4	37.8
80	2.1 ± 2.2	-0.2 ± 2.3	2.9 ± 3.2	2.7 ± 3.4	-0.1 ± 2.3	2.4 ± 3.2	0.7 ± 2.7	$-0.55^{+0.34}_{-0.45}$	$-0.46^{+0.61}_{-0.99}$	$0.61^{+0.52}_{-0.69}$	-	-	-	0.7	36.9
81	≤ 16.9	-	-	-	-	-	-	-	-	-	-	-	-	0.8	≤ 37.8
82	≤ 0.9	-	-	-	-	-	-	-	-	-	-	-	-	1.9	≤ 36.5
83	≤ 5.1	-	-	-	-	-	-	-	-	-	-	-	-	0.5	≤ 37.3
84	23.0 ± 4.5	5.0 ± 3.8	14.2 ± 5.1	19.2 ± 5.9	4.1 ± 3.6	16.1 ± 5.5	5.9 ± 4.0	$-0.53^{+0.20}_{-0.21}$	$-0.32^{+0.24}_{-0.30}$	$0.51^{+0.35}_{-0.27}$	N	N	-	1.4	37.9
85	≤ 20.5	-	-	-	-	-	-	-	-	-	-	-	-	0.2	≤ 37.9
86	≤ 8.4	-	-	-	-	-	-	-	-	-	-	-	-	0.3	≤ 37.5
87	≤ 9.0	-	-	-	-	-	-	-	-	-	-	-	-	0.0	≤ 37.5
88	≤ 8.6	-	-	-	-	-	-	-	-	-	-	-	-	0.9	≤ 37.5
89	≤ 4.1	-	-	-	-	-	-	-	-	-	-	-	-	0.7	≤ 37.2
90	≤ 5.4	-	-	-	-	-	-	-	-	-	-	-	-	0.0	≤ 37.3
91	≤ 5.1	-	-	-	-	-	-	-	-	-	-	-	-	0.0	≤ 37.3
92	10.0 ± 4.4	0.6 ± 2.3	5.7 ± 3.6	6.3 ± 3.8	3.6 ± 3.2	5.5 ± 3.6	4.6 ± 3.4	$-0.16^{+0.29}_{-0.32}$	$-0.61^{+0.46}_{-0.77}$	$0.21^{+0.30}_{-0.29}$	-	-	-	1.2	37.5
93	≤ 9.1	-	-	-	-	-	-	-	-	-	-	-	-	1.0	≤ 37.5
94	≤ 9.0	-	-	-	-	-	-	-	-	-	-	-	-	1.5	≤ 37.5
95	≤ 3.6	-	-	-	-	-	-	-	-	-	-	-	-	0.8	≤ 37.1
96	93.3 ± 11.1	28.0 ± 6.5	50.1 ± 8.3	78.1 ± 10.1	15.2 ± 5.3	62.2 ± 9.1	23.0 ± 6.2	$-0.51^{+0.08}_{-0.10}$	$-0.14^{+0.08}_{-0.13}$	$0.55^{+0.13}_{-0.15}$	N	P	-	1.0	38.5
97	≤ 3.9	-	-	-	-	-	-	-	-	-	-	-	-	2.0	≤ 37.1
98	19.6 ± 4.3	4.3 ± 3.8	12.7 ± 5.0	17.0 ± 5.8	3.1 ± 3.4	13.1 ± 5.2	6.0 ± 4.0	$-0.44^{+0.22}_{-0.25}$	$-0.35^{+0.30}_{-0.37}$	$0.56^{+0.46}_{-0.32}$	N	N	-	0.9	37.8
99	39.2 ± 9.1	8.5 ± 5.4	25.0 ± 6.8	33.5 ± 8.2	5.7 ± 4.5	29.0 ± 7.7	9.8 ± 5.1	$-0.56^{+0.18}_{-0.17}$	$-0.35^{+0.24}_{-0.34}$	$0.62^{+0.37}_{-0.28}$	N	N	-	1.2	38.1
100	6.8 ± 3.0	3.6 ± 3.4	3.2 ± 3.2	6.8 ± 4.1	0.5 ± 2.7	5.6 ± 3.8	2.3 ± 3.2	$-0.55^{+0.21}_{-0.30}$	$0.13^{+0.46}_{-0.45}$	$0.46^{+0.84}_{-0.61}$	-	-	-	0.1	37.4
101	≤ 23.4	-	-	-	-	-	-	-	-	-	-	-	-	0.1	≤ 37.9

TABLE 10 — *Continued*

Masterid	B-band	S1-band	S2-band	Net Counts S-band	H-band	Sc-band	Hc-band	HR	C21	C32	BB	Variability k-S	signif.	Log L_x (0.3–8.0 keV)	
(1)	(2)	(3)	(4)	(5)	(6)	(7)	(8)	(9)	(10)	(11)	(12)	(13)	(14)	(15)	
102	<1.7	-	-	-	-	-	-	-	-	-	-	-	-	0.0	<36.8
103	19.8±6.1	4.2±3.6	9.3±4.4	13.5±5.2	6.2±4.0	11.5±4.8	8.0±4.3	-0.25 ^{+0.23} _{-0.25}	-0.21 ^{+0.26} _{-0.35}	0.19 ^{+0.27} _{-0.24}	-	-	0.8	37.8	
104	<22.5	-	-	-	-	-	-	-	-	-	-	-	-	0.0	<37.9
105	<2.6	-	-	-	-	-	-	-	-	-	-	-	-	1.4	<37.0
106	<29.0	-	-	-	-	-	-	-	-	-	-	-	-	0.8	<38.0
107	<3.6	-	-	-	-	-	-	-	-	-	-	-	-	1.2	<37.1
108	9.6±5.0	2.6±3.2	7.3±4.1	9.9±4.7	-0.4±2.7	8.9±4.4	1.4±3.2	-0.82 ^{+0.15} _{-0.18}	-0.29 ^{+0.37} _{-0.49}	0.84 ^{+0.99} _{-0.46}	-	-	0.1	37.5	
109	<15.2	-	-	-	-	-	-	-	-	-	-	-	-	0.9	<37.7
110	11.2±6.0	1.3±3.2	8.9±4.6	10.2±5.1	1.0±3.7	8.2±4.8	1.8±3.9	-0.74 ^{+0.21} _{-0.26}	-0.53 ^{+0.45} _{-0.77}	0.59 ^{+0.83} _{-0.46}	-	-	0.6	37.6	
111	10.9±5.6	8.3±4.4	4.4±4.0	12.7±5.5	-1.8±2.3	9.3±4.9	0.5±3.2	-0.89 ^{+0.13} _{-0.11}	0.32 ^{+0.43} _{-0.35}	0.84 ^{+1.07} _{-0.69}	-	-	0.2	37.6	
112	<1.6	-	-	-	-	-	-	-	-	-	-	-	-	0.6	<36.8
113	<1.8	-	-	-	-	-	-	-	-	-	-	-	-	0.0	<36.8
114	<33.9	-	-	-	-	-	-	-	-	-	-	-	-	1.2	<38.1
115	<5.1	-	-	-	-	-	-	-	-	-	-	-	-	0.6	<37.3
116	<23.5	-	-	-	-	-	-	-	-	-	-	-	-	2.9	<37.9
117	3211.3±58.0	1245.6±36.5	1644.8±41.8	2890.4±55.1	320.9±19.1	2525.5±51.5	5474.0±23.0	-0.72 ^{+0.01} _{-0.01}	-0.03 ^{+0.01} _{-0.02}	0.74 ^{+0.03} _{-0.03}	N	N	6.3	40.1	
118	32.7±7.9	7.8±4.5	20.0±6.2	27.8±7.2	4.9±3.8	19.9±6.3	9.8±4.8	-0.40 ^{+0.18} _{-0.21}	-0.29 ^{+0.21} _{-0.25}	0.59 ^{+0.32} _{-0.24}	N	N	0.7	38.1	
119	139.5±14.1	31.5±7.7	80.7±10.7	112.2±12.8	27.3±6.6	91.9±11.8	44.1±8.0	-0.41 ^{+0.08} _{-0.09}	-0.32 ^{+0.10} _{-0.11}	0.50 ^{+0.11} _{-0.09}	N	N	0.6	38.7	
120	50.2±6.9	18.4±6.6	26.8±7.2	45.1±9.3	6.0±4.1	38.5±8.7	9.5±4.7	-0.65 ^{+0.12} _{-0.13}	-0.09 ^{+0.10} _{-0.15}	0.70 ^{+0.24} _{-0.29}	N	N	0.2	38.3	
121	7.2±4.6	1.8±2.9	2.8±3.2	4.6±3.8	2.6±3.4	4.8±3.6	2.2±3.4	-0.52 ^{+0.24} _{-0.25}	-0.05 ^{+0.59} _{-0.67}	0.03 ^{+0.67} _{-0.57}	-	-	0.8	37.4	
122	7.8±4.7	3.1±3.2	3.7±3.4	6.8±4.1	1.1±3.2	6.5±4.0	1.8±3.4	-0.69 ^{+0.20} _{-0.31}	0.03 ^{+0.43} _{-0.46}	0.32 ^{+0.86} _{-0.56}	-	-	1.6	37.4	
123	<58.3	-	-	-	-	-	-	-	-	-	-	-	-	1.6	<38.3
124	<19.4	-	-	-	-	-	-	-	-	-	-	-	-	1.0	<37.8
125	7.1±4.9	0.2±2.7	6.2±4.0	6.4±4.3	0.7±3.2	4.2±3.8	3.5±3.8	-0.21 ^{+0.43} _{-0.49}	-0.61 ^{+0.53} _{-0.84}	0.56 ^{+0.83} _{-0.51}	-	-	0.0	37.4	
126	<4.9	-	-	-	-	-	-	-	-	-	-	-	-	0.5	<37.2
127	<9.8	-	-	-	-	-	-	-	-	-	-	-	-	0.3	<37.5
128	<15.3	-	-	-	-	-	-	-	-	-	-	-	-	0.1	<37.7
129	25.8±4.9	10.3±4.8	10.1±5.1	20.4±6.6	4.3±3.6	18.7±6.3	5.5±4.0	-0.61 ^{+0.18} _{-0.21}	0.11 ^{+0.24} _{-0.24}	0.38 ^{+0.34} _{-0.33}	N	N	2.7	38.0	
130	<9.2	-	-	-	-	-	-	-	-	-	-	-	-	0.1	<37.5
131	<2.2	-	-	-	-	-	-	-	-	-	-	-	-	0.0	<36.9
132	34.9±8.1	12.4±5.3	15.0±5.7	27.4±7.3	7.5±4.3	22.5±6.8	10.0±4.7	-0.44 ^{+0.16} _{-0.20}	-0.02 ^{+0.23} _{-0.18}	0.32 ^{+0.24} _{-0.24}	N	Y	0.2	38.1	
133	34.5±7.3	9.5±4.4	17.7±5.4	27.2±6.5	7.3±4.1	26.3±6.4	8.0±4.3	-0.58 ^{+0.14} _{-0.16}	-0.16 ^{+0.16} _{-0.19}	0.40 ^{+0.22} _{-0.19}	N	N	0.8	38.1	
134	<12.3	-	-	-	-	-	-	-	-	-	-	-	-	0.3	<37.6
135	<24.9	-	-	-	-	-	-	-	-	-	-	-	-	1.0	<37.9
136	<3.1	-	-	-	-	-	-	-	-	-	-	-	-	0.0	<37.0
137	<10.3	-	-	-	-	-	-	-	-	-	-	-	-	0.0	<37.6
138	<10.6	-	-	-	-	-	-	-	-	-	-	-	-	0.2	<37.6
139	<6.0	-	-	-	-	-	-	-	-	-	-	-	-	0.9	<37.3
140	31.1±7.5	9.2±4.6	12.8±5.1	22.0±6.4	9.1±4.6	22.2±6.3	9.5±4.7	-0.46 ^{+0.16} _{-0.12}	-0.05 ^{+0.21} _{-0.22}	0.16 ^{+0.24} _{-0.19}	N	N	2.1	38.0	
141	12.4±5.4	2.2±3.2	11.7±4.7	13.8±5.2	-1.4±2.3	11.9±4.8	1.4±3.2	-0.87 ^{+0.12} _{-0.13}	-0.54 ^{+0.38} _{-0.53}	1.22 ^{+1.00} _{-0.46}	-	-	0.5	37.7	
142	11.0±4.9	0.5±2.3	6.9±4.0	7.4±4.1	3.5±3.4	6.9±4.0	3.3±3.4	-0.47 ^{+0.30} _{-0.33}	-0.69 ^{+0.46} _{-0.76}	0.29 ^{+0.38} _{-0.32}	-	-	1.2	37.6	
143	<5.2	-	-	-	-	-	-	-	-	-	-	-	-	1.6	<37.3
144	<2.7	-	-	-	-	-	-	-	-	-	-	-	-	1.0	<37.0
145	<2.5	-	-	-	-	-	-	-	-	-	-	-	-	0.0	<36.9
146	155.3±13.9	24.3±6.4	95.0±10.9	119.3±12.3	36.0±7.2	103.2±11.5	50.7±8.3	-0.40 ^{+0.07} _{-0.08}	-0.48 ^{+0.09} _{-0.13}	0.45 ^{+0.10} _{-0.07}	N	N	0.1	38.7	
147	25.0±6.5	4.4±3.6	14.4±5.1	18.8±5.8	6.2±3.8	16.1±5.4	9.0±4.3	-0.34 ^{+0.18} _{-0.20}	-0.38 ^{+0.23} _{-0.32}	0.38 ^{+0.21} _{-0.22}	N	N	0.2	37.9	
148	29.7±7.3	4.7±3.8	18.4±5.7	23.0±6.4	6.6±4.3	22.2±6.2	8.2±4.6	-0.52 ^{+0.17} _{-0.19}	-0.46 ^{+0.25} _{-0.34}	0.46 ^{+0.24} _{-0.25}	N	N	0.8	38.0	
149	<18.7	-	-	-	-	-	-	-	-	-	-	-	-	2.4	<37.8
150	<7.1	-	-	-	-	-	-	-	-	-	-	-	-	0.4	<37.4
151	<3.3	-	-	-	-	-	-	-	-	-	-	-	-	0.7	<37.1
152	<1.9	-	-	-	-	-	-	-	-	-	-	-	-	3.2	<36.8
153	<2.9	-	-	-	-	-	-	-	-	-	-	-	-	0.0	<37.0

TABLE 10 — *Continued*

Masterid	B-band	S1-band	S2-band	Net Counts S-band	H-band	Sc-band	Hc-band	HR	C21	C32	BB	Variability k-S	signif.	Log L_x (0.3–8.0 keV)	
(1)	(2)	(3)	(4)	(5)	(6)	(7)	(8)	(9)	(10)	(11)	(12)	(13)	(14)	(15)	
154	25.3±6.4	5.0±3.6	13.8±5.0	18.8±5.7	6.5±3.8	18.1±5.6	7.5±4.0	-0.47 ^{+0.16} _{-0.18}	-0.32 ^{+0.21} _{-0.27}	0.35 ^{+0.19} _{-0.22}	-	-	0.3	38.0	
155	12.4±5.4	2.3±3.2	7.4±4.1	9.7±4.7	2.8±3.4	10.6±4.7	2.6±3.4	-0.72 ^{+0.14} _{-0.17}	-0.32 ^{+0.37} _{-0.57}	0.38 ^{+0.51} _{-0.38}	-	-	0.3	37.6	
156	≤1.4	-	-	-	-	-	-	-	-	-	-	-	-	0.0	≤36.7
157	32.3±7.4	9.0±4.4	20.5±5.9	29.6±6.9	2.7±3.6	24.7±6.4	5.4±4.1	-0.71 ^{+0.16} _{-0.17}	-0.27 ^{+0.19} _{-0.19}	0.78 ^{+0.56} _{-0.32}	N	N	1.7	38.1	
158	84.0±7.1	20.7±5.8	44.8±7.8	65.6±9.3	17.7±5.4	54.2±8.5	24.5±6.2	-0.43 ^{+0.09} _{-0.11}	-0.22 ^{+0.10} _{-0.13}	0.41 ^{+0.16} _{-0.09}	N	N	0.1	38.5	
159	23.2±6.6	4.6±3.6	10.7±4.7	15.3±5.4	7.9±4.4	10.6±4.7	10.4±4.8	-0.08 ^{+0.24} _{-0.25}	-0.24 ^{+0.24} _{-0.32}	0.16 ^{+0.24} _{-0.24}	N	N	3.3	37.9	
160	19.7±6.2	0.9±2.9	9.5±4.4	10.4±4.8	9.3±4.6	11.4±4.8	9.1±4.6	-0.18 ^{+0.23} _{-0.26}	-0.61 ^{+0.38} _{-0.84}	0.03 ^{+0.24} _{-0.19}	-	-	0.6	37.9	
161	≤5.9	-	-	-	-	-	-	-	-	-	-	-	-	1.1	≤37.3
162	17.6±6.1	3.8±3.6	7.8±4.3	11.6±5.1	5.9±4.0	10.9±4.9	5.6±4.0	-0.40 ^{+0.26} _{-0.28}	-0.19 ^{+0.35} _{-0.40}	0.13 ^{+0.33} _{-0.26}	-	-	0.1	37.8	
163	39.3±5.2	5.9±3.8	23.5±6.1	29.4±6.7	9.8±4.4	25.0±6.3	12.6±4.8	-0.39 ^{+0.14} _{-0.16}	-0.48 ^{+0.19} _{-0.24}	0.40 ^{+0.16} _{-0.16}	N	N	0.9	38.2	
164	6.1±4.5	0.7±2.7	2.6±3.2	3.3±3.6	2.8±3.4	3.0±3.4	2.5±3.4	-0.21 ^{+0.35} _{-0.53}	-0.23 ^{+0.69} _{-0.92}	0.00 ^{+0.64} _{-0.62}	-	-	0.6	37.3	
165	≤8.1	-	-	-	-	-	-	-	-	-	-	-	-	0.2	≤37.5
166	11.2±5.4	1.2±2.9	9.2±4.4	10.4±4.8	0.8±3.2	9.4±4.6	0.3±3.2	-0.90 ^{+0.12} _{-0.10}	-0.53 ^{+0.38} _{-0.77}	0.70 ^{+0.83} _{-0.43}	-	-	0.0	37.6	
167	≤6.7	-	-	-	-	-	-	-	-	-	-	-	-	0.2	≤37.4
168	≤6.7	-	-	-	-	-	-	-	-	-	-	-	-	1.1	≤37.4
169	≤10.8	-	-	-	-	-	-	-	-	-	-	-	-	3.1	≤37.6
170	8.9±5.0	5.5±3.8	4.3±3.6	9.8±4.7	-0.9±2.7	6.8±4.1	0.0±2.9	-0.89 ^{+0.15} _{-0.11}	0.19 ^{+0.35} _{-0.35}	0.69 ^{+0.99} _{-0.54}	-	-	0.7	37.5	
171	≤7.8	-	-	-	-	-	-	-	-	-	-	-	-	0.9	≤37.4
172	≤2.4	-	-	-	-	-	-	-	-	-	-	-	-	1.4	≤36.9
173	6.7±4.8	7.3±4.1	-0.1±2.7	7.2±4.4	-0.5±2.7	4.4±3.8	-1.0±2.7	-0.88 ^{+0.18} _{-0.12}	0.92 ^{+0.84} _{-0.54}	0.08 ^{+1.07} _{-1.07}	-	-	1.4	37.4	
174	≤3.3	-	-	-	-	-	-	-	-	-	-	-	-	0.0	≤37.1
175	≤1.1	-	-	-	-	-	-	-	-	-	-	-	-	2.1	≤36.6
176	≤3.3	-	-	-	-	-	-	-	-	-	-	-	-	0.0	≤37.1
177	≤2.0	-	-	-	-	-	-	-	-	-	-	-	-	0.0	≤36.9
178	≤0.9	-	-	-	-	-	-	-	-	-	-	-	-	0.0	≤36.5
179	13.9±5.5	3.0±3.2	9.6±4.4	12.5±5.0	1.4±3.2	9.2±4.4	5.2±4.0	-0.37 ^{+0.29} _{-0.29}	-0.35 ^{+0.30} _{-0.40}	0.64 ^{+0.75} _{-0.40}	-	-	1.6	37.7	
180	≤1.0	-	-	-	-	-	-	-	-	-	-	-	-	1.4	≤36.6
181	6.5±4.5	1.6±2.9	1.6±2.9	3.2±3.6	3.3±3.4	4.0±3.6	3.2±3.4	-0.21 ^{+0.43} _{-0.49}	0.11 ^{+0.80} _{-0.81}	-0.19 ^{+0.59} _{-0.75}	-	-	0.6	37.4	
182	≤9.1	-	-	-	-	-	-	-	-	-	-	-	-	1.2	≤37.5
183	10.2±4.9	0.1±2.3	7.7±4.1	7.8±4.3	2.4±3.2	5.6±3.8	5.0±3.8	-0.14 ^{+0.35} _{-0.37}	-0.84 ^{+0.53} _{-0.84}	0.46 ^{+0.51} _{-0.38}	-	-	0.3	37.6	
184	149.5±13.5	23.4±6.1	81.0±10.2	104.4±11.4	45.1±8.0	89.3±10.6	55.9±8.7	-0.29 ^{+0.08} _{-0.08}	-0.42 ^{+0.08} _{-0.13}	0.28 ^{+0.09} _{-0.08}	N	N	0.1	38.7	
185	97.7±11.2	12.7±4.8	58.5±8.8	71.2±9.6	26.5±6.5	63.3±9.1	31.1±6.9	-0.40 ^{+0.08} _{-0.10}	-0.55 ^{+0.12} _{-0.16}	0.35 ^{+0.13} _{-0.07}	N	N	5.6	38.6	
186	≤12.3	-	-	-	-	-	-	-	-	-	-	-	-	2.1	≤37.6
187	20.3±6.1	5.8±3.8	9.8±4.4	15.6±5.3	4.7±3.8	11.3±4.7	6.5±4.1	-0.34 ^{+0.24} _{-0.26}	-0.13 ^{+0.24} _{-0.25}	0.32 ^{+0.32} _{-0.29}	N	N	0.0	37.9	
188	≤2.3	-	-	-	-	-	-	-	-	-	-	-	-	0.9	≤36.9
189	3.2±2.3	0.4±2.3	0.9±2.7	1.3±2.9	3.0±3.2	1.8±2.9	2.7±3.2	0.16 ^{+0.52} _{-0.46}	-0.08 ^{+0.92} _{-0.99}	-0.31 ^{+0.62} _{-0.76}	-	-	1.3	37.1	
190	20.3±6.1	2.9±3.2	17.4±5.4	20.3±5.9	-0.1±2.7	14.8±5.2	3.8±3.6	-0.68 ^{+0.19} _{-0.20}	-0.62 ^{+0.30} _{-0.37}	1.15 ^{+0.91} _{-0.39}	N	N	0.5	37.9	
191	9.8±5.0	2.0±2.9	4.4±3.6	6.4±4.1	3.4±3.6	4.1±3.6	4.2±3.8	-0.08 ^{+0.46} _{-0.47}	-0.19 ^{+0.46} _{-0.59}	0.11 ^{+0.51} _{-0.43}	-	-	0.2	37.5	
192	≤3.4	-	-	-	-	-	-	-	-	-	-	-	-	2.0	≤37.1
193	≤3.2	-	-	-	-	-	-	-	-	-	-	-	-	0.7	≤37.1
194	41.8±5.3	10.4±4.4	23.3±6.0	33.7±7.0	8.8±4.3	28.1±6.5	12.6±4.8	-0.44 ^{+0.14} _{-0.15}	-0.26 ^{+0.17} _{-0.15}	0.43 ^{+0.19} _{-0.16}	N	N	0.9	38.2	
195	19.2±6.1	4.8±3.6	12.4±4.8	17.2±5.6	1.9±3.4	10.2±4.6	6.7±4.3	-0.30 ^{+0.28} _{-0.27}	-0.29 ^{+0.24} _{-0.27}	0.67 ^{+0.67} _{-0.38}	-	-	0.7	37.8	
196	≤11.7	-	-	-	-	-	-	-	-	-	-	-	-	1.9	≤37.6
197	7.0±4.6	-0.2±2.3	6.6±4.0	6.3±4.1	0.6±2.9	4.1±3.6	3.3±3.6	-0.22 ^{+0.44} _{-0.47}	-0.76 ^{+0.45} _{-1.00}	0.61 ^{+0.84} _{-0.46}	-	-	0.7	37.4	
198	≤1.5	-	-	-	-	-	-	-	-	-	-	-	-	0.0	≤36.7
199	≤1.8	-	-	-	-	-	-	-	-	-	-	-	-	2.3	≤36.8
200	≤0.8	-	-	-	-	-	-	-	-	-	-	-	-	0.0	≤36.5
201	≤4.2	-	-	-	-	-	-	-	-	-	-	-	-	1.5	≤37.2
202	13.0±5.4	-0.3±2.3	7.7±4.1	7.4±4.3	5.5±4.0	8.5±4.3	5.2±4.0	-0.33 ^{+0.31} _{-0.30}	-0.84 ^{+0.46} _{-0.99}	0.16 ^{+0.32} _{-0.27}	-	-	0.2	37.7	
203	11.0±5.0	0.7±2.7	10.0±4.4	10.7±4.7	0.4±2.7	9.6±4.4	0.2±2.7	-0.94 ^{+0.10} _{-0.06}	-0.76 ^{+0.45} _{-0.77}	0.92 ^{+0.84} _{-0.46}	-	-	0.1	37.6	
204	≤0.7	-	-	-	-	-	-	-	-	-	-	-	-	0.0	≤36.4

TABLE 10 — *Continued*

Masterid	B-band	S1-band	S2-band	Net Counts			HR	C21	C32	Variability			Log L_X		
(1)	(2)	(3)	(4)	S-band	H-band	Sc-band	Hc-band	(9)	(10)	(11)	BB	k-S	signif.	(0.3–8.0 keV)	
				(5)	(6)	(7)	(8)				(12)	(13)	(14)	(15)	
205	14.0±5.4	1.1±2.7	8.8±4.3	9.8±4.6	4.2±3.6	9.5±4.4	4.0±3.6	-0.50 ^{+0.27} _{-0.28}	-0.61 ^{+0.38} _{-0.69}	0.32 ^{+0.35} _{-0.29}	-	-	1.1	37.7	
206	4.2±4.2	0.6±2.7	4.8±3.6	5.4±4.0	-1.2±2.3	4.4±3.6	-0.5±2.7	-0.87 ^{+0.17} _{-0.13}	-0.46 ^{+0.54} _{-0.84}	0.84 ^{+0.99} _{-0.53}	-	-	0.0	37.2	
207	≤3.2	-	-	-	-	-	-	-	-	-	-	-	-	0.0	≤37.1
208	≤2.6	-	-	-	-	-	-	-	-	-	-	-	-	1.5	≤37.0
209	20.3±6.0	3.1±3.2	10.2±4.4	13.3±5.0	7.1±4.1	9.0±4.3	9.8±4.6	-0.03 ^{+0.25} _{-0.25}	-0.38 ^{+0.30} _{-0.34}	0.19 ^{+0.24} _{-0.24}	N	N	1.4	37.9	
210	≤3.6	-	-	-	-	-	-	-	-	-	-	-	-	1.4	≤37.1
211	≤4.4	-	-	-	-	-	-	-	-	-	-	-	-	0.0	≤37.2
212	≤10.3	-	-	-	-	-	-	-	-	-	-	-	-	1.6	≤37.6
213	6.1±2.9	0.1±2.3	2.3±2.9	2.4±3.2	4.1±3.4	2.2±2.9	4.0±3.4	0.27 ^{+0.45} _{-0.43}	-0.38 ^{+0.69} _{-0.92}	-0.19 ^{+0.43} _{-0.45}	-	-	0.1	37.4	
214	≤0.9	-	-	-	-	-	-	-	-	-	-	-	-	0.9	≤36.5
215	≤3.7	-	-	-	-	-	-	-	-	-	-	-	-	0.0	≤37.1
216	11.3±5.1	1.9±2.9	9.9±4.4	11.8±4.8	-0.5±2.7	11.8±4.7	0.1±2.9	-0.94 ^{+0.08} _{-0.06}	-0.51 ^{+0.38} _{-0.54}	0.99 ^{+0.92} _{-0.46}	-	-	0.2	37.6	
217	3.6±2.2	-0.8±1.9	3.5±3.2	2.7±3.2	0.2±2.3	3.3±3.2	1.1±2.7	-0.60 ^{+0.24} _{-0.40}	-0.84 ^{+0.69} _{-0.92}	0.61 ^{+0.92} _{-0.53}	-	-	0.0	37.1	
218	≤0.8	-	-	-	-	-	-	-	-	-	-	-	-	1.6	≤36.5
219	≤6.2	-	-	-	-	-	-	-	-	-	-	-	-	1.5	≤37.3
220	38.6±7.5	8.7±4.1	22.1±5.9	30.8±6.7	7.8±4.1	24.1±6.1	11.7±4.7	-0.41 ^{+0.15} _{-0.15}	-0.29 ^{+0.16} _{-0.19}	0.46 ^{+0.21} _{-0.17}	N	N	1.6	38.4	
221	≤5.7	-	-	-	-	-	-	-	-	-	-	-	-	0.1	≤37.3
222	1.4±3.8	0.1±2.7	-0.2±2.3	-0.1±2.9	1.5±3.2	1.6±2.9	1.0±3.2	-0.23 ^{+0.23} _{-0.77}	0.23 ^{+1.07} _{-1.07}	-0.31 ^{+0.84} _{-1.14}	-	-	0.3	36.7	
223	12.8±5.1	0.9±2.7	6.2±3.8	7.1±4.1	5.7±3.8	6.6±4.0	6.5±4.0	-0.08 ^{+0.29} _{-0.32}	-0.53 ^{+0.45} _{-0.77}	0.05 ^{+0.27} _{-0.26}	-	-	0.6	37.7	
224	≤4.4	-	-	-	-	-	-	-	-	-	-	-	-	0.0	≤37.2
225	13.1±5.4	-0.3±2.3	12.3±4.8	12.0±5.0	1.1±2.9	12.1±4.8	1.5±3.2	-0.86 ^{+0.12} _{-0.14}	-1.07 ^{+0.46} _{-0.92}	0.83 ^{+0.75} _{-0.43}	-	-	1.5	37.7	
226	11.4±5.1	4.2±3.4	4.9±3.6	9.2±4.4	2.2±3.4	6.1±3.8	3.8±3.8	-0.38 ^{+0.38} _{-0.34}	0.03 ^{+0.32} _{-0.32}	0.29 ^{+0.65} _{-0.45}	-	-	2.1	37.6	
227	19.4±3.8	4.5±3.4	12.5±4.7	17.0±5.3	3.9±3.4	15.2±5.1	4.9±3.6	-0.56 ^{+0.17} _{-0.11}	-0.32 ^{+0.21} _{-0.27}	0.48 ^{+0.32} _{-0.24}	Y	N	2.9	37.8	
228	61.3±6.2	11.5±4.6	37.3±7.2	48.9±8.1	13.9±5.0	39.1±7.4	19.8±5.7	-0.38 ^{+0.11} _{-0.13}	-0.43 ^{+0.16} _{-0.14}	0.42 ^{+0.17} _{-0.11}	N	N	7.3	38.3	
229	25.6±6.7	5.7±3.8	13.6±5.0	19.3±5.8	6.4±4.1	18.4±5.6	7.0±4.3	-0.51 ^{+0.19} _{-0.20}	-0.27 ^{+0.24} _{-0.24}	0.32 ^{+0.27} _{-0.21}	N	N	0.8	38.0	
230	10.1±5.0	1.8±2.9	7.6±4.1	9.4±4.6	0.7±2.9	10.3±4.6	0.2±2.9	-0.93 ^{+0.11} _{-0.07}	-0.43 ^{+0.40} _{-0.56}	0.69 ^{+0.84} _{-0.46}	-	-	0.3	37.6	
231	5.2±2.5	0.5±2.3	2.3±2.9	2.8±3.2	2.8±3.2	1.2±2.7	3.7±3.4	0.49 ^{+0.51} _{-0.27}	-0.31 ^{+0.62} _{-0.91}	-0.05 ^{+0.51} _{-0.51}	-	-	0.0	37.3	
232	≤4.7	-	-	-	-	-	-	-	-	-	-	-	-	1.0	≤37.2
233	6.7±5.7	-0.1±2.3	5.6±3.8	5.5±4.0	0.8±2.9	7.4±4.1	0.4±2.9	-0.88 ^{+0.14} _{-0.12}	-0.69 ^{+0.54} _{-0.91}	0.53 ^{+0.85} _{-0.45}	-	-	0.6	37.4	
234	≤9.9	-	-	-	-	-	-	-	-	-	-	-	-	0.3	≤37.6
235	≤3.9	-	-	-	-	-	-	-	-	-	-	-	-	0.0	≤37.1
236	≤9.6	-	-	-	-	-	-	-	-	-	-	-	-	1.7	≤37.5

NOTE. — Col. (1): Master ID, cols. (2)–(8): net counts, in each of the 7 energy bands (see Table 2 for definitions of these bands), col. (9): hardness ratio, cols. (10) and (11) color values, errors are given as 1σ , cols. (12) and (13): short-term variability, where (BB) indicate Bayesian block analysis and (K-S) indicates the Kolmogorov-Smirnov test, in both columns symbols indicate - (N) non-variable in all observations, (V) variable in at least one observation, (P) possible variability in at least one observation, col. (14): the significance of the change in L_X between the previous observation and the current observation respectively (equation 2), col. (15): $\log L_X$ (0.3–8.0 keV). Upper limit values of net B and L_X are at the 68% confidence level.

TABLE 11
 PROPERTIES OF OPTICAL SOURCES THAT ARE CORRELATED WITH AN X-RAY POINT
 SOURCE

Masterid	V	I	V-I	GC separation (arcsec)	Ratio
(1)	(2)	(3)	(4)	(5)	(6)
51	21.21±0.01	20.11±0.01	1.11±0.02	0.40	1.02
63	22.31±0.02	21.17±0.03	1.14±0.03	0.48	1.73
68	20.25±0.01	19.21±0.01	1.04±0.01	0.38	1.45
76	22.75±0.03	21.66±0.05	1.09±0.06	0.26	1.01
81	22.10±0.02	20.94±0.04	1.16±0.04	0.23	0.70
83	21.63±0.01	20.63±0.02	1.00±0.02	0.19	0.76
84	22.14±0.02	20.91±0.03	1.23±0.04	0.19	0.72
85	22.29±0.02	21.39±0.05	0.90±0.05	0.33	1.22
96	20.96±0.01	19.94±0.01	1.03±0.02	0.27	1.16
98	22.68±0.04	21.71±0.06	0.97±0.07	0.18	0.70
108	21.64±0.01	20.54±0.02	1.10±0.02	0.35	1.27
118	21.97±0.02	20.91±0.03	1.06±0.04	0.24	0.98
134	23.80±0.11	22.62±0.13	1.18±0.17	0.13	0.39
148	22.89±0.04	21.69±0.06	1.19±0.07	0.11	0.46
153	22.66±0.03	21.59±0.05	1.08±0.06	0.49	1.10
154	20.61±0.01	19.47±0.01	1.14±0.01	0.04	0.15
161	23.34±0.04	22.11±0.06	1.24±0.07	0.17	0.35
162	23.31±0.06	22.06±0.07	1.26±0.09	0.13	0.45
163	21.80±0.02	20.68±0.02	1.12±0.03	0.09	0.39
165	22.53±0.02	21.30±0.03	1.23±0.04	0.14	0.45
167	22.06±0.02	20.83±0.02	1.23±0.03	0.44	1.04
172	21.40±0.01	20.41±0.02	0.98±0.02	0.22	0.45
173	23.17±0.04	22.18±0.07	0.99±0.08	0.53	0.76
174	21.40±0.01	20.31±0.01	1.09±0.02	0.26	0.67
179	21.73±0.01	20.60±0.02	1.13±0.02	0.34	1.19
185	22.30±0.02	21.15±0.03	1.15±0.03	0.07	0.32
187	24.19±0.08	22.87±0.11	1.32±0.14	0.29	1.11
190	22.42±0.02	21.25±0.03	1.16±0.04	0.20	0.72
191	22.83±0.03	21.81±0.04	1.02±0.05	0.08	0.28
193	24.07±0.07	23.14±0.11	0.93±0.13	0.02	0.06
194	21.75±0.01	20.78±0.02	0.97±0.03	0.15	0.64
199	22.14±0.02	21.08±0.03	1.06±0.03	0.16	0.40
202	23.08±0.03	21.88±0.04	1.20±0.05	0.35	1.32
203	22.30±0.02	21.16±0.03	1.14±0.03	0.28	0.91
208	22.65±0.02	21.71±0.04	0.94±0.04	0.27	0.85
214	21.34±0.01	20.28±0.01	1.06±0.02	0.16	0.33
215	22.79±0.02	21.93±0.04	0.86±0.05	0.36	0.93
216	21.32±0.01	20.35±0.02	0.97±0.02	0.37	1.39
217	21.03±0.01	20.14±0.01	0.89±0.01	0.48	1.38
117	19.39±0.02	18.58±0.03	0.81±0.03	0.09	0.44
128	24.15±0.22	22.80±0.24	1.35±0.33	0.51	1.96
129	24.43±0.28	23.32±0.38	1.12±0.47	0.16	0.56
147	24.00±0.14	23.28±0.29	0.73±0.32	0.45	1.86
189	19.73±0.01	18.52±0.01	1.21±0.01	0.16	0.61
213	21.77±0.02	20.53±0.02	1.23±0.03	0.42	1.44

NOTE. — The sources in the top section of the table, denoted by the horizontal line, have been confirmed as globular clusters, while those in the bottom section of the table have all been identified as background objects.

TABLE 12
 PROPERTIES OF OPTICAL SOURCES THAT HAVE BEEN CLASSIFIED AS ‘EXCLUDED
 MATCHES’; SOURCES DETECTED BETWEEN 0.6'' AND 3'' OF AN X-RAY POINT
 SOURCE

Masterid	V	I	V-I	GC separation (arcsec)	Ratio
(1)	(2)	(3)	(4)	(5)	(6)
75	23.21±0.04	22.09±0.06	1.12±0.07	0.66	1.13
88	23.35±0.06	22.22±0.10	1.13±0.12	0.66	1.99
93	22.76±0.03	21.70±0.04	1.07±0.05	1.61	2.49
99	22.11±0.03	20.78±0.03	1.33±0.04	0.98	3.91
104	22.56±0.04	21.52±0.07	1.04±0.08	2.26	8.64
105	22.97±0.07	21.76±0.08	1.21±0.10	2.23	5.57
106	22.16±0.17	21.09±0.23	1.07±0.29	2.27	8.92
113	23.96±0.08	22.73±0.11	1.24±0.14	1.68	3.42
119	23.90±0.17	22.90±0.26	1.00±0.31	2.25	9.99
120	22.31±0.04	21.61±0.09	0.70±0.10	1.66	7.15
124	23.66±0.10	22.67±0.15	0.98±0.18	2.31	8.96
125	24.18±0.14	23.49±0.26	0.69±0.29	2.46	8.41
127	21.78±0.03	20.81±0.03	0.97±0.04	2.22	7.07
135	23.93±0.12	22.63±0.16	1.29±0.20	1.69	6.09
136	23.64±0.07	22.32±0.08	1.31±0.11	1.34	2.23
137	20.75±0.01	19.66±0.02	1.09±0.02	1.50	5.19
139	23.79±0.11	23.01±0.24	0.78±0.26	2.70	10.53
149	23.46±0.08	22.22±0.11	1.24±0.14	1.33	3.73
151	21.28±0.01	20.30±0.01	0.97±0.02	0.77	1.77
152	24.38±0.16	23.42±0.27	0.95±0.31	1.90	4.37
157	22.07±0.02	21.09±0.03	0.98±0.04	1.99	8.19
158	23.73±0.11	22.96±0.19	0.77±0.22	2.76	12.18
166	24.57±0.16	23.64±0.27	0.92±0.31	2.52	8.55
168	21.70±0.01	20.57±0.02	1.14±0.02	1.72	4.74
170	23.62±0.05	22.71±0.08	0.91±0.10	1.64	6.10
171	23.56±0.05	22.59±0.07	0.97±0.09	2.59	8.24
176	22.45±0.02	21.24±0.03	1.20±0.03	0.99	2.06
177	21.02±0.01	19.88±0.01	1.14±0.01	1.95	2.02
180	22.81±0.03	21.53±0.04	1.28±0.05	2.11	4.58
184	23.82±0.06	22.98±0.10	0.84±0.12	1.97	8.84
198	20.85±0.01	19.92±0.01	0.93±0.01	0.67	1.24
78	23.71±0.05	21.87±0.05	1.84±0.07	1.60	6.18
82	20.99±0.01	19.95±0.02	1.04±0.02	1.80	3.44
100	26.52±0.92	25.16±1.61	1.36±1.86	0.87	2.84
132	23.21±0.11	21.85±0.12	1.35±0.16	1.63	6.72
145	24.41±0.14	23.23±0.18	1.18±0.23	1.97	5.07
197	25.11±0.18	23.20±0.12	1.91±0.21	1.55	4.56
218	24.12±0.07	21.42±0.03	2.70±0.08	0.80	1.78

NOTE. — The sources in the top section of the table, denoted by the horizontal line, have been confirmed as globular clusters, while those in the bottom section of the table have all been identified as background objects.

TABLE 13
RATIO VALUES OF POTENTIAL TRANSIENT CANDIDATES

Masterid	Mode Ratio	Lower Bound Ratio	Variability
27	5.0	3.6	V
30	3.2	2.2	V
32	4.5	3.7	V
59	4.8	3.5	V
83	57.8	35.5	TC
91	9.0	8.3	PTC
92	5.8	4.3	V
113	3.5	2.4	V
139	26.1	18.9	TC
152	5.3	4.2	V
156	6.2	5.5	PTC
159	13.6	5.8	PTC
204	871.7	202.9	TC

NOTE. — The 13 sources that were identified as potential transients candidates. Mode ratios and lower bound ratios were derived from Bayesian modeling, see §2.4 for more details. Sources were determined to be transient candidates (TC) if the lower bound >10, possible transient candidates (PTC) if the lower bound >5 and variable (V), if lower than 5.

TABLE 14
SUMMARY OF LONG-TERM AND SHORT-TERM SOURCE VARIABILITY

Short-Term Variability	N	Long-Term Variability				Total
		V	TC	PTC	U	
N	7 (7)	11 (9)	0 (0)	0 (0)	0 (0)	18 (16)
V	3 (2)	6 (5)	0 (0)	0 (0)	0 (0)	9 (7)
P	11 (7)	14 (10)	0 (0)	0 (0)	0 (0)	25 (17)
U	76 (54)	66 (52)	3 (3)	3 (3)	36 (28)	184 (140)
Total	97 (70)	97 (76)	3 (3)	3 (3)	36 (28)	236 (180)

NOTE. — The long-term variability definitions: N-non-variable, V-variable, TC-transient candidate, PTC-possible transient candidate and U unable to determine variability as all individual observations were upper limits. Short-term variability definitions: N-non-variable in all six observation, V-variable in a least one observation, P-possible variability in at least one observation (see §2.4 for full definition), U too few counts in all six observations to determine variability. Bold values in brackets indicate the number of sources within the D_{25} ellipse.

TABLE 15
 RAW SOURCE AND BACKGROUND COUNTS FROM THE CO-ADDED OBSERVATION

Masterid (1)	Net B Counts (2)	Raw Counts													
		B-band		S1-band		S2-band		H-band		Bc-band		Sc-band		Hc-band	
		(Src) (3)	(Bkg) (4)	(Src) (5)	(Bkg) (6)	(Src) (7)	(Bkg) (8)	(Src) (9)	(Bkg) (10)	(Src) (11)	(Bkg) (12)	(Src) (13)	(Bkg) (14)	(Src) (15)	(Bkg) (16)
1	139.8	198.0	58.2	13.0	15.3	61.0	13.0	124.0	29.8	191.0	48.5	54.0	14.9	137.0	33.6
2	386.2	458.0	71.3	74.0	16.5	254.0	16.6	130.0	38.2	438.0	61.9	278.0	19.4	160.0	42.5
3	7.8	69.0	61.9	15.0	15.8	25.0	15.5	29.0	30.6	61.0	53.1	29.0	18.7	32.0	34.3
4	266.1	333.0	66.6	94.0	15.2	162.0	16.7	77.0	34.8	312.0	58.1	215.0	19.3	97.0	38.9
5	725.7	787.0	61.3	217.0	14.8	413.0	14.7	157.0	31.8	737.0	53.6	527.0	18.4	210.0	35.3
6	17.5	75.0	58.1	9.0	15.7	23.0	13.9	43.0	28.6	72.0	49.4	22.0	17.3	50.0	32.1
7	-	-	-	-	-	-	-	-	-	-	-	-	-	-	-
8	128.6	180.0	51.4	44.0	11.1	89.0	12.4	47.0	28.0	169.0	45.0	108.0	14.2	61.0	30.9
9	46.7	108.0	61.3	31.0	14.6	39.0	15.4	38.0	31.3	97.0	52.7	52.0	17.1	45.0	35.6
10	7.7	44.0	36.3	13.0	8.1	15.0	9.9	16.0	18.4	39.0	32.4	21.0	11.6	18.0	20.7
11	67.4	99.0	31.6	14.0	8.1	41.0	7.7	44.0	15.8	95.0	27.4	41.0	10.0	54.0	17.3
12	-	-	-	-	-	-	-	-	-	-	-	-	-	-	-
13	1110.4	1164.0	53.6	296.0	14.0	618.0	14.2	250.0	25.4	1113.0	46.4	785.0	17.9	328.0	28.5
14	258.4	303.0	44.6	79.0	10.2	147.0	12.0	77.0	22.4	288.0	38.9	193.0	13.4	95.0	25.5
15	80.6	114.0	33.4	19.0	7.1	53.0	8.7	42.0	17.6	109.0	29.4	58.0	9.7	51.0	19.6
16	31.9	66.0	34.1	14.0	8.2	23.0	8.7	29.0	17.2	58.0	30.2	22.0	11.2	36.0	19.0
17	159.3	212.0	52.7	38.0	13.9	108.0	13.7	66.0	25.1	206.0	45.5	124.0	16.5	82.0	29.0
18	-	-	-	-	-	-	-	-	-	-	-	-	-	-	-
19	56.7	88.0	31.3	18.0	7.9	47.0	7.5	23.0	15.9	83.0	27.0	55.0	9.2	28.0	17.8
20	22.4	55.0	32.6	20.0	7.8	15.0	8.9	20.0	15.9	50.0	28.6	29.0	10.9	21.0	17.7
21	35.3	69.0	33.7	14.0	7.1	28.0	9.1	27.0	17.5	66.0	30.4	33.0	10.9	33.0	19.5
22	22.8	55.0	32.2	16.0	8.6	23.0	8.0	16.0	15.7	50.0	27.5	32.0	10.1	18.0	17.4
23	45.2	76.0	30.8	22.0	7.4	34.0	7.6	20.0	15.8	71.0	26.7	48.0	9.2	23.0	17.5
24	38.3	71.0	32.7	11.0	7.4	25.0	8.6	35.0	16.7	64.0	28.4	21.0	10.1	43.0	18.3
25	20.9	51.0	30.1	9.0	7.9	26.0	7.8	16.0	14.4	50.0	25.7	27.0	9.5	23.0	16.2
26	78.9	111.0	32.1	9.0	7.6	61.0	8.9	41.0	15.5	104.0	28.0	55.0	9.8	49.0	18.2
27	25.0	50.0	24.1	10.0	6.3	19.0	6.3	21.0	11.5	45.0	21.1	21.0	8.2	24.0	12.9
28	27.0	53.0	26.9	11.0	6.9	20.0	7.1	22.0	12.8	49.0	23.4	22.0	8.8	27.0	14.5
29	106.9	139.0	32.1	23.0	7.1	70.0	8.6	46.0	16.3	132.0	27.7	76.0	9.6	56.0	18.1
30	29.5	63.0	33.5	17.0	8.3	21.0	9.2	25.0	16.0	57.0	29.4	24.0	11.1	33.0	18.2
31	454.7	486.0	31.3	104.0	6.8	264.0	9.6	118.0	14.9	472.0	27.7	303.0	10.3	169.0	17.4
32	19.1	54.0	34.9	33.0	9.9	6.0	9.0	15.0	16.0	35.0	30.4	18.0	12.5	17.0	17.9
33	14.2	49.0	34.8	21.0	9.4	10.0	8.7	18.0	16.7	40.0	30.3	20.0	11.9	20.0	18.4
34	13.0	23.0	10.0	8.0	2.5	7.0	2.7	8.0	4.8	16.0	8.7	7.0	3.2	9.0	5.5
35	167.1	199.0	31.9	37.0	9.0	105.0	8.0	57.0	15.0	194.0	27.6	124.0	10.4	70.0	17.2
36	33.4	70.0	36.6	22.0	8.4	30.0	9.8	18.0	18.4	63.0	32.8	40.0	12.0	23.0	20.7
37	23.5	57.0	33.5	16.0	9.1	25.0	8.8	16.0	15.6	54.0	29.0	35.0	11.2	19.0	17.8
38	64.3	74.0	9.7	23.0	2.4	34.0	2.7	17.0	4.5	66.0	8.6	40.0	3.4	26.0	5.2
39	139.8	153.0	13.2	41.0	3.4	73.0	3.7	39.0	6.0	145.0	11.6	93.0	4.8	52.0	6.8
40	126.8	139.0	12.2	27.0	3.3	76.0	3.5	36.0	5.5	133.0	10.7	88.0	4.6	45.0	6.1
41	662.3	698.0	35.7	136.0	9.5	389.0	9.4	173.0	16.9	671.0	31.6	439.0	12.6	232.0	19.0
42	430.0	462.0	32.0	105.0	8.1	253.0	8.6	104.0	15.2	441.0	28.3	308.0	11.1	133.0	17.2
43	141.4	177.0	35.6	46.0	9.7	85.0	10.1	46.0	15.8	167.0	31.0	116.0	12.3	51.0	18.7
44	30.4	61.0	30.6	11.0	6.7	25.0	8.5	25.0	15.5	57.0	26.7	28.0	8.9	29.0	17.8
45	35.6	69.0	33.4	11.0	8.8	28.0	9.1	30.0	15.5	65.0	29.7	23.0	12.2	42.0	17.5
46	39.2	78.0	38.8	19.0	12.8	38.0	9.9	21.0	16.1	70.0	33.8	45.0	16.0	25.0	17.9
47	-	-	-	-	-	-	-	-	-	-	-	-	-	-	-
48	72.4	113.0	41.6	35.0	11.9	51.0	11.0	27.0	18.7	102.0	36.7	70.0	15.2	32.0	21.6
49	20.8	53.0	32.2	11.0	7.9	29.0	8.7	13.0	15.6	50.0	27.8	28.0	10.5	22.0	17.3
50	151.3	186.0	34.7	47.0	9.1	95.0	9.3	44.0	16.3	177.0	30.6	118.0	11.5	59.0	19.1
51	57.5	93.0	35.5	25.0	9.8	46.0	10.1	22.0	15.6	87.0	31.3	59.0	13.3	28.0	18.0
52	17.9	65.0	47.7	19.0	14.2	28.0	13.5	18.0	19.9	58.0	42.5	37.0	19.0	21.0	23.5
53	75.6	91.0	15.4	22.0	4.8	38.0	4.2	31.0	6.3	80.0	13.6	41.0	6.3	39.0	7.3

TABLE 15 — *Continued*

Masterid	Net B Counts	Raw Counts													
		B-band		S1-band		S2-band		H-band		Bc-band		Sc-band		Hc-band	
(1)	(2)	(Src)	(Bkg)	(Src)	(Bkg)	(Src)	(Bkg)	(Src)	(Bkg)	(Src)	(Bkg)	(Src)	(Bkg)	(Src)	(Bkg)
54	63.1	107.0	43.9	34.0	13.9	46.0	12.1	27.0	17.9	96.0	39.1	59.0	18.8	37.0	20.2
55	30.7	67.0	36.3	19.0	9.7	28.0	10.7	20.0	15.9	62.0	32.1	37.0	13.9	25.0	18.2
56	94.4	141.0	46.6	32.0	14.9	76.0	13.1	33.0	18.6	135.0	41.3	87.0	20.1	48.0	21.2
57	54.7	98.0	43.3	15.0	12.9	43.0	11.2	40.0	19.2	90.0	38.1	44.0	16.5	46.0	21.6
58	17.0	59.0	41.3	19.0	12.0	23.0	11.6	17.0	17.6	52.0	36.2	32.0	16.1	20.0	20.1
59	34.7	86.0	50.8	18.0	17.9	48.0	15.0	20.0	17.9	82.0	45.6	53.0	24.8	29.0	20.8
60	48.9	79.0	30.1	25.0	6.9	30.0	8.7	24.0	14.5	69.0	27.1	38.0	10.7	31.0	16.4
61	-	-	-	-	-	-	-	-	-	-	-	-	-	-	-
62	25.9	35.0	9.1	21.0	3.1	11.0	2.7	3.0	3.4	26.0	8.4	22.0	4.5	4.0	3.9
63	142.9	178.0	35.1	35.0	10.0	86.0	9.4	57.0	15.6	172.0	31.1	107.0	13.5	65.0	17.6
64	29.5	37.0	7.5	13.0	2.1	16.0	2.1	8.0	3.3	35.0	6.6	26.0	2.8	9.0	3.7
65	103.3	118.0	14.7	31.0	5.0	61.0	4.2	26.0	5.5	111.0	13.1	76.0	7.0	35.0	6.1
66	155.7	168.0	12.3	42.0	4.0	89.0	3.6	37.0	4.7	162.0	10.9	115.0	5.7	47.0	5.2
67	139.1	173.0	33.9	16.0	9.2	92.0	9.2	65.0	15.6	167.0	29.8	85.0	11.8	82.0	18.0
68	205.5	246.0	40.7	66.0	11.7	111.0	10.7	69.0	18.3	228.0	35.5	140.0	14.9	88.0	20.6
69	78.7	109.0	30.3	23.0	8.2	55.0	8.3	31.0	13.9	101.0	26.3	60.0	10.4	41.0	15.9
70	34.5	89.0	54.9	23.0	18.5	38.0	17.4	28.0	19.0	80.0	49.3	40.0	27.9	40.0	21.4
71	110.5	142.0	31.5	28.0	7.4	63.0	9.0	51.0	15.2	133.0	28.2	70.0	10.0	63.0	18.2
72	244.3	276.0	31.7	74.0	7.7	128.0	9.6	74.0	14.4	262.0	28.2	172.0	11.2	90.0	16.9
73	141.3	185.0	44.3	43.0	14.6	96.0	12.9	46.0	16.7	174.0	38.8	114.0	19.7	60.0	19.1
74	77.0	88.0	11.0	24.0	3.4	40.0	3.0	24.0	4.6	80.0	9.4	53.0	4.1	27.0	5.3
75	27.3	61.0	33.7	15.0	8.0	26.0	8.9	20.0	16.9	51.0	30.2	24.0	11.8	27.0	18.5
76	268.2	317.0	49.0	83.0	16.0	160.0	15.1	74.0	17.9	301.0	43.0	204.0	22.8	97.0	20.2
77	14.7	59.0	43.5	9.0	13.1	26.0	12.2	24.0	18.2	57.0	38.6	30.0	17.7	27.0	20.8
78	245.7	282.0	36.3	68.0	9.4	140.0	9.9	74.0	17.0	271.0	32.1	181.0	12.5	90.0	19.5
79	-	-	-	-	-	-	-	-	-	-	-	-	-	-	-
80	53.6	67.0	13.4	21.0	4.8	30.0	3.8	16.0	4.7	61.0	11.6	41.0	6.4	20.0	5.2
81	71.9	99.0	27.1	30.0	11.3	36.0	8.3	33.0	7.5	92.0	24.0	55.0	16.0	37.0	8.1
82	26.0	35.0	9.0	9.0	3.3	16.0	2.5	10.0	3.2	32.0	7.9	21.0	4.3	11.0	3.6
83	240.9	288.0	48.0	86.0	15.4	144.0	14.9	58.0	17.7	275.0	41.8	193.0	21.9	82.0	19.9
84	168.7	184.0	15.3	46.0	6.0	92.0	4.6	46.0	4.7	177.0	13.8	119.0	8.5	58.0	5.3
85	154.0	171.0	17.0	39.0	6.6	95.0	5.3	37.0	5.1	164.0	15.2	117.0	9.2	47.0	5.9
86	54.5	71.0	16.5	17.0	6.5	42.0	5.6	12.0	4.3	66.0	14.8	47.0	10.0	19.0	4.8
87	59.8	94.0	33.7	11.0	8.5	40.0	8.6	43.0	16.7	91.0	30.0	43.0	11.3	48.0	18.7
88	76.5	107.0	30.5	33.0	13.3	54.0	9.2	20.0	8.1	99.0	28.1	72.0	19.2	27.0	9.0
89	-	-	-	-	-	-	-	-	-	-	-	-	-	-	-
90	22.9	59.0	36.1	16.0	10.0	24.0	10.5	19.0	15.7	55.0	31.8	31.0	13.4	24.0	18.3
91	93.1	128.0	34.9	56.0	14.2	55.0	12.3	17.0	8.4	114.0	31.0	92.0	21.3	22.0	9.7
92	25.5	34.0	8.5	4.0	3.0	19.0	2.5	11.0	3.0	33.0	7.4	19.0	4.1	14.0	3.3
93	25.6	69.0	43.4	24.0	12.3	20.0	11.9	25.0	19.2	61.0	38.4	31.0	17.3	30.0	21.1
94	35.9	55.0	19.5	6.0	4.9	24.0	4.9	25.0	9.7	54.0	17.3	26.0	6.5	28.0	10.8
95	11.9	46.0	34.1	7.0	8.9	18.0	10.3	21.0	14.8	44.0	30.5	18.0	13.1	26.0	17.4
96	859.2	908.0	48.8	194.0	14.6	512.0	15.0	202.0	19.1	867.0	43.0	595.0	21.4	272.0	21.7
97	43.9	76.0	32.1	16.0	7.9	30.0	9.1	30.0	15.1	71.0	28.5	35.0	11.1	36.0	17.4
98	306.4	348.0	41.6	75.0	18.7	194.0	13.2	79.0	9.7	335.0	36.9	226.0	25.5	109.0	11.4
99	256.7	347.0	90.3	119.0	43.4	160.0	30.5	68.0	16.5	324.0	82.2	240.0	62.8	84.0	19.4
100	118.8	179.0	59.4	58.0	23.0	77.0	16.7	44.0	19.7	162.0	53.3	103.0	30.9	59.0	22.4
101	175.3	263.0	87.7	88.0	43.9	121.0	31.4	54.0	12.4	228.0	79.7	159.0	64.2	69.0	15.6
102	26.5	103.0	76.2	47.0	29.6	35.0	25.0	21.0	21.5	91.0	67.7	65.0	43.5	26.0	24.2
103	175.2	218.0	42.8	46.0	11.8	101.0	12.6	71.0	18.4	204.0	37.8	123.0	17.1	81.0	20.7
104	134.2	200.0	65.8	69.0	32.3	92.0	22.3	39.0	11.2	190.0	59.8	137.0	46.8	53.0	13.0
105	-	-	-	-	-	-	-	-	-	-	-	-	-	-	-
106	139.1	258.0	118.9	103.0	57.3	125.0	47.3	30.0	14.2	242.0	108.1	202.0	90.9	40.0	17.2
107	46.6	76.0	29.4	15.0	6.8	40.0	7.8	21.0	14.9	73.0	26.2	46.0	9.6	27.0	16.6

TABLE 15 — *Continued*

Masterid	Net B Counts	Raw Counts													
		B-band		S1-band		S2-band		H-band		Bc-band		Sc-band		Hc-band	
(1)	(2)	(Src)	(Bkg)	(Src)	(Bkg)	(Src)	(Bkg)	(Src)	(Bkg)	(Src)	(Bkg)	(Src)	(Bkg)	(Src)	(Bkg)
108	133.5	172.0	38.5	37.0	10.2	93.0	10.1	42.0	18.2	166.0	34.2	113.0	13.7	53.0	20.5
109	73.4	159.0	85.2	55.0	35.9	74.0	26.8	30.0	22.5	147.0	76.4	108.0	50.0	39.0	26.4
110	81.9	147.0	65.0	43.0	19.4	75.0	22.7	29.0	22.9	137.0	59.2	98.0	33.0	39.0	26.2
111	81.4	134.0	52.6	48.0	18.5	67.0	16.0	19.0	18.2	124.0	47.0	97.0	26.3	27.0	20.7
112	8.2	42.0	33.6	11.0	7.3	10.0	9.7	21.0	16.6	38.0	30.1	15.0	11.4	23.0	18.7
113	13.4	57.0	43.6	21.0	12.3	20.0	12.8	16.0	18.4	47.0	38.6	28.0	18.0	19.0	20.6
114	192.6	248.0	55.4	87.0	27.3	118.0	19.0	43.0	9.1	239.0	50.3	185.0	39.7	54.0	10.5
115	30.7	83.0	52.3	23.0	17.7	36.0	15.2	24.0	19.4	78.0	46.6	49.0	24.7	29.0	21.9
116	89.0	146.0	57.0	40.0	28.6	79.0	19.3	27.0	9.1	140.0	51.3	106.0	41.1	34.0	10.3
117	48772.2	49127.0	354.8	17276.0	166.9	25183.0	129.9	6668.0	58.1	45815.0	321.1	36317.0	251.7	9498.0	69.4
118	372.0	415.0	43.0	95.0	18.2	228.0	12.6	92.0	12.2	390.0	38.2	270.0	23.8	120.0	14.4
119	1275.8	1532.0	256.2	358.0	125.6	809.0	105.9	365.0	24.6	1482.0	235.3	1007.0	204.5	475.0	30.8
120	621.0	946.0	325.0	314.0	154.4	479.0	135.4	153.0	35.1	897.0	298.1	692.0	253.5	205.0	44.6
121	55.0	90.0	34.8	25.0	8.0	37.0	9.5	28.0	17.4	87.0	30.9	55.0	11.5	32.0	19.4
122	20.8	53.0	32.2	17.0	7.4	22.0	7.3	14.0	17.6	50.0	28.5	32.0	9.3	18.0	19.2
123	-	-	-	-	-	-	-	-	-	-	-	-	-	-	-
124	164.1	242.0	77.9	90.0	36.2	129.0	27.1	23.0	14.5	230.0	70.4	197.0	53.8	33.0	16.6
125	101.4	148.0	46.4	32.0	13.2	71.0	13.9	45.0	19.4	140.0	41.0	81.0	19.9	59.0	21.1
126	69.4	125.0	55.6	46.0	20.5	45.0	17.3	34.0	17.8	110.0	49.6	69.0	28.7	41.0	20.8
127	72.7	98.0	25.3	36.0	10.8	49.0	9.0	13.0	5.5	92.0	22.7	71.0	15.8	21.0	7.0
128	120.6	209.0	88.4	104.0	41.9	75.0	35.2	30.0	11.4	197.0	79.7	161.0	65.8	36.0	13.9
129	114.4	156.0	41.6	62.0	17.3	73.0	16.7	21.0	7.6	148.0	37.1	126.0	26.3	22.0	10.7
130	65.1	116.0	50.9	28.0	16.8	54.0	15.9	34.0	18.1	110.0	46.1	72.0	25.0	38.0	21.1
131	30.7	42.0	11.3	20.0	4.4	15.0	3.5	7.0	3.4	38.0	10.0	30.0	6.1	8.0	4.0
132	264.8	446.0	181.2	169.0	83.7	203.0	80.1	74.0	17.4	422.0	166.3	325.0	145.2	97.0	21.0
133	311.9	346.0	34.1	74.0	8.2	175.0	9.3	97.0	16.6	339.0	30.5	219.0	11.6	120.0	18.9
134	64.2	76.0	11.8	23.0	3.2	33.0	3.7	20.0	4.9	72.0	10.6	49.0	5.0	23.0	5.5
135	113.6	154.0	40.4	55.0	18.8	71.0	13.9	28.0	7.7	149.0	37.0	112.0	28.2	37.0	8.8
136	-	-	-	-	-	-	-	-	-	-	-	-	-	-	-
137	96.6	118.0	21.4	28.0	8.4	76.0	9.0	14.0	4.0	114.0	19.3	91.0	13.9	23.0	5.4
138	79.5	126.0	46.5	40.0	20.1	61.0	19.3	25.0	7.1	115.0	42.5	84.0	34.3	31.0	8.1
139	161.6	186.0	24.4	56.0	10.1	112.0	9.7	18.0	4.7	181.0	22.0	152.0	15.8	29.0	6.2
140	296.5	324.0	27.5	81.0	9.6	165.0	8.9	78.0	9.0	310.0	25.1	215.0	14.4	95.0	10.7
141	98.1	141.0	43.2	38.0	13.6	79.0	11.9	24.0	17.7	137.0	38.0	102.0	18.0	35.0	20.0
142	48.7	80.0	31.3	16.0	7.2	37.0	9.0	27.0	15.0	75.0	27.5	47.0	10.2	28.0	17.3
143	98.7	130.0	31.3	7.0	6.8	53.0	8.1	70.0	16.4	127.0	28.0	44.0	9.8	83.0	18.2
144	40.4	82.0	41.7	30.0	11.7	31.0	12.2	21.0	17.8	78.0	36.9	49.0	16.8	29.0	20.1
145	55.0	138.0	83.0	77.0	40.1	44.0	22.8	17.0	20.1	119.0	74.0	97.0	49.9	22.0	24.1
146	1120.3	1192.0	71.7	258.0	32.9	668.0	25.4	266.0	13.4	1169.0	64.0	813.0	49.3	356.0	14.7
147	391.9	460.0	68.1	149.0	30.0	242.0	24.5	69.0	13.6	443.0	61.6	349.0	46.8	94.0	14.8
148	295.1	315.0	19.9	74.0	5.5	161.0	6.8	80.0	7.5	303.0	18.1	200.0	9.3	103.0	8.8
149	-	-	-	-	-	-	-	-	-	-	-	-	-	-	-
150	32.7	41.0	8.3	8.0	2.5	19.0	2.3	14.0	3.5	40.0	7.4	25.0	3.4	15.0	3.9
151	23.0	57.0	34.0	13.0	7.7	31.0	9.9	13.0	16.5	54.0	30.6	34.0	12.0	20.0	18.6
152	28.9	36.0	7.1	21.0	2.0	8.0	2.4	7.0	2.7	32.0	6.4	25.0	3.4	7.0	3.0
153	39.6	113.0	73.4	35.0	28.1	52.0	28.4	26.0	16.9	103.0	67.7	71.0	46.4	32.0	21.3
154	247.9	292.0	44.1	75.0	17.8	142.0	16.0	75.0	10.3	282.0	39.9	186.0	28.6	96.0	11.4
155	138.5	175.0	36.5	52.0	9.9	79.0	11.3	44.0	15.3	162.0	32.5	110.0	15.3	52.0	17.2
156	52.4	98.0	45.6	28.0	12.0	52.0	15.2	18.0	18.4	89.0	41.1	62.0	20.2	27.0	20.9
157	287.7	342.0	53.9	76.0	16.1	192.0	17.6	74.0	20.2	323.0	49.4	231.0	26.3	92.0	23.2
158	1181.3	1238.0	56.9	267.0	19.7	722.0	17.7	249.0	19.4	1186.0	52.0	840.0	29.6	346.0	22.4
159	34.3	45.0	10.7	8.0	2.8	19.0	3.4	18.0	4.5	42.0	9.7	21.0	4.6	21.0	5.1
160	103.2	147.0	43.8	33.0	12.5	70.0	13.4	44.0	17.9	138.0	39.8	84.0	18.8	54.0	21.0
161	23.7	67.0	42.3	22.0	12.1	28.0	11.8	17.0	18.4	56.0	37.7	32.0	16.6	24.0	21.0

TABLE 15 — *Continued*

Masterid	Net B Counts	Raw Counts													
		B-band		S1-band		S2-band		H-band		Bc-band		Sc-band		Hc-band	
(1)	(2)	(Src)	(Bkg)	(Src)	(Bkg)	(Src)	(Bkg)	(Src)	(Bkg)	(Src)	(Bkg)	(Src)	(Bkg)	(Src)	(Bkg)
162	105.3	155.0	49.7	54.0	16.6	69.0	15.9	32.0	17.2	137.0	45.2	100.0	25.6	37.0	19.6
163	583.0	641.0	57.2	133.0	20.1	346.0	17.3	162.0	19.8	615.0	52.2	396.0	29.8	219.0	22.4
164	48.2	84.0	35.8	20.0	8.0	39.0	10.9	25.0	16.9	79.0	32.5	50.0	13.3	29.0	19.2
165	62.3	73.0	10.7	30.0	2.6	35.0	3.6	8.0	4.5	66.0	9.7	55.0	4.5	11.0	5.2
166	101.3	149.0	47.7	44.0	12.4	60.0	15.4	45.0	19.9	137.0	43.9	88.0	20.4	49.0	23.5
167	39.6	50.0	10.4	16.0	3.0	19.0	3.1	15.0	4.4	48.0	9.2	32.0	4.2	16.0	5.0
168	41.0	51.0	10.0	10.0	2.4	28.0	3.4	13.0	4.2	51.0	9.2	33.0	4.2	18.0	5.0
169	140.6	178.0	37.4	64.0	8.2	89.0	11.1	25.0	18.1	166.0	33.7	132.0	13.2	34.0	20.5
170	109.3	146.0	36.7	37.0	9.0	68.0	11.6	41.0	16.0	136.0	32.7	91.0	14.2	45.0	18.5
171	62.5	98.0	35.5	30.0	8.1	46.0	10.8	22.0	16.6	90.0	31.5	63.0	12.5	27.0	19.1
172	35.3	74.0	39.1	24.0	10.9	22.0	11.9	28.0	16.3	66.0	35.2	38.0	16.3	28.0	18.8
173	-	-	-	-	-	-	-	-	-	-	-	-	-	-	-
174	32.8	74.0	41.0	19.0	10.7	44.0	13.1	11.0	17.2	69.0	36.8	53.0	17.4	16.0	19.5
175	34.4	78.0	43.2	24.0	11.0	30.0	14.6	24.0	17.5	72.0	39.3	42.0	18.3	30.0	20.9
176	16.0	49.0	33.0	11.0	7.2	18.0	9.2	20.0	16.6	45.0	29.6	18.0	10.9	27.0	18.7
177	-	-	-	-	-	-	-	-	-	-	-	-	-	-	-
178	29.2	78.0	48.8	32.0	14.7	23.0	15.3	23.0	18.8	68.0	44.6	41.0	23.6	27.0	21.0
179	113.5	127.0	13.5	30.0	3.4	66.0	4.4	31.0	5.7	119.0	12.2	73.0	5.7	46.0	6.5
180	31.2	79.0	47.8	28.0	14.7	28.0	14.1	23.0	19.0	76.0	43.1	44.0	22.0	32.0	21.1
181	64.2	102.0	38.3	18.0	11.2	56.0	11.2	28.0	15.9	96.0	33.7	63.0	15.9	33.0	17.9
182	56.8	68.0	11.2	15.0	3.5	36.0	3.1	17.0	4.6	63.0	10.0	41.0	4.9	22.0	5.1
183	64.9	98.0	33.1	19.0	9.0	43.0	8.8	36.0	15.4	89.0	29.0	47.0	11.4	42.0	17.6
184	1109.6	1148.0	38.4	206.0	9.7	638.0	11.7	304.0	17.1	1114.0	33.9	717.0	14.5	397.0	19.4
185	538.6	586.0	47.0	100.0	14.0	338.0	13.0	148.0	20.0	568.0	42.4	371.0	20.3	197.0	22.2
186	46.3	89.0	42.7	25.0	12.1	38.0	13.1	26.0	17.5	79.0	38.8	48.0	19.0	31.0	19.8
187	143.7	186.0	42.3	45.0	11.6	93.0	12.6	48.0	18.0	179.0	37.9	119.0	17.5	60.0	20.4
188	13.0	50.0	37.0	14.0	8.7	19.0	11.2	17.0	17.1	46.0	32.6	27.0	13.1	19.0	19.5
189	136.2	176.0	40.1	45.0	13.0	89.0	11.1	42.0	16.0	166.0	35.4	113.0	17.4	53.0	18.0
190	139.3	176.0	36.7	36.0	8.7	101.0	10.6	39.0	17.4	168.0	33.4	111.0	13.6	57.0	19.8
191	103.3	142.0	38.7	39.0	11.3	61.0	10.8	42.0	16.6	129.0	34.6	81.0	16.5	48.0	18.1
192	32.8	70.0	37.2	15.0	9.2	29.0	11.7	26.0	16.3	67.0	33.9	37.0	15.0	30.0	18.9
193	28.2	67.0	38.8	19.0	10.8	22.0	10.4	26.0	17.6	61.0	34.8	30.0	15.3	31.0	19.5
194	598.4	636.0	37.3	150.0	11.6	343.0	9.4	143.0	16.3	608.0	33.1	419.0	14.6	189.0	18.5
195	117.5	153.0	35.5	36.0	7.3	80.0	9.6	37.0	18.6	143.0	31.9	90.0	11.1	53.0	20.8
196	41.9	71.0	29.1	27.0	7.5	27.0	6.8	17.0	14.8	65.0	26.0	40.0	9.6	25.0	16.4
197	58.5	94.0	35.5	20.0	10.2	46.0	9.9	28.0	15.5	87.0	32.0	44.0	14.4	43.0	17.7
198	15.5	49.0	33.5	8.0	7.9	18.0	8.6	23.0	17.0	45.0	29.6	18.0	11.1	27.0	18.5
199	34.5	70.0	35.5	20.0	9.9	24.0	9.7	26.0	15.8	68.0	32.0	35.0	14.0	33.0	18.0
200	15.3	49.0	33.7	15.0	8.8	11.0	8.5	23.0	16.4	44.0	29.7	20.0	10.9	24.0	18.7
201	42.3	75.0	32.7	11.0	8.5	21.0	8.1	43.0	16.1	70.0	29.7	20.0	12.0	50.0	17.7
202	91.8	124.0	32.2	20.0	7.4	67.0	7.9	37.0	16.8	120.0	28.7	75.0	10.0	45.0	18.7
203	72.1	103.0	30.9	26.0	7.5	50.0	7.8	27.0	15.6	95.0	26.9	63.0	9.4	32.0	17.5
204	336.2	370.0	33.8	111.0	9.9	200.0	8.6	59.0	15.2	348.0	30.1	264.0	13.0	84.0	17.0
205	77.2	112.0	34.8	20.0	8.0	63.0	10.0	29.0	16.8	106.0	30.9	72.0	11.6	34.0	19.3
206	31.4	66.0	34.6	16.0	8.0	26.0	10.3	24.0	16.3	62.0	30.5	35.0	11.6	27.0	18.9
207	12.9	48.0	35.1	13.0	8.2	23.0	9.7	12.0	17.2	42.0	32.0	28.0	12.4	14.0	19.6
208	45.6	79.0	33.4	13.0	7.5	42.0	8.6	24.0	17.2	73.0	30.1	41.0	10.6	32.0	19.5
209	196.9	230.0	33.1	18.0	7.9	119.0	8.9	93.0	16.4	225.0	29.4	107.0	10.9	118.0	18.5
210	50.2	59.0	8.8	16.0	2.0	27.0	2.5	16.0	4.3	58.0	7.6	38.0	2.7	20.0	5.0
211	57.1	90.0	32.9	19.0	8.1	42.0	9.3	29.0	15.5	84.0	29.8	50.0	11.7	34.0	18.1
212	22.3	54.0	31.9	14.0	7.0	23.0	9.4	17.0	15.4	50.0	28.4	30.0	10.5	20.0	17.9
213	89.3	122.0	32.8	30.0	7.3	37.0	8.9	55.0	16.6	117.0	29.1	59.0	10.0	58.0	19.2
214	18.5	24.0	5.5	6.0	1.3	8.0	1.5	10.0	2.8	24.0	4.8	14.0	1.5	10.0	3.3
215	25.1	57.0	31.9	10.0	7.8	26.0	7.9	21.0	16.2	54.0	28.7	30.0	10.1	24.0	18.7

TABLE 15 — *Continued*

Masterid	Net B Counts	Raw Counts													
		B-band		S1-band		S2-band		H-band		Bc-band		Sc-band		Hc-band	
(1)	(2)	(Src) (3)	(Bkg) (4)	(Src) (5)	(Bkg) (6)	(Src) (7)	(Bkg) (8)	(Src) (9)	(Bkg) (10)	(Src) (11)	(Bkg) (12)	(Src) (13)	(Bkg) (14)	(Src) (15)	(Bkg) (16)
216	102.3	139.0	36.7	30.0	8.7	74.0	9.8	35.0	18.2	134.0	32.9	92.0	12.8	42.0	20.2
217	46.4	79.0	32.0	17.0	7.7	44.0	8.5	18.0	15.8	74.0	28.4	50.0	10.2	24.0	18.2
218	22.8	53.0	30.0	11.0	7.2	22.0	8.1	20.0	14.7	50.0	26.0	26.0	8.8	24.0	17.2
219	29.5	67.0	37.5	16.0	9.2	26.0	10.2	25.0	18.1	62.0	33.4	33.0	12.6	29.0	20.8
220	340.2	370.0	29.8	104.0	7.7	189.0	7.6	77.0	14.5	351.0	26.7	256.0	10.2	95.0	16.5
221	-	-	-	-	-	-	-	-	-	-	-	-	-	-	-
222	-	-	-	-	-	-	-	-	-	-	-	-	-	-	-
223	79.2	109.0	29.8	19.0	7.1	49.0	8.2	41.0	14.5	105.0	26.4	59.0	9.6	46.0	16.8
224	-	-	-	-	-	-	-	-	-	-	-	-	-	-	-
225	188.2	224.0	35.8	57.0	9.4	111.0	9.5	56.0	16.8	213.0	31.8	145.0	13.1	68.0	18.7
226	50.1	81.0	30.9	20.0	7.1	35.0	8.3	26.0	15.5	74.0	27.0	39.0	9.2	35.0	17.8
227	325.0	358.0	33.7	75.0	7.6	184.0	9.0	99.0	17.1	355.0	30.4	227.0	11.6	128.0	18.7
228	506.0	541.0	34.7	88.0	7.7	310.0	9.9	143.0	17.1	528.0	31.2	334.0	12.0	194.0	19.1
229	158.3	192.0	33.7	45.0	7.8	92.0	9.0	55.0	16.9	185.0	30.5	122.0	11.6	63.0	18.9
230	104.6	136.0	31.4	27.0	7.3	74.0	8.9	35.0	15.3	130.0	28.0	85.0	10.7	45.0	17.3
231	120.7	150.0	29.3	29.0	7.1	80.0	8.3	41.0	13.9	142.0	25.9	93.0	9.5	49.0	16.3
232	35.8	70.0	33.3	39.0	8.3	12.0	10.3	19.0	14.7	49.0	29.4	25.0	12.1	24.0	17.3
233	62.3	93.0	30.5	19.0	6.9	49.0	8.2	25.0	15.3	87.0	27.2	57.0	9.4	30.0	17.8
234	43.9	55.0	11.1	4.0	2.5	20.0	3.3	31.0	5.3	55.0	9.9	18.0	3.7	37.0	6.2
235	7.5	36.0	28.5	6.0	7.7	18.0	7.3	12.0	13.5	33.0	25.2	17.0	9.9	16.0	15.4
236	28.9	62.0	33.1	8.0	8.7	27.0	8.2	27.0	16.1	60.0	29.3	28.0	11.4	32.0	17.9

NOTE. — Col. (1): Master ID, cols. (2): net broad-band counts. Cols. (3), (5), (7), (9), (11), (13) and (15): raw source counts in each of the 7 energy bands (see Table 2 for definitions of these bands), cols. (4), (6), (8), (10), (12), (14) and (16): background counts in each of the 7 energy bands. In some instances background counts are very low. For these sources standard aperture photometry results in negative net counts, so, instead, the source cell determined by *wavdetect* has been used. This results in a large area ratio between the background and source regions and therefore a low background count value is derived.

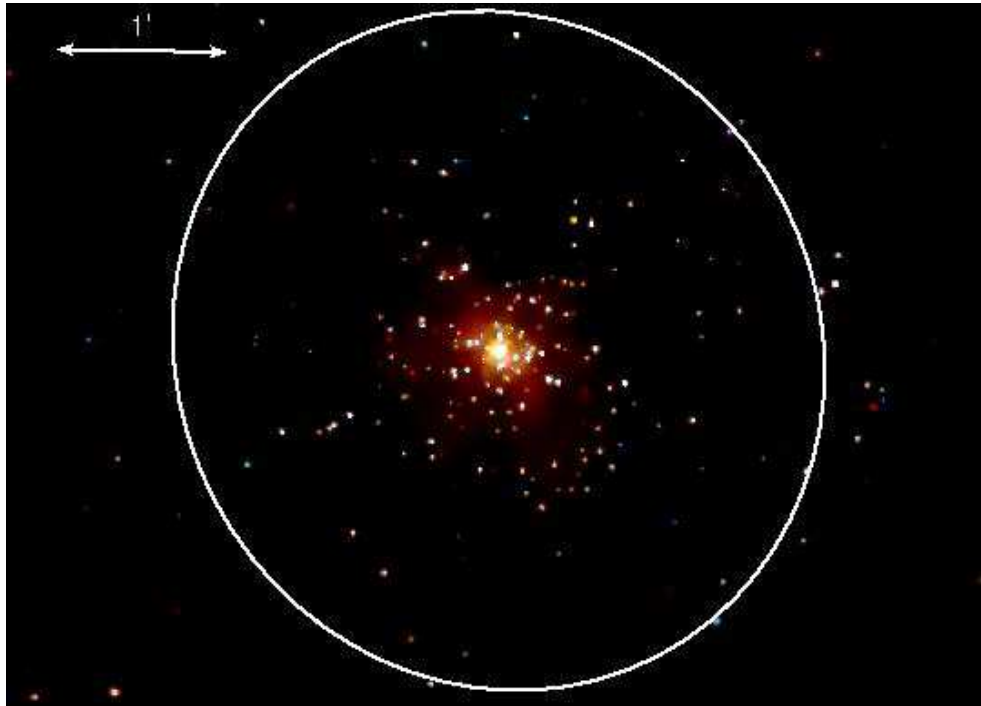
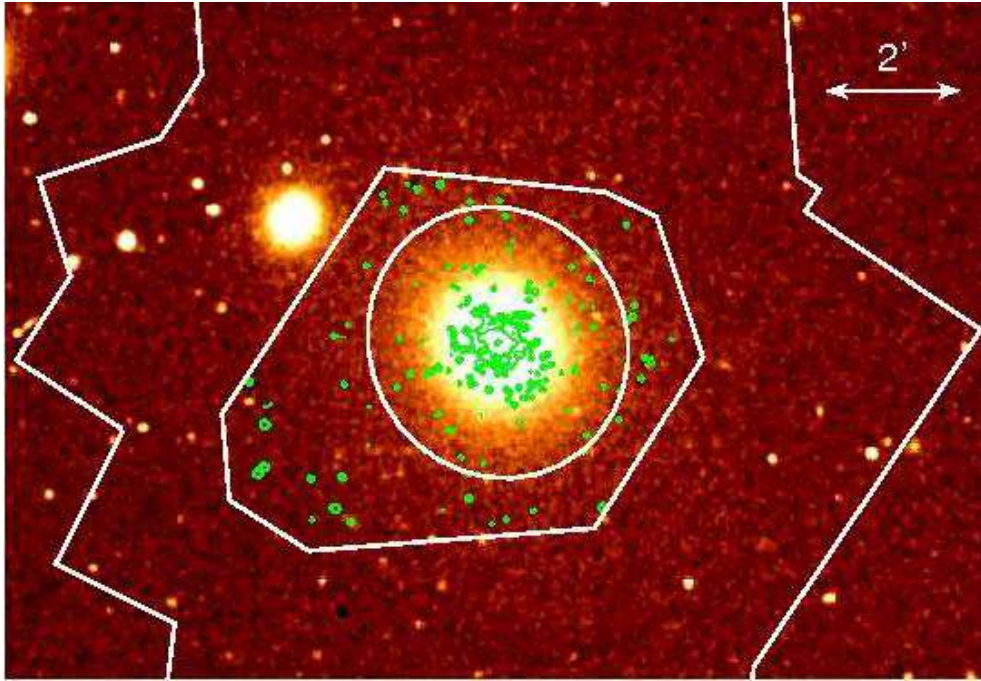


FIG. 1.— Top: An optical image of NGC 4278, with the outline of the total area covered by the ACIS-S3 chips, the region overlapped by all six of the pointings and the D_{25} ellipse of this galaxy shown in white. Also overlaid within the overlap region are the full band adaptively smoothed, X-ray contours. Bottom: A ‘true color’ image of the galaxy, where red corresponds to 0.3–0.9 keV, green to 0.9–2.5 keV and blue to 2.5–8.0 keV. The D_{25} ellipse of this galaxy is also shown.

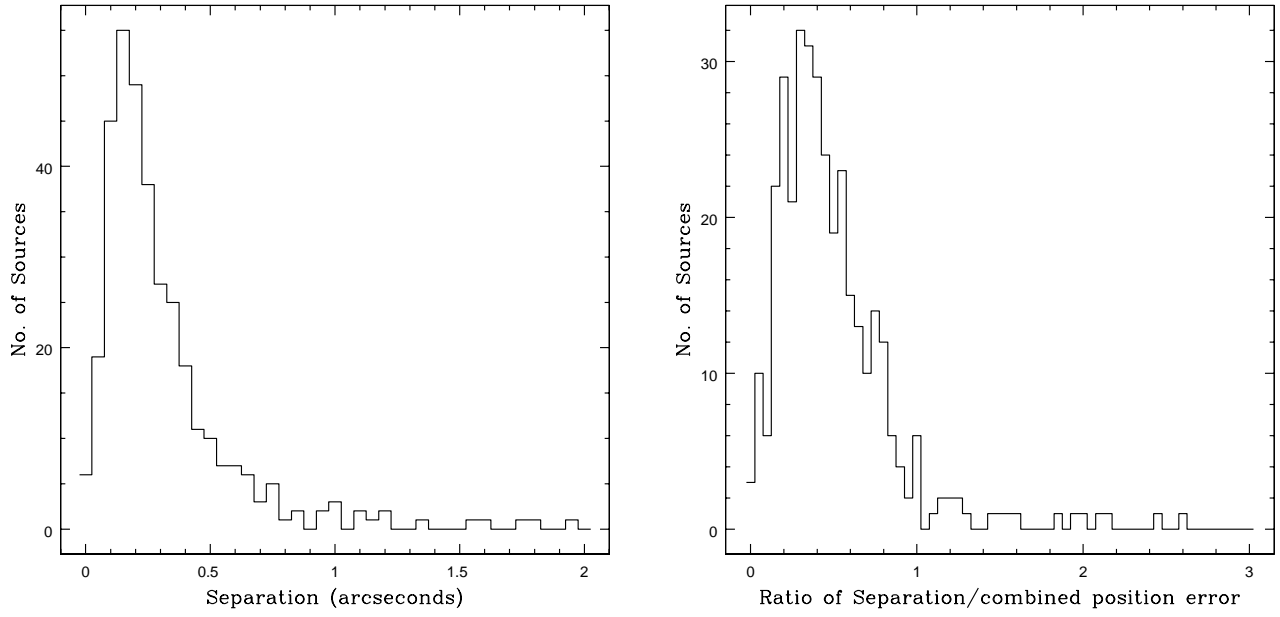


FIG. 2.— Left: Histogram of the separation between sources detected in the co-added observation and sources detected in single observations. Right: Histogram of the ratio of separation between sources detected in the co-added observation and sources detected in single observations, divided by the combined position uncertainty of these sources.

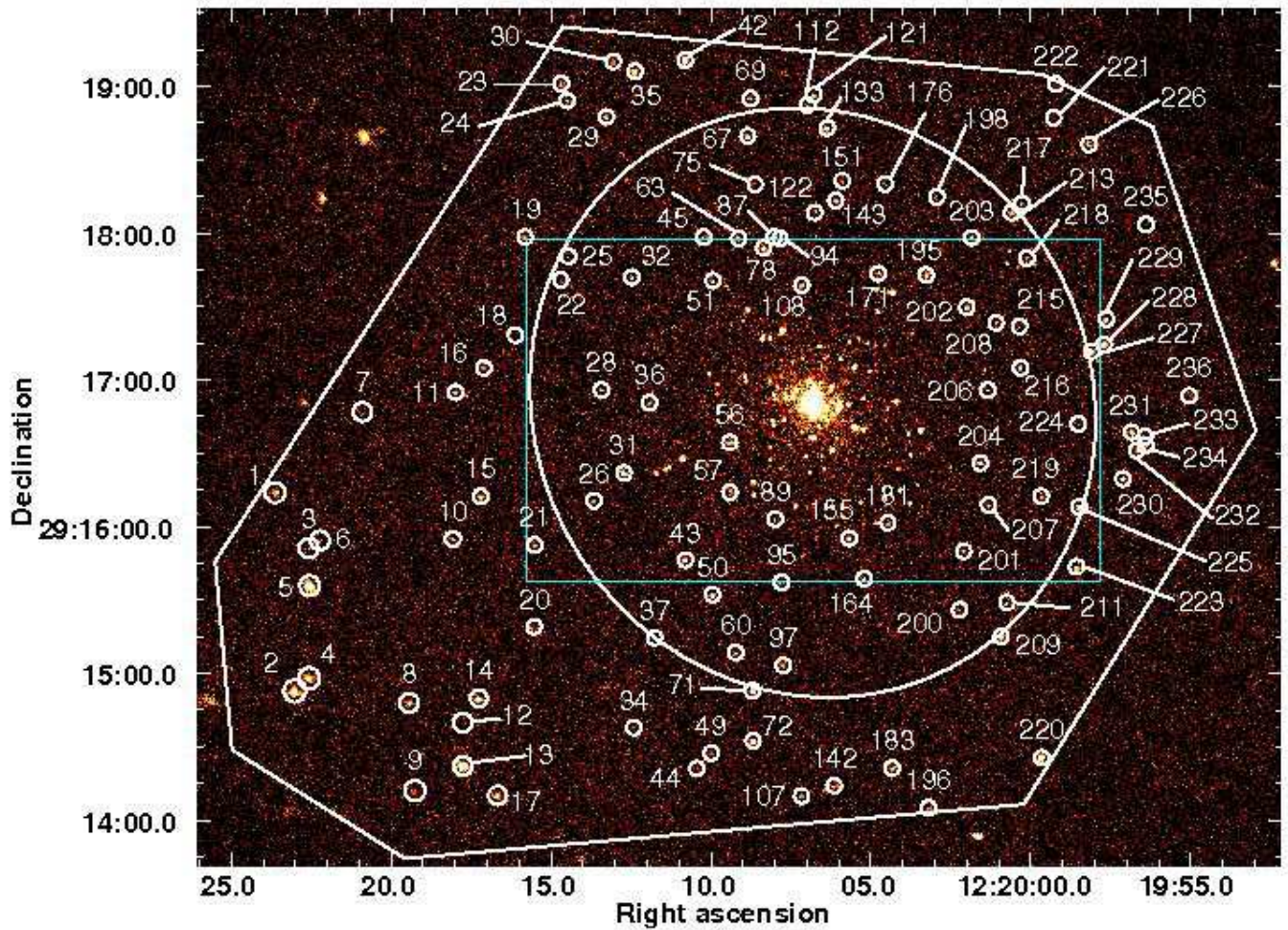
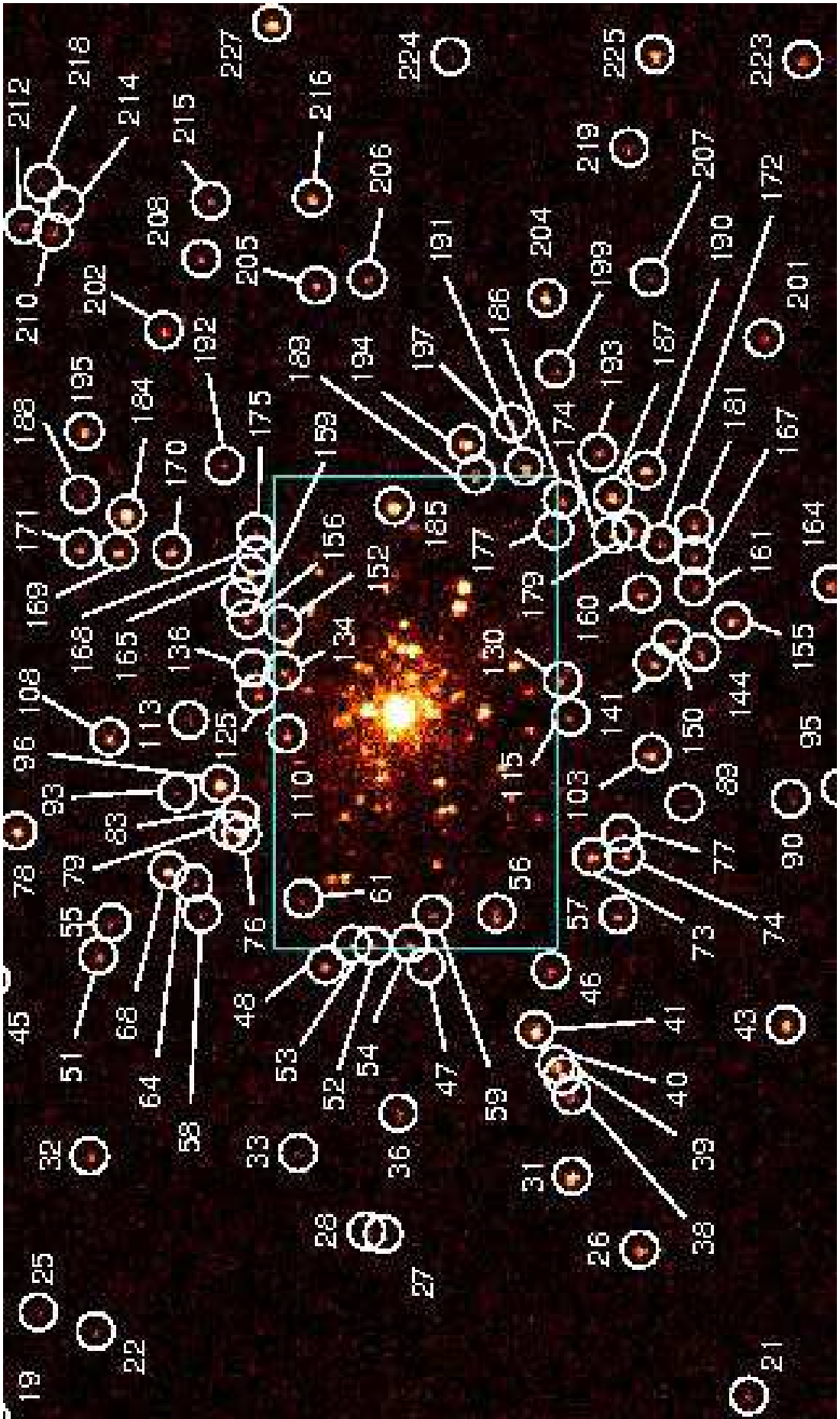
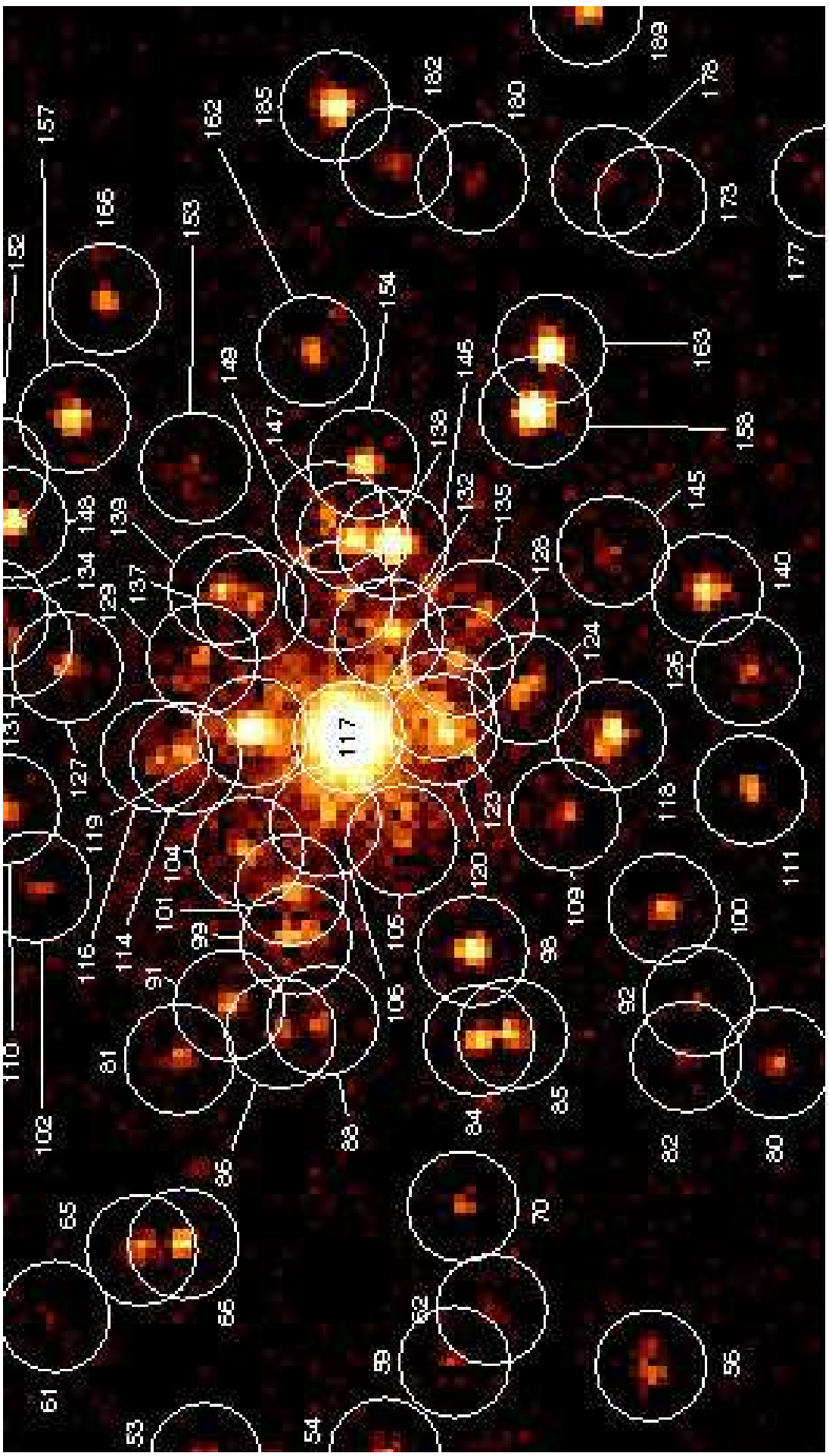


FIG. 3.— The main image presents a full band, raw (unsmoothed, with no exposure correction) image from the co-added observation of NGC 4278, with the D_{25} ellipse and the region overlapped by all six observations overlaid. Source region numbering corresponds to the naming convention in Table 3 and regions represent the 95% encircled energy radius at 1.5 keV. The box in the central region indicates the area shown in the next image, the central region of the galaxy, with sources labeled with the same convention as in the main image. The box shown here encloses the nuclear region of the galaxy, where there is a dense population of sources. This is presented in the final image, where these individual sources can be more clearly seen.





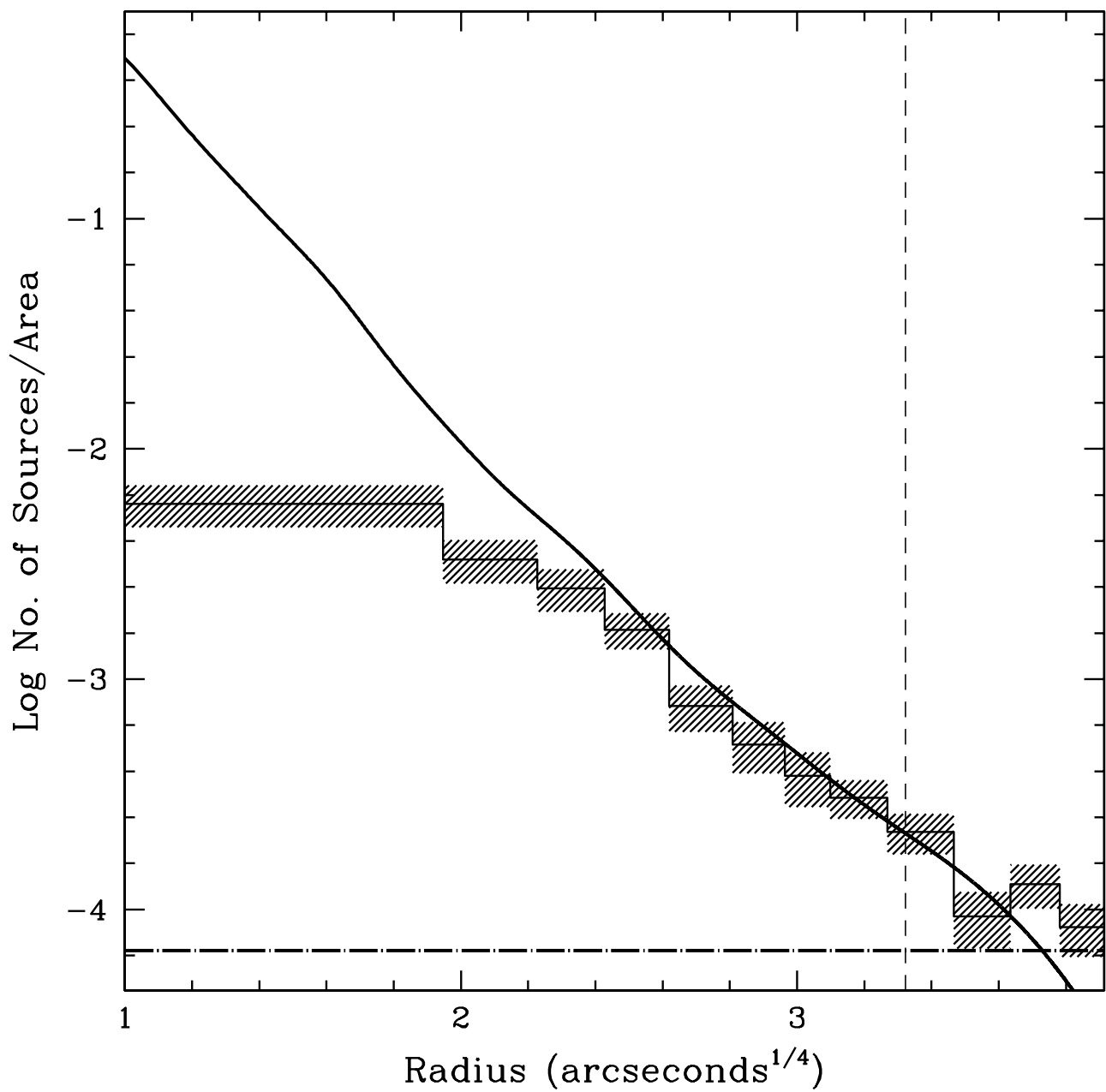


FIG. 4.— X-ray source density profile compared to the optical profile. The histogram indicates the X-ray data and the thick black line is the I-band surface brightness best fit of Cappellari *et al.* (2006). The vertical dashed line is the D_{25} ellipse and the horizontal dot-dashed line indicates the expected number of background sources. The central $1''$ has been excluded in this plot due to the excess optical light contribution from the LINER at the center of this galaxy.

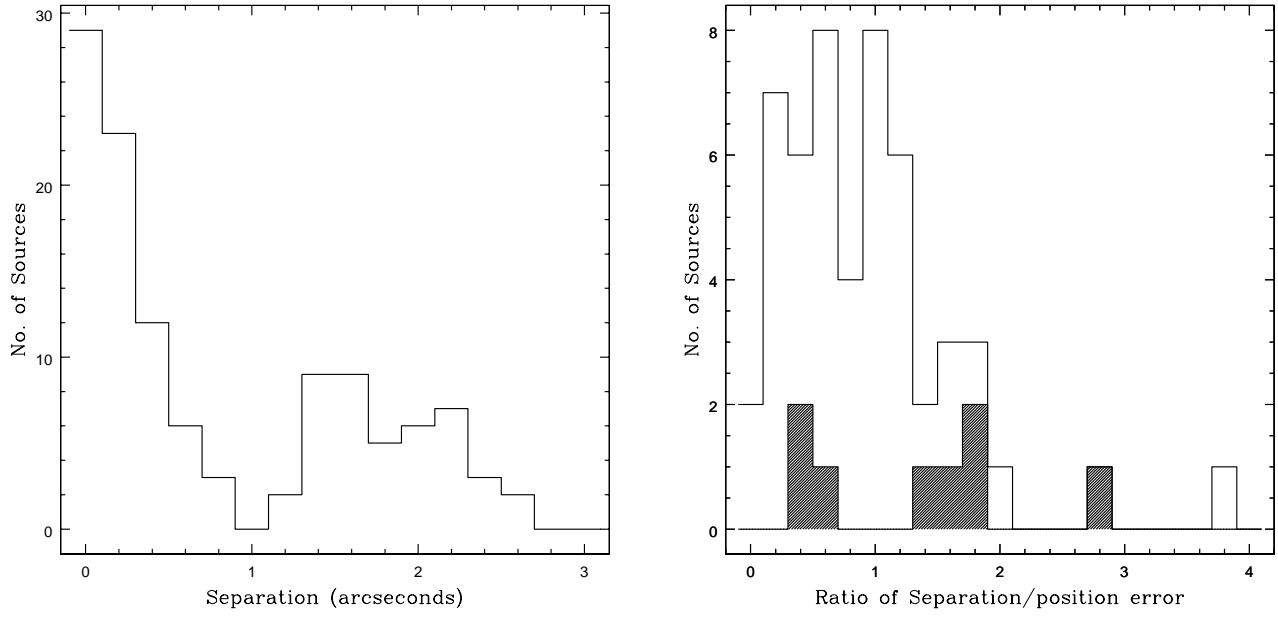


FIG. 5.— Left: A histogram of the separation between the co-added X-ray source position and the optical counterpart. Right: Histogram of the ratio of separation divided by the position uncertainty from the X-ray point source for all optical-X-ray correlations with separations smaller than $1''$. Shaded regions indicate correlations with optical objects that have been classified as background sources (details of this classification are given in the text).

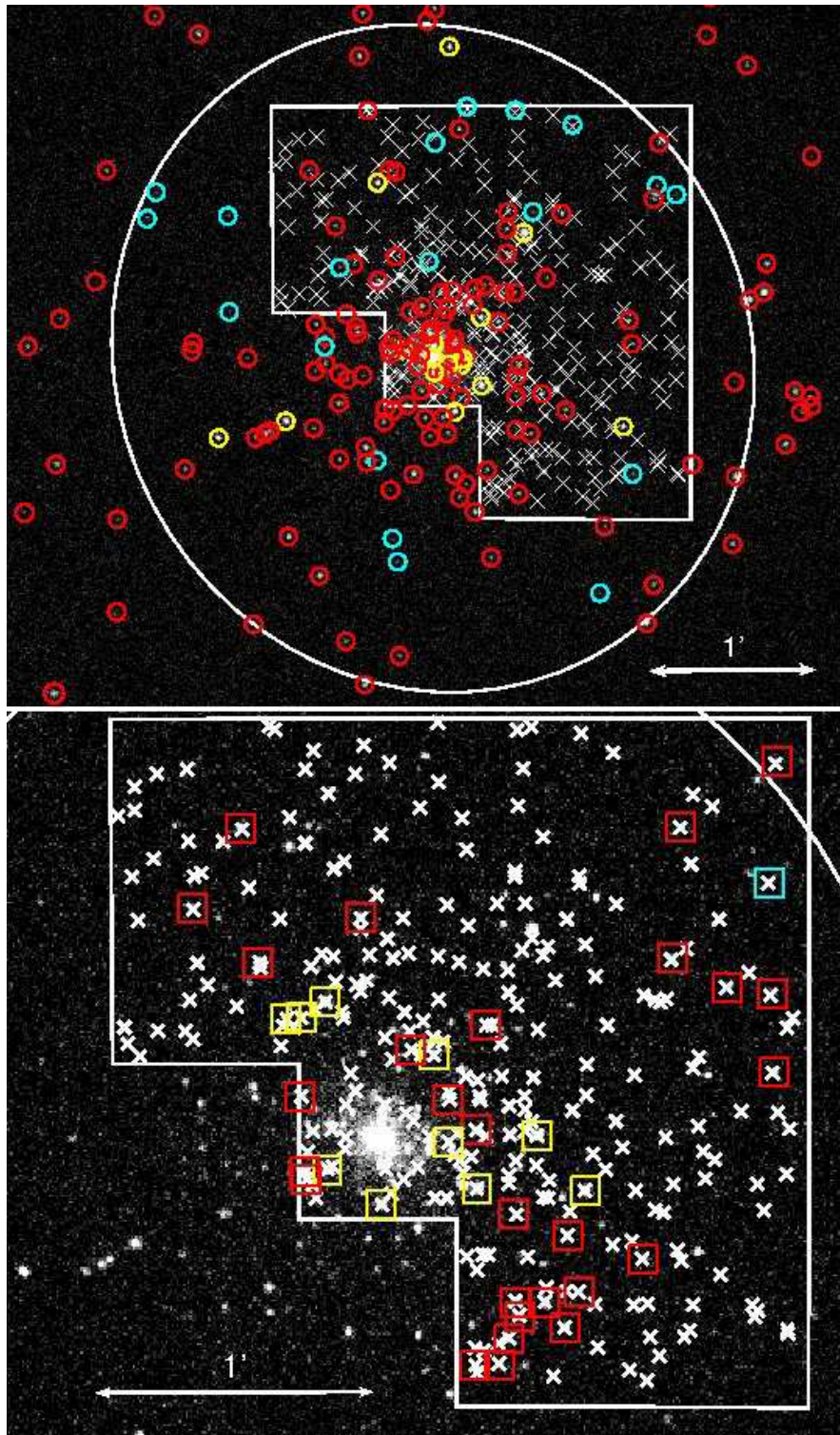


FIG. 6.— Full band X-ray images from the co-added observation of NGC 4278. Both images show confirmed GCs from the *HST* observation indicated by white ‘X’ marks. The top image shows all X-ray sources *not* correlated with a GC and the bottom image indicates all correlated X-ray sources. Region colors indicate the 0.3–8.0 keV luminosity of the source from the co-added observation; yellow regions indicate $L_X \geq 1 \times 10^{38} \text{ erg s}^{-1}$, red regions have $1 \times 10^{38} \geq L_X \geq 1 \times 10^{37} \text{ erg s}^{-1}$, and cyan regions show sources with $L_X \leq 1 \times 10^{37} \text{ erg s}^{-1}$. Also shown in white are the D_{25} ellipse and the *HST* FOV.

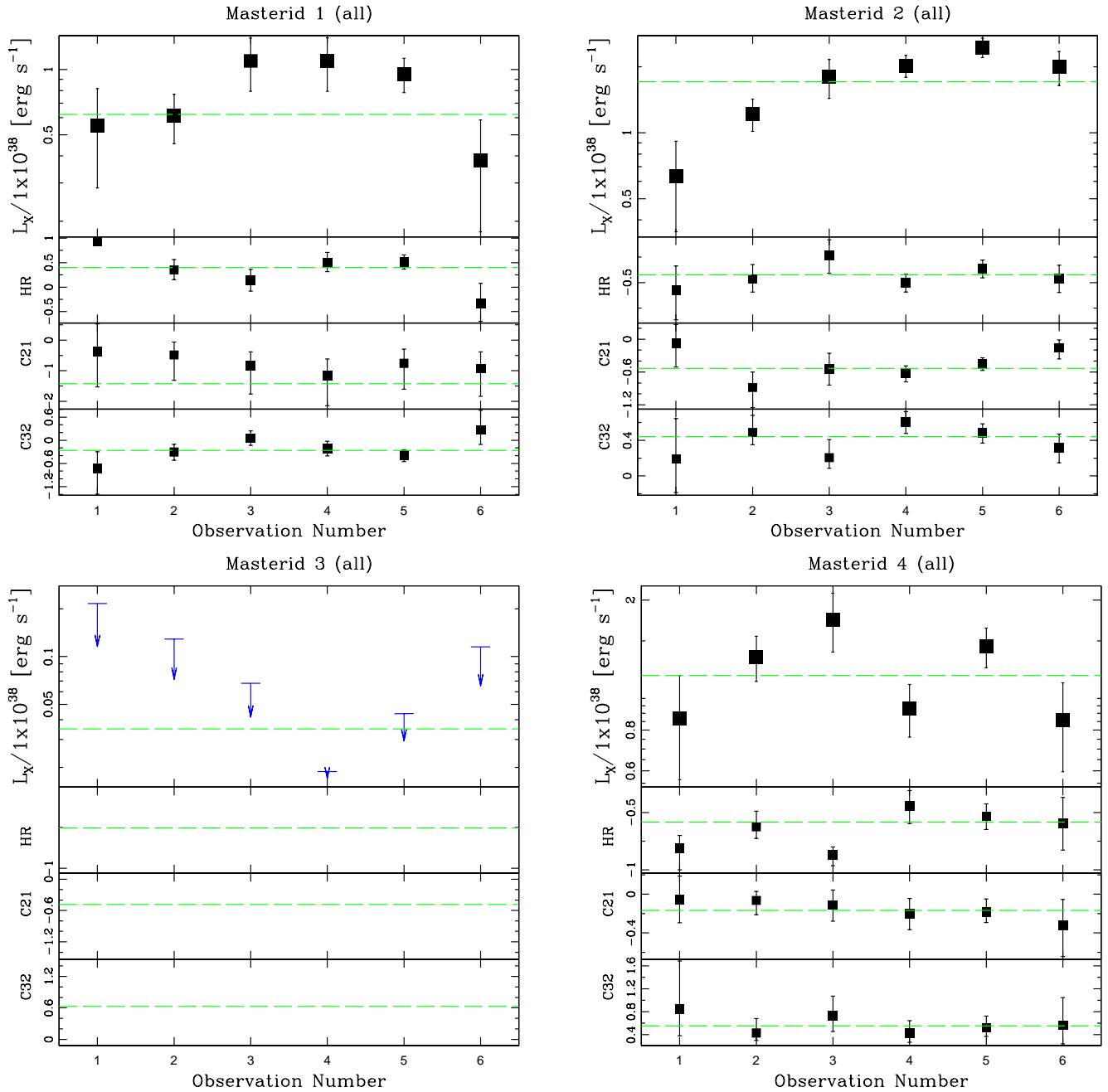
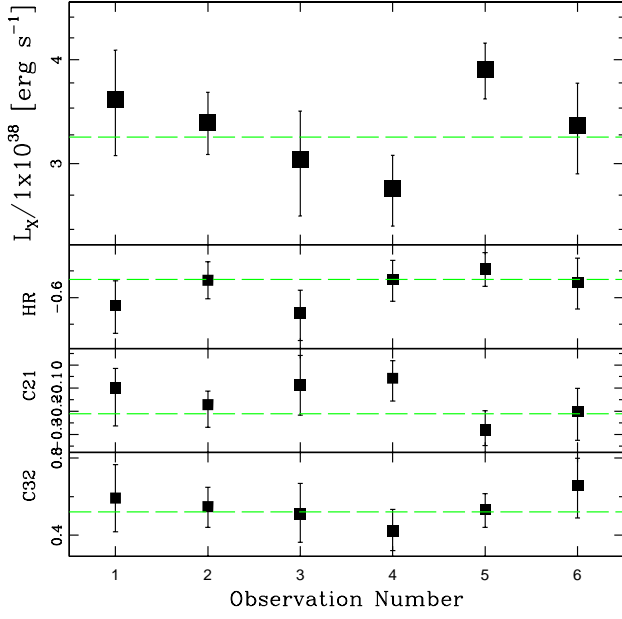
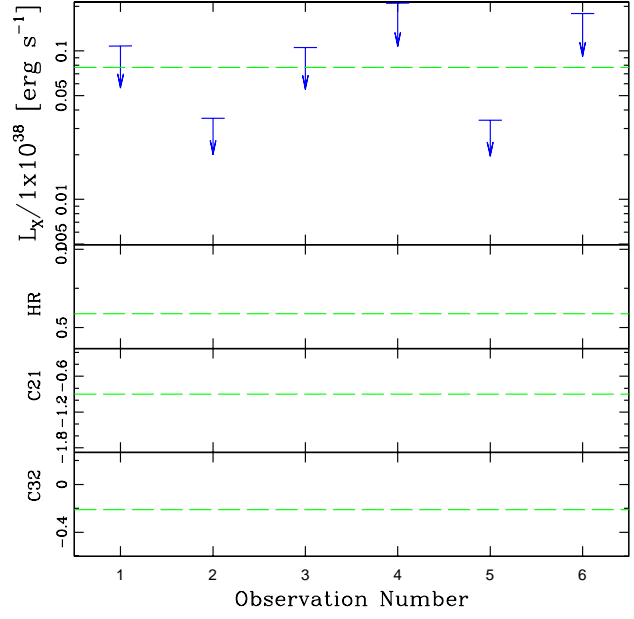


FIG. 7.— Plots of the 236 detected sources, summarizing the variations in properties of each source between each observation. In the top panel the long-term light curves are shown. In the second panel down, the hardness ratios are indicated. These are defined to be $HR = H_c - S_c / H_c + S_c$, where H_c is the number of counts in the hard band (2.0–8.0 keV) and S_c is the number of counts in the soft band (0.5–2.0 keV). These bands have been selected to show comparisons with HR ratios derived in the literature. In the third and fourth panels the color ratios; C21 and C32, are plotted, where $C21 = \log S2 + \log S1$ and $C32 = -\log H + \log S2$. For the color ratios the bandwidths are defined to be $S1 = 0.3 - 0.9$ keV, $S2 = 0.9 - 2.5$ keV and $H = 2.5 - 8.0$ keV. In cases where a source was not detected in a single observation, an upper limit of the X-ray luminosity is indicated, this is the 90% completeness limit for that observation. In all panels the green horizontal line indicates the value derived from the co-added observation. The blue horizontal line indicates the 90% completeness limit for instances where no source was detected in the co-added observation.

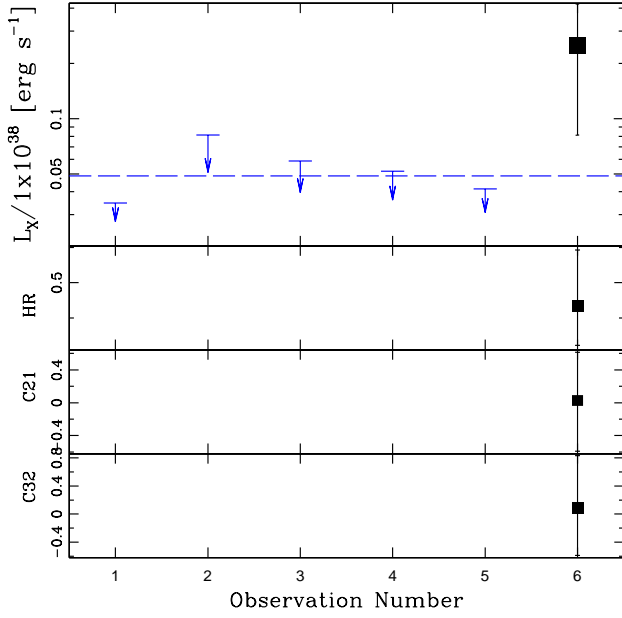
Masterid 5 (all)



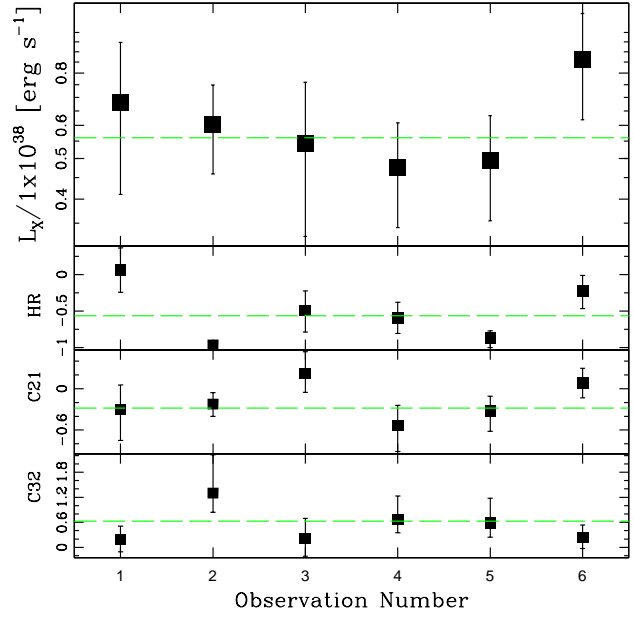
Masterid 6 (all)



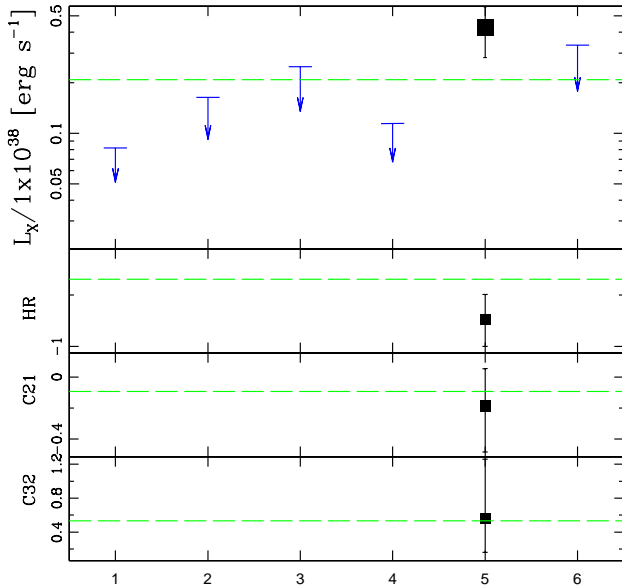
Masterid 7 (all)



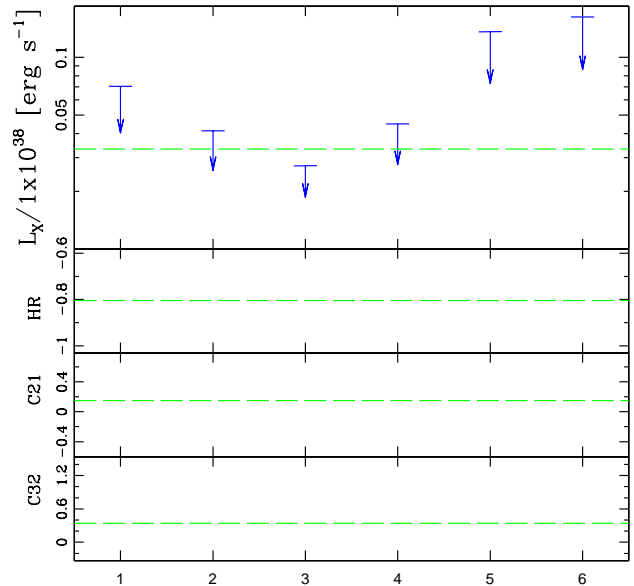
Masterid 8 (all)



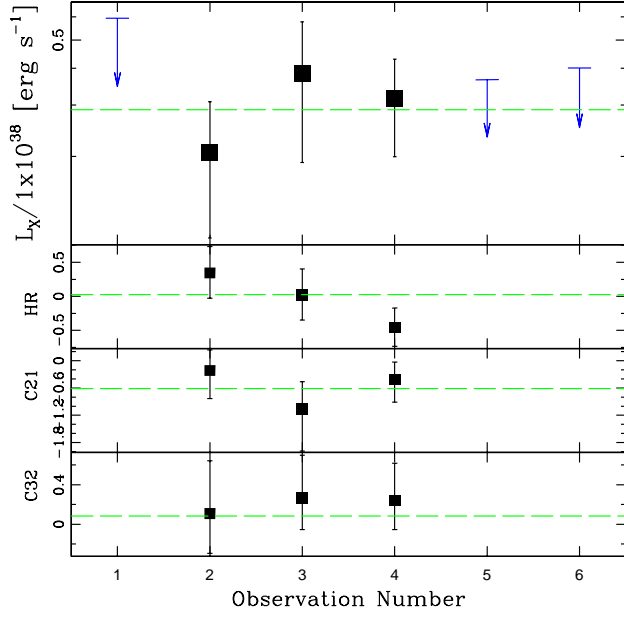
Masterid 9 (all)



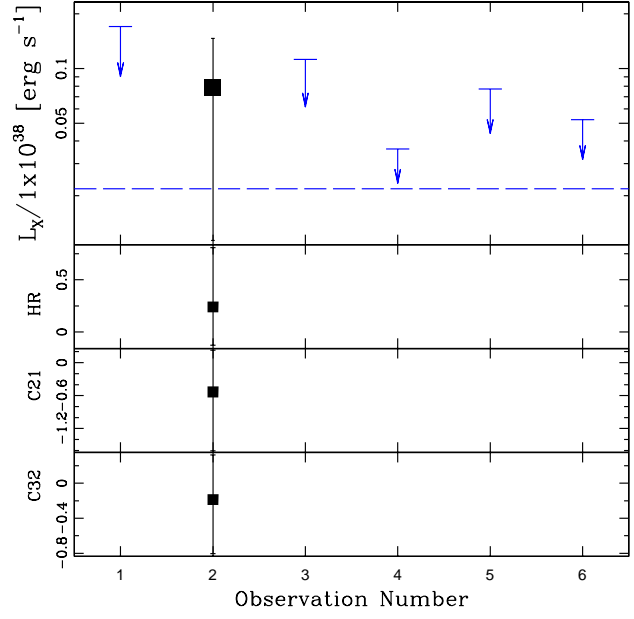
Masterid 10 (all)



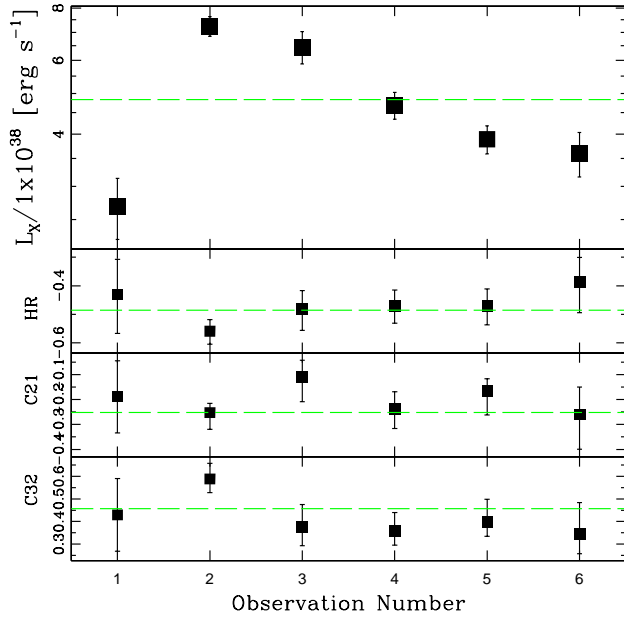
Masterid 11 (all)



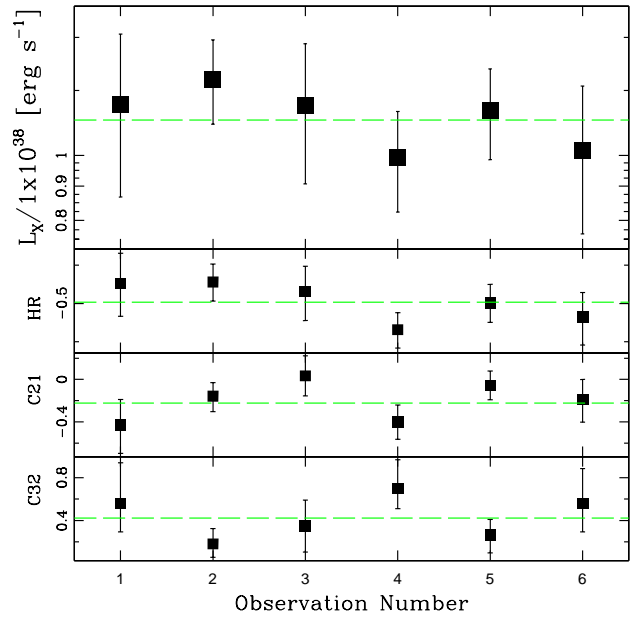
Masterid 12 (all)



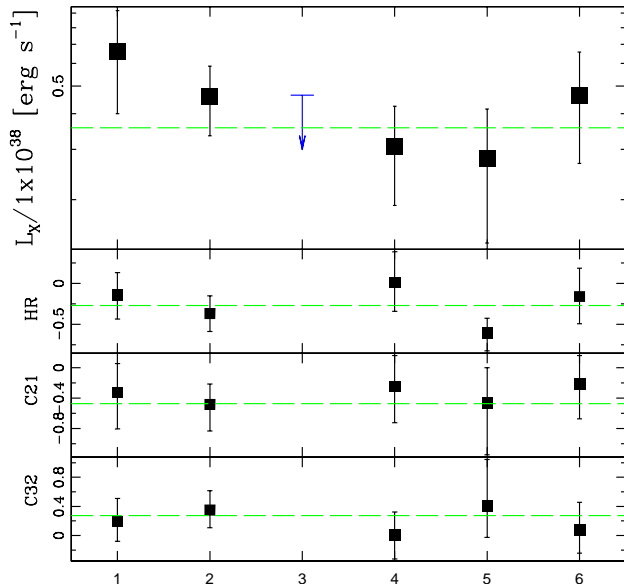
Masterid 13 (all)



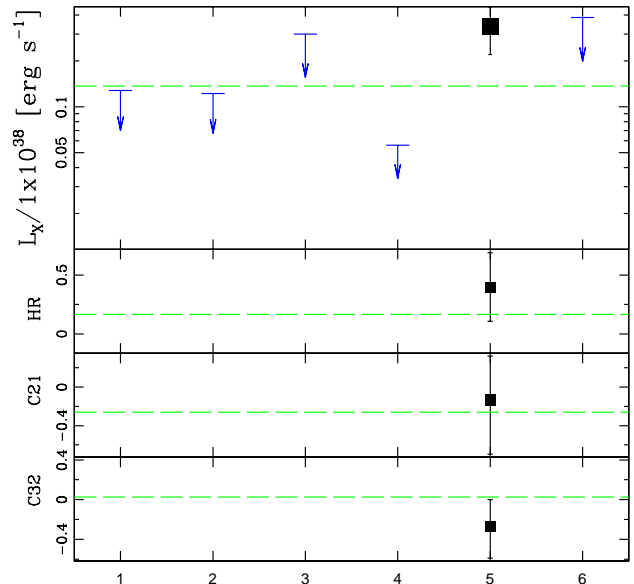
Masterid 14 (all)



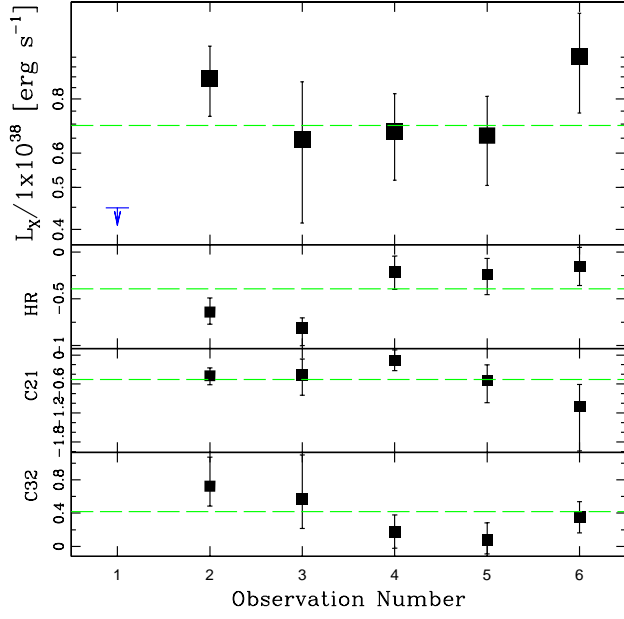
Masterid 15 (all)



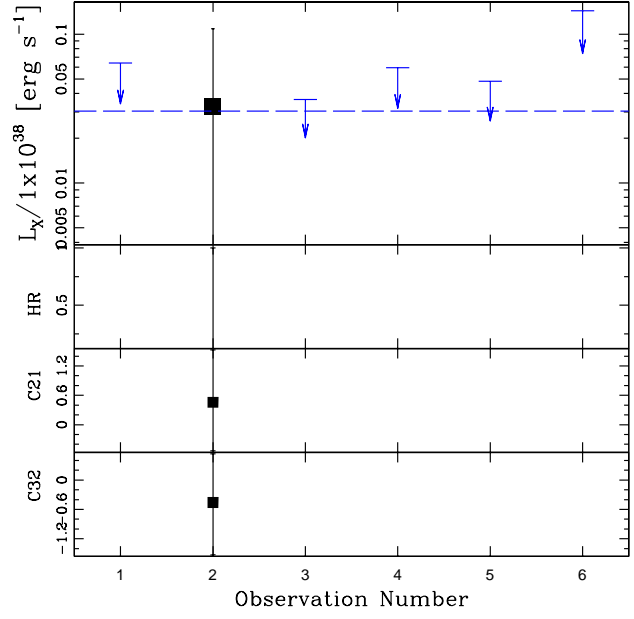
Masterid 16 (all)



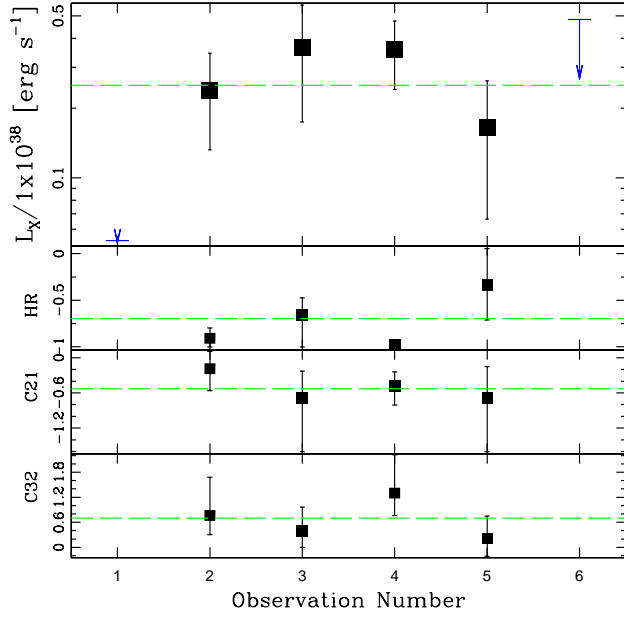
Masterid 17 (all)



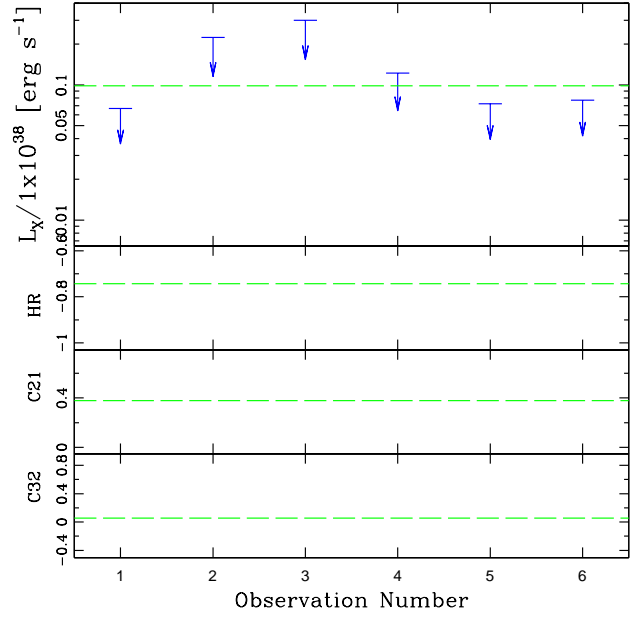
Masterid 18 (all)



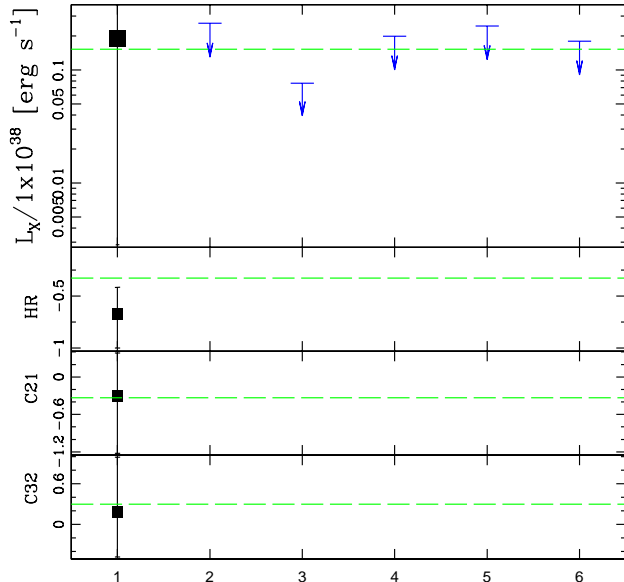
Masterid 19 (all)



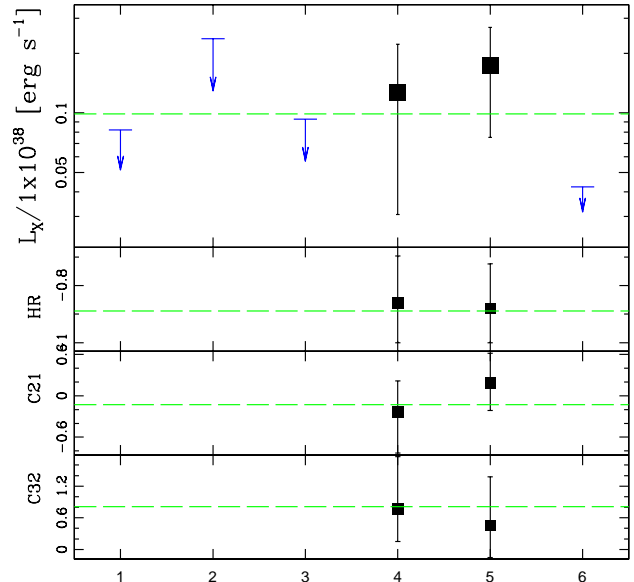
Masterid 20 (all)

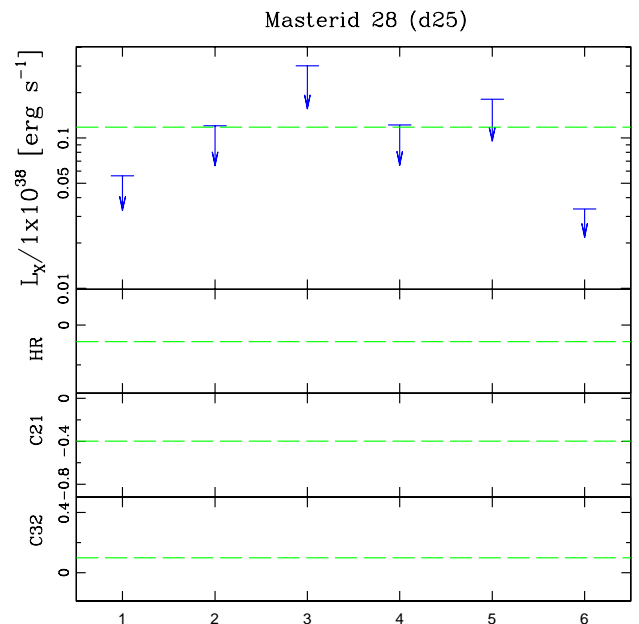
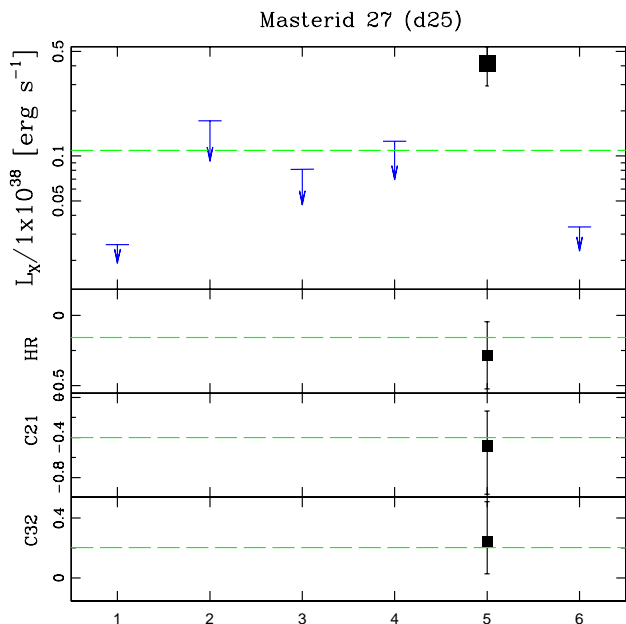
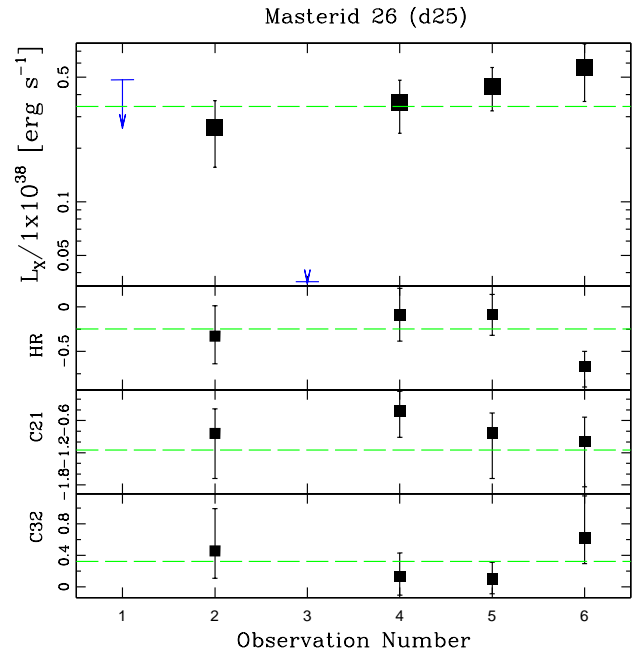
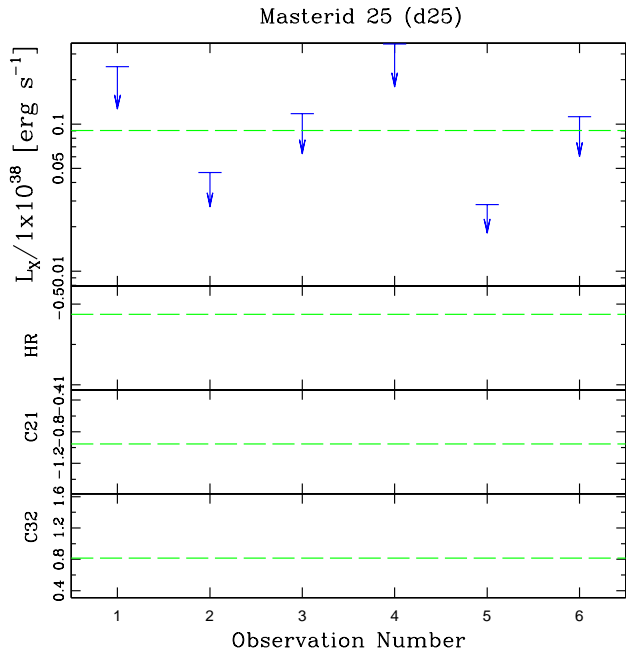
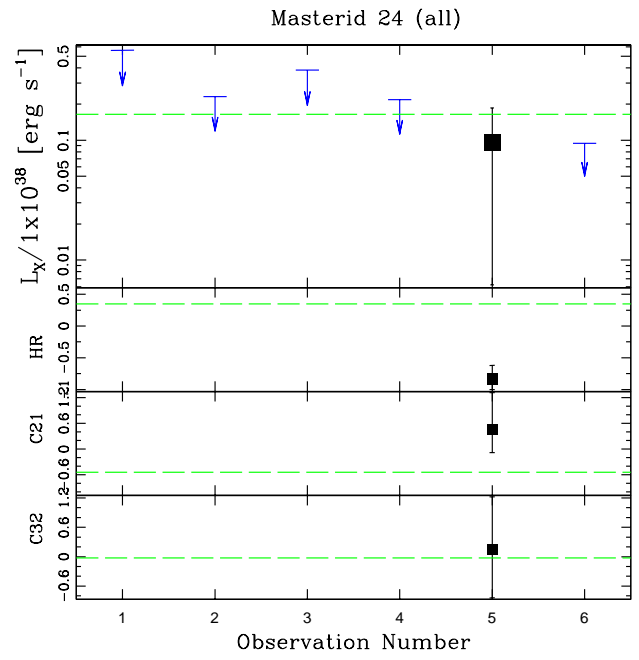
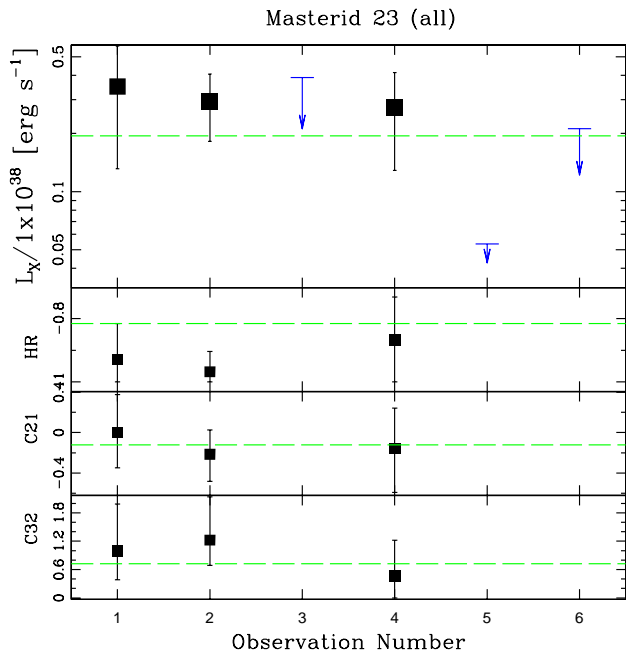


Masterid 21 (all)

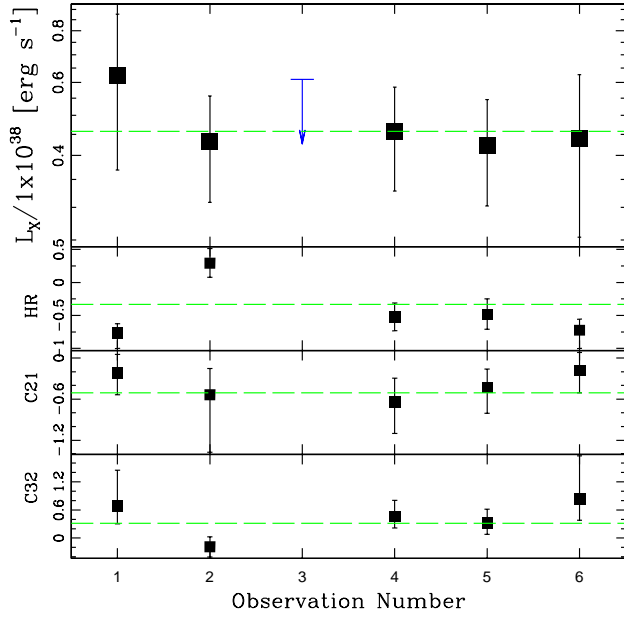


Masterid 22 (d25)

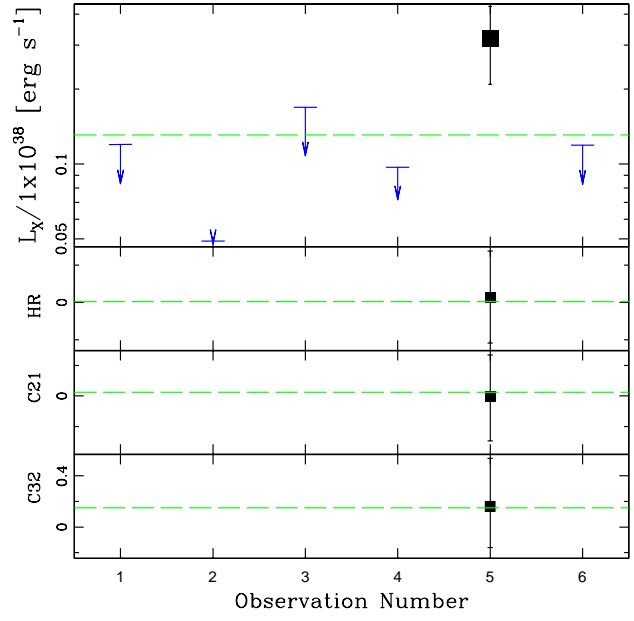




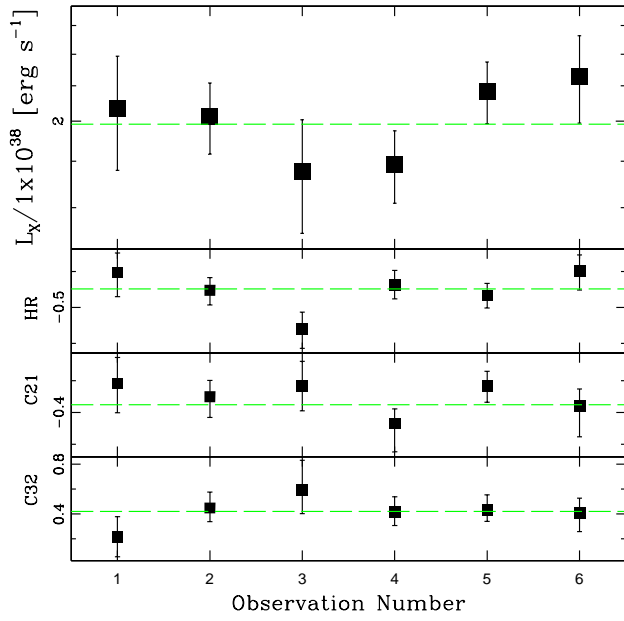
Masterid 29 (all)



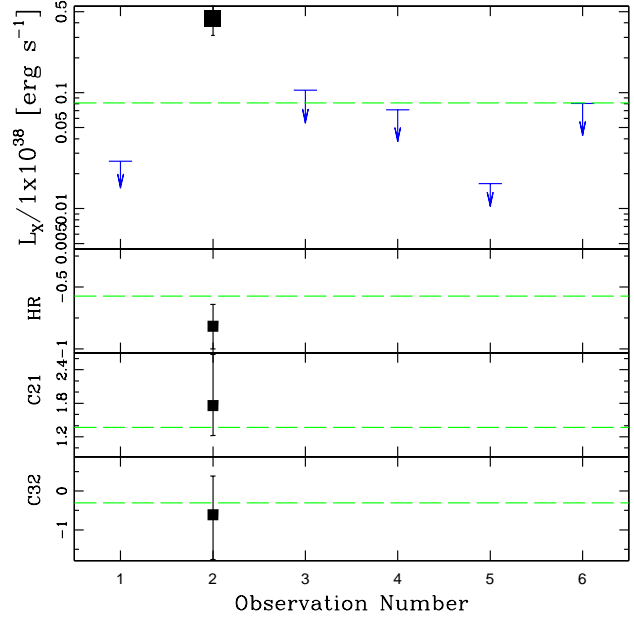
Masterid 30 (all)



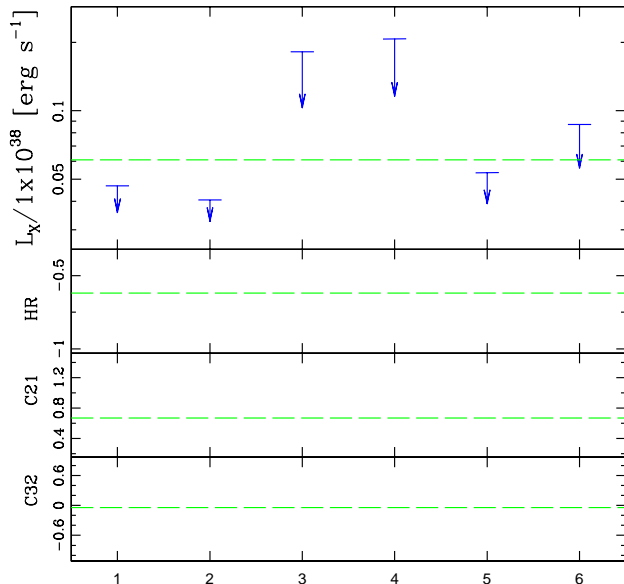
Masterid 31 (d25)



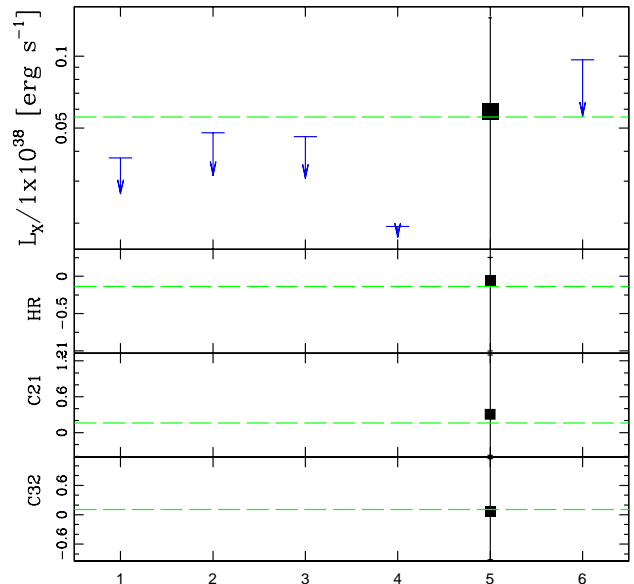
Masterid 32 (d25)



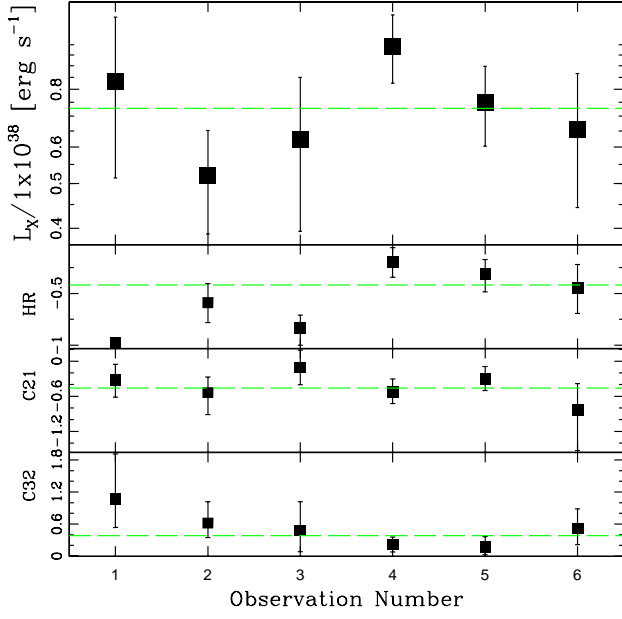
Masterid 33 (d25)



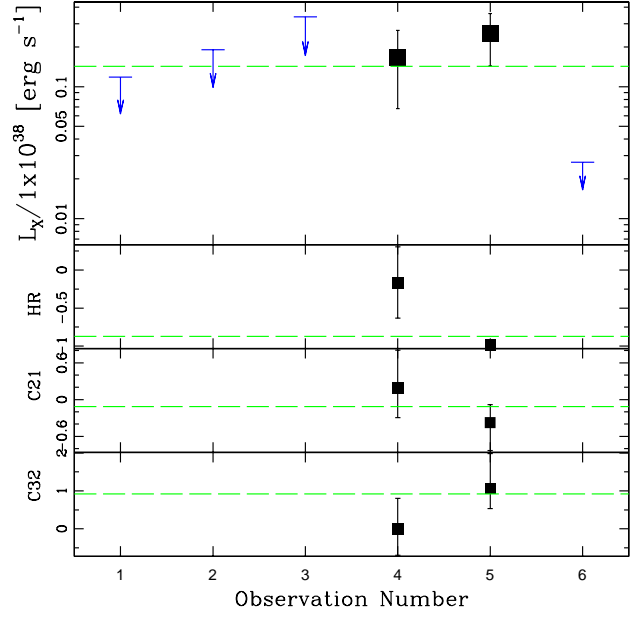
Masterid 34 (all)



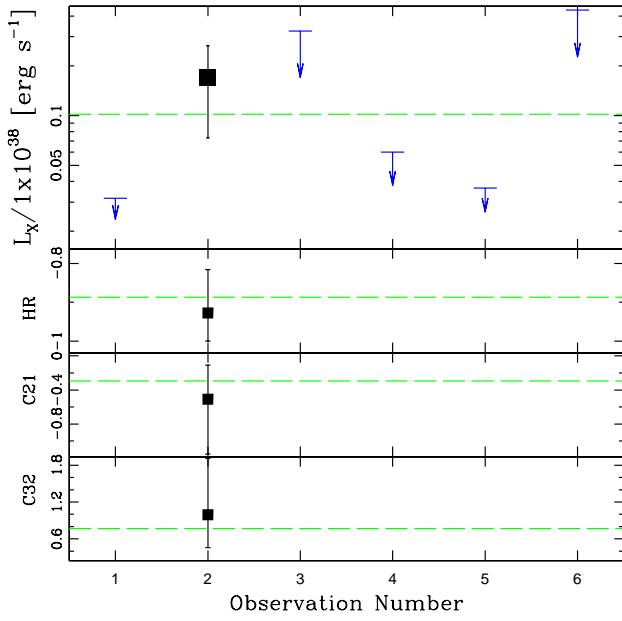
Masterid 35 (all)



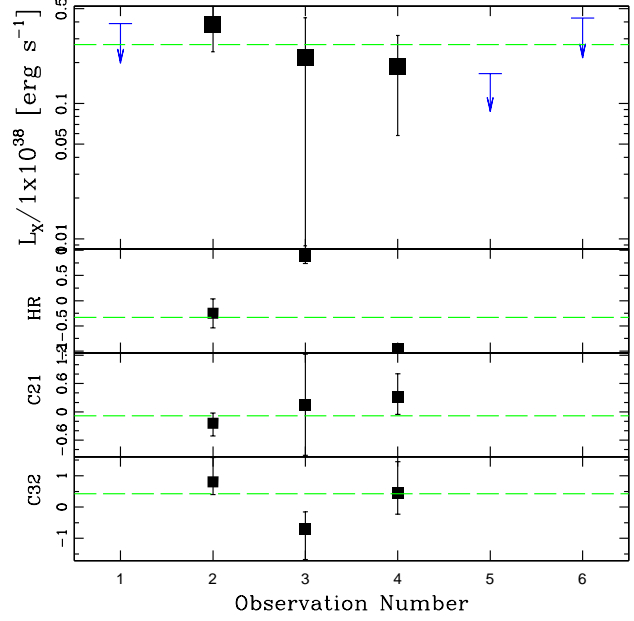
Masterid 36 (d25)



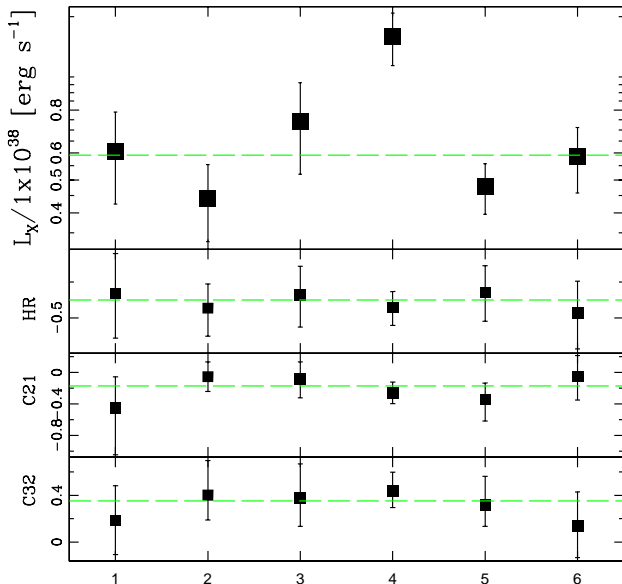
Masterid 37 (d25)



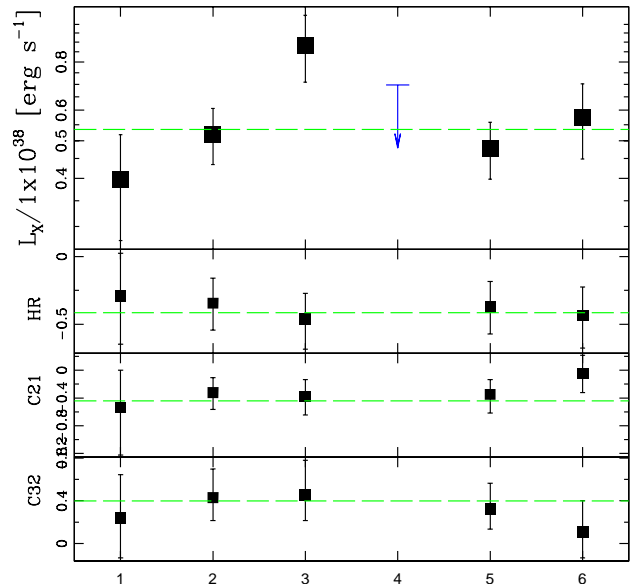
Masterid 38 (d25)



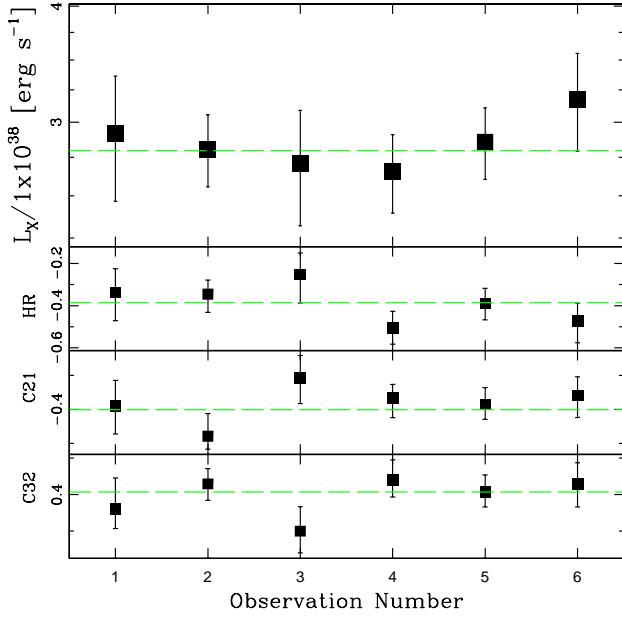
Masterid 39 (d25)



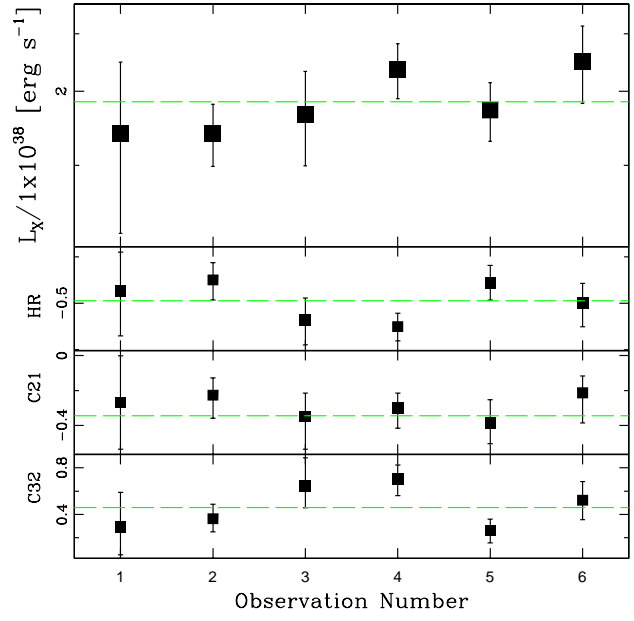
Masterid 40 (d25)



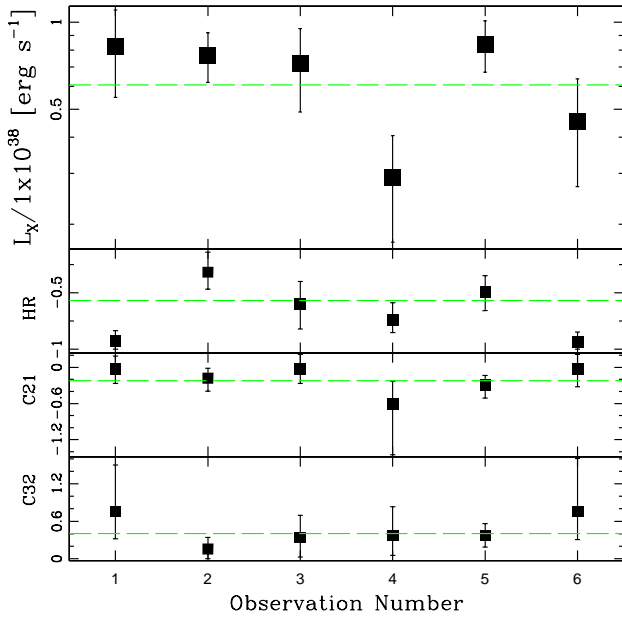
Masterid 41 (d25)



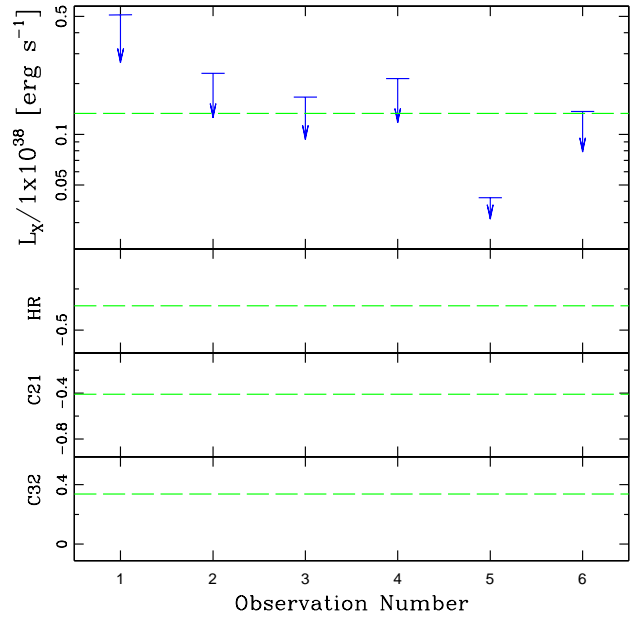
Masterid 42 (all)



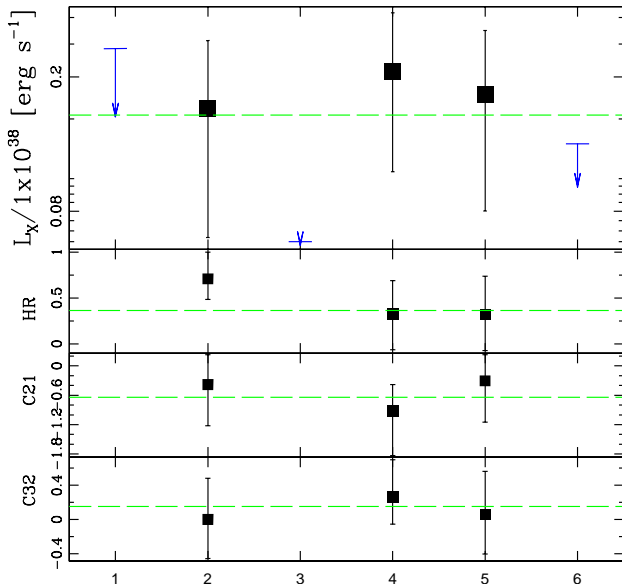
Masterid 43 (d25)



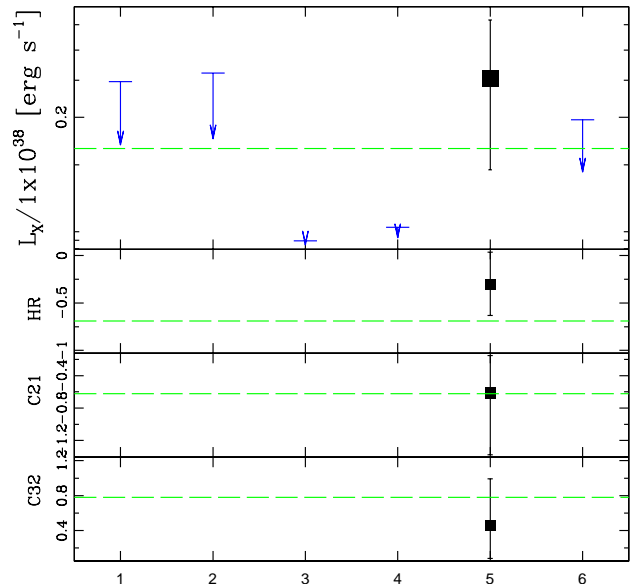
Masterid 44 (all)



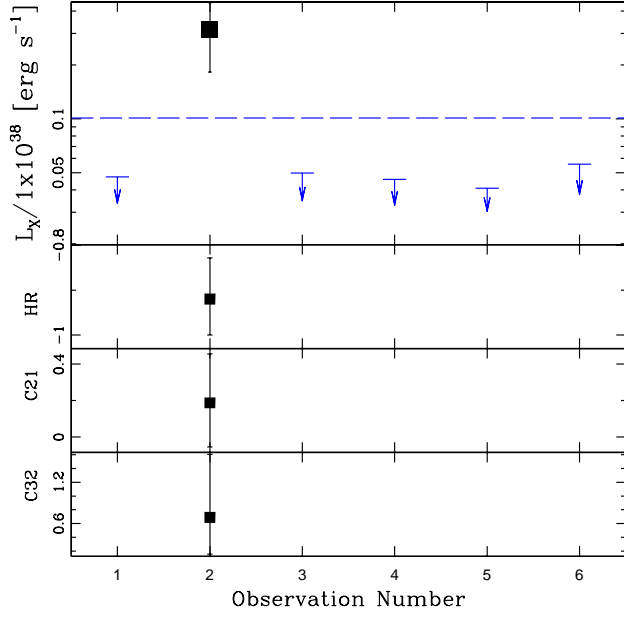
Masterid 45 (d25)



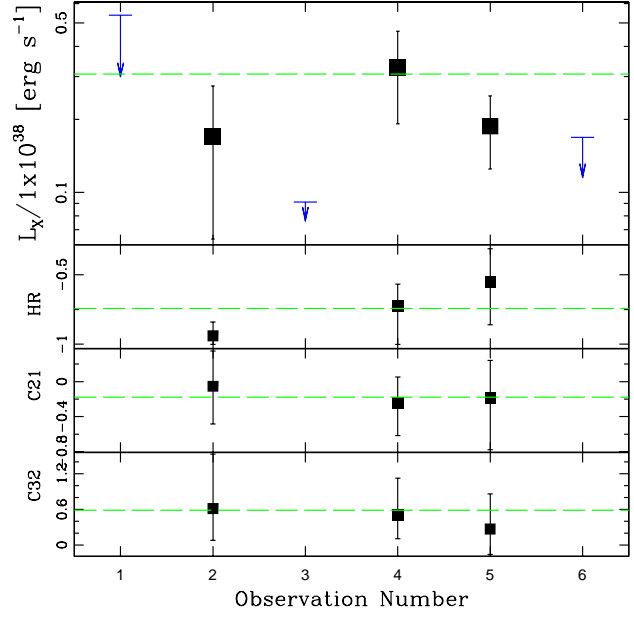
Masterid 46 (d25)



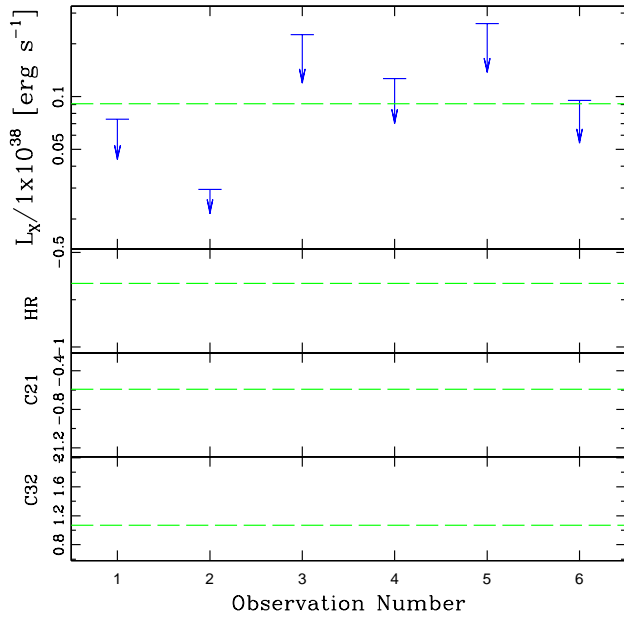
Masterid 47 (d25)



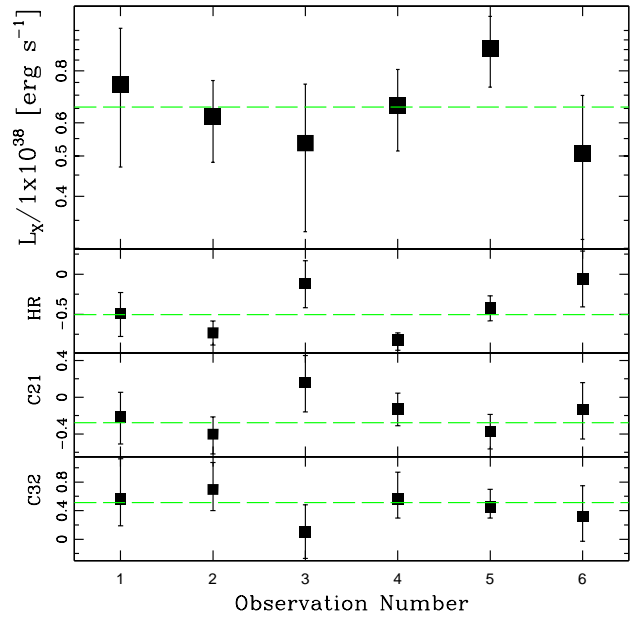
Masterid 48 (d25)



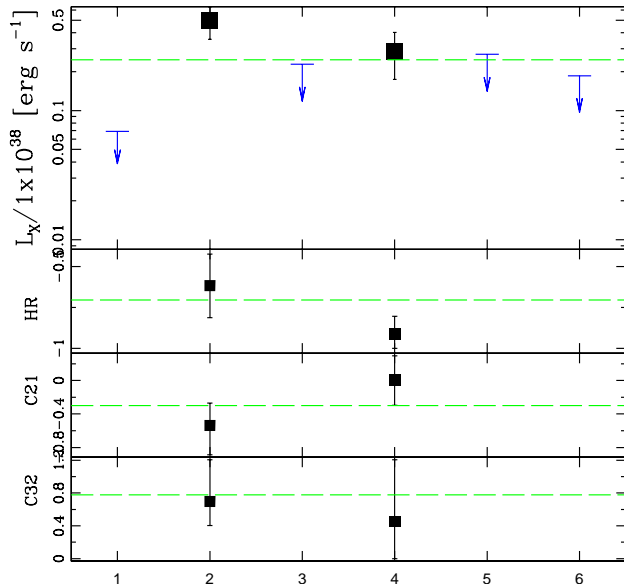
Masterid 49 (all)



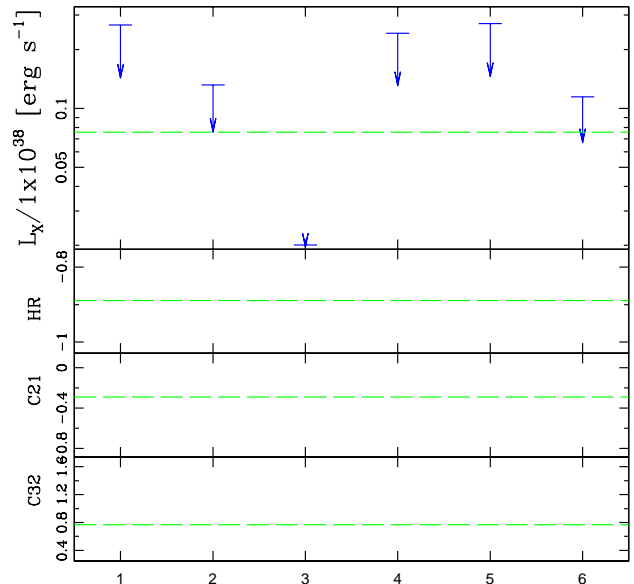
Masterid 50 (d25)



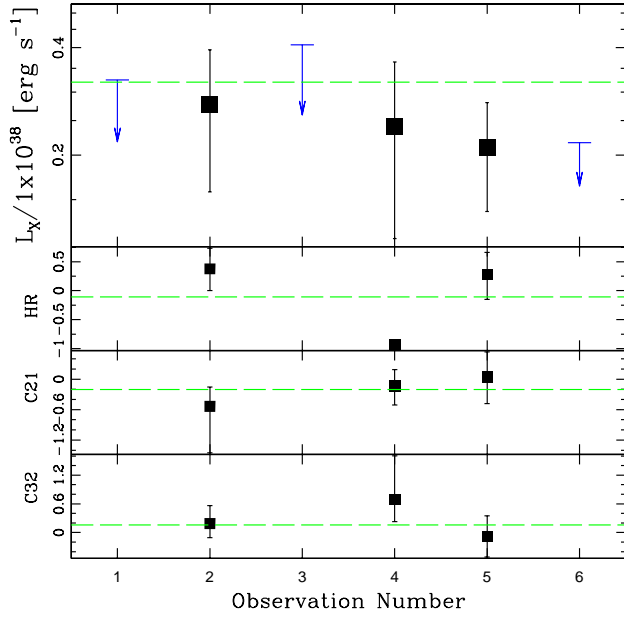
Masterid 51 (d25)



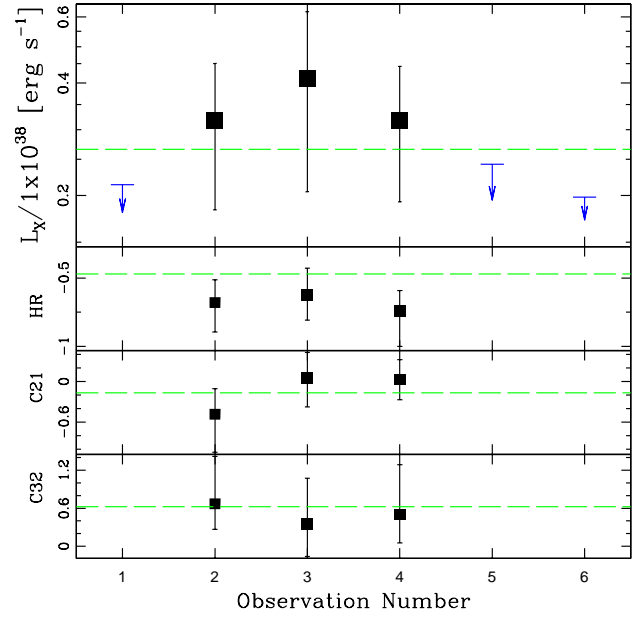
Masterid 52 (d25)



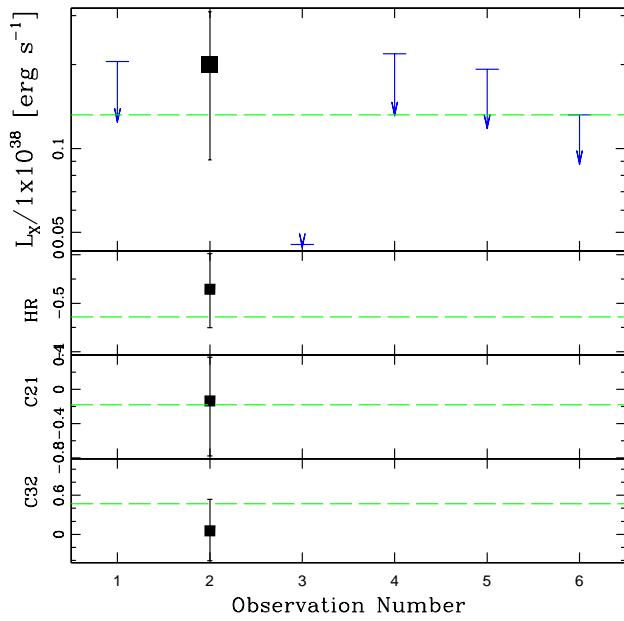
Masterid 53 (d25)



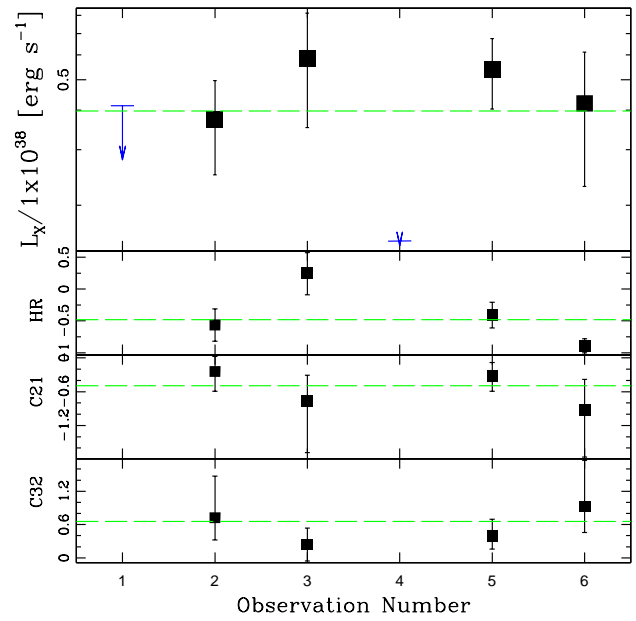
Masterid 54 (d25)



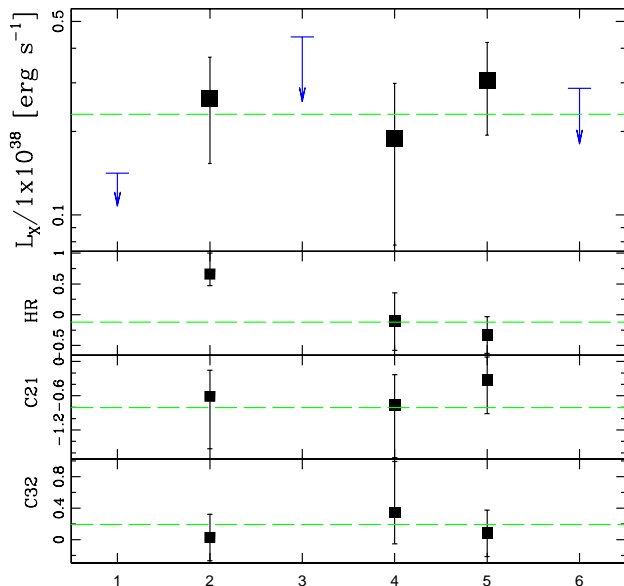
Masterid 55 (d25)



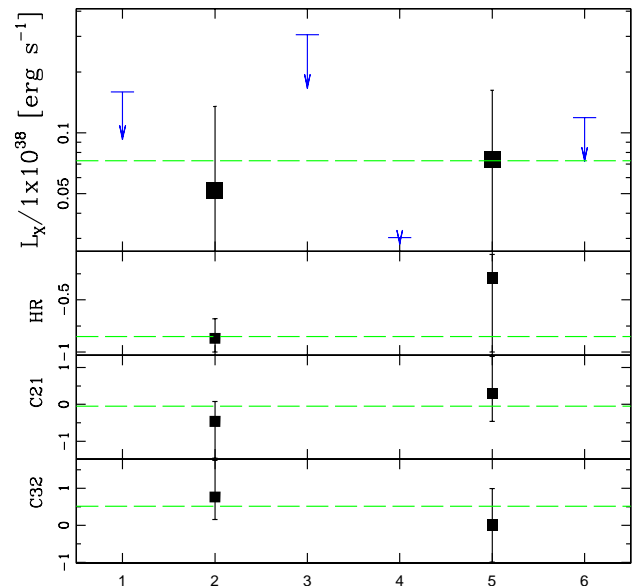
Masterid 56 (d25)

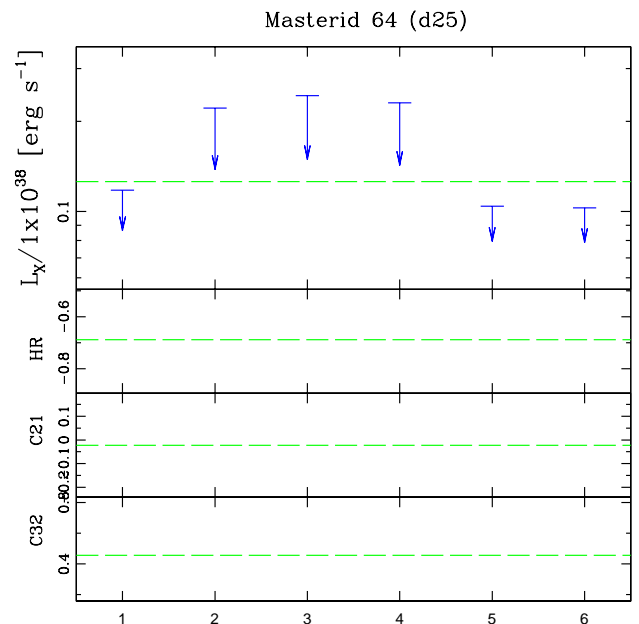
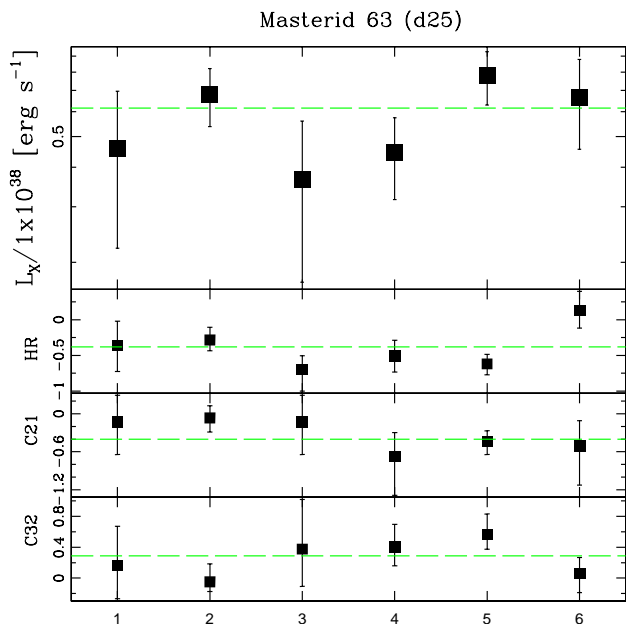
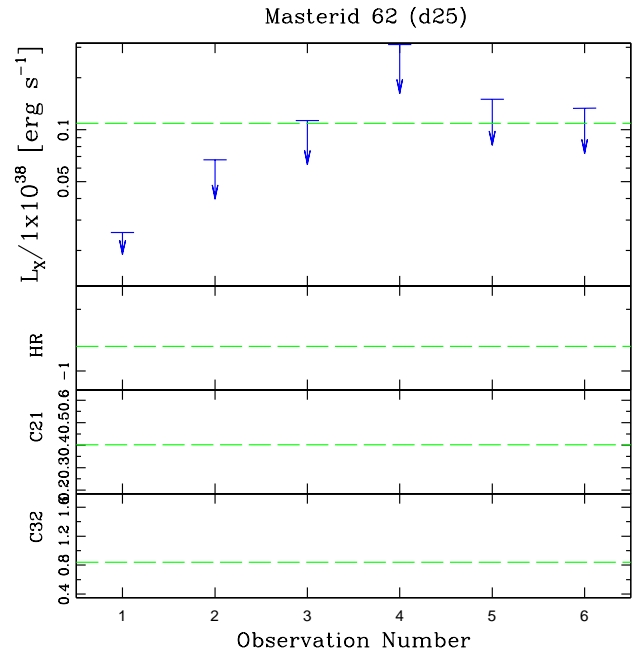
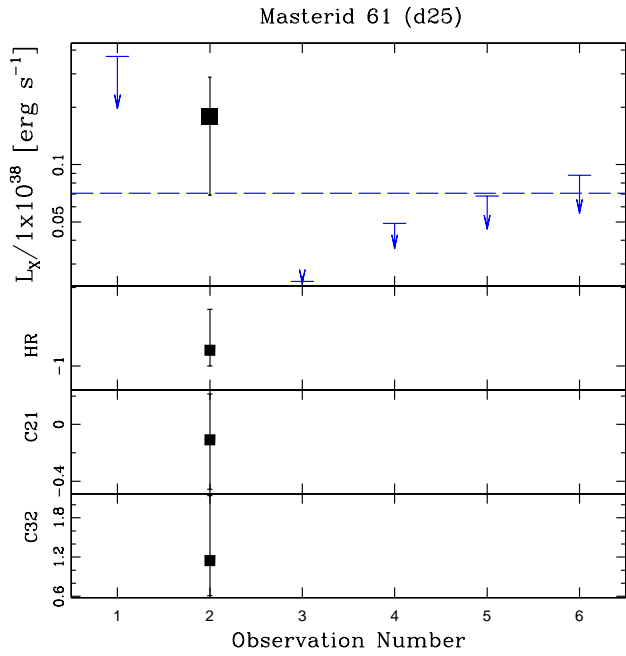
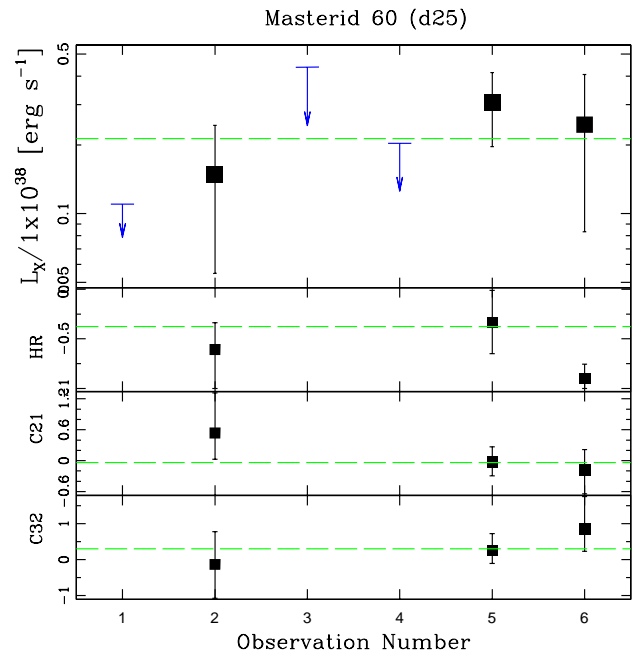
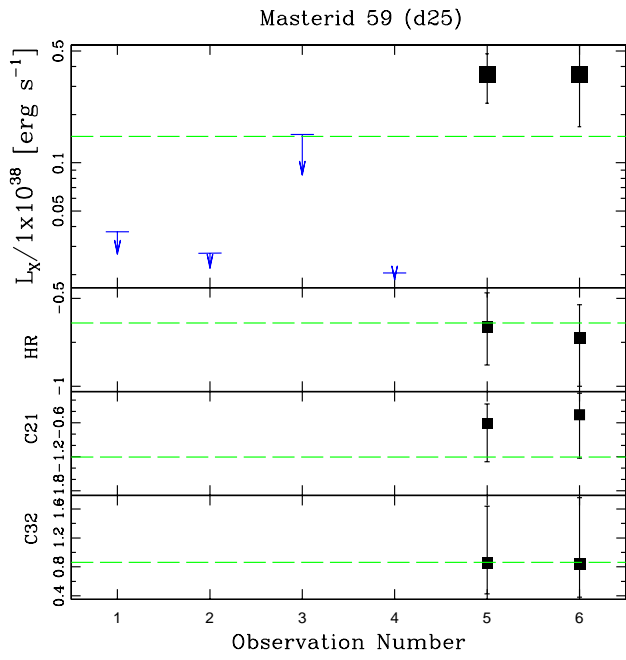


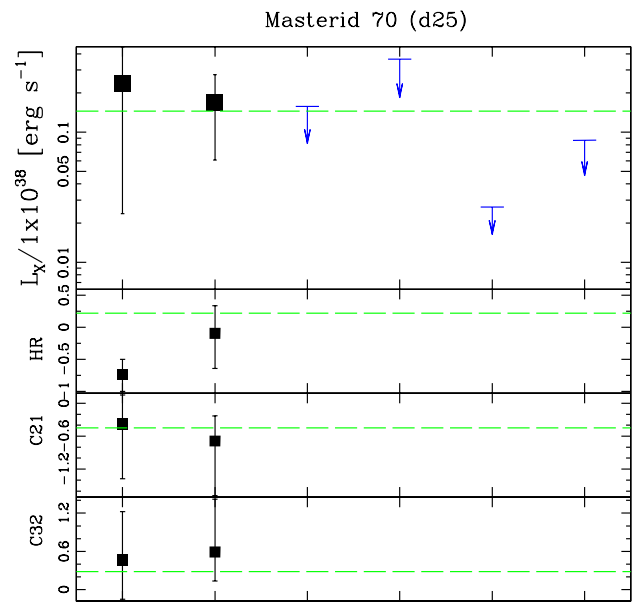
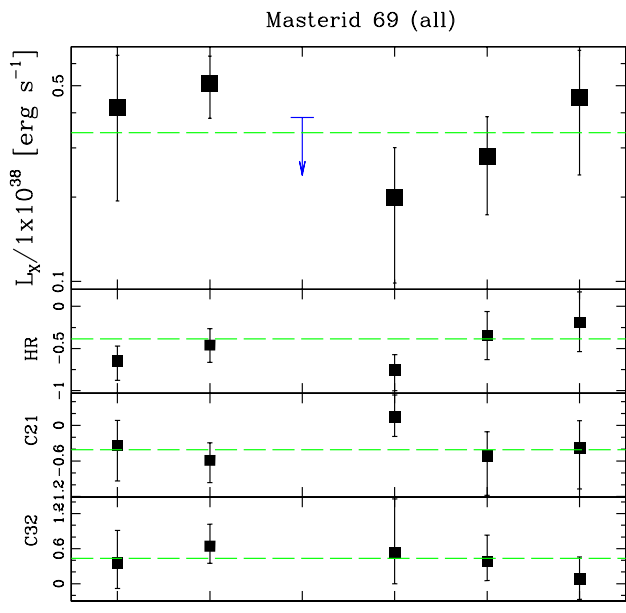
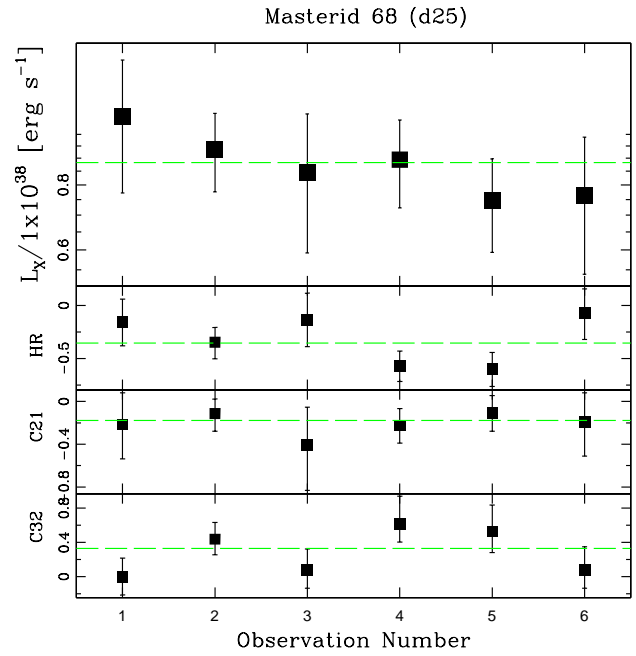
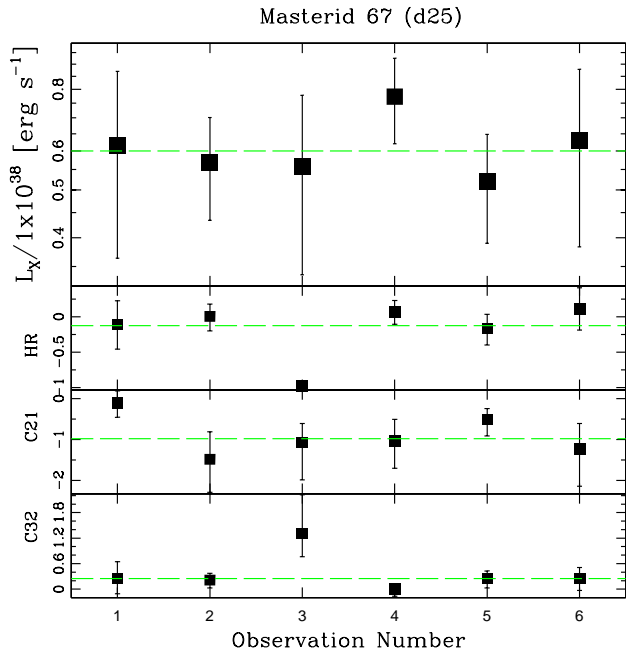
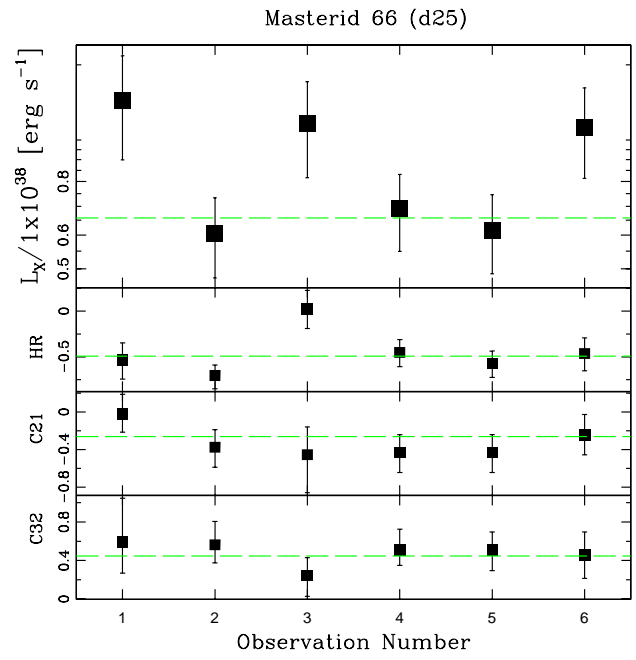
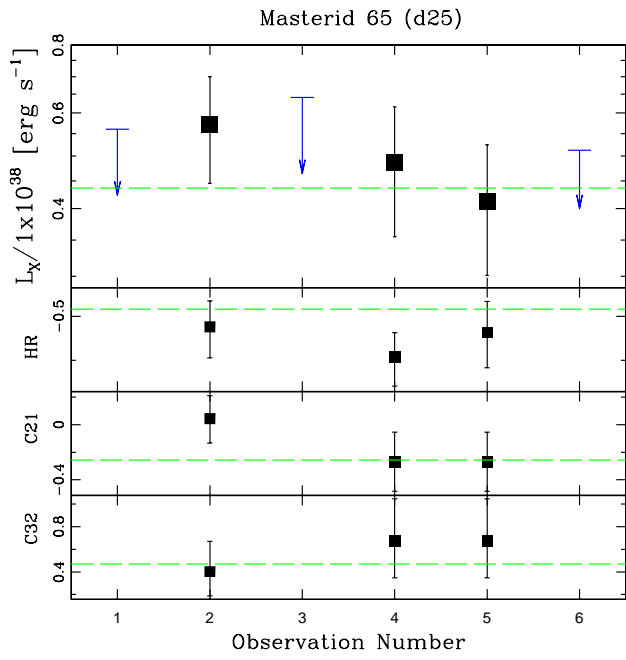
Masterid 57 (d25)



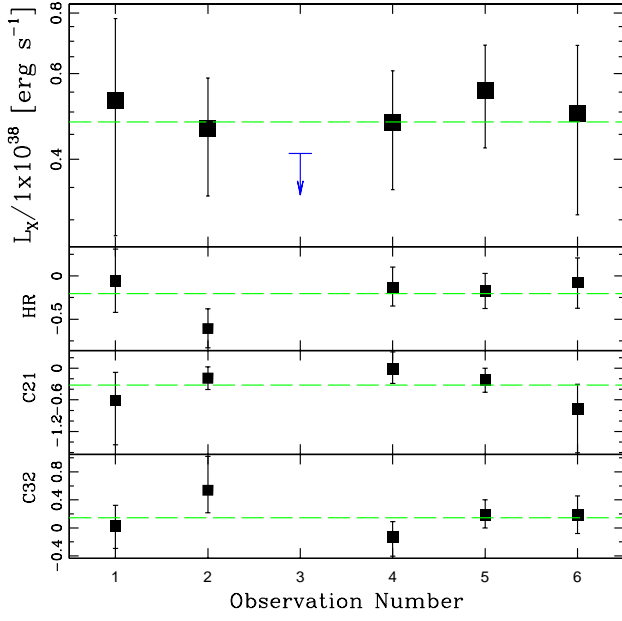
Masterid 58 (d25)



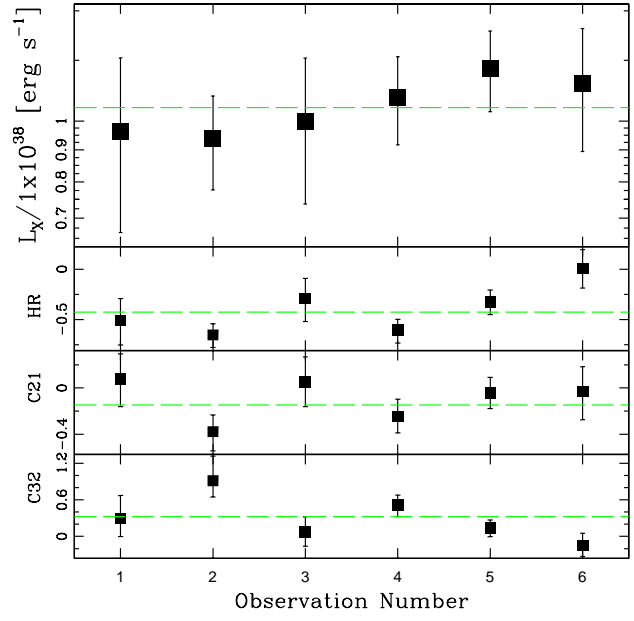




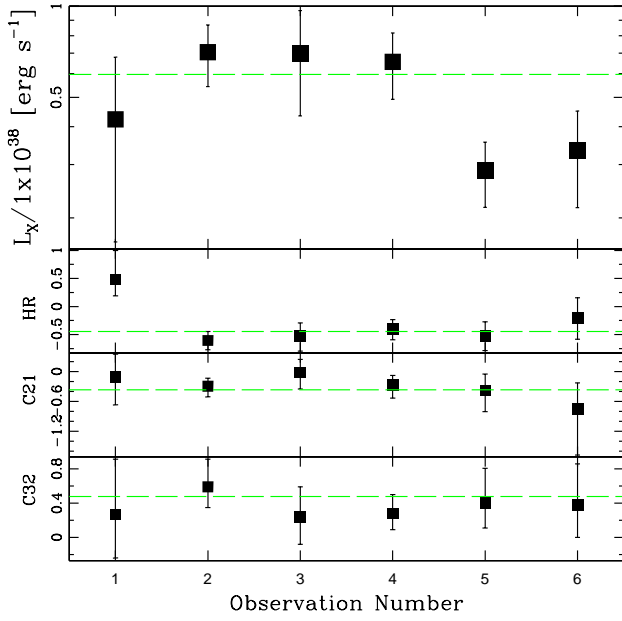
Masterid 71 (all)



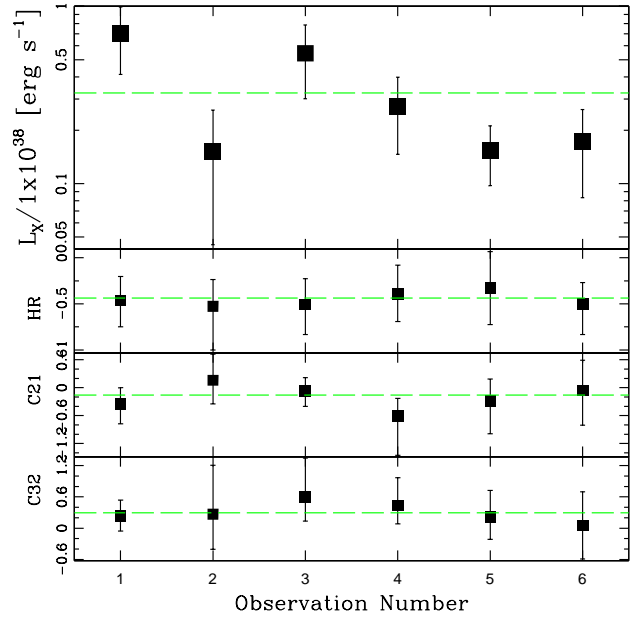
Masterid 72 (all)



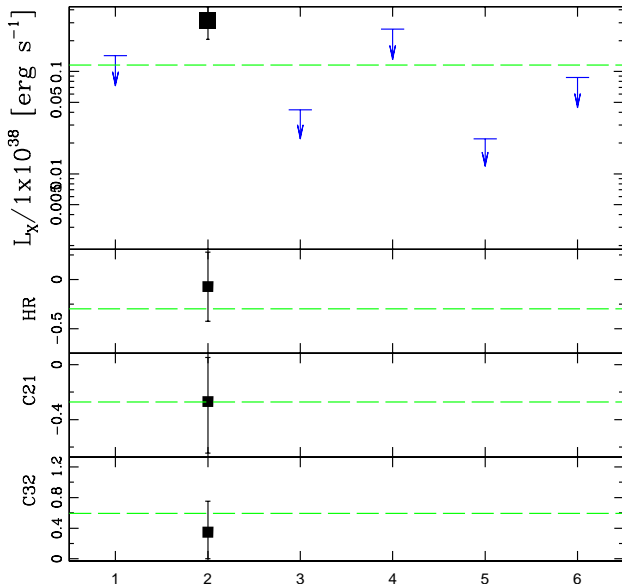
Masterid 73 (d25)



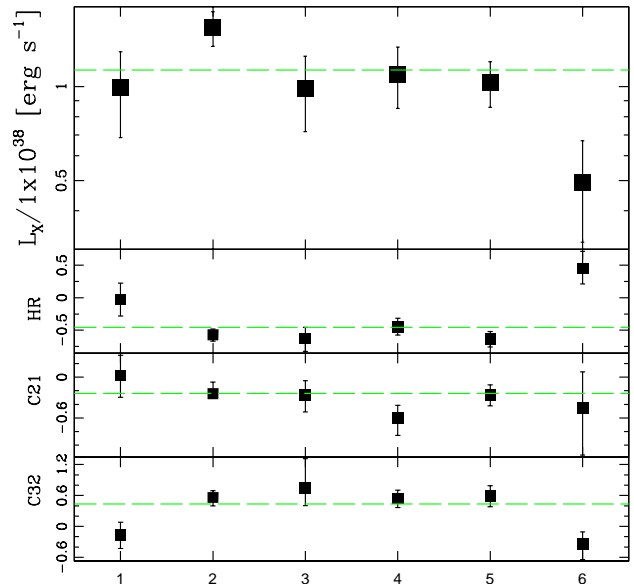
Masterid 74 (d25)



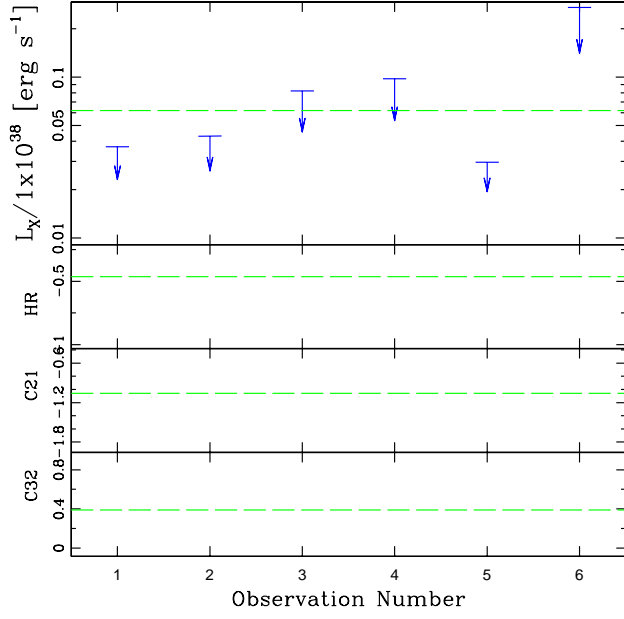
Masterid 75 (d25)



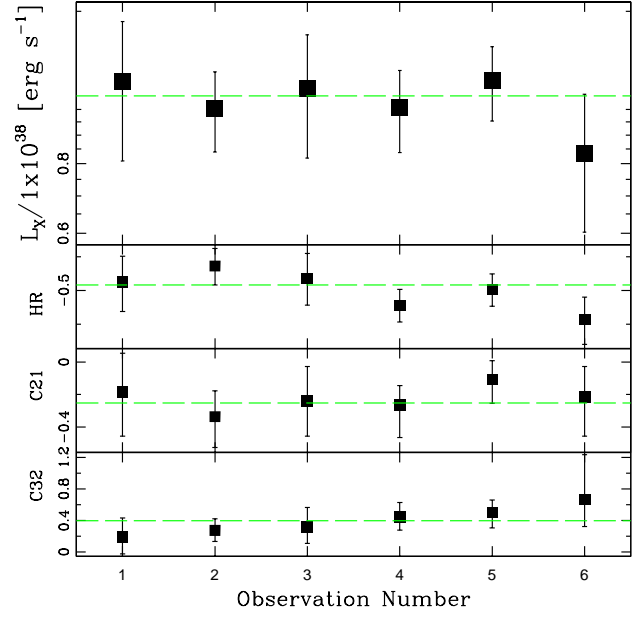
Masterid 76 (d25)



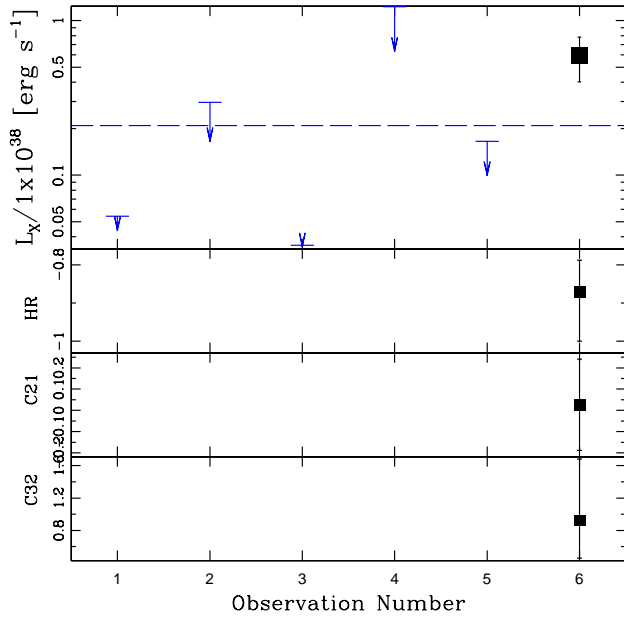
Masterid 77 (d25)



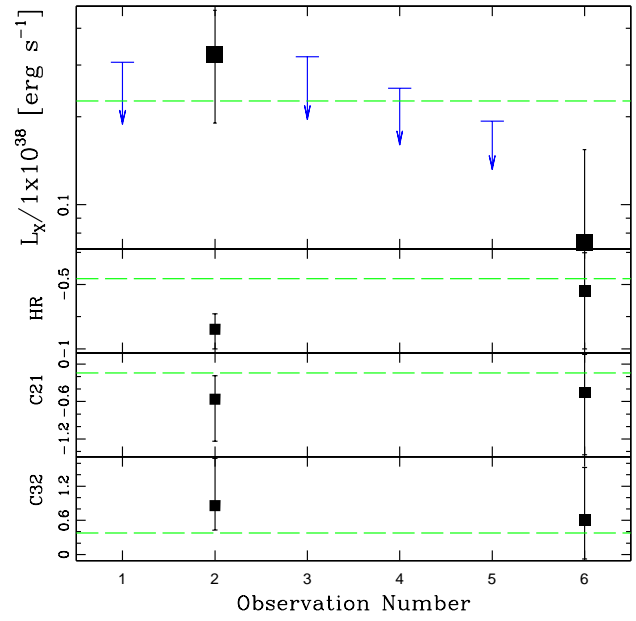
Masterid 78 (d25)



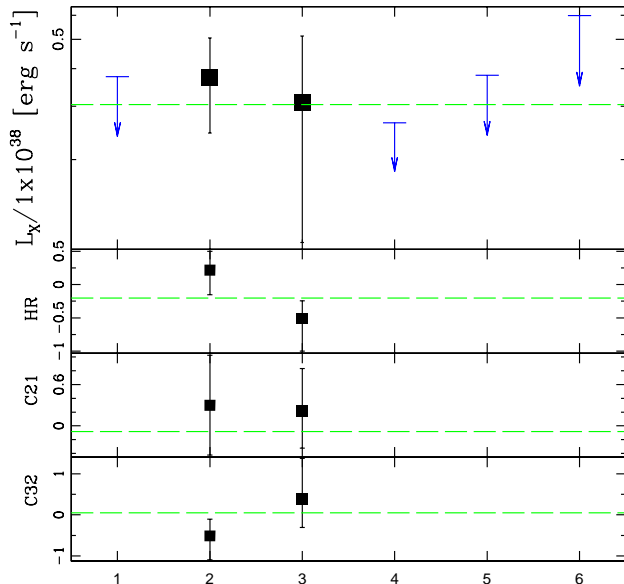
Masterid 79 (d25)



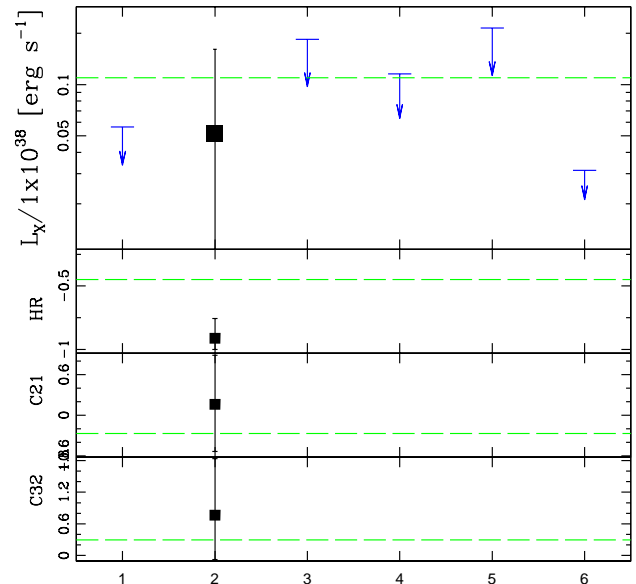
Masterid 80 (d25)

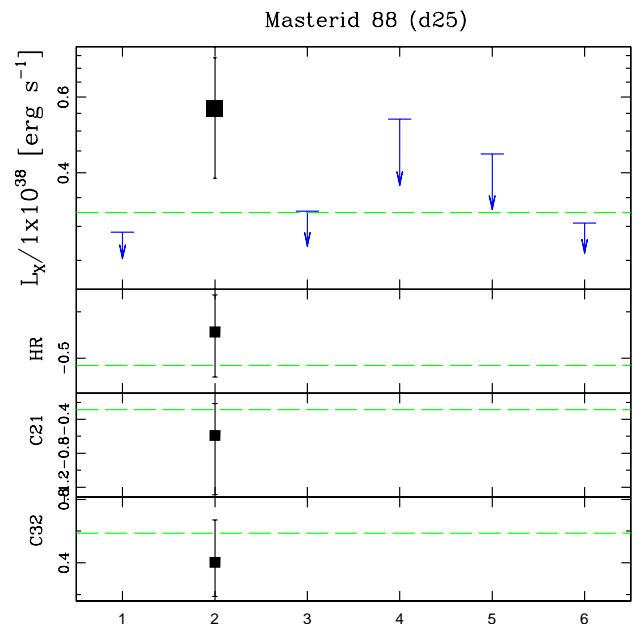
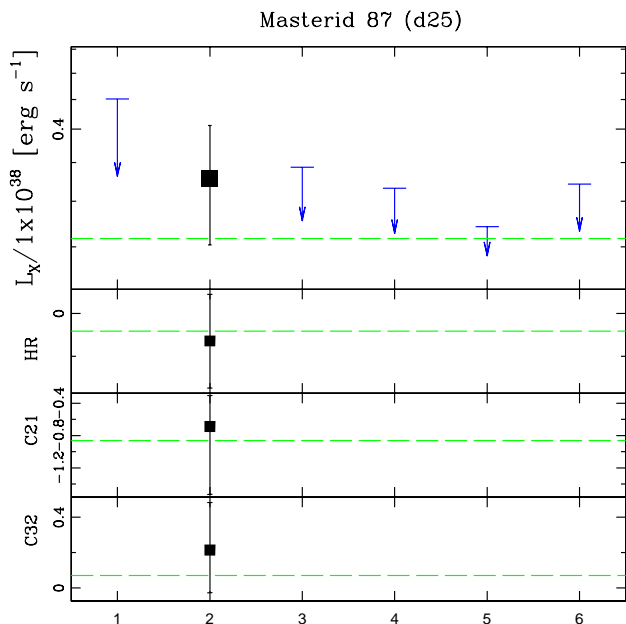
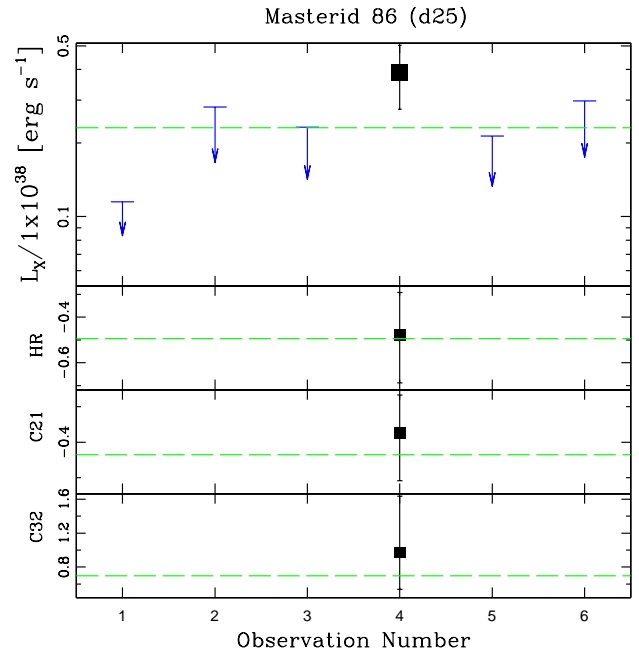
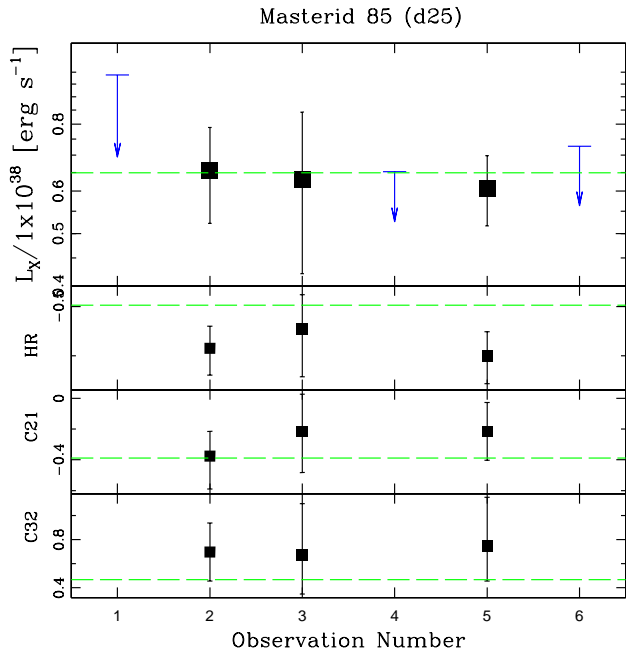
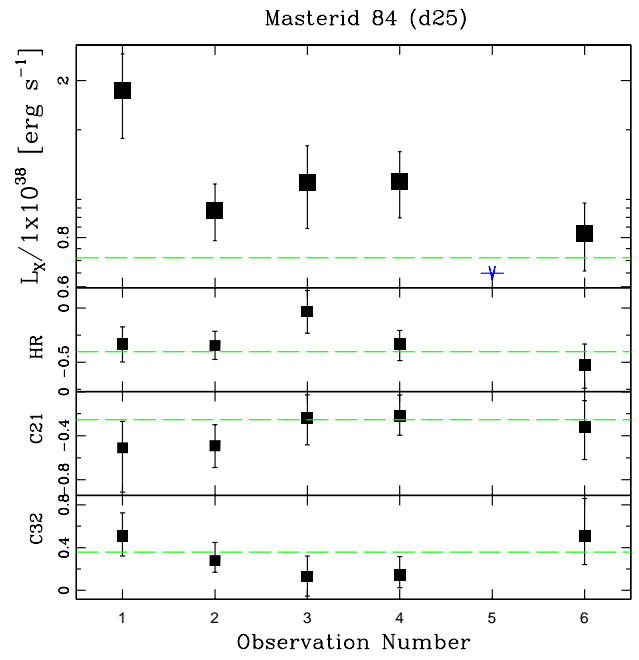
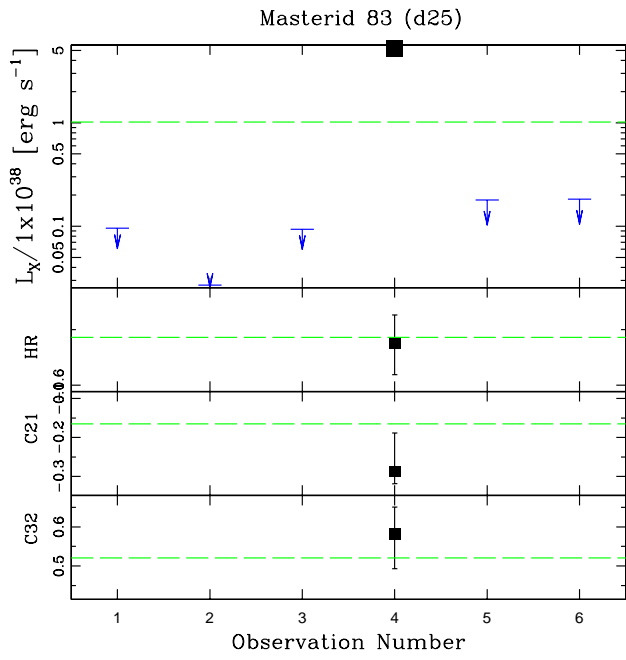


Masterid 81 (d25)

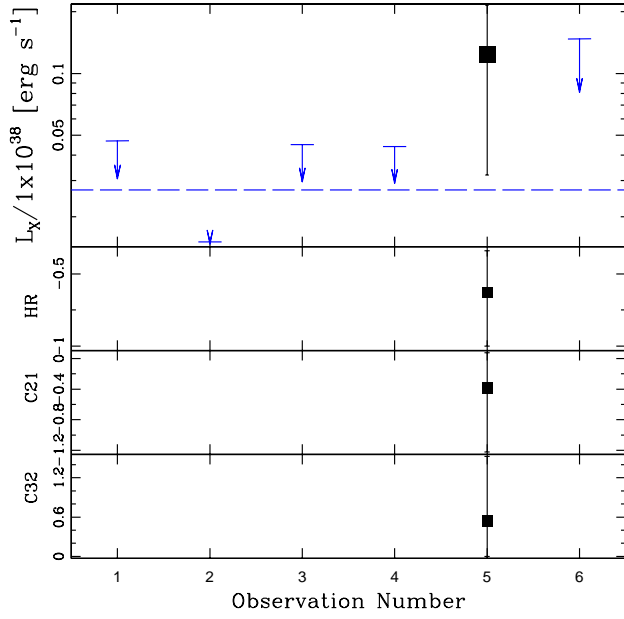


Masterid 82 (d25)

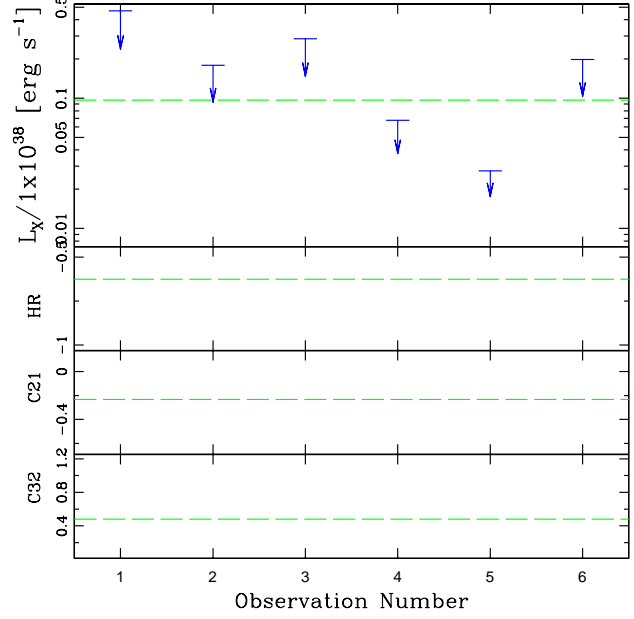




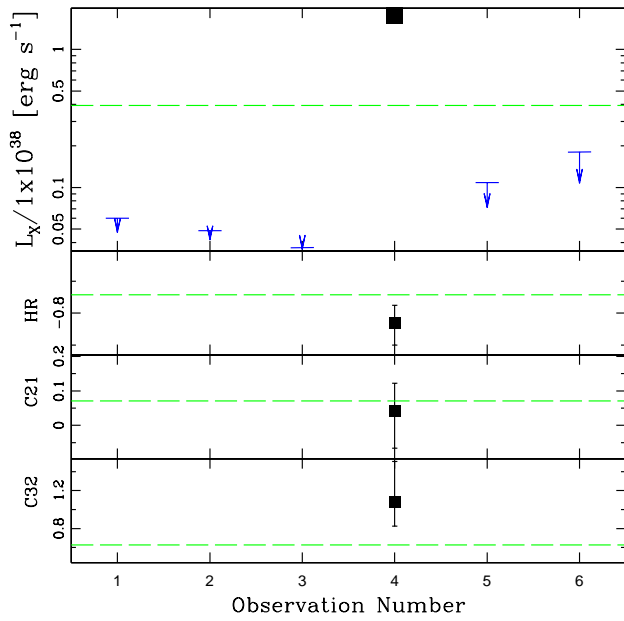
Masterid 89 (d25)



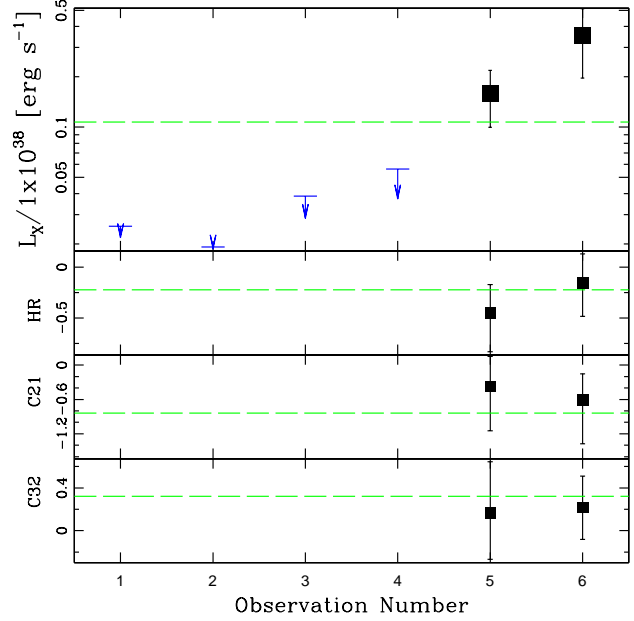
Masterid 90 (d25)



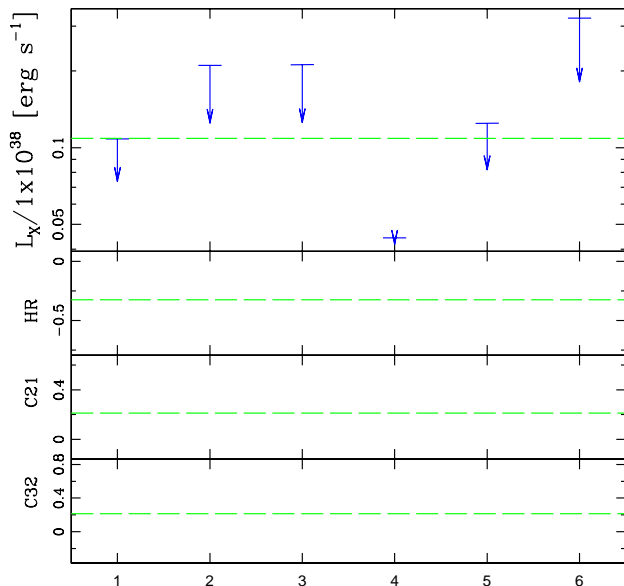
Masterid 91 (d25)



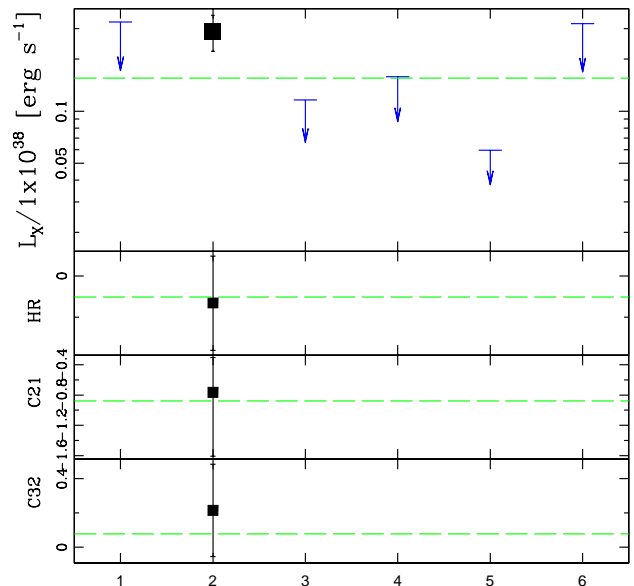
Masterid 92 (d25)



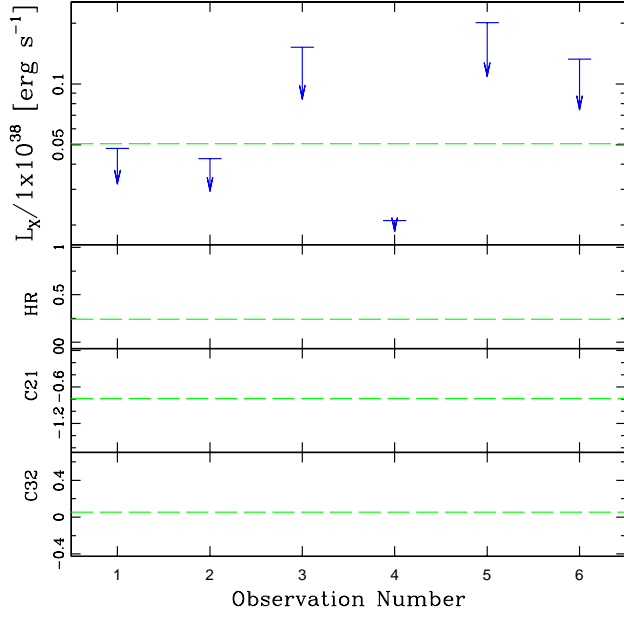
Masterid 93 (d25)



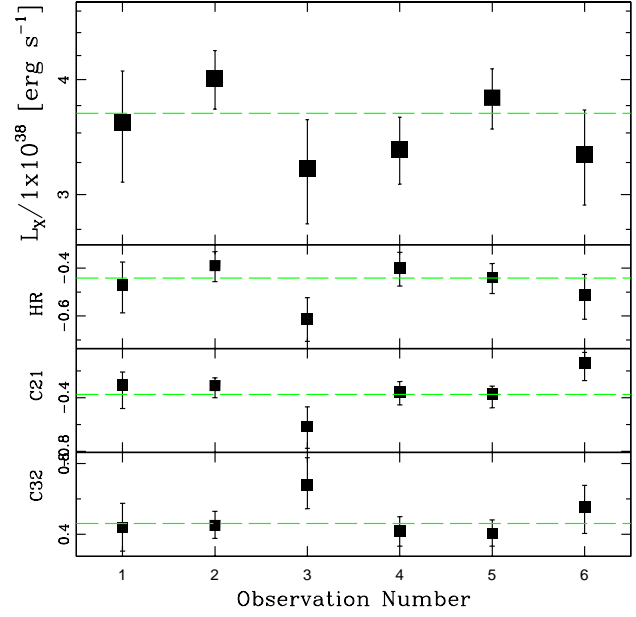
Masterid 94 (d25)



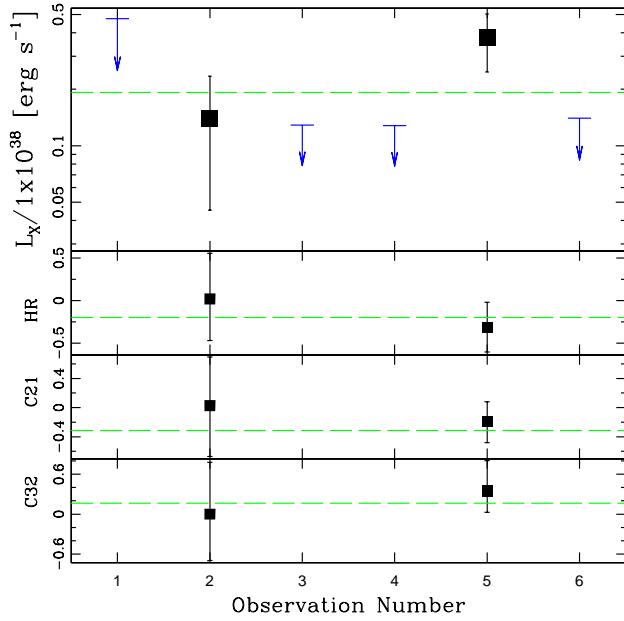
Masterid 95 (d25)



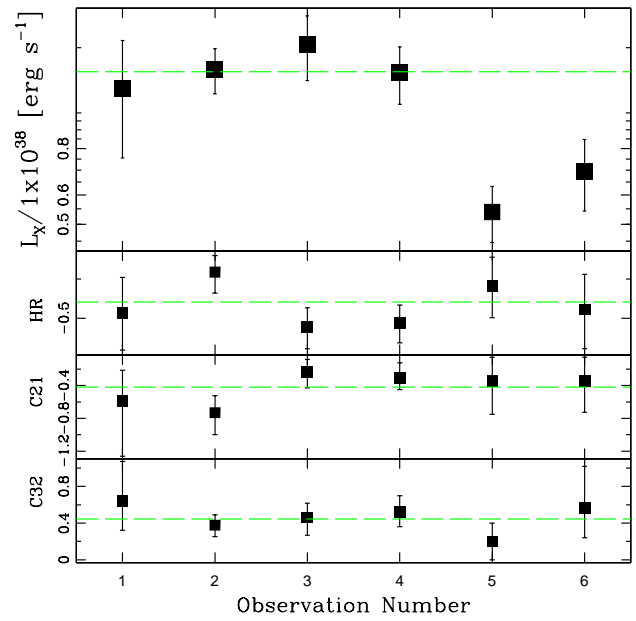
Masterid 96 (d25)



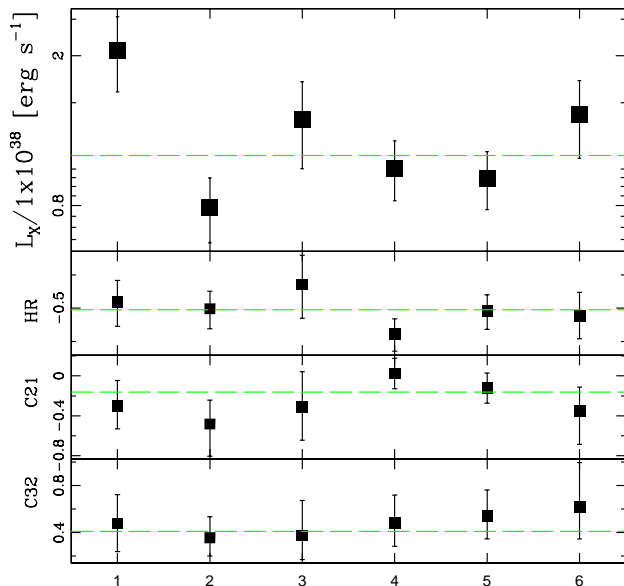
Masterid 97 (d25)



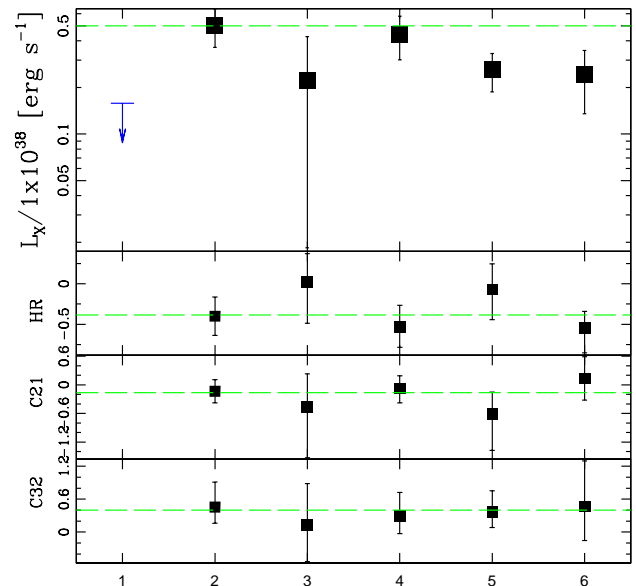
Masterid 98 (d25)



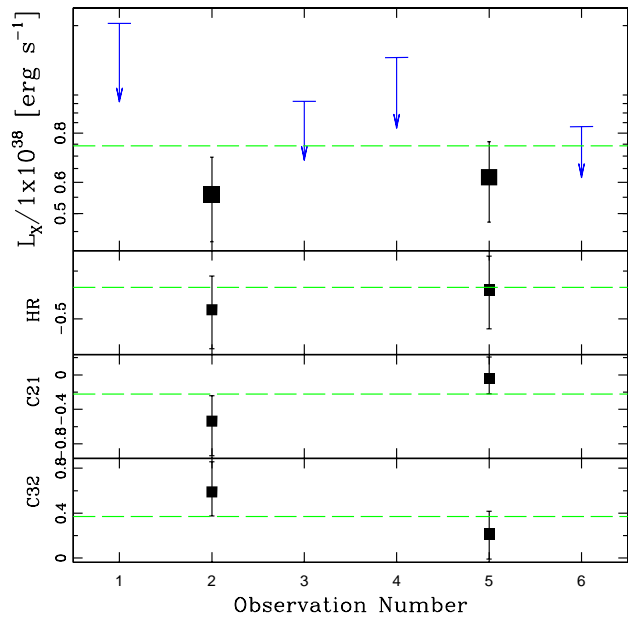
Masterid 99 (d25)



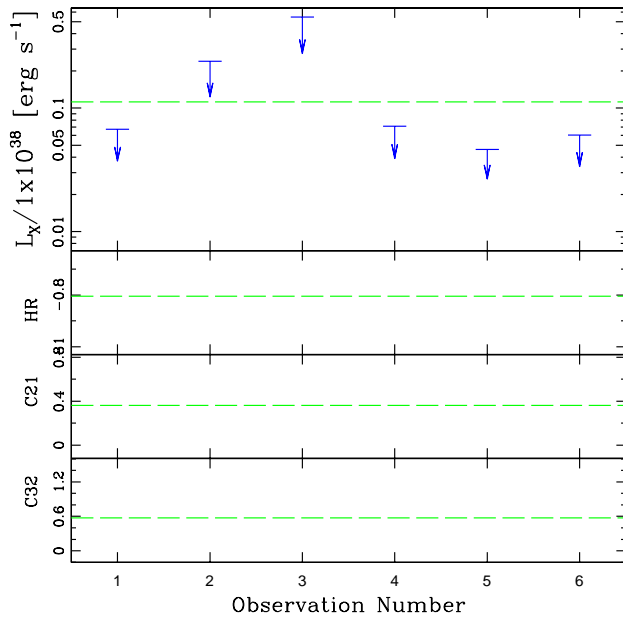
Masterid 100 (d25)



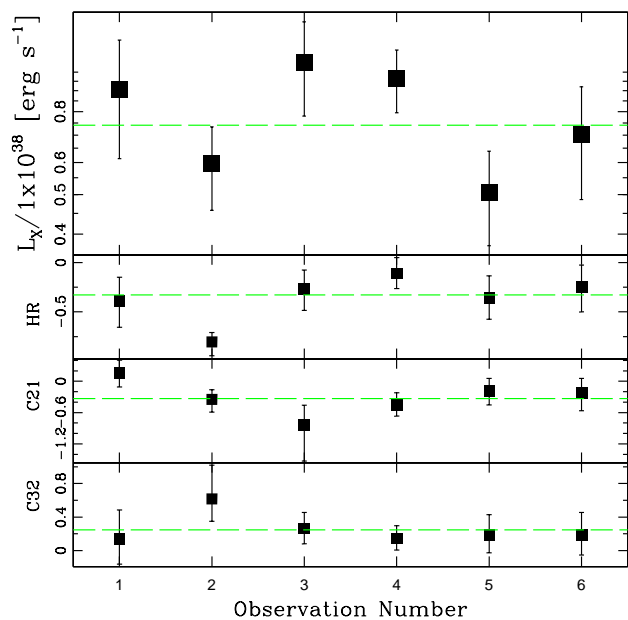
Masterid 101 (d25)



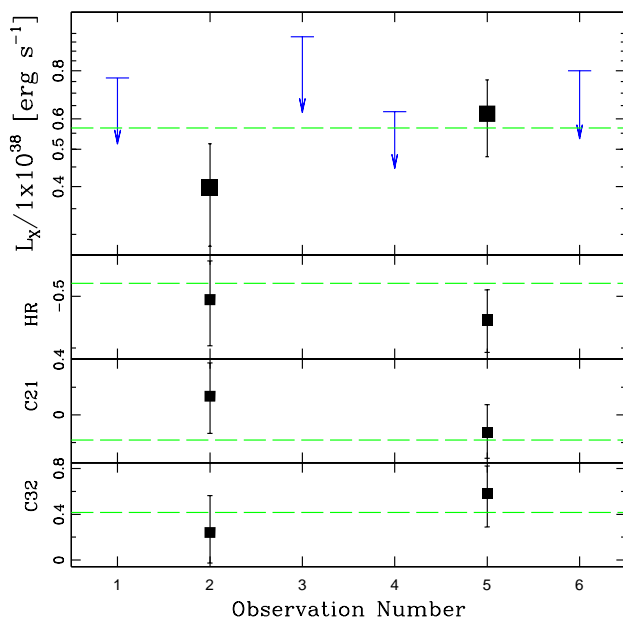
Masterid 102 (d25)



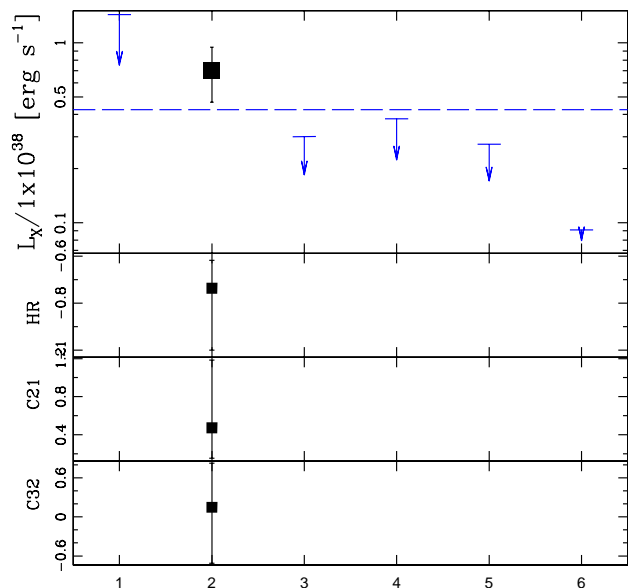
Masterid 103 (d25)



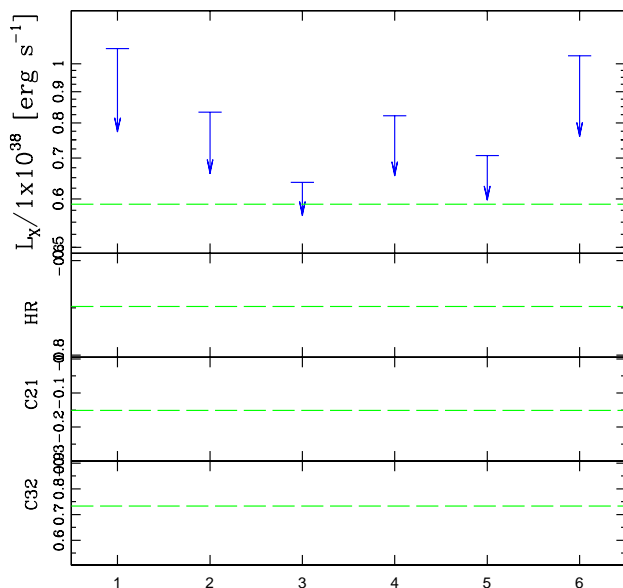
Masterid 104 (d25)



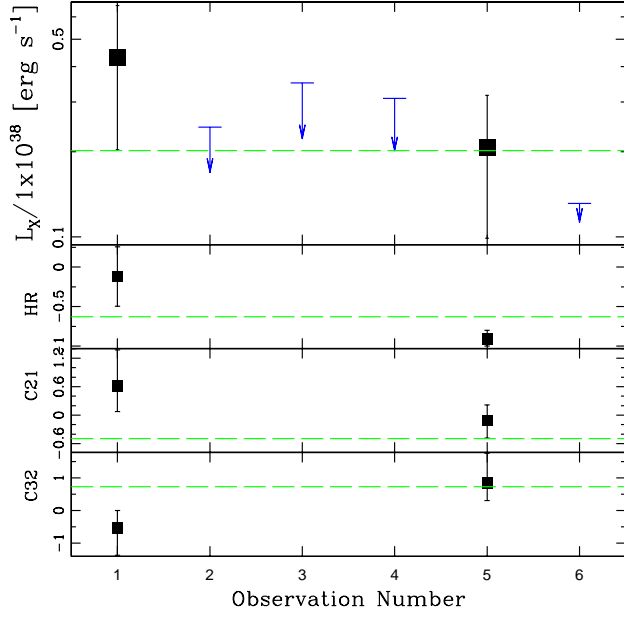
Masterid 105 (d25)



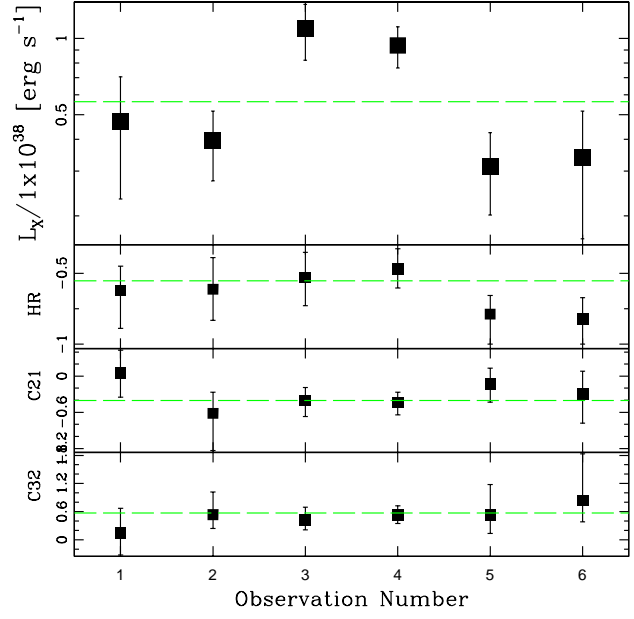
Masterid 106 (d25)



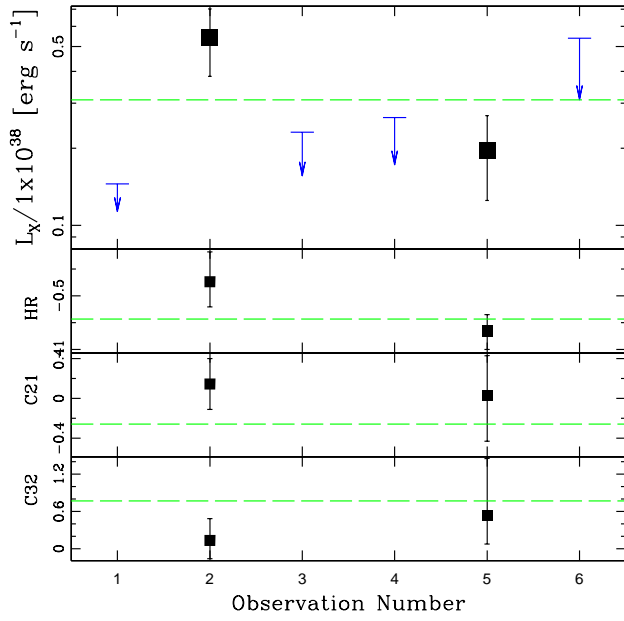
Masterid 107 (all)



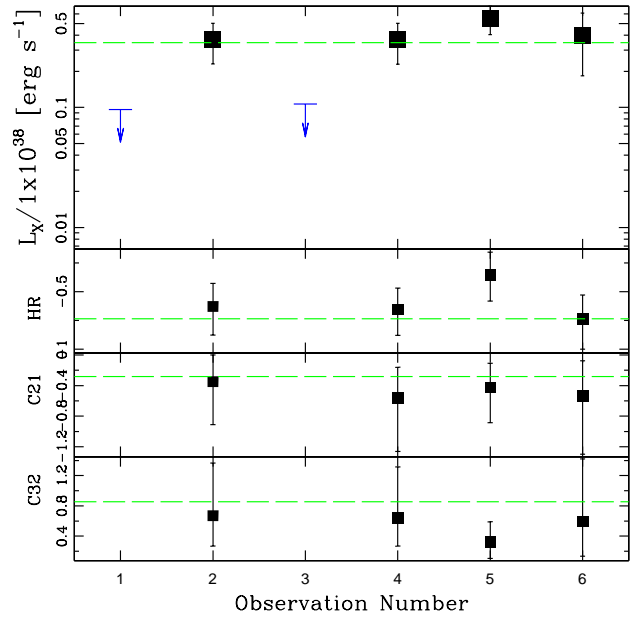
Masterid 108 (d25)



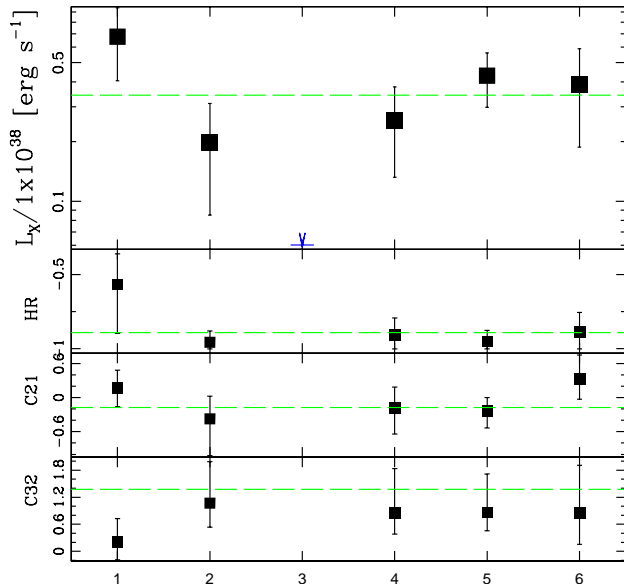
Masterid 109 (d25)



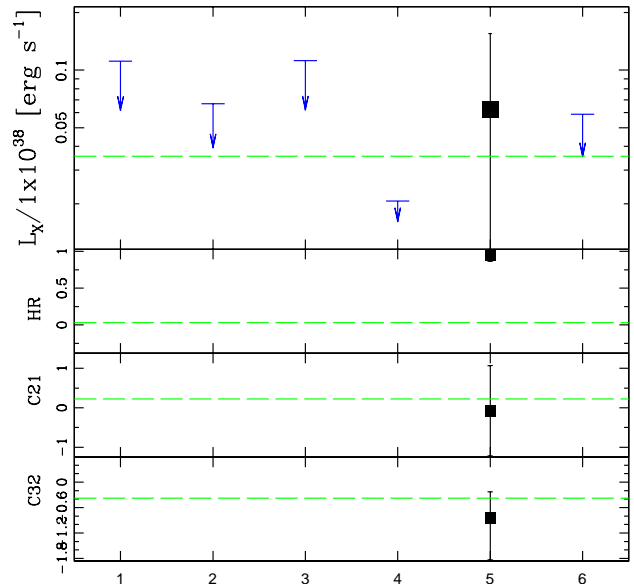
Masterid 110 (d25)



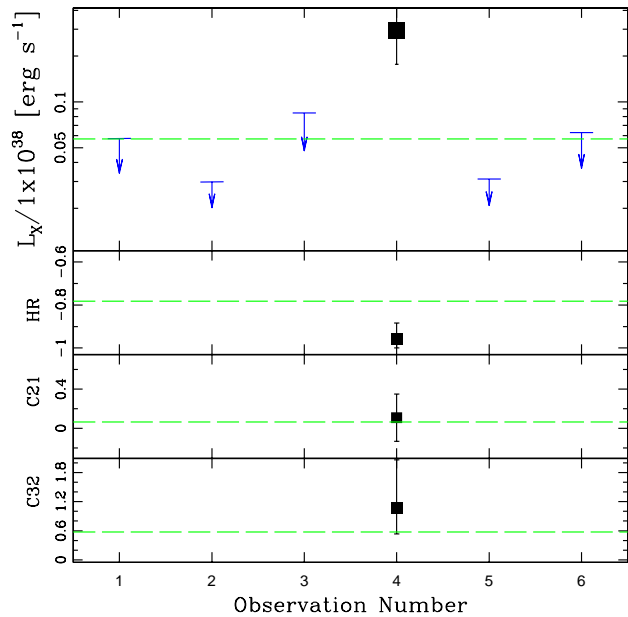
Masterid 111 (d25)



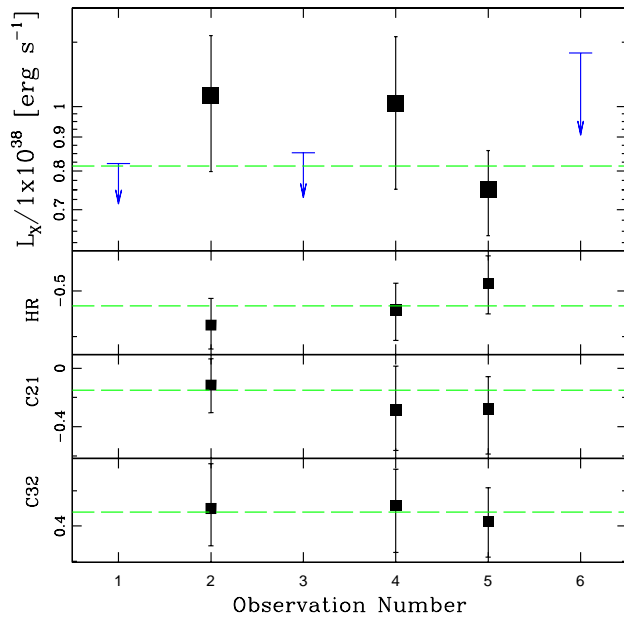
Masterid 112 (all)



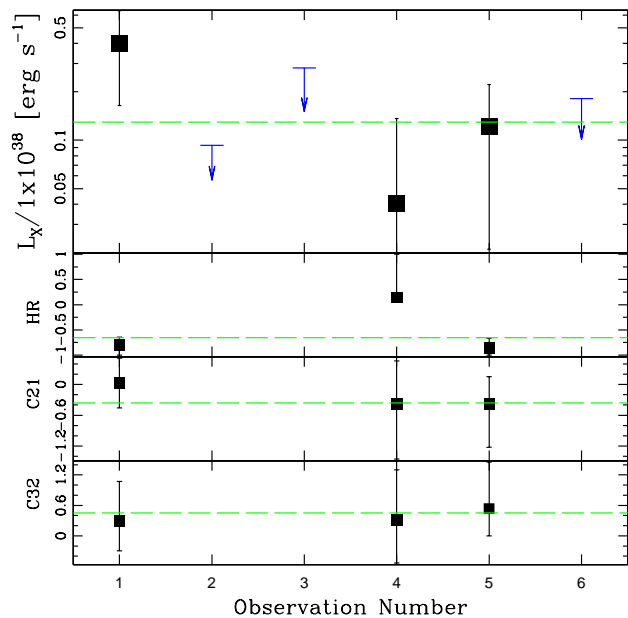
Masterid 113 (d25)



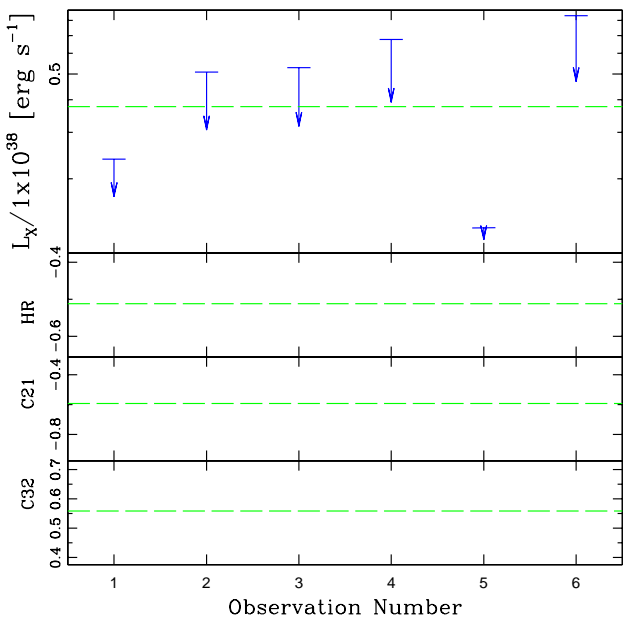
Masterid 114 (d25)



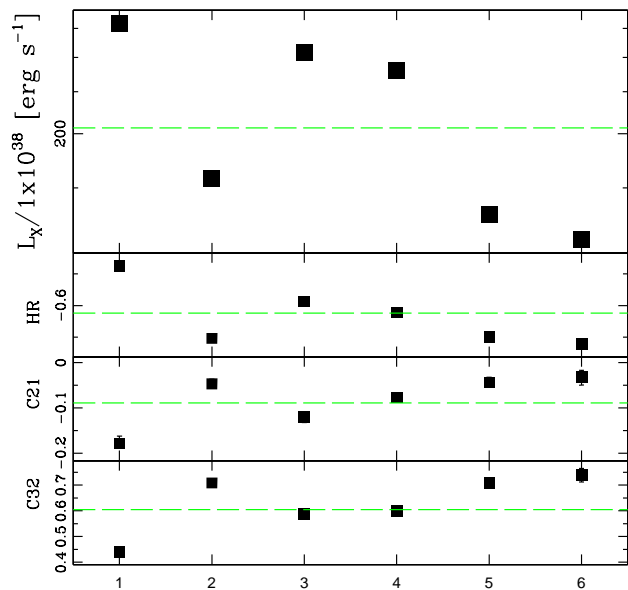
Masterid 115 (d25)



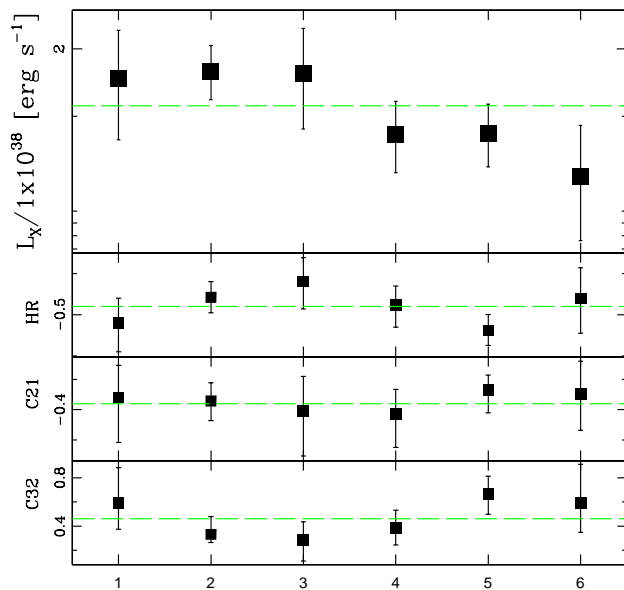
Masterid 116 (d25)



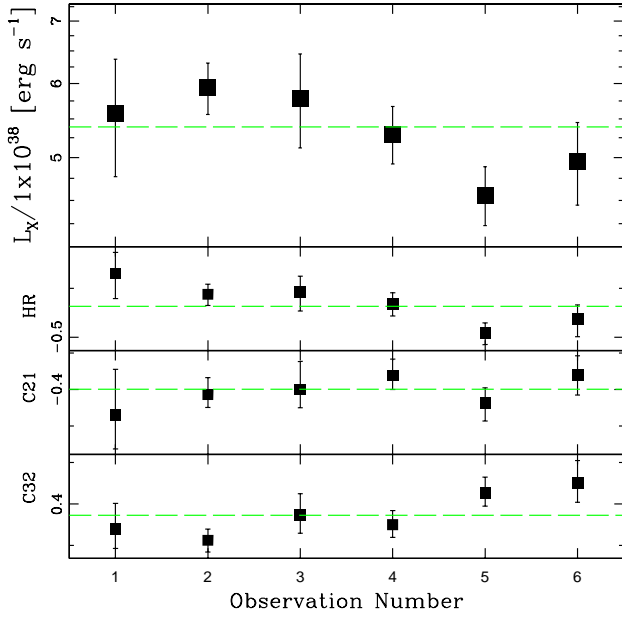
Masterid 117 (d25)



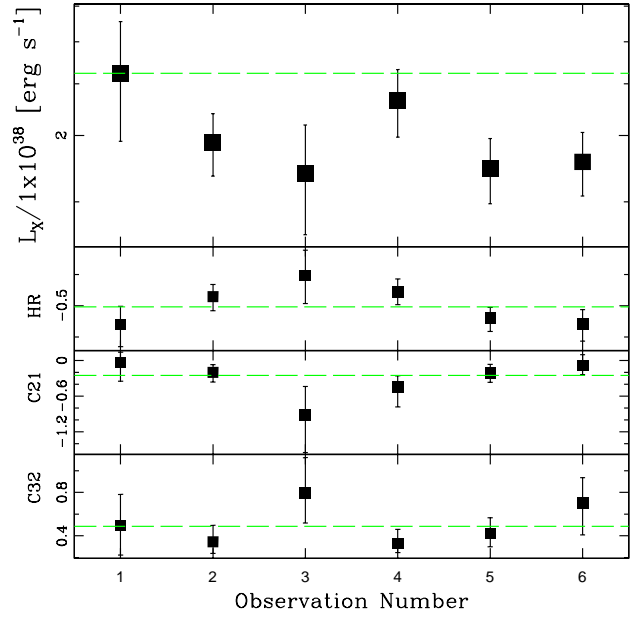
Masterid 118 (d25)



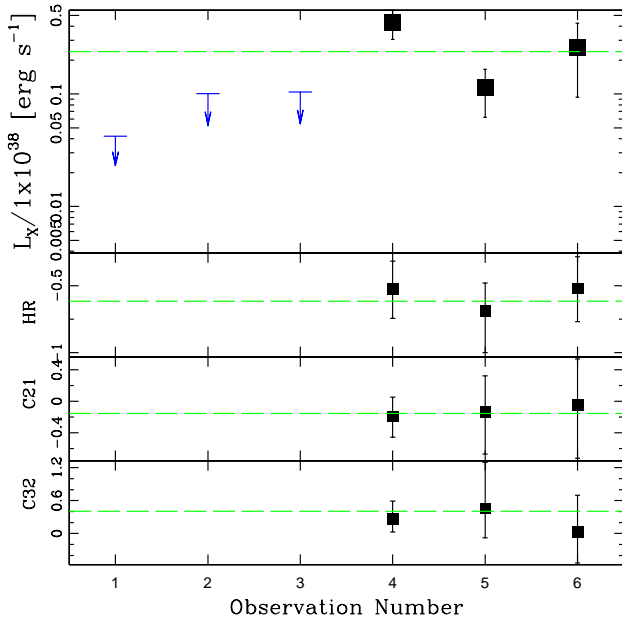
Masterid 119 (d25)



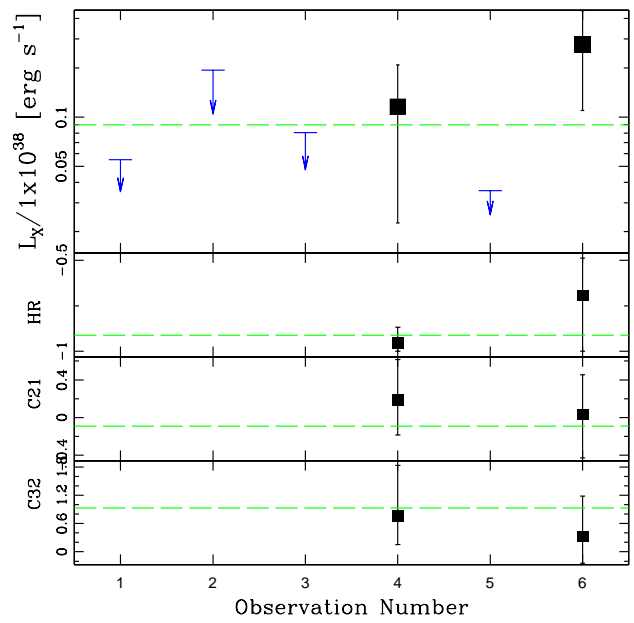
Masterid 120 (d25)



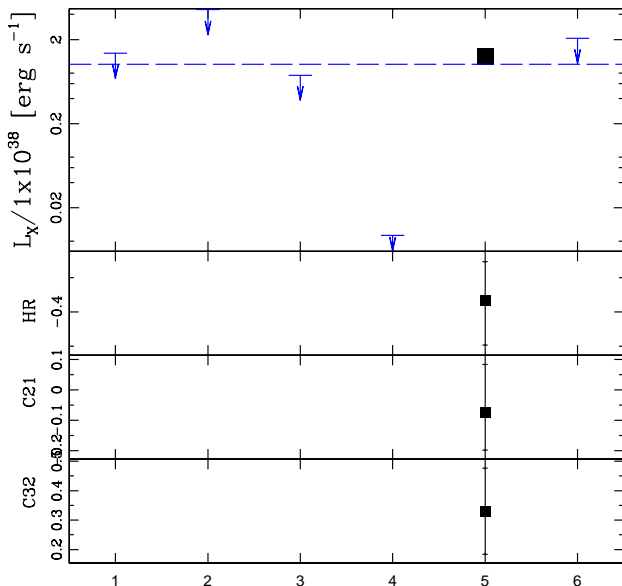
Masterid 121 (all)



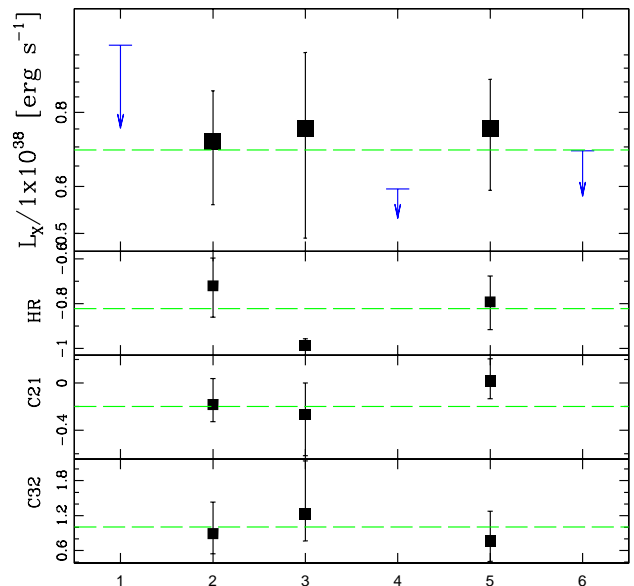
Masterid 122 (d25)



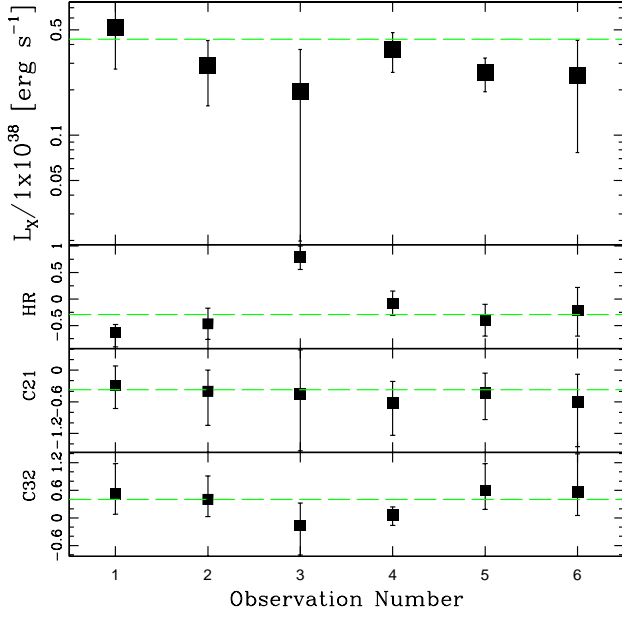
Masterid 123 (d25)



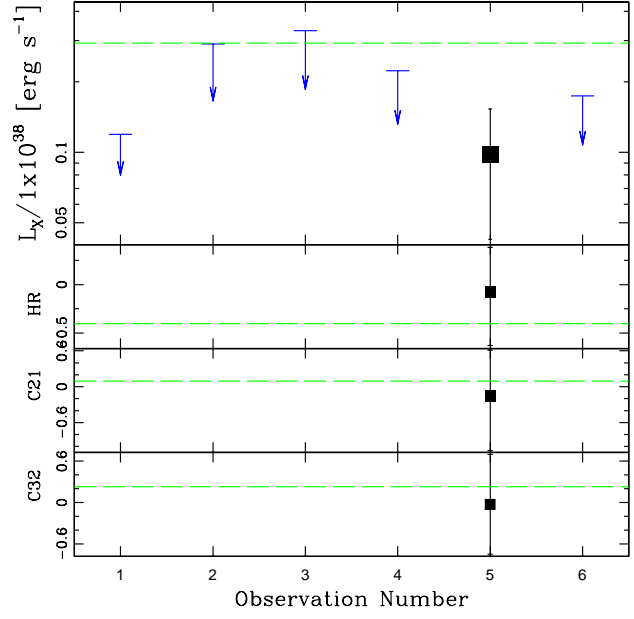
Masterid 124 (d25)



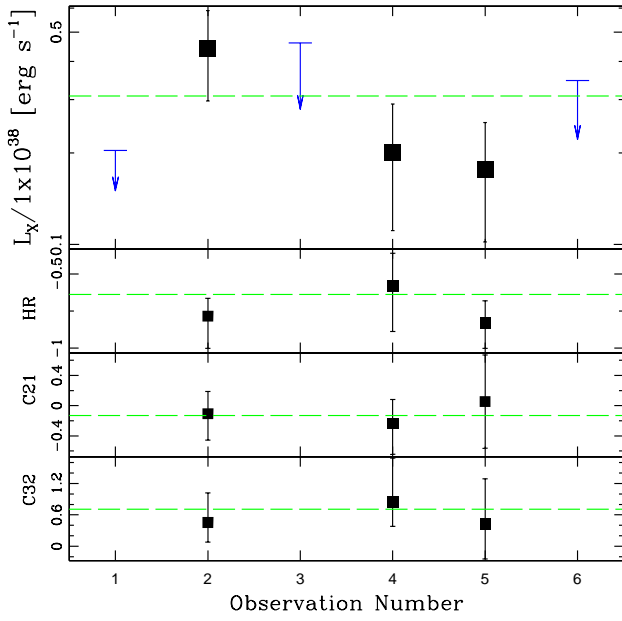
Masterid 125 (d25)



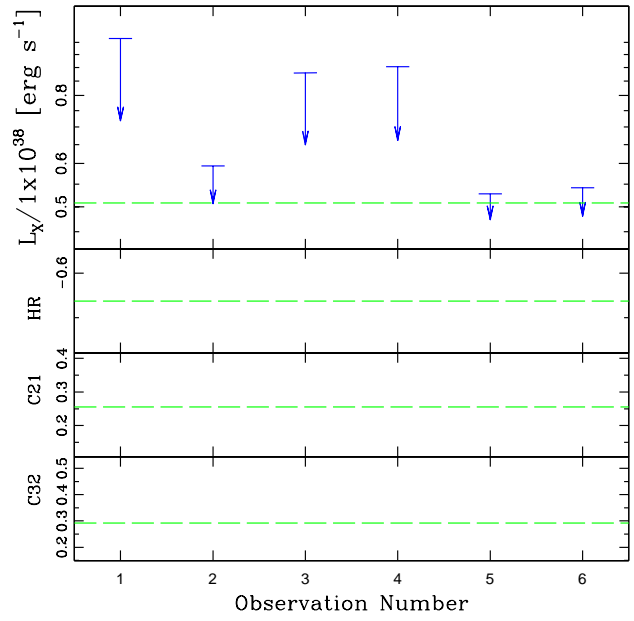
Masterid 126 (d25)



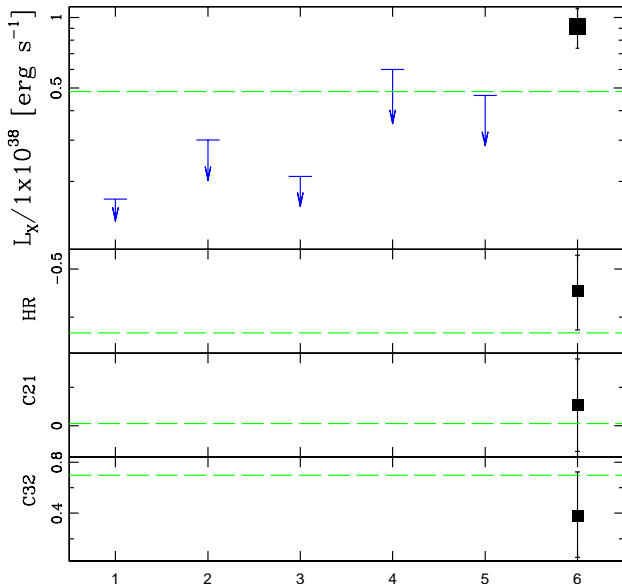
Masterid 127 (d25)



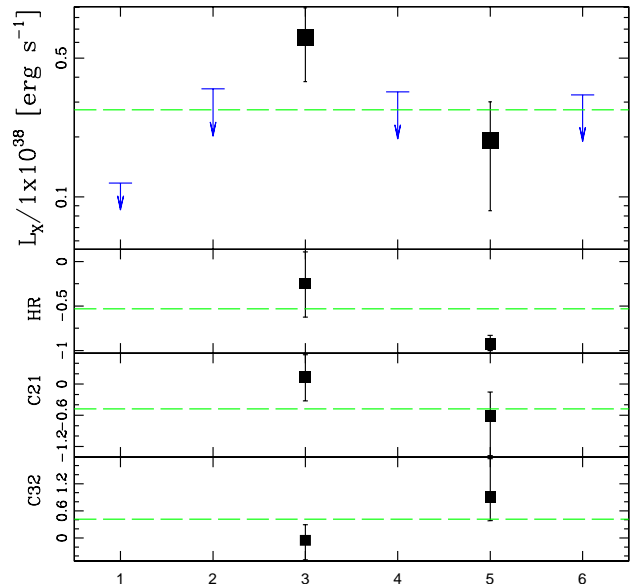
Masterid 128 (d25)



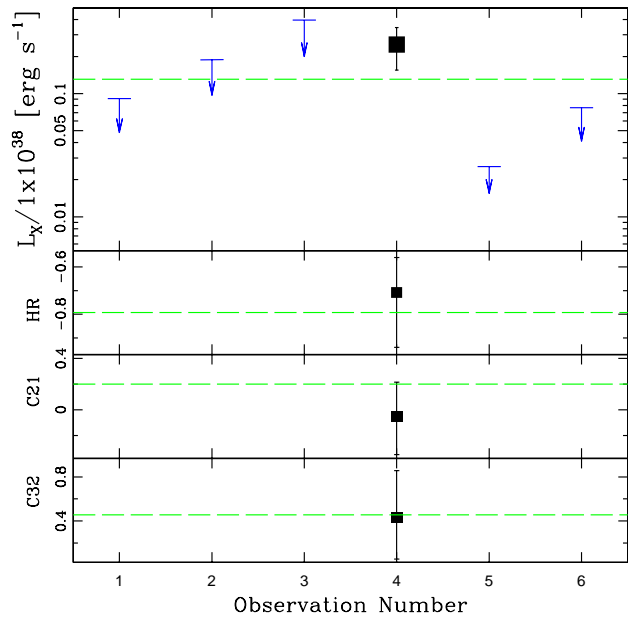
Masterid 129 (d25)



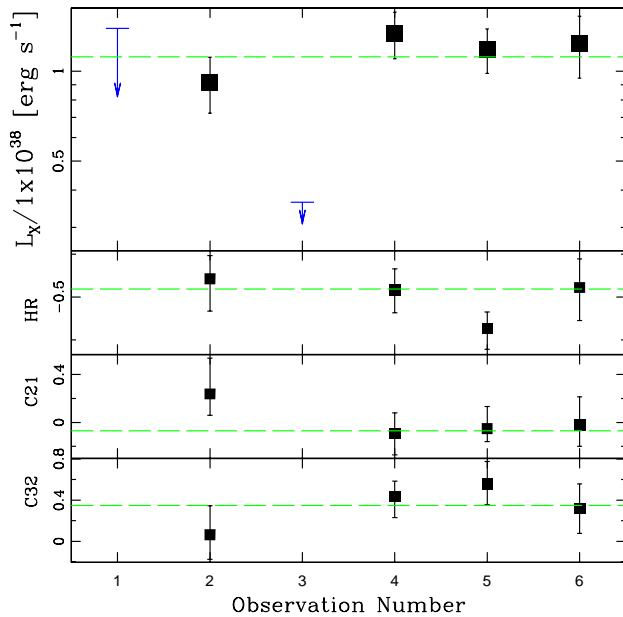
Masterid 130 (d25)



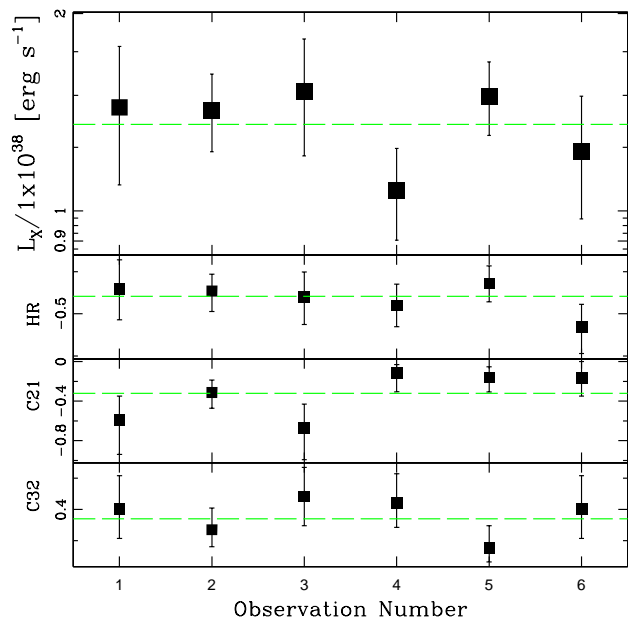
Masterid 131 (d25)



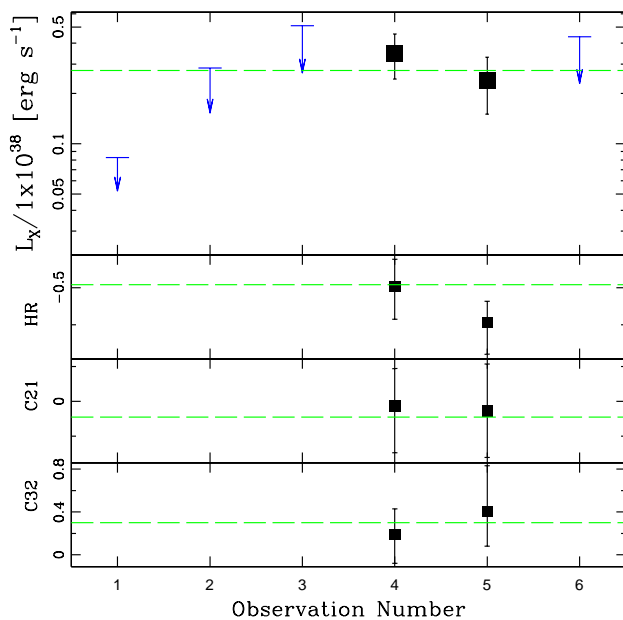
Masterid 132 (d25)



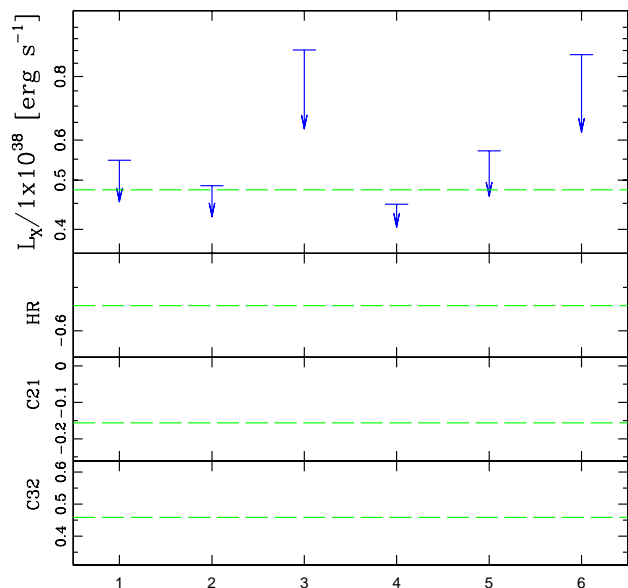
Masterid 133 (d25)



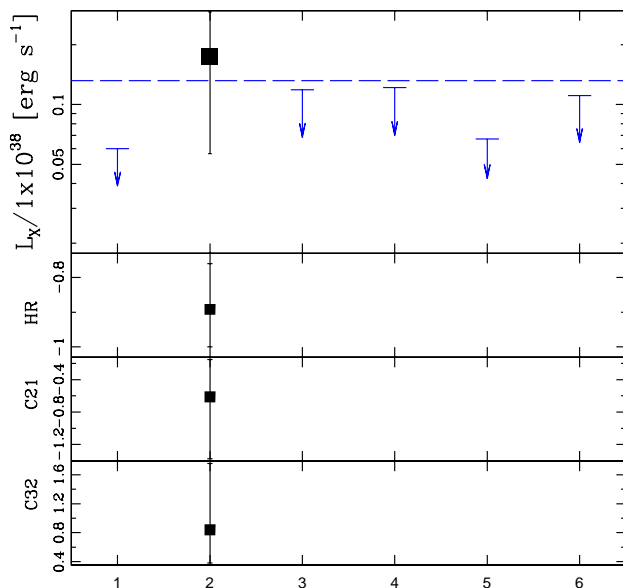
Masterid 134 (d25)



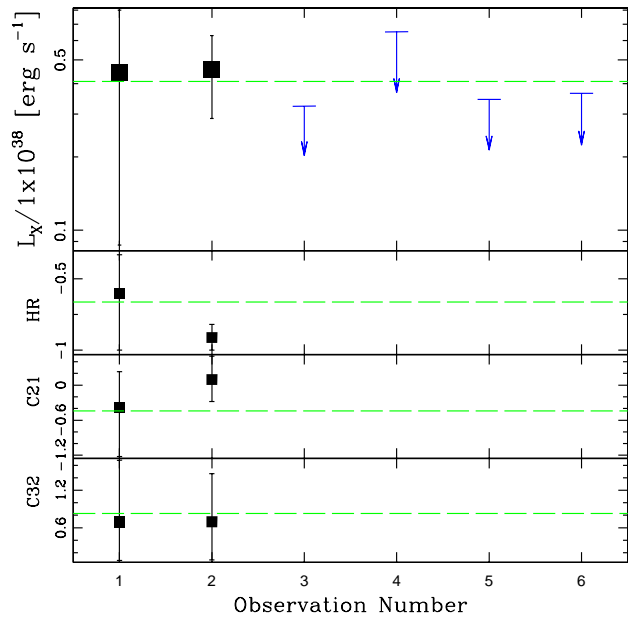
Masterid 135 (d25)



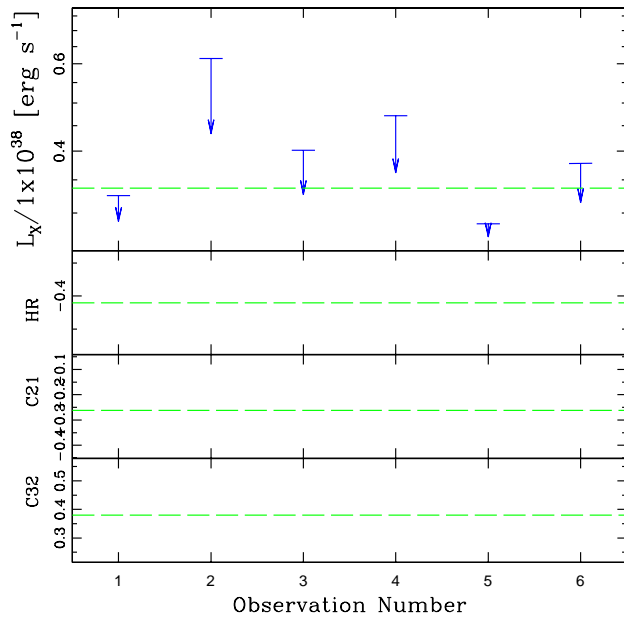
Masterid 136 (d25)



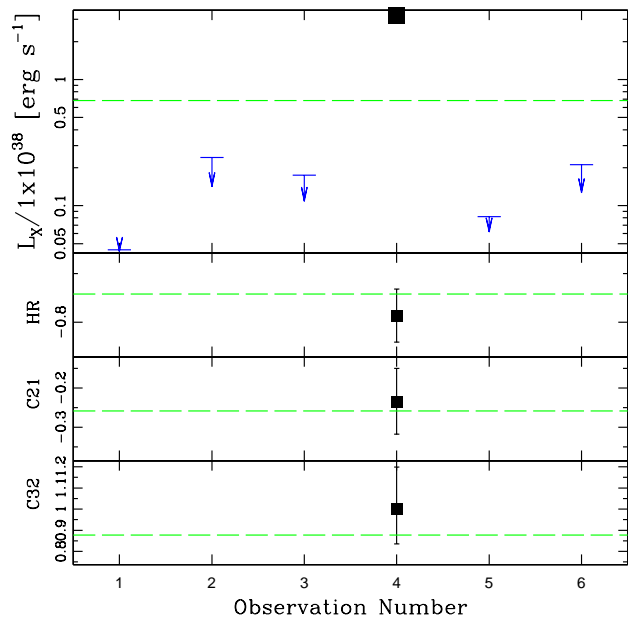
Masterid 137 (d25)



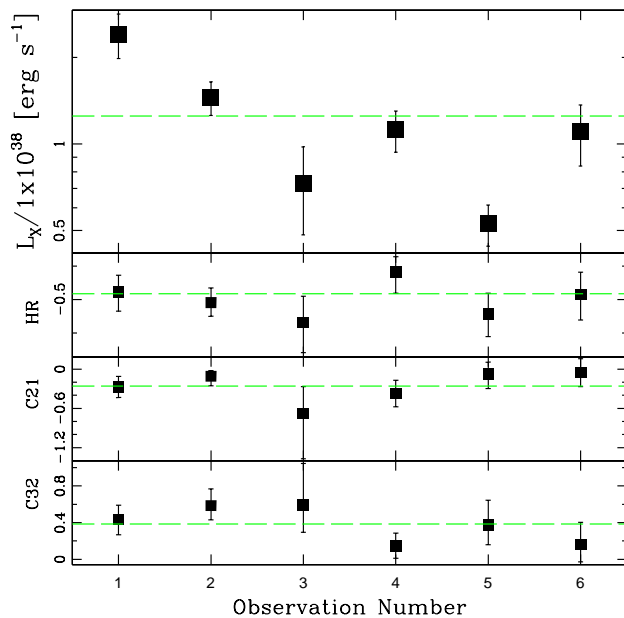
Masterid 138 (d25)



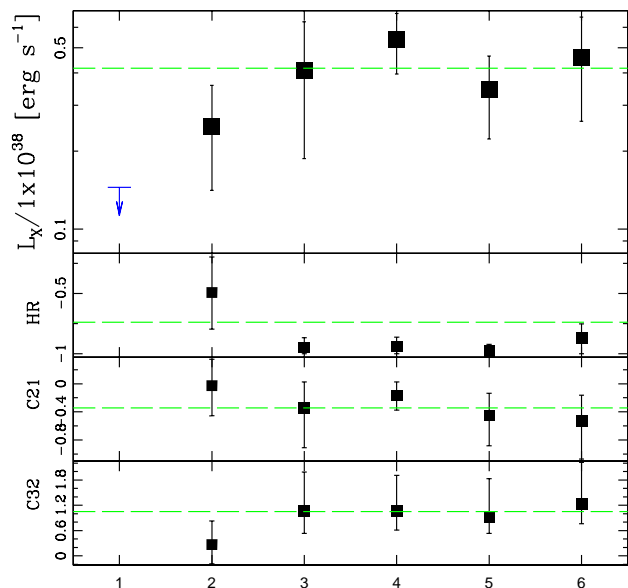
Masterid 139 (d25)



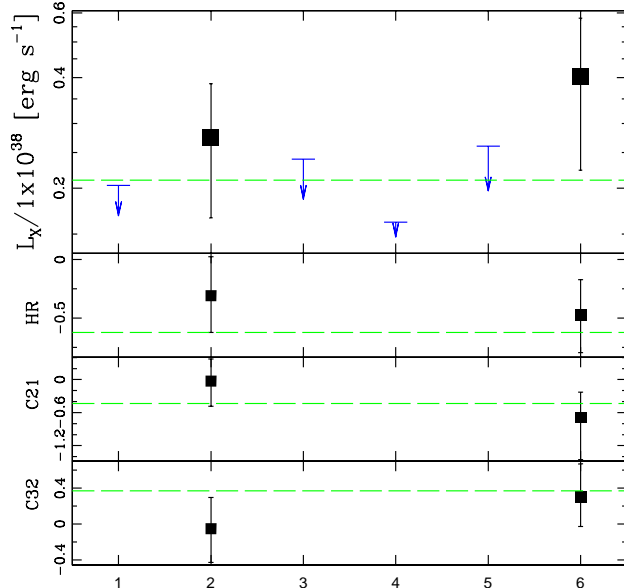
Masterid 140 (d25)



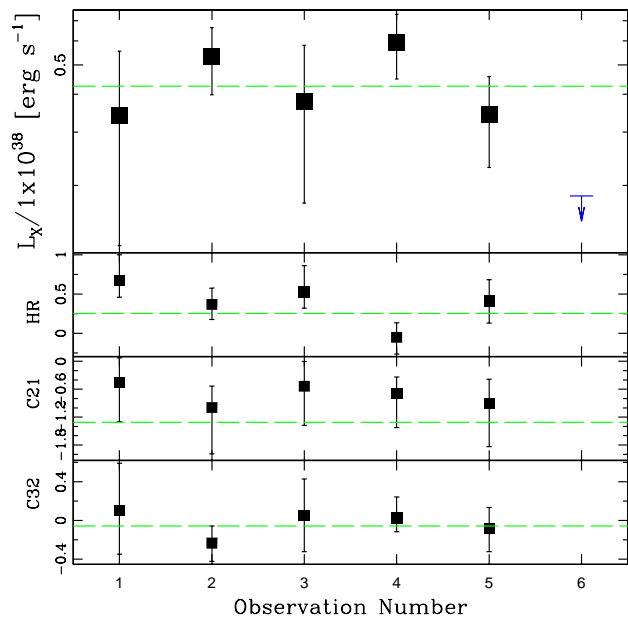
Masterid 141 (d25)



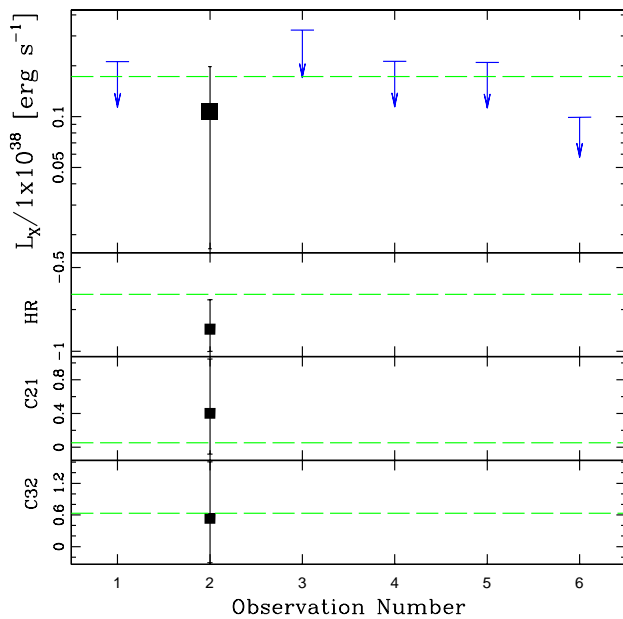
Masterid 142 (all)



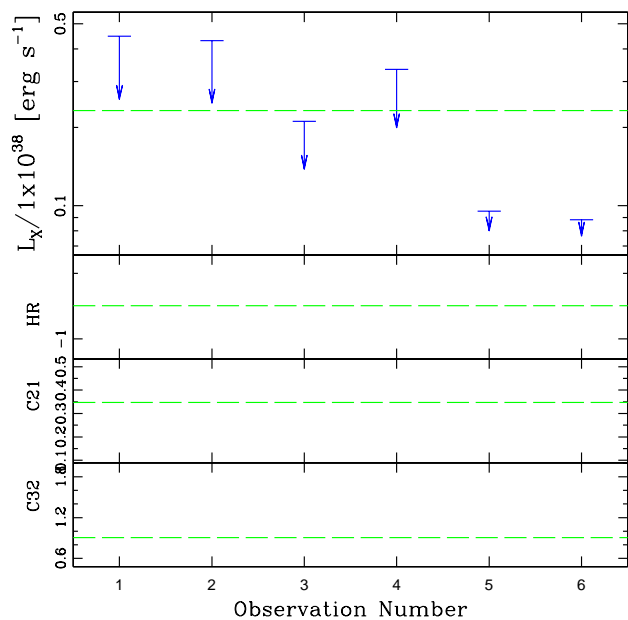
Masterid 143 (d25)



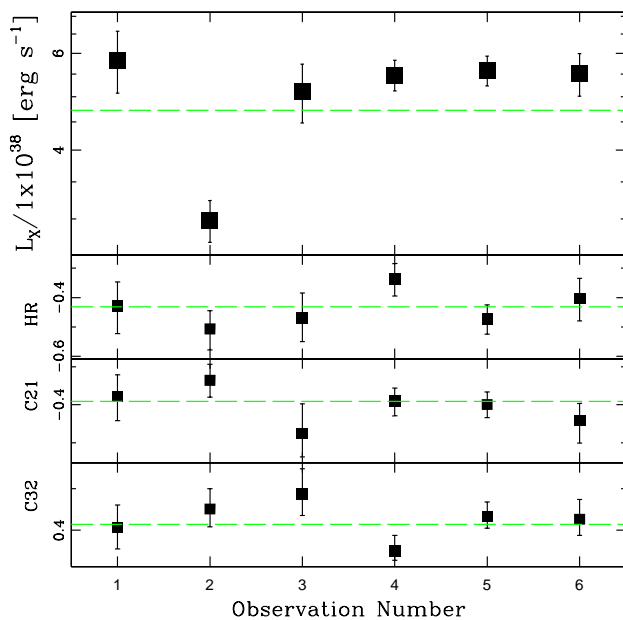
Masterid 144 (d25)



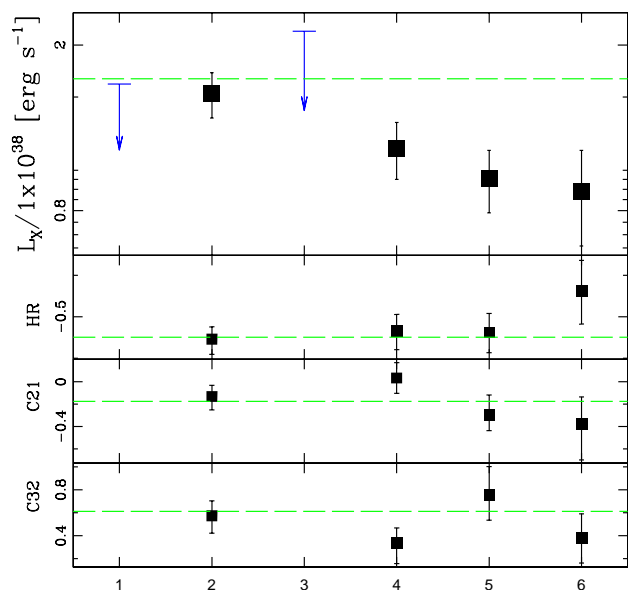
Masterid 145 (d25)



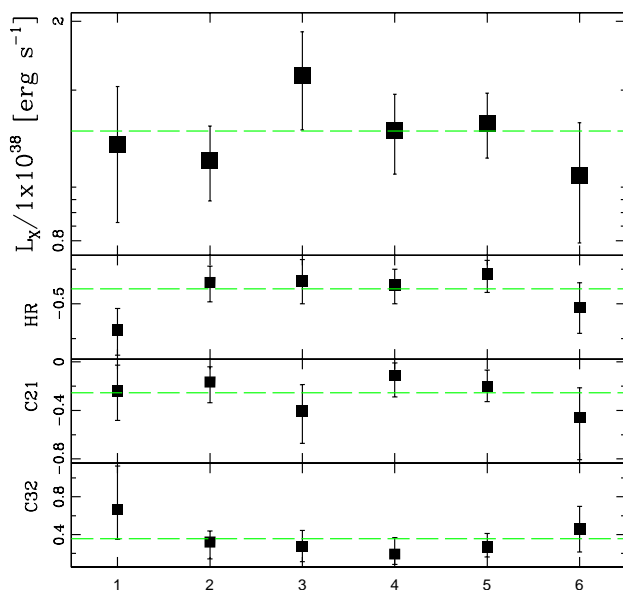
Masterid 146 (d25)



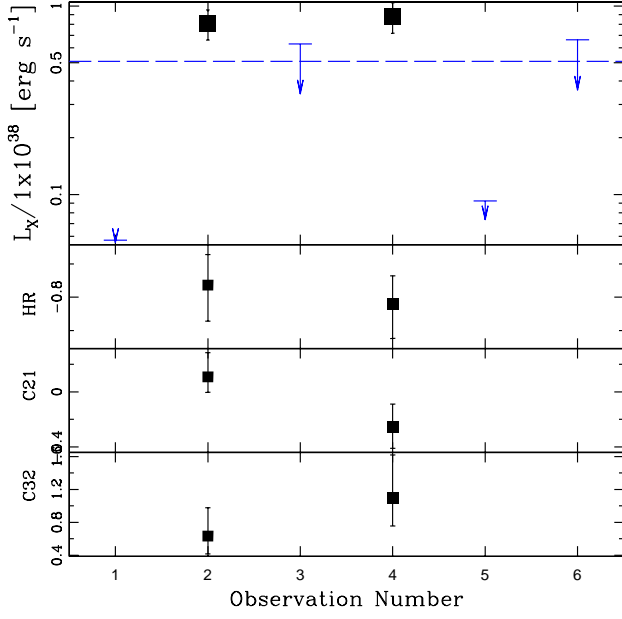
Masterid 147 (d25)



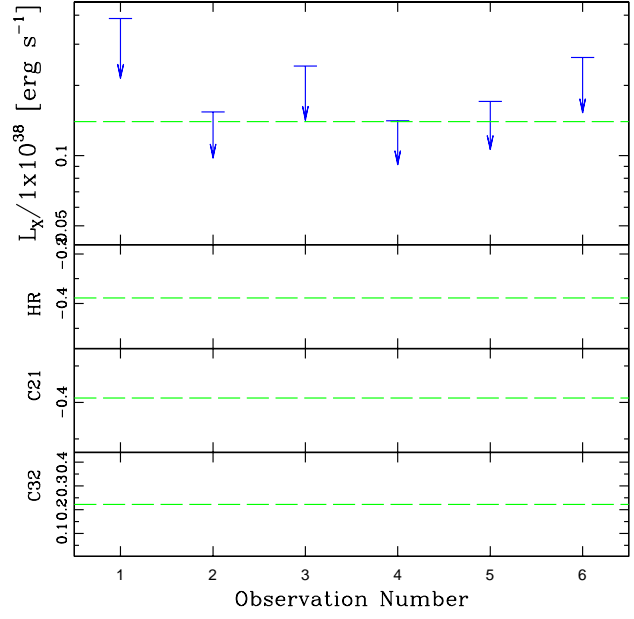
Masterid 148 (d25)



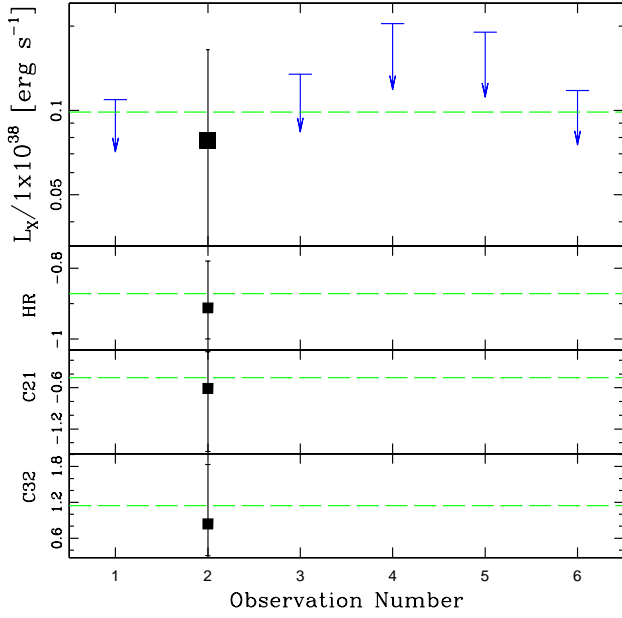
Masterid 149 (d25)



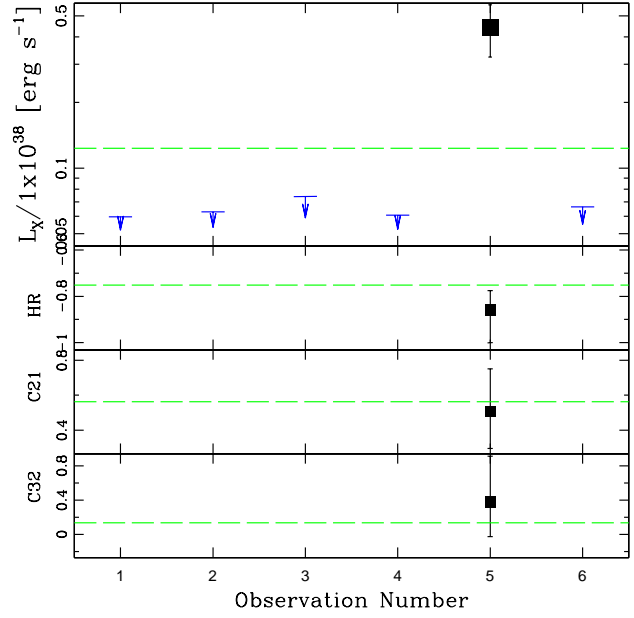
Masterid 150 (d25)



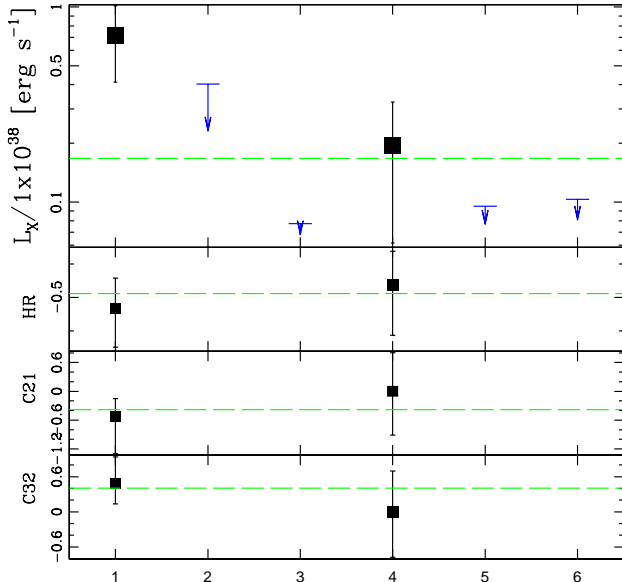
Masterid 151 (d25)



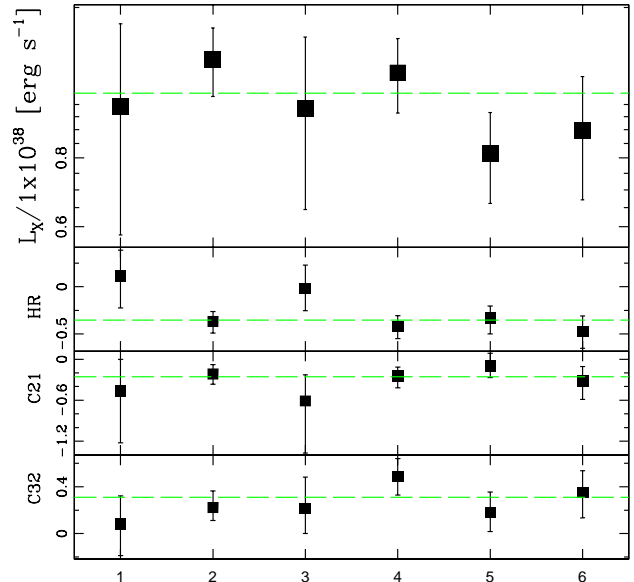
Masterid 152 (d25)



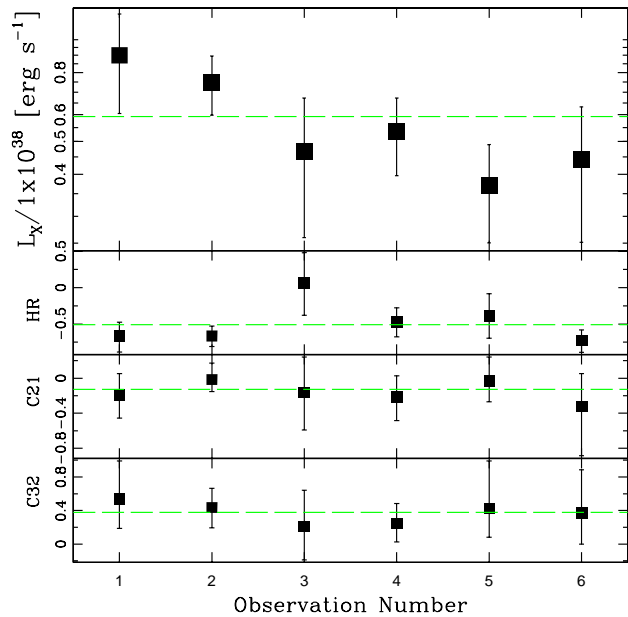
Masterid 153 (d25)



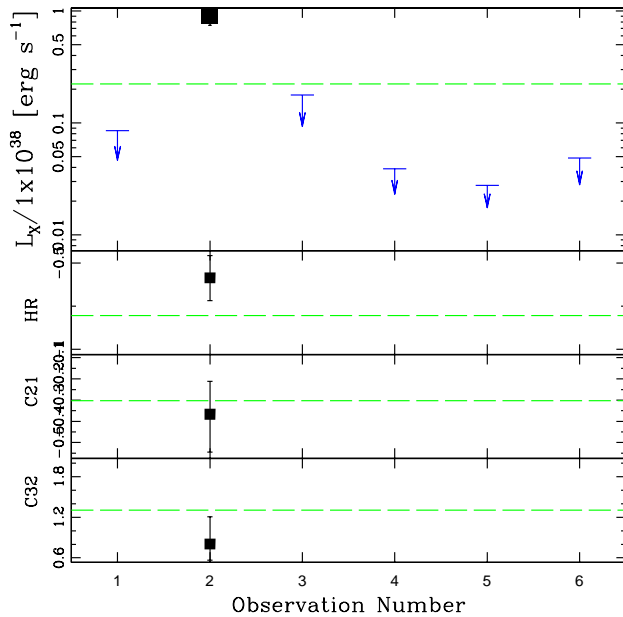
Masterid 154 (d25)



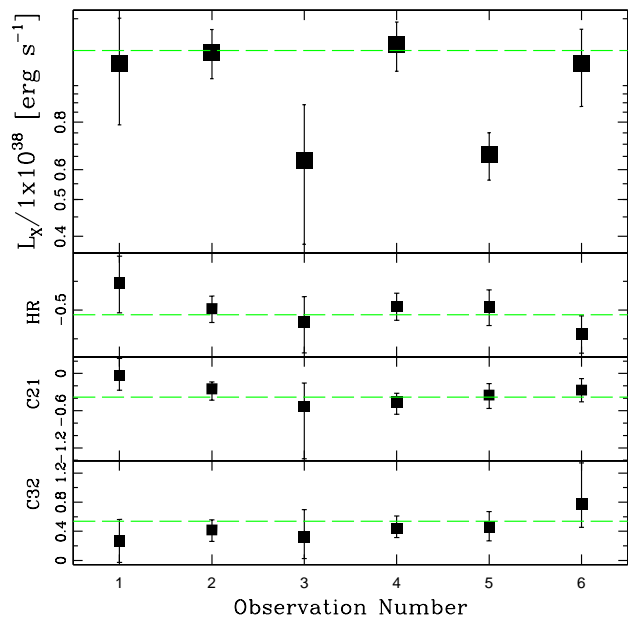
Masterid 155 (d25)



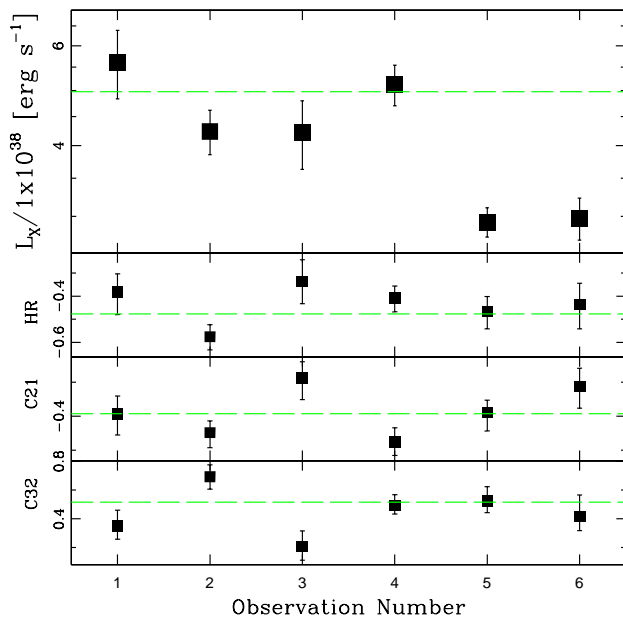
Masterid 156 (d25)



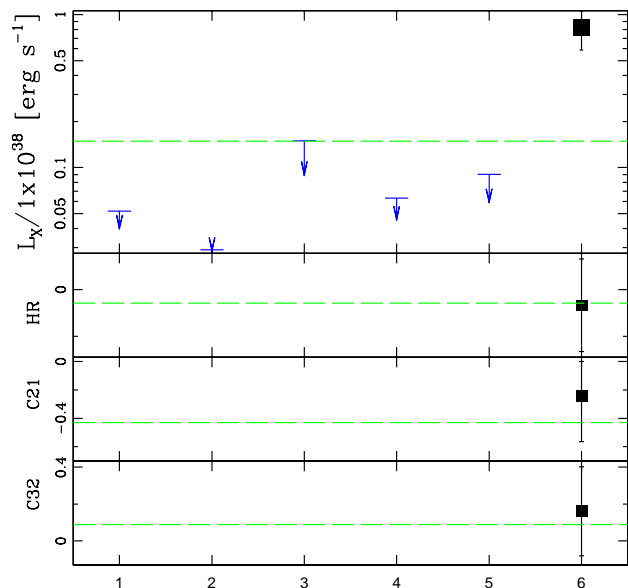
Masterid 157 (d25)



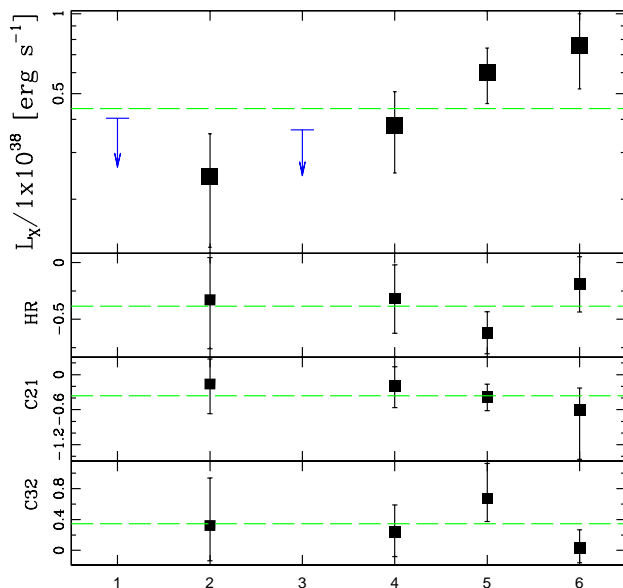
Masterid 158 (d25)

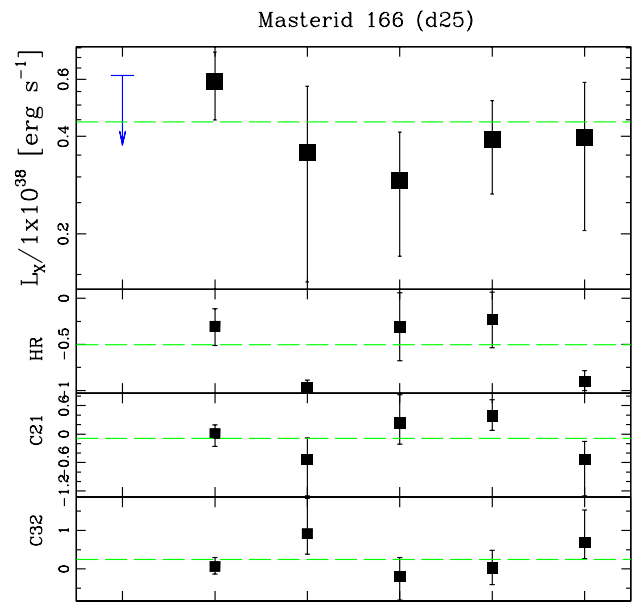
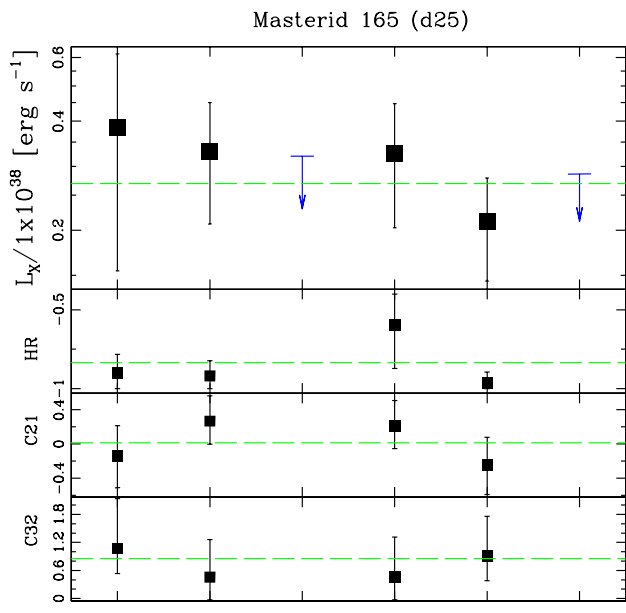
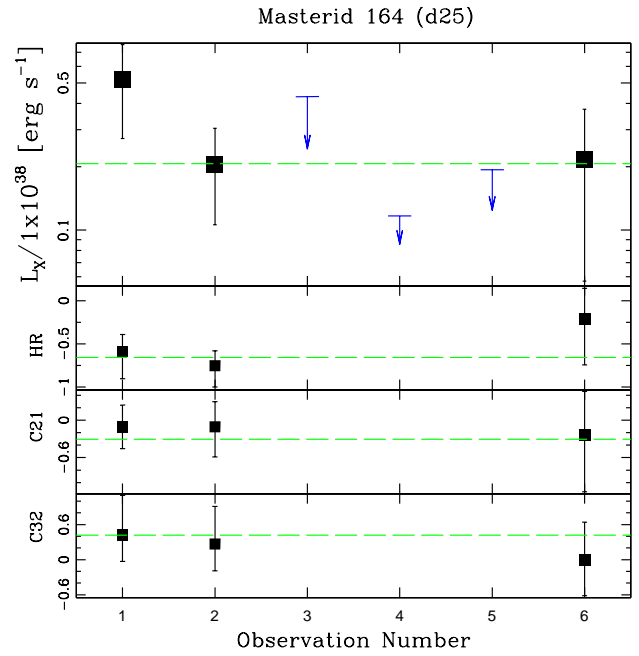
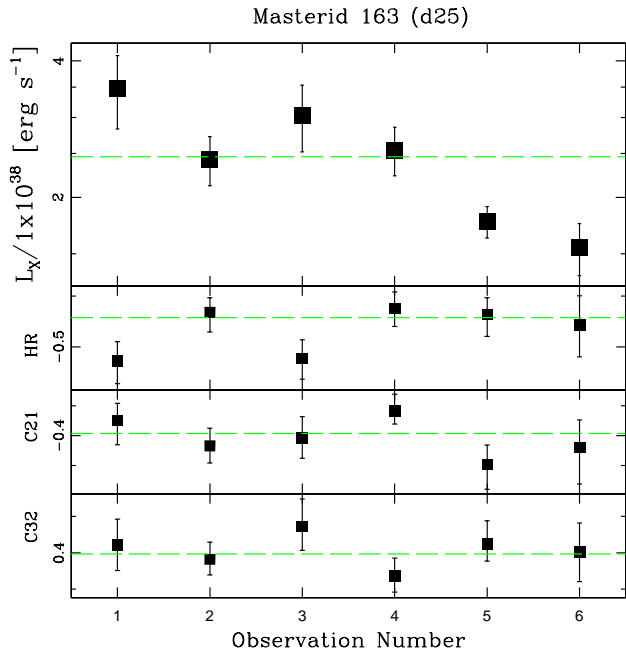
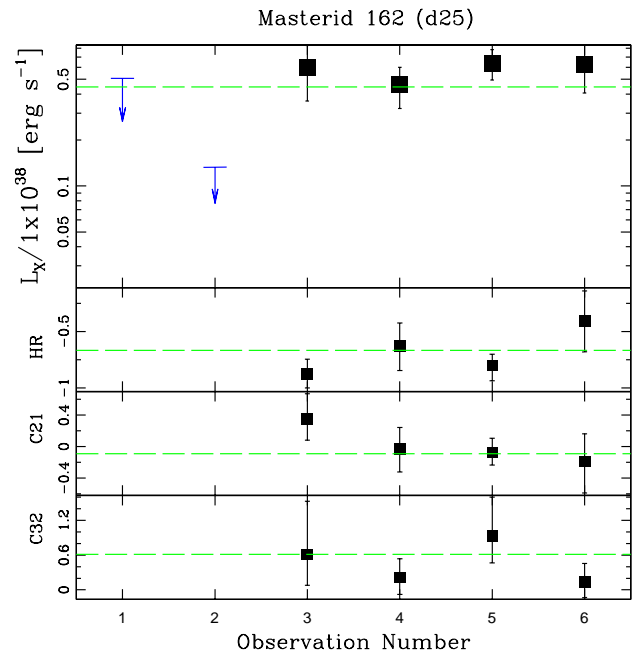
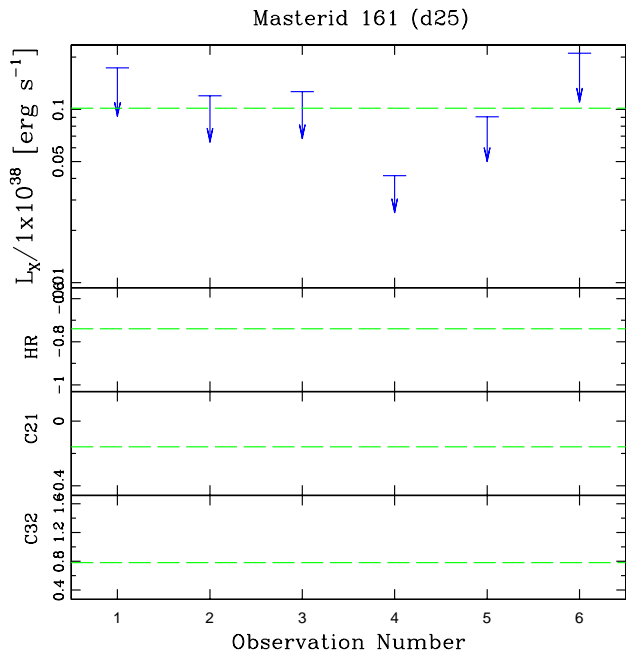


Masterid 159 (d25)

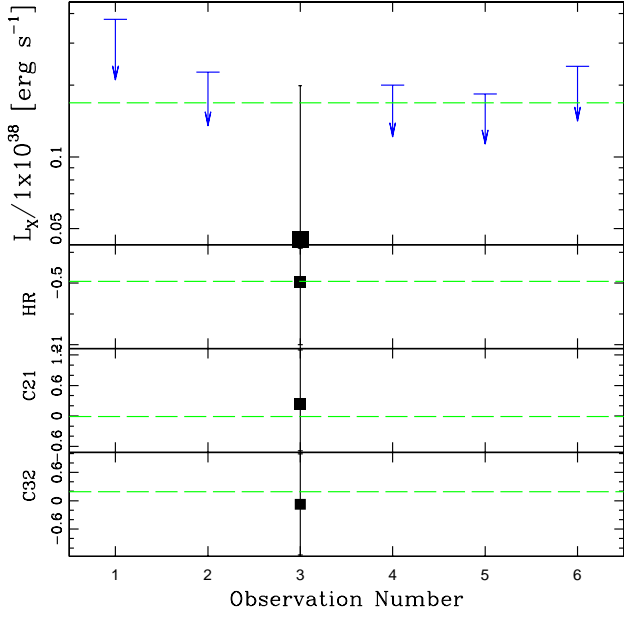


Masterid 160 (d25)

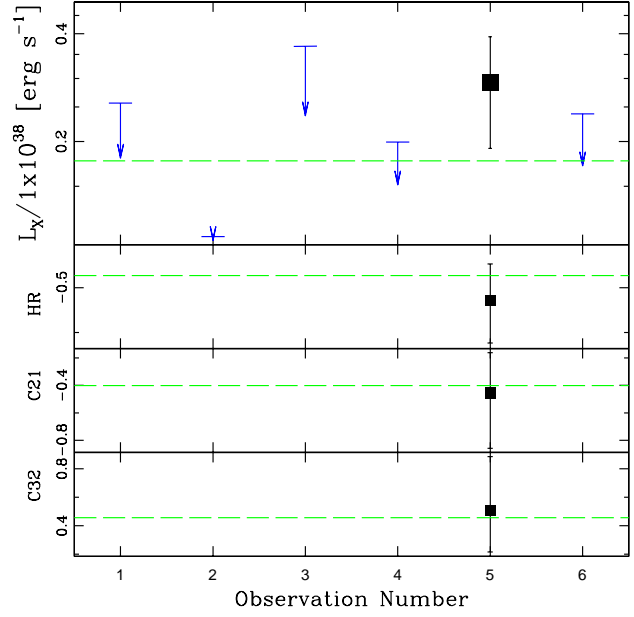




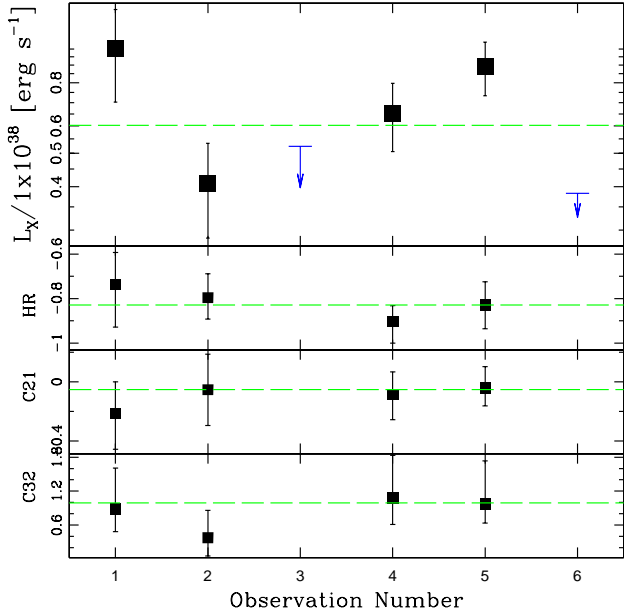
Masterid 167 (d25)



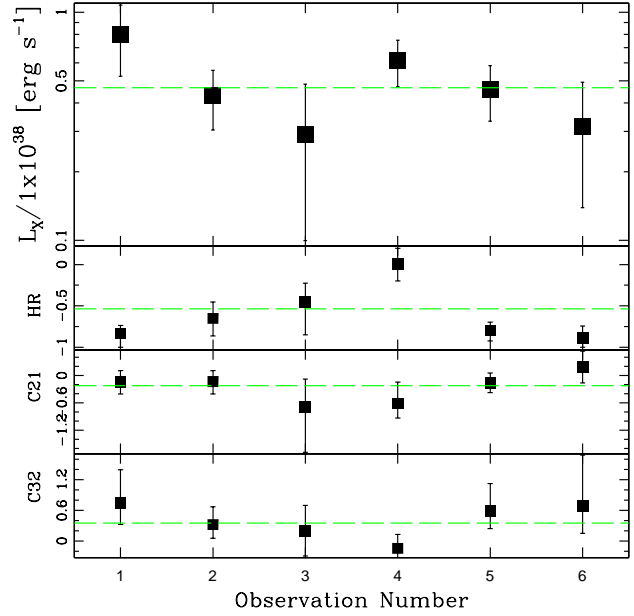
Masterid 168 (d25)



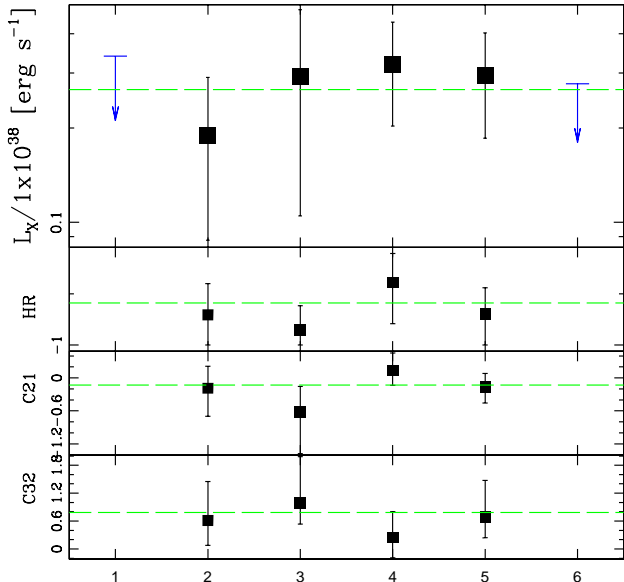
Masterid 169 (d25)



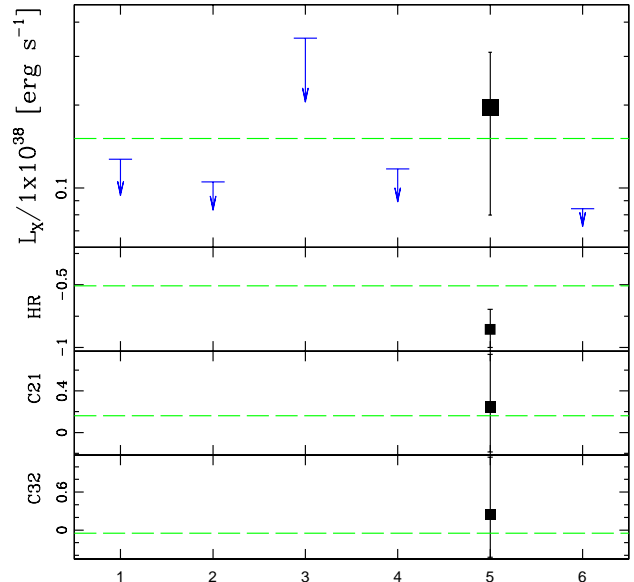
Masterid 170 (d25)

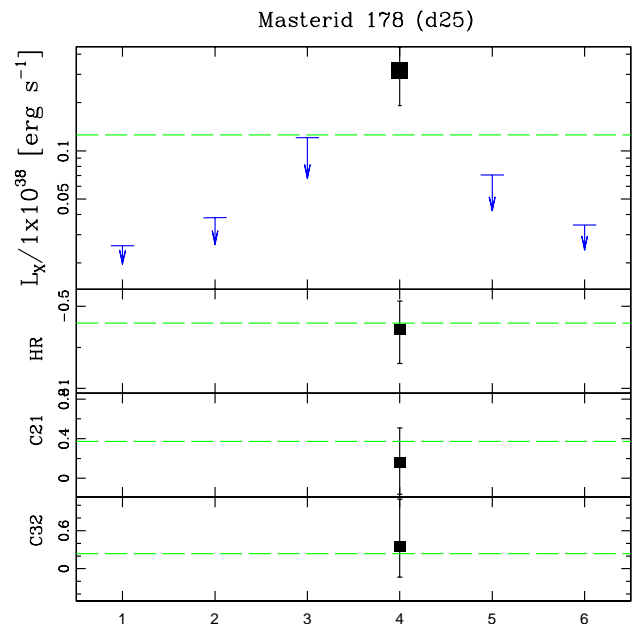
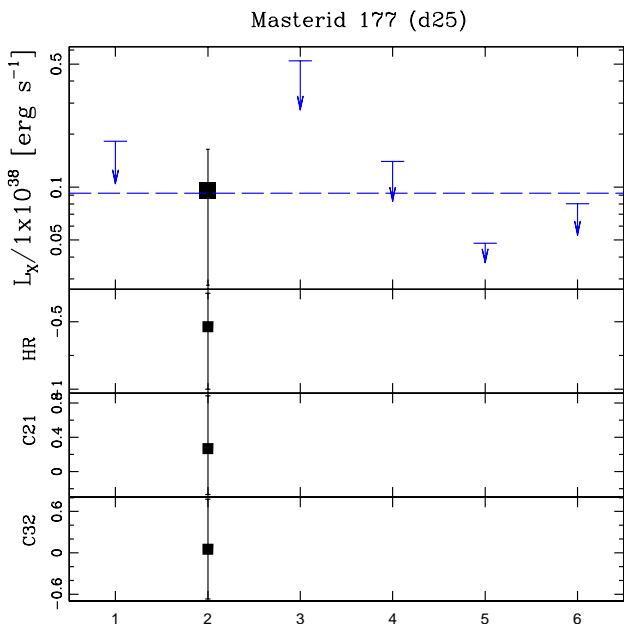
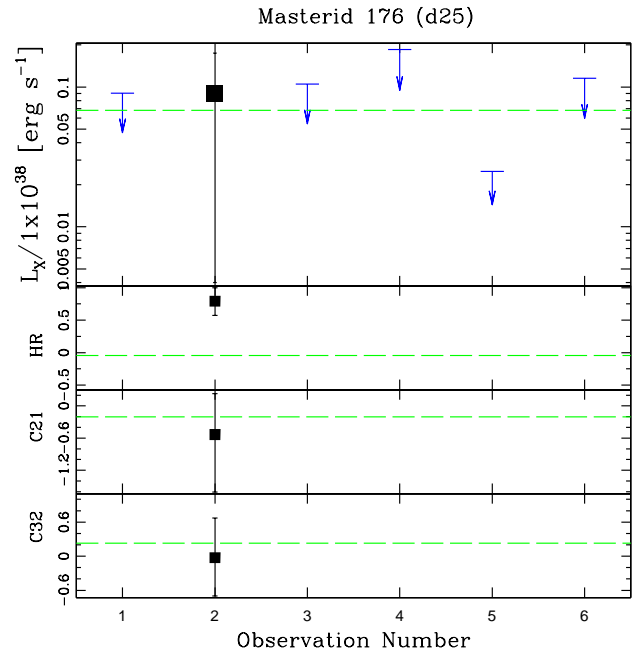
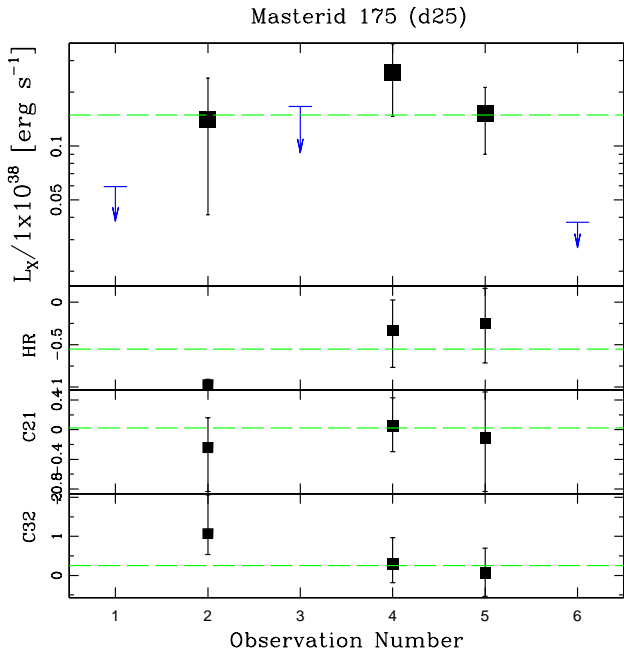
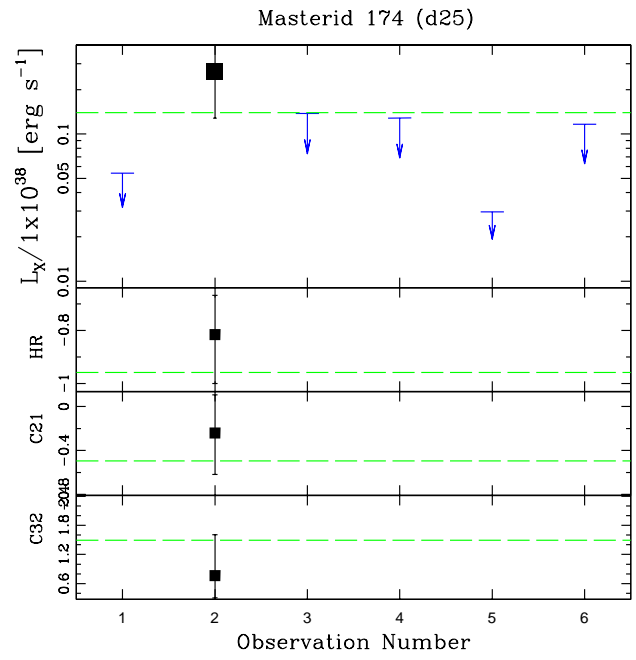
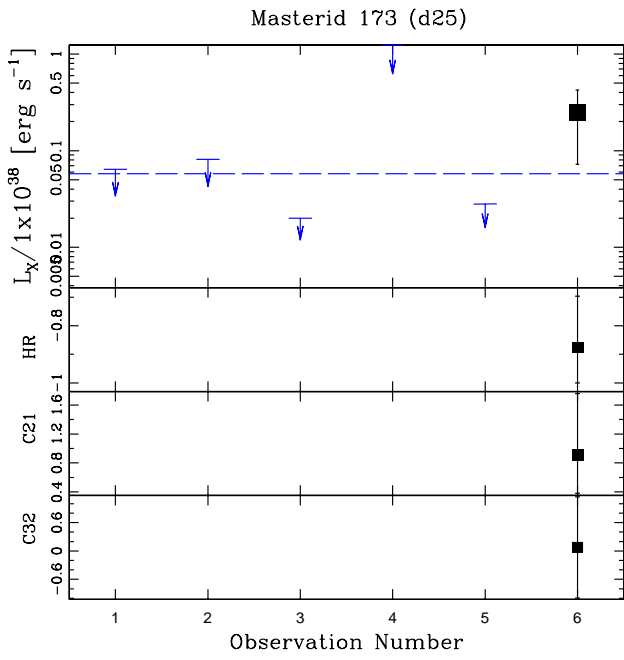


Masterid 171 (d25)

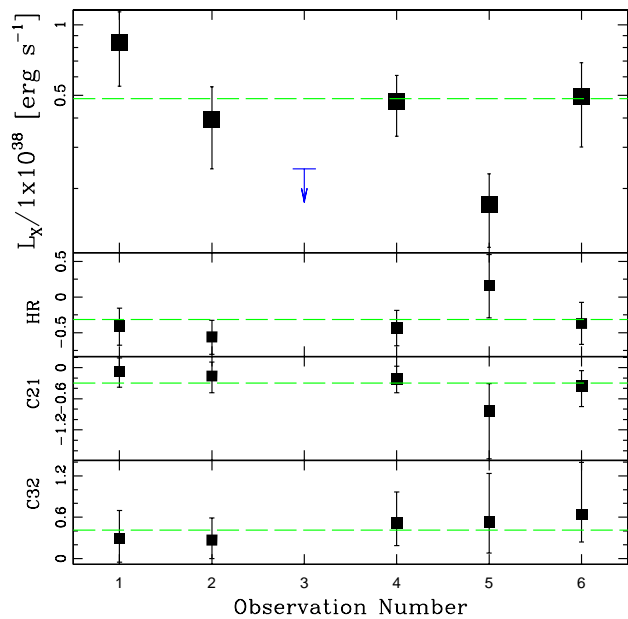


Masterid 172 (d25)

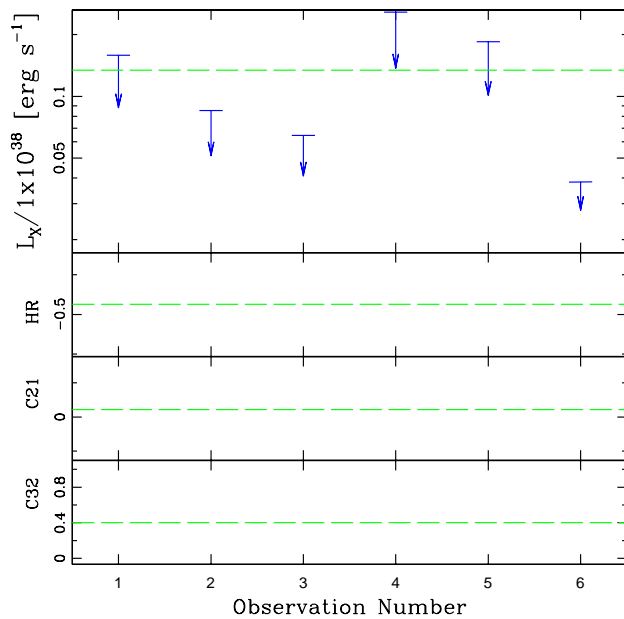




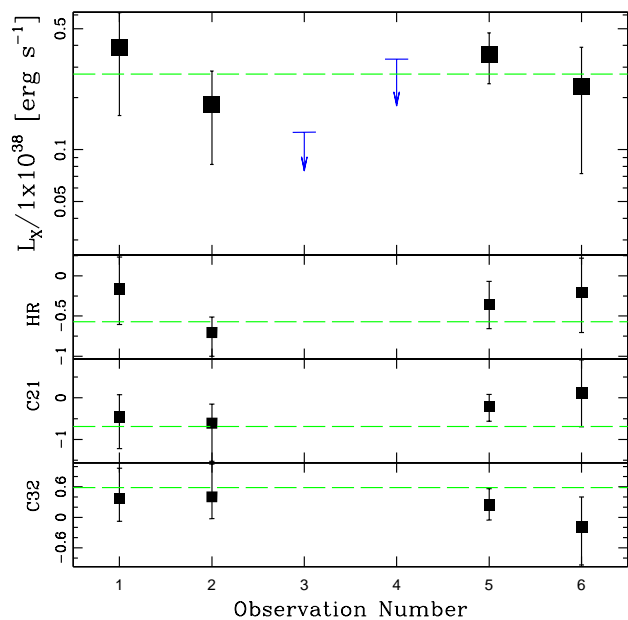
Masterid 179 (d25)



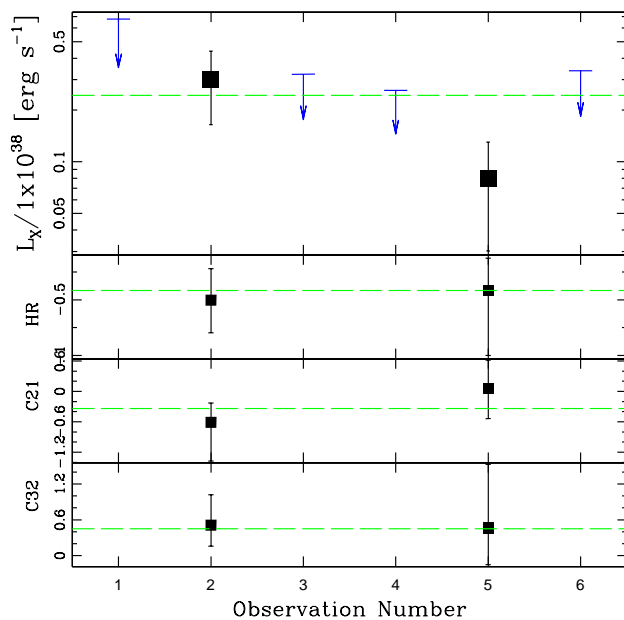
Masterid 180 (d25)



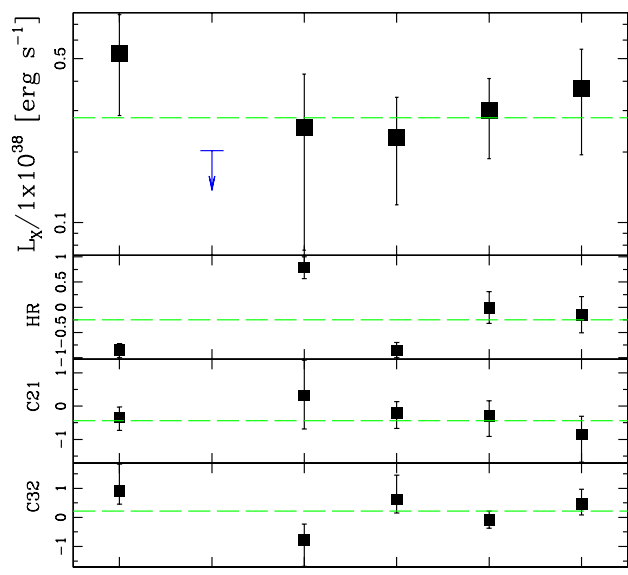
Masterid 181 (d25)



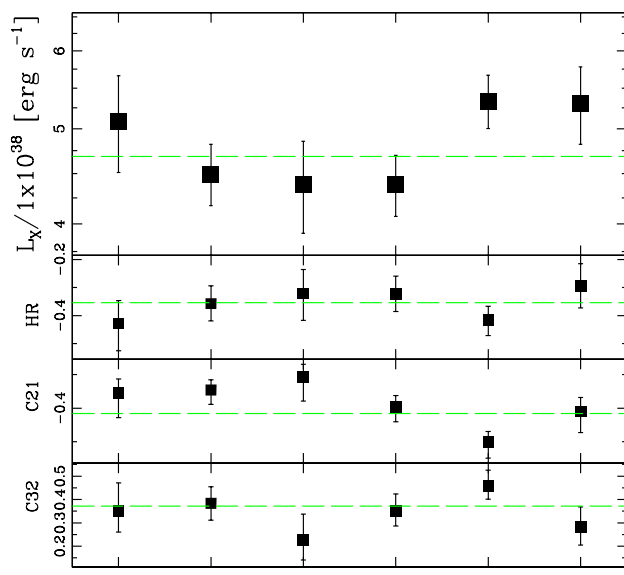
Masterid 182 (d25)



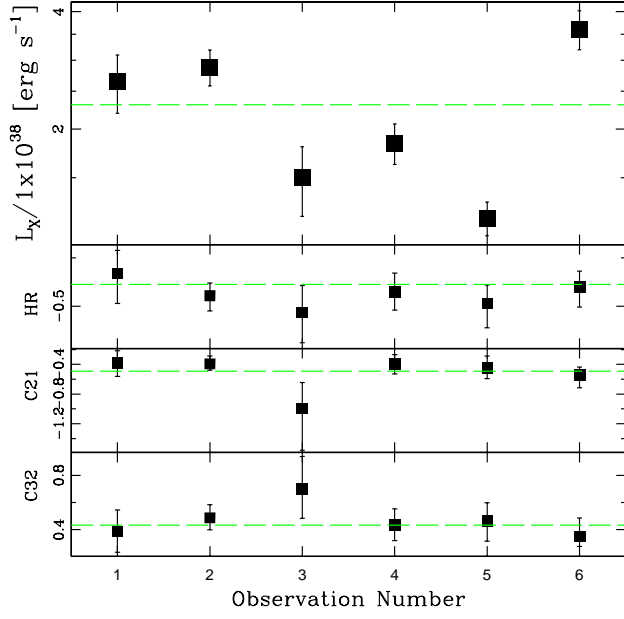
Masterid 183 (all)



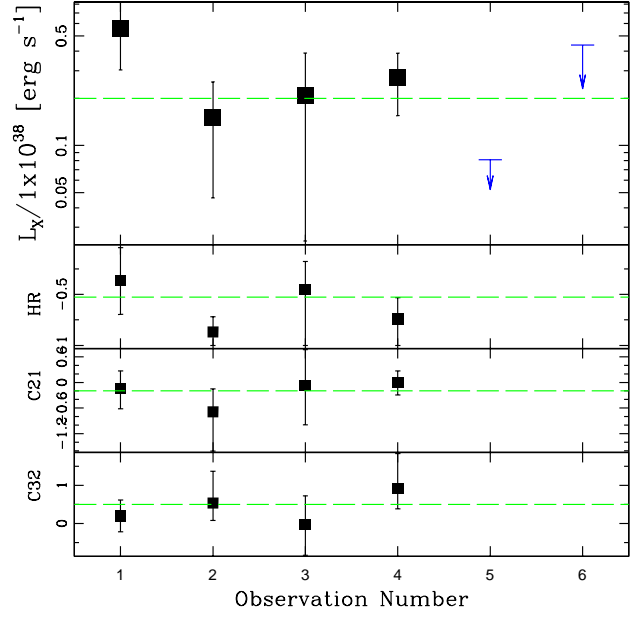
Masterid 184 (d25)



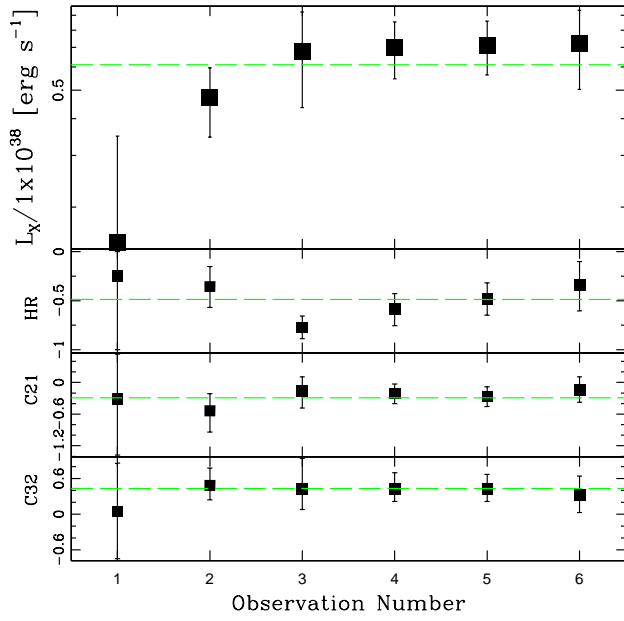
Masterid 185 (d25)



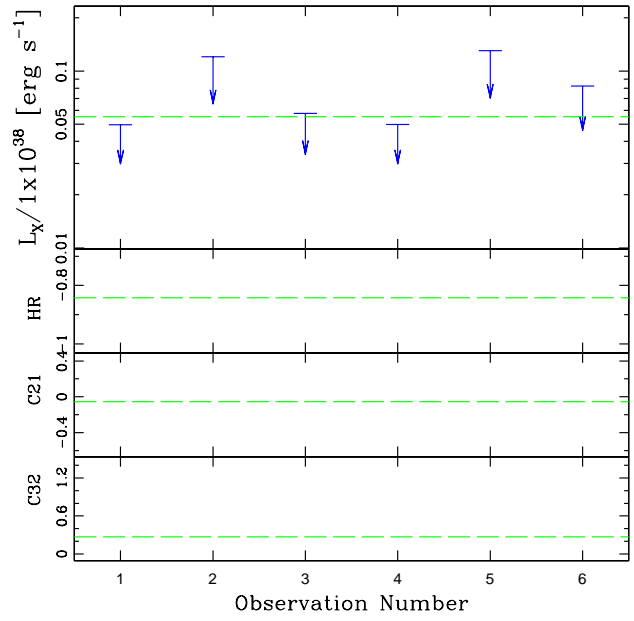
Masterid 186 (d25)



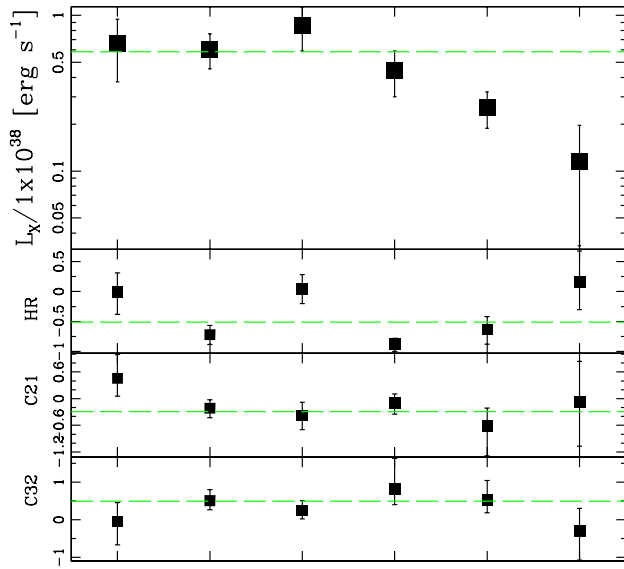
Masterid 187 (d25)



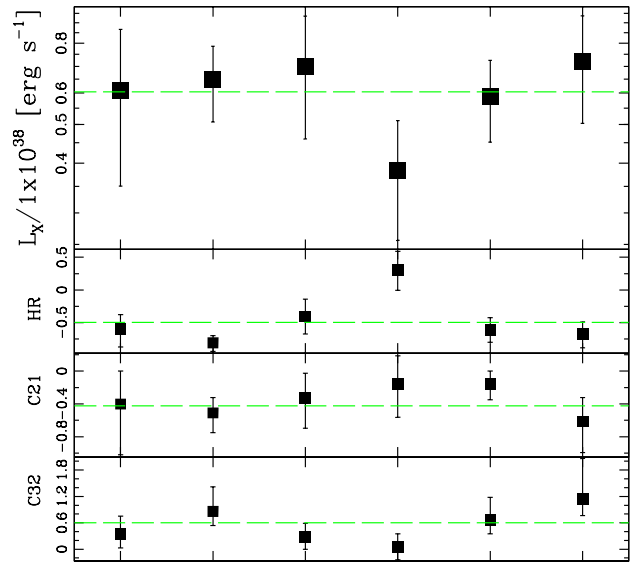
Masterid 188 (d25)



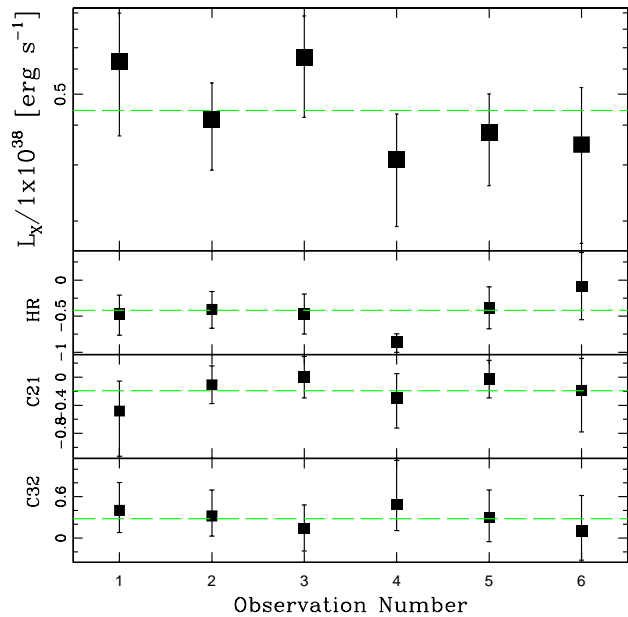
Masterid 189 (d25)



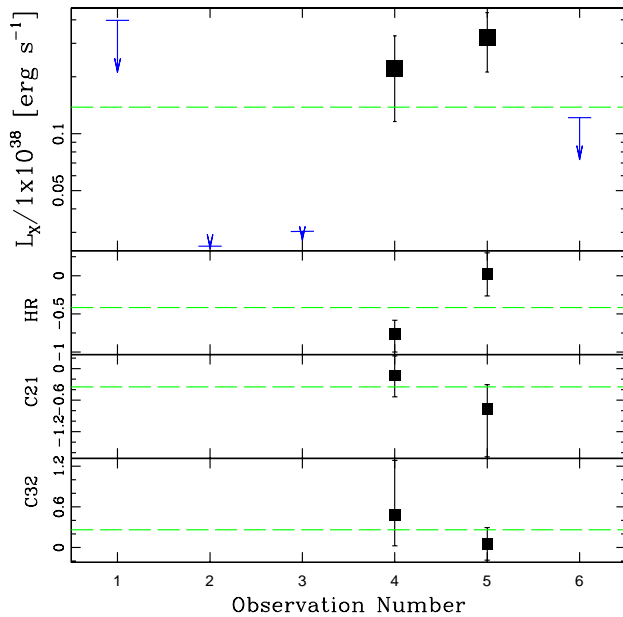
Masterid 190 (d25)



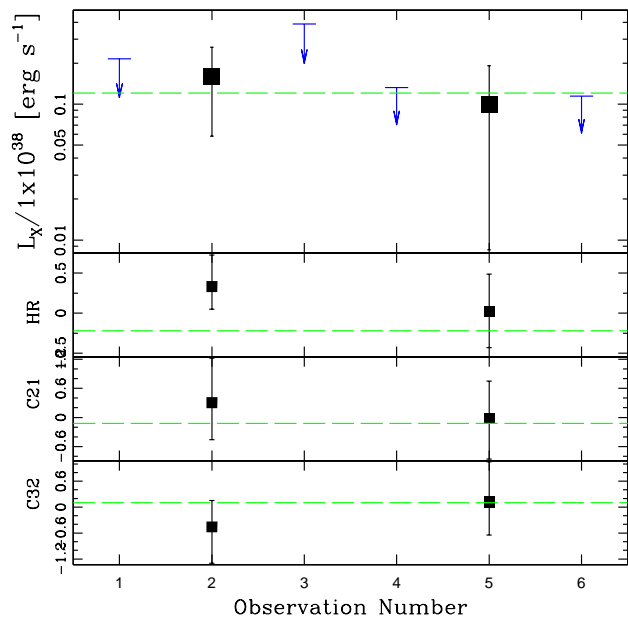
Masterid 191 (d25)



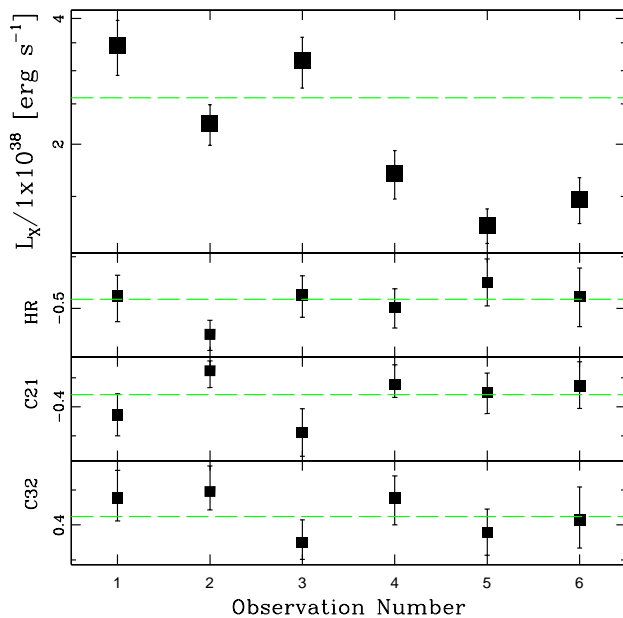
Masterid 192 (d25)



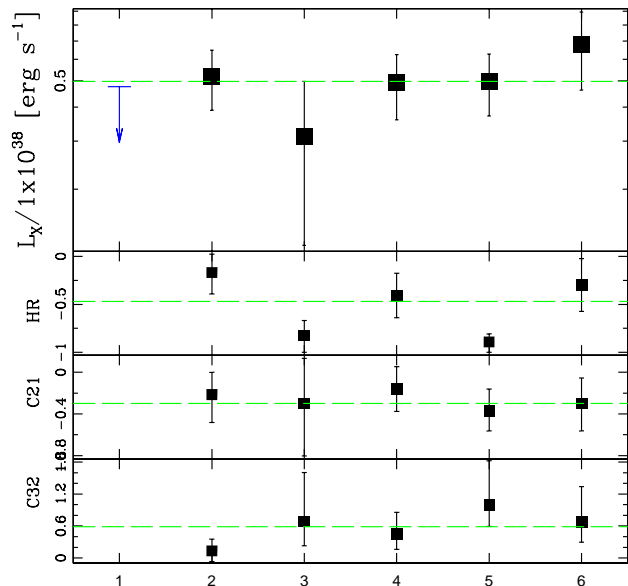
Masterid 193 (d25)



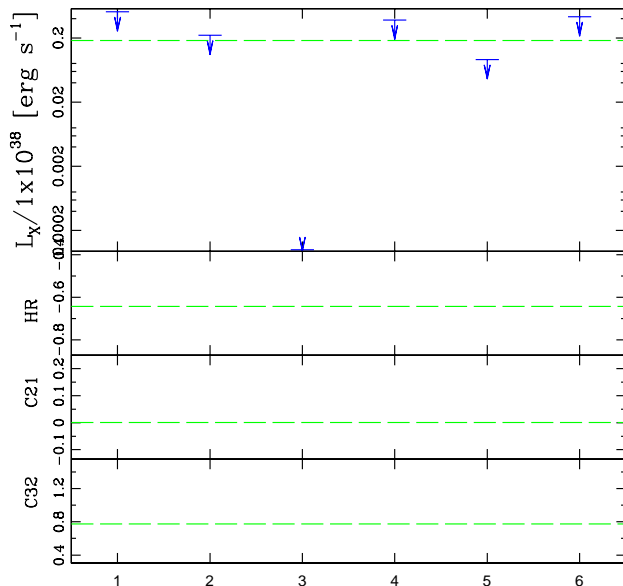
Masterid 194 (d25)



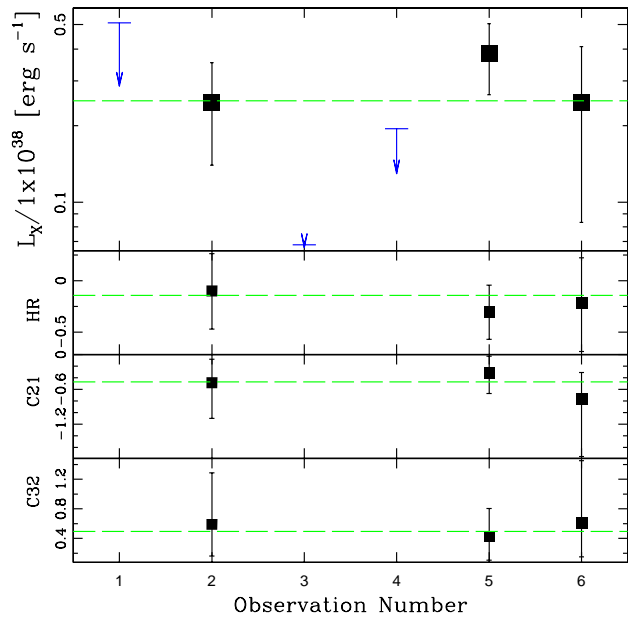
Masterid 195 (d25)



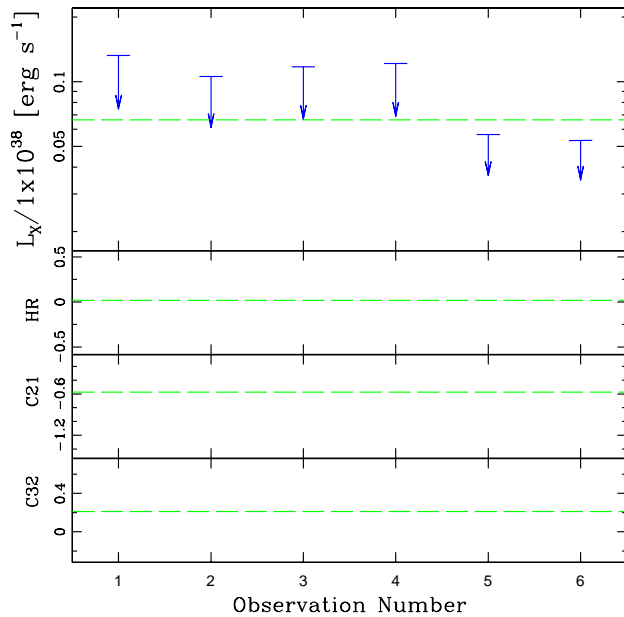
Masterid 196 (all)



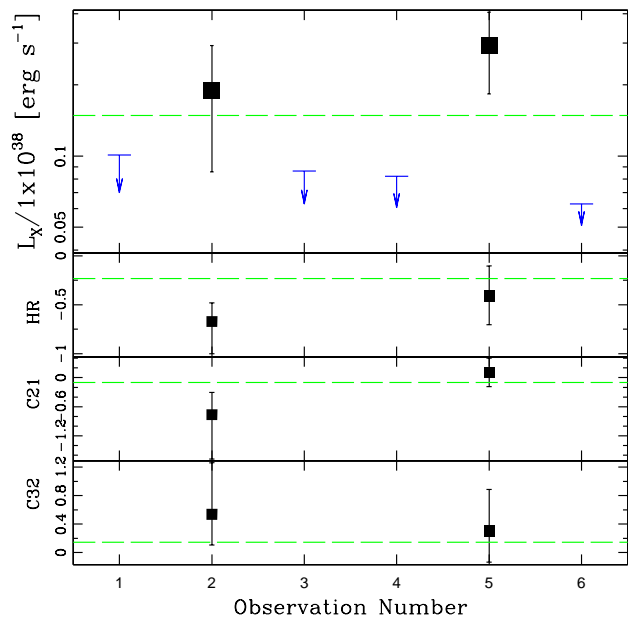
Masterid 197 (d25)



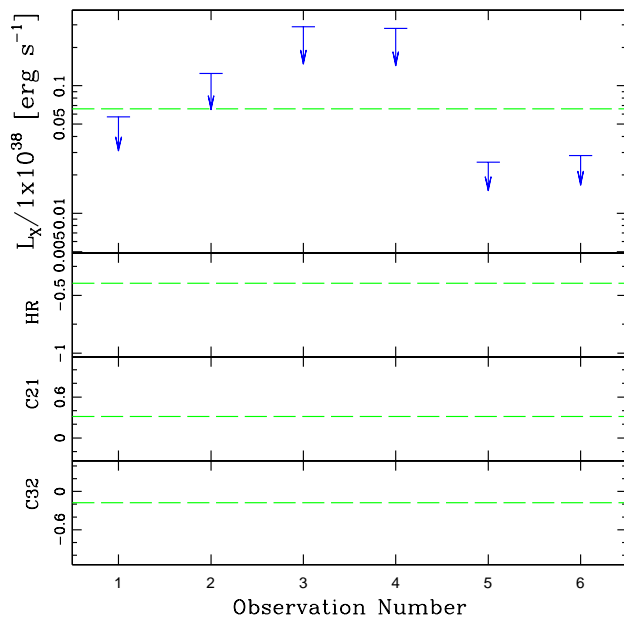
Masterid 198 (d25)



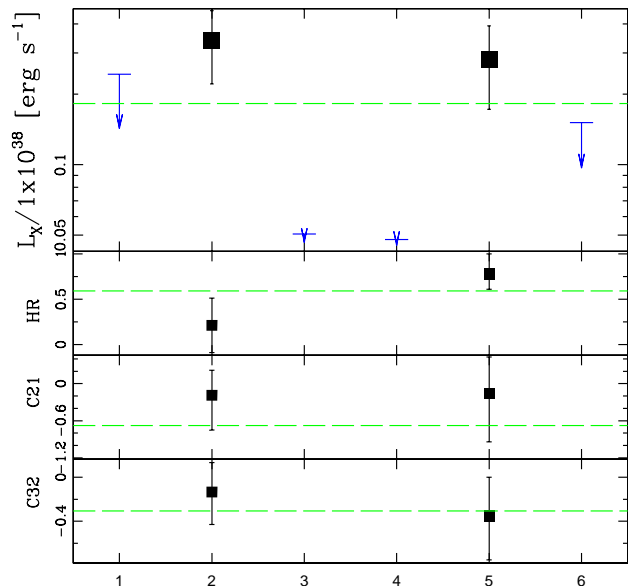
Masterid 199 (d25)



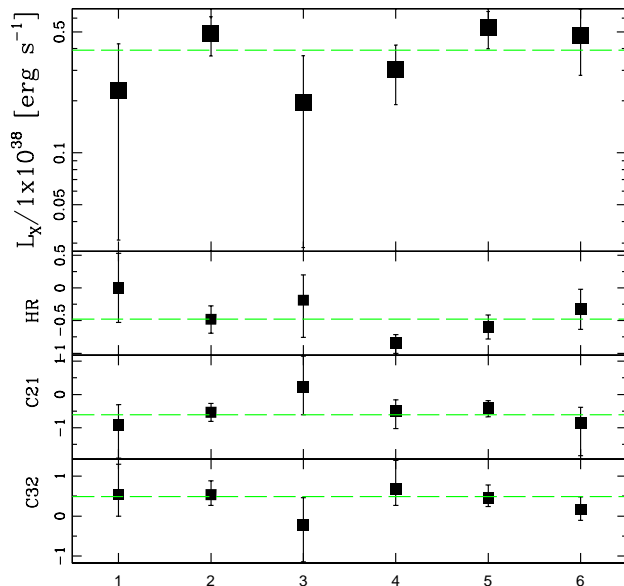
Masterid 200 (d25)



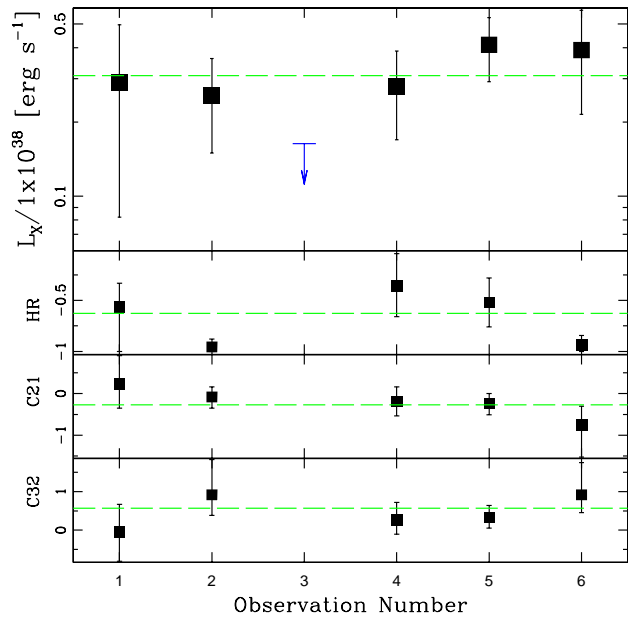
Masterid 201 (d25)



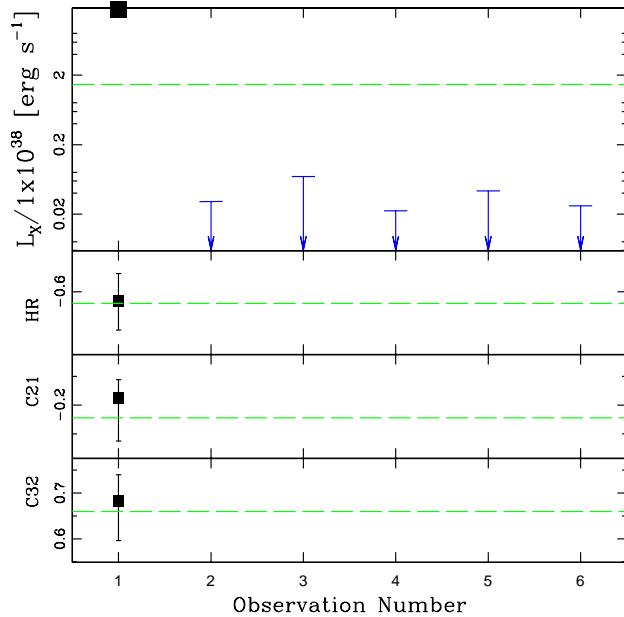
Masterid 202 (d25)



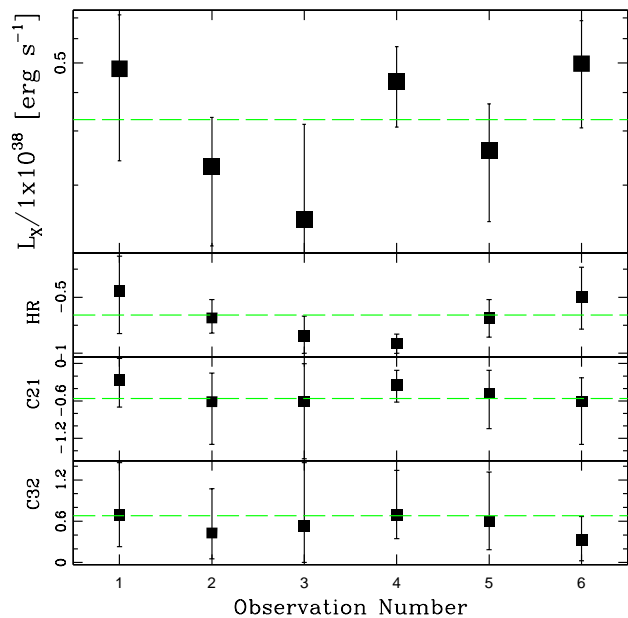
Masterid 203 (d25)



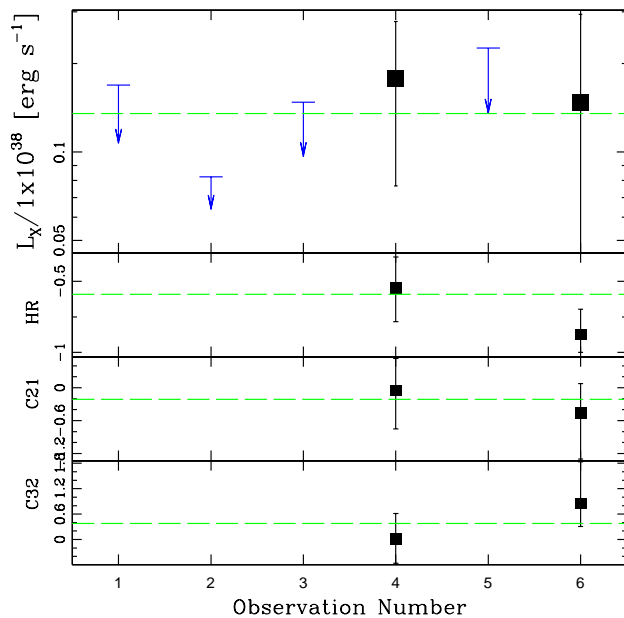
Masterid 204 (d25)



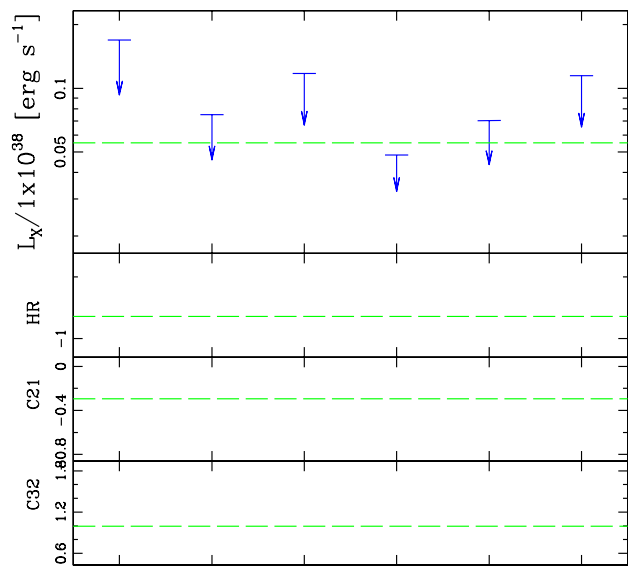
Masterid 205 (d25)



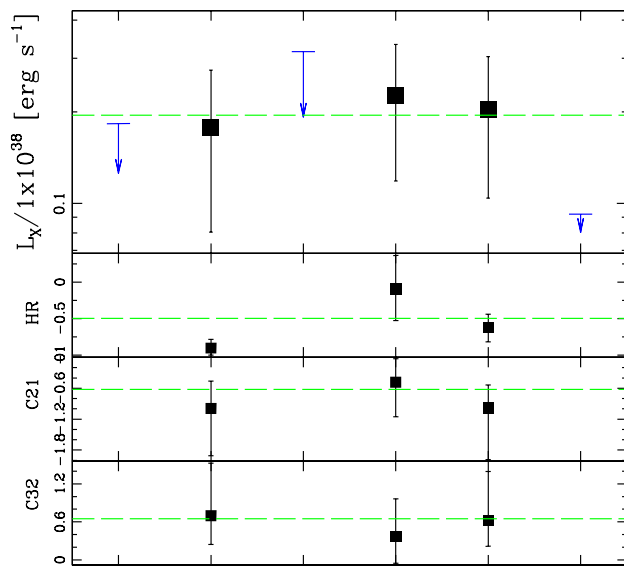
Masterid 206 (d25)

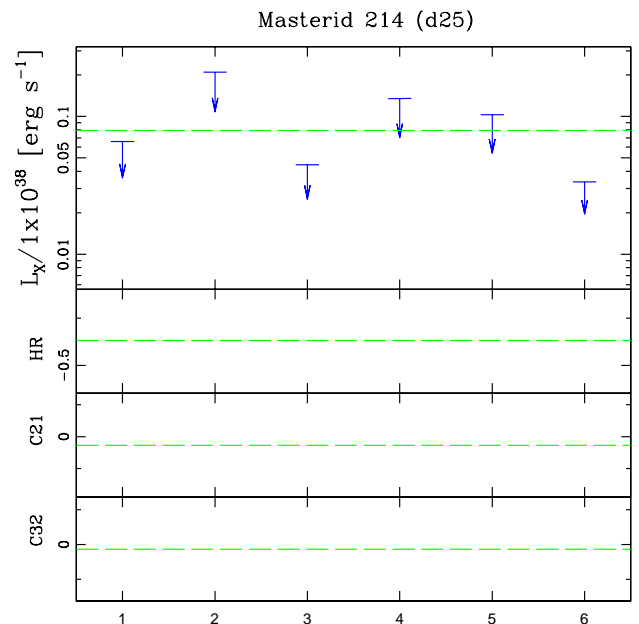
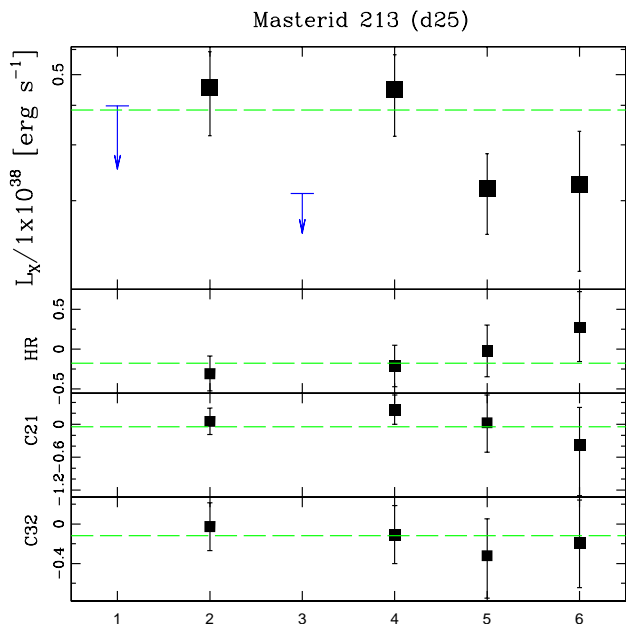
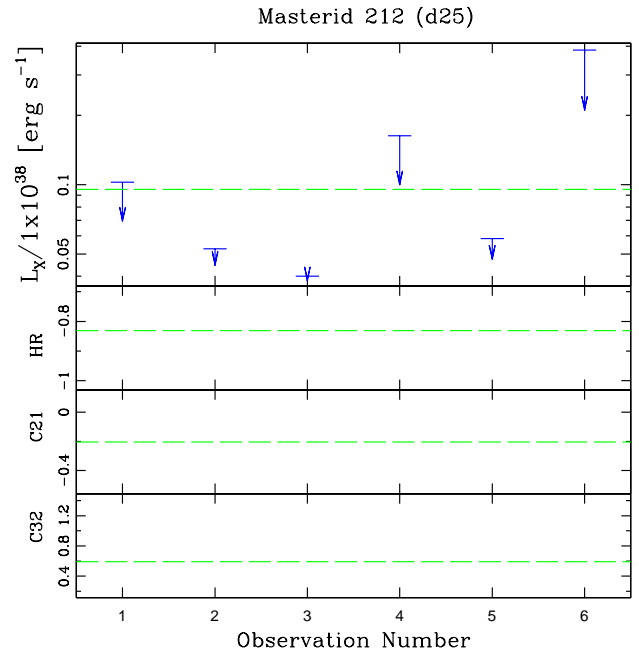
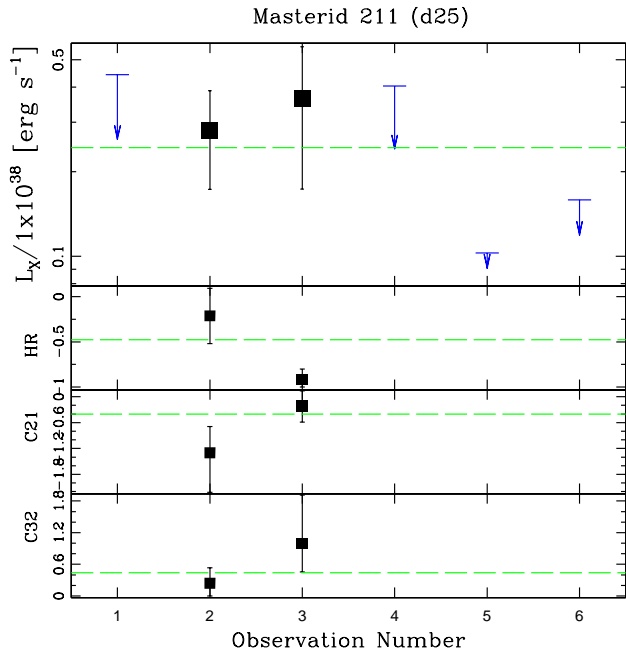
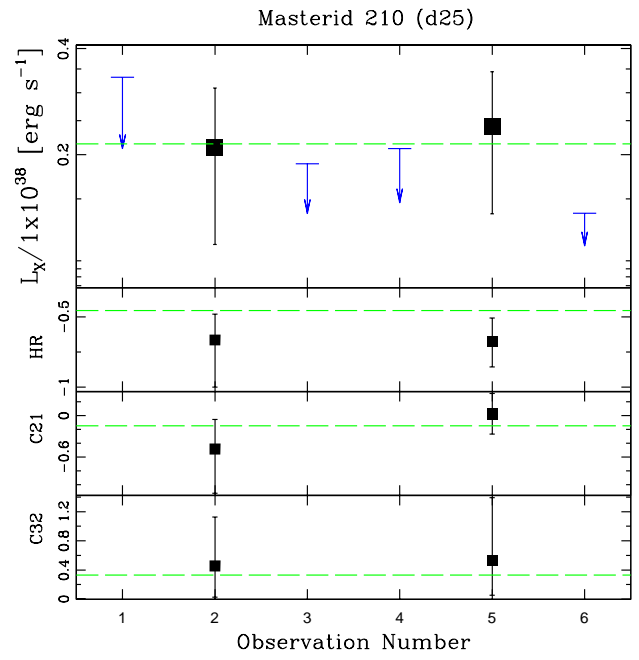
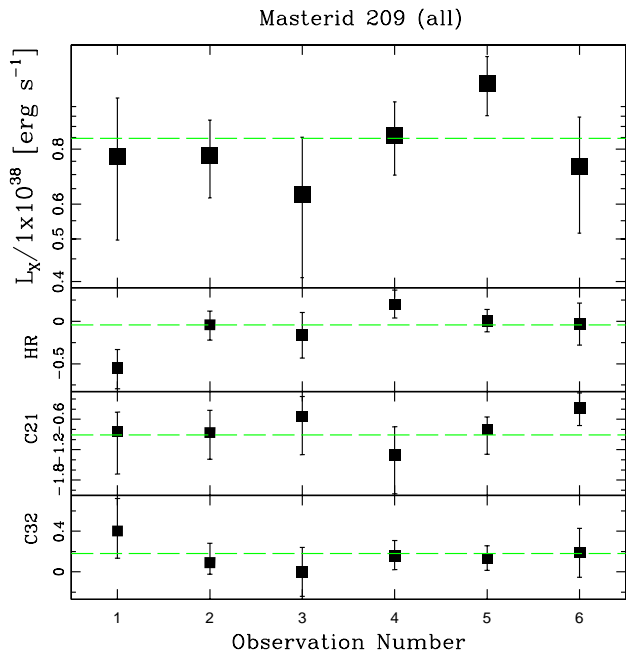


Masterid 207 (d25)

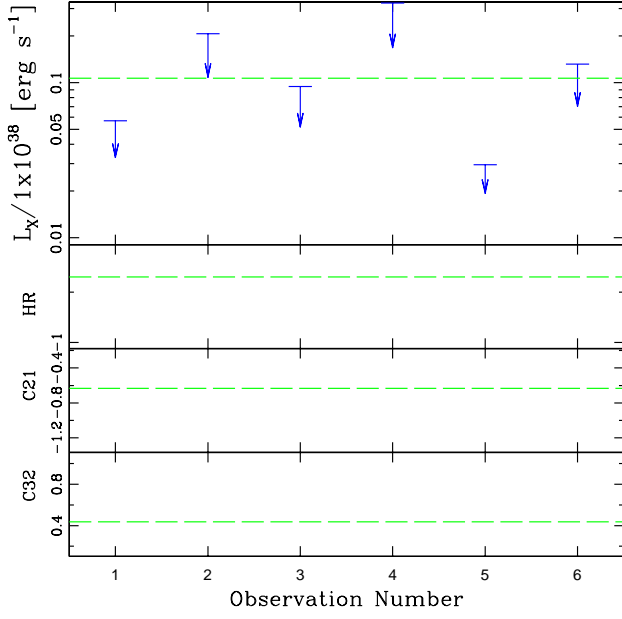


Masterid 208 (d25)

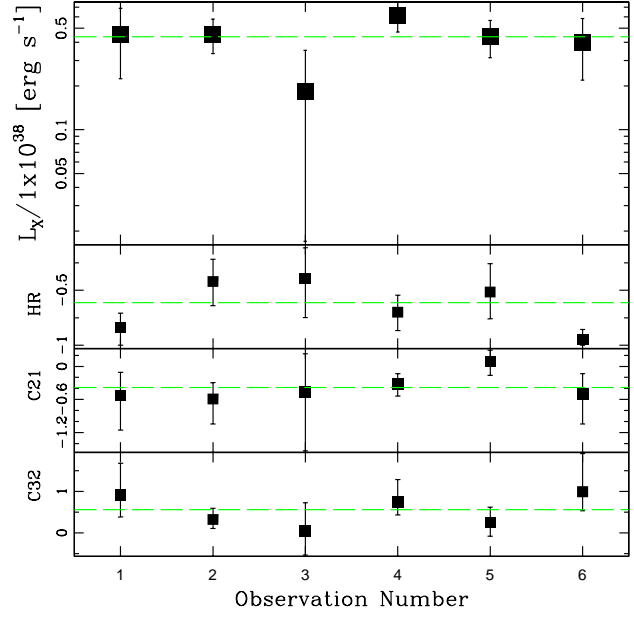




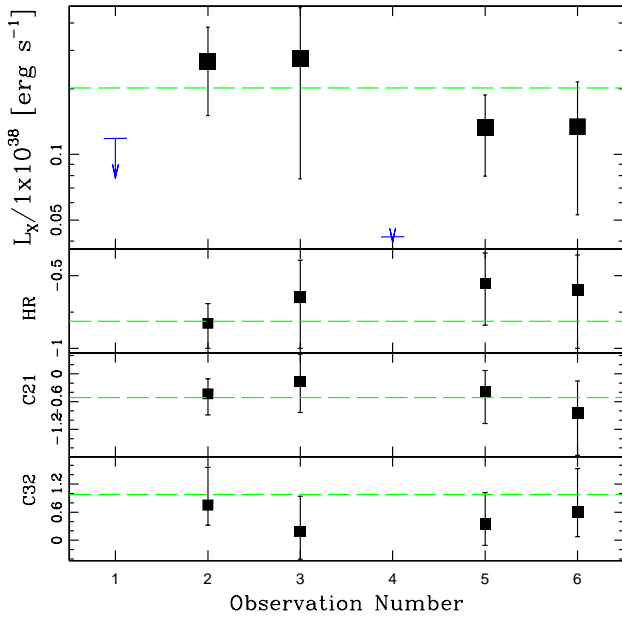
Masterid 215 (d25)



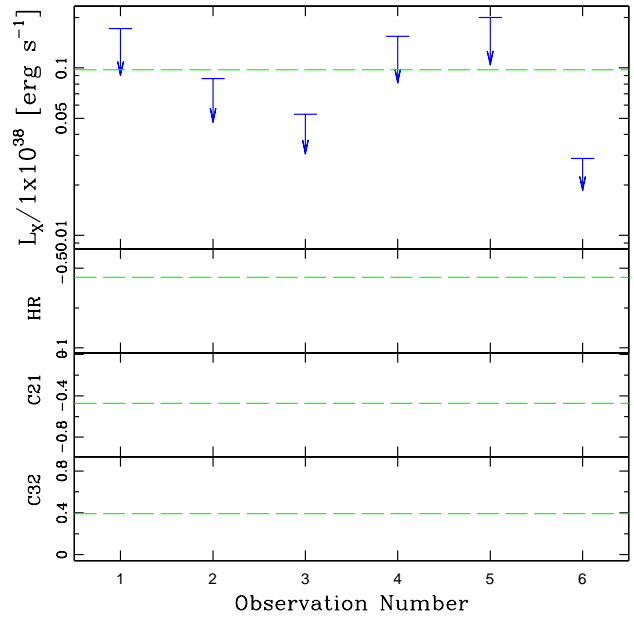
Masterid 216 (d25)



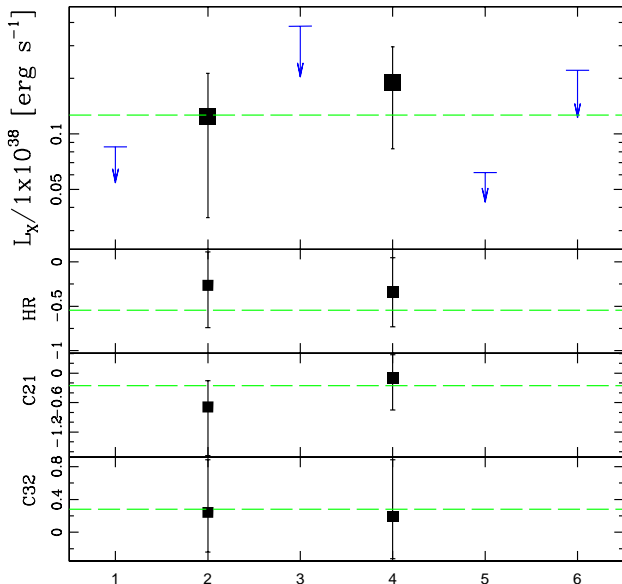
Masterid 217 (all)



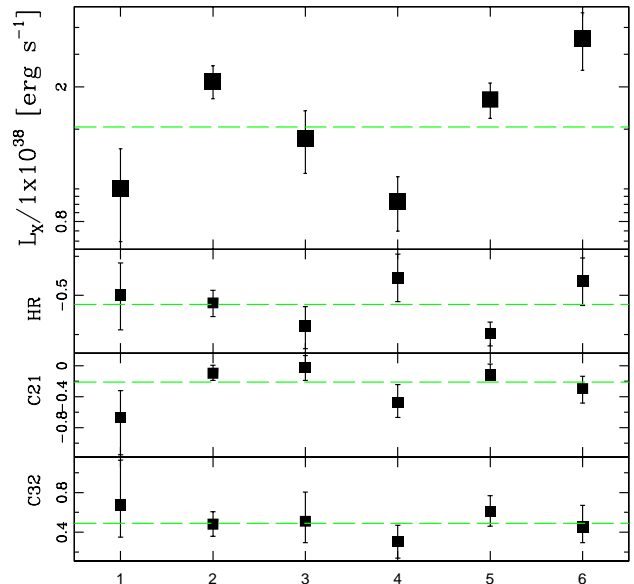
Masterid 218 (d25)



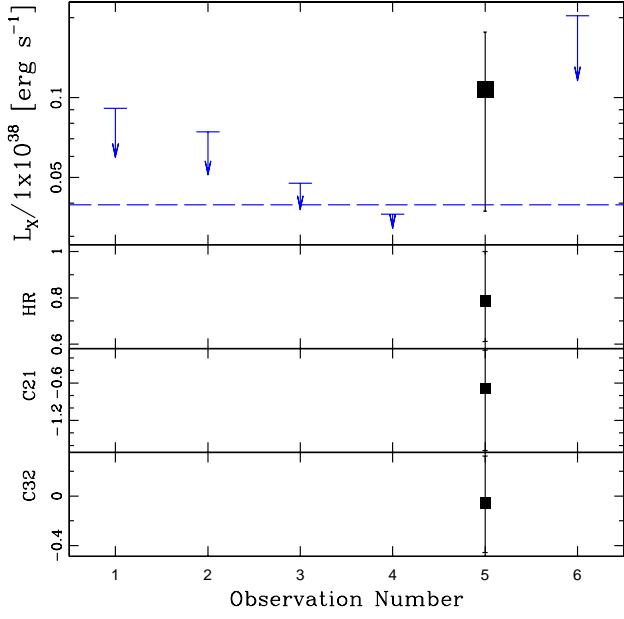
Masterid 219 (d25)



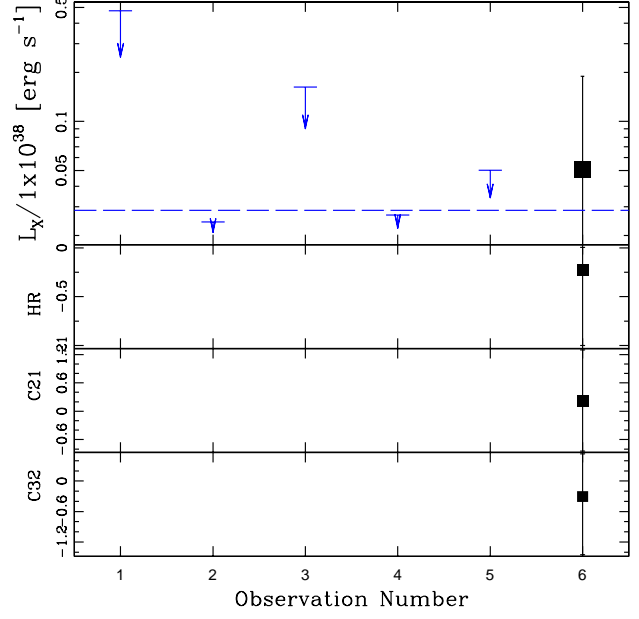
Masterid 220 (all)



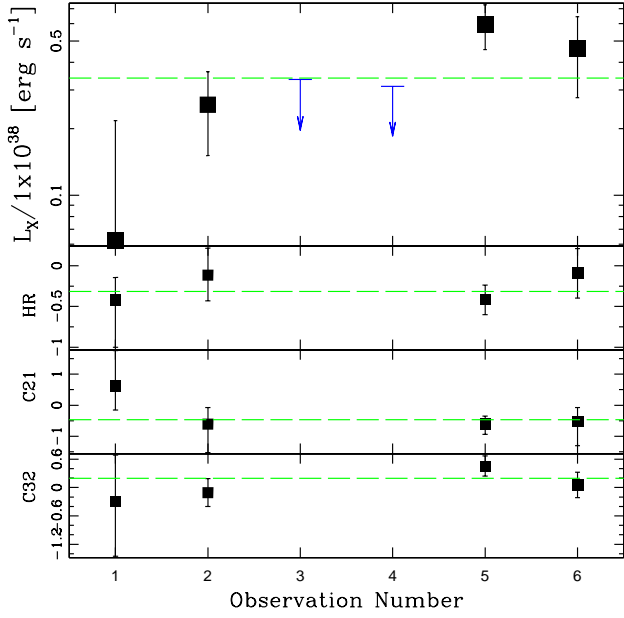
Masterid 221 (all)



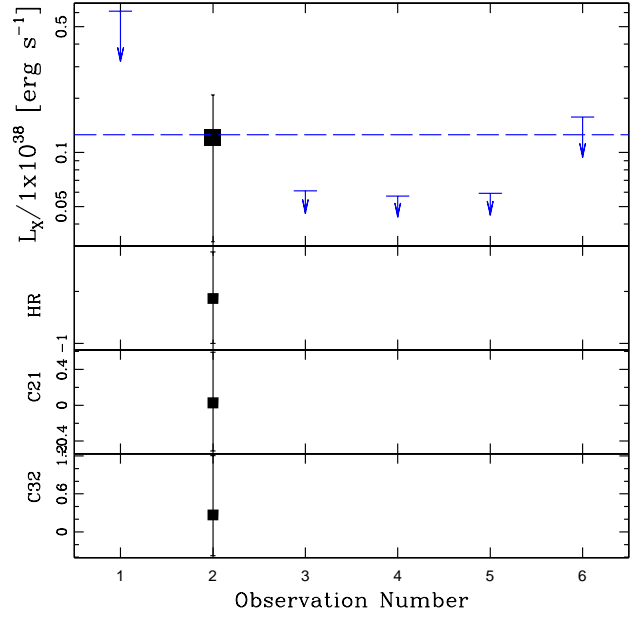
Masterid 222 (all)



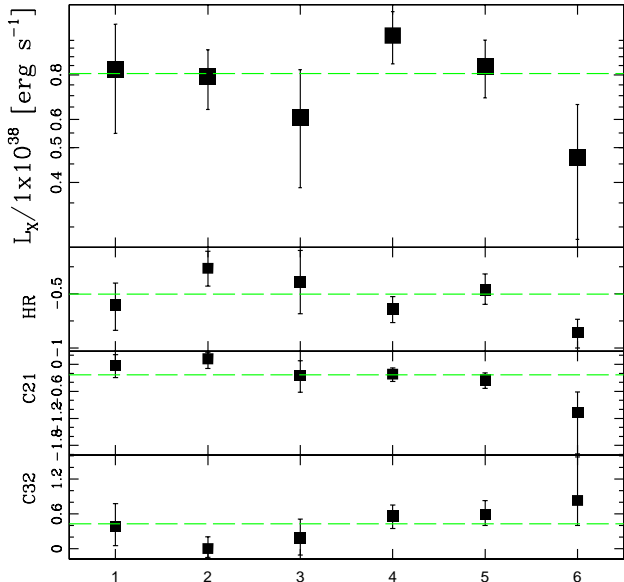
Masterid 223 (all)



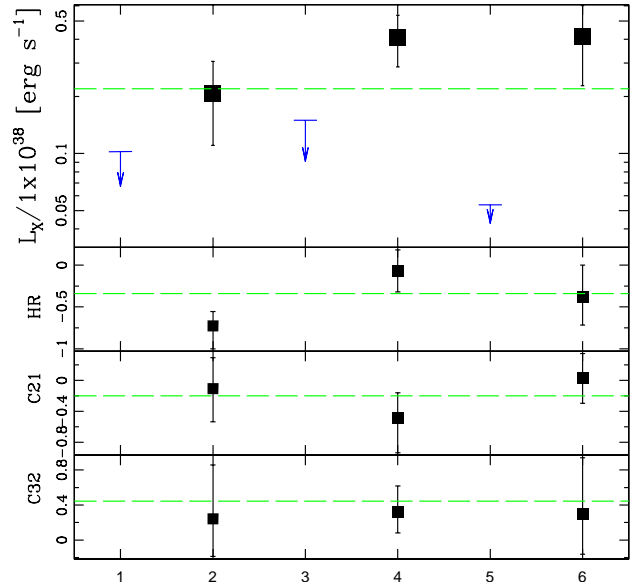
Masterid 224 (d25)



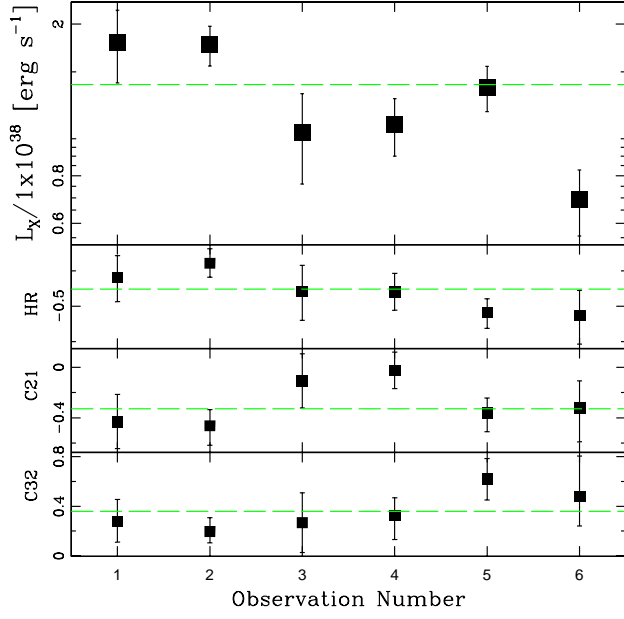
Masterid 225 (d25)



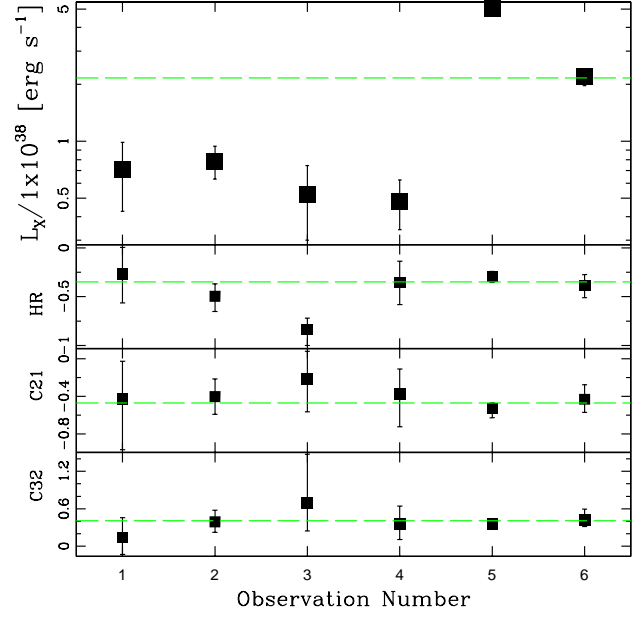
Masterid 226 (all)



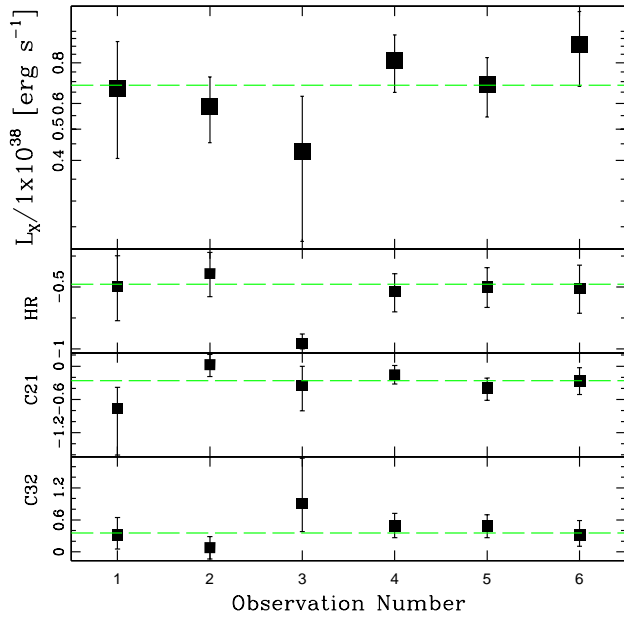
Masterid 227 (all)



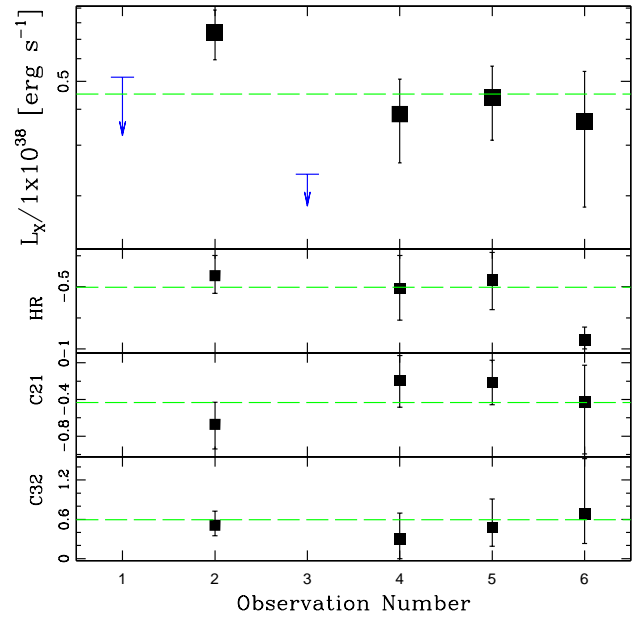
Masterid 228 (all)



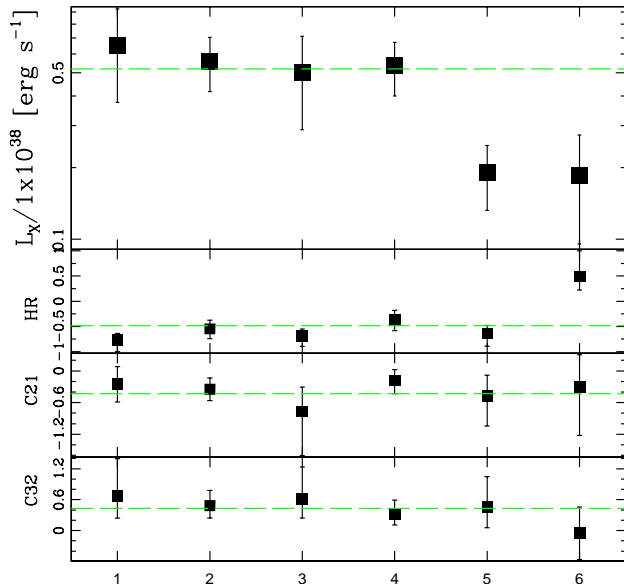
Masterid 229 (all)



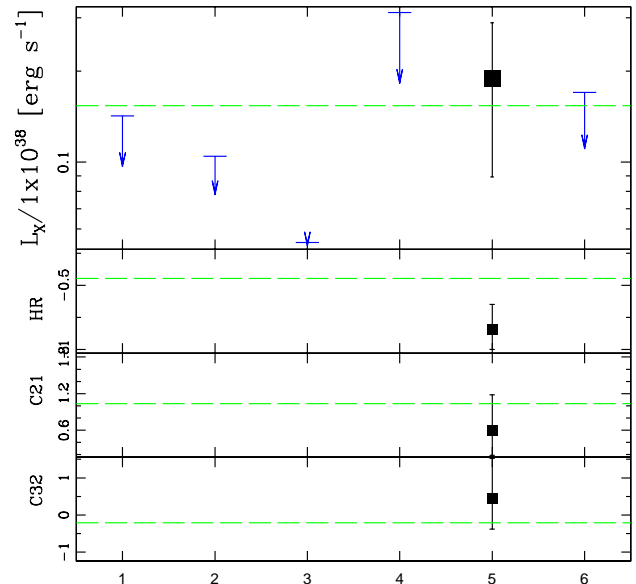
Masterid 230 (all)



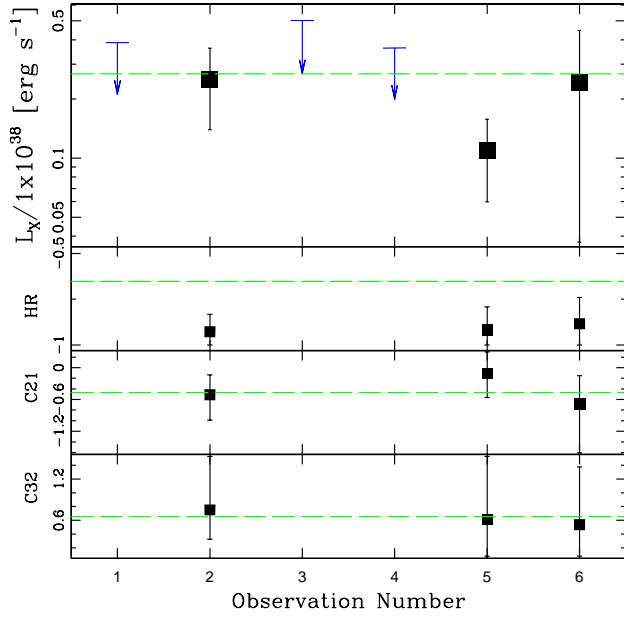
Masterid 231 (all)



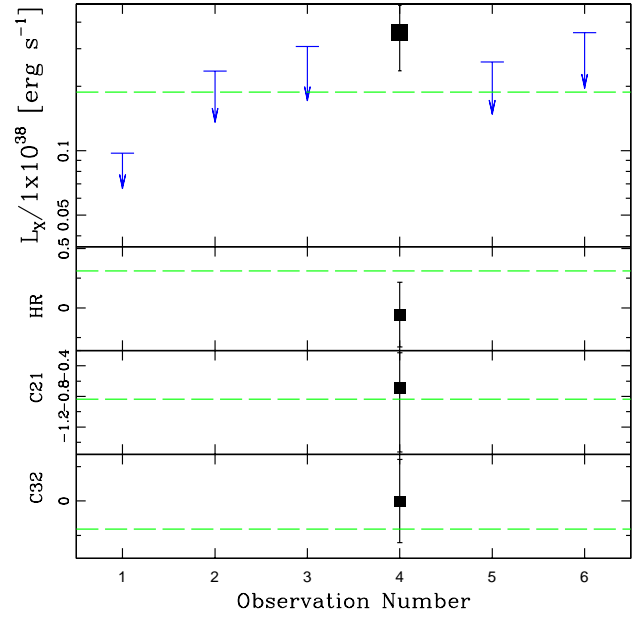
Masterid 232 (all)



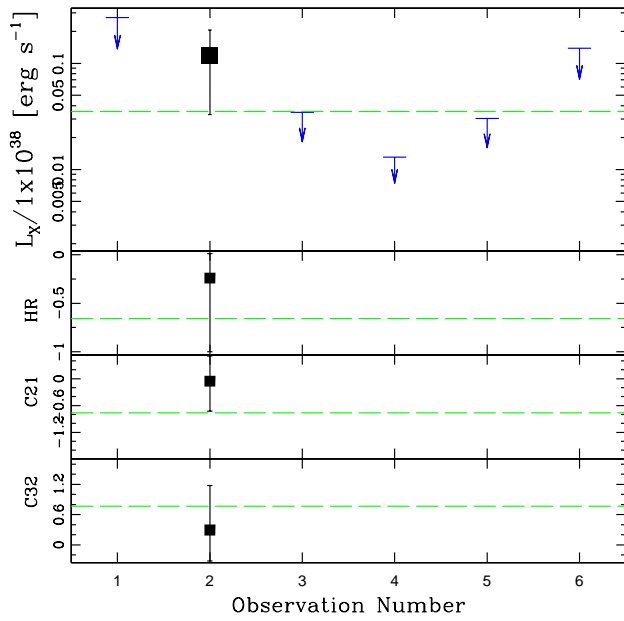
Masterid 233 (all)



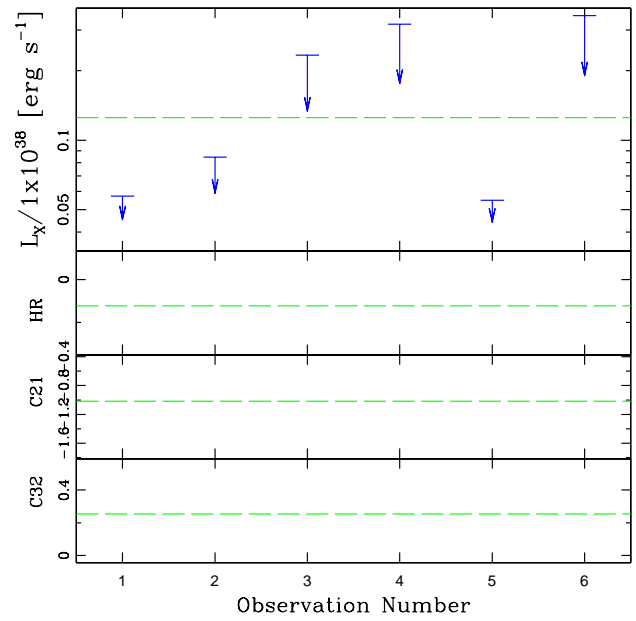
Masterid 234 (all)



Masterid 235 (all)



Masterid 236 (all)



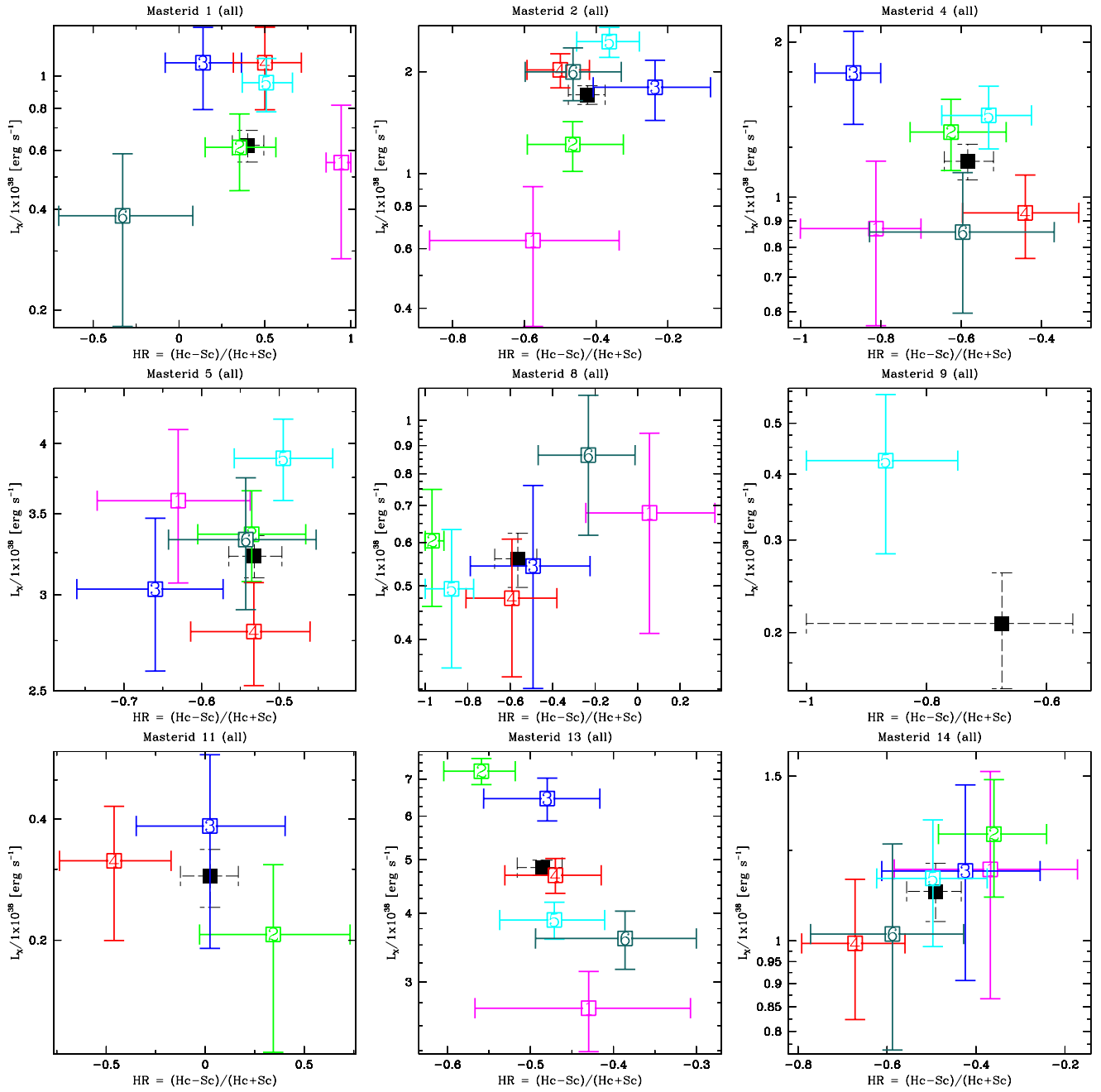
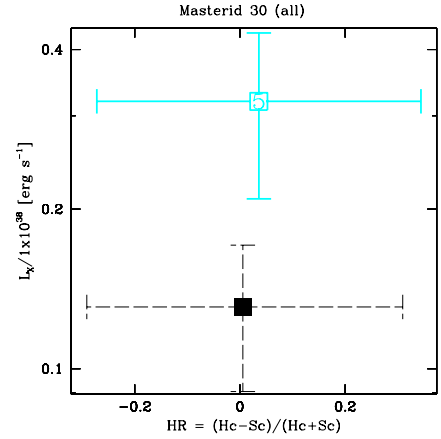
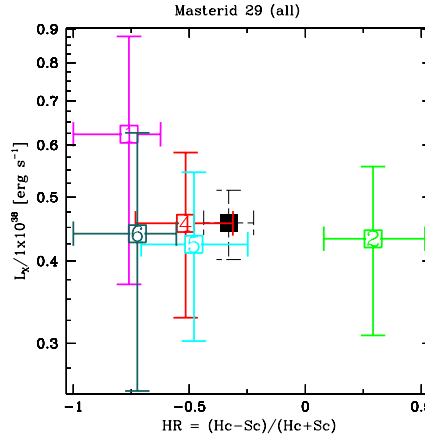
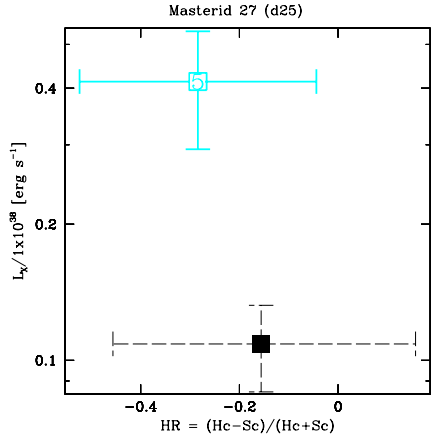
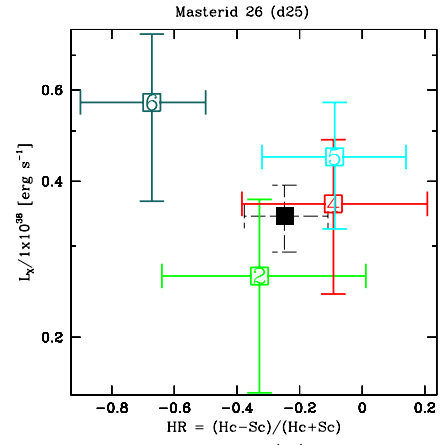
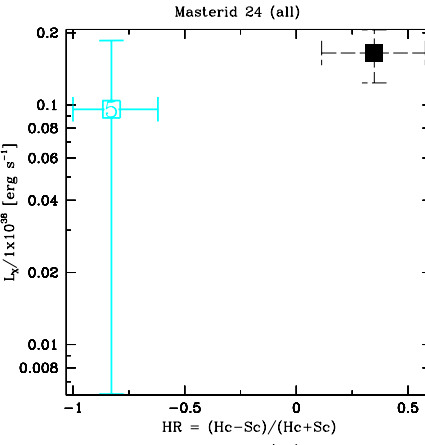
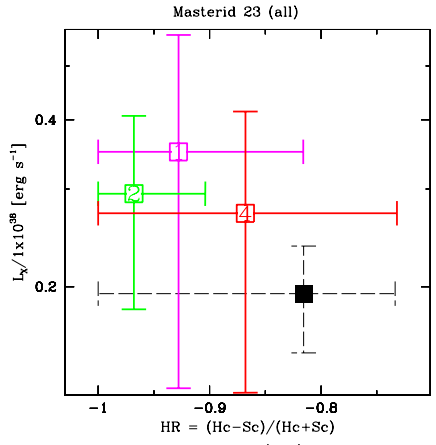
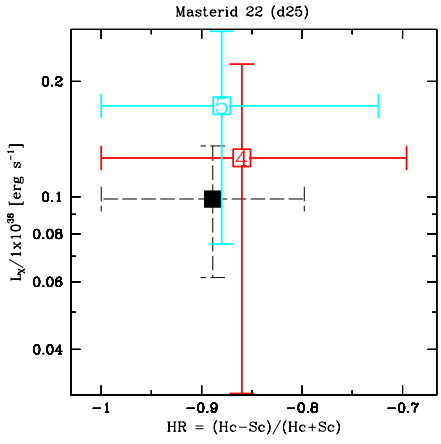
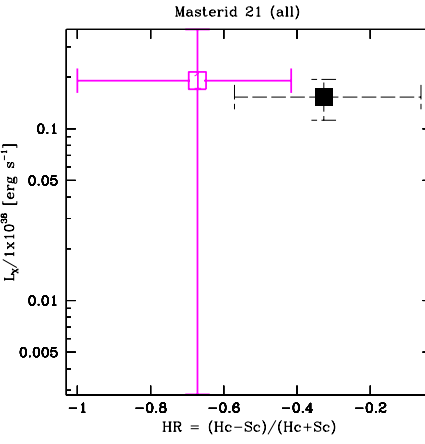
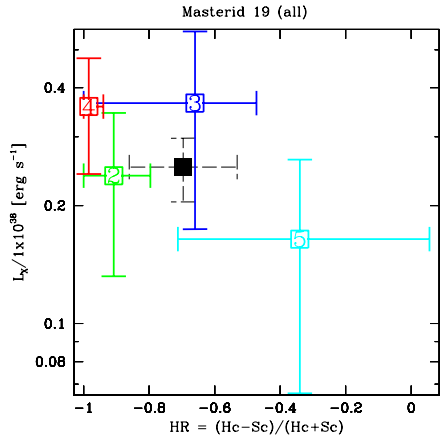
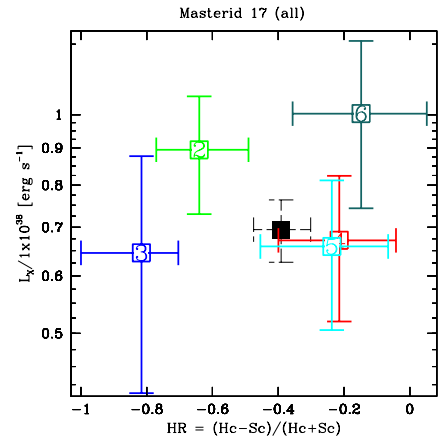
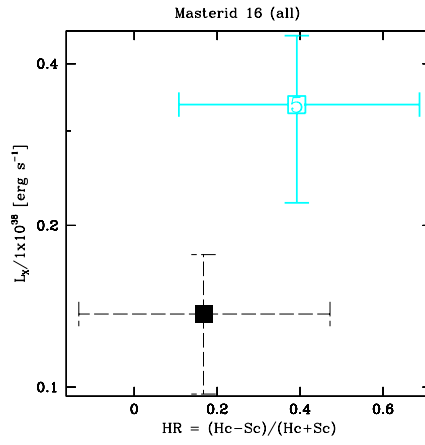
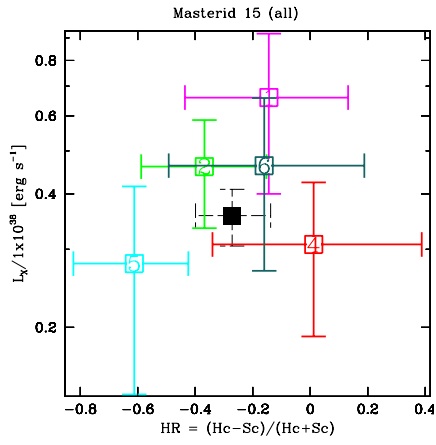
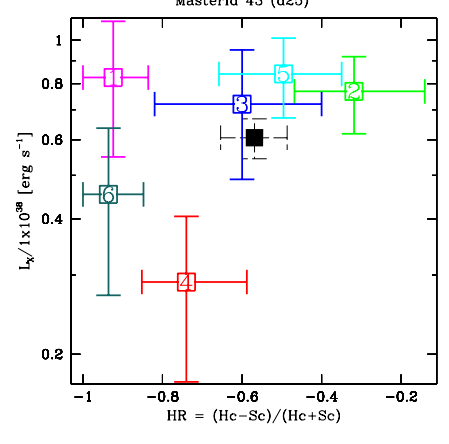
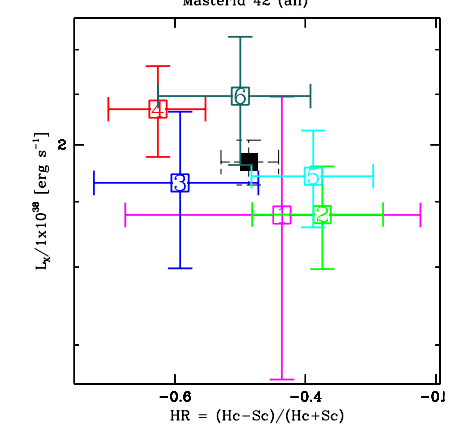
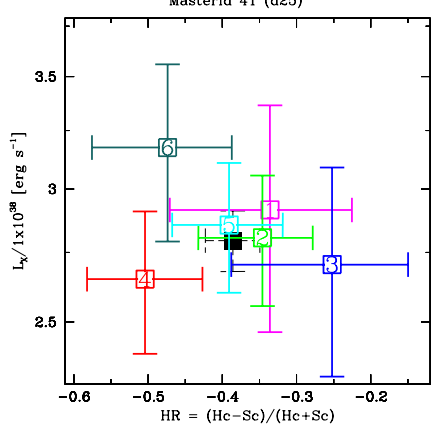
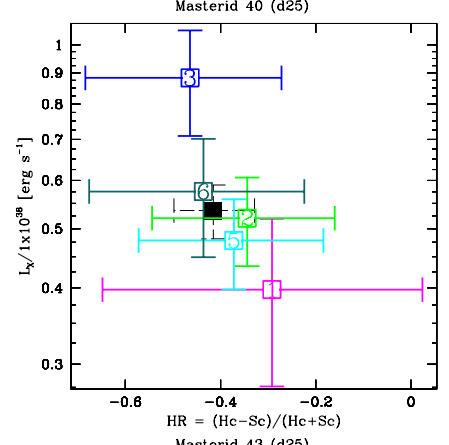
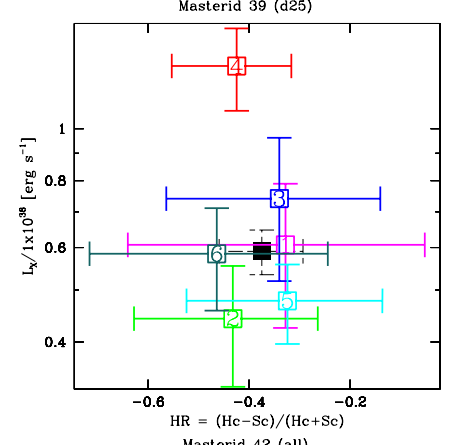
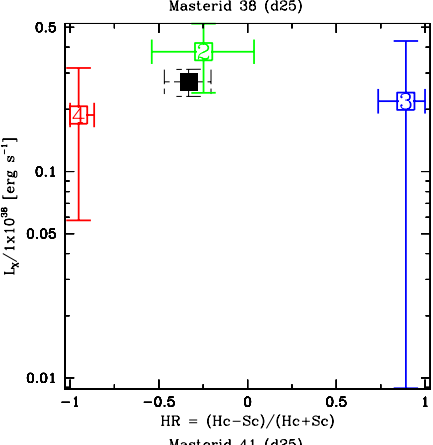
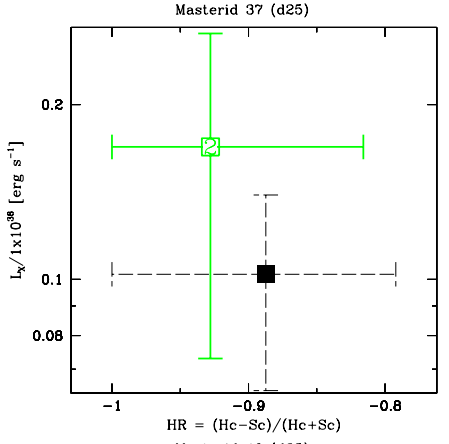
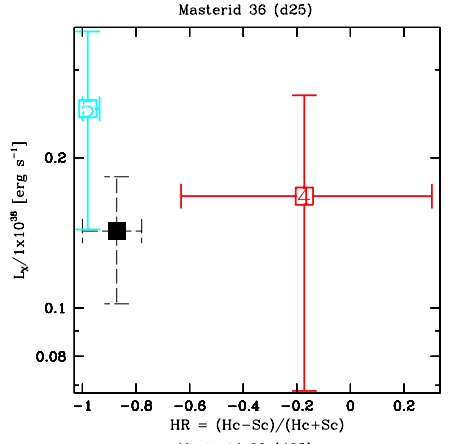
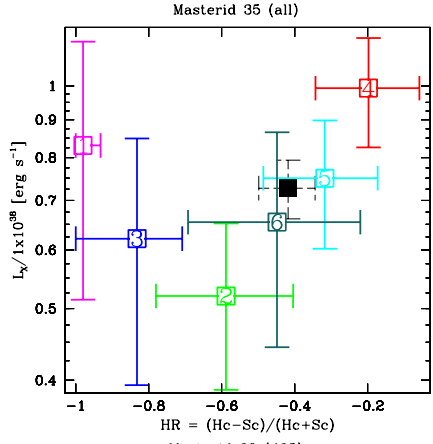
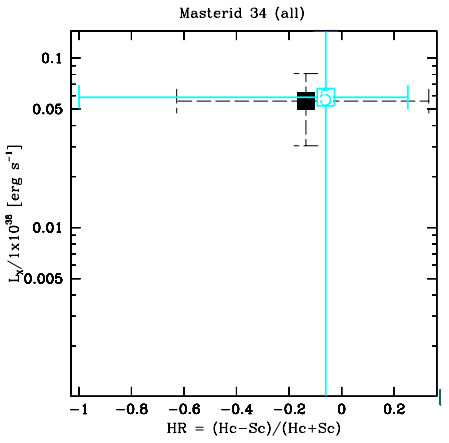
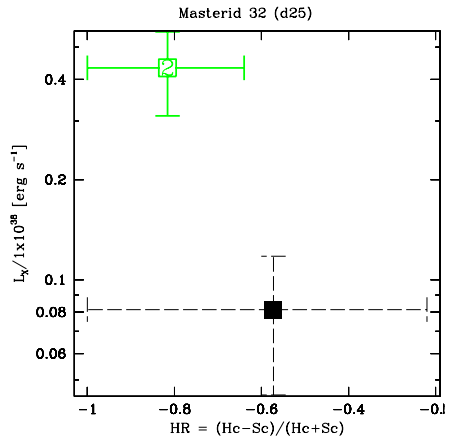
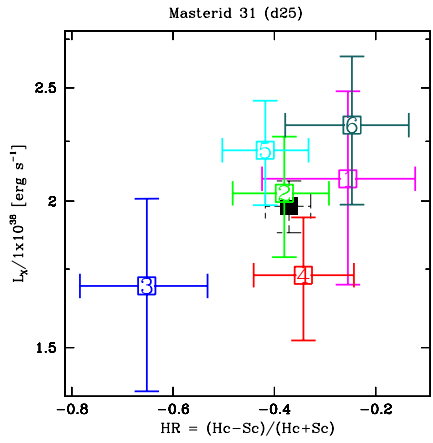
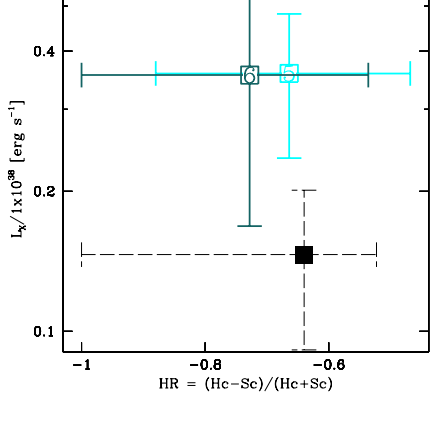
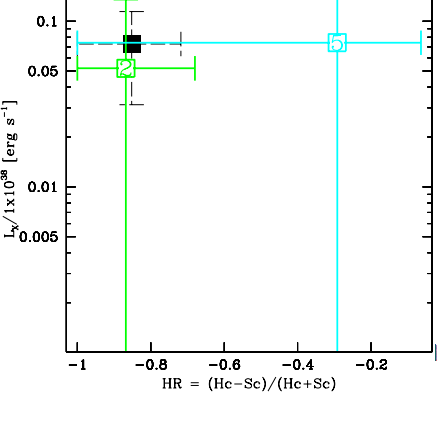
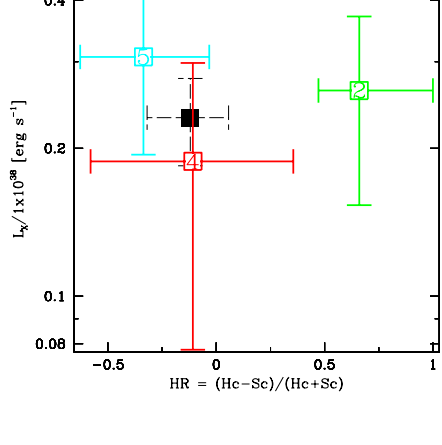
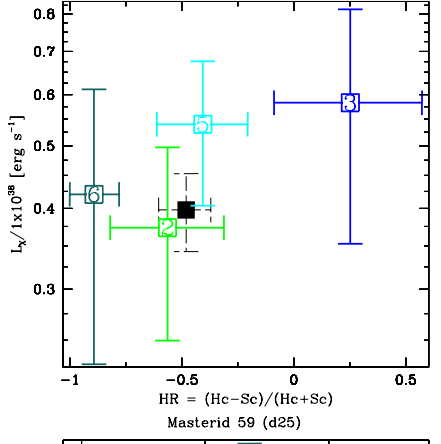
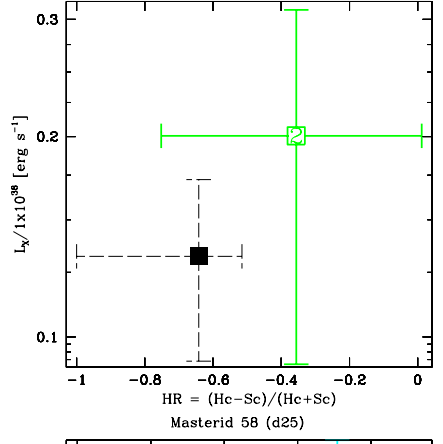
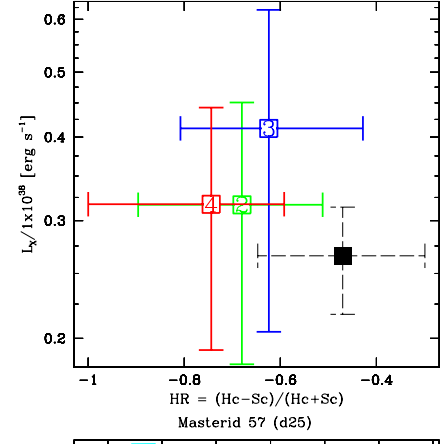
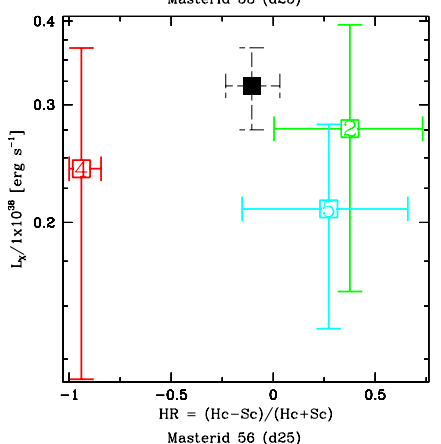
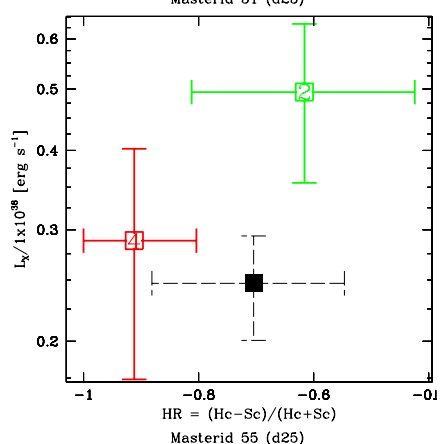
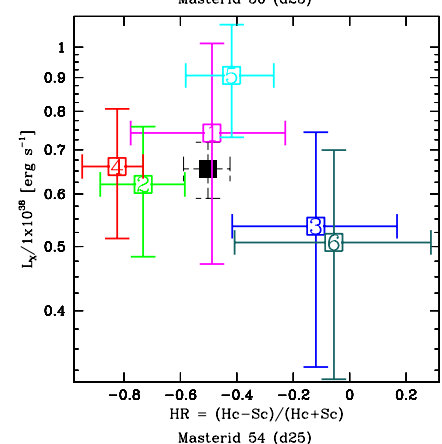
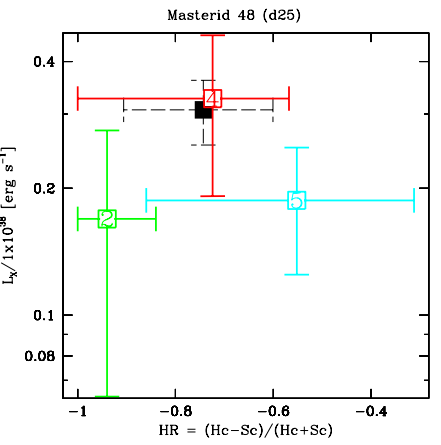
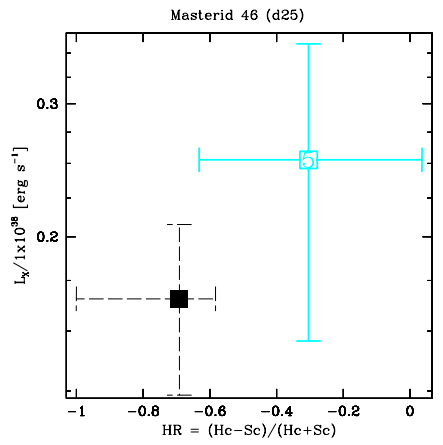
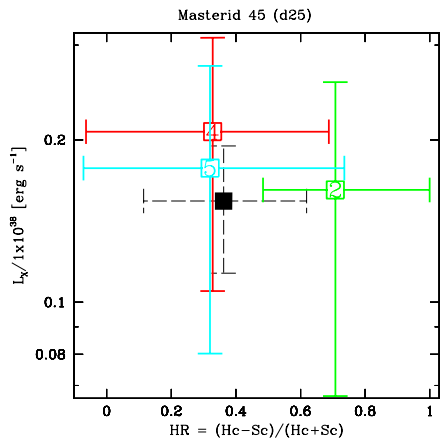
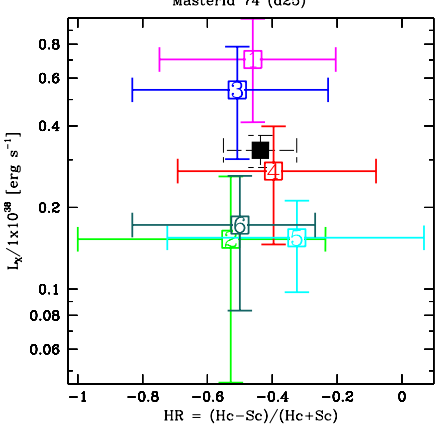
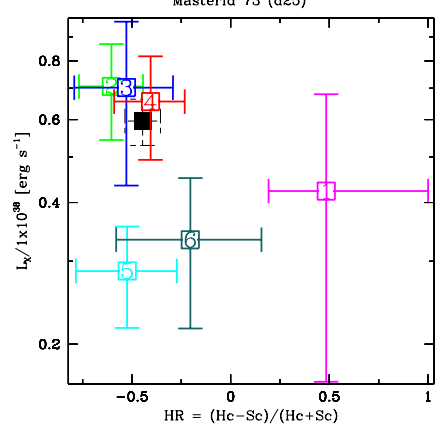
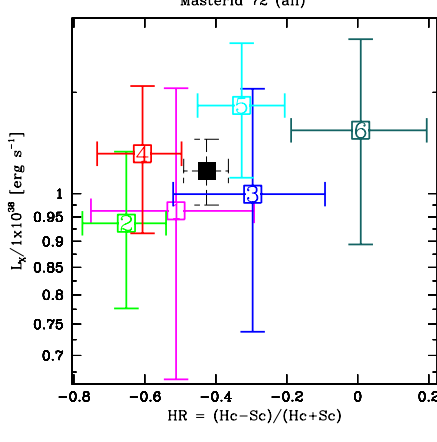
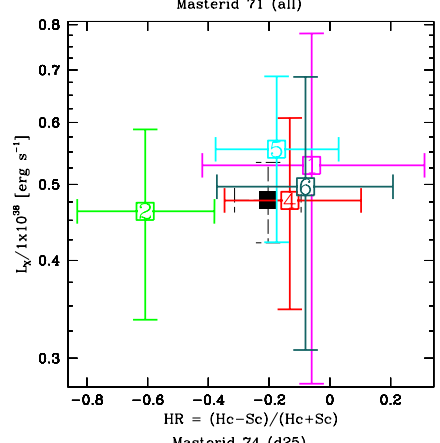
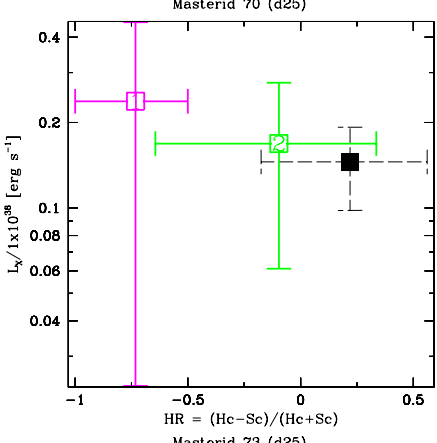
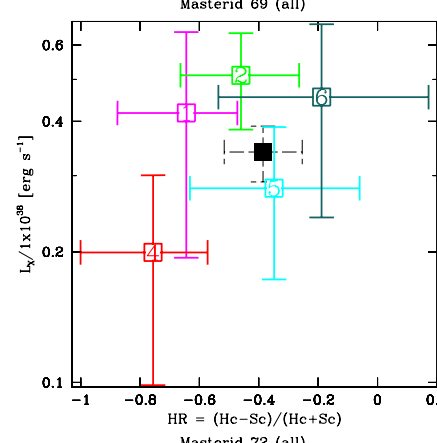
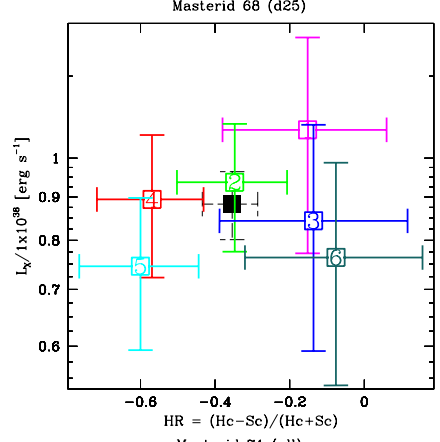
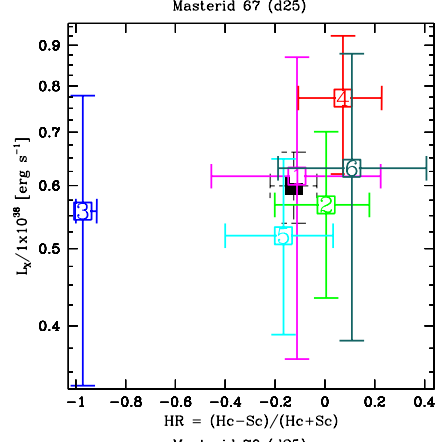
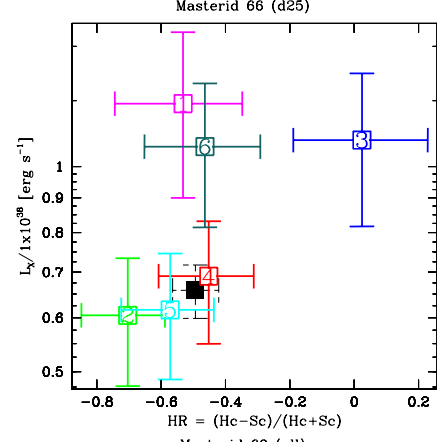
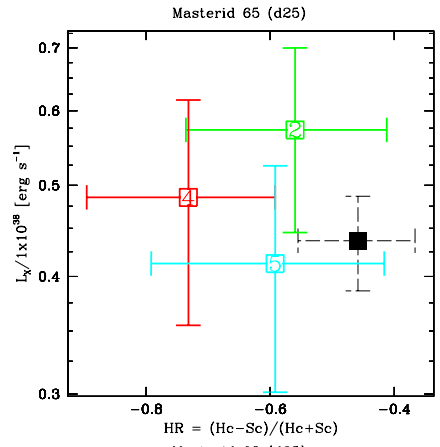
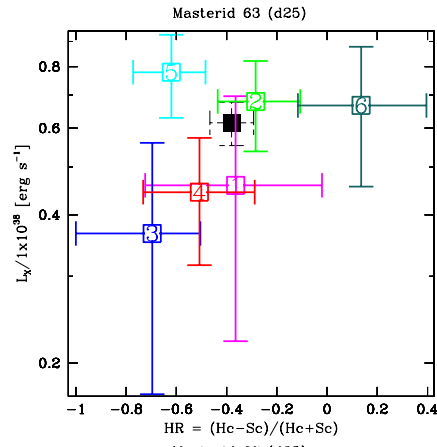
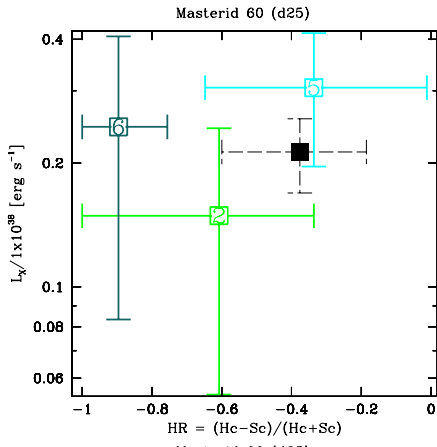


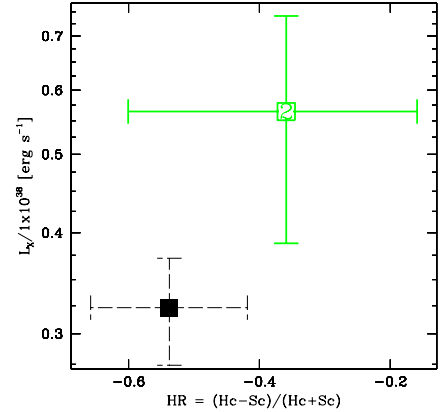
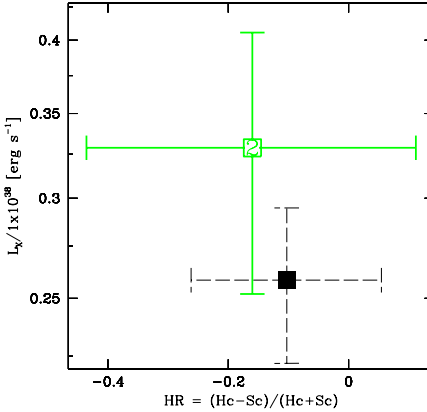
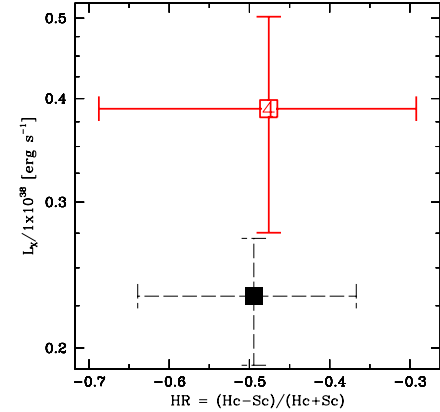
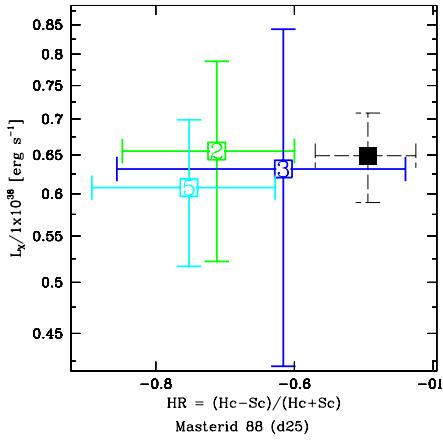
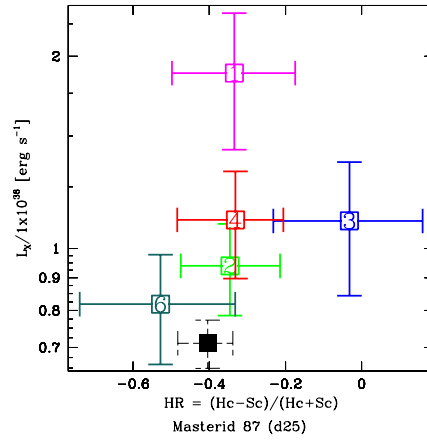
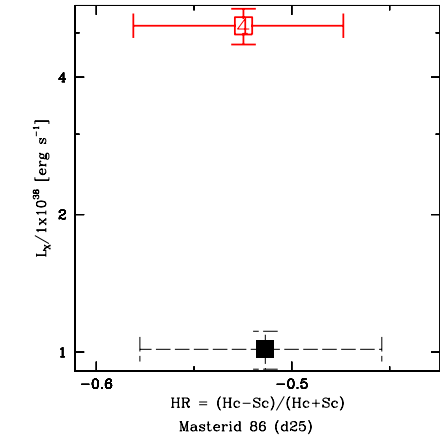
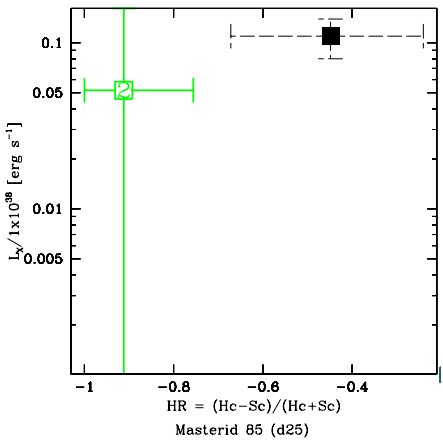
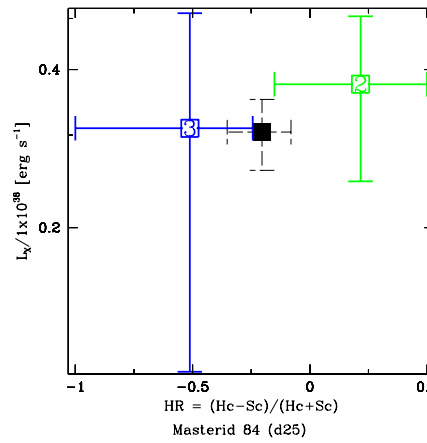
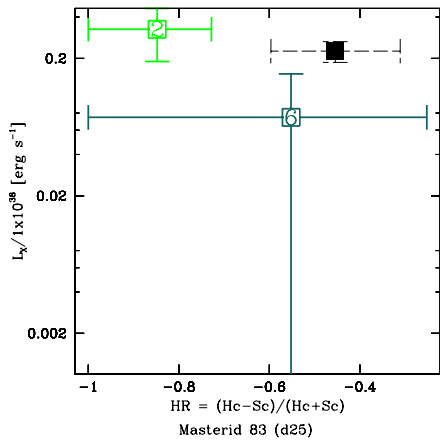
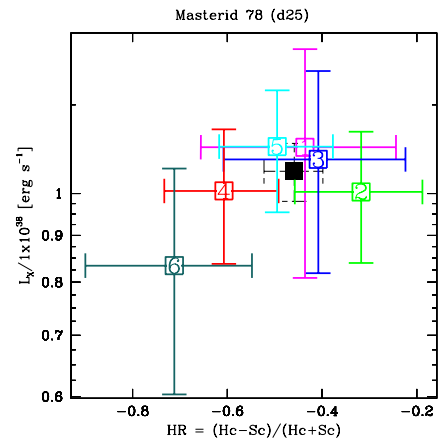
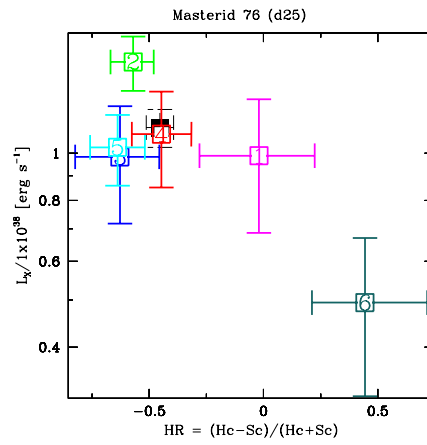
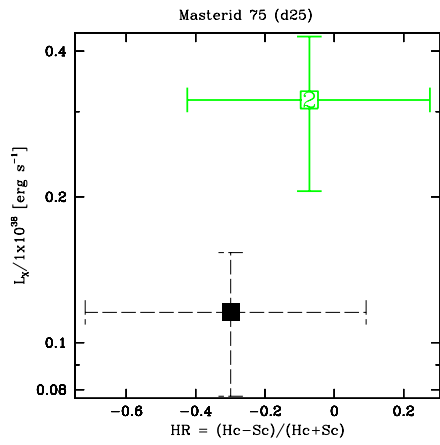
FIG. 8.— HR- L_X plots for each source detected in more than one individual observation, with each observation plotted in a different color; observation 1 is magenta, observation 2 is green, observation 3 blue, observation 4 red, observation 5 cyan and observation 6 is dark green. The HR and L_X values for the co-added observation are also shown, plotted in black. The hardness ratios are defined to be $HR = Hc-Sc/Hc+Sc$, where Hc is the number of counts in the hard band (2.0–8.0 keV) and Sc is the number of counts in the soft band (0.5–2.0 keV).

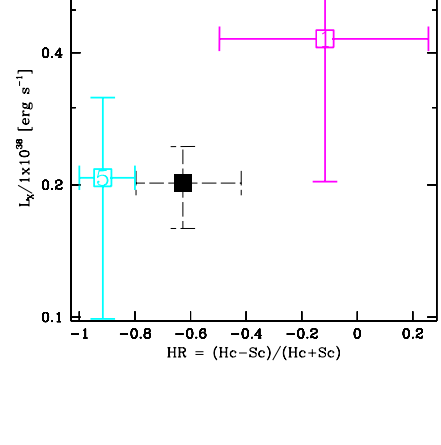
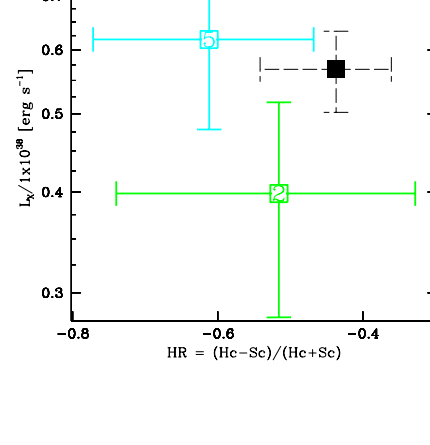
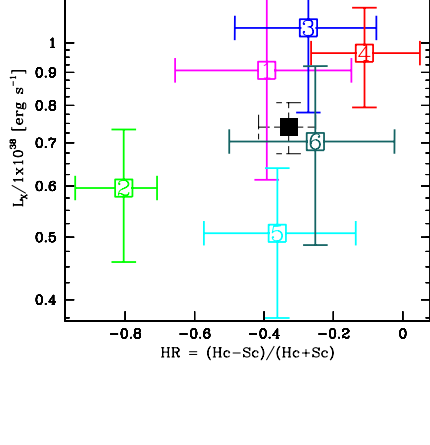
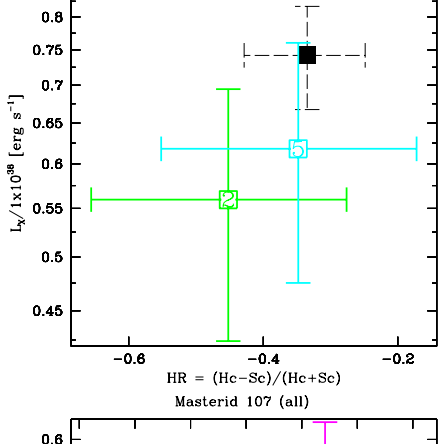
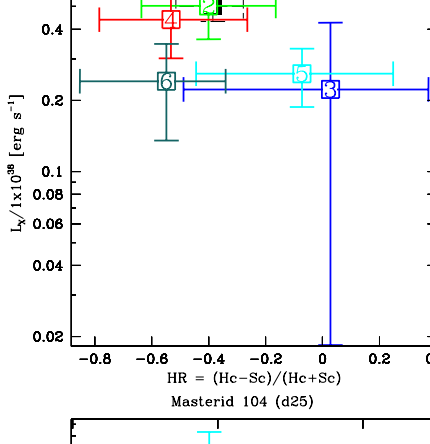
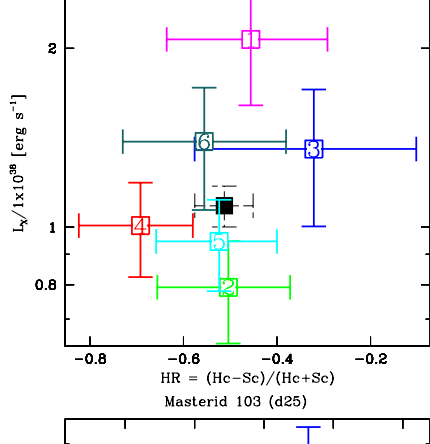
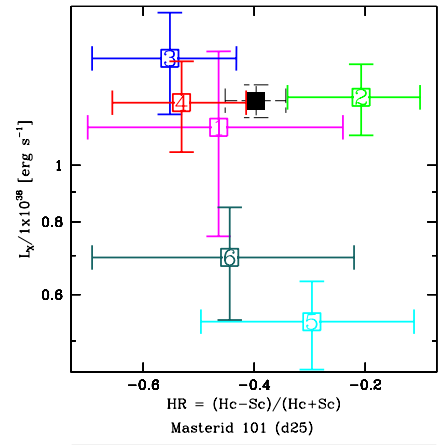
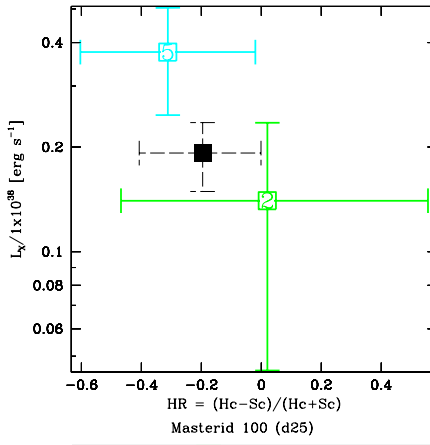
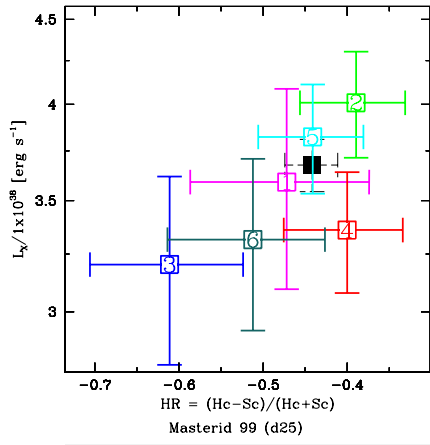
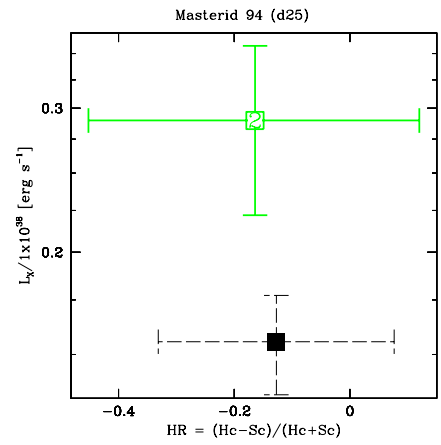
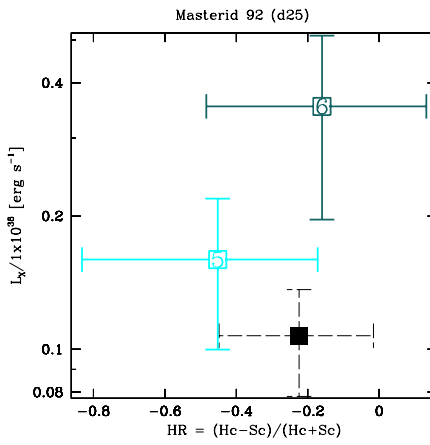
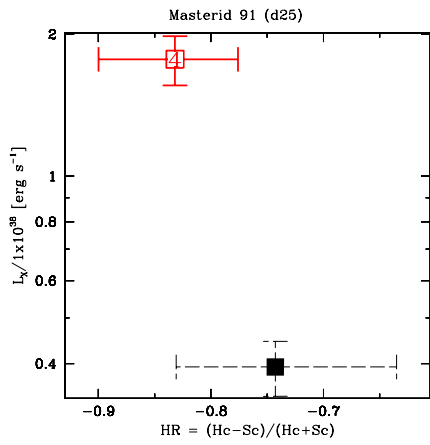


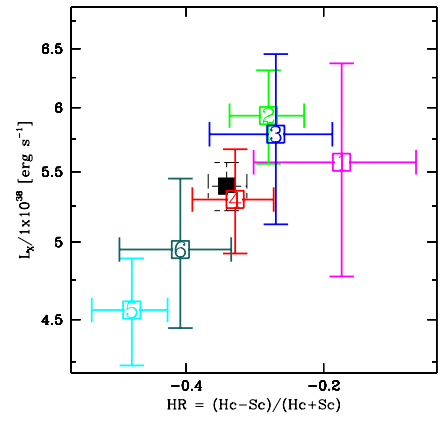
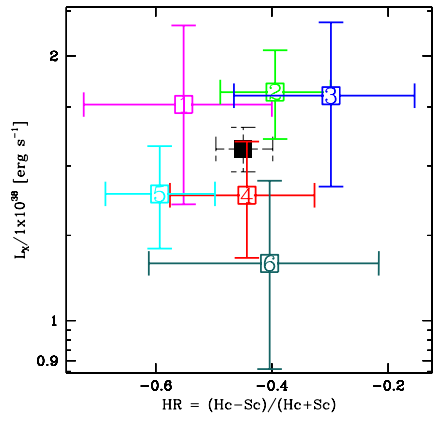
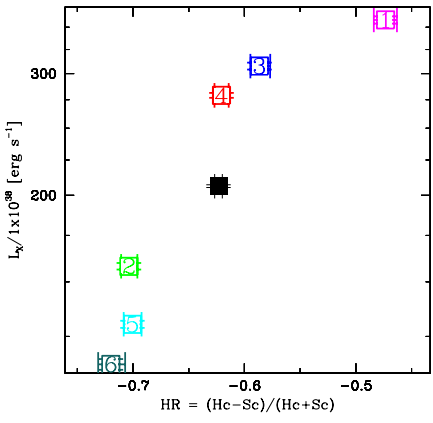
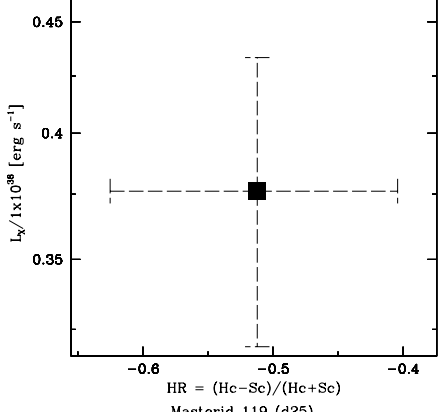
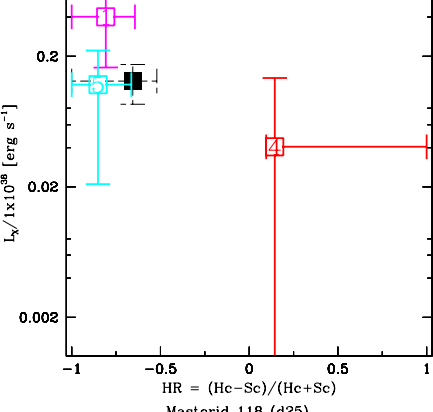
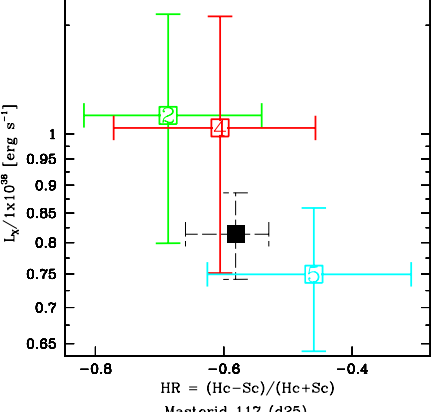
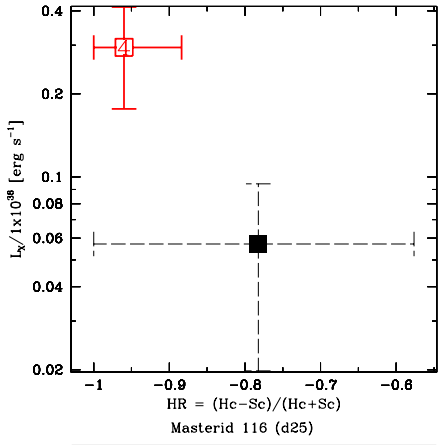
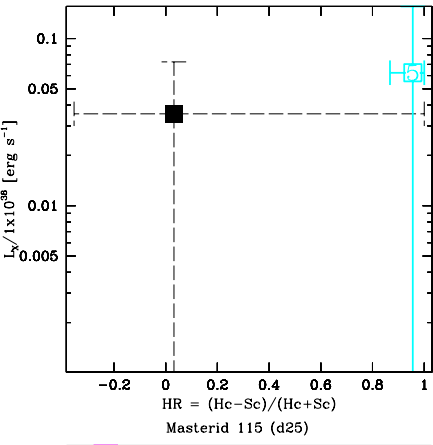
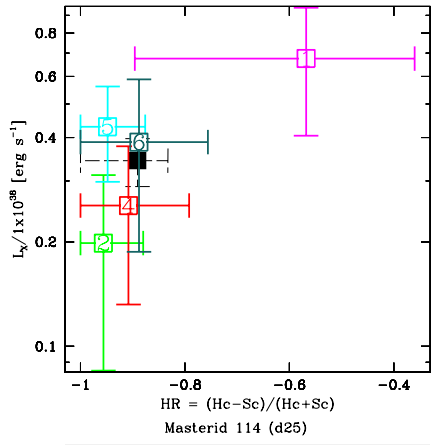
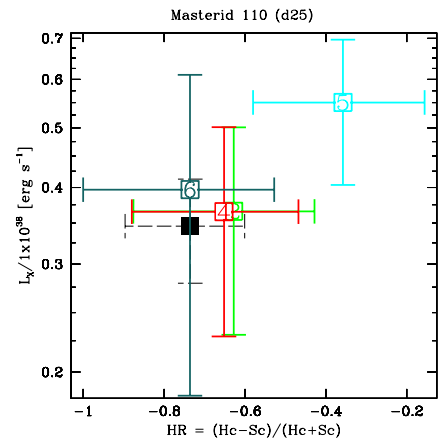
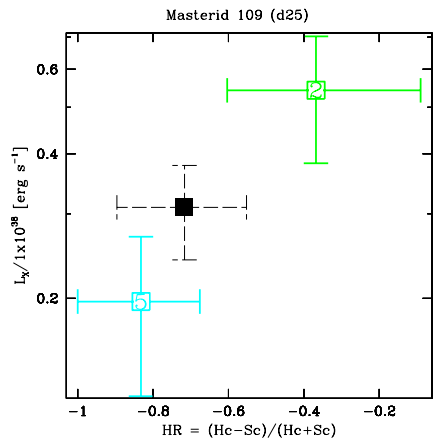
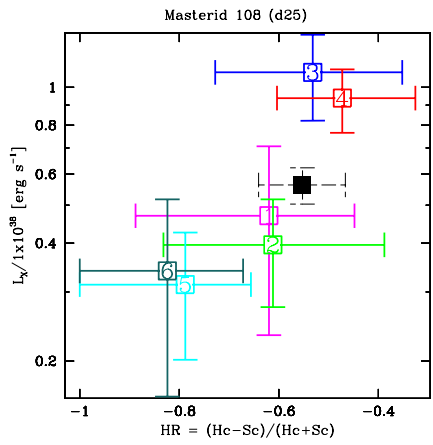


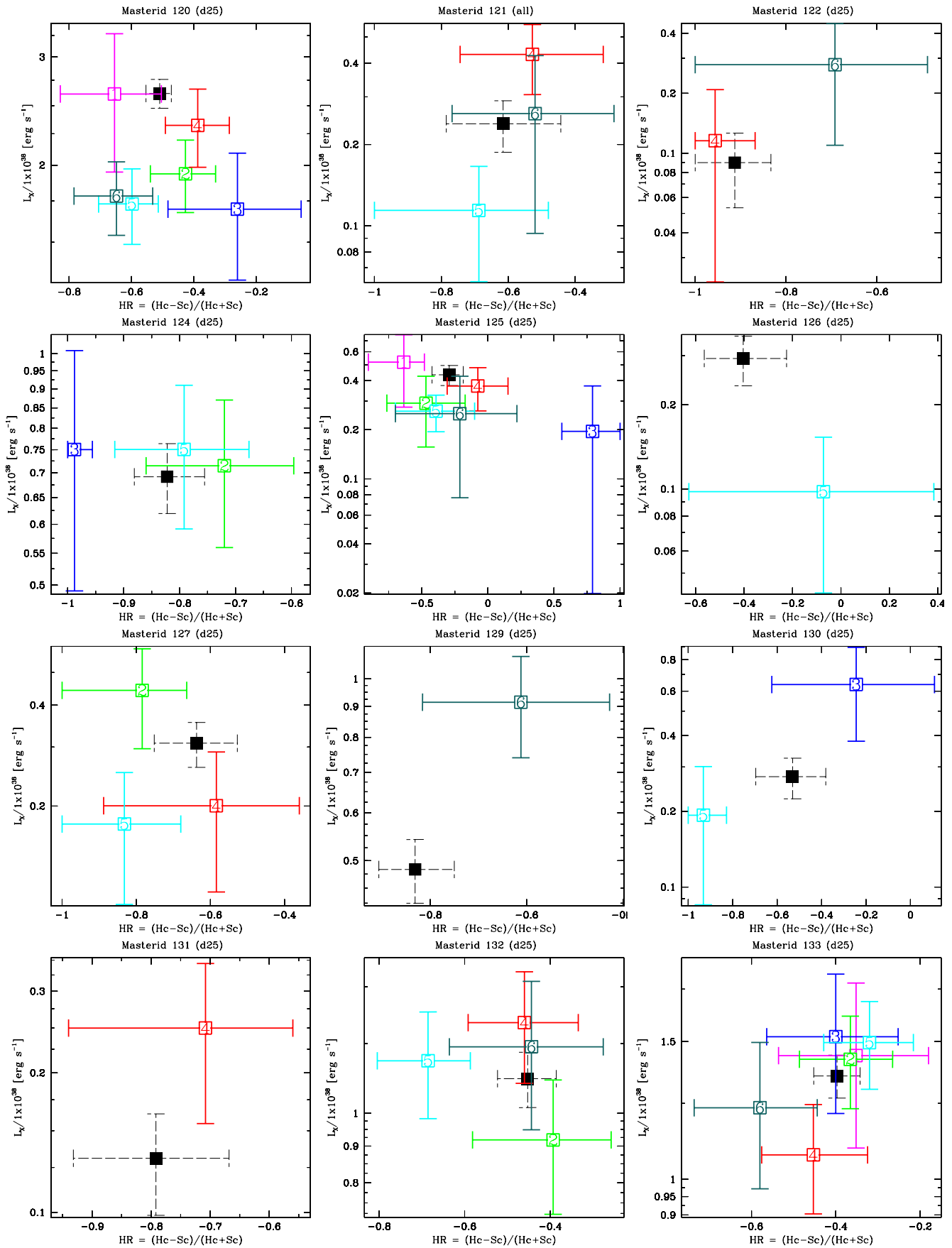


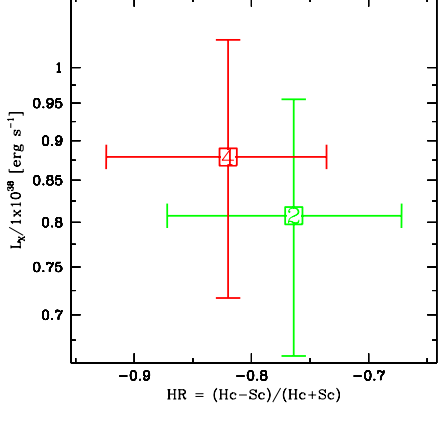
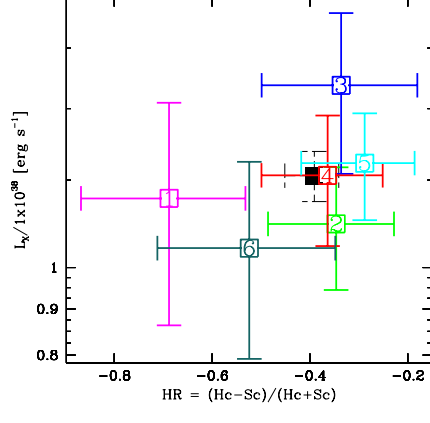
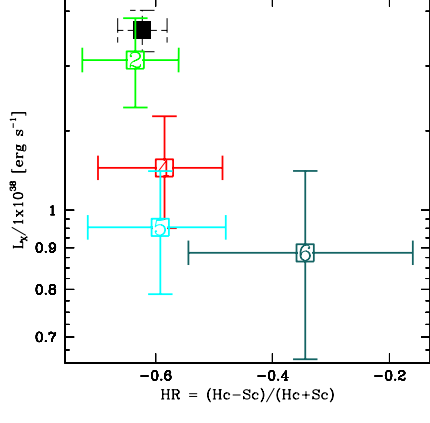
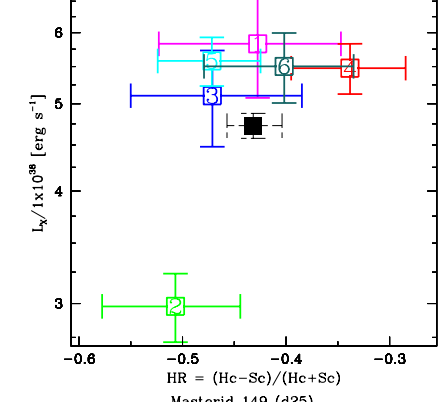
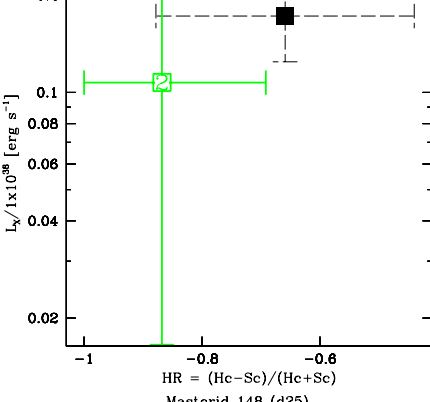
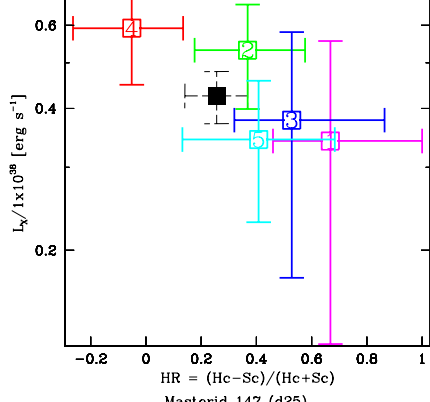
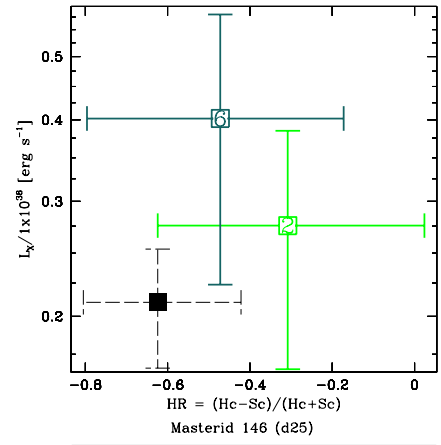
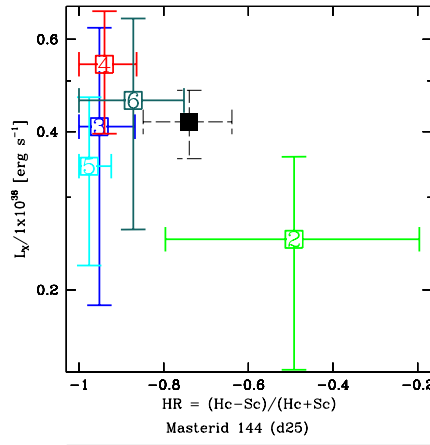
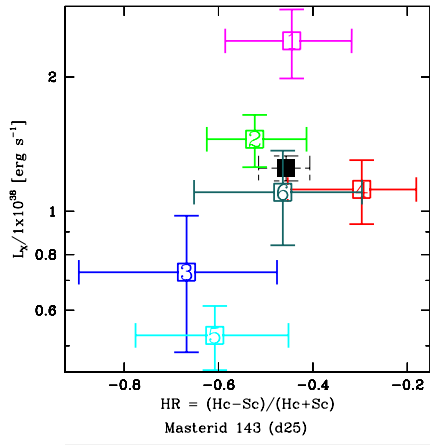
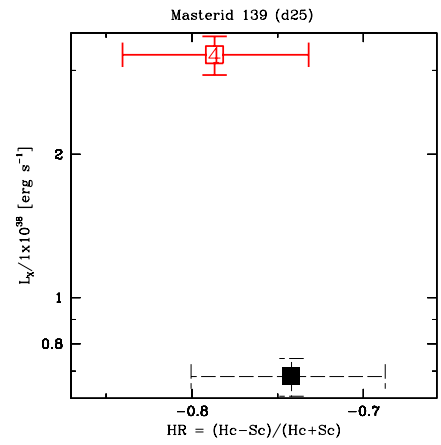
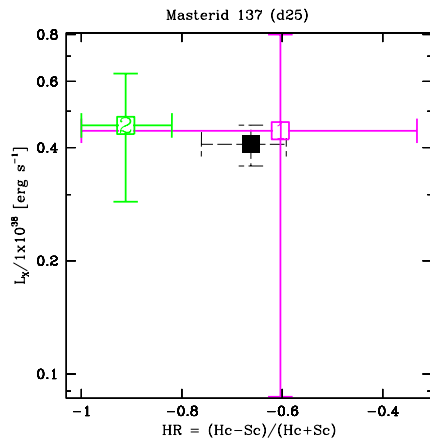
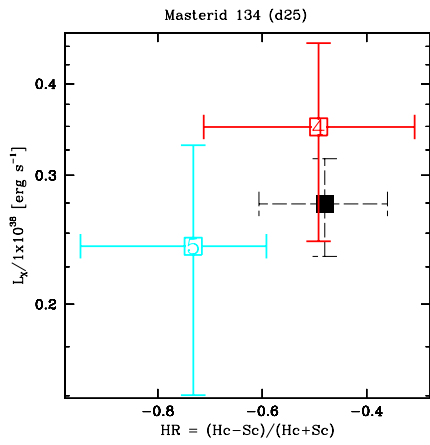


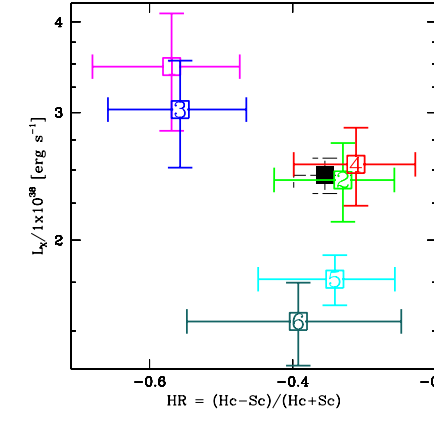
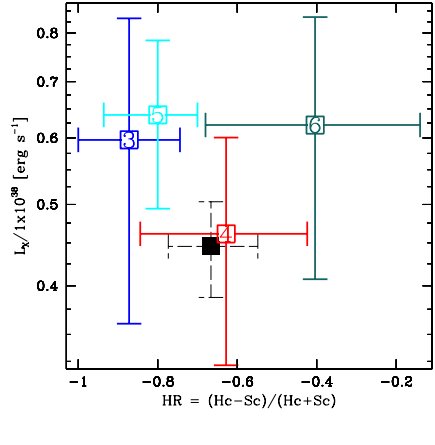
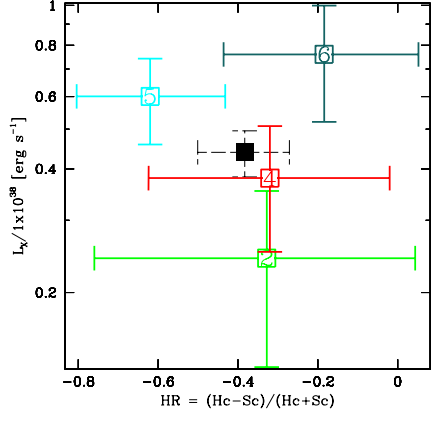
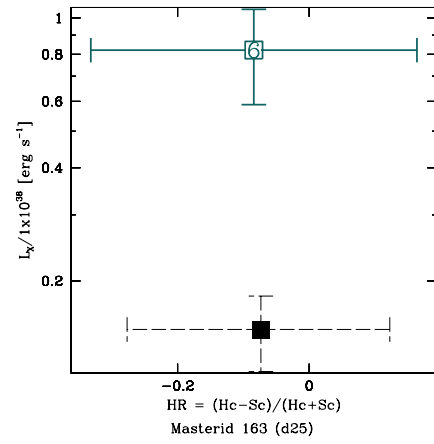
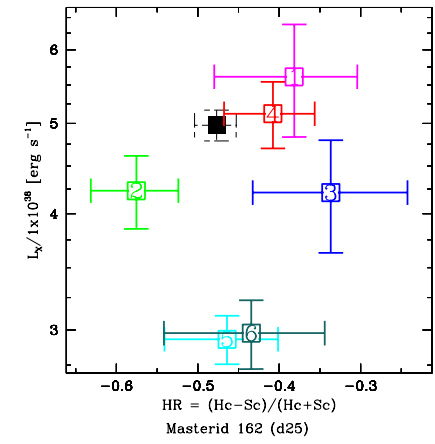
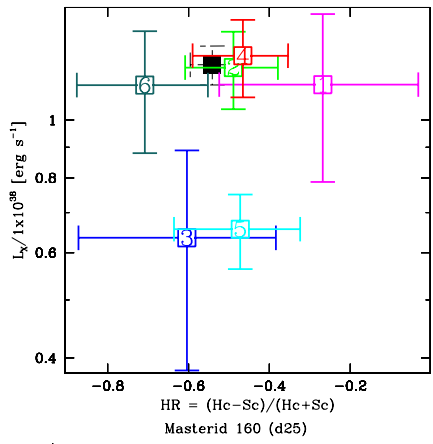
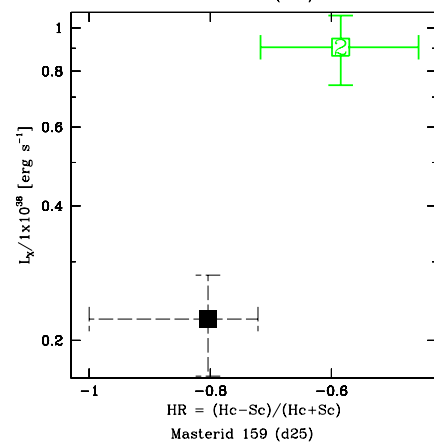
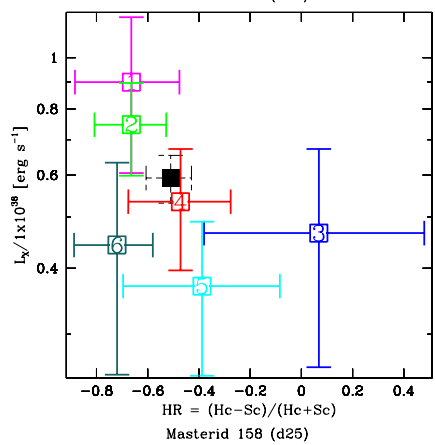
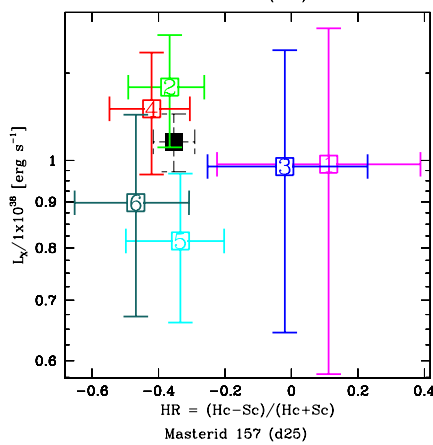
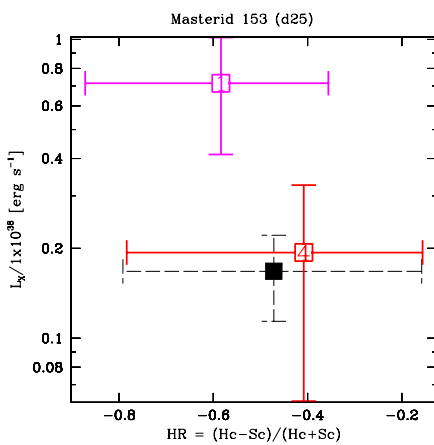
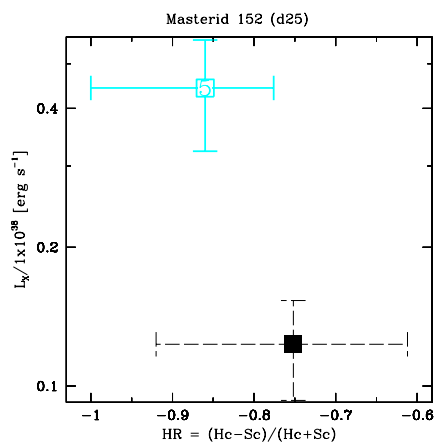
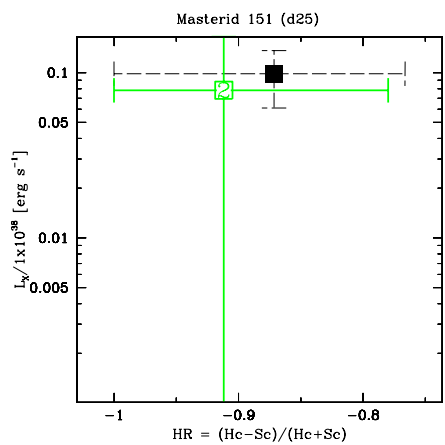


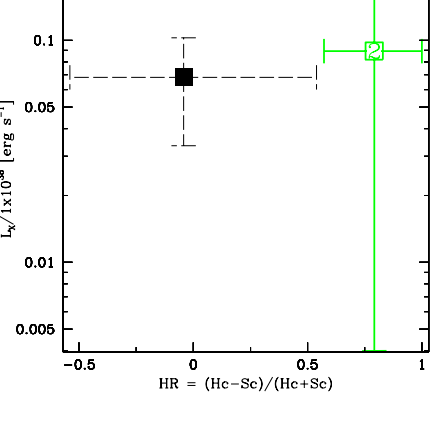
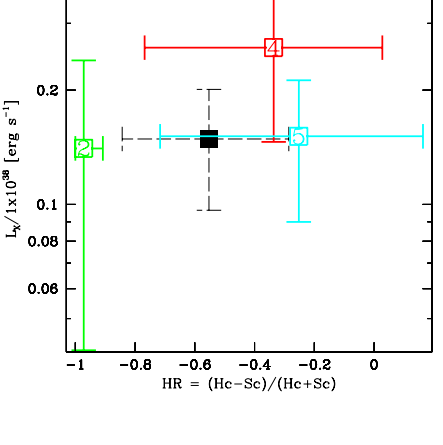
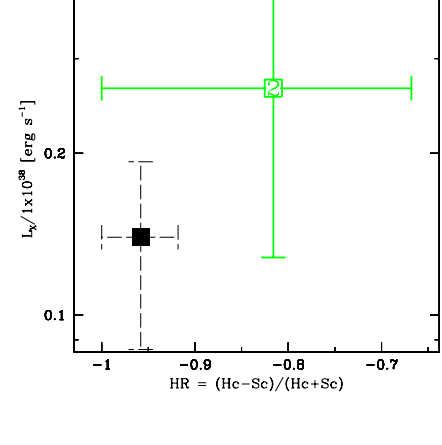
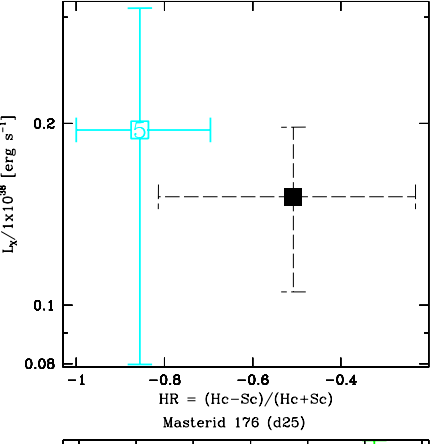
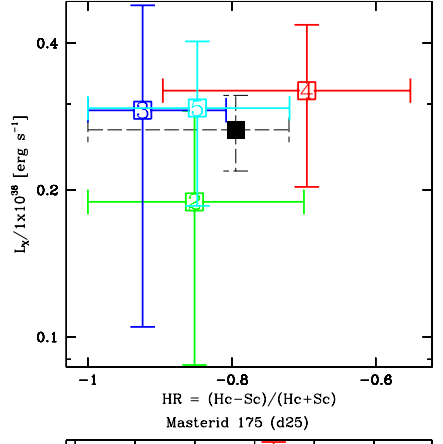
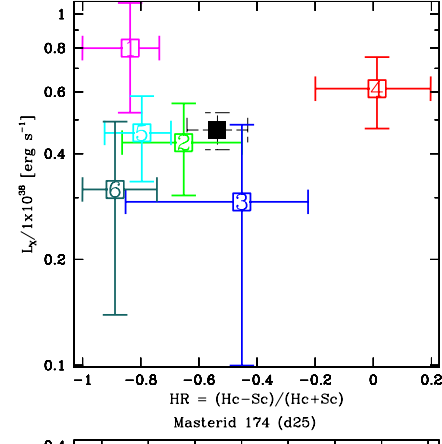
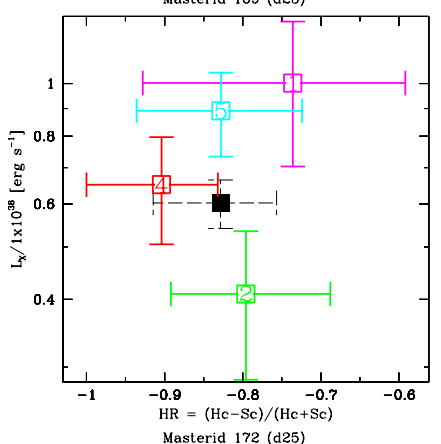
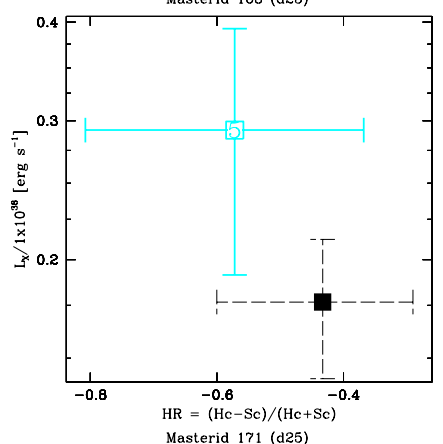
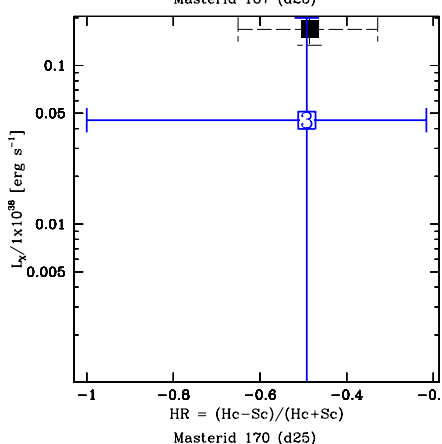
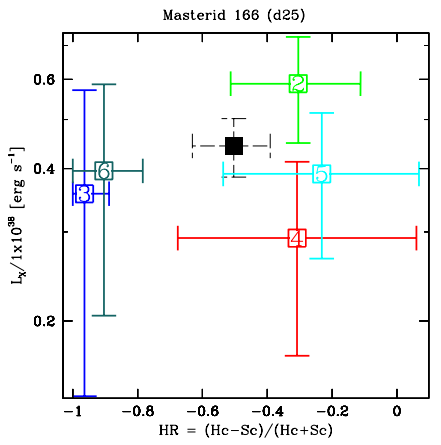
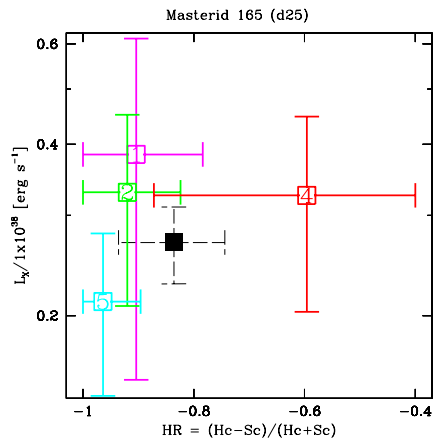
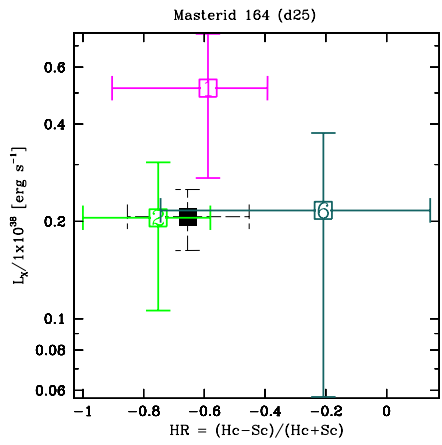


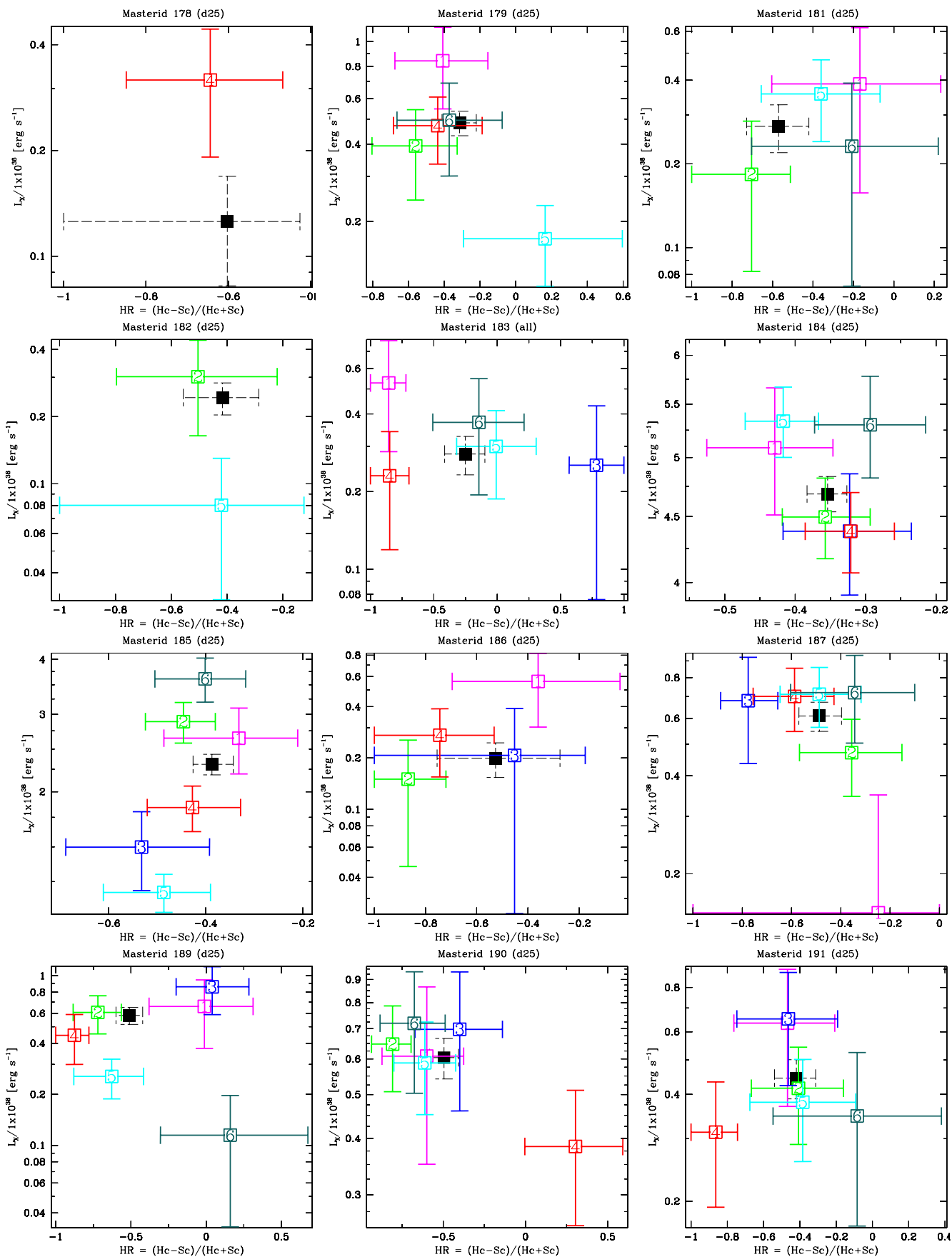


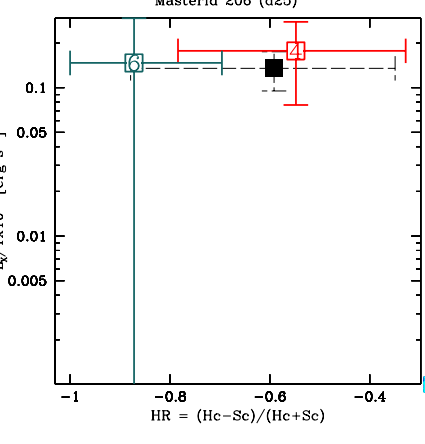
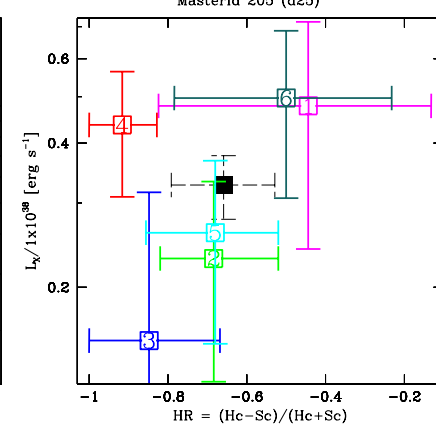
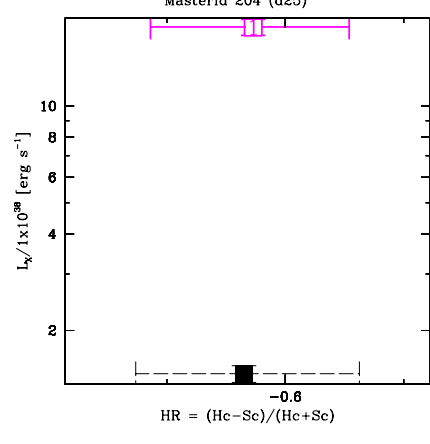
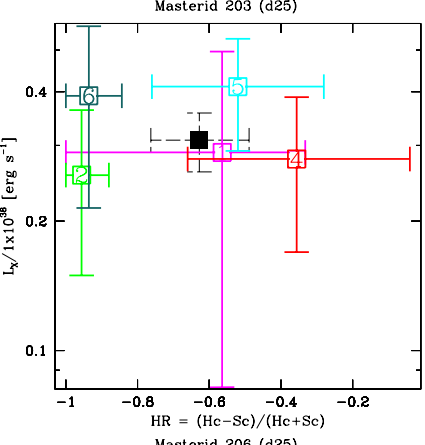
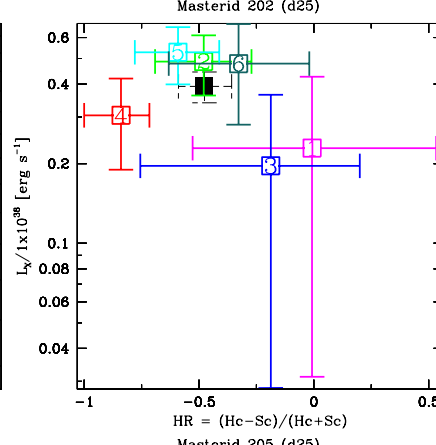
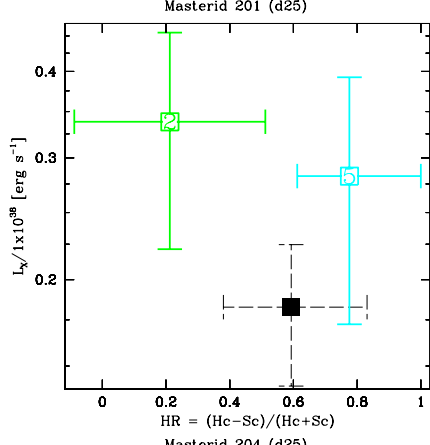
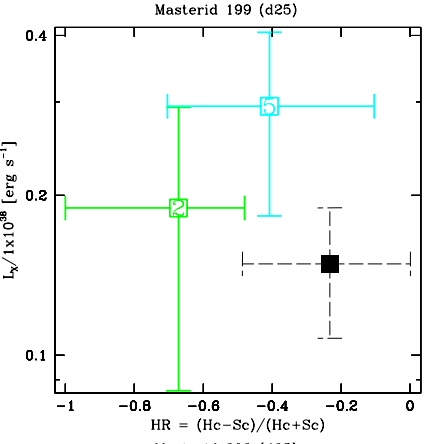
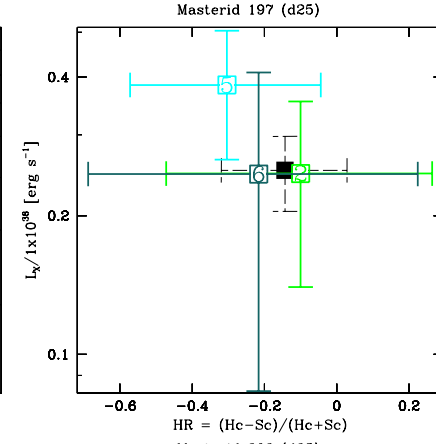
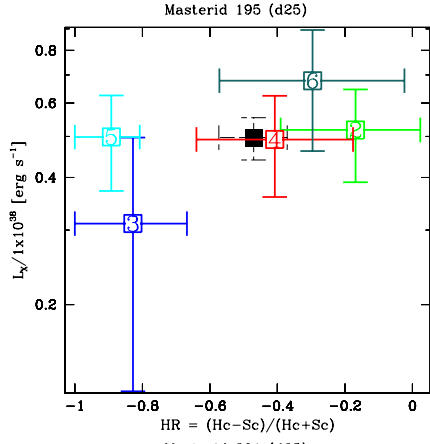
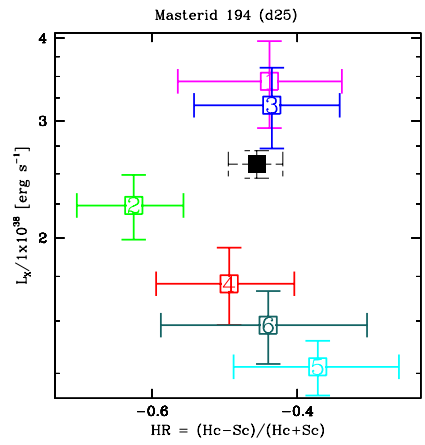
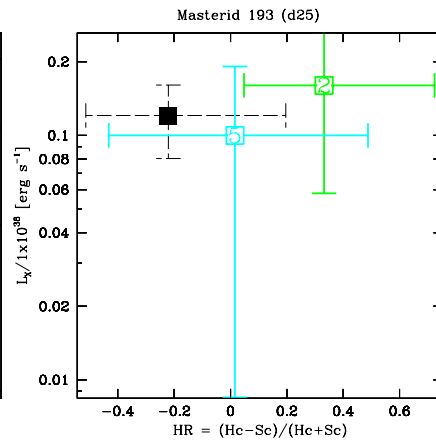
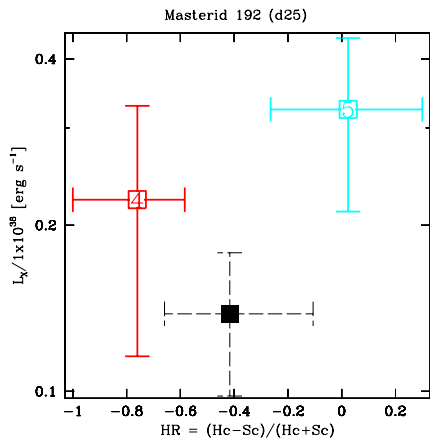


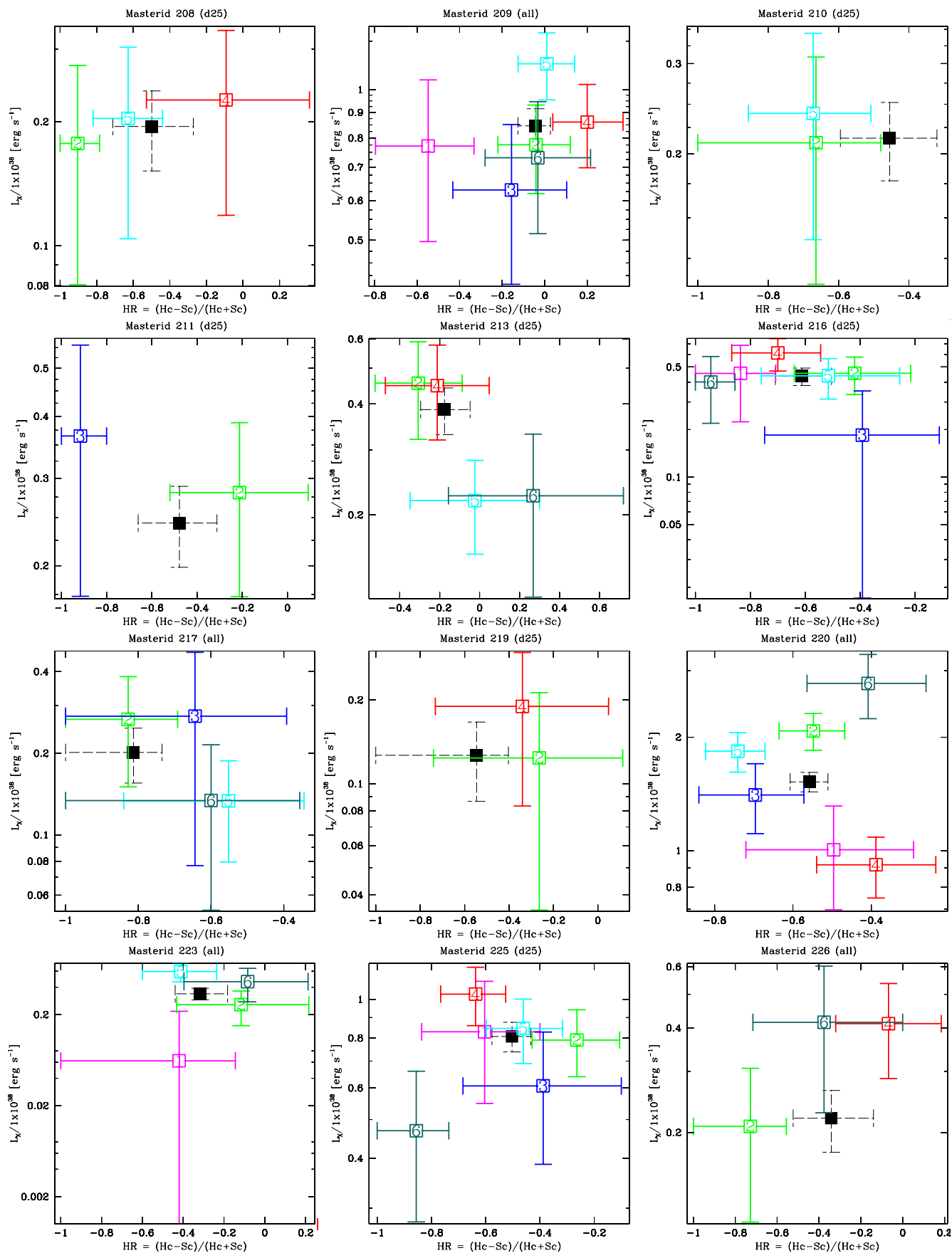


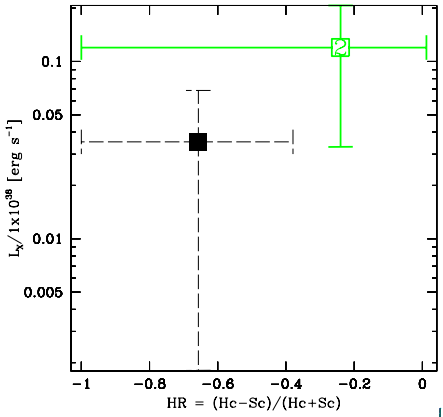
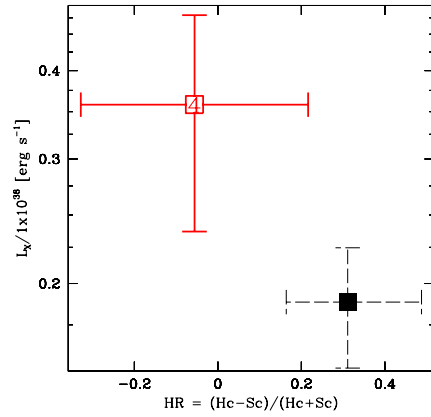
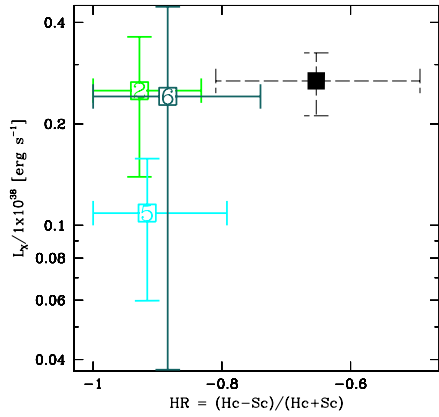
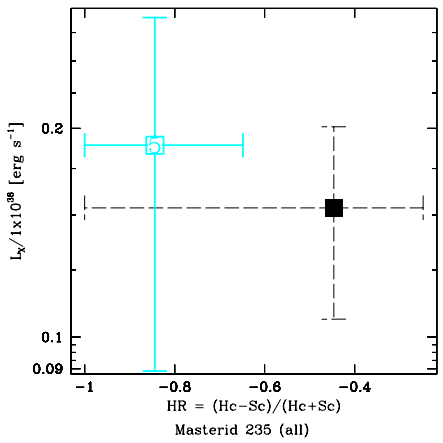
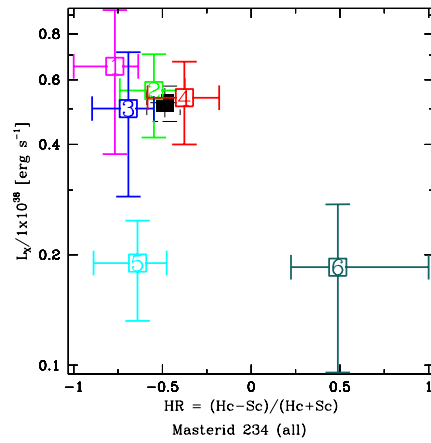
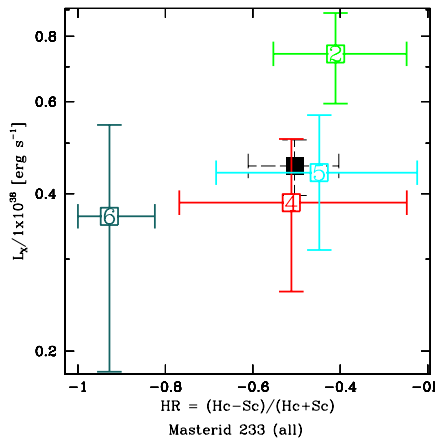
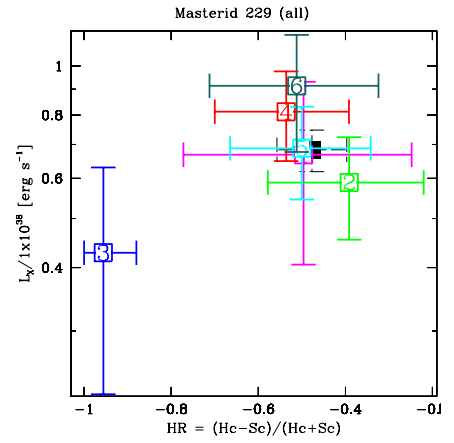
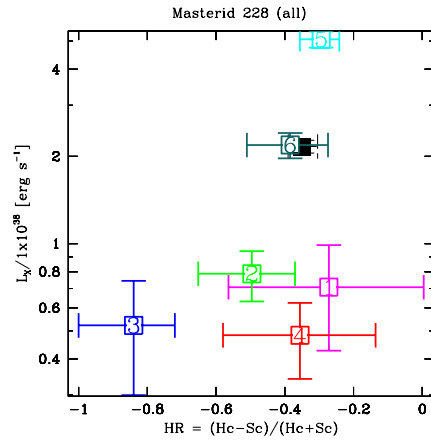
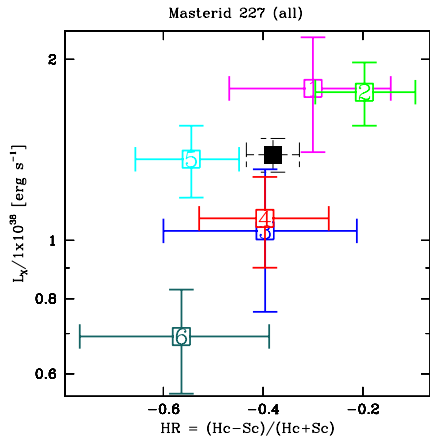












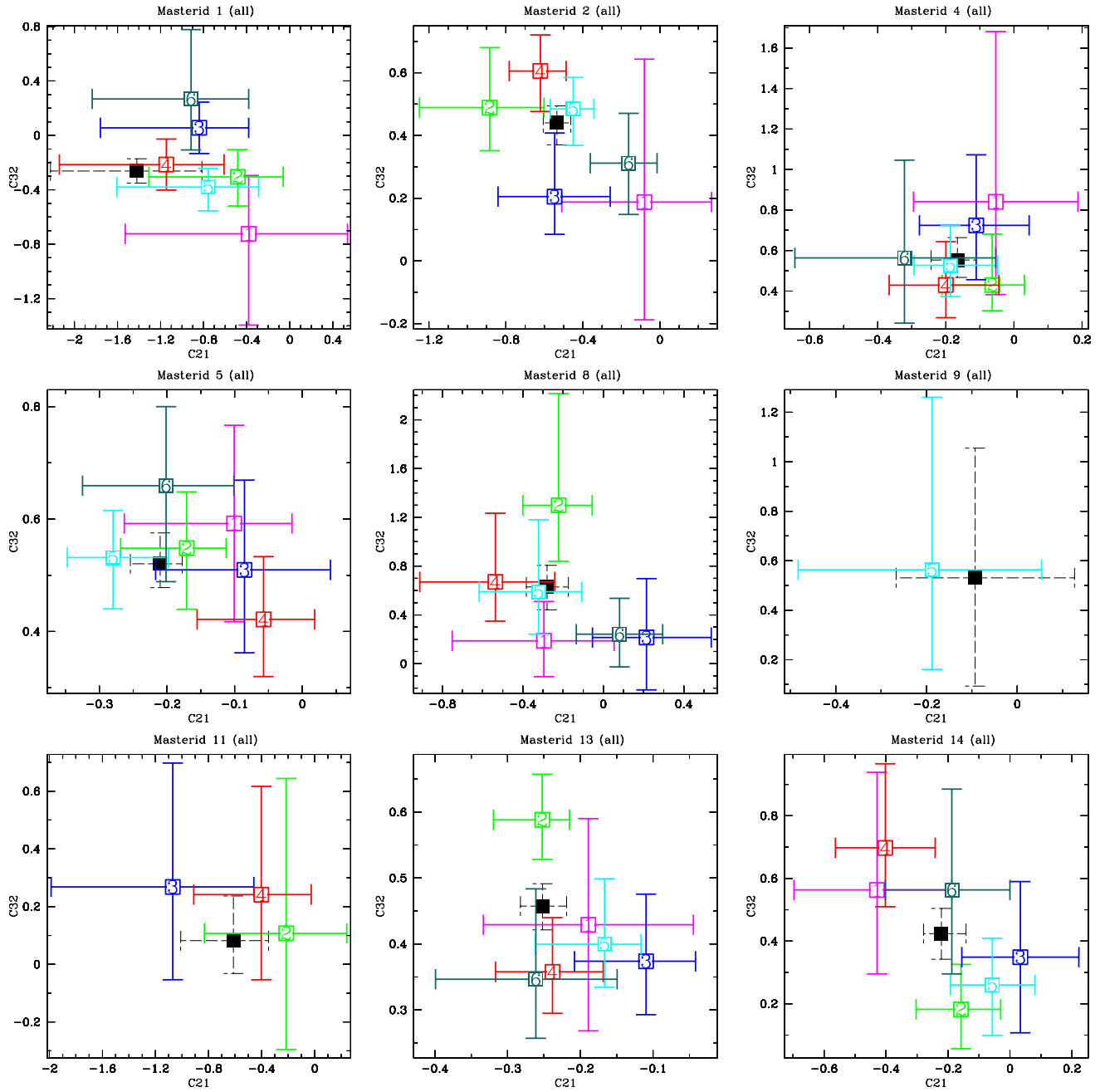
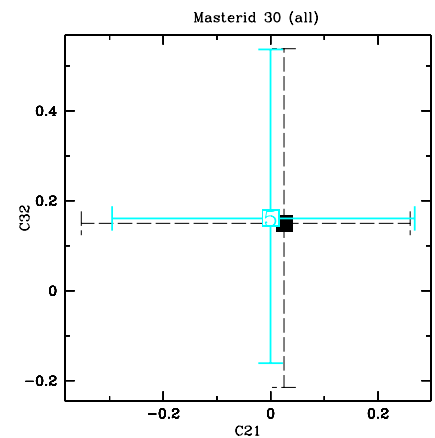
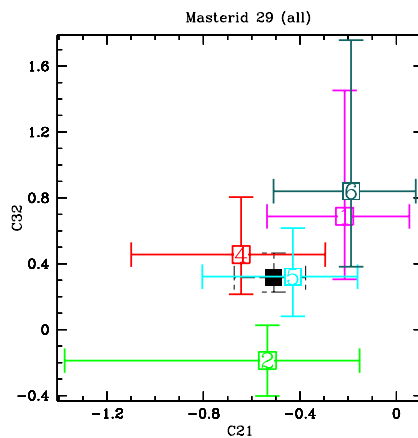
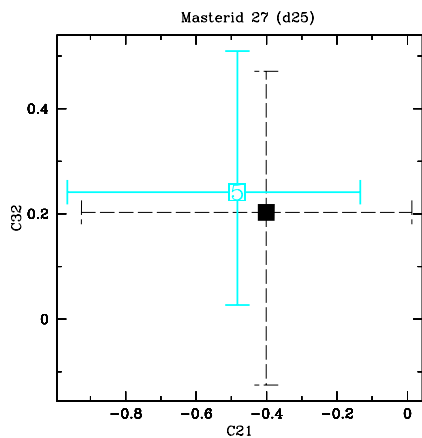
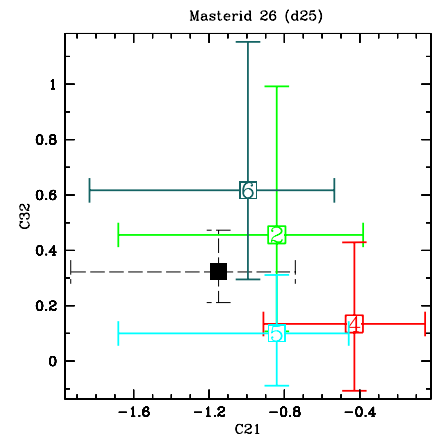
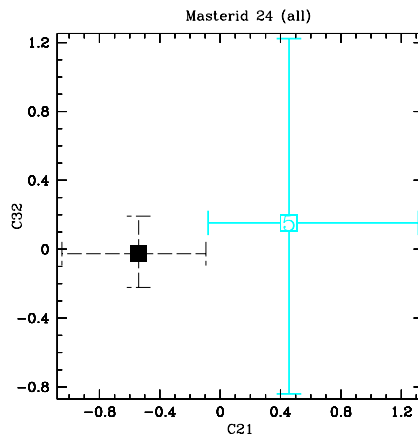
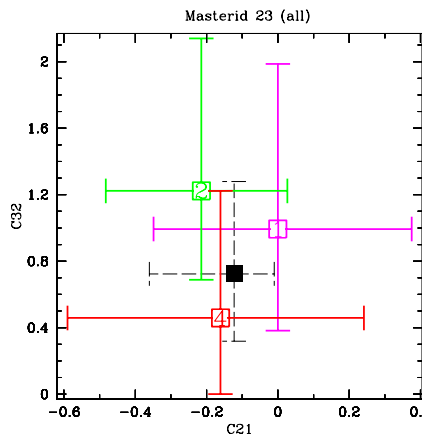
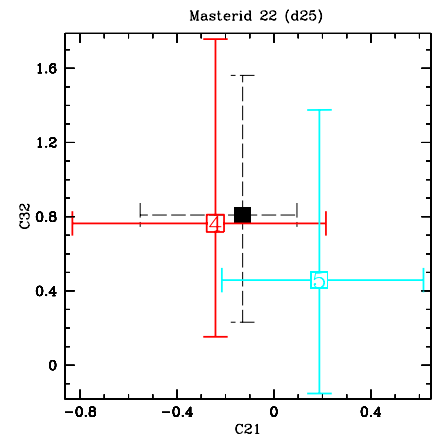
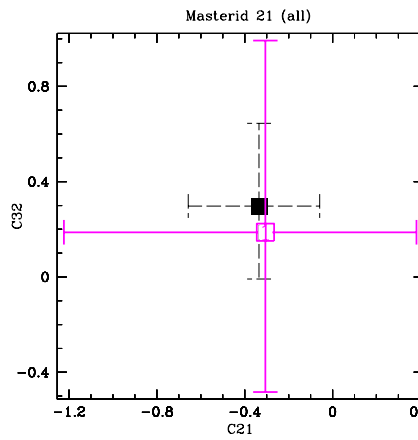
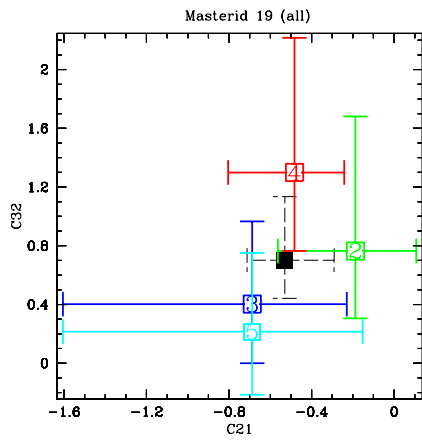
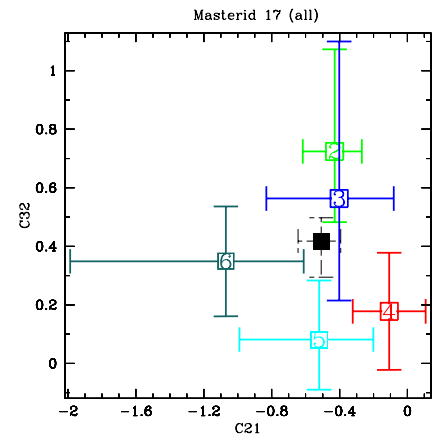
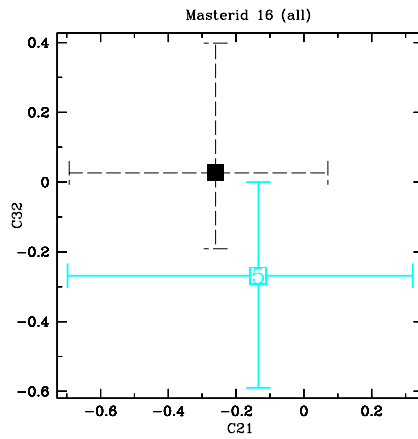
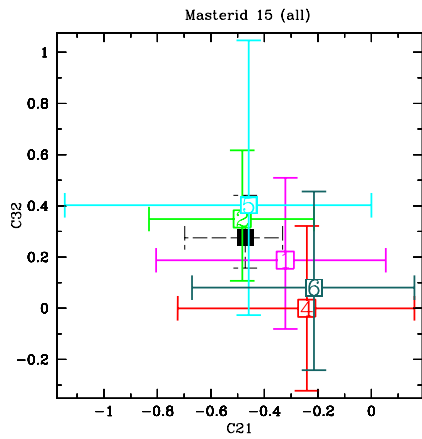
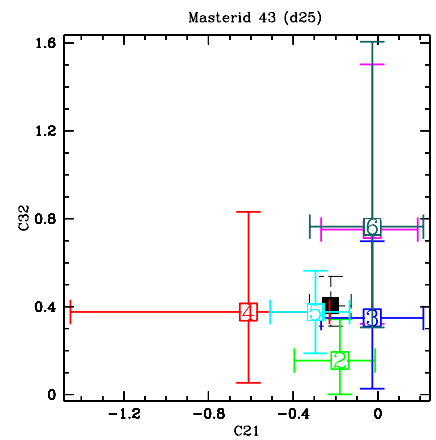
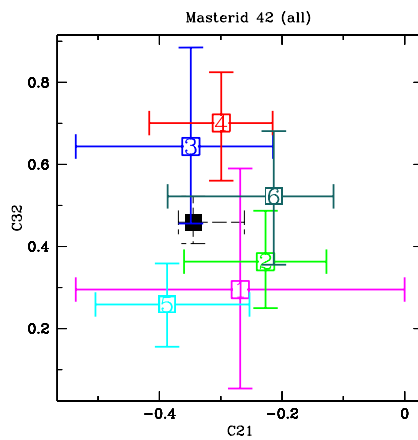
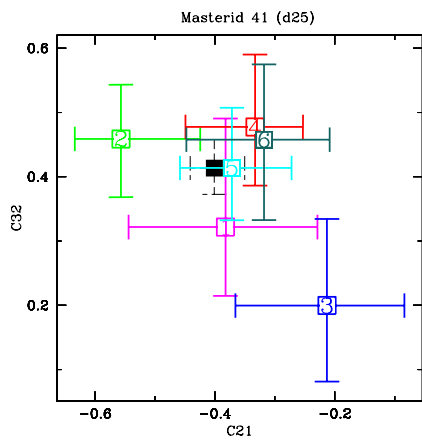
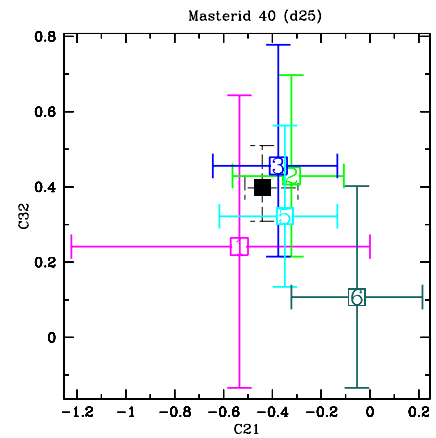
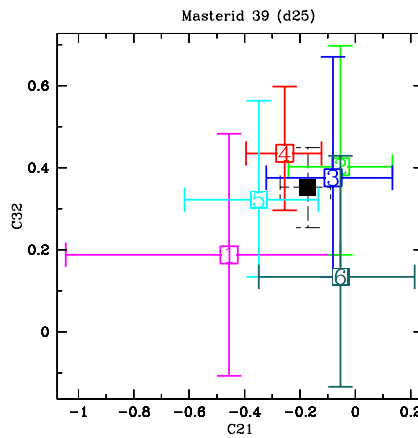
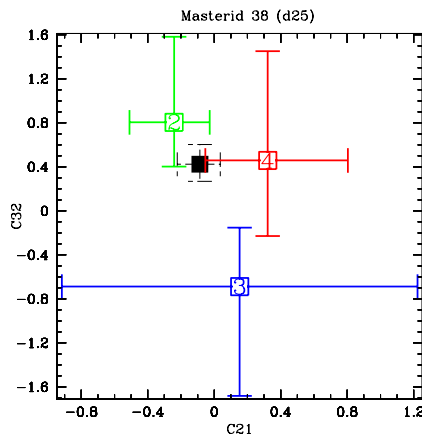
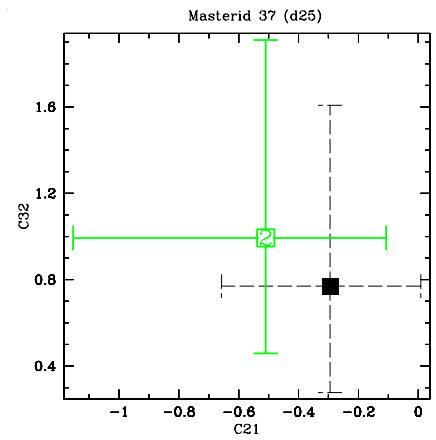
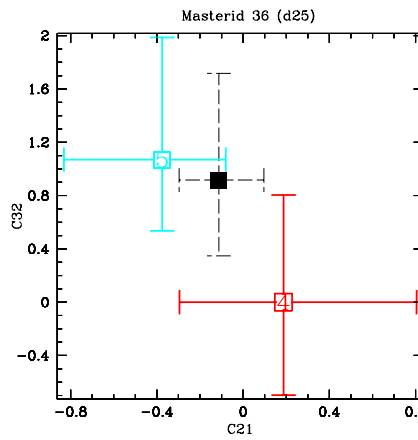
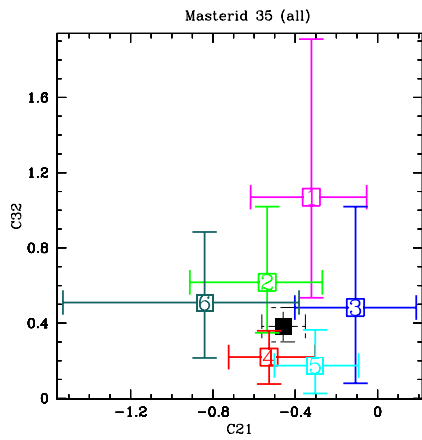
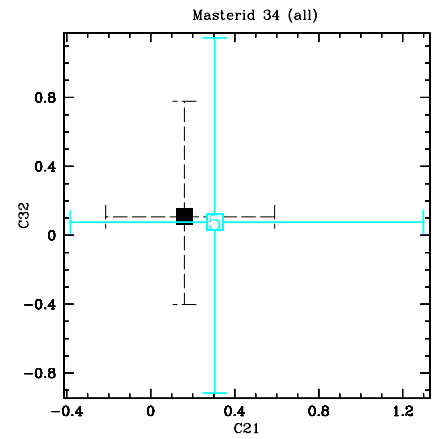
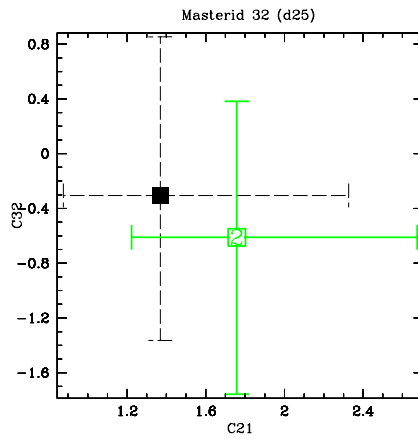
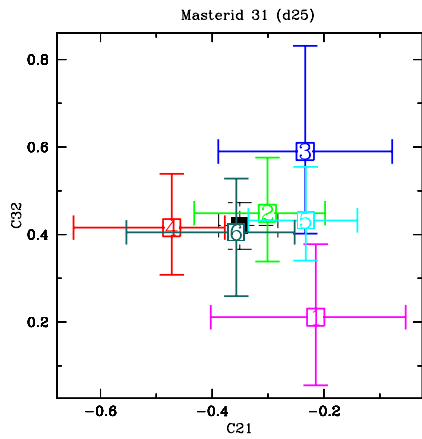
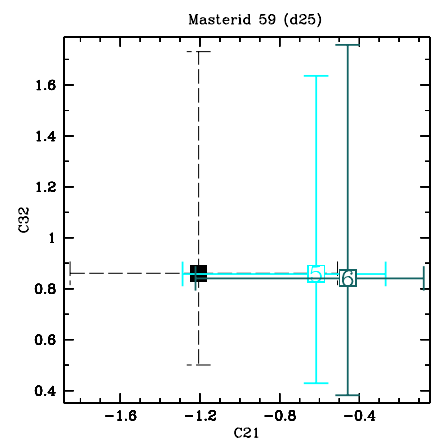
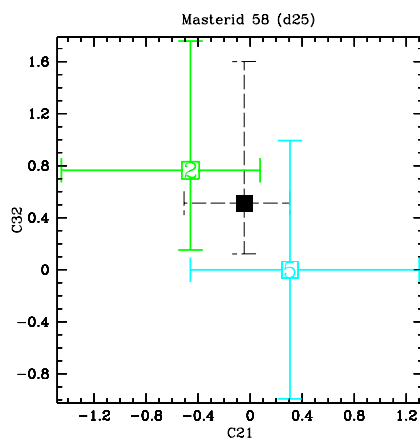
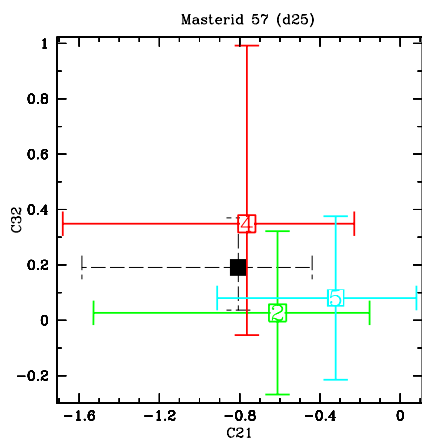
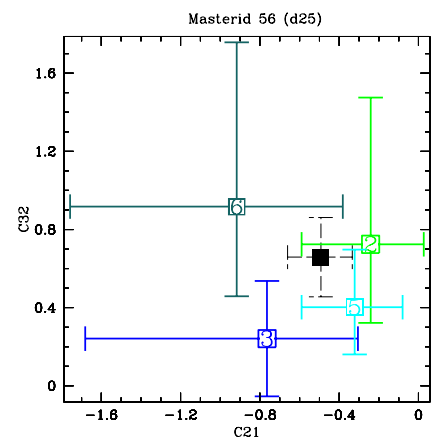
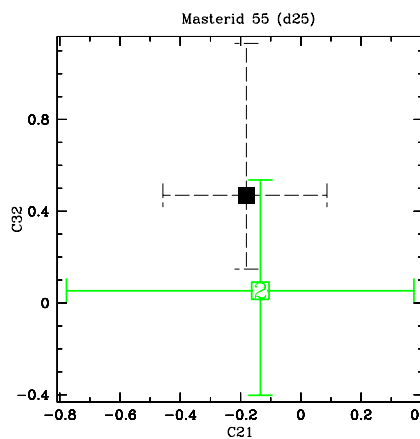
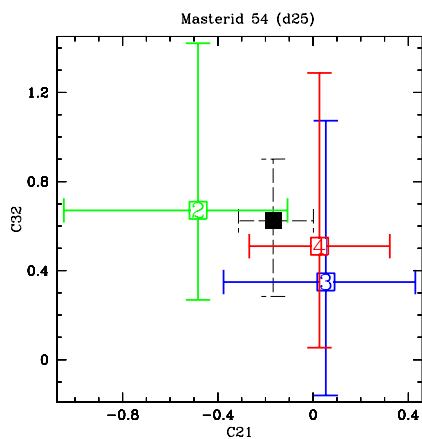
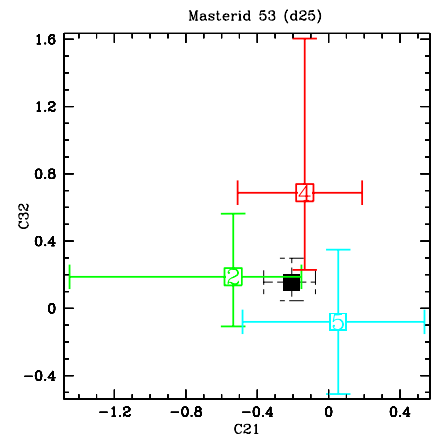
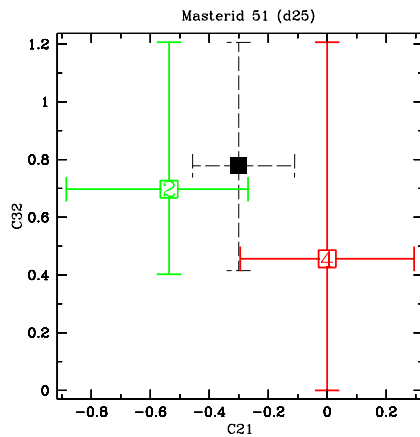
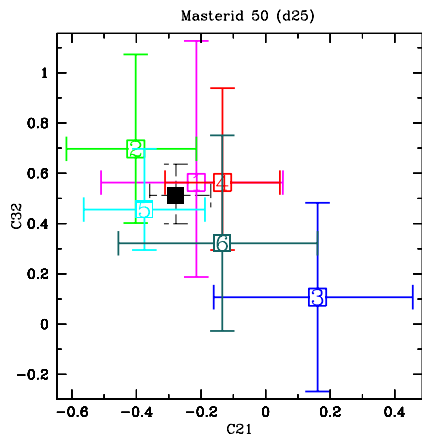
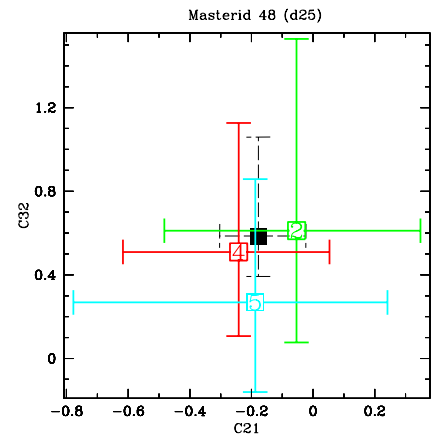
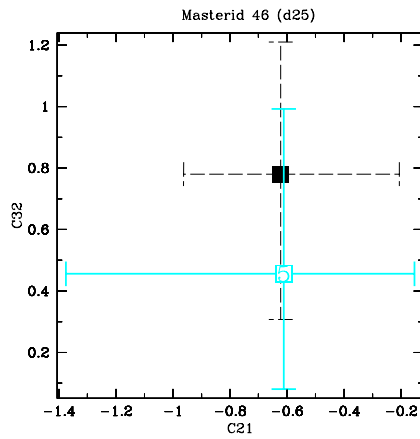
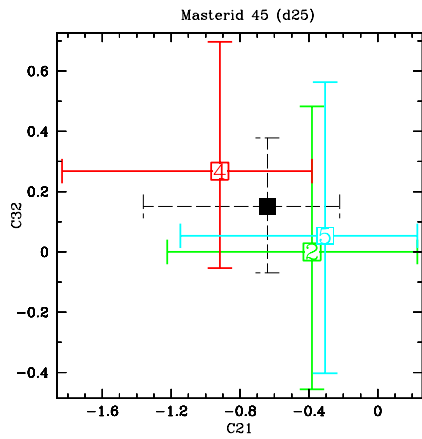
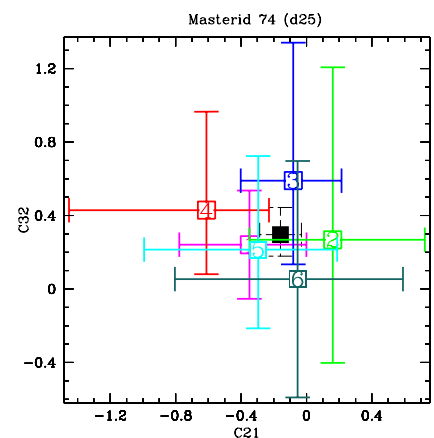
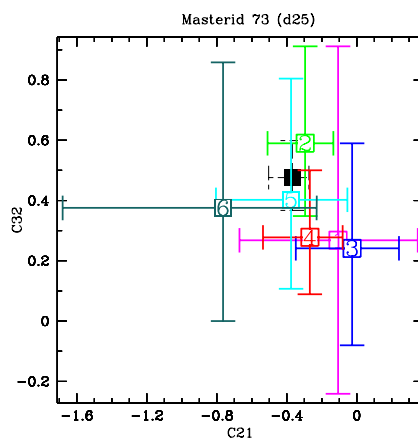
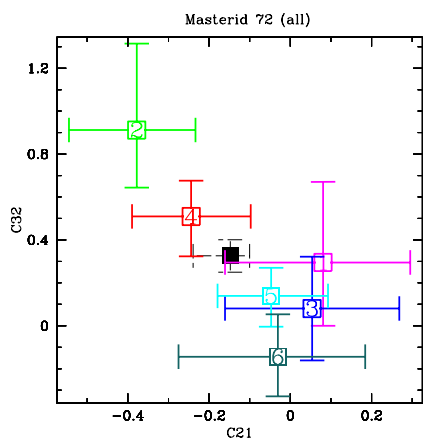
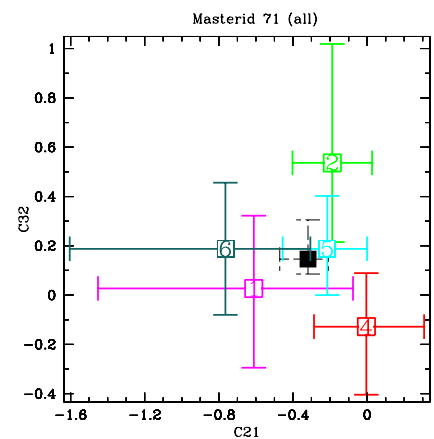
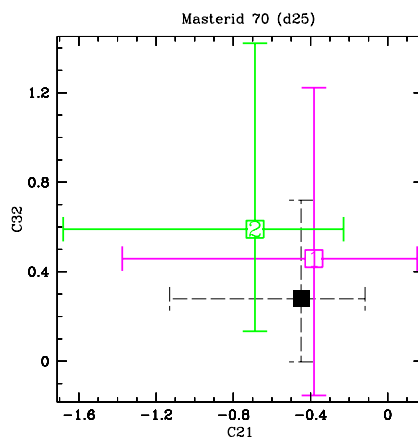
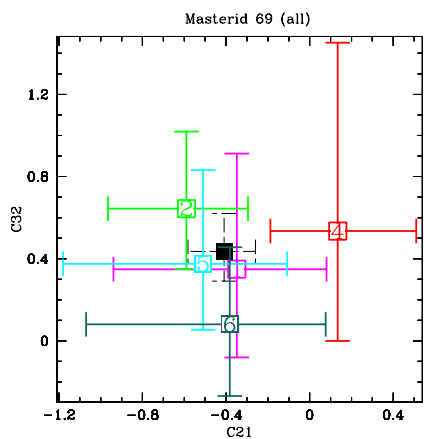
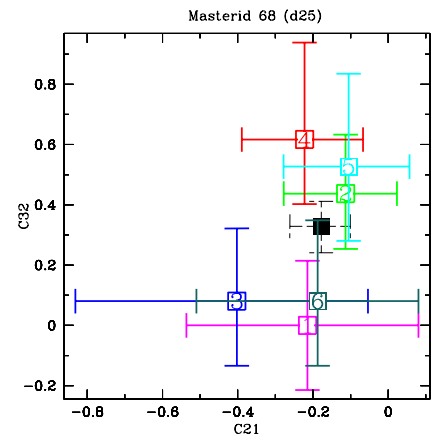
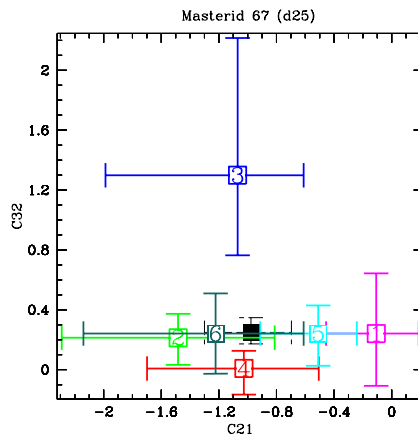
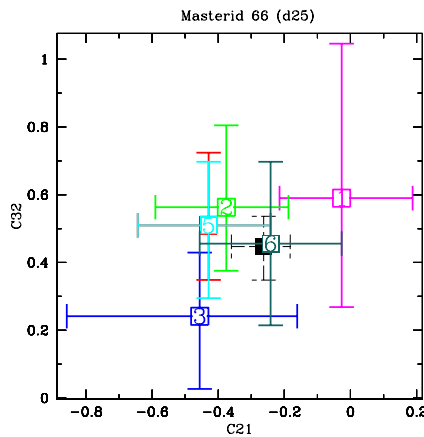
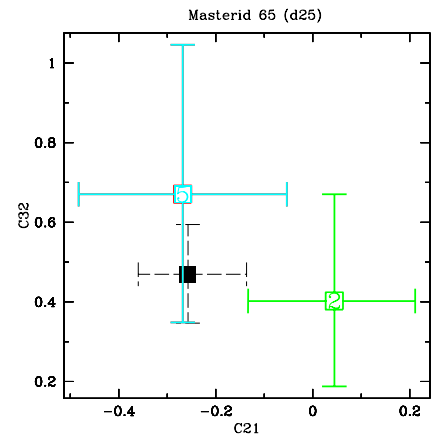
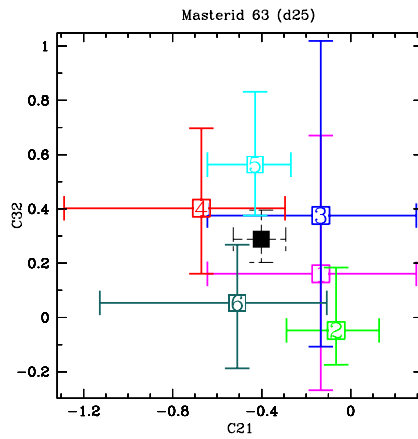
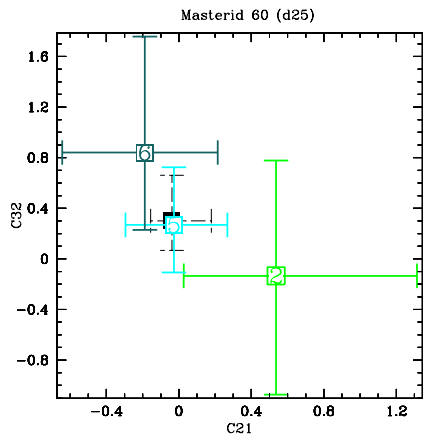


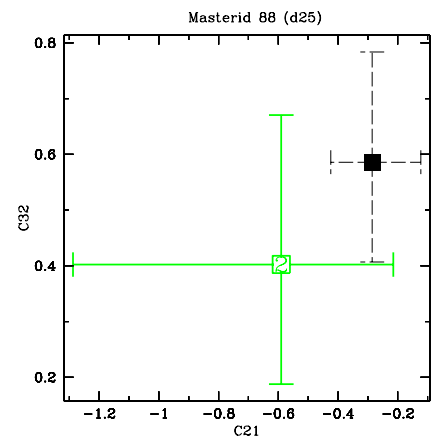
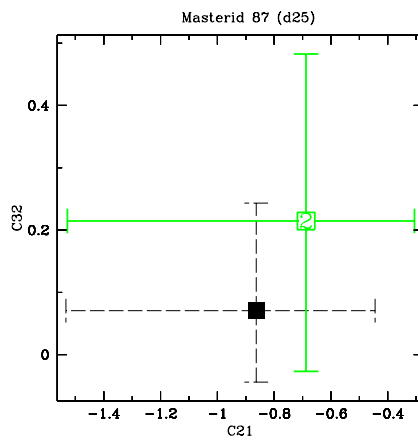
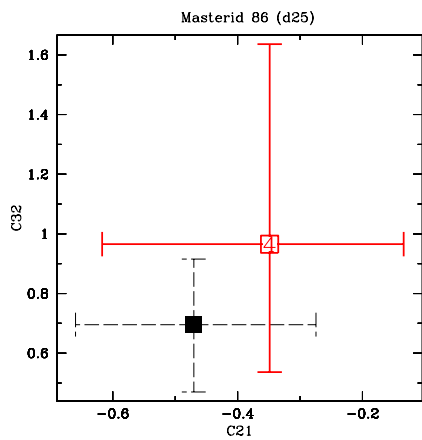
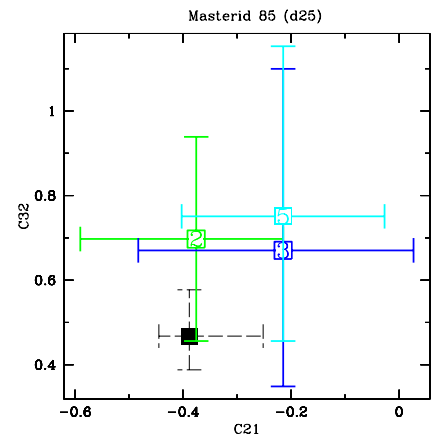
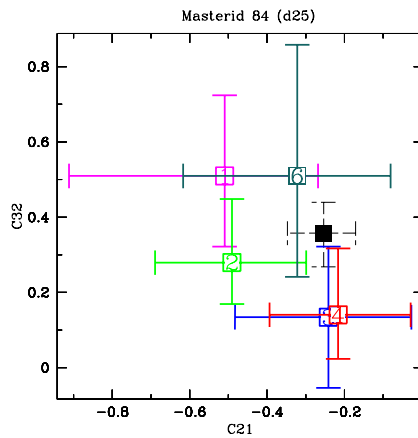
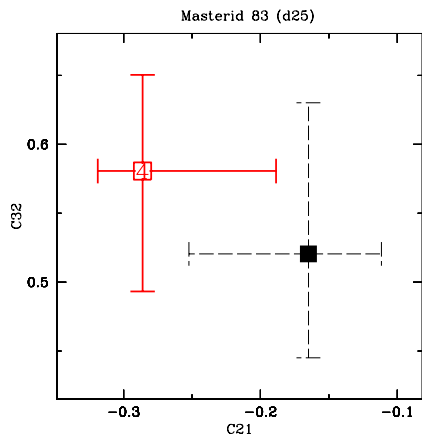
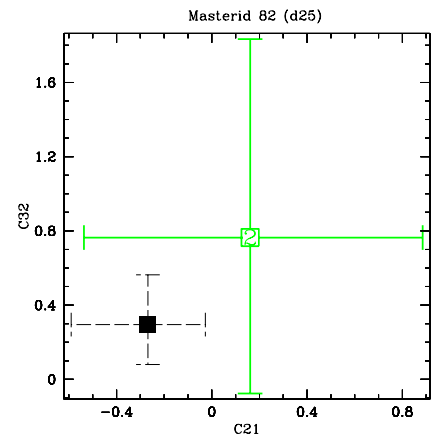
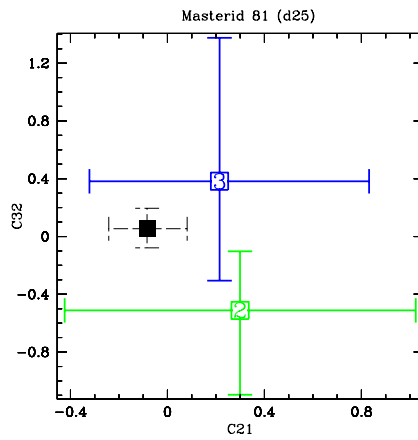
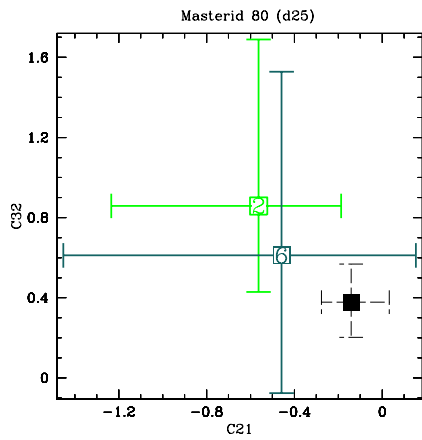
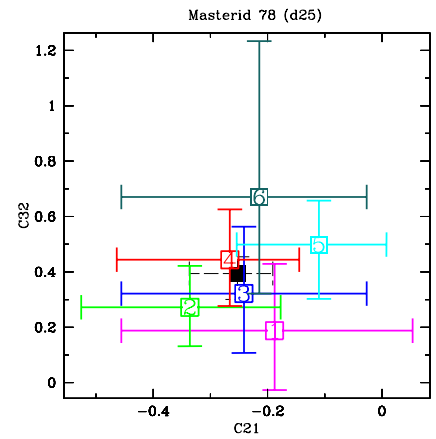
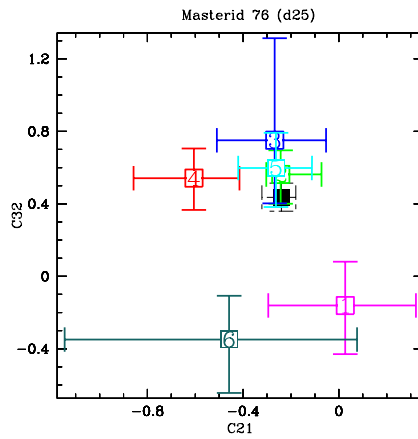
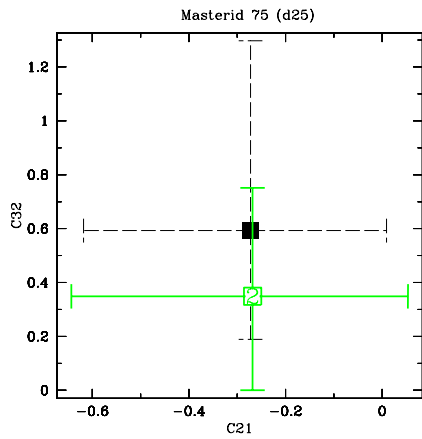
FIG. 9.— Color-color plots for each source that has been detected in more than one pointing. Each individual observation is plotted in a different color; observation 1 is magenta, observation 2 is green, observation 3 blue, observation 4 red, observation 5 is cyan and observation 6 is dark green. The co-added observation is also plotted in black. The color ratios; C21 and C32, are plotted, where $C21 = \log S2 + \log S1$ and $C32 = -\log H + \log S2$. For the color ratios the bandwidths are defined to be $S1 = 0.3 - 0.9$ keV, $S2 = 0.9 - 2.5$ keV and $H = 2.5 - 8.0$ keV.

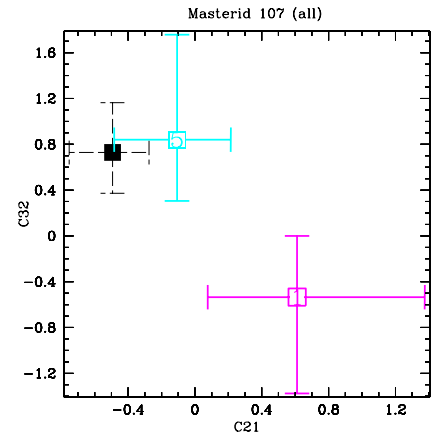
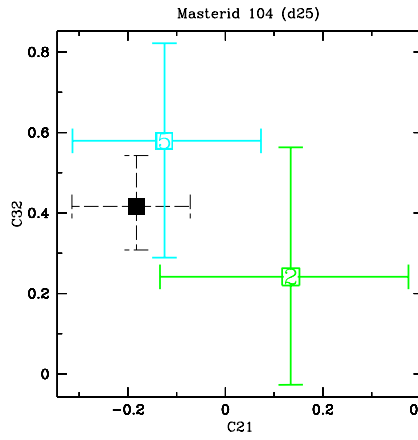
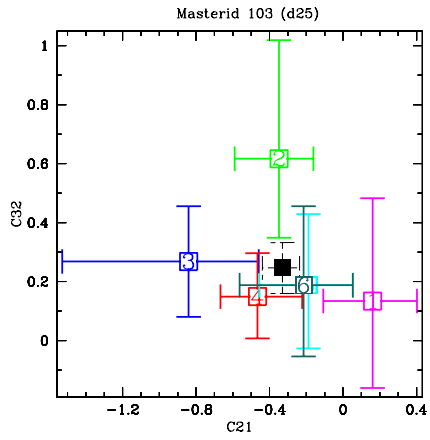
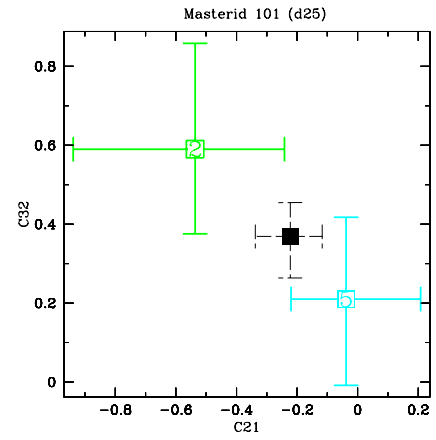
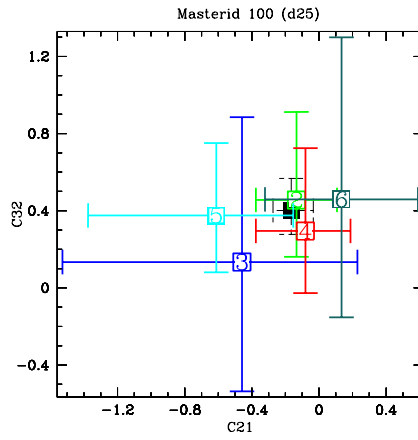
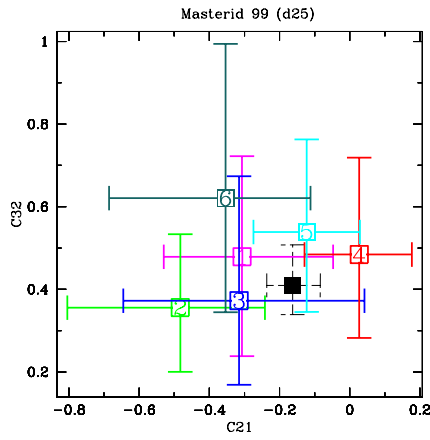
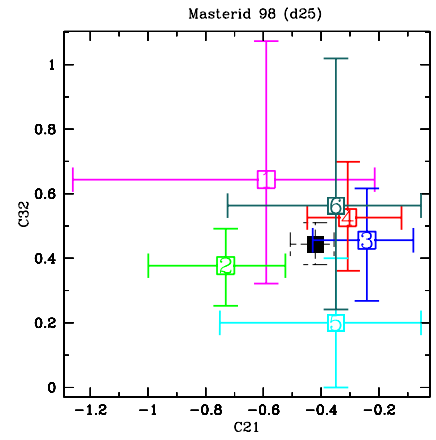
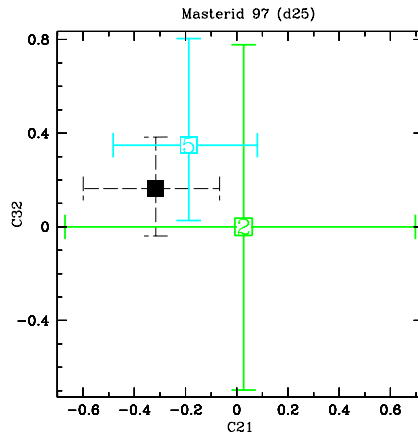
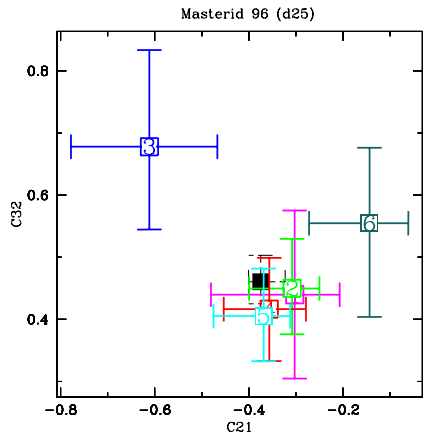
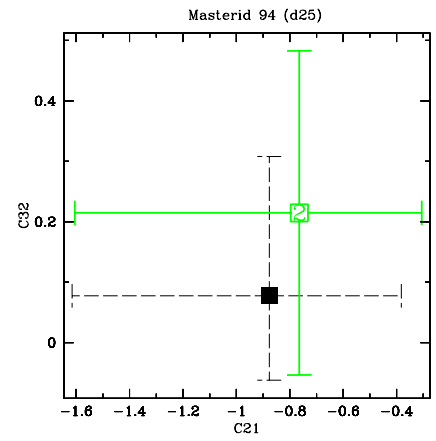
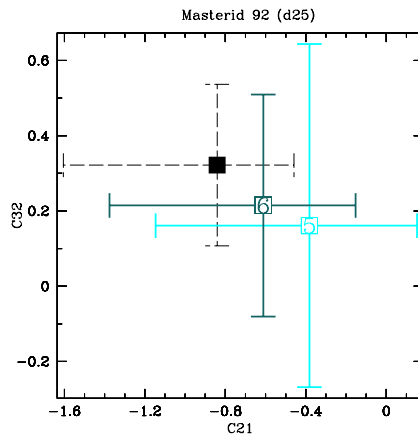
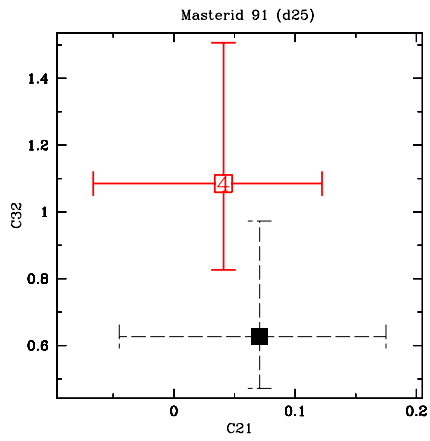


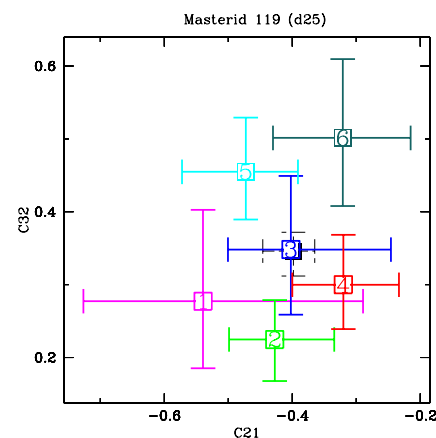
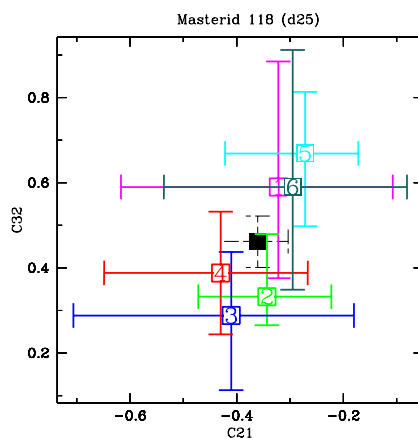
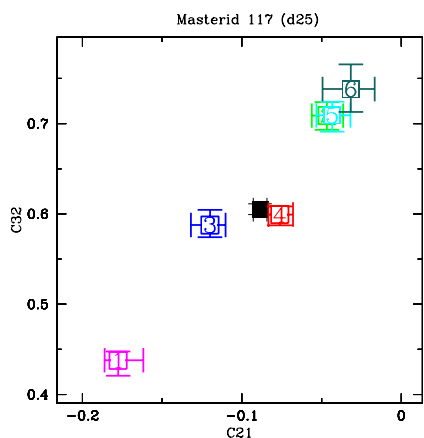
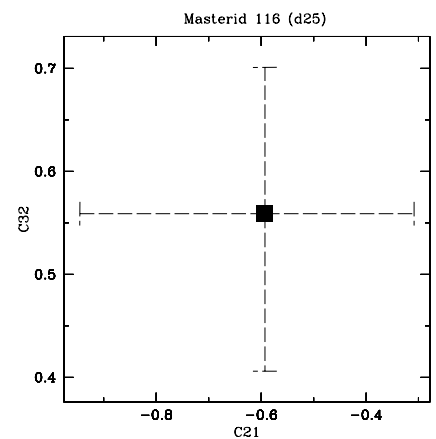
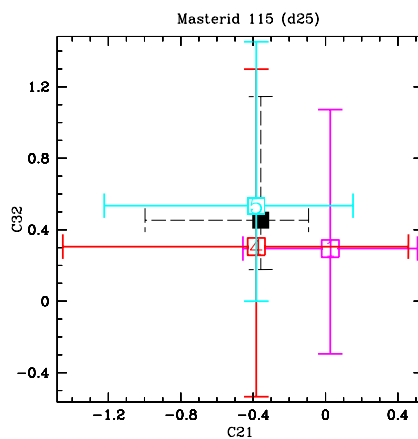
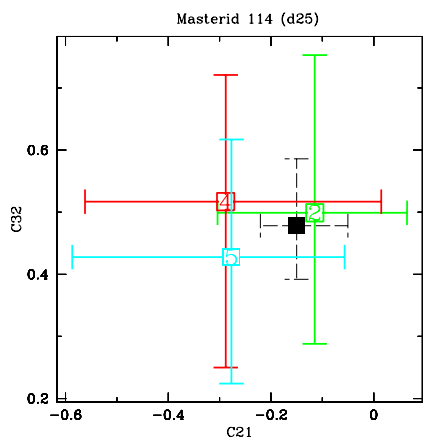
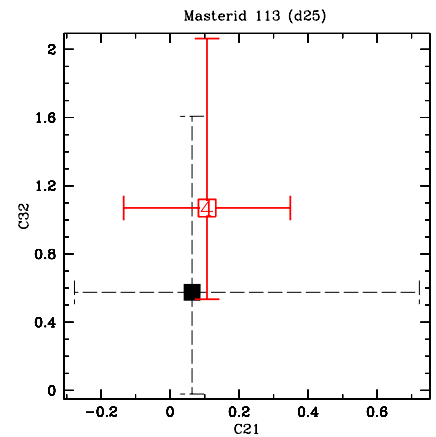
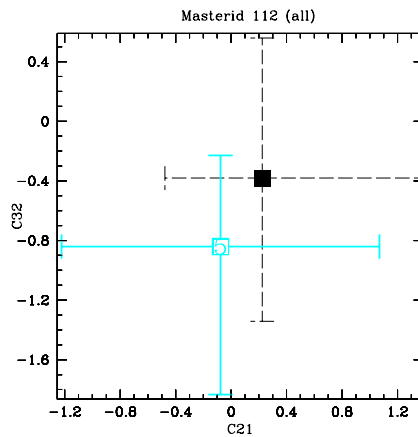
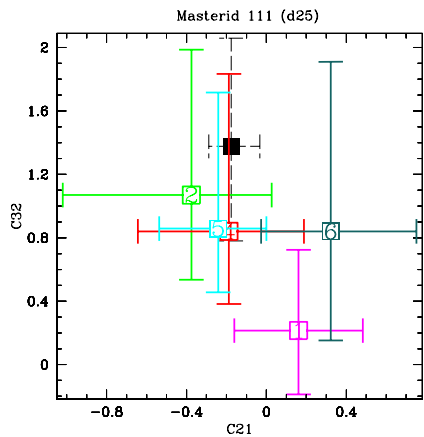
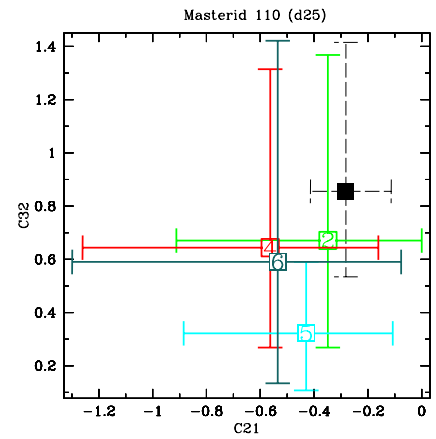
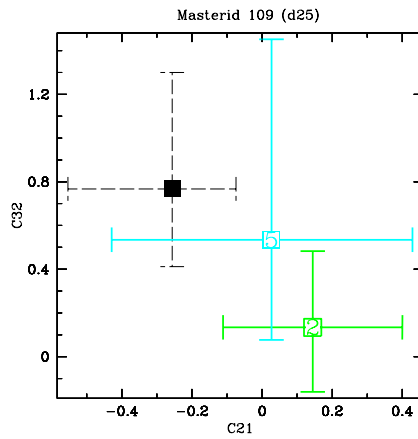
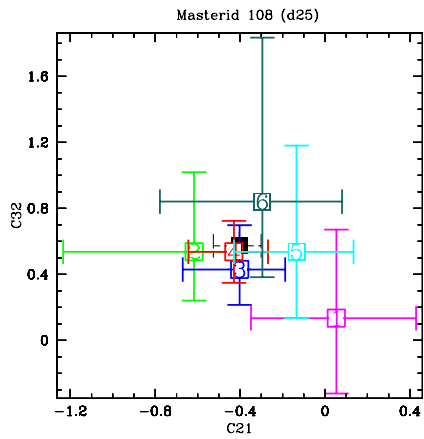


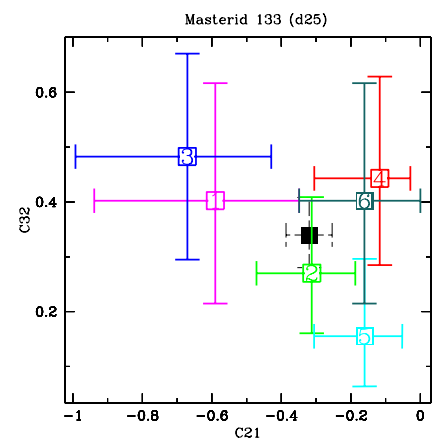
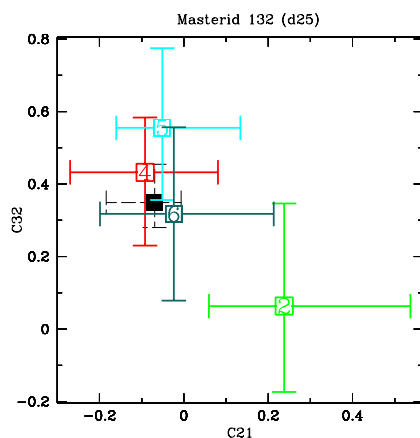
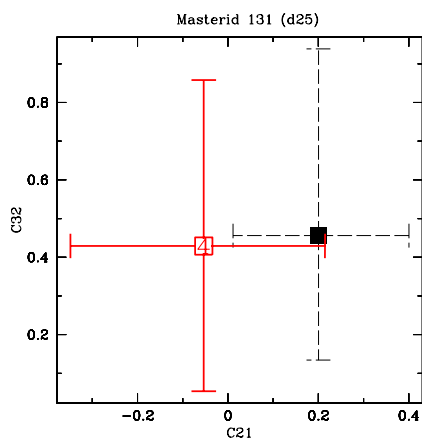
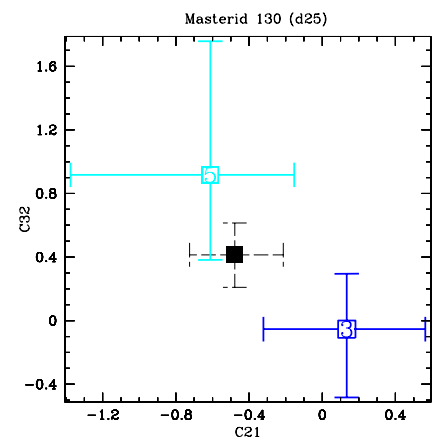
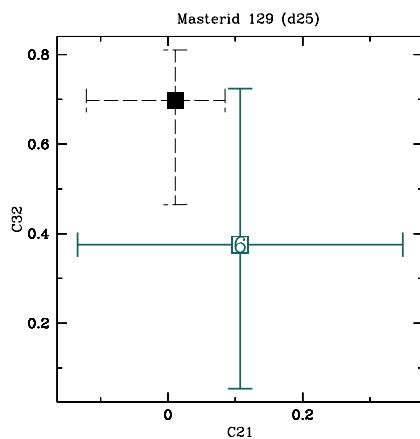
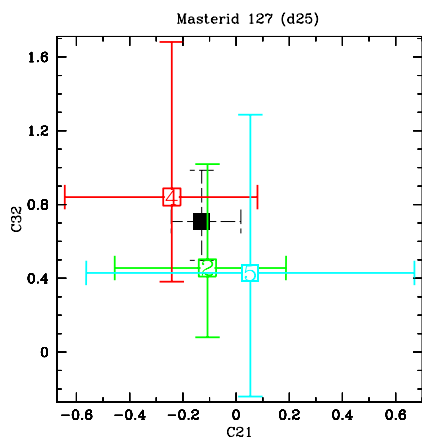
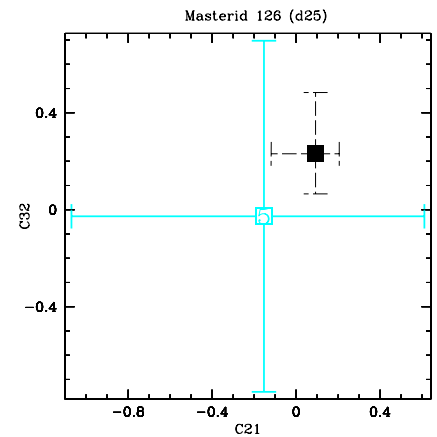
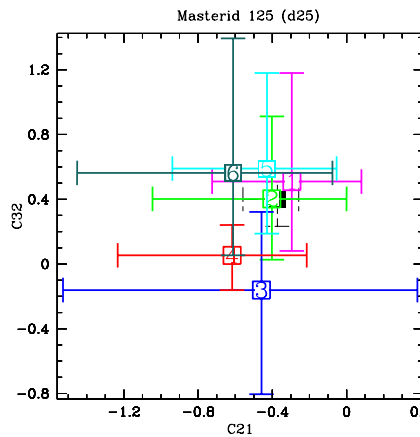
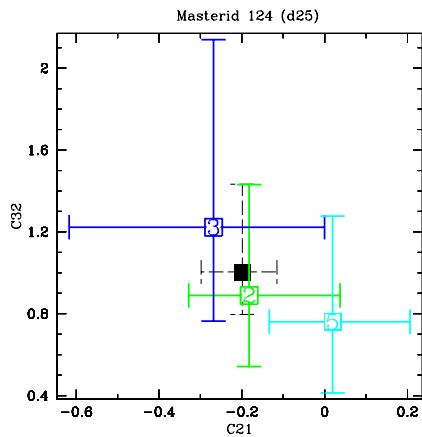
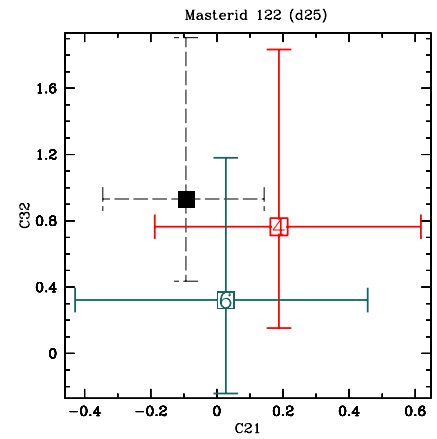
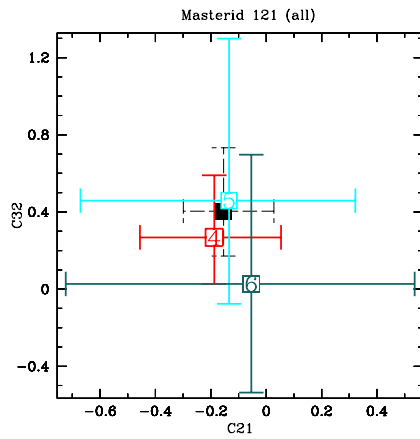
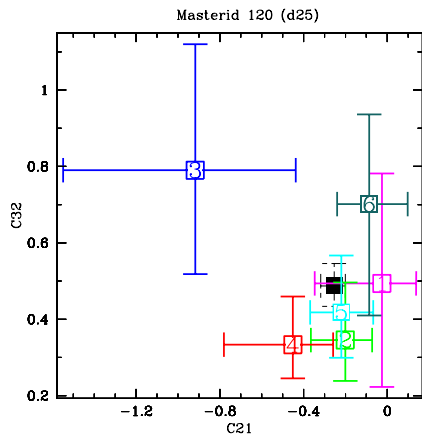


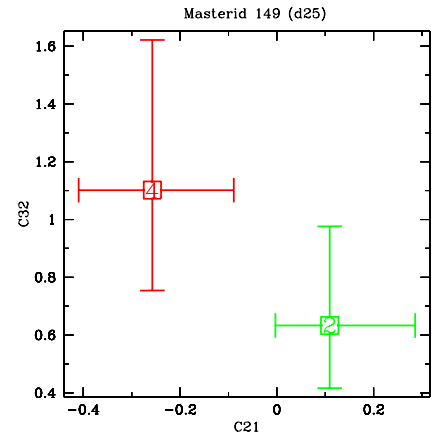
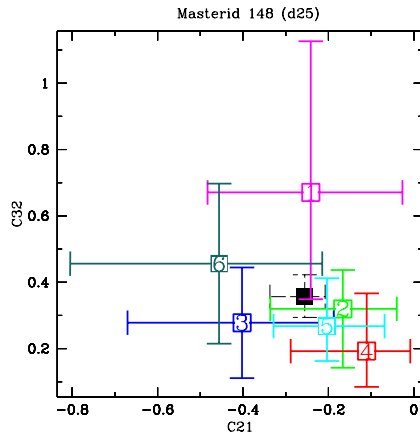
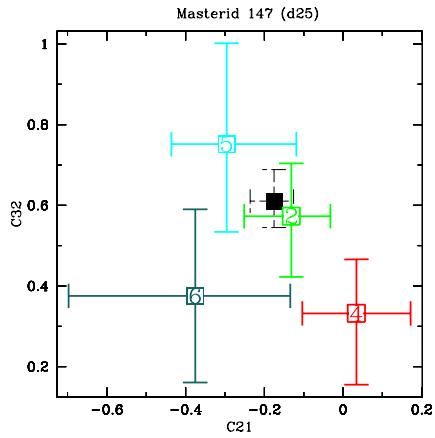
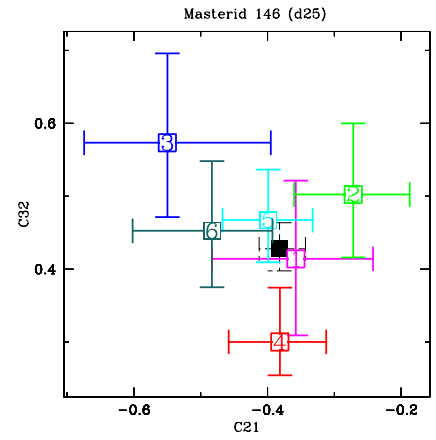
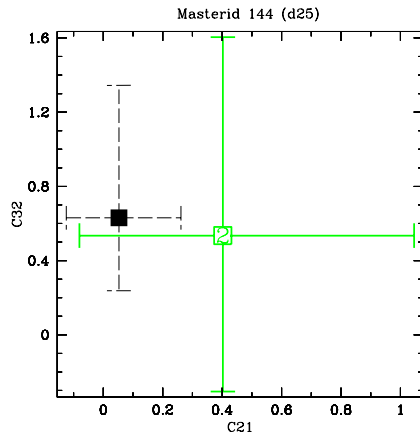
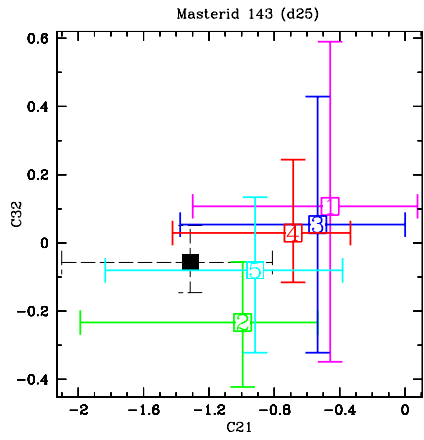
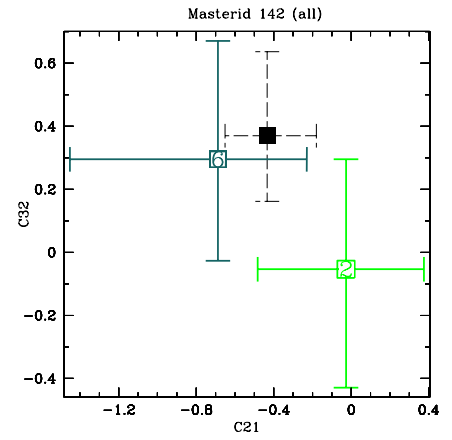
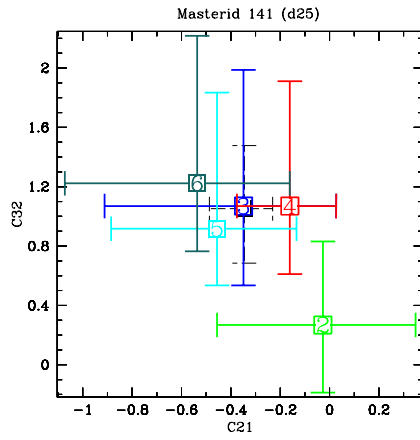
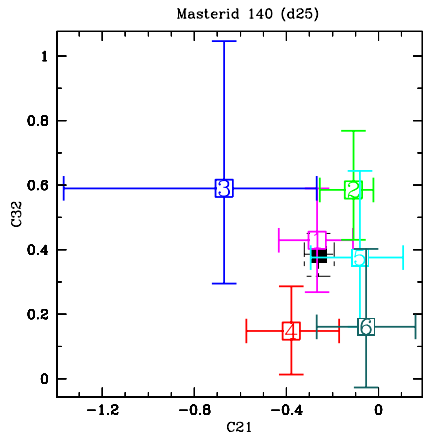
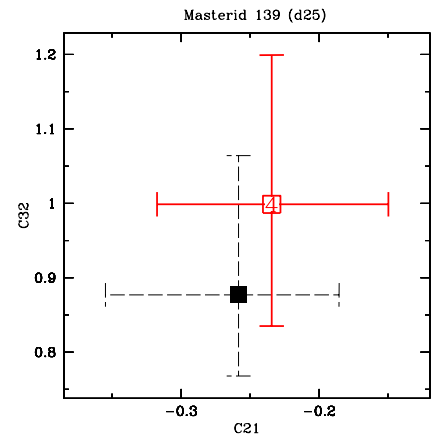
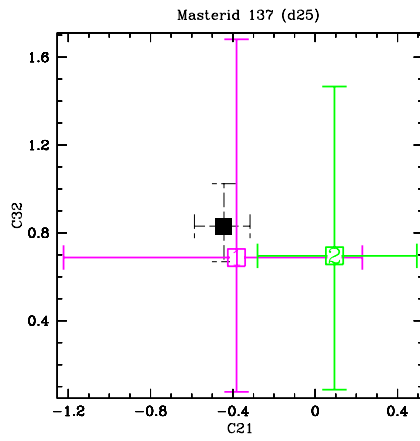
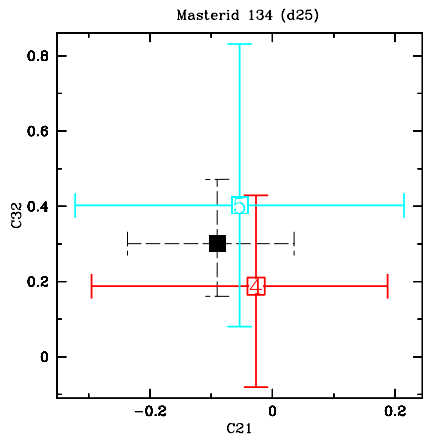


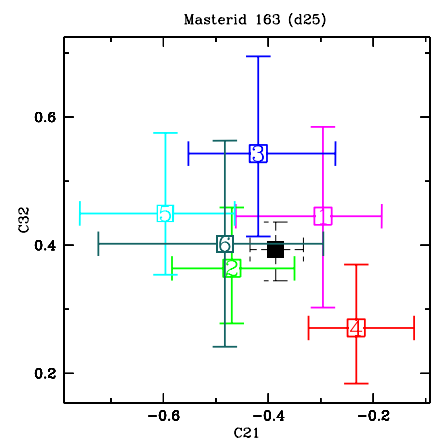
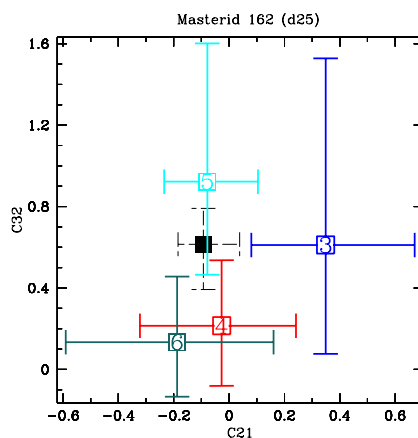
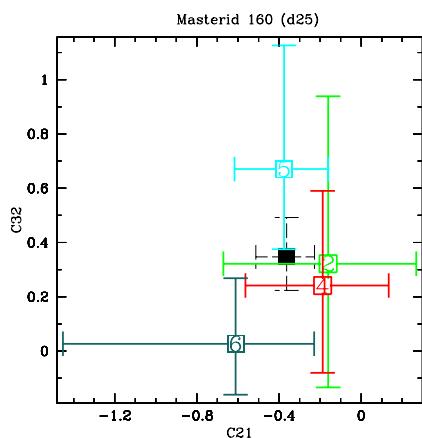
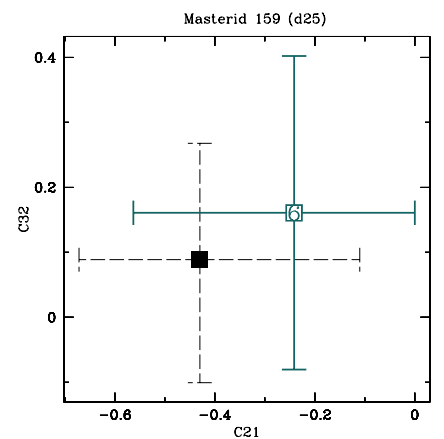
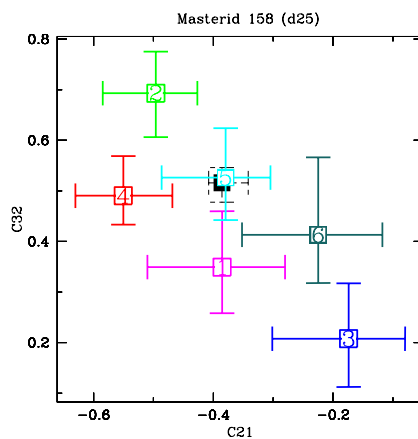
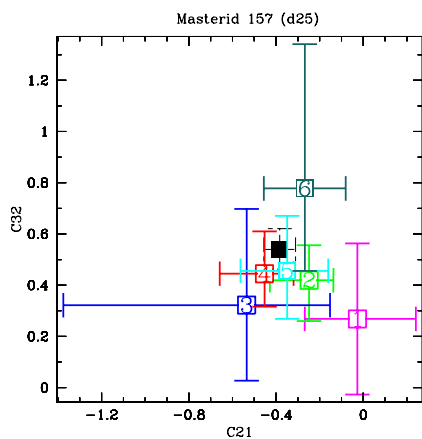
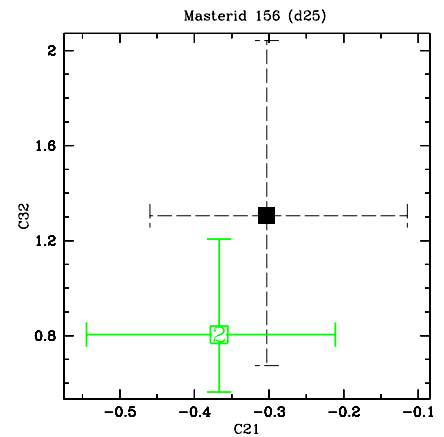
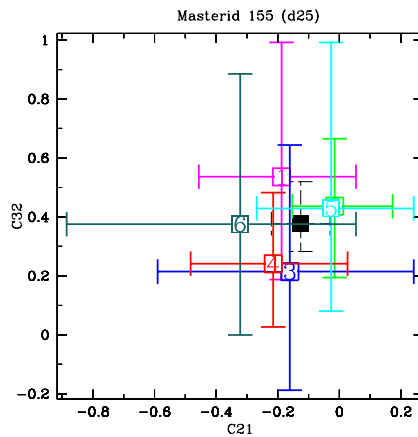
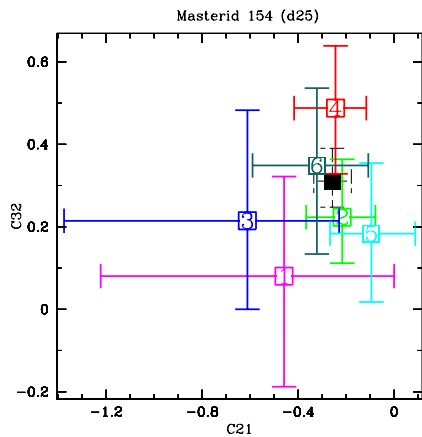
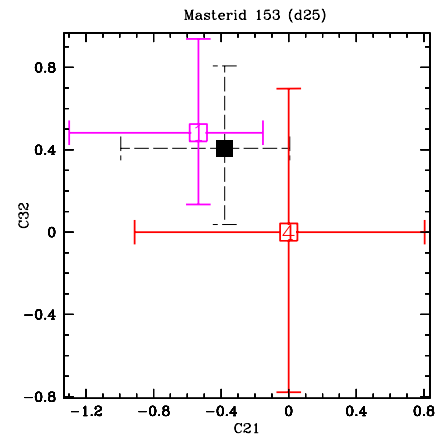
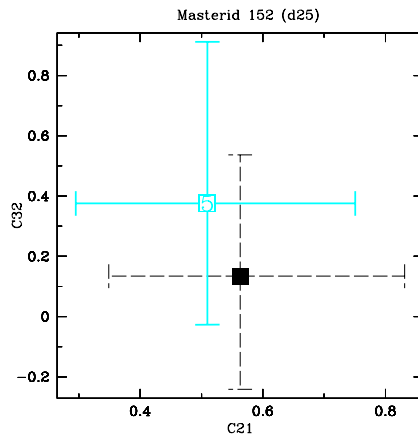
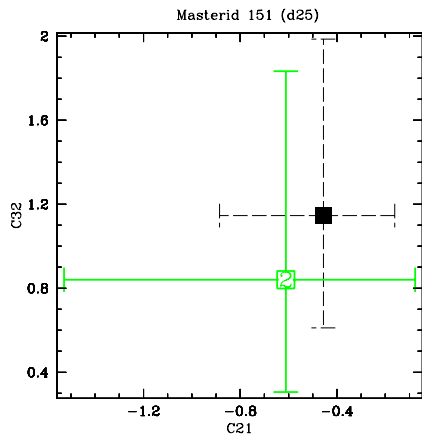


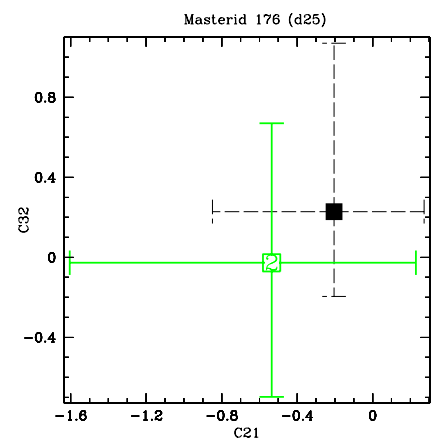
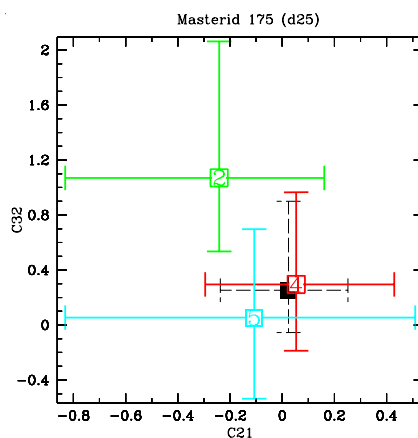
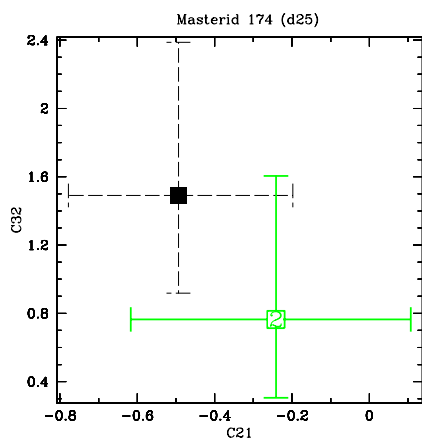
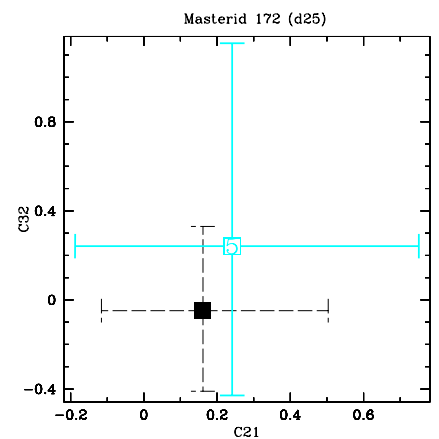
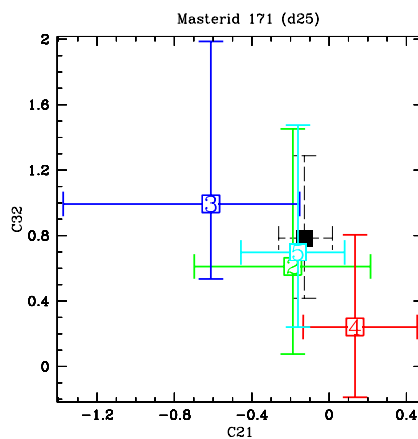
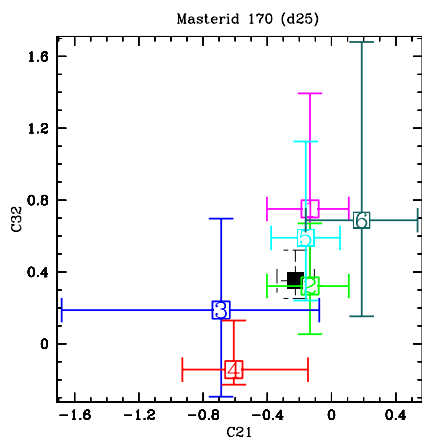
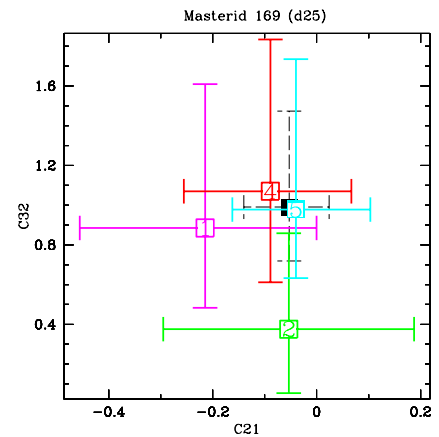
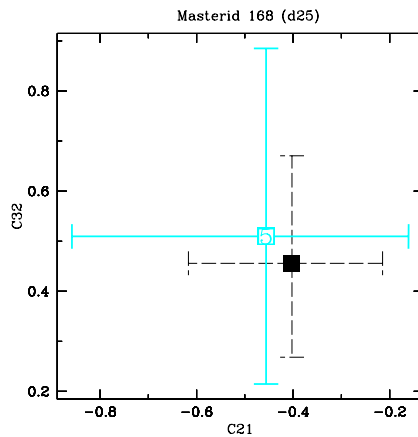
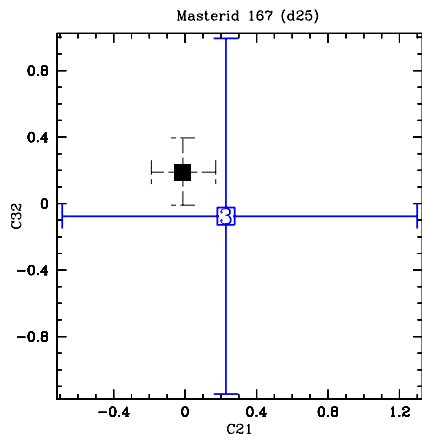
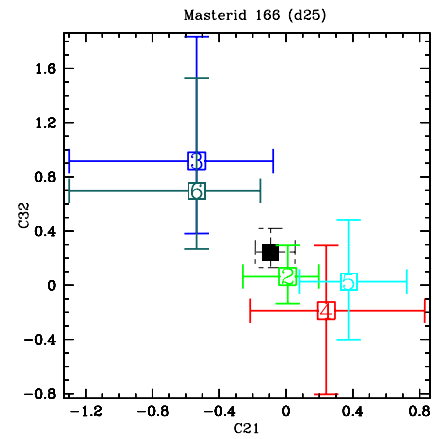
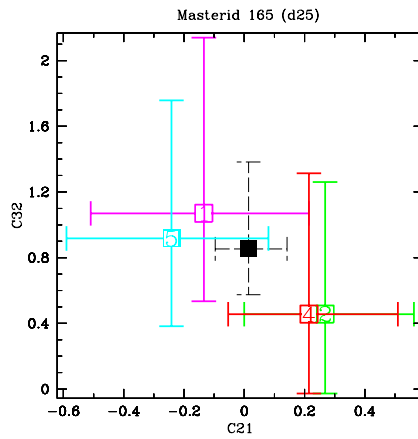
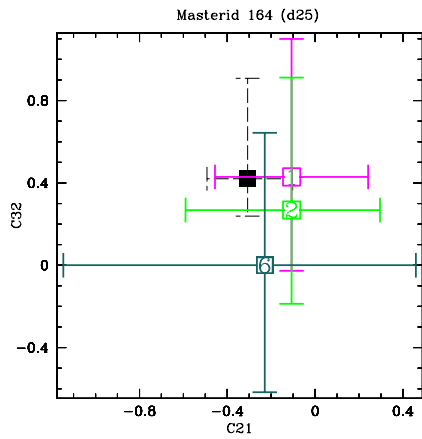


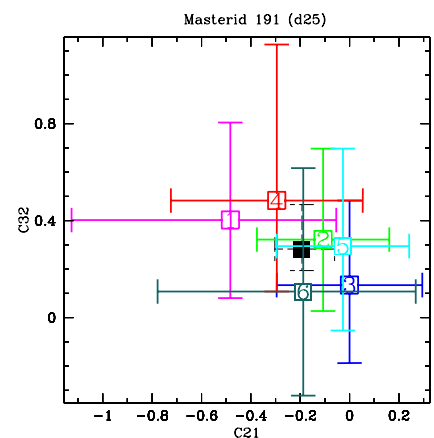
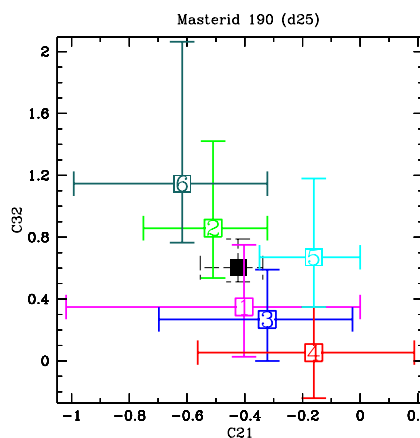
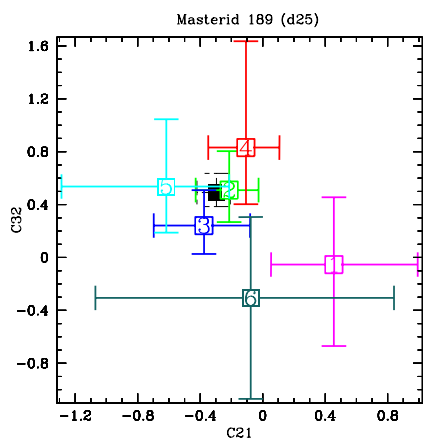
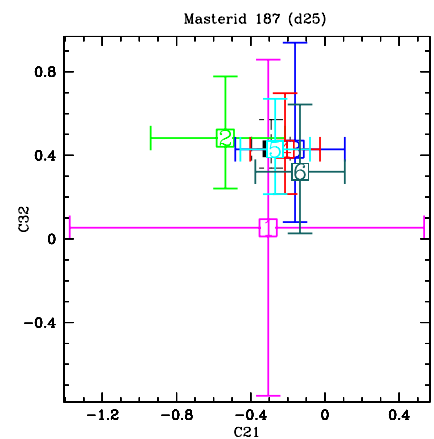
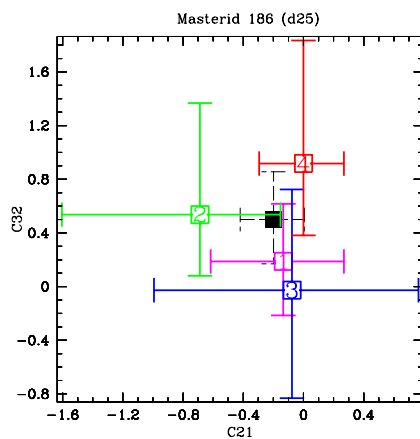
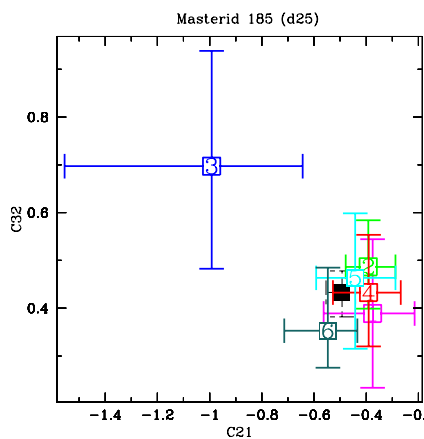
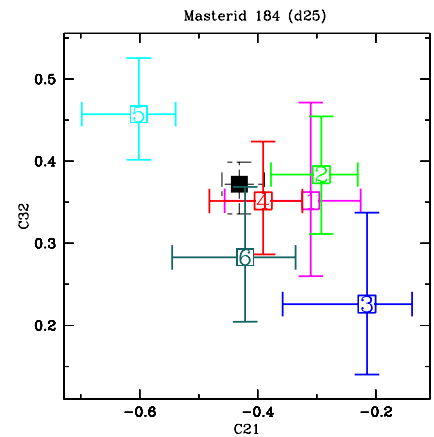
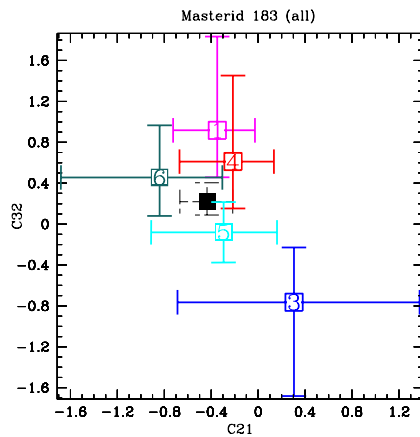
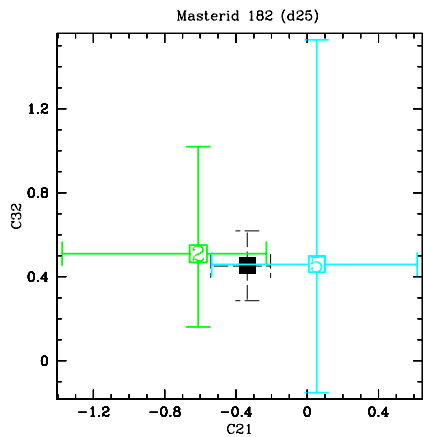
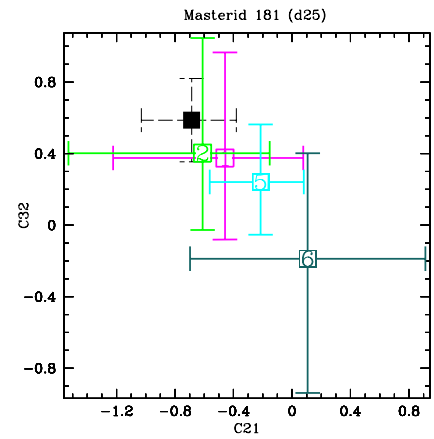
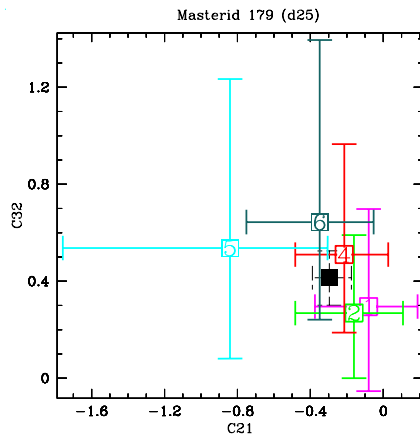
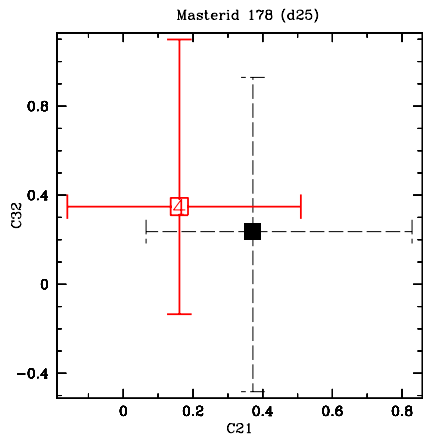


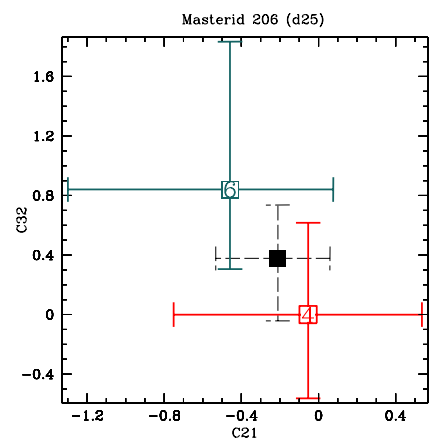
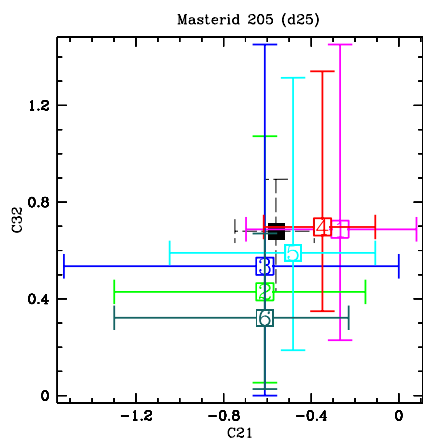
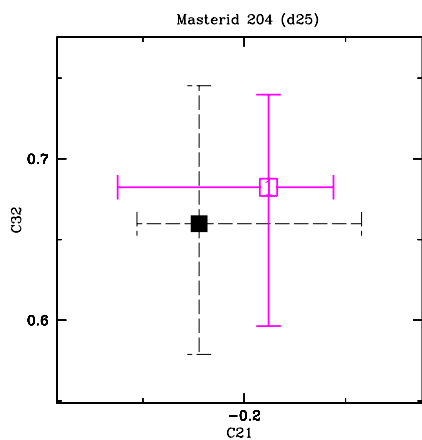
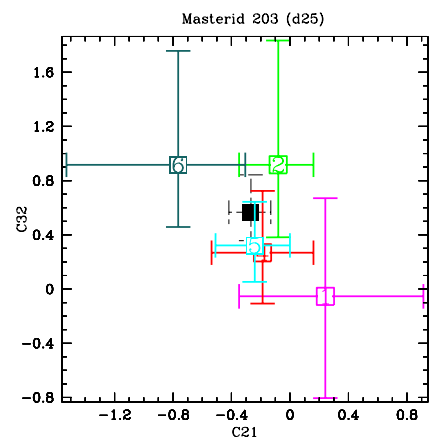
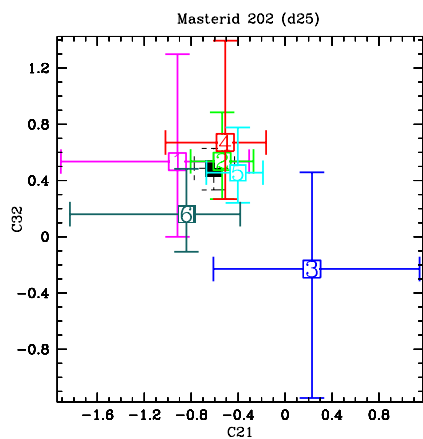
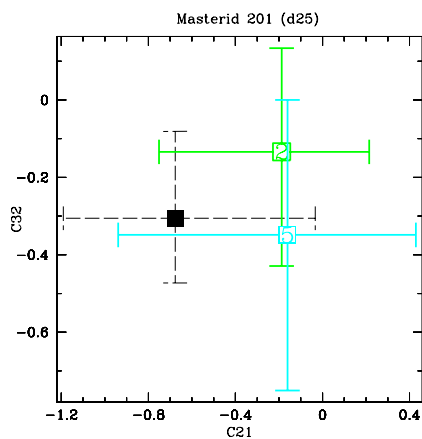
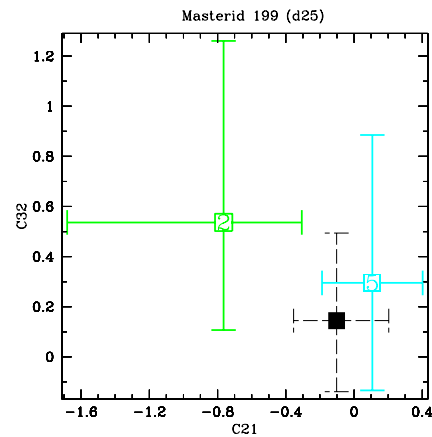
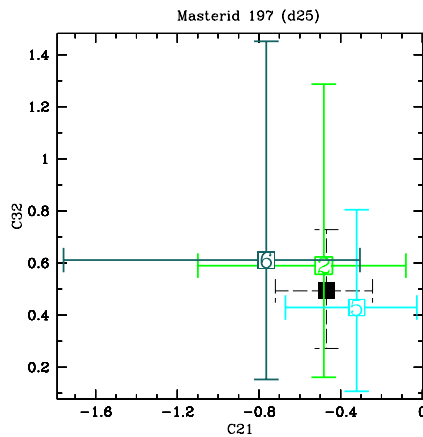
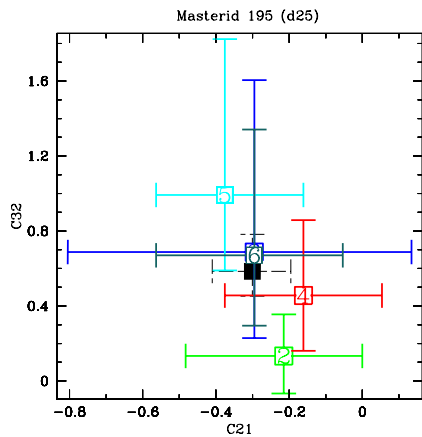
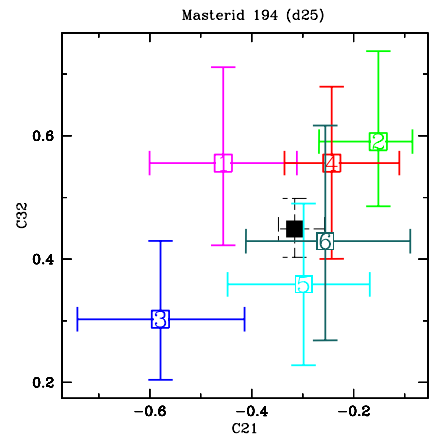
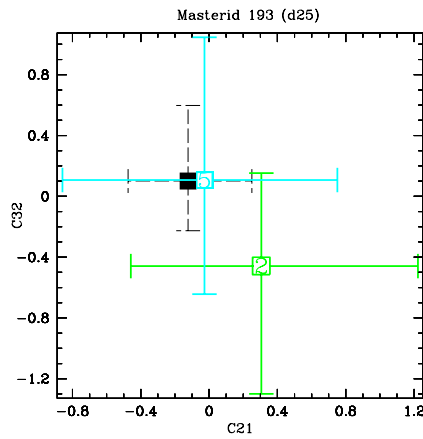
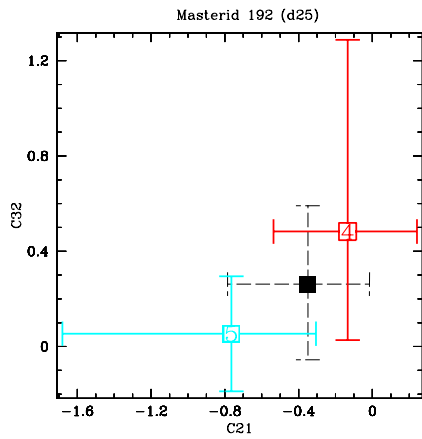


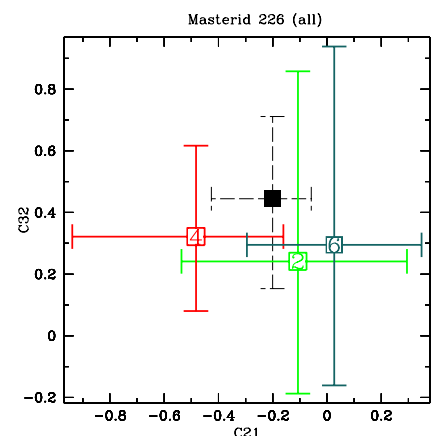
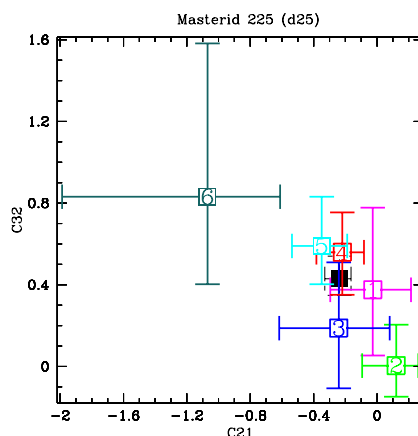
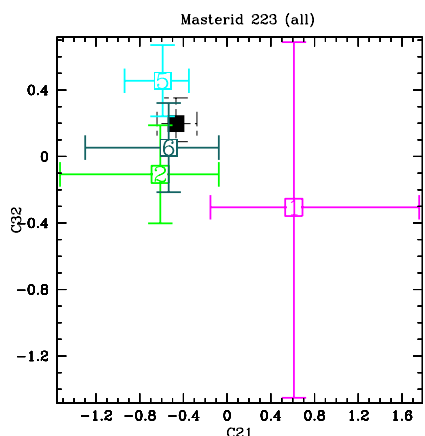
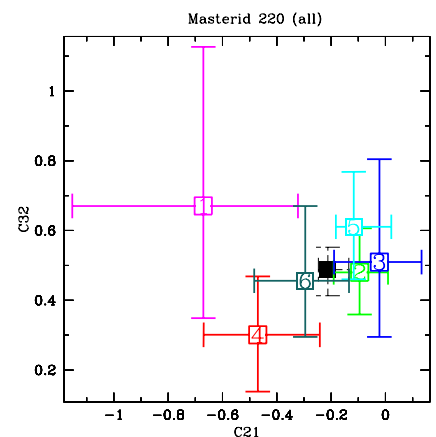
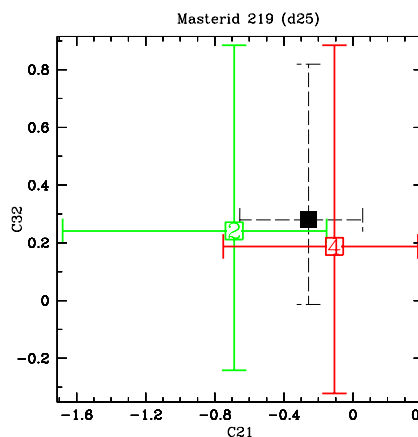
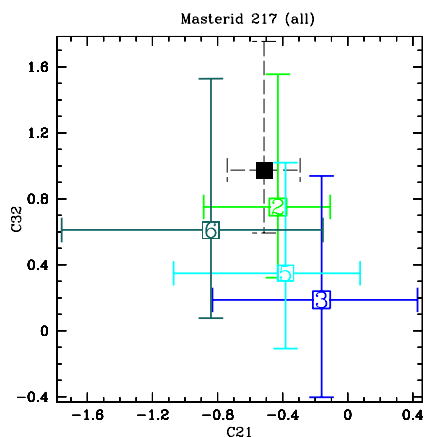
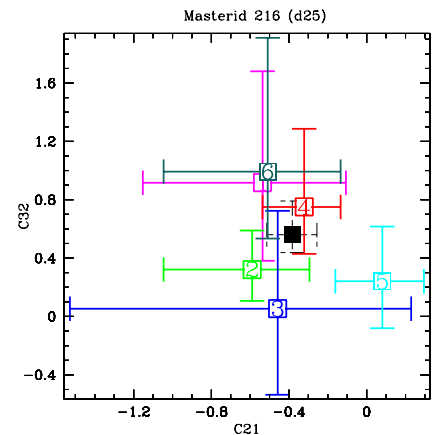
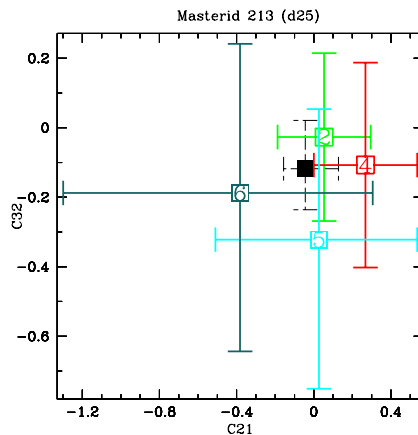
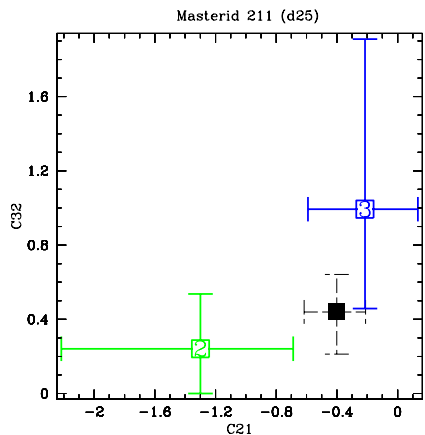
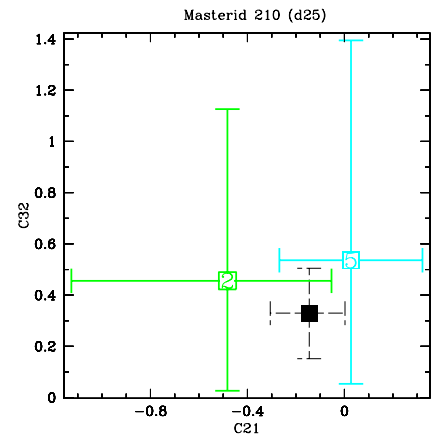
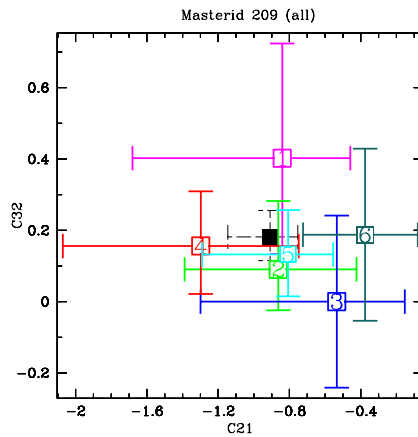
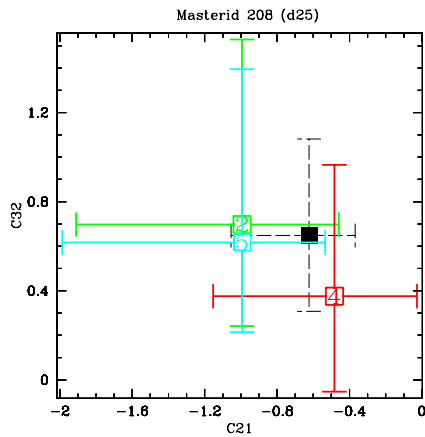


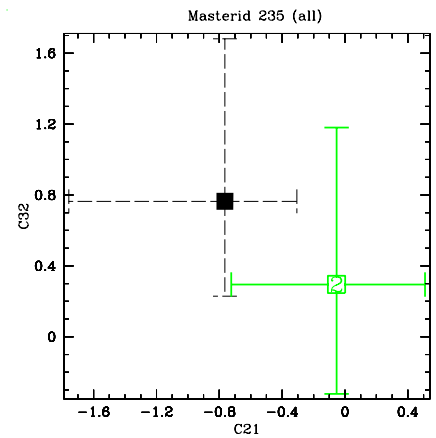
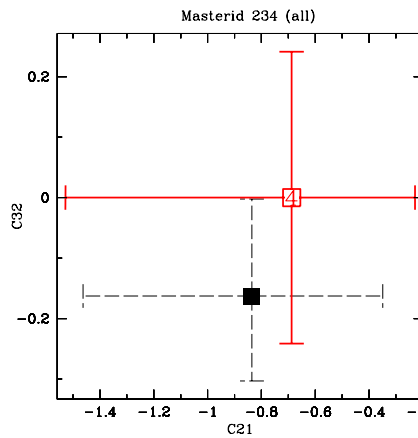
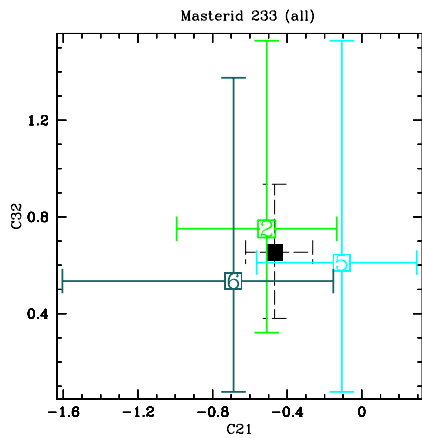
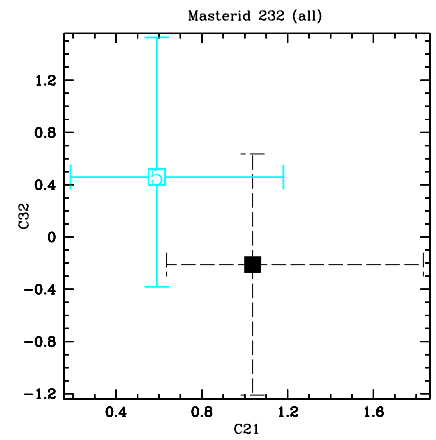
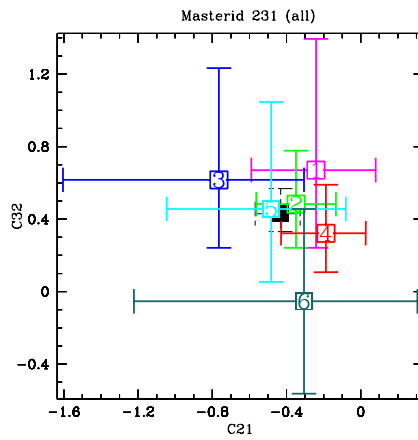
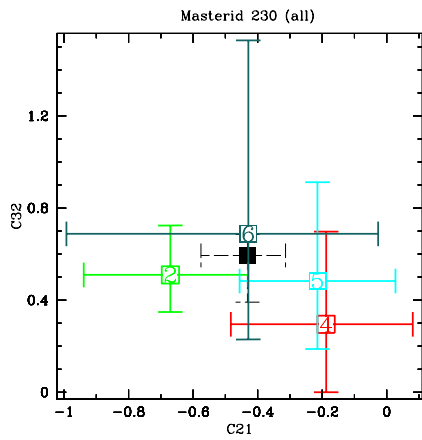
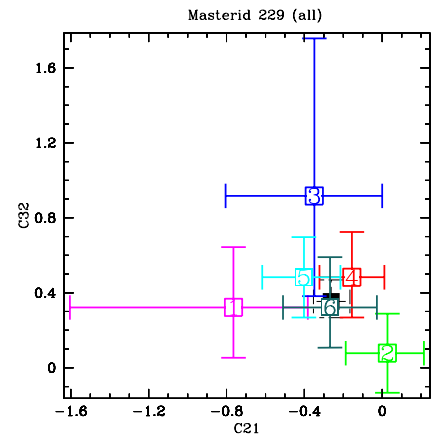
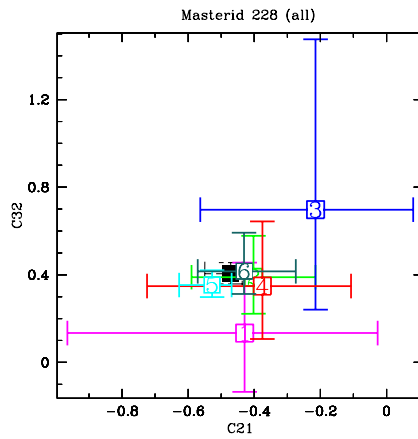
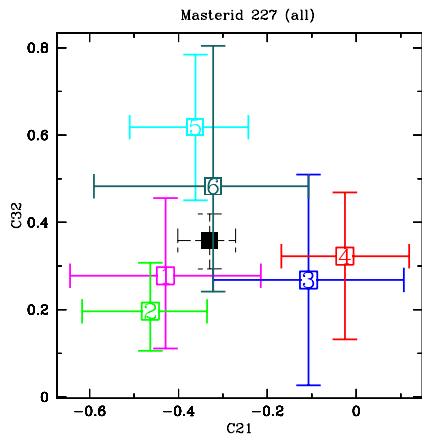












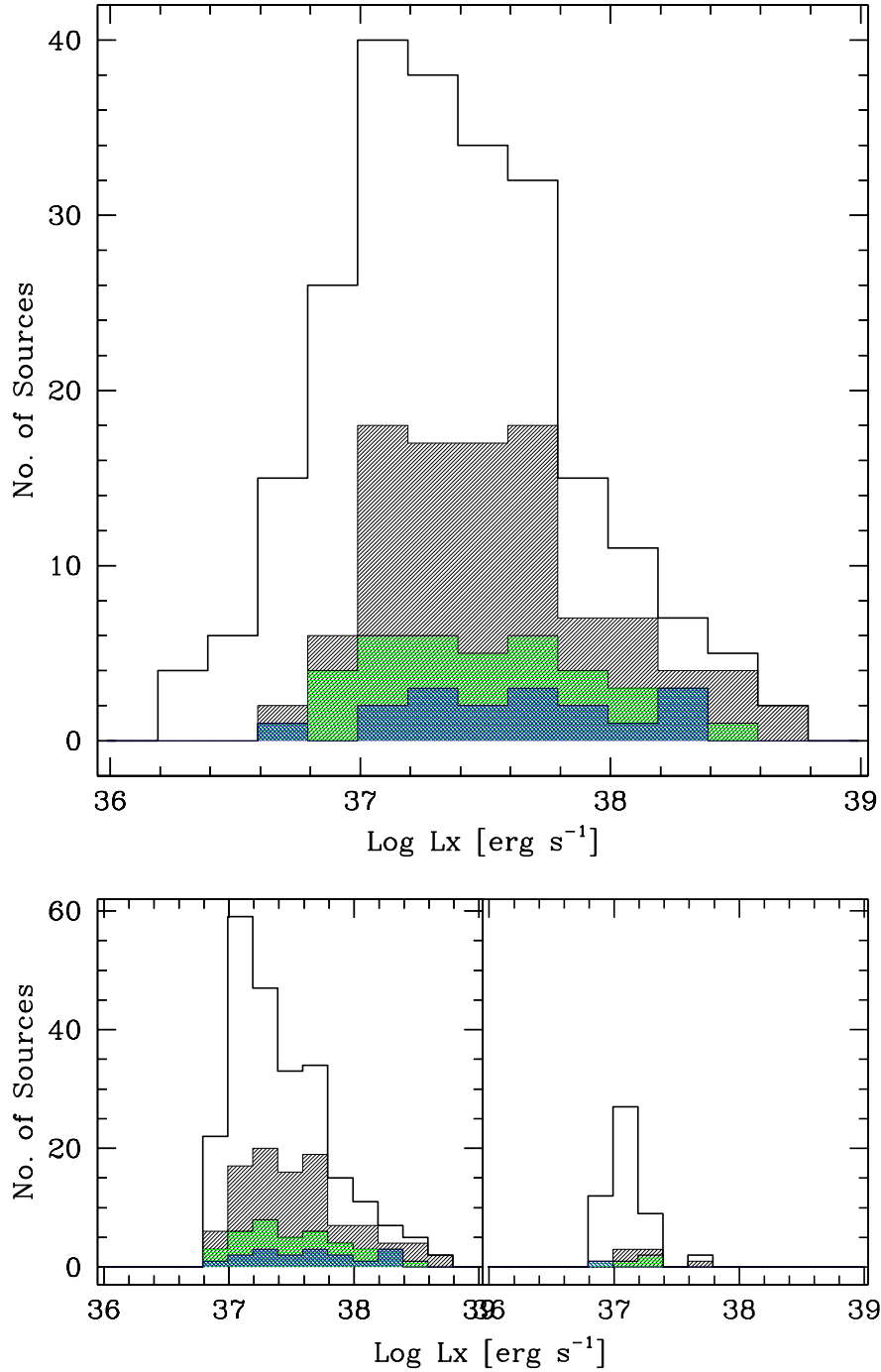


FIG. 10.— The top figure presents the L_X distribution of the 236 sources detected within the overlapping region, covered by all six *Chandra* pointings. The unshaded histogram indicates all detected sources. The lightly shaded (gray) region shows all variable sources (including both transient classes). The darker (green) histogram indicates sources associated with a GC and the darkest (blue) histogram shows varying sources that have a confirmed GC counterpart. The bottom left image indicates the same 236 sources, but for those with $S/N < 3$, 3σ upper limit values have been used in place of L_X . The bottom right image presents these upper limit values only. The shading for these two figures are the same as described for the main histogram.

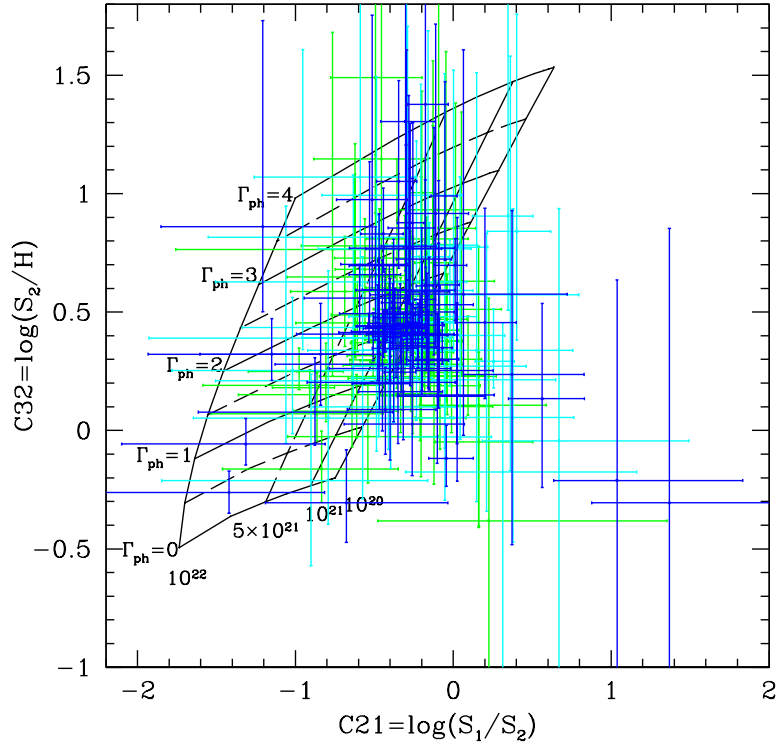
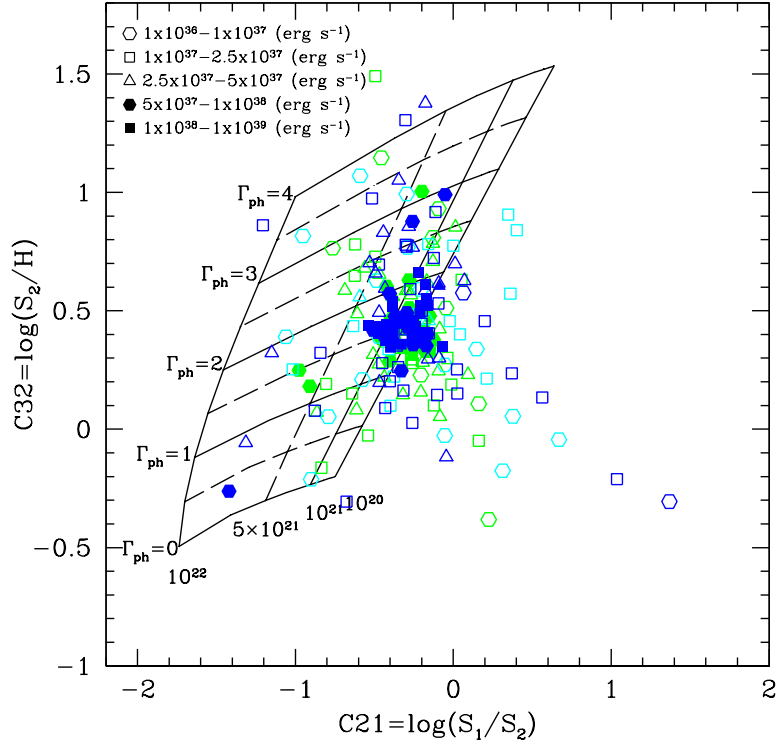


FIG. 11.— The color-color diagram of the X-ray point sources detected in the co-added observation. In the top panel color-color values are plotted, with the sources divided into luminosity bins, with symbols of each bin indicated by the labeling in the panel. Variability is also indicated, where variable sources are shown in blue, non-variable source are indicated in green and source that have insufficient counts to identify variability are shown in cyan. In the lower panel the error values for each of the sources are presented. In both of the panels, the grid indicates the predicted locations of the sources at redshift $z=0$ with various photon indices ($0 \leq \Gamma_{ph} \leq 4$, from top to bottom.) and absorption column densities ($10^{20} \leq N_H \leq 10^{22} \text{ cm}^{-2}$, from right to left).

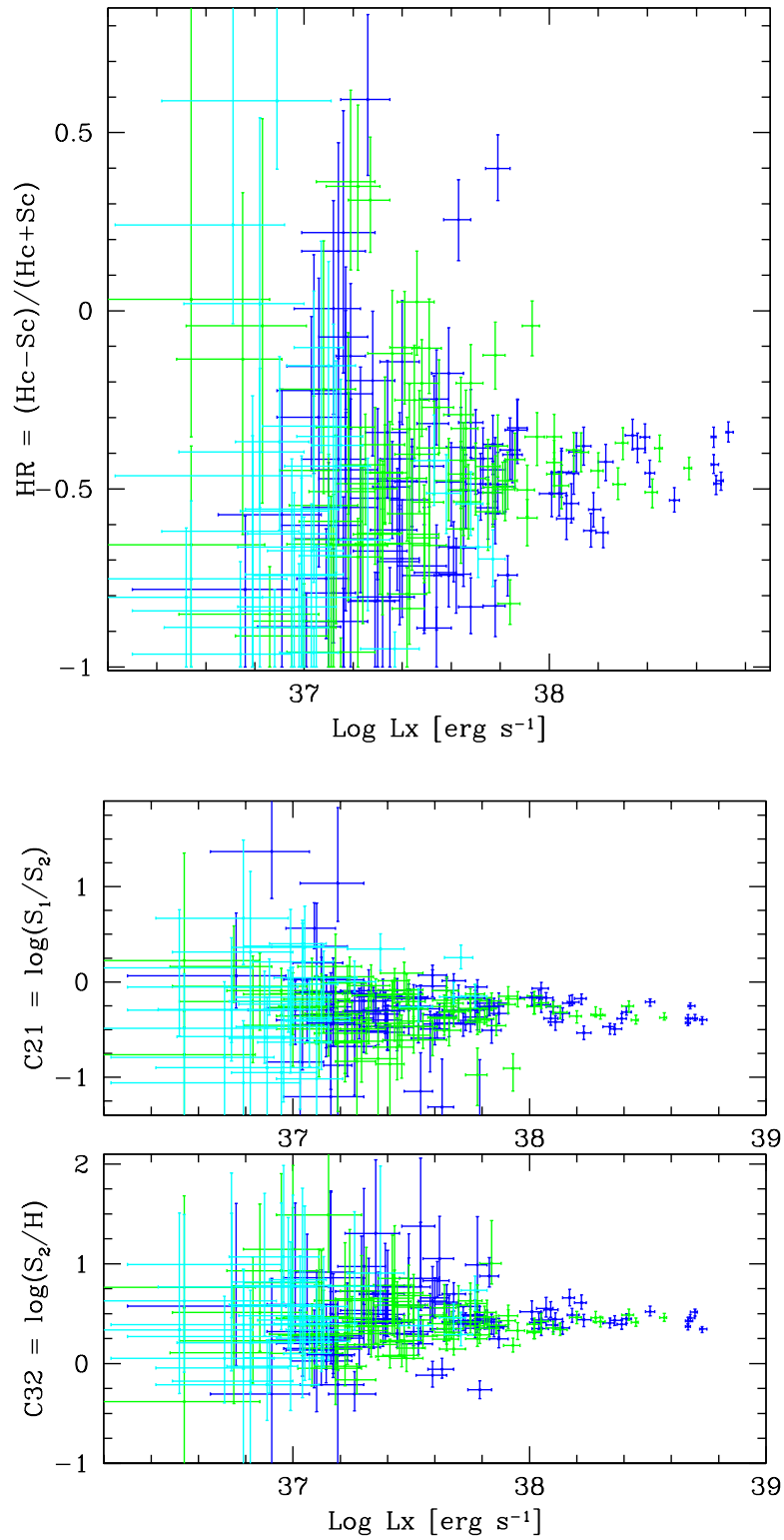


FIG. 12.— The top panel presents the L_X -HR diagram of the X-ray point sources detected in the co-added observation. The second panel shows the L_X -C21 plot for this population and the bottom panel shows the L_X -C32 values. In all three panels the variable sources are plotted in blue, non-variable sources in green and the sources without determined variability are plotted in cyan.